ZooKeys 1230: 1–24 (2025)
DOI: 10.3897/zookeys.1230.134516

Checklist

An annotated checklist and the first Red List of harvestmen (Opiliones) of Slovakia

Juraj Litavský[1], Slavomír Stašiov[2], Ivan Mihál[3], Martin Šalkovič[1]

1 *Department of Environmental Ecology and Landscape Management, Faculty of Natural Sciences, Comenius University, Ilkovičova 6, SK 842 15 Bratislava, Slovakia*
2 *Department of Biology and General Ecology, Faculty of Ecology and Environmental Sciences, Technical University in Zvolen, T. G. Masaryka 24, SK 960 01 Zvolen, Slovakia*
3 *Institute of Forest Ecology, Slovak Academy of Sciences, Štúrova 2, SK 960 53 Zvolen, Slovakia*
Corresponding author: Juraj Litavský (juraj.litavsky@uniba.sk)

Abstract

Although harvestmen are a significant group of terrestrial invertebrates, their effective protection has not been ensured in Slovakia to this day. Not a single species belonging to the order Opiliones has been included in the "Red Data Book of threatened and rare plant and animal species of the Czech and Slovak Federal Republic". Harvestmen have also not been included in the Red List of plants and animals of Slovakia. Since a new Red Data Book of invertebrates of Slovakia is currently under production, a checklist and the first Red List of harvestmen of Slovakia were prepared. Thirty-five species of harvestmen were identified based on the analysis of all records published since 1873 and our unpublished records. A total of 5,254 records of harvestman species from 2,772 locations were analysed across 318 grid cells, each measuring 10 × 10 km. Two species were recorded exclusively in the Pannonian and six in the Alpine biogeographical region, while the remaining species occurred in both regions. All 35 species were assessed based on the current IUCN Red List criteria, categorising them as follows: Critically Endangered (*Holoscotolemon jaqueti*), Endangered (*Siro carpaticus*), Vulnerable (*Gyas titanus*, *Ischyropsalis manicata*, *Paranemastoma kochii*, *Paranemastoma quadripunctatum*), Near Threatened (*Lacinius dentiger*, *Lacinius horridus*, *Opilio parietinus*, *Platybunus pallidus*), Least Concern (22 species), Data Deficient (2), and Not Evaluated (1). A brief overview of the history of Opiliones research in Slovakia is also provided.

Key words: Arachnida, diversity, IUCN categories, species conservation, zoogeography

Academic editor: Gonzalo Giribet
Received: 12 August 2024
Accepted: 5 January 2025
Published: 5 March 2025

ZooBank: https://zoobank.org/F1E5EC26-E7AA-4A0A-B015-344DB29297DF

Citation: Litavský J, Stašiov S, Mihál I, Šalkovič M (2025) An annotated checklist and the first Red List of harvestmen (Opiliones) of Slovakia. ZooKeys 1230: 1–24. https://doi.org/10.3897/zookeys.1230.134516

Introduction

The order Opiliones consists of 6,757 species belonging to 1,704 genera, 71 families, and 4 suborders: Cyphophthalmi, Dyspnoi, Eupnoi, and Laniatores (Kury et al. 2024), to which an extinct suborder Tetrophthalmi was also assigned (Garwood et al. 2014). They are distributed on all continents except Antarctica. Their estimated diversity comprises more than 10,000 species (Pinto-Da-Rocha et al. 2005; Boyer et al. 2007).

Regarding the history of opiliofauna research in Slovakia, Sørensen's work (Sørensen 1873) represents the first and oldest publication providing data on harvestmen at the territory of today's Slovakia. Following that, Herman's work (Herman 1879) focused on findings of harvestmen around Bratislava. Petricskó (1892) in his monograph, documented the presence of seven species of harvestmen from the vicinity of Banská Štiavnica. Another study containing information on harvestmen from areas of Bratislava, Bardejov, Nitrianske Pravno, Starý Smokovec, and Popradské pleso was conducted by Daday (1918). Among the earliest works dedicated to the issue of the Slovak opiliofauna are also studies by Roewer (1923), Dudich (1928), Kolosváry (1929, 1933), Bartoš (1939a, 1939b), Kratochvíl (1933, 1934, 1939), and Dudich et al. (1940). A significant contribution to the knowledge of the opiliofauna of Slovakia was made by V. Šilhavý (Šilhavý 1949, 1950, 1956, 1966, 1968a, 1968b, 1970, 1972, 1974, 1981), who published findings on the distribution, ecology, and ontogeny of our species. He devoted himself to the taxonomy of harvestmen and resolved several ambiguities in their systematics, thereby advancing the research on Opiliones at the pan-European level. His most significant work (Šilhavý 1956) contains descriptions of 64 species of harvestmen recorded in the territory of the former Czechoslovakia, or the author assumed their distribution there. The first Slovak authors who studied the fauna of harvestmen in our country were Ferianc (1949), Lác (1957, 1990), Ložek and Gulička (1955), Gulička (1957, 1985). Jasenák (1972) also conducted studies on harvestmen in the Devínska Kobyla Nature Reserve. Hroznár (1981) described the fauna of harvestmen in the Kriváň – part of the Malá Fatra mountain. Košel (1984, 1994) published records of the species *Ischyropsalis manicata* in some caves in Slovakia. Majzlan and Hazuchová (1997) conducted research on opiliofauna in various locations in the floodplain forests of Podunajská nížina (Danubian Lowland). In the 1990s, Mašán and Mihál (1993) and Mašán (1998) dedicated himself to the research of harvestmen in Slovakia. Since the 1990s, B. Astaloš, I. Mihál, and S. Stašiov have been the most active contributors to the study of the harvestman fauna. Their collaboration, in partnerships with other specialists in this group of organisms has led to significant progress in understanding the harvestman fauna of Slovakia, particularly in terms of faunistics, the ecology of individual species, and their bioindication potential. P. Maršalek (Maršalek 2001), A. Šestáková (Šestáková and Mihál 2014), and J. Litavský (Litavský et al. 2018, 2019) later joined those authors.

The assembly of the Red List of harvestmen of Slovakia was prompted by the requirement to provide a legislative basis for a more efficient and effective protection of threatened and rare harvestman species, which is based on current knowledge about their distribution, ecology, and the threat of their populations in Slovakia.

Material and methods

Study area

The research was conducted in Slovakia, a Central European country with an area of 49,035 km^2. The lowest point of the country, at an elevation of 94 meters a.s.l., is located on the Bodrog River on the Slovak-Hungarian border. On the contrary, the highest point in Slovakia is Gerlach Peak in the

High Tatras, reaching an altitude of 2,655 meters a.s.l. Slovakia is located in the central part of the Carpathian Arc, which is divided into the Western, Eastern, and Southern Carpathians, with its territory primarily covered by the Western Carpathians, featuring diverse mountain ranges, basins, and lowlands. A significant geological region of the Western Carpathians is the Slovenské rudohorie (Slovak Ore Mountains), which was formed through complex tectonic processes associated with folding, volcanism, and erosion during older geological periods. From the perspective of the biogeographical division of Europe, Slovakia is located in two regions: Alpine and Pannonian (Fig. 1).

The climate in Slovakia is quite diverse, due to its geographical location and varied terrain. Most of the country experiences a temperate continental climate, characterised by cold winters and warm summers, with milder winters and warmer summers in the lower elevations. The High Tatras and other higher mountain ranges have a cooler climate, with long winters and shorter, cooler summers. The Pannonian Plain has a warmer climate, with drier summers and mild winters. Atmospheric precipitation in the territory of Slovakia is more influenced by the geographical location of the territory, altitude, wind direction or leeward direction of the territory to the prevailing flow, which brings moist air masses. The average yearly temperature is ~ 10 °C, with January being the coldest month, averaging -3 °C. In contrast, July and August see the highest averages, reaching 26 °C. Annual precipitation amounts to ~ 650 mm, with July being the wettest month, receiving around 73 mm of rainfall over 11 days. The northern mountainous regions of Slovakia experience cooler and wetter conditions, whereas the southern areas are characterised by a warmer and drier climate (Faško and Šťastný 2002; Lapin et al. 2002; Bochníček and Hrušková 2015).

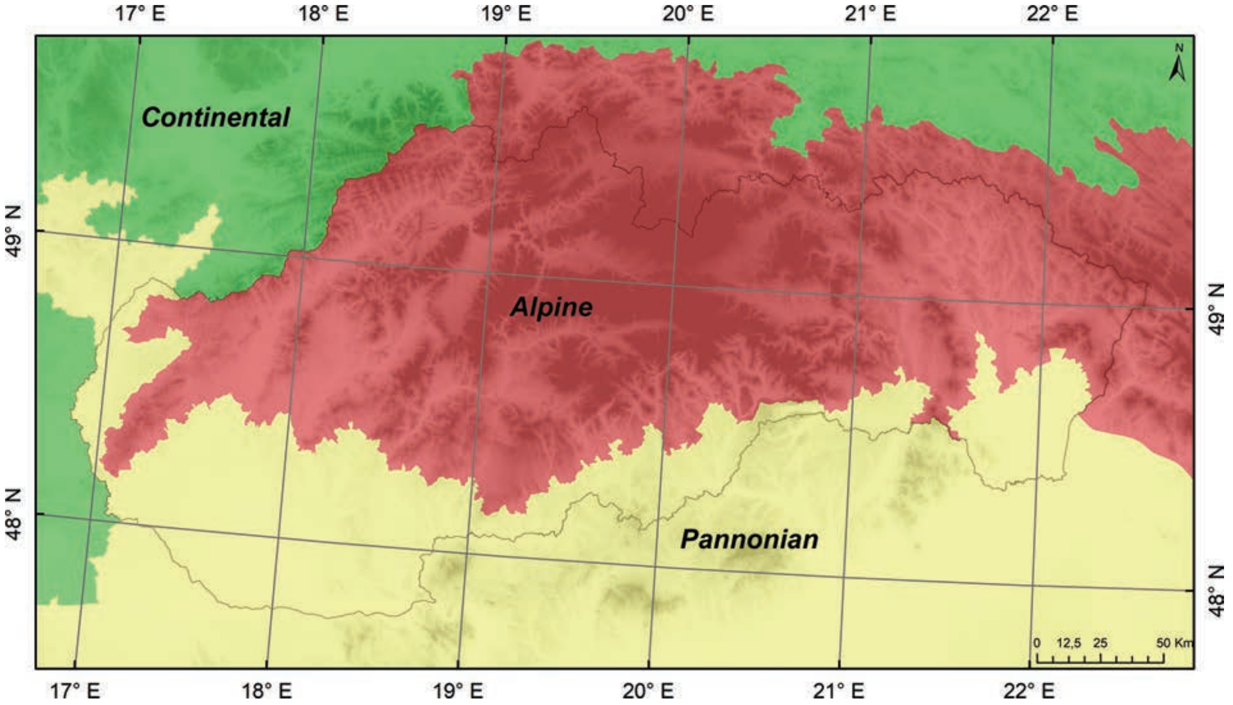

Figure 1. Biogeographical regions of Slovakia.

The landscape of Slovakia is characterised by great diversity, including mountain ranges, basins, lowlands, rivers, and lakes. The lowlands are located mainly in the south and southeast of Slovakia. The most fertile and well-known is the Danubian Lowland, while other lowlands include the East Slovak Lowland and the Záhorie Lowland. The mountain ranges include the Low Tatras and the Greater and Lesser Fatras, and the mountains feature the High Tatras. Slovakia has a wide variety of soil types, resulting from various geological and climatic conditions that also affect the diversity of the flora. In lower elevations, where chernozem and brown soils dominate, there are mainly meadows and agricultural landscape. In the middle and higher elevations, where acid podzolic soils and forest soils prevail, forests predominate, dominated by beech, oak, spruce, and fir. In mountainous areas, where peat and wet soils are found, alpine and subalpine vegetation is typical, including various types of vegetation adapted to a colder and wetter environment. This relationship between soil and flora creates various ecosystems that are characteristic of individual regional conditions in Slovakia (Lukniš 1972).

Data sampling and harvestmen mapping

We analysed all available data on harvestmen in Slovakia, including published works up to January 2024 and unpublished records from the first three authors. Building on the comprehensive work “Harvestmen of Slovakia” (Stašiov 2004), which covered data until the end of 2003, we incorporated this earlier information and added distribution records from the next 20 years (2004–2024). This allowed us to assess diversity, monitor changes in the opiliofauna, and propose a red list of harvestmen of Slovakia.

To assemble a Red List of Slovak harvestmen and the interpretation of the results using maps, we created map bases with a grid cell size of 10 × 10 km according to Murray (2017). We examined 284 literary data (from 1873 to January 2024), as well as our own previously unpublished data on the occurrence of harvestmen from a total of 2,772 locations within Slovakia. We considered the number of locations where research on harvestmen was conducted – records of harvestmen within each individual grid cell. We also assessed the species richness of harvestmen per individual grid cells covering the territory of Slovakia. Data on harvestmen records from Slovakia were processed and graphically represented for the period from 1873 to the end of 2003, and from the beginning of 2004 to January 2024. The total number of records of harvestmen in Slovakia is 5,254, which shows the total number of species-specific records during 150 years of research on this group of organisms in our country (Table 1). Most data on the occurrence of harvestmen in Slovakia were obtained using pitfall traps, hand collection, and soil and litter sieving. Due to variations in capture methods and study durations (e.g., half-year, annual, or multi-year pitfall studies versus one-day or multi-day hand collection or litter sieving), analysing and comparing the abundance of recorded individuals across these studies was not considered meaningful.

A geodatabase was created in ArcGIS Pro using descriptive data provided by the authors, including location, altitude, slope orientation, and cadastral area. Records lacking precise localisation (e.g., “the Tatras”) or involving questionable species identifications, such as *Nemastoma bidentatum* near Bardejov (Sørensen 1873) and *Opilio dinaricus* in Bratislava (Hajková 1995), were excluded from the analysis.

Table 1. Checklist of harvestman species recorded in Slovakia up to 2024 with IUCN Red list categories and criteria. Acronyms of Red List categories: CE – Critically Endangered, EN – Endangered, VU – Vulnerable, NT – Near Threatened, LC – Least Concern, DD – Data Deficient, NE – Not Evaluated (for non-native species). Total number of records shows the total number of species-specific records since 1873 to January 2024. Share of records from 2004–2024 [%] – share of records obtained in the years 2004–2024 relative to the total number of records. Share of records until 2004 [%] – share of records obtained until 2004 relative to the total number of records. Number of grid cells occupied – the number of grid cells in which the species has been recorded. BR – biogeographical region; Red List of Austria (Komposch 2009), Red List of the Czech Republic (Bezděčka and Bezděčková 2017) and Red List of Poland (Głowaciński 2002).

	Red List Category	Red List Criteria	Number of records before 2004	Number of records since 2004	Total number of records	Share of records from 2004–2024 [%]	Share of records until 2004 [%]	Number of grid cells occupied	Distribution in the Alpine BR	Distribution in the Pannonian BR	Red List of Austria (2009)	Red List of the Czech Republic (2017)	Red List of Poland (2002)
Suborder, family, species													
Cyphophthalmi Simon, 1879													
Sironidae Simon, 1879													
Siro carpaticus Rafalski, 1956	EN	B1ab (iii.v)	8	2	10	20.0	80.0	9	10	0			EN
Eupnoi Hansen & Sørensen, 1904													
Sclerosomatidae Simon, 1879													
Astrobunus laevipes (Canestrini, 1872)	LC		65	125	190	65.8	34.2	70	102	88	VU		EN
Gyas titanus Simon, 1879	VU	B1ab (iii.v)	69	18	87	20.7	79.3	48	87	0	EN		
Leiobunum limbatum Koch, 1861	LC		0	6	6	100.0	0.0	6	6	0	LC		EN
Leiobunum rotundum (Latreille, 1798)	LC		44	41	85	48.2	51.8	50	62	23	NT		
Leiobunum gracile Thorell, 1876	LC		123	94	217	43.3	56.7	112	194	23	LC		
Nelima sempronii Szalay, 1951	LC		8	120	128	93.8	6.3	44	49	79	LC		
Phalangiidae Latreille, 1801													
Dicranopalpus sp. Doleschall, 1852	DD		1	0	1	0.0	100.0	1	1	0	LC		
Egaenus convexus (Koch, 1835)	LC		76	142	218	65.1	34.9	79	121	97	VU	NT	EN
Lacinius dentiger (Koch, 1848)	NT		38	27	65	41.5	58.5	31	27	38	LC		VU
Lacinius ephippiatus (Koch, 1835)	LC		154	175	329	53.2	46.8	131	280	49	NT		
Lacinius horridus (Panzer, 1794)	NT		64	40	104	38.5	61.5	55	81	23	VU		
Lophopilio palpinalis (Herbst, 1799)	LC		131	96	227	42.3	57.7	103	192	35	LC		
Mitopus morio (Fabricius, 1799)	LC		266	103	369	27.9	72.1	139	339	28	LC		
Oligolophus tridens (Koch, 1836)	LC		169	148	317	46.7	53.3	131	248	69	LC		
Opilio canestrinii (Thorell, 1876)	NE		2	44	46	95.7	4.3	21	20	26	NE		
Opilio dinaricus Šilhavý, 1938	DD		1	0	1	0.0	100.0	1	1	0	NT		
Opilio parietinus (De Geer, 1778)	NT		68	14	82	17.1	82.9	59	53	29	EN		
Opilio saxatilis Koch, 1839	LC		56	66	122	54.1	45.9	50	54	68	LC		
Phalangium opilio Linnaeus, 1761	LC		177	138	315	43.8	56.2	122	239	76	LC		
Platybunus bucephalus (Koch, 1835)	LC		224	92	316	29.1	70.9	120	301	15	LC		
Platybunus pallidus Šilhavý, 1938	NT		37	28	65	43.1	56.9	44	65	0			EN
Rilaena triangularis (Herbst, 1799)	LC		86	155	241	64.3	35.7	109	165	76	LC		
Zachaeus crista (Brullé, 1832)	LC		88	132	220	60.0	40.0	78	150	70		NT	
Dyspnoi Hansen & Sørensen, 1904													
Dicranolasmatidae Simon, 1879													
Dicranolasma scabrum (Herbst, 1799)	LC		77	83	160	51.9	48.1	76	127	33	EN	VU	
Ischyropsalididae Simon, 1879													
Ischyropsalis manicata Koch, 1869	VU	B1ab (i.iii.v)	66	24	90	26.7	73.3	50	85	5		VU	VU

	Red List Category	Red List Criteria	Number of records before 2004	Number of records since 2004	Total number of records	Share of records from 2004–2024 [%]	Share of records until 2004 [%]	Number of grid cells occupied	Distribution in the Alpine BR	Distribution in the Pannonian BR	Red List of Austria (2009)	Red List of the Czech Republic (2017)	Red List of Poland (2002)
Nemastomatidae Simon, 1871													
Carinostoma elegans (Sørensen, 1894)	LC		0	14	14	100.0	0.0	8	0	14			
Mitostoma chrysomelas (Hermann, 1804)	LC		143	91	234	38.9	61.1	107	177	57	LC		
Nemastoma bidentatum sparsum Gruber & Martens, 1968	LC		9	42	51	82.4	17.6	10	0	51	NT	VU	
Nemastoma lugubre (Müller, 1776)	LC		218	167	385	43.4	56.6	161	323	62	EN		
Paranemastoma kochii (Nowicki, 1870)	VU	B1ab (iii.v)	74	35	109	32.1	67.9	58	105	4		VU	
Paranemastoma quadripunctatum (Perty, 1833)	VU	B1ab (i.iii.v)	1	1	2	50.0	50.0	2	2	0	NT		
Trogulidae Sundevall, 1833													
Trogulus nepaeformis (Scopoli, 1763)	LC		112	122	234	52.1	47.9	107	191	43	DD		VU
Trogulus tricarinatus (Linnaeus, 1767)	LC		51	155	206	75.2	24.8	73	112	94	DD		
Laniatores Thorell, 1876													
Cladonychiidae Hadži, 1935													
Holoscotolemon jaqueti (Corti, 1905)	CR	B1ab (iii.v)	4	4	8	50.0	50.0	2	0	8			

Species list and nomenclature

The presented list includes all species of Opiliones known from Slovakia, divided into higher taxonomic units; suborders are indicated in bold, families are underlined, and species are in italics (Table 1). The species richness of harvestmen within individual grid cells is also provided. Since Slovakian harvestman species are not listed on the IUCN Red List, threat categories were determined based on the official criteria of the IUCN Standards and Petitions Committee (IUCN 2022). During our study of harvestmen, we identified specimens using the keys provided by Šilhavý (1956), Martens (1978), and Wijnhoven (2009). The nomenclature of harvestmen follows Kury et al. (2024).

Results and discussion

Regarding the opiliofauna of Slovakia, 35 species from eight families and four suborders have been recorded (Table 1). The suborders Cyphophthalmi (family Sironidae) and Laniatores (family Cladonychiidae) are represented in Slovakia by a single species each (Figs 2–5). From the suborder Dyspnoi, 10 species from 4 families are known in Slovakia. Their distribution in Slovakia is shown in Figs 2, 3. There is one species each documented in our territory from the families Dicranolasmatidae and Ischyropsalididae, while there are two species from the family Trogulidae and four genera with six species from the family Nematostomatidae. More than half of the harvestman fauna in Slovakia is in the suborder Eupnoi: the family Phalangiidae is represented by 11 genera with 17 species (Figs 3, 4), and the family Sclerosomatidae includes four genera with six species (Fig. 5). The genus *Dicranopalpus* is known from Slovakia (Vtáčnik Mountains) only from immature individuals, which do not allow for reliable species identification.

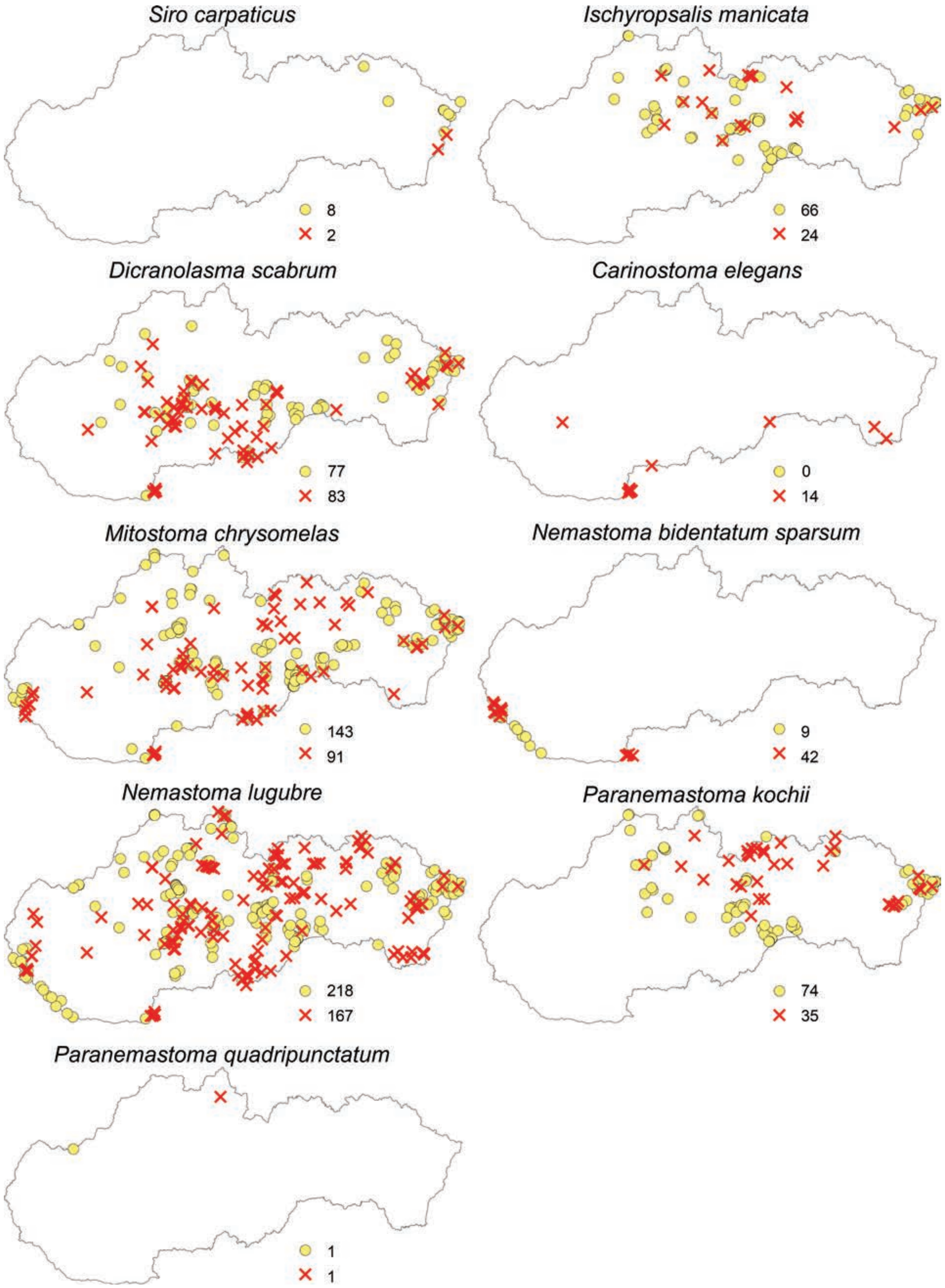

Figure 2. Distribution of harvestmen (Opiliones) in Slovakia belonging to the families Sironidae, Ischyropsalididae, Dicranolasmatidae, and Nemastomatidae (yellow circles represent the locations of individual species recorded before 2004, and red X marks indicate the locations of species recorded since 2004; the numbers next to these symbols represent the total number of records).

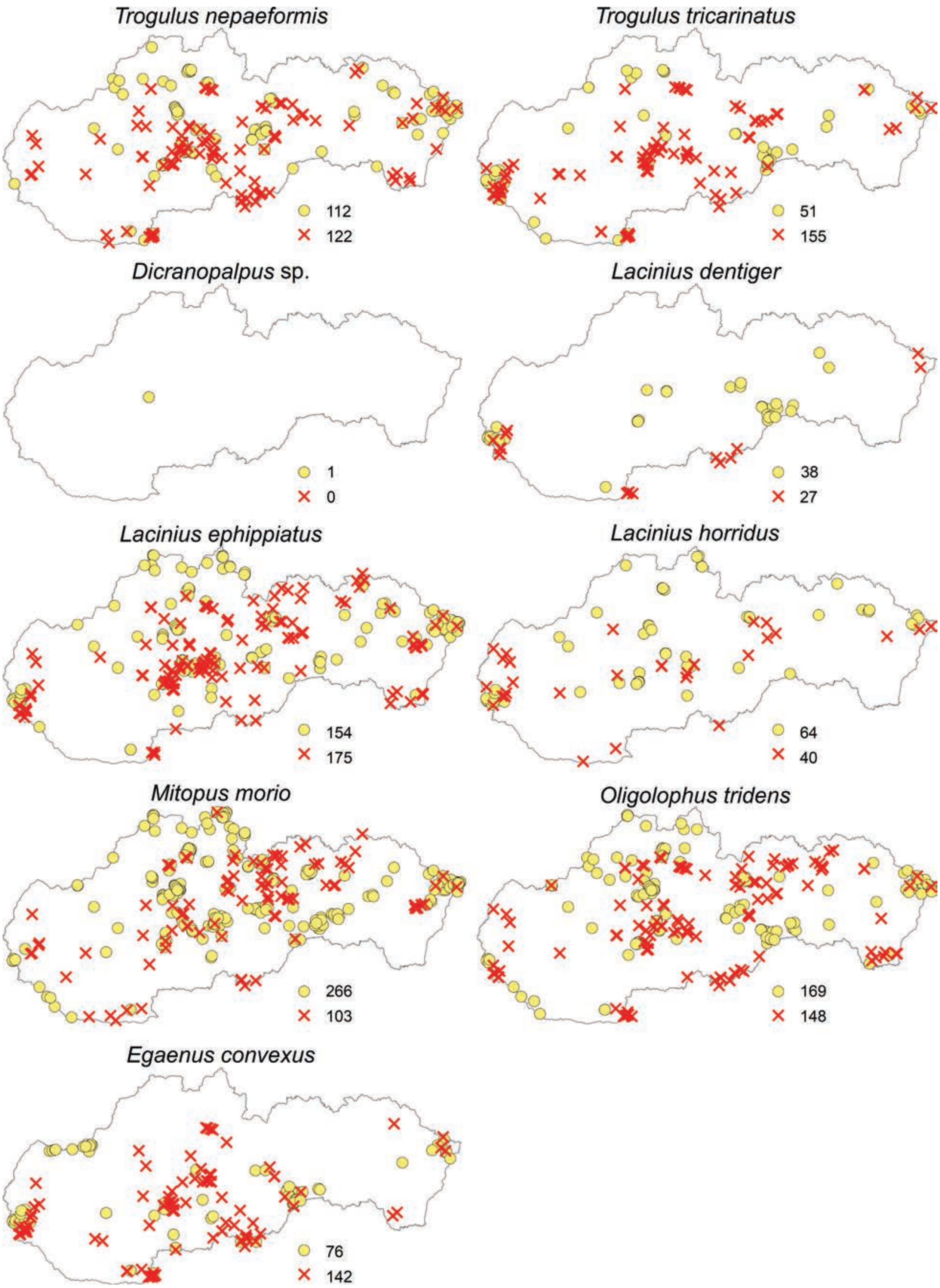

Figure 3. Distribution of harvestmen (Opiliones) in Slovakia belonging to the families Trogulidae and Phalangiidae (yellow circles represent the locations of individual species recorded before 2004, and red X marks indicate the locations of species recorded since 2004; the numbers next to these symbols represent the total number of records).

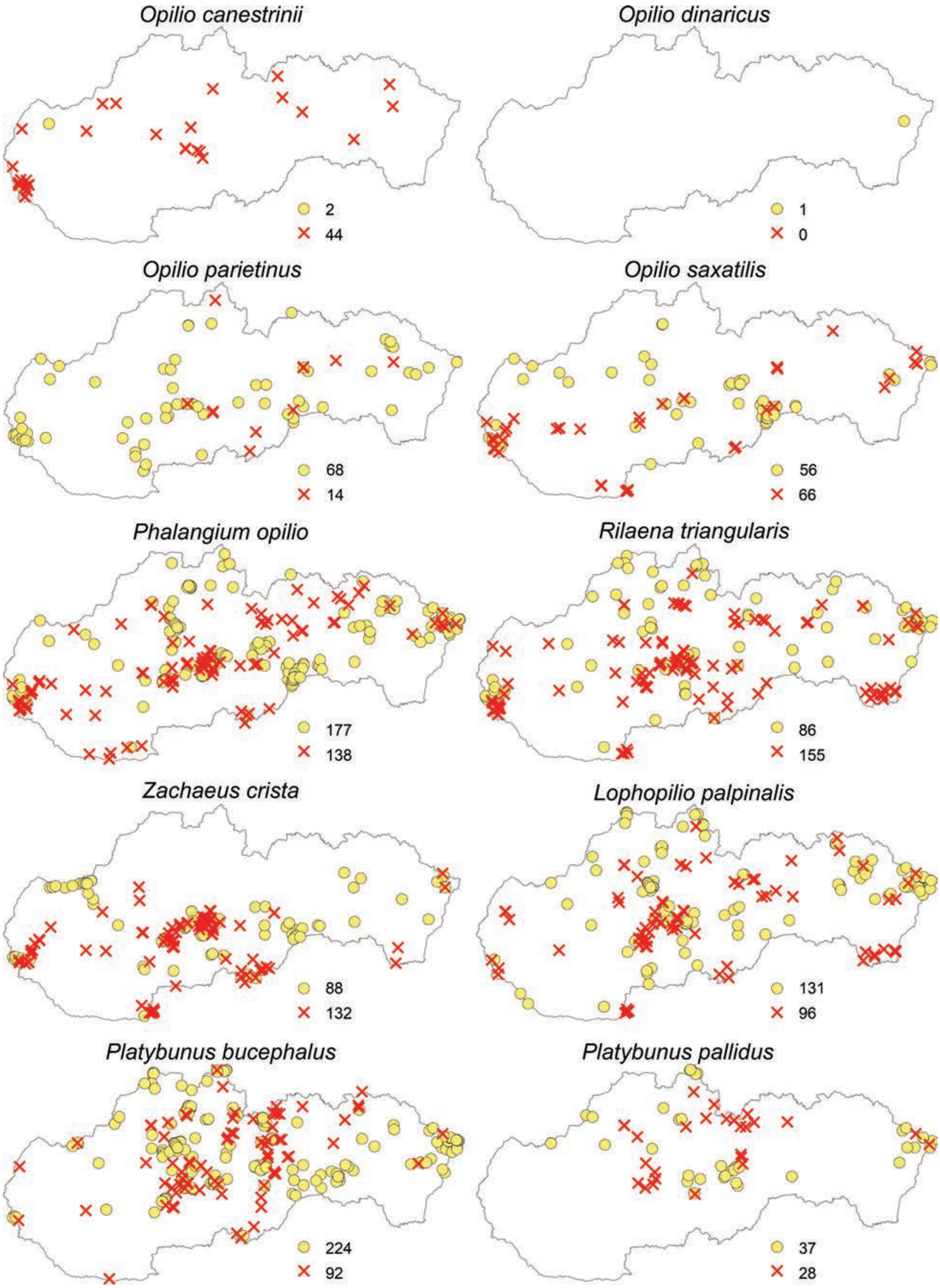

Figure 4. Distribution of harvestmen (Opiliones) in Slovakia belonging to the family Phalangiidae (yellow circles represent the locations of individual species recorded before 2004, and red X marks indicate the locations of species recorded since 2004; the numbers next to these symbols represent the total number of records).

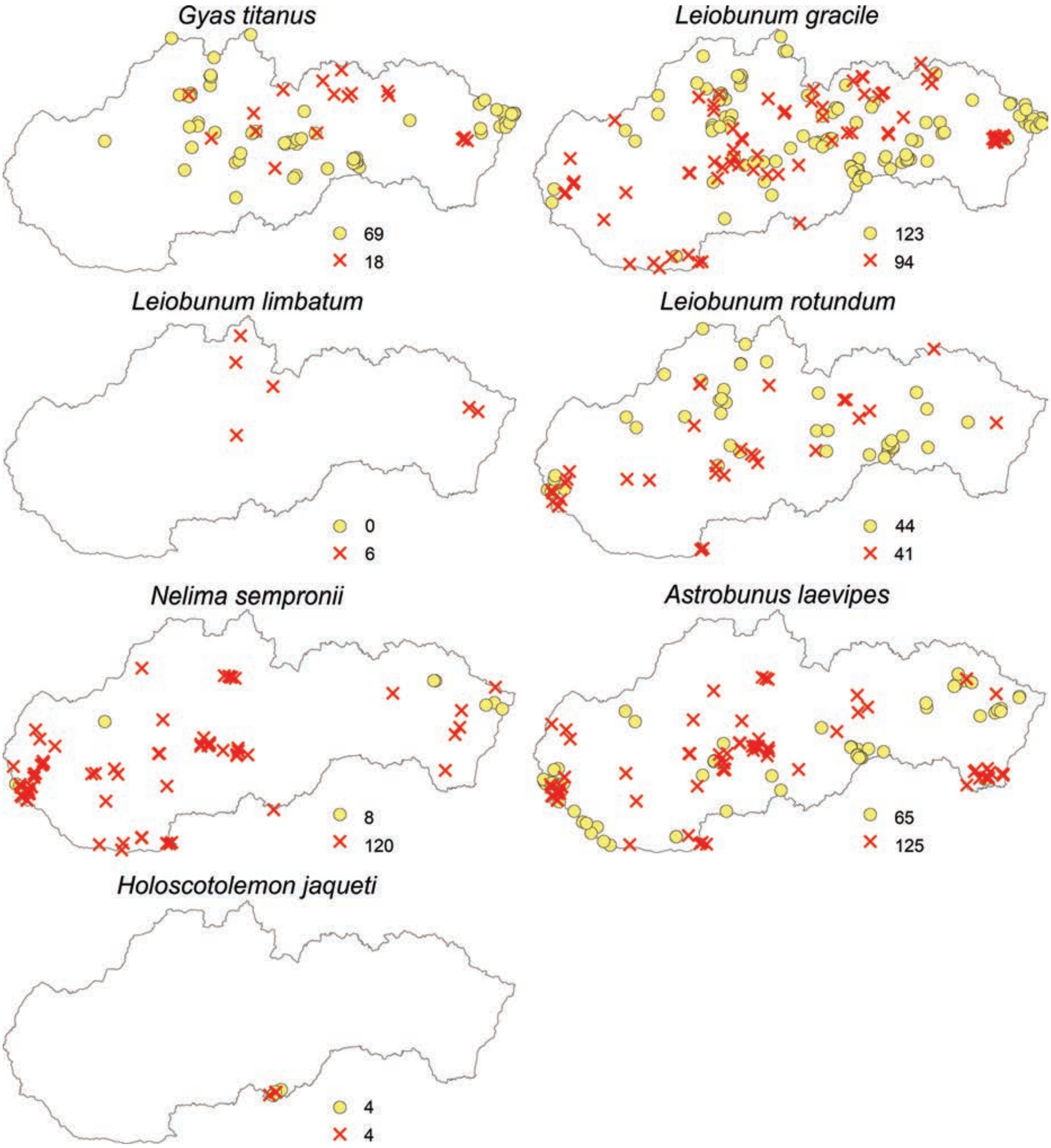

Figure 5. Distribution of harvestmen (Opiliones) in Slovakia belonging to the families Sclerosomatidae and Cladonychiidae (yellow circles represent the locations of individual species recorded before 2004, and red X marks indicate the locations of species recorded since 2004; the numbers next to these symbols represent the total number of records).

So far, 56.6% of the 562 grid cells (10 × 10 km) covering the Slovak territory have been examined at least at one site (Fig. 6). No harvestmen surveys have been conducted in 244 grid cells so far. Of a total of 2,772 studied localities, there is one record per cell in 82 grid cells, 2–5 records per cell in 112 grid cells, 6–15 records per cell in 73 grid cells, 16–50 records per cell in 44 grid cells, and 51–130 records per cell were documented in 7 grid cells covering the territory of Slovakia.

Regarding the species richness of harvestmen within the grid cells of Slovakia, one species per cell was recorded in 56 grid cells, two species per cell in 29 grid cells, 3–5 species per cell in 78 grid cells, 6–15 species per cell in 118 grid cells, and 16–24 species per cell in 37 grid cells across the territory of Slovakia (Fig. 7).

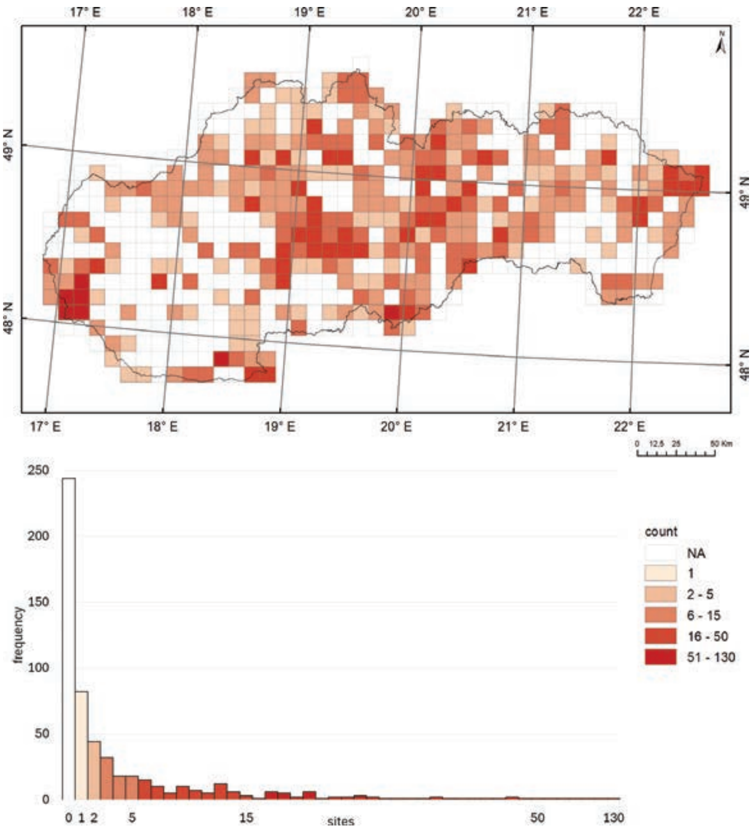

Figure 6. The frequency of sampled sites within 10 × 10 km grid cells in Slovakia, categorised into six levels (*n* = 562 grid cells; NA – not applicable).

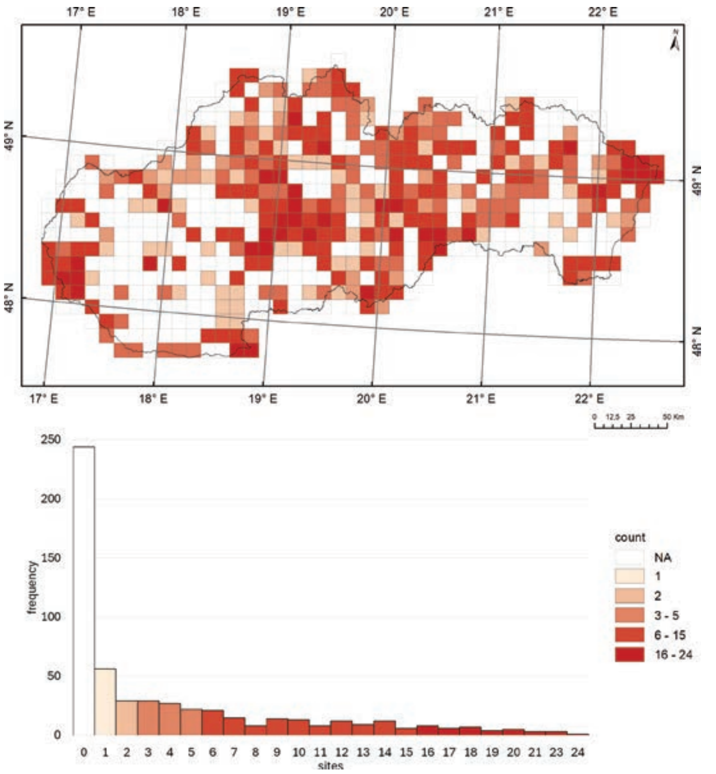

Figure 7. Number of recorded species within 10 × 10 km grid cells in Slovakia. The histogram illustrates the frequency of counts categorised into six levels (*n* = 562 grid cells; NA – not applicable).

Based on the IUCN Red List criteria (IUCN 2022), we assessed all 35 species. The species were red-listed as follows: one Critically Endangered – CE (*Holoscotolemon jaqueti*), one Endangered – EN (*Siro carpaticus*) and four Vulnerable – VU (*Gyas titanus*, *Ischyropsalis manicata*, *Paranemastoma kochii*, *Paranemastoma quadripunctatum*). Four species were assessed as Near Threatened – NT, (*Lacinius dentiger*, *Lacinius horridus*, *Opilio parietinus*, *Platybunus pallidus*), 22 as Least Concern – LC, two as Data Deficient – DD, and one Not Evaluated – NE for a non-native species – *Opilio canestrinii* (Table 1).

Comments on the distribution and ecology of the most endangered species of harvestmen in Slovakia

We have classified six species of harvestmen (Opiliones) in this group (Fig. 8).

Cyphophthalmi Simon, 1879
Sironidae Simon, 1879

Siro carpaticus Rafalski, 1956

Siro carpaticus (Rafalski, 1956): 49–52 (Poland, Bieszczady). Mašán 1998: 650. Mašán 2005: 28. Mihál et al. 2003: 129. Mihál and Mašán 2006: 92. Stašiov et al. 2003a: 263, 265.

Current distribution in Europe. This species has a relatively small known range and was described in the second half of the 20th century from southeastern Poland (Rafalski 1956). In addition to Poland, it has been found in northeastern Slovakia. It is highly likely that *S. carpaticus* also occurs in Ukraine, but it has not yet been scientifically confirmed there.

Current distribution in Slovakia. In Slovakia, *S. carpaticus* is very rare and it is distributed only in the Eastern Carpathians (Mihál et al. 2003; Rozwałka 2012). It has been found in Slovakia using the leaf litter sieving method in the northeast part of the country within nine grid cells, namely in the geomorphological units (Lehotský et al. 2022): Bukovské vrchy, Ondavská vrchovina, Vihorlatské vrchy, and Východoslovenská pahorkatina (Mašán 1998, 2005; Mihál et al. 2003; Stašiov et al. 2003a; Mihál and Mašán 2006).

Altitude range and habitat. The lowest recorded altitude within its known range in Slovakia is 280 m a.s.l.in Bukovské vrchy near Ulič. The highest recorded location is in the National Nature Reserve Stužica, Bukovské vrchy, at 1100 m a.s.l. (Mihál et al. 2003). *Siro carpaticus* is a forest species that prefers dense and preserved submontane and montane deciduous and mixed forests, particularly beech and oak forests. The species lives primarily in soil and under stones and fallen wood, but it can also be found in detritus, moss, and among decayed rocks (Stašiov 2004).

Threats and conservation measures. Among the most common impacts and threats of its population are improper management of forest habitats (e.g., extensive clear-cut logging followed by soil desiccation) – primarily in beech forests, and the planting of tree species that do not occur naturally in the area (e.g., *Pinus sylvestris*, *Pinus nigra*, *Larix* sp., *Picea* sp.).

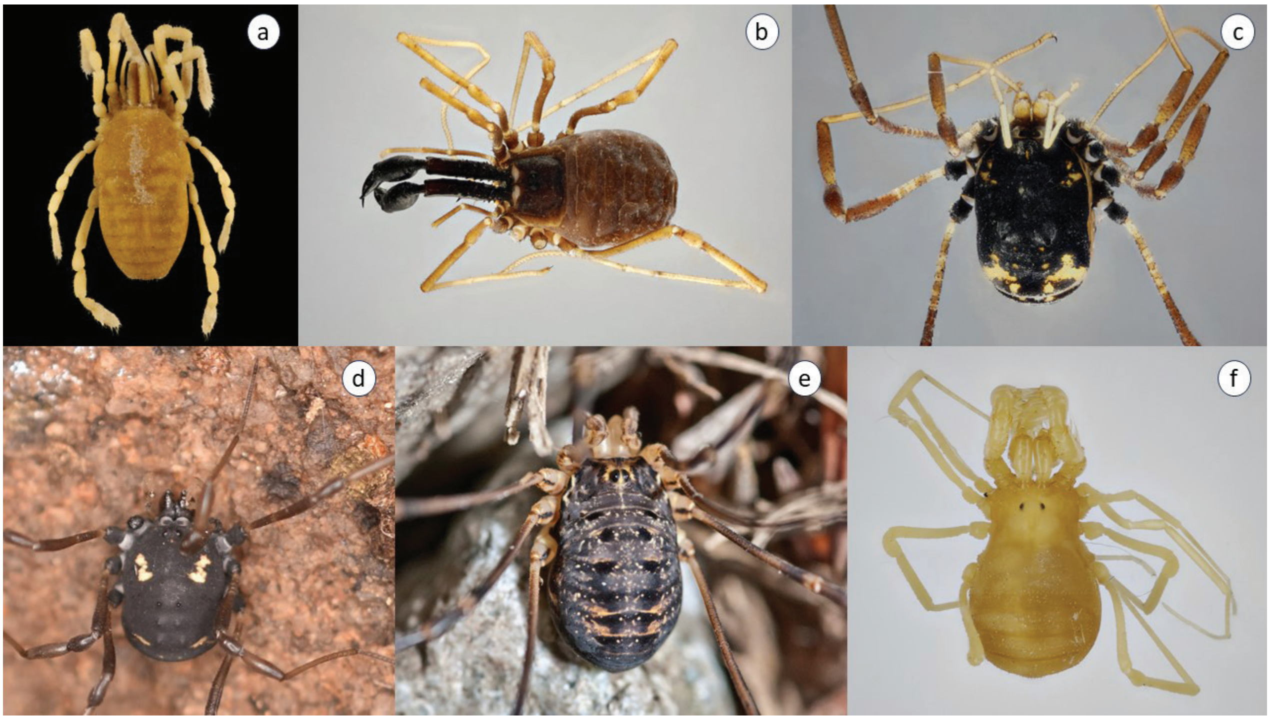

Figure 8. Critically endangered, endangered, and vulnerable species of harvestmen in Slovakia **a** *Siro carpaticus* (photo by A. Christophoryová) **b** *Ischyropsalis manicata* (photo by A. Christophoryová) **c** *Paranemastoma kochii* (photo by A. Christophoryová) **d** *Paranemastoma quadripunctatum* (photo by: O. Machač) **e** *Gyas titanus* (photo by A. Šestáková) **f** *Holoscotolemon jaqueti* (photo by D. Selnekovič).

Laniatores Thorell, 1876
Cladonychiidae Hadži, 1935

Holoscotolemon jaqueti (Corti, 1905)

Holoscotolemon jaqueti (Corti, 1905): 204–226 (Romania, Negreni). Franc (2008), Franc and Mlejnek (1999), Mihál et al. (2009), Stašiov et al. (2003b).
Current distribution in Europe

Holoscotolemon jaqueti has a disjunct southeastern European and Carpathian distribution, found in Hungary, Slovakia, Romania, Ukraine, Bosnia and Herzegovina, and Serbia (Raspotnig et al. 2011).

Current distribution in Slovakia. This is a rare species recorded in only two grid cells in Slovakia (in the Cerová vrchovina upland). It has a very small population size that cannot be precisely defined, exposing it to an exceptionally high risk of extinction.

Altitude range and habitat. It inhabits sub-montane and montane forests, preferring wetter and cooler habitats. Suitable conditions are also found in caves with ample food, high relative humidity, lack of drafts, and temperatures that do not drop below 9 °C year-round. It primarily lives in cave environments, deep talus slopes, or rock crevices. It is found in the upper layers of the soil, detritus, moss, under decaying wood, and stones (Stašiov 2004). In Slovakia, it has been found in Cerová vrchovina upland: National Nature Reserve Pohanský hrad (Labyrintová jaskyňa), Dunivá hora, National Nature Reserve Ragáč (well at Ragáč), and National Nature Reserve Šomoška (alluvium of the Bukovinský stream) (Franc and Mlejnek 1999; Stašiov et al. 2003b; Franc 2008; Mihál et al. 2009).

Threats and conservation measures. Factors that may negatively impact *H. jaqueti* populations include tourism, illegal cave entries, and illegal collection by enthusiasts. The cave vestibules where these individuals are active have relatively small areas, which makes the activities of collectors a threat to the small local population. To preserve their habitats, it is essential to refrain from any forestry activities in the immediate vicinity of cave entrances.

Dyspnoi Hansen & Sørensen, 1904
Nemastomatidae Simon, 1871

Paranemastoma kochii (Nowicki, 1870)

Nemastoma kochi Nowicki, 1870: 57. Ložek and Gulička (1955), Staręga (1966). Šilhavý 1950: 99–106. Šilhavý (1968a,b), Šilhavý (1974).
Nemastoma kochi Sørensen (1873), Daday (1918).
Nemastoma quadripunctatum kochi Now., Kratochvíl (1933, 1934).
Nemastoma werneri Kulczyński (1903), Šilhavý (1974).
Paranemastoma kochii Nowicki (1870) (mostly Slovakia, High Tatras Mts.), Astaloš (2000), Astaloš and Jarab (2005) Astaloš et al. (1998), Gulička (1985), Hroznár (1981), Kluka and Krumpál (2009), Mihál and Korenko (2010), Maršalek 2004, 2012a,b, 2017, 2018, Maršalek and Stašiov (2015), Mašán and Mihál (1993), Mihál and Astaloš (2011), Mihál and Hrúz (1998), Mihál et al. (2003, 2015), Stašiov (2004), Stašiov et al. (1997, 2003b, 2021), Šilhavý (1970, 1972).

Current distribution in Europe. This is a Carpathian endemic species found in Slovakia, the Czech Republic, Poland, Romania, and Ukraine.

Current distribution in Slovakia. In the southwestern part of Slovakia, this species has not yet been recorded. Overall, it has been recorded in 58 grid cells. Post-2004, additional records of this species' occurrence have been contributed by works such as Astaloš and Jarab (2005), Kluka and Krumpál (2009), Mihál and Korenko (2010), Mihál and Astaloš (2011), Maršalek (2004, 2012a, 2012b, 2017, 2018), Maršalek and Stašiov (2015), Mihál et al. (2015), and Stašiov et al. (2021).

Altitude range and habitat. *Paranemastoma kochii* is a hygrophilous montane species that prefers shaded and sufficiently moist habitats without specific preferences for slope exposure. It thrives in forested areas with diverse tree compositions at mid- and higher elevations. Suitable conditions are generally found near springs and streams, in areas with surface seepage, and similar environments. In Slovakia, it prefers mainly beech and fir-beech forests. It has also been found in canyon valleys, peat bogs, spruce forests, riparian vegetation, caves (in the aphotic zone), and other moist habitats. It seeks shelter under stones, decaying wood, moss, and similar substrates (Stašiov 2004).

Threats and conservation measures. *Paranemastoma kochii* is a hygrophilous montane species highly sensitive to environmental changes. Its habitats, including shaded, moist areas near springs and streams, are increasingly degraded due to anthropogenic influences. Key threats include inappropriate forest management, altered hydrological conditions, and water pollution. These activities lead to habitat thinning, soil compaction from heavy logging machinery, and changes in stream quality, often due to pollutants like oil. Effective conservation measures are essential to protect its populations.

***Paranemastoma quadripunctatum* (Perty, 1833)**

Paranemastoma quadripunctatum (Perty 1833) (Germany), Bezděčka (2009), Dudich et al. (1940), Šilhavý (1972).
Paranemastoma quadripunctatum kochi Now.: Kratochvíl (1934).
Paranemastoma quadripunctatum werneri Kulczyński Kratochvíl (1933, 1934). Current distribution in Europe
Paranemastoma. *quadripunctatum* is a sub-Atlantic to Central European montane species, distributed from eastern France to eastern Poland. Its range extends across northern Germany, Belgium, the Netherlands, the Alpine and Central European countries, and reaches the northern parts of the Balkan and Apennine Peninsulas (Martens 1978).

Current distribution in Slovakia. The eastern boundary of its range passes through Slovakia, making it one of the rarest harvestmen species in the country (Stašiov 2003). The oldest records of this species in Slovakia were published by Kratochvíl (1934) from the Tatra Mountains and Turčianske Teplice, Dudich et al. (1940) from the vicinity of Kremnica, and Šilhavý (1972) from the Slovak Karst. These older records are not precisely localised and cannot be assigned to a specific geographical point. Therefore, we omitted these records and did not mark them on the distribution map of *P. quadripunctatum*. The occurrence of this species in Slovakia was later confirmed by Bezděčka (2009) from the Stará Turá locality in the White Carpathians. The most recent record in Slovakia was made by P. Gajdoš and P. Purgat in 2021 in the cadastral area of Ťapešovo, within the Orava Basin (Litavský unpubl.). So, in Slovakia this species is officially confirmed in two grid cells.

Altitude range and habitat. *Paranemastoma quadripunctatum* prefers shaded and moist habitats in mixed forests of middle and higher elevations. It is also found at the edge of forests and occasionally penetrates shrub areas of open landscapes. It has been recorded in caves as well. It occurs from lowlands to mountainous areas but prefers altitudes ranging from 400 to 1200 metres (Martens 1978).

Threats and conservation measures. *Paranemastoma quadripunctatum* is a rare, hygrophilous species found in mid- to high-elevation areas, highly sensitive to environmental changes. It serves as an indicator of undisturbed and ecologically valuable environments that provide suitable conditions for various protected and endangered flora and fauna species. Currently, anthropogenic impacts are leading to the degradation of habitats on which this species depends. The main threats of high or medium intensity include improper forest management practices and changes in landscape hydrological conditions. These impacts result in the clearing or removal of forest habitats, alteration of their species and spatial structure, soil compaction due to the use of heavy machinery during logging, and changes in the water regime and quality of streams.

Ischyropsalididae Simon, 1879

Ischyropsalis manicata Koch, 1869

Ischyropsalis carli Lessert (1905), Dudich et al. (1940), Šilhavý (1956).

Ischyropsalis dacica Roewer, 1916: 90–158. Ložek and Gulička (1955), Šilhavý (1950, 1956).

Ischyropsalis helvetica Roewer (1916), Dudich et al. (1940).

Ischyropsalis helvetica milleri Kratochvíl (1933), Kratochvíl (1934).

Ischyropsalis hellwigii Panzer (1794), Kolosváry (1929), Kratochvíl (1934), Šilhavý (1956).

Ischyropsalis manicata Koch (1869) (Romania, Transylvania), Astaloš (2000, 2002), Astaloš and Mihál (2009), Astaloš et al. (1998), Gulička (1985), Hroznár (1981), Košel (1984), Kováč et al. (2007), Kratochvíl (1933, 1934), Maršalek (2012b), Mihál and Hrúz (1998), Mihál and Korenko (2010), Mihál et al. (2003, 2015), Melega et al. (2022), Roewer (1923). Roušar (1999), Staręga (1966), Stašiov (1999, 2004), Stašiov and Bitušík (2001), Stašiov et al. (1997), Stašiov et al. (2003b), Šilhavý (1956, 1968b, 1972 1974).

Ischyropsalis milleri Kratochvíl (1933), Prantl and Mařan (1957).

Current distribution in Europe. *Ischyropsalis manicata* is a Carpathian endemic species found in Slovakia, the Czech Republic, Poland, Romania, and Ukraine.

Current distribution in Slovakia. In Slovakia, this species is moderately common. It is primarily distributed in the northern part of central Slovakia, the Slovak Karst, and the eastern tip of the country. To date, it has been recorded in 50 grid cells. Post-2004 research contributing to the distribution records includes works by Kováč et al. (2007), Astaloš and Mihál (2009), Maršalek (2012b), Mihál and Korenko (2010), Mihál et al. (2015), and Melega et al. (2022).

Altitude range and habitat. This harvestman is a hygrophilous mountain species that prefers moist and shaded habitats. It is mainly found in forested mountain areas, often near streams and springs. In Slovakia, it has also been recorded in caves, occupying both the dysphotic and aphotic zones. Outside of caves, it is primarily found in spruce forests, fir-beech-spruce forests, fir-beech forests, beech forests, and dwarf pine areas. It is less commonly found in open habitats such as alpine and moist meadows. This species lives in detritus, moss, under stones, wood fragments, and in the cavities of decaying stumps (Stašiov 2004).

Threats and conservation measures. *Ischyropsalis manicata* is a hygrophilous mountain species that inhabits shaded habitats near streams and springs, as well as cave environments. Significant negative anthropogenic impacts and threats to its populations include improper forest management and changes in the hydrological conditions of the landscape. The primary threats are habitat loss due to logging, environmental pollution, natural disasters, climate change, and similar factors.

Gyas titanus Simon, 1879

Gyas annulatus Olivier (1791), Astaloš (1993, 2000), Dudich (1928), Dudich et al. (1940), Gulička (1985), Hroznár (1981), Kolosváry (1929), Kratochvíl (1933. 1934), Lác (1990), Mašán and Mihál (1993), Staręga (1966), Stašiov (2004), Stašiov et al. (2003b), Šilhavý (1950, 1956, 1968 a,b, 1972, 1974).

Gyas titanus Simon (1879), (France), Astaloš (2000), Astaloš et al. (1998), Mihál (1996, 1998), Mihál and Hrúz (1998), Mihál et al. (2003), Stašiov and Mihál (2001).

Current distribution in Europe. *Gyas titanus* is a European species found in Portugal, Spain, France, Switzerland, Austria, Germany, the Czech Republic, Poland, Hungary, Romania, Italy, Slovenia, Croatia, Bosnia and Herzegovina, Montenegro, Serbia, Slovakia, and Ukraine (Novak et al. 2000; Stašiov 2004).

Current distribution in Slovakia. In Slovakia, this species is moderately common in suitable habitats, avoiding extensive lowland areas such as the Danubian lowland and the eastern Slovak lowland. It has been recorded in 48 grid cells. Post-2004 research that expanded the records of this species is presented in works by Astaloš and Jarab (2005), Mihál and Korenko (2010), Maršalek (2004, 2012b, 2017, 2018), Maršalek and Stašiov (2015), and Mihál et al. (2015).

Altitude range and habitat. *Gyas titanus* is a hygrophilous harvestman species that thrives in shaded, humid mountain environments. It predominantly inhabits mixed moist forests, particularly beech, fir-beech, fir-spruce-beech, and spruce forests in Slovakia, often near streams. This species avoids lowland areas and anthropogenic habitats, favouring moist microhabitats such as rock crevices, moss, fallen wood, and old stumps. Additionally, it has been observed in canyon-like valleys and caves, occupying both dysphotic and aphotic zones (Stašiov 2004).

Threats and conservation measures. *Gyas titanus* is a moderately common hygrophilous mountain species sensitive to environmental changes. Its habitats, characterised by shaded areas with high humidity and stable temperatures, are currently threatened by intense anthropogenic influences. Key threats to local populations include improper forest management and changes in hydrological conditions, exacerbated by deforestation and climate change. These factors lead to habitat degradation, which significantly affects the survival of the species.

The current status of the protection of harvestmen in Slovakia

Although harvestmen are a significant group of animals, their effective protection in Slovakia was not ensured until 2003. None of the species belonging to the order Opiliones were included in the Red Data Book of threatened and rare plant and animal species of the Czech and Slovak Federal Republic 3. Invertebrates published in 1992 (Škapec et al. 1992). Harvestmen were also not included in the Red List of plants and animals of Slovakia published in 2001 (Baláž et al. 2001). Later, some species of harvestmen were included in the list of protected animal species (species of national environmental significance) in Annex 6 of the Decree of the Ministry of the Environment of the Slovak Republic No. 24/2003 Coll., implementing Act No. 543/2002 Coll. on nature and landscape protection, as amended (Ministry of the Environment of the Slovak Republic 2003). This included the following species: *Egaenus convexus*, *Gyas titanus*, *Ischyropsalis manicata*, *Opilio dinaricus*, *Platybunus pallidus*, and *Siro carpaticus*. The currently valid regulation is the Ministry of Environment of the Slovak Republic Decree No. 170/2021 Coll. (effective from January 1, 2023), implementing Act No. 543/2002 Coll. on

Nature and Landscape Protection, as amended by subsequent regulations. In table 5 of this Decree, the list of protected animal species includes the following species: *Opilio dinaricus*, *Holoscotolemon jaqueti*, *Carinostoma elegans*, *Leiobunum limbatum*, and *Siro carpaticus* (Ministry of Environment of the Slovak Republic 2021).

Many European countries have long-established and regularly updated Red Lists of harvestmen, such as Germany (Muster et al. 2016), Austria (Komposch 2009), the Czech Republic (Bezděčka and Bezděčková 2017), and Poland (Głowaciński 2002), among others. Among other reasons, this was also one of the motivations for preparing the first Red List of harvestmen in Slovakia.

Although *Leiobunum limbatum* has so far been recorded in only six locations in Slovakia (Bezděčka and Bezděčková 2011; Stašiov and Tuf 2016; Stašiov and Diviaková 2022; Litavský unpubl.), we have classified this species under the category LC (Least Concern). The reason is that *L. limbatum* can be considered a species, which primary habitats are rocks and rocky outcrops in forests. Currently, it inhabits various types of habitats.

We included two species of harvestmen in the Data Deficient category. Occurrence of *Opilio dinaricus* has been reliably documented only at two localities in the Vihorlat Mountains (Šilhavý 1966, 1968a). The second harvestman is the genus *Dicranopalpus* sp. In Slovakia, only juvenile individuals from the genus *Dicranopalpus* have been found so far, and they were reliably identified only to the genus *Dicranopalpus*. So far, this genus has only been recorded in Slovakia at two locations, situated in the Vtáčnik Mountains and in the High Tatras (Stašiov 2004).

We have classified *Lacinius dentiger*, *Lacinius horridus*, *Platybunus pallidus*, and *Opilio parietinus* as Near Threatened, as they become increasingly rare over time. It is likely that *Opilio parietinus* is gradually being displaced from its original habitats by *Opilio canestrinii*, which is more frequently observed in Slovakia. In this matter, Bliss et al. (1996) had previously mentioned this in the Red List of harvestmen of Germany. Since *Opilio canestrinii* is considered a non-native invasive species in Slovakia, we have classified it under the category NE (Not Evaluated).

Given the ongoing climate change, increasingly intense negative human impact on the environment, as well as the penetration of invasive species into our territory, which suppress populations of our native species (e.g., *Opilio canestrinii*), it can be expected that the current Red List of proposed harvestman species will need to be updated in the near future.

Conclusions

By applying the IUCN Red List criteria, we have identified several species of harvestmen that are at varying levels of endangerment, including one critically endangered species, *Holoscotolemon jaqueti*, and several others that are endangered or vulnerable in Slovakia. The inclusion of these species in a Red List for the first time highlights the urgent need for targeted conservation measures to protect both the species themselves and the habitats they depend on. This checklist and the Red List can serve as foundational tools for conservation planning and policy making in Slovakia, paving the way for more effective protection of this important group of terrestrial invertebrates.

Acknowledgements

We would like to thank all members of the Slovak Arachnological Society, especially opilionologists, for their valuable advice and suggestions that have improved our work. We would also like to thank A. Šestáková and O. Machač for providing photographs of harvestmen in the field, and A. Chistophoryová and D. Selnekovič for photographing harvestmen in the laboratory. The work was supported by research grants 1/0076/22 and 1/0255/23 of the Slovak Grant Agency (VEGA) and by the Operational Programme Integrated Infrastructure (OPII) funded by the ERDF [ITMS 313011T721].

Additional information

Conflict of interest

The authors have declared that no competing interests exist.

Ethical statement

No ethical statement was reported.

Funding

This study was funded by research grants 1/0076/22 and 1/0255/23 of the Slovak Grant Agency (VEGA) and by the Operational Programme Integrated Infrastructure (OPII) funded by the ERDF [ITMS 313011T721].

Author contributions

Formal analysis: MŠ. Writing - original draft: SS, JL, IM.

Author ORCIDs

Juraj Litavský https://orcid.org/0000-0003-1229-1098
Slavomír Stašiov https://orcid.org/0000-0002-4914-4465
Ivan Mihál https://orcid.org/0000-0003-4582-0750
Martin Šalkovič https://orcid.org/0000-0001-7300-2603

Data availability

All of the data that support the findings of this study are available in the main text.

References

Astaloš B (2000) Kosce (Opiliones) Národnej prírodnej rezervácie Veľká Skalná vo Veľkej Fatre. Kmetianum, zborník SNM – Múzeum Andreja Kmeťa, Martin 9: 69–74.

Astaloš B (2002) História a súčasný stav výskumu koscov (Arachnida, Opiliones) vo Veľkej Fatre. Matthias Belivs Univ. Proc., Banská Bystrica 2(1): 135–138.

Astaloš B, Jarab M (2005) K faune koscov (Arachnida, Opiliones) Lúčanskej Fatry. Entomofauna carpathica 17: 37–39.

Astaloš B, Mihál I, Mašán P, Staňková E (1998) Kosce (Opiliones) Chránenej krajinnej oblasti Kysuce. Vlastivedný zborník Považia. Považské múzeum, Žilina 19: 93–99. https://doi.org/10.1080/08897079809511378

Astaloš B (1993) Kosce (Opiliones) v Štátnej prírodnej rezervácii Šútovská dolina v Národnom parku Malá Fatra. Zborník Oravského Múzea 10: 31–33.

Astaloš B, Mihál I (2009) Príspevok k poznaniu koscov (Arachnida, Opiliones) Veľkého Choča v Chočských vrchoch. Naturae Tutela 13(1): 59–64.

Baláž D, Marhold K, Urban P [Eds] (2001) Červený zoznam rastlín a živočíchov Slovenska. Ochrana Prírody, ŠOP SR, Banská Bystrica, 20 (Supplement), 160 pp.

Bartoš E (1939a) Die Weberknechte (Opiliones) des östlichen Carpaticums. Folia zoologica et hydrobiologica 9: 308–310.

Bartoš E (1939b) Sekáči bratislavského okolí. Entomologické listy, Brno 2: 47–49.

Bezděčka P (2009) Kosec *Paranemastoma quadripunctatum* potvrdený pre Slovensko. Folia faunistica Slovaca 14(9): 59–62.

Bezděčka P, Bezděčková K (2011) *Leiobunum limbatum* – nový sekáč (Opiliones) pro Slovensko. Folia faunistica Slovaca 16: 31–34.

Bezděčka P, Bezděčková K (2017) Opiliones (sekáči). In: Hejda R, Farkač J, Chobot K (Eds) Červený seznam ohrožených druhů České republiky. Bezobratlí. Příroda 36: 80–82.

Bliss P, Martens J, Blick T (1996) Rote Liste der Weberknechte Deutschlands (Arachnida: Opiliones). Arachnologische Mitteilungen 11: 32–35. https://doi.org/10.5431/aramit1103

Bochníček O, Hrušková K (2015) Climate atlas of Slovakia. Slovak Hydrometeorological Institute, Bratislava, 131 pp.

Boyer SL, Clouse RM, Benavides LR, Sharma P, Schwendinger PJ, Karunarathna I, Giribet G (2007) Biogeography of the world: a case study from cyphophthalmid Opiliones, a globally distributed group of arachnids. Journal of Biogeography 34: 2070–2085. https://doi.org/10.1111/j.1365-2699.2007.01755.x

Daday E (1918) Opiliones. Fauna Regni Hungariae, Budapest, 3 pp.

Dudich E (1928) Faunisztikai jegyzetek III. Állattani Közlemények 25: 38–45.

Dudich E, Kolosváry G, Szalay L (1940) Bars vármegye pókszabású (Arachnoidea) faunájának alapvetése. – Matematikai és természettudományi közlemények, Budapest 30: 1–71.

Faško P, Šťastný P (2002) Priemerné ročné úhrny zrážok 1: 2 000 000, Atlas krajiny Slovenskej republiky, 1. vyd., Bratislava: Ministerstvo životného prostredia SR, Slovenská agentúra životného prostredia, Banská Bystrica, 344 pp.

Ferianc O (1949) Fauna Zvolenského okresu so zreteľom na stavovce. Prírodovedný zborník Bratislava 4: 35–76.

Franc V (2008) The distribution and ecology of rare harvestman *Holoscotolemon jaqueti* in Central Europe. Matthias Belivs University Proceedings 4: 51–54.

Franc V, Mlejnek R (1999) First record of *Holoscotolemon jaqueti* (Opiliones, Erebomastidae) from Slovakia. Biologia 542: 134.

Garwood RJ, Sharma PP, Dunlop JA, Giribet GA (2014) Paleozoic stem group of mite harvestmen revealed through integration of phylogenetics and development. Current Biology 24: 1017–1023. https://doi.org/10.1016/j.cub.2014.03.039

Głowaciński Z [Ed.] (2002) Red list of threatened animals in Poland. Polish Academy of Sciences, Institute of Nature Conservation, Kraków, 155 pp.

Gulička J (1957) Kvalitatívno-kvantitatívny rozbor pôdnej fauny Čierneho lesa (Ostrov) (Myriapoda, Isopoda, Opiliones). Acta Facultatis Rerum Naturalium Universitatis Comenianae, Zoologia 2: 119–139.

Gulička J (1985) Pôdna a jaskynná makrofauna krasových pohorí Západných Karpát (I). – Slovenský kras, Martin 23: 89–129.

Hajková K (1995) Pôdna makrofauna Karlovej Vsi (Bratislava). Diploma Thesis. Prírodovedecká fakulta Univerzity Komenského, Bratislava.

Herman O (1879) Opiliones, Ungarns Spinnen–Fauna, III. Band, Verlag der K. U. Naturwissenschaftlichen Gesellschaft. Budapest, 326–331.

Hroznár P (1981) Kosce (Opilionidea) Štátnej prírodnej rezervácie Rozsutec. In: Janík M, Štollmann A (Eds) Rozsutec, Štátna prírodná rezervácia. Osveta. Martin, 707–718.

IUCN (2022) Standards and Petitions Committee. Guidelines for Using the IUCN Red List Categories and Criteria. – Version 15.1. Prepared by the Standards and Petitions Committee. – Internet: https://www.iucnredlist.org/documents/RedListGuidelines.pdf [Accessed on 10 August 2023]

Jasenák L (1972) Pôdna makrofauna Devínskej Kobyly. Diploma Thesis. Prírodovedecká fakulta Univerzity Komenského, Bratislava.

Kluka V, Krumpál M (2009) Kosce v Čiernej Lehote (Strážovské vrchy). In: Krumpálová Z (Ed.) 7. Arachnologická konferencia – Vplyv ľudských aktivít na pavúkovce a Progres v taxonómii pavúkovcov, Východná, Ústav zoológie SAV Bratislava, 45pp.

Kolosváry G (1929) Die Weberknechte Ungarns. Studium, Budapest, 112 pp.

Kolosváry G (1933) Über eine neue Weberknechtart: *Roeweriolus hungaricus* n. gen. n. sp. Zoologischer Anzeiger, Leipzig 102: 310–313.

Komposch C (2009) Rote Liste der Weberknechte (Opiliones) Österreichs. In: Zulka KP (Ed.) Rote Liste gefährdeter Tiere Österreichs. Checklisten, Gefährdungsanalysen, Handlungsbedarf. Teil 3: Flusskrebse, Köcherfliegen, Skorpione, Weberknechte, Zikaden. Grüne Reihe des Lebensministeriums (Gesamtherausgeberin Ruth Wallner) Band 14/3. Böhlau, Wien, 397–483.

Košel V (1984) Súčasný stav poznania fauny v jaskyniach Slovenského raja. Spravodaj Slovenskej spelelogickej spoločnosti 15: 38–40.

Košel V (1994) Živočíšstvo jaskýň. In: Rozložník M, Karasová E (Eds) Slovenský kras Chránená krajinná oblasť–biosférická rezervácia. Osveta, Martin, 240–244.

Kováč Ľ, Mock A, Višňovská A, Ľuptáčik P (2007) Spoločenstvá fauny Brestovskej jaskyne (Západné Tatry). Slovenský kras 46(1): 97–110.

Kratochvíl J (1933) Přehled zeměpisného rozšíření našich sekáčů. Věda přírodní 16: 5–12.

Kratochvíl J (1934) Sekáči (Opilionides) Československé republiky. Práce Moravské Přírodovědecké Společnosti 9: 1–35.

Kratochvíl J (1939) Druhy skupiny *Nemastoma quadripunctatum* (Perty) a několik nových sekáčů pro ČSR. Sborník Přírodovědeckého klubu v Třebíči 3: 73–81.

Kury, AB, Mendes AC, Cardoso L, Kury MS, Granado AdA, Giribet G, Cruz-López JA, Longhorn SJ, Medrano MA, de Oliveira ABR (2024) World Catalogue of Opiliones. In: Bánki O, Roskov Y, Döring M, Ower G, Hernández Robles DR, Plata Corredor CA, Stjernegaard Jeppesen T, Örn A, Vandepitte L, Hobern D, Schalk P, DeWalt RE, Ma K, Miller J, Orrell T, Aalbu R, Abbott J, Adlard R, Adriaenssens EM et al. (Eds) Catalogue of Life Checklist (Version 2024-11-18). https://doi.org/10.48580/dgjy9-4pt

Lác J (1957) Rozšírenie *Dicranolasma scabrum* Herbst, 1799 (Opilionidea) na Slovensku. Biológia, Bratislava 12: 939–941.

Lác J (1990) Živočíšstvo. In: Bolfík J (Ed.) Gemer-Malohont I. Príroda. Osveta, Martin, 446–603.

Lapin M, Faško P, Melo M, Šťastný P & Tolmain J (2002) Klimatické oblasti. In: Atlas krajiny Slovenskej republiky M 1: 1 000 000. Ministerstvo životného prostredia; Slovenská agentúra životného prostredia, Bratislava, Banská Bystrica, 344 pp.

Lehotský M, Rusnák M, Novotný J (2022) Short History of Geomorphological Research and Geomorphological Division of Slovakia. In: Lehotský M, Boltižiar M (eds) Landscapes and Landforms of Slovakia. World Geomorphological Landscapes. Springer, Cham, 480 pp. https://doi.org/10.1007/978-3-030-89293-7

Litavský J, Stašiov S, Svitok M, Michalková E, Majzlan O, Žarnovičan H, Fedor P (2018) Epigean communities of harvestmen (Opiliones) in Pannonian Basin floodplain forests: an interaction with environmental parameters. Biologia 73: 753–763. https://doi.org/10.2478/s11756-018-0084-8

Litavský J, Stašiov S, Fedor P (2019) Taxocenózy koscov (Opiliones) a ich bioindikačný potenciál v evaluácii ekologických a environmentálnych parametrov krajiny Podunajska. Technická univerzita vo Zvolene, Zvolen, 112 pp.

Ložek V, Gulička J (1955) Zoologický výskum pralesní reservace Stužica ve slovenských Východních Karpatech (Mollusca, Myriapoda). Ochrana přírody 10: 202–209.

Lukniš M (1972) Reliéf. In: Lukniš, M. (ed.) Slovensko 2. Príroda, Obzor, Bratislava, 124–203.

Majzlan O, Hazuchová A (1997) Abundancia a sezónna dynamika koscov (Opiliones) v pôde lužných lesov Podunajska. Folia faunistica Slovaca 2: 47–51.

Maršalek P (2001) Kosce (Opiliones) Levočských vrchov. Natura Carpatica 42: 187–190.

Maršalek P (2004) Opiliofauna Volovských vrchov. Natura Carpatica 45: 117–124.

Maršalek P (2012a) Kosce (Opiliones) okolia mesta Bardejov. Folia faunistica Slovaca 17(4): 305–307.

Maršalek P (2012b) Kosce (Opiliones) Vihorlatských vrchov. Naturae Tutela 16(1): 51–56.

Maršalek P (2017) Niekoľko poznámok o faune koscov (Opiliones) Spišskej Magury. Folia Oecologica 9(1): 32–38.

Maršalek P (2018) Kosce (Opiliones) Levočských vrchov a Spišskej Magury. Vlastivedný zborník SPIŠ 9: 368–375.

Maršalek P, Stašiov S (2015) Kosce (Arachnida, Opiliones) pohoria Čergov. Folia faunistica Slovaca 20(2): 131–134.

Martens J (1978) Spinnentiere, Arachnida: Weberknechte, Opiliones. Die Tierwelt Deutschlands. 64. VEB Gustav Fischer Verlag, Jena, 464 pp.

Mašán P (1998) First record of *Siro carpaticus* (Opiliones, Cyphophtalmi, Sironidae) from Slovakia. Biologia, Bratislava 53(5): 650.

Mašán P (2005) Prvý nález kosca *Siro carpaticus* (Opiliones, Cyphophtalmi, Sironidae) vo Vihorlate. Telekia, Spravodaj CHKO Vihorlat 3: 28.

Mašán P, Mihál I (1993) Contribution to the knowledge of harvestmen (Opiliones) in Slovakia. Entomological Problems 24: 75–80.

Melega M, Parimuchová A, Ľuptáčik P, Jászay T, Košel V, Čech V, Šestáková A, Mock A (2022) Fauna bezstavovcov jaskýň planiny Galmus (Volovské vrchy), Slovenský kras, (Acta Carsologica Slovaca) 60(1): 63–92.

Mihál I (1996) Kosce (Opilionida). In: Sláviková D, Slávik D (Eds) Ochrana biodiverzity a obhospodarovanie trvalých trávnatých porastov CHKO – BR Poľana. Nadácia IUCN, Svetová únia ochrany prírody, Bratislava, 45–46.

Mihál I (1998) Kosce (Opiliones) lesných porastov a lúk na Poľane. Ochrana prírody 16: 119–124.

Mihál I, Astaloš B (2011) Harvestmen (Arachnida, Opiliones) in disturbed forest ecosystems of the Low and High Tatras Mts. Folia oecologica 38(1): 89–95.

Mihál I, Hrúz V (1998) Opiliofauna PR Havranie skaly v CHKO – BR Poľana. Chránené územia Slovenska 38: 23.

Mihál I, Korenko S (2010) Kosce (Arachnida, Opiliones) Starohorských vrchov (stredné Slovensko). Naturae Tutela 14(2): 201–206.

Mihál I, Mašán P (2006) Príspevok k poznaniu koscov (Opiliones) stredného a východného Slovenska. Natura Carpatica 47: 89–96.

Mihál I, Mašán P, Astaloš B (2003) Kosce – Opiliones. In: Mašán P, Svatoň J (Eds) Pavúkovce Národného parku Poloniny (Arachnida: Araneae, Pseudoscorpiones, Opiliones, Acari – Parasitiformes). Štátna ochrana prírody SR Banská Bystrica, Správa Národného parku Poloniny, Snina, 127–141.

Mihál I, Mašán P, Astaloš B (2009) Kosce – Opiliones. In: Mašán P, Mihál I (Eds) Pavúkovce Cerovej vrchoviny (Arachnida: Araneae, Pseudoscorpiones, Opiliones, Acari). Štátna ochrana prírody SR Banská Bystrica, Správa CHKO Cerová vrchovina Rimavská Sobota, Ústav zoológie SAV Bratislava, Ústav ekológie lesa SAV Zvolen, 137–151.

Mihál I, Astaloš B, Černecká Ľ, Gajdoš P, Šestáková A, Žila P (2015) K poznaniu koscov (Arachnida, Opiliones) vybraných lokalít na strednom a východnom Slovensku. Folia faunistica Slovaca 20(1): 31–35.

Ministry of Environment of the Slovak Republic (2021) Decree No. 170/2021 Coll. implementing Act No. 543/2002 Coll. on Nature and Landscape Protection, as amended by subsequent regulations (Annex 5). Effective from 1 January 2023.

Ministry of the Environment of the Slovak Republic (2003) Decree No. 24/2003 Coll. implementing Act No. 543/2002 Coll. on nature and landscape protection, as amended (Annex 6).

Murray N (2017) Global 10 × 10-km grids suitable for use in IUCN Red List of Ecosystems assessments (vector and raster format). https://doi.org/10.6084/m9.figshare.4653439.v1

Muster C, Blick T, Schönhofer A (2016) Rote Liste und Gesamtartenliste der Weberknechte (Arachnida: Opiliones) Deutschlands. In: Gruttke H, Balzer S, Binot-Hafke M, Haupt H, Hofbauer N, Ludwig G, Matzke-Hajek G, Ries M (Eds) Rote Liste der gefährdeten Tiere, Pflanzen und Pilze Deutschlands. Band 4: Wirbellose Tiere (Teil 2). Bonn (Bundesamt für Naturschutz). Naturschutz und Biologische Vielfalt 70(4): 513–536.

Novak T, Lipovšek S, Slana Lj (2000) Biogeographical remarks on *Gyas titanus* Simon, 1879 (Opiliones, Phalangiidae) in the Balkans. Natura Croatica 9(3): 189–194.

Petricskó J (1892) Selmeczbánya vidéké állattani tekintetben. Kiadja saját költségén a selmeczbányai gyógyászati és természettudományi egyesòlet, Selmeczbánya, 133 pp.

Pinto-Da-Rocha R, Da Silva MB, Bragagnolo C (2005) Faunistic similarity and historic biogeography of the harvestmen of southern and southeastern Atlantic Rain Forest of Brazil. Journal of Arachnology 33: 290–299. https://doi.org/doi:10.1636/04-114.1 https://doi.org/10.1636/04-114.1

Prantl F, Mařan J (1957) Sekáči (Opilionidea). In: Štěpánek O (Ed.) Přírodopis živočíšstva. Orbis, Praha, 521 pp.

Rafalski J (1956) Opis *Siro carpaticus* sp. n. wraz z uwagami o morfologii i systematice Cyphophthalmi (Opiliones). Sprawozdania Poznanski Towarzystwa Przyjaciół Nauk 22: 49–52.

Raspotnig G, Schaider M, Föttinger P, Komposch C, Karaman I (2011) Nitrogen-containing compounds in the scent gland secretions of European cladonychiid harvestmen (Opiliones, Laniatores, Travunioidea). Journal of Chemical Ecology 37(8): 912–921. https://doi.org/10.1007/s10886-011-9996-2

Roewer CF (1923) Die Webernechte der Erde. Fischer Verlag, Jena, 1116 pp.

Roušar A (1999) Nález klepítníka členeného v Krušných horách. Živa 2: 82.

Rozwałka R (2012) Is *Siro carpaticus* Rafalski, 1956 (Arachnida: Opiliones) really a rare harvestmen species? Fragmenta Faunistica 55(2): 169–175. https://doi.org/10.3161/00159301FF2012.55.2.169

Sørensen W (1873) Bidrag til Phalangidernes Morphologi og Systematik samt Beskrivelse af nogle nye, herhen høhre Former. Naturhistorisk Tidssk 3: 489–526.

Staręga W (1966) Kosarze (Opiliones) Bieszczad. Fragmenta Faunistica 13: 145–157. https://doi.org/10.3161/00159301FF1966.13.6.145

Stašiov S (1999) Rozšírenie *Ischyropsalis manicata* (Opilionida) na Slovensku. Entomofauna carpathica 11(1): 9–12.

Stašiov S (2003) Výskyt *Paranemastoma quadripunctatum* (Opiliones) na Slovensku. In: Roller L (Ed.) Entomologická konferencia 2003. Zborník abstraktov z konferencie, Mošovce, Slovenská entomologická spoločnosť pri SAV, Bratislava, Ústav zoológie SAV, Bratislava, 22 pp.

Stašiov S (2004) Kosce (Opiliones) Slovenska. Technická univerzita vo Zvolene, Zvolen, 119 pp.

Stašiov S, Diviaková A (2022) Kosce (Opiliones) rôzne obhospodarovaných podhorských lúk. Zborník abstraktov z vedeckého kongresu "Zoológia 2022". Technická univerzita vo Zvolene, Zvolen, 68 pp.

Stašiov S, Mihál I (2001) Rozšírenie a ekológia koscov (Opilionida) Ostrôžok (juh stredného Slovenska). Acta Facultatis Ecologiae 8: 99–104.

Stašiov S, Tuf IH (2016) Nový nález sekáče obroubeného (Opiliones: Sclerosomatidae: Leiobuninae: *Leiobunum limbatum*) na Slovensku. Acta Carpathica Occidentalis 7: 56–57. https://doi.org/10.62317/aco.2016.008

Stašiov S, Bitušík P, Šamaj J (1997) Kosce (Opiliones) NPR Malý Polom (CHKO Kysuce). Ochrana prírody, Banská Bystrica 15: 119–125.

Stašiov S, Maršalek P, Mihál I, Mašán P, Astaloš B, Jarab M (2003a) Kosce (Opiliones) Ondavskej vrchoviny. Natura Carpatica 44: 261–266.

Stašiov S, Mock A, Mlejnek R (2003b) Nové nálezy koscov (Opiliones) v jaskyniach Slovenska. Slovenský kras, Acta Carsologica Slovaca 41: 199–207.

Stašiov S, Kubovčík V, Čiliak M, Diviaková A, Lukáčik I, Dovciak M (2021) Harvestmen (Opiliones) community structure varies across forest-meadow ecotones in a biodiverse karst region. Biodiversty and Conservation 30: 1101–1117. https://doi.org/10.1007/s10531-021-02135-5

Šestáková A, Mihál I (2014) *Carinostoma elegans* new to the Slovakian harvestmen fauna (Opiliones, Dyspnoi, Nemastomatidae). Arachnologische Mitteilungen 48: 16–23. https://doi.org/10.5431/aramit4804

Šilhavý V (1950) Sekáči východního Slovenska. Entomologické listy 13: 99–106.

Šilhavý V (1956) Sekáči – Opilionidea. Fauna ČSR 7. Nakladatelství ČSAV, Praha, 274 pp.

Šilhavý V (1966) Fragmenta Opilionidologica II (Arachn., Opilionidea). Zprávy Československé společnosti entomologické při ČSAV, Praha 2: 104–105.

Šilhavý V (1968a) Příspěvek k faunistice sekáčů (Opilionidea) Slovenska. Zprávy Československé společnosti entomologické při ČSAV, Praha 4: 63–64.

Šilhavý V (1968b) Sekáči (Opilionideae) Slovenského krasu. Zborník Východoslovenského múzea 9: 101–103.

Šilhavý V (1970) Faunistický příspěvek o sekáčích (Opilionidea) Československa. Fragmenta opilionidologica IV. Zprávy Československé společnosti entomologické při ČSAV 6: 107–108

Šilhavý V (1972) Druhý příspěvek k poznání Československých sekáčů (Opilionidea). Zprávy Československé společnosti entomologické při ČSAV, Praha 8: 93–96.

Šilhavý V (1974) Opilionidea. Zborník prác o Tatranskom národnom parku 16: 81–85.

Šilhavý V (1981) Occurrence of *Leiobunum glabrum* in Czechoslovakia (Arachn., Opilionidea). Věstník Československé Společnosti Zoologické, Praha 45: 204–208.

Šilhavý V (1949) Sekáč *Astrobunus meadi* (Thor.) v Československé republice. Časopis Československé společnosti entomologické, Praha 46: 151–155.

Škapec L, Beneš K, Bílý S, Brtek J, Buchar J, Čaputa A, Čepelák J, Gulička J, Jelínek J, Korbel L, Lauterer P, Ložek V, Lukáš J, Novák I, Novák K, Raušer J, Rozkošný R, Soldán T, Spitzer K, Štys P, Tkalců B, Zelený J (1992) Red Data Book of Threatened and Rare Plant and Animal Species of the Czech and Slovak Federal Republic 3. Invertebrates. Príroda, Bratislava, 150 pp.

Wijnhoven H (2009) De Nederlandse hooiwagens (Opiliones). Entomol Tabellen 3: 1–118.

ZooKeys 1230: 25–36 (2025)
DOI: 10.3897/zookeys.1230.140329

Research Article

Ambusher in sponge: a new species of *Eunice* (Annelida, Eunicidae) commensal within deep-sea Farreidae (Porifera, Hexactinellida) on northwest Pacific seamounts

Yadong Zhou[1,2], Ruiyan Zhang[1], Chengcheng Shen[1], Qin Mao[1], Mouyingke Zhang[1], Dongsheng Zhang[1,2,3]

1 *Key Laboratory of Marine Ecosystem Dynamics, Second Institute of Oceanography, Ministry of Natural Resources, Hangzhou, Zhejiang, China*
2 *Southern Marine Science and Engineering Guangdong Laboratory (Zhuhai), Zhuhai Guangdong, China*
3 *School of Oceanography, Shanghai Jiao Tong University, Shanghai, China*
Corresponding author: Dongsheng Zhang (dszhang@sio.org.cn)

Abstract

Deep-sea sponges create complex biogenic structures and attract a wide array of deep-sea organisms, including symbionts. In this study, we describe *Eunice siphoninsidiator* **sp. nov.**, a new eunicid species living in the central cavity of deep-sea farreid glass sponges found on northwest Pacific seamounts. The new species closely resembles the Atlantic *Eunice norvegica* both morphologically and molecularly, but it differs in the relative length of palp compared to peristomium, starting points of subacicular hooks, and shape of pectinate chaetae. A 13% *COI* genetic distance between the two species further supports the establishment of *E. siphoninsidiator* as a distinct species. Gut content analyses reveals fragments of barnacles and brittle stars, suggesting a carnivorous diet and a sit-and-wait predatory strategy. The eunicid gains protection from living inside the sponge, which consistently harbored the polychaete in all specimens examined, while the sponge benefits from the cleaning of epibionts, pointing to a potentially mutualistic relationship.

Key words: Gut content, morphology, Polychaeta, sponge associated species, taxonomy

OPEN ACCESS

Academic editor: Christopher Glasby
Received: 27 October 2024
Accepted: 15 January 2025
Published: 5 March 2025

ZooBank: https://zoobank.org/91A22F26-5E7B-4C51-A00A-435913E00E3B

Citation: Zhou Y, Zhang R, Shen C, Mao Q, Zhang M, Zhang D (2025) Ambusher in sponge: a new species of *Eunice* (Annelida, Eunicidae) commensal within deep-sea Farreidae (Porifera, Hexactinellida) on northwest Pacific seamounts. ZooKeys 1230: 25–36. https://doi.org/10.3897/zookeys.1230.140329

Introduction

Eunice Cuvier, 1817 is a diverse genus with more than 200 currently accepted species (Read and Fauchald 2024) occurring worldwide in a wide variety of marine habitats, from shallow water to deep sea and including, among others, soft sediments, rocky bottoms, sponge conglomerates, coral rubble, and deep-sea hydrothermal vents (Hutchings 1986; Fauchald 1992; Desbruyères et al. 2006; Martin and Britayev 2018; Zanol et al. 2020). However, the associations involving species of *Eunice* and sponges are exclusively known from shallow waters (Zanol et al. 2021). In the nutrient-limited deep sea, glass sponges are important habitat modifiers, which increase the three-dimensional habitat complexity and attract a wide variety of organisms (Maldonado et al. 2015; Hanz et al. 2022).

Numerous species of polychaetes are known to live in association with these deep-sea sponges, but a few belong to *Eunice*. Among them, there are *Eunice goodei* Fauchald, 1992 (as *Nicidion kinbergi* Webster), *Eunice denticulata* Webster, 1884 (as *Leodice denticulata* Webster), and *Eunice spongicola* (Treadwell, 1921) (as *Leodice spongicola* Treadwell, 1921) (Treadwell 1921), all of them found in soft bottoms of the Caribbean Sea (Treadwell 1921). Notably, this study reports and formally describes new species of *Eunice* living as a commensal of glass sponges (Porifera, Farreidae) found on deep-sea seamounts in the northwest Pacific. In addition to describing the characteristics of the association, we have analyzed the gut contents of the worms to uncover their potential food sources to support defining the type of association with its host sponges. These results expand our view of sponge-dwelling biodiversity in the largely unknown deep sea.

Material and methods

Sample collection, treatment, and observation

Seven farreid sponges were collected from O-Hakucho Guyot, Albo Guyot; DD seamount (Fig. 1), using the manipulator of the human-occupied vehicle (HOV) *Jiaolong* during cruises DY80 and DY86 onboard R/V *Shenhaiyihao*. Onboard, single eunicids were picked out from the central cavity of six sponges, while two specimens were extracted from the seventh sponge (RSIOPOLY86001 and RSIOPOLY86003) (Fig. 2A, B). All specimens were preserved in 100% (v/v) ethanol prior to being observed and photographed under a Zeiss Discovery V.16/V.20 stereomicroscope. The maxillary apparatus and parapodia were dissected and examined under a stereomicroscope (Carl Zeiss SteREO Discovery V.20). Selected parapodia from anterior, middle, and posterior regions were dissected and prepared for morphological examinations of dorsal cirri, ventral cirri, and chaetae under a microscope (Carl Zeiss Imager. A2). Two specimens were dissected to extract the gut contents, which were then examined under a stereomicroscope. Undigested tissues were picked out, photographed, and analyzed to determine their potential origins.

Type specimens and material examined are deposited at the repository of the Second Institute of Oceanography (**RSIO**), Ministry of Natural Resources, Hangzhou, China.

Molecular analysis

Total genomic DNA was extracted from a dissected parapodium using the Mollusc DNA kit (Omega, USA) following manufacturer instructions. Gene fragments of the cytochrome *c* oxidase subunit I gene (*COI*) were amplified using the primer pairs HCO2198/LCO1490 for (Folmer et al. 1994), following the thermal program 95 °C for 4 min, 35 cycles of 95 °C for 30 s, 45 °C for 45 s, and 72 °C for 1 min, and 72 °C for 7 min. Purifications and bidirectional Sanger sequencing of the polymerase chain reaction (PCR) products were then conducted in Sangon (Shanghai China). Consensus sequences (ca 660 bp) were assembled in Geneious R11 after examination of the raw sequences by eye (Kearse et al. 2012). A *COI* dataset (Suppl. material 1), in-

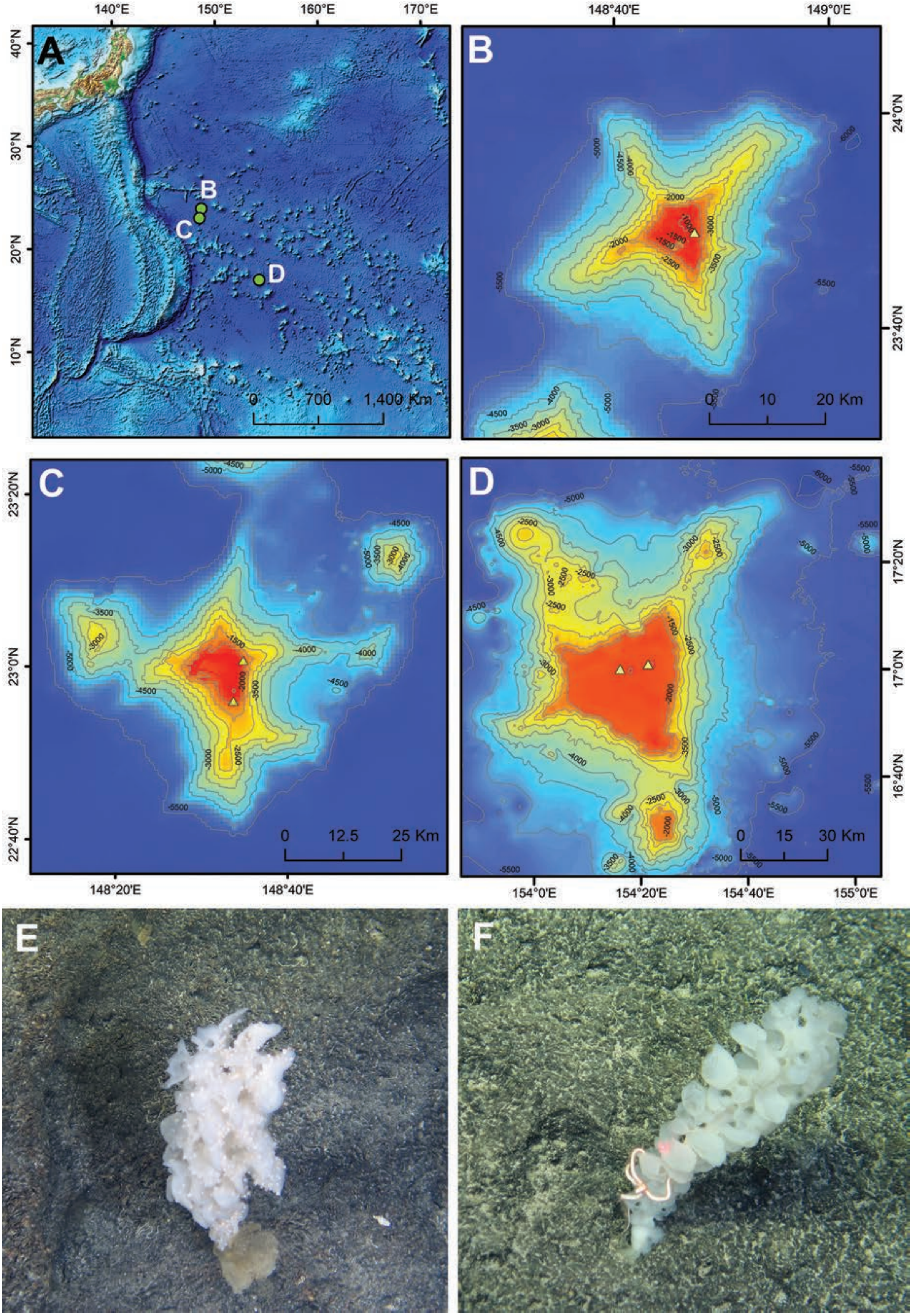

Figure 1. Map of sampling locations (**A–D**) and *in situ* images of farreid glass sponges captured during the *Jiaolong* dive JL230 (**E**) and JL233 (**F**) **B** DD Seamount **C** O-Hakucho Guyot **D** Albo Guyot.

cluding the newly generated and publicly available sequences, was created and aligned using the MUSCLE algorithm (Edgar 2004) within Geneious R11. The result was then used to estimate the genetic distances between the new species and its congeners in MEGA v. 11 (Tamura et al. 2021), with the Kimura 2-parameters (K2P) substitution model (Suppl. material 2).

Results

Systematics

Eunicidae Berthold, 1827
***Eunice* Cuvier, 1817**

***Eunice siphoninsidiator* Zhou, Zhang, Shen & Zhang, sp. nov.**
https://zoobank.org/3351F071-3A6F-483E-8591-1102FE2FA028
Figs 2, 3

Type material. ***Holotype*:** • RSIOPOLY80001, O-Hakucho Guyot, Northwest Pacific, 23.01°N, 148.58°E, 1135 m depth; *Jiaolong* dive JL230, R/V *Shenhaiyihao* cruise DY80-I; 27 June 2023; fixed in 100% (v/v) ethanol. ***Paratype*:** • two specimens. Paratype 1#, RSIOPOLY80002, O-Hakucho Guyot, Northwest Pacific, 22.93°N, 148.56°E, 1175 m depth; *Jiaolong* dive JL233, R/V *Shenhaiyihao* cruise DY80-I; 30 June 2023; fixed in 100% (v/v) ethanol; • ***Paratype*** 2#, RSIOPOLY86005, Albo Guyot, Northwest Pacific, 17.0001°N, 154.2679°E, 1057 m depth, *Jiaolong* dive JL311, R/V *Shenhaiyihao* cruise DY86-II, 3 September 2024, fixed in 10% (v/v) formalin, partial tissue fixed in 100% (v/v) ethanol.

Additional material. Five specimens, incomplete. • RSIOPOLY86001 and RSIOPOLY86003, Albo Guyot, Northwest Pacific, 16.9998°N, 154.7687°E, 1107 m depth, *Jiaolong* dive JL311, R/V *Shenhaiyihao* cruise DY86-II, 3 September 2024, anterior part fixed in 100% (v/v) ethanol; • RSIOPOLY86014, DD Seamount, Northwest Pacific, 23.8150°N, 148.7926°E, 1055 m depth, *Jiaolong* dive JL302, R/V *Shenhaiyihao* cruise DY86-II, 20 August 2024, anterior part fixed in 100% (v/v) ethanol; • RSIOPOLY86015, DD Seamount, Northwest Pacific, 23.8150°N, 148.7915°E, 1047 m depth, *Jiaolong* dive JL302, R/V *Shenhaiyihao* cruise DY86-II, 20 August 2024, anterior part fixed in 100% (v/v) ethanol; • RSIOPOLY86016, Albo Guyot, Northwest Pacific, 17.0143°N, 154.3549°E, 1126 m depth, *Jiaolong* dive JL312, R/V *Shenhaiyihao* cruise DY86-II, 4 September 2024, anterior part fixed in 100% (v/v) ethanol.

Measurements (before fixation). Holotype complete, with 95 chaetigers, total length 177 mm, first 10 chaetigers 11.5 mm in length, width at chaetiger 10 without parapodia 10 mm. Paratype 1# complete, with 107 chaetigers, total length 140 mm, first 10 chaetigers 8.1 mm in length, width at chaetiger 10 without parapodia 6.1 mm. Paratype 2# complete, with 103 chaetigers, total length 151 mm, first 10 chaetigers 11.2 mm in length, width at chaetiger 10 without parapodia 6.7 mm.

Description. Live specimens iridescent brownish or slightly pinkish with lighter patches along the body. Preserved specimens pale white, slightly iridescent. Body long, dorsally convex, and ventrally flat (Fig. 2C, D).

Prostomium narrower and shorter than first peristomial ring, bilobed anteriorly with round anterior ends and deep median sulcus (Fig. 2E, F). Prostomial

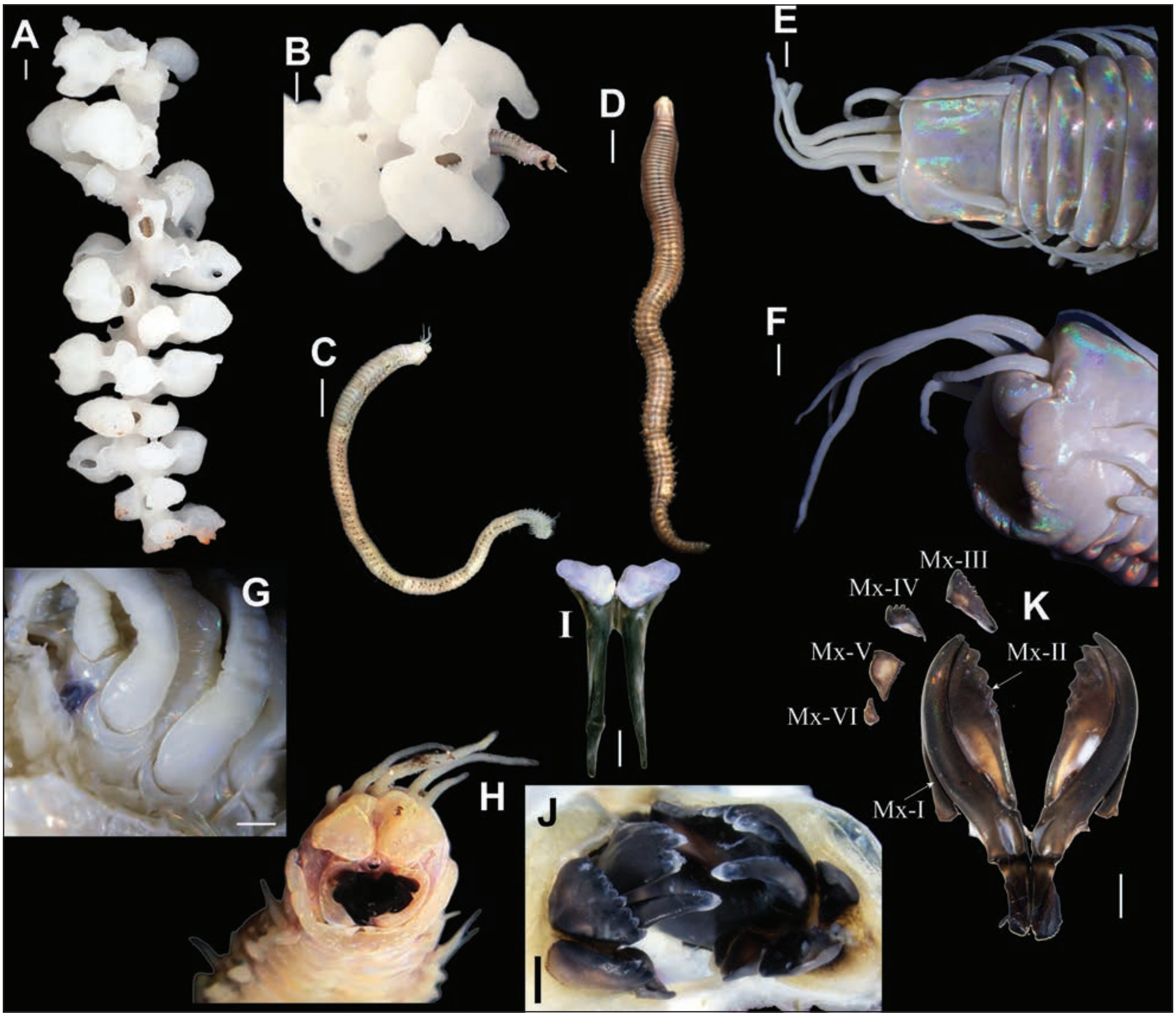

Figure 2. *Eunice siphoninsidiator* sp. nov. **A** paratype (RSIOPOLY80002) commensal within a farreid sponge collected during the dive JL233 **B** anterior part of paratype (RSIOPOLY80002), anterior-ventral view **C** paratype (RSIOPOLY80002, before fixation), lateral view **D** holotype (RSIOPOLY80001, before fixation), dorsal view **E** anterior end of holotype, dorsal view (fixed in 100% (v/v) ethanol) **F** detail of anterior end of holotype, lateral view (fixed in 100% (v/v) ethanol) **G** location of eye in the paratype, dorsal view (fixed in 100% (v/v) ethanol) **H** anterior end of paratype, frontal view (fixed in 100% ethanol) **I** mandible of paratype, ventral view **J** maxillae apparatus of paratype (RSIOPOLY80002), frontal view (before digestion with Proteinase K) **K** maxillae apparatus of paratype (RSIOPOLY80002), dorsal view (after digestion with Proteinase K). Scale bars: 1 cm (**A–D**); 1 mm (**E, F**); 0.5 mm (**G, J**); 1 mm (**I, K**).

appendages in semicircle, with lateral antennae closer to palps than to median antennae (Fig. 2E–H). Antennae 2 × longer than palps, reaching anterior end of chaetiger 5 when reversing; median antennae about 1.5 × as long as lateral antennae (Fig. 2E, F). Ceratophores of antennae and palps short and ring-shaped, usually covered by prostomium; ceratostyles long, tapering, with indistinct articulations; palpstyles tapering digitiform distally with indistinct articulations (Fig. 2E–G). Eyes dark, lateral to ceratophores of lateral antennae (Fig. 2G).

Peristomium cylindrical, separation between first and second ring visible on both dorsal and ventral sides (Fig. 2E, F); first ring more than 5/6 as long as of whole peristomium; peristomial cirri tapering, indistinctly articulated, reaching anterior end (middle in paratype) of first peristomial ring (Fig. 2E, F).

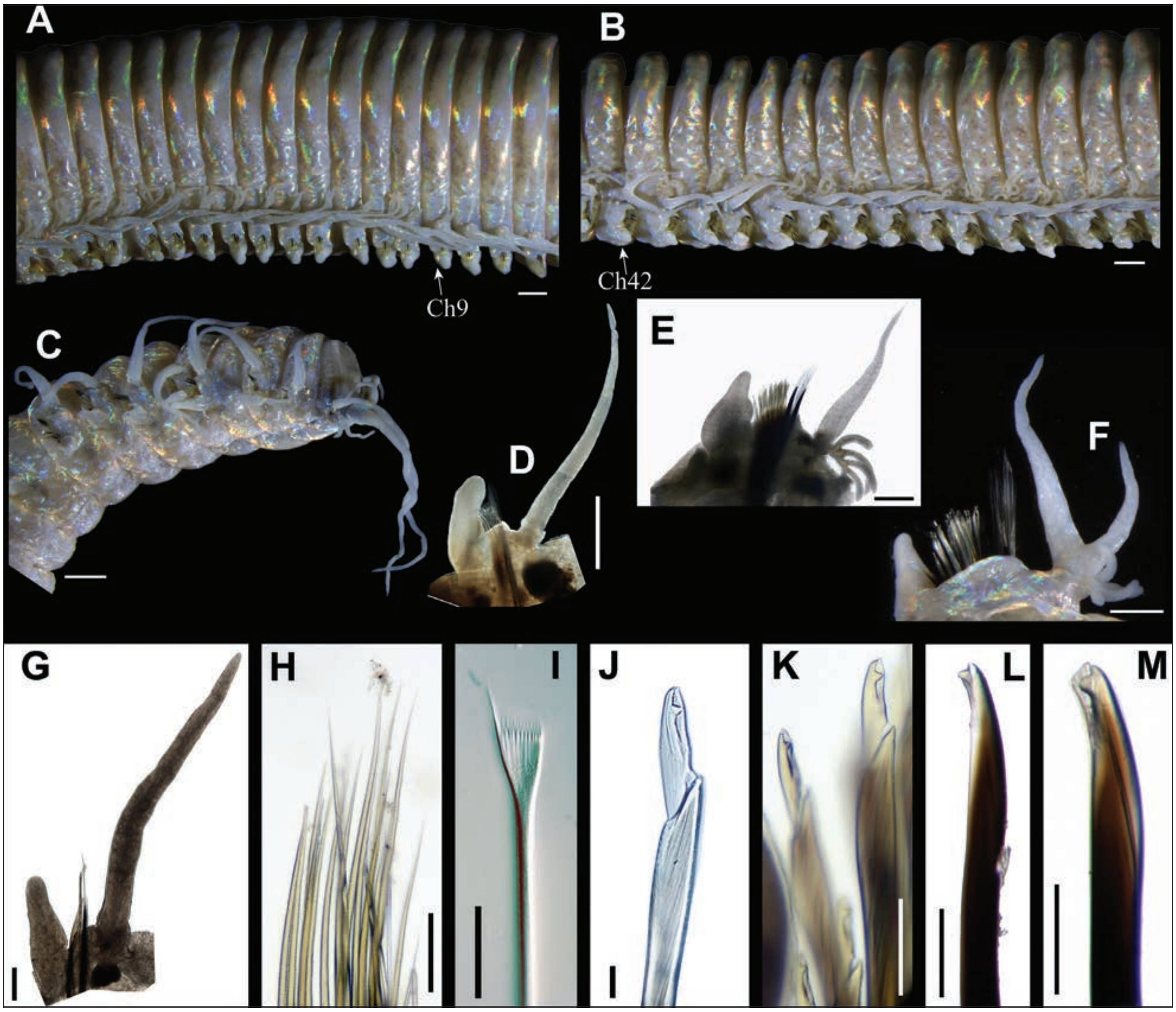

Figure 3. *Eunice siphoninsidiator* sp. nov. **A** middle frontal segments of holotype, lateral view (right side) **B** middle segments of paratype in lateral view (right side) **C** posterior end of holotype, lateral view (left side) **D** right parapodium of chaetiger 4 of paratype (RSIOPOLY86005, frontal view) **E** right parapodium of chaetiger 30 of holotype (frontal view) **F** right parapodium of chaetiger 44 of holotype (frontal view) **G** right parapodium of chaetiger 103 of paratype (RSIOPOLY86005, frontal view) **H** limbate chaetae on chaetiger 30 **I** pectinate chaetae on chaetiger 64 of paratype (RSIOPOLY86005) **J** compound falcigers on chaetiger 54 of paratype (RSIOPOLY80002) **K** compound falcigers on chaetiger 30 of paratype (RSIOPOLY80002) **L** subacicular hooks on a posterior chaetiger of paratype (RSIOPOLY80002) **M** subacicular hooks on chaetiger 50 of paratype (RSIOPOLY80002). Scale bars: 1 mm (**A–D**); 0.5 mm (**E, F**); 0.2 mm (**G**); 0.1 mm (**H, J–L**); 50 µm (**I**).

Mandibles dark brown, with white wing-shaped calcareous cutting edges (Fig. 2I). Maxillary apparatus brown to dark brown. Maxillae formula MxI 1+1, MxII 6+5, MxIII 8+0, MxIV 5+5, MxV 1+1, MxVI 1+1. All teeth with blunt ends. Mx-I about 3 × as long as carrier. MxV with a large square ridge; MxVI reduced to a plate with a minute tooth (Fig. 2J, K).

Branchiae from chaetiger 9 to near posterior end (Fig. 3A–C), pectinate, always shorter and slender than dorsal cirri (Fig. 3A, B), with 1–2 short filaments on most anterior and most posterior branchial segments, increasing to 4–5 filaments on following parapodia and reaching a maximum of 7–8 at middle region (Fig. 3D–F).

Dorsal cirri tapering, indistinctly articulated distally in anterior chaetigers, then smooth, slightly thicker on prebranchial segments and slender on posterior segments (Fig. 3A–G). Ventral cirri 1/4–1/3 and 2–3 as long as dorsal cirri and chaetal lobes, respectively, gradually shortening from anterior to posterior regions. First four ventral cirri short, digitiform, strong; following ones with suboval basal inflation and a short tapering tip from chaetiger 5 through 37; subsequent ventral cirri digitiform (Fig. 3D–G).

Chaetal lobs obliquely truncate, longer dorsally than ventrally, with aciculae emerging dorsal to midline. Prechaetal lobe low transverse fold. Postchaetal lobes round or obliquely truncate, inflated on all chaetigers. Limbate chaetae supracicular, tapering and slender (Fig. 3 H). Thin pectinate chaetae emerging from chaetiger 5 to last chaetiger, tapering, flat with 12–16 teeth; one marginal teeth longer than others (Fig. 3I). Shafts of compound falcigers smooth, slender at basal part, expanded distally; blades bidentate, with proximal tooth triangular, similar to distal tooth in length, directed laterally; distal tooth slightly curved, slightly slenderer than proximal tooth (Fig. 3J, K). Aciculae dark brown, straight or slightly bent, tapering with blunt or pointed tips, 1–3 in each parapodium (Fig. 3E). Subacicular hook bidentate, dark brown, from chaetiger 27 to last segment, 1–2 per parapodium; proximal tooth triangular, directed laterally; distal tooth, smaller than proximal tooth, directed upwards (Fig. 3L, M).

Pygidium with two pairs of smooth anal cirri, most ventral pair short and slender; dorsal pair much longer and thicker, extending to last 6th chaetiger when folded anteriorly (Fig. 3C).

Variation. Relative length of peristomial cirri to first ring of peristomium close to 1:1 in holotype, paratype 2# and 4 other individuals, but close to 1:2 in paratype 1#. Holotype with bifurcated dorsal cirri in left parapodia of chaetigers 14 and 45 and in right parapodia of chaetiger 44, absent in paratype (Fig. 3B, F). Starting of branchiae and subacicular hook ranging from chaetiger 8–11 and 27–32, respectively, in all examined specimens.

Etymology. A combination of two Latin words: ‘*siphon-*’ meaning ‘tube’ or ‘pipe’ and ‘*insidiator*’ meaning ‘ambusher’. This is a reference to the behavior of the species as ambush predator living within tubular structure of glass sponges. This name is to be treated as noun in apposition.

Distribution. Found living in association with deep-sea glass sponges on seamounts in the northwest Pacific.

Remarks. *Eunice siphoninsidiator* sp. nov. belongs to group B-2 as proposed by Fauchald (1992) based on its dark bidentate subacicular hooks and high percentage of branchial chaetigers (>65%). It has indistinctly articulated prostomial appendages and anterior dorsal cirri, and reduced branchiae with only a few short branchial filaments (<8 and shorter than the notopodial dorsal cirri), thus most closely resembles *Eunice norvegica* (Linnaeus, 1767). However, *E. siphoninsidiator* sp. nov. has a ~1/1 relative length of palps compared to peristomium (1/2 in *E. norvegica*), subacicular hooks starting from chaetiger 27–32 (42/44 in *E. norvegica*) and pectinate chaetae asymmetric, with one marginal tooth much longer than others (symmetric, with two slight-

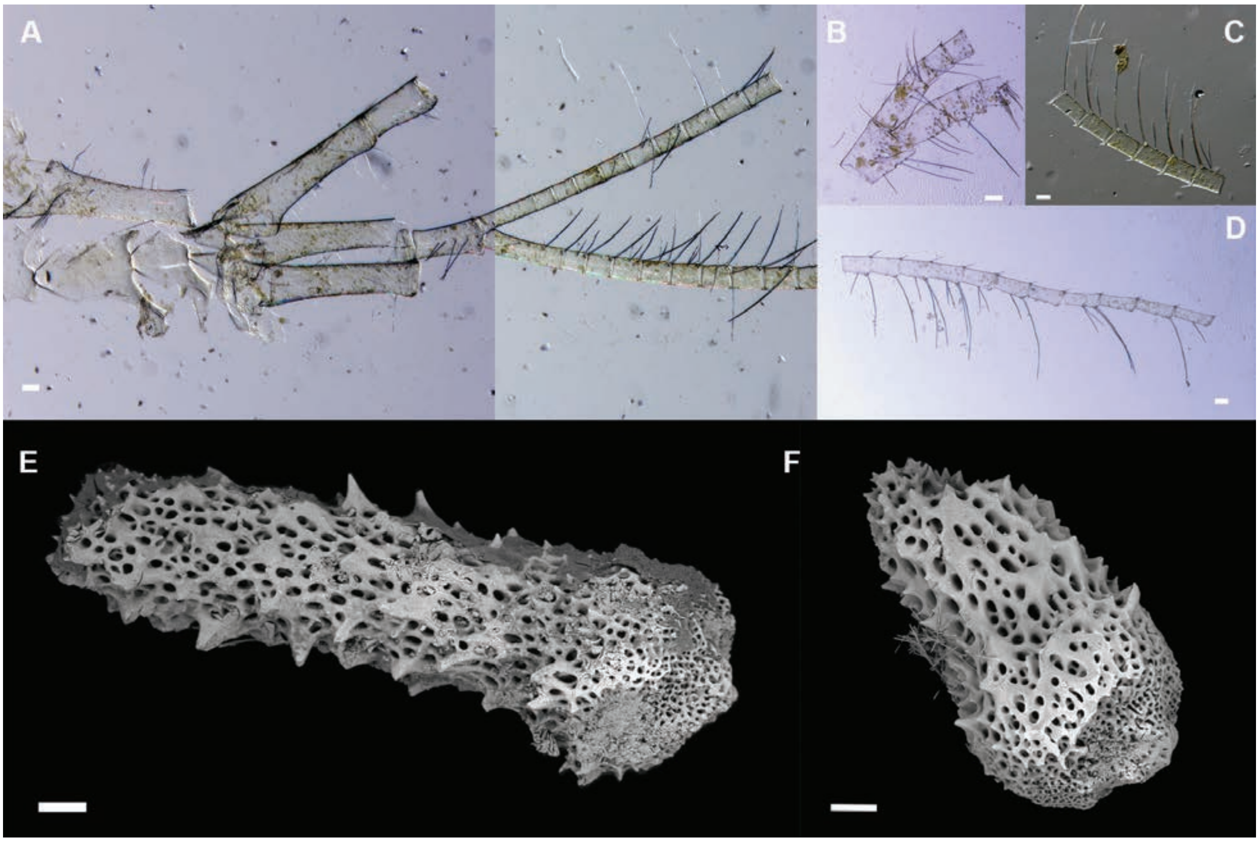

Figure 4. Gut contents of paratype **A–D** fragments of stalked-barnacle ctenopod cirri **E, F** fragments as brittle star arm spines. Scale bars: 0.1 mm (**A–F**).

ly longer marginal teeth in *E. norvegica*). Moreover, they differ by 13% in K2P genetic distance (Suppl. material 2).

Gut content analyses

It was not possible to identify gut content fragments to species level, but some were ctenopod cirri of stalked-barnacles and arm spines of brittle stars (Fig. 4).

Discussion

Habitat forming species (HFS) living in the food-limited deep sea, such as sponges and corals, significantly enhance small-scale environmental heterogeneity, providing various ecological functions for other animals, such as protection from predation, refugia, nursery habitats and feeding grounds (De La Torriente et al. 2020). A wide variety of animals have been found to be associated with deep-sea sponges, including fish, echinoderms, crustaceans, and polychaetes, the latter mainly represented by polynoids and syllids and more rarely by eunicids (Martin and Britayev 1998, 2018; Maldonado et al. 2015; Taboada et al. 2021).

Among eunicids, *Eunice* species are considered either as free-living (Jumars et al. 2015) or as symbionts, which are associated with cnidarians (including deep-sea cold-water corals), gastropods, echiurids, and shallow-water sponges (Treadwell 1921; Fauchald 1992; Martin and Britayev 1998, 2018). Therefore, this study marks the first documented case of a eunicid inhabiting deep-sea sponges.

Symbiotic eunicids were initially regarded as commensals or inquilines, obtaining shelter from their hosts (Martin and Britayev 1998). However, mutualistic characters were revealed in the association between *E. norvegica* and the cold-water reef-coral *Desmophyllum pertusum* (Linnaeus, 1758). The eunicid contributes to reef-patch formation by connecting coral fragments, to reef cleaning by active sediment transport and to protect host coral from sea urchin's predation (Mortensen 2001; Roberts 2005; Mueller et al. 2013). In return, the eunicid obtains more available food either thanks to the water flow produced by the hosts or by stealing food captured by the hosts (Mortensen 2001). Thus, we speculate that *E. siphoninsidiator* sp. nov. might not only use its farreid host as a shelter but also avail the host's water circulation for feeding.

Moreover, *E. siphoninsidiator* sp. nov. seems to obtain additional food from species "attracted" by the refuge provided by its host, as glass sponges are key HFS in the barren deep sea. This increases possibilities of inter- and intra-specific interactions, including predation. Thus, we cannot discard *E. siphoninsidiator* sp. nov. behaving as a sit-and-wait predator. Its gut content contained remains of barnacles and brittle stars, which inhabit the sponge outer surface to elevate themselves off the seafloor and improve their filtering efficiency. Inadvertently, this places themselves within reach of the ambushing worm hidden inside the sponge, which may obtain prey while avoiding being predated. Such a feeding strategy may also play a key role in cleaning the sponge from unwanted epibionts, thereby supporting the sponge's filtration efficiency. This potentially reciprocal benefit suggests a mutualistic relationship, which appears to be obligate, as all farreid sponges examined hosted specimens of *E. siphoninsidiator* sp. nov. Nevertheless, further research is needed to confirm the nature of this interaction and the extent of its ecological implications.

Acknowledgements

We thank all the crew and scientists onboard R/V Shenhaiyihao and the HOV Jiaolong team during the cruise DY80 and DY86. Special thanks go to Xiaojun Xie, Hiromi Kayama Watanabe and Zhibin Gan for their expertise and assistance with gut content identification, and to Runxuan Yan for his contributions in constructing the bathymetric maps of the seamounts. We extend our gratitude to three reviewers for their overall and insightful comments on the manuscript.

Additional information

Conflict of interest

The authors have declared that no competing interests exist.

Ethical statement

No ethical statement was reported.

Funding

This research was supported by the National Key Research and Development Program of China (2022YFC2804001), National Natural Science Foundation of China (42276132), International Seabed Authority's Sustainable Seabed Knowledge Initiative: One Thousand Reasons Campaign (co-financed by the European Maritime and Fisheries Fund of the European Union, Project 101071214 — SSKI-I — EMFAF-2021-ISA-SSKI-IBA), and the UN Ocean Decade Programme Digital DEPTH.

Author contributions

Dongsheng Zhang and Yadong Zhou conceived and designed the project. YZ, RZ, CS, QM and DZ collected and preserved specimens onboard. YZ and CS performed morphological examinations of the specimens. QM and MZ carried out DNA sequencing and analysed the molecular data. YZ interpreted the data and drafted the manuscript. All authors contributed to the final version.

Author ORCIDs

Yadong Zhou https://orcid.org/0000-0002-3577-1118
Ruiyan Zhang https://orcid.org/0000-0001-8556-8145
Chengcheng Shen https://orcid.org/0000-0002-2505-0974
Dongsheng Zhang https://orcid.org/0000-0002-2736-3229

Data availability

Molecular data of the new species is deposited in NCBI GenBank, with the accession numbers PQ517215-PQ517222.

References

Berthold AA (1827) Latreille's Natürliche Familien des Thierreichs aus dem Französischen. Mit Anmerkungen und Zusätzen. Landes-Industrie Comptoirs, Weimar, 606 pp. https://doi.org/10.5962/bhl.title.11652

Cuvier G (1817) Le règne animal distribué d'après son organisation, pour servir de base a l'histoire naturelle des animaux et d'introduction a l'anatomie comparée. Vol. 2. Contenant les reptiles, les poissons, les mollusques et les annélides. Deterville, Paris, 532 pp.

De La Torriente A, Aguilar R, González-Irusta JM, Blanco M, Serrano A (2020) Habitat forming species explain taxonomic and functional diversities in a Mediterranean seamount. Ecological Indicators 118: 106747. https://doi.org/10.1016/j.ecolind.2020.106747

Desbruyères D, Segonzac M, Bright M (2006) Handbook of Deep-Sea Hydrothermal Vent Fauna. Denisia 18, Linz-Dornach, 544 pp.

Edgar RC (2004) MUSCLE: multiple sequence alignment with high accuracy and high throughput. Nucleic Acids Research 32: 1792–1797. https://doi.org/10.1093/nar/gkh340

Fauchald K (1992) A review of the genus *Eunice* (Eunicidae: Polychaeta) based upon type material. Smithsonian Contributions to Zoology 523: 1–422. https://doi.org/10.5479/si.00810282.523

Folmer O, Black M, Hoeh W, Lutz R, Vrijenhoek R (1994) DNA primers for amplification of mitochondrial cytochrome c oxidase subunit I from diverse metazoan invertebrates. Molecular Marine Biology and Biotechnology 3: 294–299.

Hanz U, Riekenberg P, de Kluijver A, van der Meer M, Middelburg JJ, de Goeij JM, Bart MC, Wurz E, Colaço A, Duineveld GCA, Reichart GJ, Rapp HT, Mienis F (2022) The important role of sponges in carbon and nitrogen cycling in a deep-sea biological hotspot. Functional Ecology 36: 2188–2199. https://doi.org/10.1111/1365-2435.14117

Hutchings PA (1986) Biological destruction of coral reefs. Coral Reefs 4: 239–252. https://doi.org/10.1007/BF00298083

Jumars PA, Dorgan KM, Lindsay SM. (2015) Diet of worms emended: an update of polychaete feeding guilds. Annual Review of Marine Sciences 7: 497–520. https://doi.org/10.1146/annurev-marine-010814-020007

Kearse M, Moir R, Wilson A, Stones-Havas S, Cheung M, Sturrock S, Buxton S, Cooper A, Markowitz S, Duran C, Thierer T, Ashton B, Meintjes P, Drummond A (2012) Geneious Basic: an integrated and extendable desktop software platform for the organization and analysis of sequence data. Bioinformatics 28: 1647–1649. https://doi.org/10.1093/bioinformatics/bts199

Linnaeus C (1767) Systema naturae per regna tria naturae: secundum classes, ordines, genera, species, cum characteribus, differentiis, synonymis, locis. Editio Duodecima, Reformata, Tomus I, Pars II. Regnum Animale. Holmiae [Stockholm]: Laurentii Salvii, 533–1327. https://doi.org/10.5962/bhl.title.156772

Maldonado M, Aguilar R, Bannister RJ, Bell JJ, Conway KW, Dayton PK, Díaz C, Gutt J, Kelly M, Kenchington ELR, Leys SP, Pomponi SA, Rapp HT, Rützler K, Tendal OS, Vacelet J, Young CM (2015) Sponge grounds as key marine habitats: A synthetic review of types, structure, functional roles, and conservation concerns. In: Rossi S, Bramanti L, Gori A, Orejas Saco del Valle C (Eds) Marine Animal Forests. Springer, Cham. https://doi.org/10.1007/978-3-319-17001-5_24-1

Martin D, Britayev TA (1998) Symbiotic polychaetes: review of known species. In: Ansell A, Barnes M, Gibson RN (Eds) Oceanography and Marine Biology: an Annual Review. CRC Press, London. https://doi.org/10.1201/b12646

Martin D, Britayev TA (2018) Symbiotic polychaetes revisited: an update of the known species and relationships (1998–2017). In: Hawkins SJ, Evans AJ, Dale AC, Firth LB, Smith IP (Eds) Oceanography and Marine Biology: an Annual Review. CRC Press, Boca Raton, 371–448. https://doi.org/10.1201/9780429454455

Mortensen PB (2001) Aquarium observations on the deep-water coral *Lophelia pertusa* (L., 1758) (Scleractinia) and selected associated invertebrates. Ophelia 54: 83–104. https://doi.org/10.1080/00785236.2001.10409457

Mueller CE, Lundälv T, Middelburg JJ, van Oevelen D (2013) The symbiosis between *Lophelia pertusa* and *Eunice norvegica* stimulates coral calcification and worm assimilation. PLoS ONE 8(3): e58660. https://doi.org/10.1371/journal.pone.0058660

Read G, Fauchald K [Ed.] (2024) World Polychaeta Database. *Eunice* Cuvier, 1817. [Accessed through: World Register of Marine Species at:] https://www.marinespecies.org/aphia.php?p=taxdetails&id=129278 on 2024-10-15

Roberts JM (2005) Reef-aggregating behaviour by symbiotic eunicid polychaetes from cold-water corals: do worms assemble reefs? Journal of the Marine Biological Association of the UK 85: 813–819. https://doi.org/10.1017/S0025315405011756

Taboada S, Silva AS, Díez-Vives C, Neal L, Cristobo J, Ríos P, Hestetun JT, Clark B, Rossi ME, Junoy J, Navarro J, Riesgo A (2021) Sleeping with the enemy: unravelling the symbiotic relationships between the scale worm *Neopolynoe chondrocladiae* (Annelida: Polynoidae) and its carnivorous sponge hosts. Zoological Journal of the Linnean Society 193(1): 295–318. https://doi.org/10.1093/zoolinnean/zlaa146

Tamura K, Stecher G, Kumar S (2021) MEGA11: Molecular Evolutionary Genetics Analysis Version 11. Molecular Biology and Evolution 38(7): 3022–3027. https://doi.org/10.1093/molbev/msab120

Treadwell AL (1921) Leodicidae of the West Indian region. Carnegie Institute of Washington Publication 15(293): 1–131. https://doi.org/10.5962/bhl.part.20335

Zanol J, Hutchings P, Fauchald K (2020) *Eunice sensu latu* (Annelida: Eunicidae) from Australia: description of seven new species and comments on previously reported species of the genera *Eunice*, *Leodice* and *Nicidion*. Zootaxa 4748: 1–43. https://doi.org/10.11646/zootaxa.4748.1.1

Zanol J, Carrera-Parra LF, Steiner TM, Amaral ACZ. Wiklund H, Ravara A, Budaeva N (2021) The current state of Eunicida (Annelida) systematics and biodiversity. Diversity 13(2): 74. https://doi.org/10.3390/d13020074

Supplementary material 1

COI sequences used for genetic distance calculation

Authors: Yadong Zhou, Ruiyan Zhang, Chengcheng Shen, Qin Mao, Mouyingke Zhang, Dongsheng Zhang

Data type: docx

Explanation note: Species and accession numbers of *COI* sequences used for genetic distance calculation.

Link: https://doi.org/10.3897/zookeys.1230.140329.suppl1

Supplementary material 2

Pairwise K2P distance (based on partial *COI* sequences) between known *Eunice* species with available DNA data

Authors: Yadong Zhou, Ruiyan Zhang, Chengcheng Shen, Qin Mao, Mouyingke Zhang, Dongsheng Zhang

Data type: docx

Link: https://doi.org/10.3897/zookeys.1230.140329.suppl2

ZooKeys 1230: 37–80 (2025)
DOI: 10.3897/zookeys.1230.137029

Research Article

A review of cave spiders (Arachnida, Araneae) of the Crimean Mountains, with descriptions of two new species

Anton A. Nadolny[1], Ilya S. Turbanov[2,3]

1 *A.O. Kovalevsky Institute of Biology of the Southern Seas, Nakhimov Ave. 2, Sevastopol 299011*
2 *Papanin Institute for Biology of Inland Waters Russian Academy of Sciences, Borok 152742, Yaroslavl Region, Russia*
3 *Cherepovets State University, Lunacharskogo Ave. 5, Cherepovets 162600, Vologda Region, Russia*
Corresponding author: Ilya S. Turbanov (turba13@mail.ru)

Academic editor: Miquel A. Arnedo
Received: 13 September 2024
Accepted: 24 January 2025
Published: 5 March 2025

ZooBank: https://zoobank.org/FAF5D699-E6F2-4B4C-92E1-4081187E90DD

Citation: Nadolny AA, Turbanov IS (2025) A review of cave spiders (Arachnida, Araneae) of the Crimean Mountains, with descriptions of two new species. ZooKeys 1230: 37–80. https://doi.org/10.3897/zookeys.1230.137029

Abstract

Based on a critical review of the literature and study of the authors' own collections, a survey of cave spiders of the Crimean Mountains has been conducted, resulting in 20 reliable species records in eight families. Nine species have been discovered in the Crimean caves for the first time, of which two are described as new to science. A classification of spiders by ecological groups depending on their cave lifestyle is provided; a troglomorphic spider is found and described from Crimea for the first time. The most likely scenarios of spider colonization into underground habitats of Crimea are discussed. Most species arrived during multiple Pleistocene-Holocene regressions of the Black Sea basin, when zoogeographic corridors on the exposed shelf connected Crimea with the Caucasus and the Balkans. However, four synanthropic species entered Crimean caves in historical times. High relative humidity and temperature are considered key factors that enable caves to serve as refugia for Pleistocene araneofauna. A zoogeographical analysis of cave spiders is carried out. The majority of the spider species considered, totalling 16 species, are widespread, with ranges including cosmopolitan, Holarctic, trans-Palaearctic, West and Central Palaearctic, East European, and East Mediterranean. Three species are endemic to Crimea: *Tegenaria taurica*, *Bisetifer tactus* **sp. nov.**, and *Troglohyphantes exspectatus* **sp. nov.** *Bisetifer gruzin* is a Crimean-Caucasian subendemic species.

Key words: Aranei, faunistics, subterranean biology, taxonomy, troglobiont

Introduction

The study of the subterranean fauna of the Crimean Peninsula has more than a centennial history (Turbanov et al. 2016a, b, c). The first data on cave spiders in the region in question appeared in the papers by Lebedinsky (1904, 1914), Novikov (1912) and Spassky (1927, 1936). Later, Charitonov (1947a) re-examined the material of Lebedinsky (1904, 1914) and revealed that many of his records were based on misidentifications; he also described two new species: *Tegenaria taurica* Charitonov, 1947 (Agelenidae) and *Palliduphantes khobarum* (Charitonov, 1947) (Linyphiidae). All subsequent reports on the Crimean cave spiders have been based on occasional collections (Evtushenko 2004; Zagorodniuk and Vargovitsh

2004; Kovblyuk 2004b, 2007; Nadolny and Turbanov 2014; Turbanov et al. 2019a, b, 2021). In total, there are 14 publications that have provided 11 spider species for the Crimean caves. Compared to other karst regions of the Alpine-Mediterranean foldbelt, the Crimean caves are characterised by lower spider diversity (Turbanov et al. 2016b; Mammola et al. 2018). Yet, the overall spider diversity in Crimea is equal/comparable to that of neighbouring regions of similar size (Kovblyuk and Kastrygina 2015; Nentwig et al. 2024). The level of regional species endemism remains quite low, with only 11 spider species that are confined to Crimea, including one cave species, *T. taurica*. At the same time, two monotypic endemic genera, *Deliriosa* Kovblyuk, 2009 (Lycosidae) and *Spinestis* Saaristo & Marusik, 2009 (Oonopidae), are known from the mountainous part of the peninsula (Kovblyuk 2014; see WSC 2024 for additional records). The endemism at the generic level indicates that the age of the araneofauna in the Crimean Mountains could be comparable to those of the Balkans (14 endemic genera, including cave genera) and the Caucasus (one endemic genus from an endemic subfamily; see Kovblyuk 2014).

Thus, compared to the well-studied epigean araneofauna of the Crimean Peninsula, subterranean spiders are still poorly studied. For this reason, the first thorough survey of the Crimean cave spiders is the main objective of the present paper, aiming at (1) a critical analysis of literature-derived data; (2) providing new faunistic and taxonomic data; (3) presenting a possible ecological classification of the Crimean cave species depending on their association with caves; (4) discussing the possible scenarios of spider penetration into the Crimean underground habitats; and (5) undertaking a zoogeographic analysis of the Crimean spider fauna.

Materials and methods

The material for the present study has been hand-collected from 31 the Crimean caves over the decade 2010–2021. A total of 243 spider specimens (216 adults, 5 subadults and 22 juveniles) belonging to 20 species have been collected and identified; two additional species (two specimens) were studied as comparative material. All the material was preserved in 96% alcohol directly in the caves.

For the study, the copulatory organs were dissected, boiled in a 10% aqueous solution of potassium hydroxide (KOH), and placed in glycerine on a slide with a cavity. The photos of copulatory organs and general appearances were taken using Canon EOS 550D camera mounted on MBS-1 and Olympus CX41 microscopes and a Hitachi SU3500 scanning electron microscope at the A.O. Kovalevsky Institute of Biology of the Southern Seas (Sevastopol). Resulting images were processed in the Helicon Focus 7.0.2., Adobe Photoshop CS6 and CorelDRAW 11 programs. Some maps were created using Google Earth Pro version 7.3.0.3832 and Adobe Photoshop CS6.

Types and voucher specimens have been shared between the Zoological Museum of the Moscow State University, Russia (**ZMMU**); the National Arachnological Collection, the V.I. Vernadsky Tavrida National University ("Crimean Federal University"), Simferopol, Crimea (**TNU**); and the private collection of the second author (**IT**).

When discussing ecological groups of the Crimean cave spiders, the classification by Sket (2008) has been adopted: (1) troglobiont, i.e., a species/population strictly that is bound to a hypogean habitats; (2) eutroglophile, i.e., an essentially epigeic species that is capable of maintaining a permanent subterranean population; (3) subtroglophile, i.e. inclined perpetually/temporarily to inhabiting in subterranean habitats, but requires the surface for some biological functions (e.g., feeding); (4) trogloxene, i.e., a species that only sporadically (accidentally) becomes subterranean.

Results

Class Arachnida Lamarck, 1801
Order Araneae Clerck, 1757
Family Agelenidae C.L. Koch, 1837
Genus *Tegenaria* Latreille, 1804

***Tegenaria lapicidinarum* Spassky, 1934**
Fig. 1A

Tegenaria lapicidinarum Spassky, 1934: Evtushenko 2004: 66–68; Zagorodniuk and Vargovitsh 2004: 207; Kovblyuk 2014: 44; Turbanov et al. 2016b: 1283.

Material examined. • 1 ♀ (TNU 10189), Crimea, Simferopol Distr., central part of Tshatyr-Dagh Yaila, nr Vyalovsky Forest, Alushtinskaya Cave, 11.II.2015, I.S. Turbanov leg. • 3 ♀♀ (TNU 10187), Crimea, Belogorsk Distr., northeastern part of Karabi Yaila, Karani-Koba Cave, 29.I.2014, I.S. Turbanov leg.

Distribution. East European nemoral: Ukraine and the south part of European Russia. The Crimea represents the southernmost limit of the species range (Kovblyuk 2004b; Kovblyuk and Kastrygina 2015; Nentwig et al. 2024).

Records from the Crimean caves. Map (Fig. 17A – purple circle). Unnamed cave near the city of Bakhchisarai, Alushtinskaya Cave in Tshatyr-Dagh Yaila, and Karani-Koba Cave in Karabi Yaila (Evtushenko 2004; present data).

Ecology. A troglophile (Evtushenko 2004; Zagorodniuk and Vargovitsh 2004). In Crimea, *T. lapicidinarum* is a common species, occurring in all landscape zones from the seashore to yaila (Kovblyuk 2004b). In addition to the Crimean subterranean biotopes, this species has also been recorded from catacombs of Odessa, Ukraine (Deli et al. 2017). This species is common in terrestrial habitats, but is rarely found in caves, and so is here classified as a subtroglophile.

***Tegenaria parietina* (Fourcroy, 1785)**

Material examined. • 1 ♀ (TNU 10190/1), Crimea, nr Sevastopol, Khomutovaya Gorge, nr Maksimova Datsha, abandoned aqueduct carved into an unnamed cave-spring, 23.V.2015, A.A. Nadolny leg.

Distribution. Cosmopolite (Kovblyuk and Kastrygina 2015; Nentwig et al. 2024).

Records from the Crimean caves. Map (Fig. 17A – blue circle). Abandoned aqueduct carved into an unnamed cave-spring nr Maksimova Datsha, Sevastopol (present data).

Ecology. A troglophile and synanthropic species (Mammola et al. 2018; Nentwig et al. 2024). In Crimea, *T. parietina* inhabits mountainous and foothill areas (Kovblyuk and Kastrygina 2015), and has not been previously recorded from the Crimean caves. However, during our surveys of subterranean the Crimean biotopes, we have once found this species in the abandoned aqueduct of Maksimova Datsha – the site of intensive agricultural and other economic activities in the second half of the 19th and early 20th centuries (Chikin 2005). For this reason, we believe that *T. parietina* is not a permanent member of the Crimean cave fauna. This species is likely to be a facultative synanthrope that can inhabit underground biotopes as a subtroglophile.

Tegenaria taurica **Charitonov, 1947**

Figs 1B, 3–5

Tegenaria taurica Charitonov, 1947: Charitonov 1947a: 44–49, 51, 54, figs 4, 5; Charitonov 1947b: 1; Birstein 1963: 128; Tyshchenko 1971: 23, 156, 161, 163; Mikhailov 1997: 145; Mikhailov 1998: 22; Esyunin and Farzalieva 2001: 261–263, figs 1–5; Kovblyuk 2002: 105; Amelichev et al. 2004: 136, 140; Evtushenko 2004: 66, 68; Kovblyuk 2004a: 214; Kovblyuk 2004b: 43, 45, 47–48, figs 2, 3(1); Kovblyuk 2004c: 254, 256; Zagorodniuk and Vargovitsh 2004: 207; Kovblyuk 2010: 224; Mikhailov 2013: 141; Bolzern et al. 2013: 776, 803, 818, 846; Kovblyuk 2014: 34, 44, 51; Kovblyuk and Kastrygina 2015: 6; Turbanov et al. 2016b: 1283; Prokopov and Turbanov 2017: 101; Mammola et al. 2018: table S1; Samokhin et al. 2019: 247.
Tegenaria domestica (Clerck, 1757): Kovblyuk 2014: 44.
Tegenaria civilis Walk. [sic!]: Lebedinsky 1904: 77.
Tegenaria derhami (Scopoli, 1763): Charitonov 1932: 21; Charitonov 1939: 197.
Tegenaria sp.: Evtushenko 2004: 67; Zagorodniuk and Vargovitsh 2004: 208; Turbanov et al. 2019a: 218.
Meta menardi (Latreille, 1804): Lebedinsky 1914: 115, 117, 121–122; Charitonov 1932: 123; Charitonov 1939: 197; Tyshchenko 1971: 190; Mikhailov 1997: 108; Kovblyuk 2004a: 245; Mikhailov 2013: 101; Kovblyuk 2014: 44; Kovblyuk and Kastrygina 2015: 56.

Material examined. • 2 ♂♂ (TNU 10260), Crimea, Sevastopol, nr Balaklava, southern slope of Mt. Asketi, Asketi I Cave, 26.IX.2015, O.V. Kukushkin leg. • 7 ♀♀ (TNU 10259/1), Crimea, Sevastopol, nr Balaklava, Aya Cape Mt. Range, Mt. Kala-Fatlar, Izumrudnaya Cave, 20.III.2016, O.V. Kukushkin leg. • 1 ♀ (TNU 10180/1), Crimea, Sevastopol, nr Balaklava, Aya Cape Mt. Range, Mt. Kala-Fatlar, Gekkonovaya Cave, 09.X.2016, A.A. Nadolny leg. • 1 ♀ (TNU 10287/1), Crimea, Sevastopol, Tshernaya River canyon, Tshernoretshenskaya Cave, 3.VI.2021, I.S. Turbanov, A.A. Nadolny leg. • 1 ♀ (IT), Crimea, Sevastopol, northeastern slope of Baidarskaya Yaila, Baidarskaya Valley, nr Kizilovoye Vil., Mamut-Tshokrak Cave, 26.VII.2010, I.S. Turbanov leg. • 1 ♀ (TNU 10257/3), 1 ♀ (IT), Crimea, Sevastopol, northwestern slope of Ai-Petri Yaila, Baidarskaya Valley, nr Rodnikovskoye Vil., entrance to Skelskaya Cave, 29.IX.2020, A.A. Nadolny leg. • 2 ♀♀ (TNU 10197), Crimea, Sevastopol, NW slope of Ai-Petri Yaila, nr Karadagh Forest, Rodnikovskaya Cave, 4.II.2014, I.S. Turbanov leg. • 3 ♀♀ (TNU 10196), Crimea, Sevastopol, northwestern slope of Ai-Petri Yaila, nr

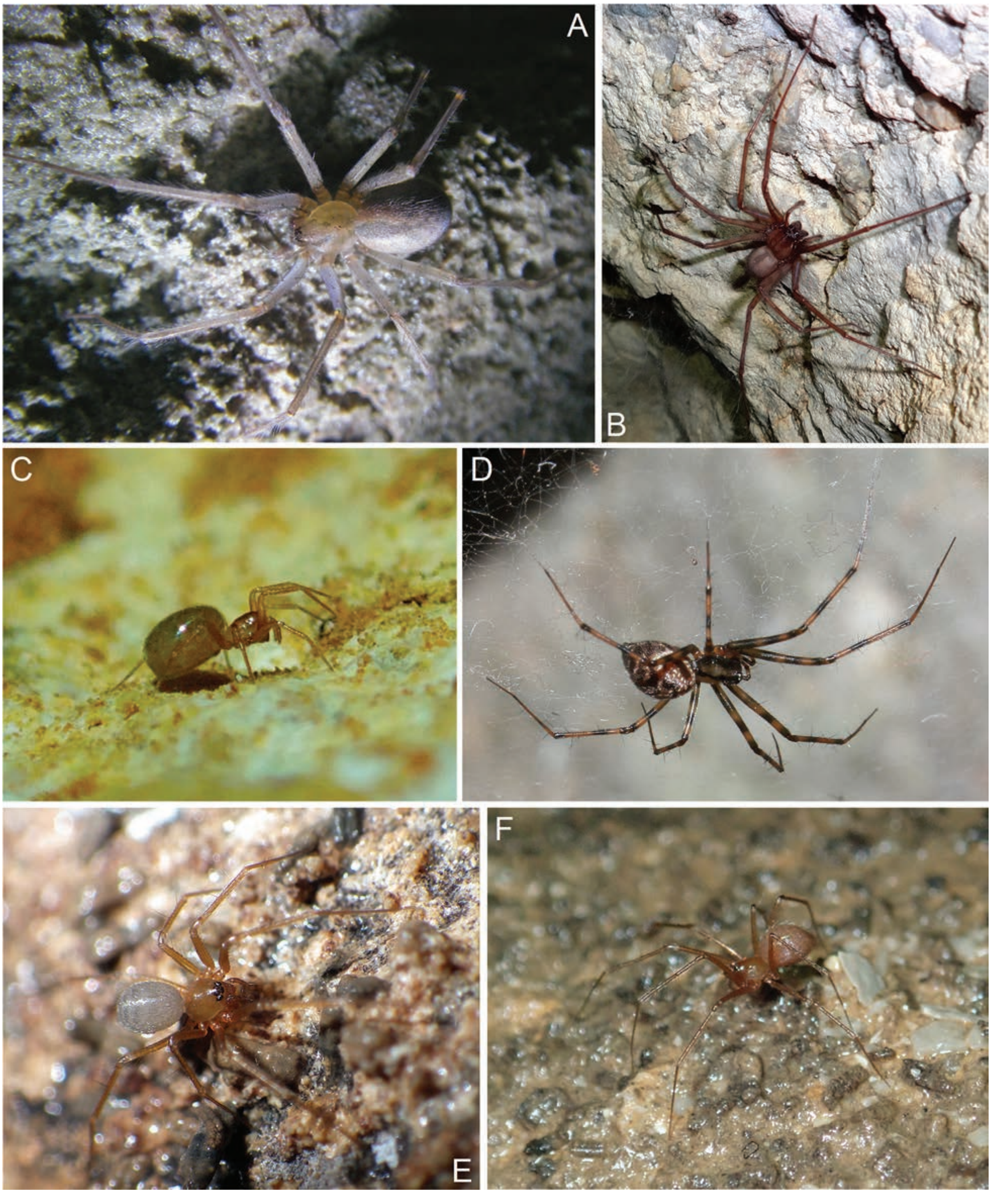

Figure 1. Spiders in situ in caves of Crimea: **A** *Tegenaria lapicidinarum*, ♀ from Karani-Koba Cave **B** *Tegenaria taurica*, ♀ from Gekkonovaya Cave **C** *Caviphantes dobrogicus*, ♀ from Tavrida Cave **D** *Megalepthyphantes pseudocollinus*, ♀ from Skelskaya Cave **E** *Palliduphantes khobarum*, ♀ from Skelskaya Cave **F** *Troglohyphantes exspectatus* sp. nov., ♀ from Druzhba Cave. Photographs by IST (**A, C, F**); AAN (**B, D**); G.A. Prokopov (**E**).

Karadagh Forest, Koryta (= Kuznetsova) Cave, 8.III.2014, I.S. Turbanov leg.• 1 ♀ (IT), Crimea, Sevastopol, southwestern part of Ai-Petri Yaila, Mortsheka Mt., Druzhba Cave, 3.X.2020, I.S. Turbanov leg. • 1 ♀ (TNU 10261/1), Crimea, Bakhchisarai Distr., northern part of Ai-Petri Yaila, Mt. Ayu-Teshik, Ayu-Teshik Cave, 8.V.2015, I.S. Turbanov leg. • 1 ♀ (TNU 10227), Crimea, Bakhchisarai Distr., nr Stshastlivoe Vil., northwestern slope of Yalta Yaila, Khaplu-Kaya Mt., Kaply-Kayanskaya (Khaplu-Khoba) Cave, 29.VI.2017, I.S. Turbanov leg. • 1 ♀ (TNU 10195/1), Crimea, Simferopol Distr., northern part of Tshatyr-Dagh Yaila, Binbash-Koba Cave, 12.II.2015, I.S. Turbanov leg. • 1 ♀ (IT), Crimea, Simferopol Distr., nr Perevalnoye Vil., western slope of Dolgorukovskaya Yaila, Kizil-Koba (= Krasnaya) Cave, 5.XI.2014, I.S. Turbanov leg.

Distribution. Endemic of the Crimean Mountains (Kovblyuk and Kastrygina 2015). However, there is a dubious record from Georgia (Mkheidze 1997), which has never been confirmed by any collected material (Kovblyuk and Kastrygina 2015).

Records from the Crimean caves. Map (Fig. 17A – orange circle). *Tegenaria taurica* is known from caves in the western and central parts of the Crimean Mountains: small unnamed cave (= ?Malaya Cave) in Nizhnie Limeny (now Goluboi Zaliv, region of Yalta; the locality for male syntype *T. taurica* – sensu Charitonov 1947a), Asketi I, Izumrudnaya, Gekkonovaya, Tshernoretshenskaya, Mamut-Tshokrak, Skelskaya, Rodnikovskaya, Koryta, Druzhba, Ayu-Teshik (= Ayutishik-Koba; the locality for female syntype *T. taurica* – sensu Charitonov 1947a), Daniltsha-Koba, Kaply-Kayanskaya, Ayu-Koba, Binbash-Koba, Kizil-Koba, and grotto in Massandra (the type locality as that of the lectotype – sensu Esyunin and Farzalieva 2001), grotto on Mt. Yuznaya Demerdzhi (Lebedinsky 1904, 1914; Charitonov 1947a; Esyunin and Farzalieva 2001; Kovblyuk 2004b; Samokhin et al. 2019; Turbanov et al. 2019a; present data).

Ecology. A troglophile (Mammola et al. 2018). There is a single record of *T. taurica* from an anthropogenic biotope (Kovblyuk 2004b), which in fact refers to *T. parietina* (1 ♂ (TNU 1630/1), Yalta, indoors, 17.X.2001 – examined), the remaining findings have been from caves (present data). Thus, this species is here referred to as eutroglophile.

Remarks. According to Charitonov (1947a, b), who described *T. taurica* on the basis of the collection of spiders reported earlier by Lebedinsky (1904, 1914), the earlier records of *T. civilis*, *T. derhami* and partly of *Meta menardi* from the Crimean caves (Lebedinsky 1904, 1914; Charitonov 1932, 1939) should in fact be assigned to *T. taurica*. Yet, a number of researchers, although with doubt, have continued to erroneously report on *M. menardi* for the Crimean caves (Tyshchenko 1971; Mikhailov 1997; Kovblyuk 2004a, 2014; Mikhailov 2013; Kovblyuk and Kastrygina 2015). The report on *T. domestica* in the Crimean caves is erroneous (Kovblyuk 2014), as it was based on the record of *T. civilis* by Lebedinsky (1904), and actually belongs to *T. taurica* (M.M. Kovblyuk, pers. comm.). The records of *Tegenaria* sp. from Mamut-Tshokrak Cave (Turbanov et al. 2019a) and Kizil-Koba Cave (Evtushenko 2004) should also be assigned to *T. taurica*, which has been confirmed by the present study (see Material examined).

Tegenaria taurica was redescribed by Esyunin and Farzalieva (2001), who also designated the lectotype based on the material from the Massandra grotto nr Yalta. Among the paralectotypes there is the specimen labelled as follows: “1 slide preparation of palp (PSU), Crimea, Nizhnie Limeny, Malaya Caves, 08–22.IX.1916, leg. L.A. Lants”. The male used for the description of *T. taurica* was collected from the same cave (see Charitonov 1947a: 47, 51).

Figure 2. Spiders in situ in caves of Crimea: **A** *Aituaria pontica*, ♀ from abandoned aqueduct carved into an unnamed cave-spring in area of the Maksimova Datsha in the nr Sevastopol **B** *Aituaria borutzkyi*, ♀ from Mangupskaya I Cave **C, D** *Metellina merianae*, ♀♀ from abandoned aqueduct carved into an unnamed cave-spring in area of the Maksimova Datsha in the nr Sevastopol (**C**) and Mamut-Tshokrak Cave (**D**); **E**, **F**, **G** *Meta bourneti*, ♀ (**E**) and juv. (**G**) from from Mangupskaya I Cave, ♂ (**F**) from Gnomov Cave. Photographs by G.A. Prokopov (**A, C**); IST (**B, D, E, G**); AAN (**F**).

The mention of *T. taurica* for Tuakskaya (= Ful-Koba) Cave was presumably based on the erroneous label "Ayu-Tishik-Koba. Tuvak. Meta spes? vois. de Menardi" (see Charitonov 1947a: 45) and "Ayutishik-Koba [caves], Tuvak, 1905, leg. Ya.N. Lebedinskii" (see Esyunin and Farzalieva 2001: 261), when two different

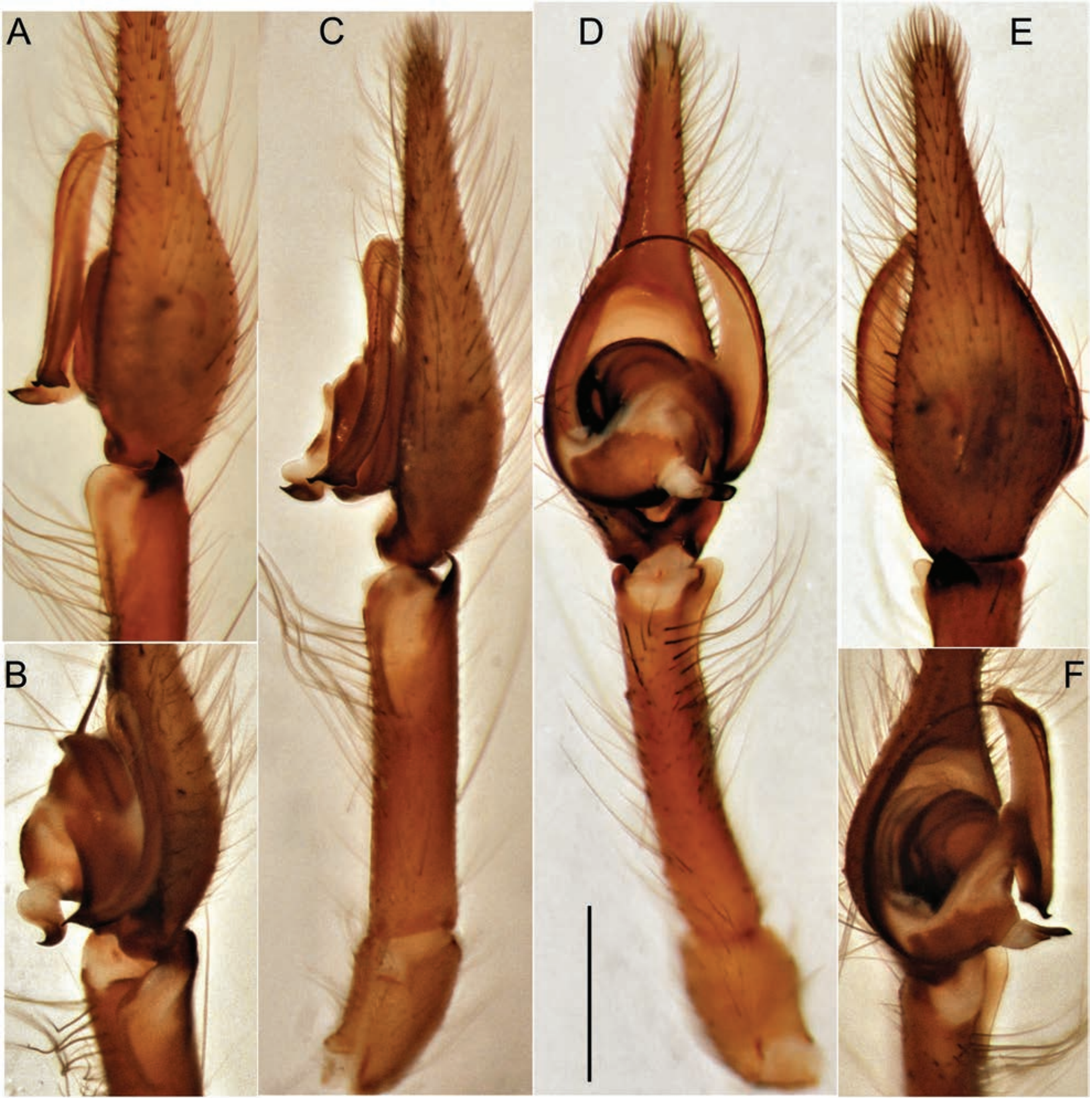

Figure 3. Male palp of *Tegenaria taurica* from Asketi I Cave: **A** dorso-retrolateral view **B** anterio-retrolateral view **C** retrolateral view **D** ventral view **E** dorsal view **F** ventro-prolateral view. Scale bar: 1.0 mm.

caves are mistakenly indicated: viz., Ayu-Teshik (as Ayu-Tishik-Koba and Ayutishik-Koba) and Tuakskaya (as Tuvak), whereas they are situated in different parts of the Crimean Mountains. However, in the original work by Lebedinsky (1914), *T. taurica* (as *Meta menardi*) is recorded from Ayu-Teshik Cave, and *Palliduphantes khobarum* (as *Lephthyphantes* [sic!] *monticola*) from Tuakskaya Cave. Our repeated survey in Tuakskaya Cave has confirmed that the only spider species occurring there is *P. khobarum*.

We consider it appropriate to provide an illustrated description of the copulatory organs of both sexes of *T. taurica* from the Crimean caves (Figs 3–5). The cymbium and tibia+patella lengths are equal (Fig. 3C). Tibia has three apophyses (Fig. 4E–G): dorsal apophysis pointed and well sclerotised (Fig. 4A, C, E), ventral and lateral – rounded and poorly sclerotised (Fig. 4A, D, E); embolus originated

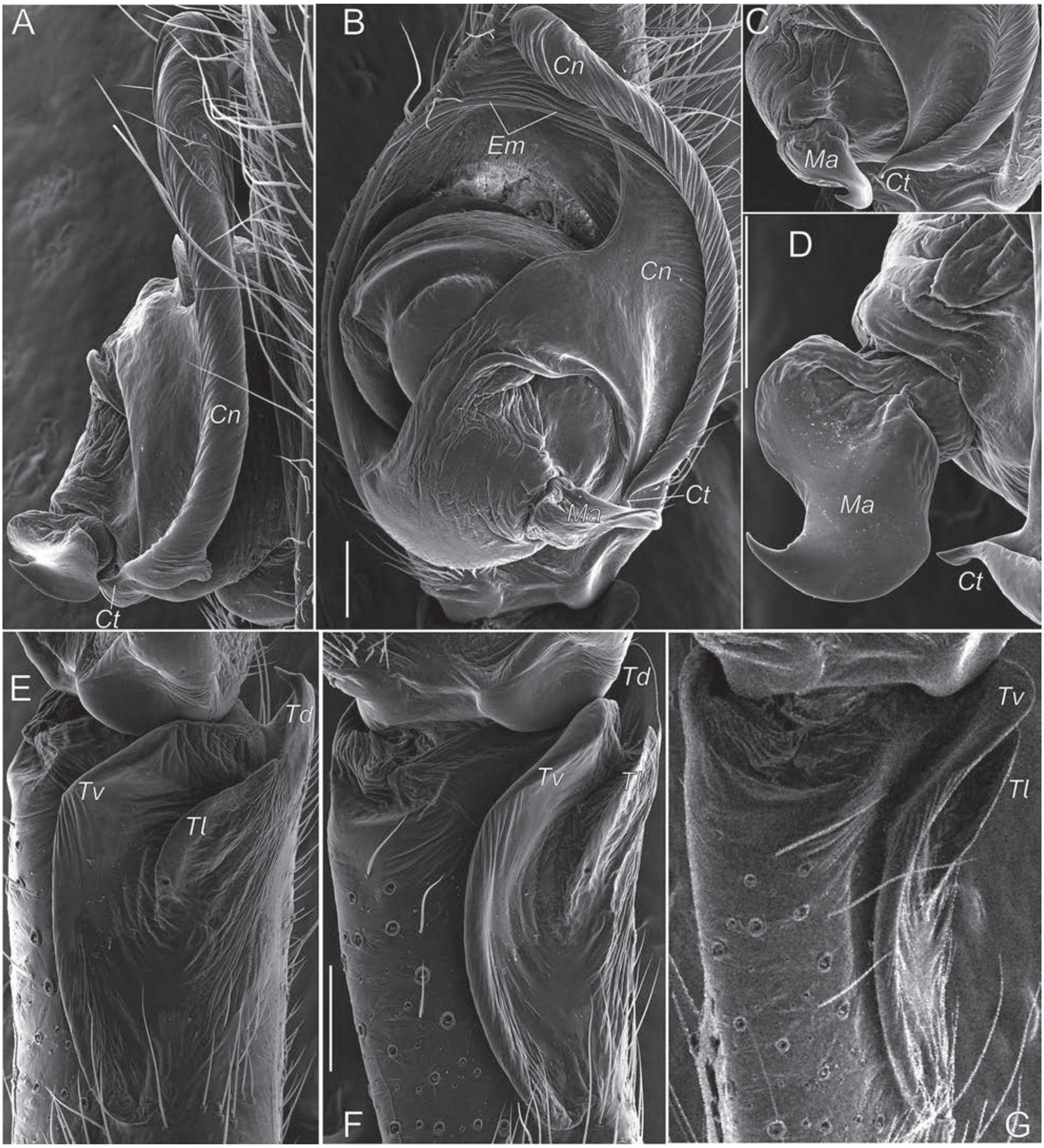

Figure 4. Male palp of *Tegenaria taurica* from Asketi I Cave: **A, B** bulbus, retrolateral and ventral views **C, D** fragment of bulbus with median apophysis and tip of conductor, anterio-retrolateral and anterior views **E–G** tibial apophyses, retrolateral, ventro-retrolateral and ventral views. Abbreviations: *Cn* – conductor, *Ct* – tip of conductor, *Em* – embolus, *Ma* – median apophysis, *Td* – dorsal tibial apophysis, *Tl* – lateral tibial apophysis, *Tv* – ventral tibial apophysis. Scale bars: 0.2 mm.

at 320° position and terminating at about 210° position, makes an ellipsoid trajectory and holds it distal part in conductor (Figs 3D, F, 4B); conductor with two arms in longitudinal position; embolic and conductor tips directed posteriorly (Figs 3A–C, 4A, B); median apophysis flat with sharped tip directed ventrally (Figs 3B, 4C, D). Epigyne with trapezoid plate (Fig. 5A); lateral borders of epigynal plate poorly recognised (Fig. 5E, F); spermatheca massive, makes two curves – ventral and sagittal (Fig. 5C, G, **I**); head of spermatheca variable (Fig. 5D, H).

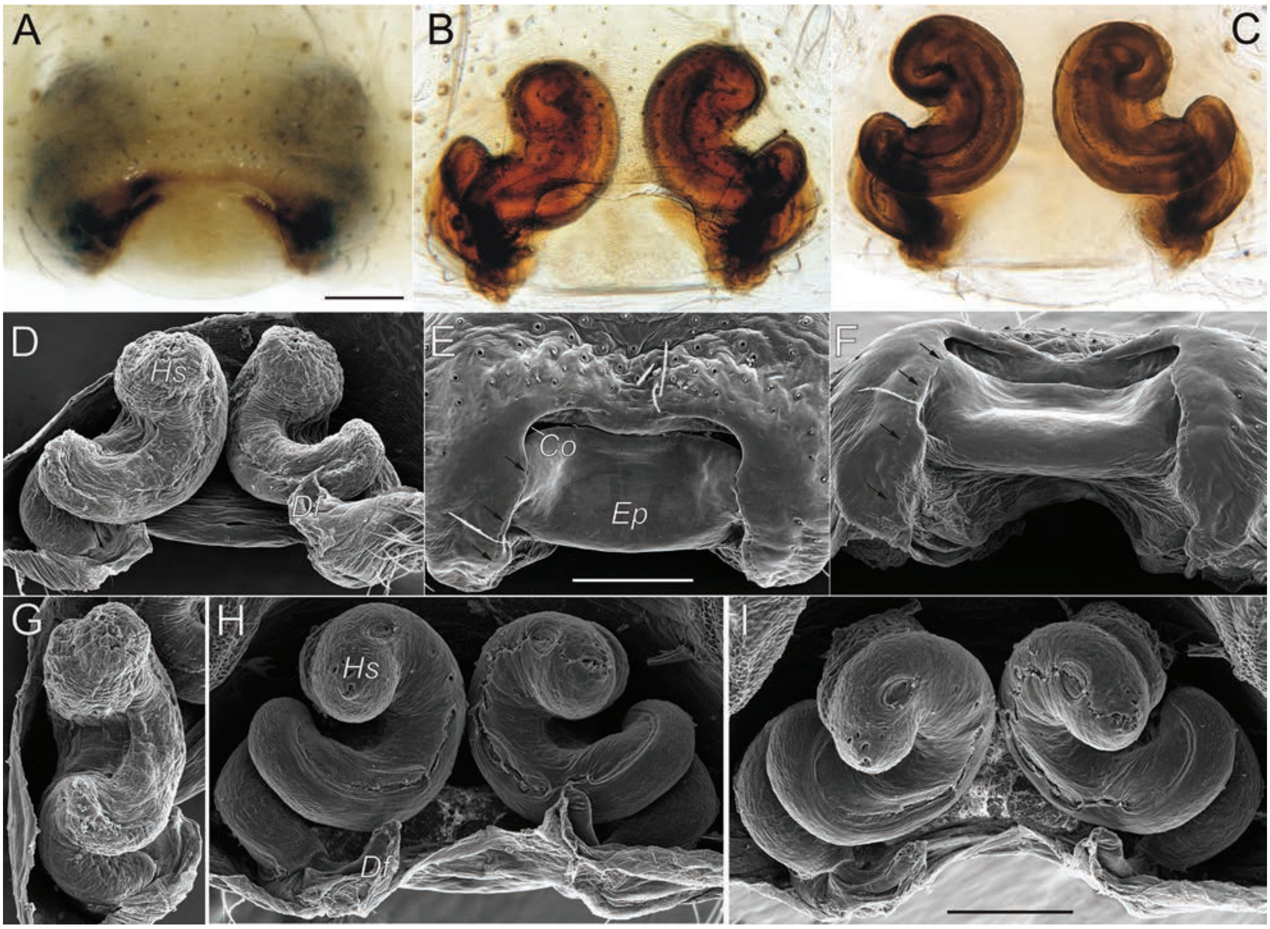

Figure 5. Epigynes of *Tegenaria taurica* from Kuznetsova Cave: **A, B, E** ventral view **C, D, H** dorsal view **F** posterior view **G** lateral view **I** anterior view. Abbreviations: *Co* – copulatory opening, *Df* – fertilization duct, *Ep* – epigynal plate, *Hs* – head of spermatheca. Arrows indicate borders of epigynal plate. Scale bars: 0.2 mm.

Family Amaurobiidae Thorell, 1869
Genus *Amaurobius* C.L. Koch, 1837

Amaurobius erberi (Keyserling, 1863)

Material examined. • 1 ♂ (TNU 10237/2), Crimea, Bakhchisarai Distr., nr Khodzha-Sala Vil., steep southern slope of Baba-Dagh Plateau (= Mangup-Kale Gorodishche), Mangupskaya I (= MK-1) Cave, 3.V.2018, I.S. Turbanov leg.

Distribution. West Palearctic nemoral-subtropical: from the Canaries to Azerbaijan and from Central Europe to Algeria (Kovblyuk and Kastrygina 2015; Nentwig et al. 2024).

Records from the Crimean caves. Map (Fig. 17A – yellow circle). Mangupskaya I Cave on steep southern slope of Baba-Dagh Plateau (present data).

Ecology. In Crimea, *Amaurobius erberi* is widespread and found in all landscape zones (Kovblyuk and Kastrygina 2015). This species has not been previously recorded from caves and it is hardly a permanent cave dweller, so it can be classified as a trogloxene.

Family Linyphiidae Blackwall, 1859
Genus *Bisetifer* Tanasevitch, 1987

Bisetifer gruzin Tanasevitch, Ponomarev & Chumachenko, 2015
Fig. 6C, D

Bisetifer cephalotus Tanasevitch, 1987: Kovblyuk 2007: 152; Mikhailov 2013: 45; Tanasevitch et al. 2015: 445–446.

Material examined. • 1 subad. ♂, 1 ♀ (TNU 10288), Crimea, Simferopol Distr., nr Perevalnoye Vil., western slope of Dolgorukovskaya Yaila, Kizil-Koba (= Krasnaya) Cave, 18.XII.2019, I.S. Turbanov leg.

Comparative material. *Bisetifer cephalotus* • 1 ♀ (TNU), Russia, Krasnodar Territory, Caucasus Nature Reserve, 20 km SSW of Psebay, 1 km SW of the cordon of Tshernoretshie, Urushten River bank, forest, 10.VI.2017, A.V. Ponomarev leg.

Distribution. The Crimean-Caucasian disjunctive: Krasnodar Territory and the Republic of Adygea, Russia. The species has been recorded from Crimea for the first time, with the Crimean Mountains being currently the westernmost part of its range (Tanasevitch et al. 2015; present data).

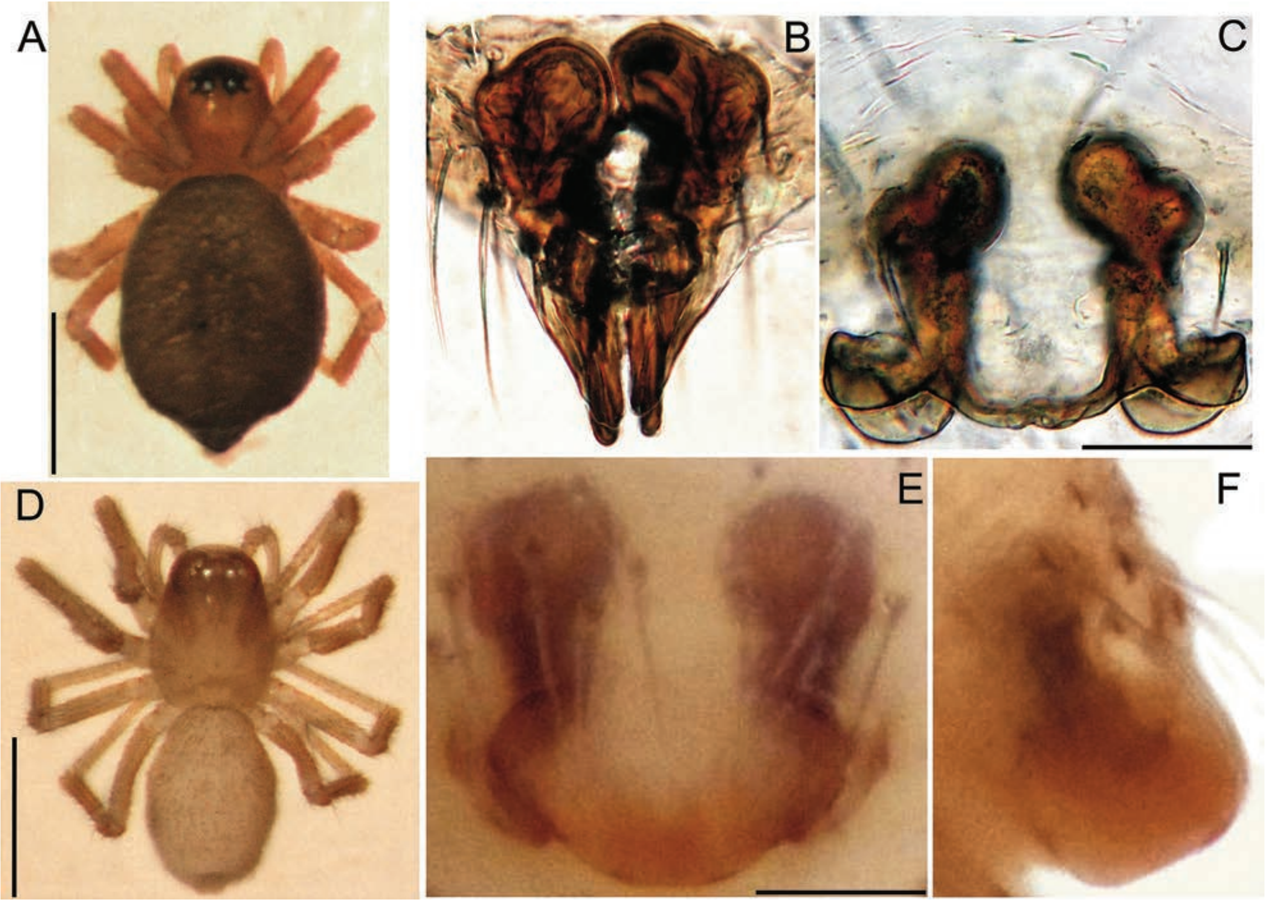

Figure 6. Females of *Bisetifer cephalotus* from the Caucasus Nature Reserve (**A, B**), *B. gruzin* from Kizil-Koba Cave (**C, D**), paratype of *B. tactus* sp. nov. from Tshernoretshenskaya Cave (**E, F**). **A, D** habitus, dorsal view **B, C, E** epigyne, ventral view **F** epigyne, lateral view. Scale bars: 0.5 mm (**A, D**); 0.05 mm (**B, C, E, F**).

Records from the Crimean caves. Map (Fig. 17B – blue circle). Kizil-Koba Cave on western slope of the Dolgorukovskaya Yaila (present data).

Ecology. In the Caucasus, *B. gruzin* inhabits humid microbiotopes (Tanasevitch 1987; Tanasevitch et al. 2015). In Crimea, it was found in the upper floors of Kizil-Koba Cave, with no permanent water flow (Kovblyuk 2007; present data). The body of the Crimean specimens is depigmented, but the eyes are well developed (see Fig. 6D). Despite the well-studied araneofauna of Crimea, *B. gruzin* has never been reported from epigeic biotopes, whereas all our findings are from caves. On this basis, this species could be preliminary considered an eutroglophile.

Remarks. In Crimea, two males of another congener, *B. cephalotus*, were collected earlier from Kizil-Koba Cave (Kovblyuk 2007); this material is currently stored by Valery A. Gnelitsa (Sumy, Ukraine). Since the earlier records of *B. cephalotus* and the newly collected specimens of *B. gruzin* come from the same cave, it could be suspected that they belong to the same species – *B. gruzin*.

In 2007, *B. gruzin* yet had not been described. This could have been the reason for erroneous identification, as *Bisetifer* species are better identified by the females (see Fig. 6B, C), while the males have a rather similar conformation of diagnostically important characters. Possible mistakes in the identification of *B. cephalotus* for Crimea were discussed by Tanasevitch et al. (2015), and their conclusion has been confirmed by present data.

Bisetifer tactus **sp. nov.**

https://zoobank.org/80D9BAAF-5BF5-4C07-BB48-8CFC1147420F
Figs 6E, F, 7–9

Type material. ***Holotype*** • ♂ (ZMMU Ta-8255), Crimea, nr Sevastopol, Tshernaya River canyon, Tshernoretshenskaya Cave, 3.III.2018, I.S. Turbanov leg. ***Paratypes*** • 3 ♀♀ (ZMMU Ta-8256), 5.V.2017 • 1 ♀ (TNU 10235), 4.V.2018, same cave and collector as for a holotype.

Diagnosis. *Bisetifer tactus* sp. nov. has reduced eyes (Figs 7A–F, 8A–D) (vs other congeners, *B. cephalotus* and *B. gruzin*, have well developed eyes, see Tanasevitch et al. 2015: figs 1–6). Additionally, *B. tactus* sp. nov. differs from its congeners in having: 1) the embolus hidden between radix and distal suprategular apophysis (Figs 8G, H, 9A, C, D) (vs not hidden, well visible, see Tanasevitch et al. 2015: figs 7, 19); 2) the hook-shaped and pointed apical part of radix (Figs 8G, 9C) (vs conical in *B. cephalotus* and flat in *B. gruzin*, see Tanasevitch et al. 2015: figs 9, 14, 23, 28–29); 3) the distal suprategular apophysis without a complicated arrangement of apophyses, with barbs on its edge (Figs 8G, 9A, C, D) (vs with apophyses, without barbs, see Tanasevitch et al. 2015: figs 7, 19); 4) the oval posterior edge of epigyne (Figs 6E, 9E) (vs with nipple-shaped outgrowths in *B. cephalotus*, with bow-shaped outgrowths in *B. gruzin*, see Fig. 6B, C and Tanasevitch et al. 2015: figs 17, 30).

Description. Male. Total length 1.5. Carapace 0.63 long, 0.5 wide, pale brown; modified as in Figs 7D, E, 8C, D: head part conical, with setae. Eyes reduced, almost completely disappeared (head part with small pale spots, visible under light microscope; no lens visible under SEM). Chelicerae 0.31, brownish, transverse shallow cuticular grooves throughout the basal segment. Legs

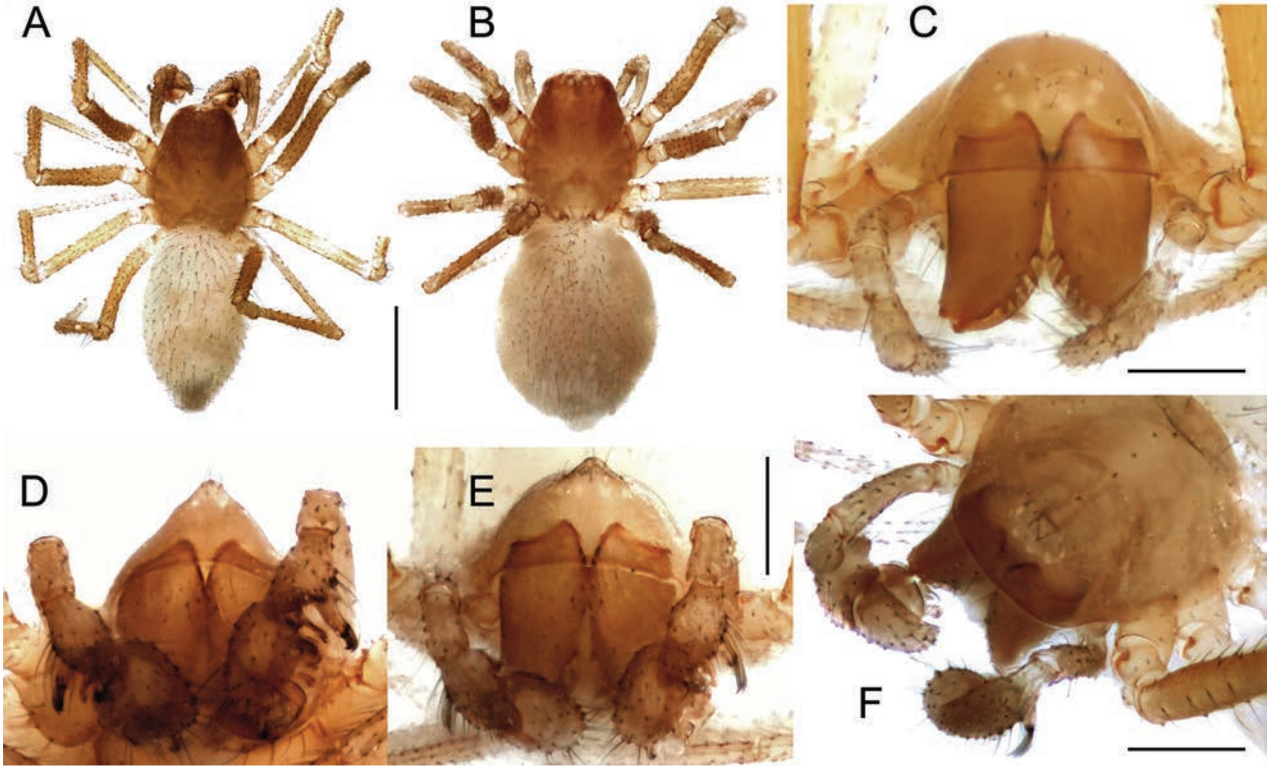

Figure 7. General appearance of male holotype and female paratype of *Bisetifer tactus* sp. nov. from Tshernoretshenskaya Cave: **A, B** male and female habitus, dorsal **C** female prosoma, anteriorly **D, E** male prosoma, anteriorly in different aspects **F** male prosoma, dorsal. Scale bars: 0.5 mm (**A, B**); 0.2 mm (**C–F**).

pale brown, chaetotaxy 2.2.1.1, metatarsi I–IV spineless, metatarsi IV without trichobothrium, TmI 0.35, leg I 2.47 long (0.69+0.18+0.63+0.52+0.45), leg IV 2.53 long (0.71+0.17+0.69+0.54+0.42). Palp as in Figs 8F–I, 9A–D: tibia with a ventro-retrolateral apophysis and two large setae on its tip, distally setae poorly serrate; paracymbium L-shaped; distal suprategular apophysis – flat, curved, and pointed, with barbs on its anterior edge; embolus small, situated in a cavity between distal suprategular apophysis and radix; apical part of radix hook-shaped and pointed distally, well-sclerotised process, retrolaterally with membrane. Abdomen pale grey.

Female. Total length 1.58. Carapace 0.77 long, 0.59 wide; unmodified. Eyes reduced, almost completely disappeared (head part with small pale spots, clearly visible under light microscope; a few poorly developed lenses visible under SEM). Chelicerae 0.36, transverse shallow cuticular grooves throughout the basal segment. TmI 0.44. Leg I 2.64 long (0.73+0.21+0.7+0.54+0.46), leg IV 2.78 long (0.8+0.2+0.77+0.59+0.42). Body colouration and spination as in the male. Epigyne as in Figs 6E, F, 9E–G: epigynal plate oval, with lateral outgrowths in which copulatory ducts open; spermathecae consists of two parts: base with copulatory duct and head with receptacle and fertilisation duct; cavity of receptacle subdivided on ventral and dorsal parts.

Variation. Females (*n* = 3): carapace width 0.53–0.59; femur I length 0.69–0.73.

Distribution and records from the Crimean caves. Map (Fig. 17B – purple circle). Only known from the type locality: Tshernoretshenskaya Cave, nr Sevastopol.

Ecology. The species has troglomorphic characteristics related to the subterranean habitat, such as the pale body and reduced eyes. Based on the mor-

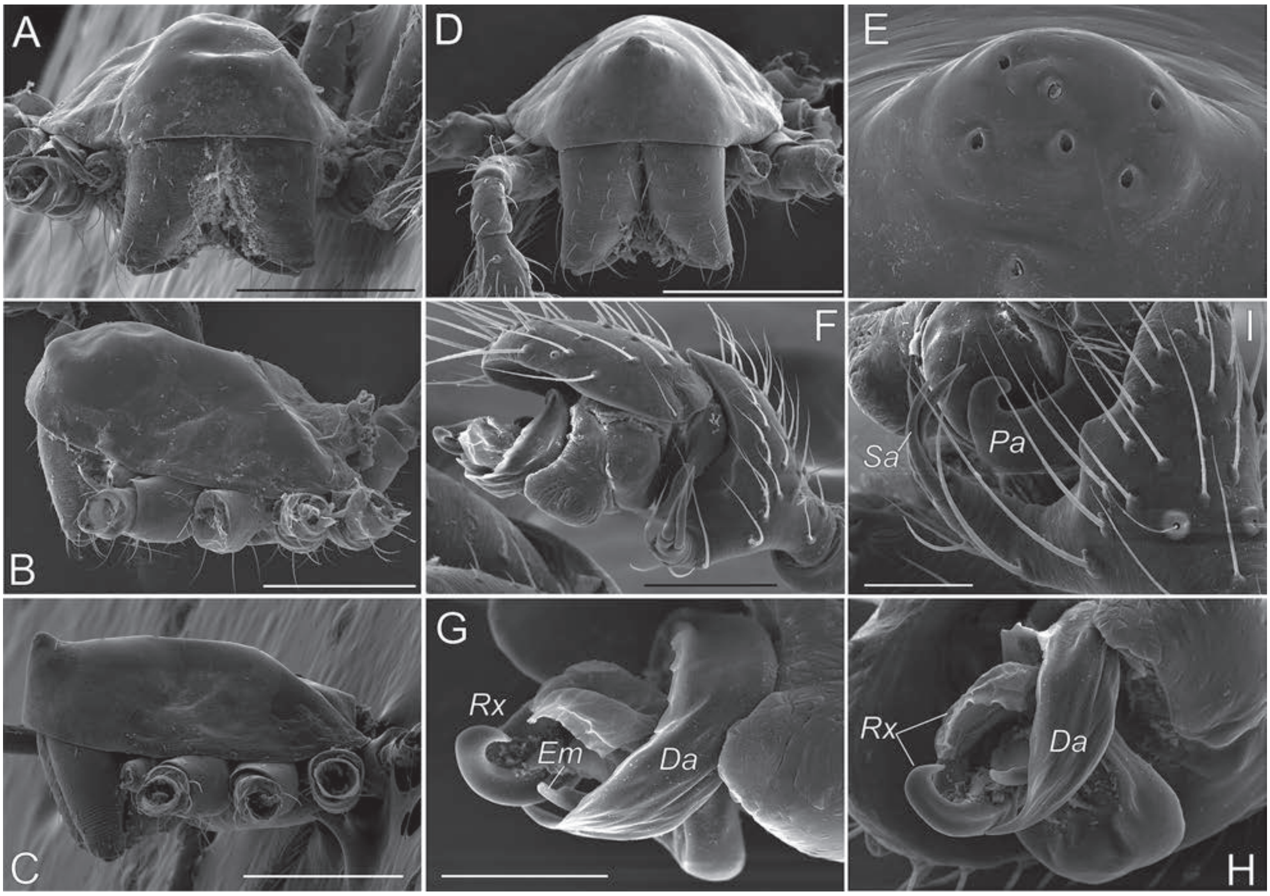

Figure 8. Details of female paratype and male holotype of *Bisetifer tactus* sp. nov. from Tshernoretshenskaya Cave: **A, B** female prosoma, anterior and lateral views **C, D** male prosoma, lateral and anterior views **E** top of head part of male carapace, anterior view **F** male palp, retrolateral view **G, H** embolic division, ventro-retrolateral and ventro-apical views **I** fragment of male palpal tibia and paracymbium, posterior view. Abbreviations: *Da* – distal suprategular apophysis, *Em* – embolus, *Pa* – paracymbium, *Rx* – radix, *Sa* – setae at apex of palpal tibial apophysis. Scale bars: 0.3 mm (**A–D**); 0.1 mm (**F**); 0.05 mm (**G–I**).

phological features and the fact that this species is known only from caves, it can be considered a troglobiont.

Etymology. From the Latin *tactus*, meaning touch, due to the fact that this species has the strongly reduced eyes and its life style as a true troglobiont relies on tactile sensations.

Genus *Caviphantes* Oi, 1960

Caviphantes dobrogicus (Dumitrescu & Miller, 1962)

Figs 1C, 10

Caviphantes dobrogicus (Dumitrescu & Miller, 1962): Turbanov et al. 2021: 180–181, 183–184, figs 2, 3.

Material examined. • 5 ♀♀ (TNU-10234), Crimea, Belogorsk Distr., nr Zuya Vil., Tavrida Cave, 29.IX.2018, I.S. Turbanov leg.

Distribution. West and Central Palaearctic nemoral-subtropical: Bulgaria, Romania, Ukraine, the southern part of European Russia, Georgia, Azerbaijan, Kyrgyzstan (Nentwig et al. 2024).

Figure 9. Male holotype and female paratype copulatory organs of *Bisetifer tactus* sp. nov. from Tshernoretshenskaya Cave: **A** male palp, retrolateral view **B** male palpal tibia, dorsal view **C, D** bulbus, ventral and prolateral views **E, F** epigyne, ventral and dorsal views **G** spermatheca, ventral view. Abbreviations: *Bs* – base of spermatheca, *Cd* – copulatory duct, *Co* – copulatory opening, *Da* – distal suprategular apophysis, *Df* – fertilisation duct, *Em* – embolus, *Fo* – fertilisation opening, *Hs* – head of spermatheca, *Me* – membrane of spermatheca, *Ou* – outgrowths of epigyne, *Pa* – paracymbium, *Rx* – radix, *Sa* – setae at apex of palpal tibial apophysis. Scale bars: 0.1 mm (**A–F**); not scaled (**G**).

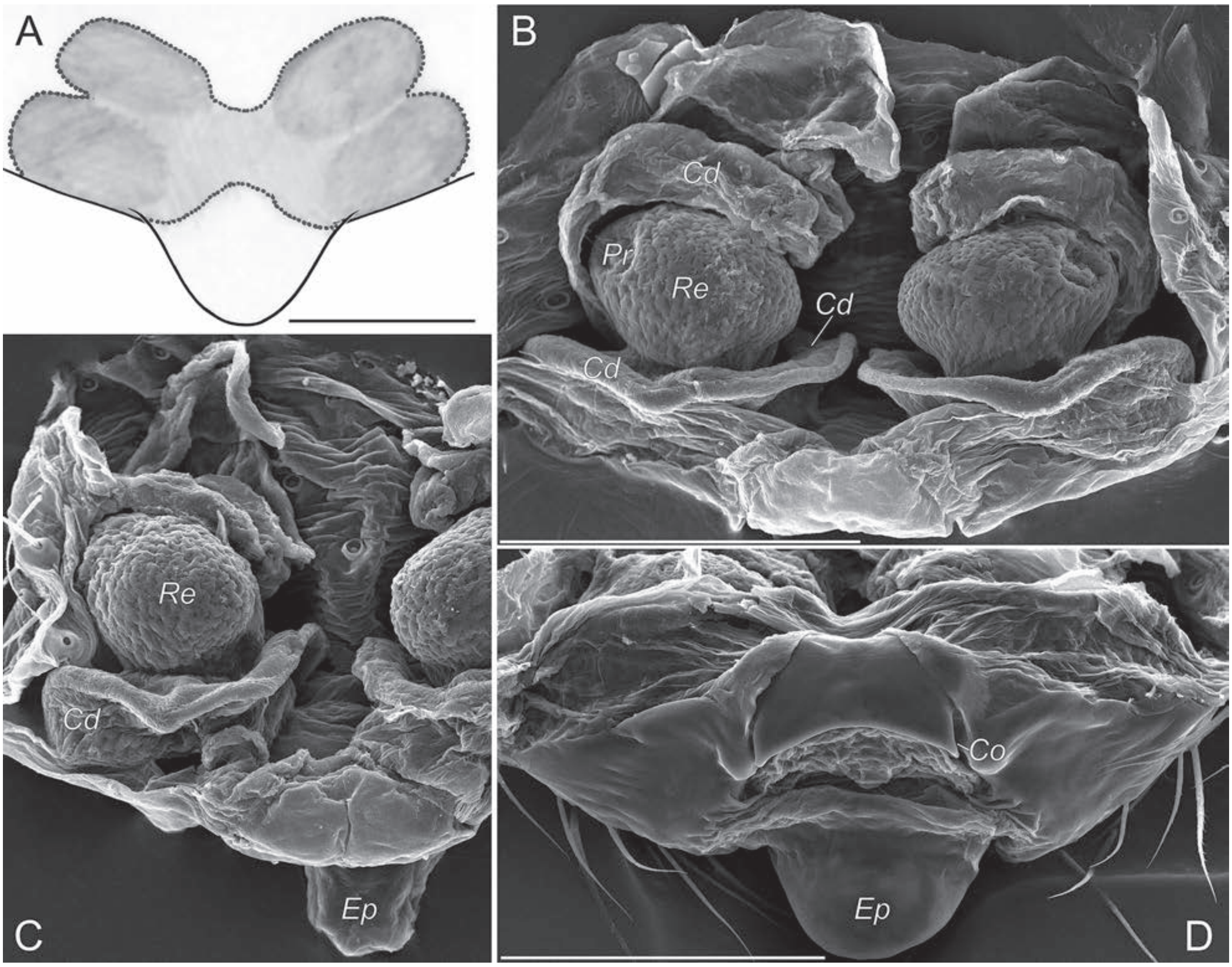

Figure 10. Epigynes of *Caviphantes dobrogicus* from Tavrida Cave: **A** ventral view **B, C** dorsal view **D** posterior view. Abbreviations: *Cd* – copulatory duct, *Co* – copulatory opening, *Ep* – epigynal plate, *Pr* – pore of receptacle, *Re* – receptacle. Scale bars: 0.1 mm.

Records from the Crimean caves. Map (Fig. 17B – green circle). Tavrida Cave nr Zuya Vil. (Turbanov et al. 2021).

Ecology. The species has been considered a troglophile (Mammola et al. 2018: table S1). In addition to caves, it inhabits sandy steppes, sea coasts and agrocenoses (Polchaninova and Prokopenko 2013). Since this species is a eurybiont that can enter caves, Turbanov et al. (2021) characterised it as a subtroglophile. Despite the Crimean araneofauna is well studied, *C. dobrogicus* has never been reported from epigeic biotopes. Based on the fact that in Crimea, the species is likely to be permanently associated with caves, it could be considered an eutroglophile.

Remarks. Only a few line drawings and digital photos of important diagnostic features of this tiny spider have been published (see WSC 2024). We present SEM micrographs of the vulva, which add to the understanding of the structure of its membranous parts (Fig. 10B–D). It is somewhat different from what can be seen under light microscope (Turbanov et al. 2021) and was provided by the original description (Dumitrescu and Miller 1962). The structures termed as the copulatory ducts are poorly sclerotised and in fact wide, but not like a twisted system of narrow ducts.

Genus *Lepthyphantes* Menge, 1866

Lepthyphantes leprosus (Ohlert, 1865)

Lepthyphantes leprosus (Ohlert, 1865): Evtushenko 2004: 66–68; Kovblyuk 2014: 44; Zagorodniuk and Vargovitsh 2004: 207; Turbanov et al. 2016b: 1283; Samokhin et al. 2019: 247.

Material examined. • 1 ♂ (TNU 10236/2), Crimea, Bakhchisarai Distr., nr Khodzha-Sala Vil., steep southern slope of Baba-Dagh Plateau (= Mangup-Kale Gorodishche), entrance to Mangupskaya I (= MK-1) Cave, 11.VI.2018, I.S. Turbanov, A.A. Nadolny leg. • 3 ♀♀ (TNU 10180/3), Crimea, Sevastopol, nr Balaklava, Aya Cape Mt. Range, Kala-Fatlar Mt., entrance to Gekkonovaya Cave, 9.X.2016, A.A. Nadolny leg. • 7 ♀♀ (IT), Crimea, nr Sevastopol, Tshernaya River canyon, entrance to Tshernoretshenskaya Cave, 3.VI.2021, I.S. Turbanov, A.A. Nadolny leg. • 4 ♂♂ 5 ♀♀ (TNU 10257/1) • 1 ♀ (IT), Crimea, nr Sevastopol, northwestern slope of Ai-Petri Yaila, Baidarskaya Valley, nr Rodnikovskoye Vil., entrance to Skelskaya Cave, 29.IX.2020, A.A. Nadolny, I.S. Turbanov A.A. Turbanova leg.

Distribution. Circum-Holarctic polyzonal (Kovblyuk and Kastrygina 2015; Nentwig et al. 2024).

Records from the Crimean caves. Map (Fig. 17B – red circle). Recorded in caves from the western and central parts of the Crimean Mountains: in unnamed cave near the city of Bakhchisarai, Mangupskaya I, Gekkonovaya, Tshernoretshenskaya, Skelskaya, and Kizil-Koba (Evtushenko 2004; present data).

Ecology. A troglophile and northward, above the 55th parallel, exclusively as a synanthropic species (Kovblyuk and Kastrygina 2015; Mammola et al. 2018; Nentwig et al. 2024). In Crimea, the species lives in the mountainous regions, except for its upper parts – mountain meadows and yaila steppes (Kovblyuk and Kastrygina 2015), and is confined to cave entrances; in our opinion, it is a subtroglophile.

Genus *Megalepthyphantes* Wunderlich, 1994

Megalepthyphantes nebulosus (Sundevall, 1830)

Material examined. • 1 ♂ (TNU 10180/2), Crimea, Sevastopol, nr Balaklava, Aya Cape Mt. Range, Kala-Fatlar Mt., Gekkonovaya Cave, 9.X.2016, A.A. Nadolny leg.

Distribution. Holarctic polyzonal (Kovblyuk and Kastrygina 2015; Nentwig et al. 2024).

Records from the Crimean caves. Map (Fig. 17B – pale blue circle). Gekkonovaya Cave of Aya Cape Mt. Range (present data).

Ecology. Above the 55th parallel northwards it is an exclusively synanthropic species (Kovblyuk and Kastrygina 2015; Nentwig et al. 2024), but southwards it can be found in natural biotopes – under stones and in rock crevices (Tyshchenko 1971). In Crimea, *M. nebulosus* is rare, recorded in Sevastopol and Feodosia (Kovblyuk and Kastrygina 2015), and only once in the subterranean biotopes (present data). Also, this species was recorded as a troglophile in the Kristalnaya Cave in Ternopol region, Ukraine (Evtushenko 2004; Zagorodniuk and Vargovitsh 2004). In the Crimean caves, the ecological confinement of *M. nebulosus* is not entirely clear, it is probably a subtroglophile.

Megalepthyphantes pseudocollinus **Saaristo, 1997**
Fig. 1D

Material examined. • 2 ♀♀ (TNU 10257/2), Crimea, nr Sevastopol, NW slope of Ai-Petri Yaila, Baidarskaya Valley, nr Rodnikovskoye Vil., entrance to Skelskaya Cave, 29.IX.2020, A.A. Nadolny leg.

Distribution. West and Central Palaearctic nemoral: from Central Europe to West Siberia and from Finland to Iran (Kovblyuk and Kastrygina 2015; Nentwig et al. 2024).

Records from the Crimean caves. Map (Fig. 17B – white circle). Skelskaya Cave in Baidarskaya Valley (present data).

Ecology. In Crimea, *M. pseudocollinus* was reported from the Karadag Nature Reserve in Feodosia District (Kovblyuk and Kastrygina 2015). Previously, this species was referred to as a trogloxene in Kungurskaya Ledyanaya (= Kungur Ice) Cave in Perm Oblast of Russia (Pankov et al. 2009). Since in Crimea the species was found at the cave entrance, it is likely to be a trogloxene species.

Genus *Palliduphantes* Saaristo & Tanasevitch, 2001

Palliduphantes khobarum **(Charitonov, 1947)**
Fig. 1E

Lephthyphantes [sic!] *khobarum* Charitonov, 1947: Charitonov 1947a: 45–47, 49, 52–53, figs 1–3; Charitonov 1947b: 1.

Lepthyphantes khobarum Charitonov, 1947: Birstein 1963: 128; Tyshchenko 1971: 23; Brignoli 1980: 190; Tanasevitch 1987: 314; Mikhailov 1997: 73; Kovblyuk 2002: 104; Amelichev et al. 2004: 133, 140; Evtushenko 2004: 66–68; Kovblyuk 2004c: 251, 253–254, 256; Zagorodniuk and Vargovitsh 2004: 207.

Palliduphantes khobarum (Charitonov, 1947): Kovblyuk 2004a: 230; Mikhailov 2013: 78; Kovblyuk 2014: 44; Kovblyuk and Kastrygina 2015: 31–32; Turbanov et al. 2016b: 1283–1284; Samokhin and Turbanov 2019: 230.

Lephthyphantes [sic!] *monticola* Kulcz.: Novikov 1912: 104; Lebedinsky 1914: 127; Mokrzecki 1914: 97.

Lepthyphantes monticola (Kulczynski, 1881): Charitonov 1932: 75; Charitonov 1939: 197; Mikhailov 1997: 74.

Anguliphantes monticola (Kulczynski, 1881): Kovblyuk 2004a: 226; Mikhailov 2013: 42; Kovblyuk 2014: 44; Turbanov et al. 2016b: 1283.

Material examined. • 1 ♂ (TNU 10264), Crimea, Sevastopol, nr Oboronnoye Vil., Ayu-Kaya Mt., Kay-Kobasy Cave, 6.IV.2019, S.V. Arefiev leg. • 1 ♀ (TNU 10231/2), Crimea, nr Sevastopol, Tshernaya River canyon, Tshernoretshenskaya Cave, 3.III.2018, A.A. Nadolny leg. • 2 ♀♀ (TNU 10262), same cave, 15.I.2020, I.S. Turbanov leg. • 1 ♀ (TNU 10287/2), same cave, 3.VI.2021, I.S. Turbanov, A.A. Nadolny leg. • 1 ♀ (TNU 10224), Crimea, nr Sevastopol, northwestern slope of Ai-Petri Yaila, Baidarskaya Valley, nr Pavlovka Vil., Baidar-Tshokrak Cave, 28.V.2015, I.S. Turbanov leg. • 1 ♀ (TNU 10183), Crimea, nr Sevastopol, northwestern slope of Ai-Petri Yaila, Baidarskaya Valley, nr Rodnikovskoye Vil., Skelskaya Cave, 3.III.2015, I.S. Turbanov leg. • 1 ♂ 5 ♀♀ (IT), same cave, 29.IX.2020, I.S. Turbanov, A.A. Turbanova leg. • 1 ♀ (TNU 10232), same cave, 4.III.2018, I.S. Turbanov, A.A. Turbanova leg. • 2 ♀♀ (TNU 10238/1), same cave, 25.IX.2018, I.S. Turbanov, A.A. Turbanova leg. • 1 ♀ (IT), Crimea, nr Sevastopol, western part of Ai-Petri Yaila, Karadagh Forest, Zemlyanitshnaya Cave, 18.VI.2011, I.S. Turbanov leg. • 2 ♀♀ (TNU 10199/1), Crimea, nr Sevastopol, western part of Ai-Petri Yaila, Karadagh Forest, Kristalnaya (= Maksimovitcha) Cave, 1.V.2013, I.S. Turbanov leg. • 1 ♂ (TNU 10183) • 1 ♂, 2 ♀♀ (IT), same cave, 6.X.2020, I.S. Turbanov leg.• 2 ♂♂ 4 ♀♀ (TNU 10263), Crimea, Bakhchisarai Distr., northern part of Ai-Petri Yaila, nr Maly Babulghan, Villyaburunskaya Cave, 6.V.2015, I.S. Turbanov leg. • 1 ♂ (TNU 10222), Crimea, Bakhchisarai Distr., northeastern slope of Ai-Petri Yaila, nr Bash-Dere, Avantyura Cave, 15.XI.2014, I.S. Turbanov leg. • 1 ♂ 1 ♀ (TNU 10186), Crimea, Simferopol Distr., central part of Tshatyr-Dagh Yaila, Vyalovsky Forest, Paskhalnaya Cave, 12.II.2015, I.S. Turbanov leg. • 1 ♀ (TNU 10195/3), Crimea, Simferopol Distr., northern part of Tshatyr-Dagh Yaila, Binbash-Koba Cave, 12.II.2015, I.S. Turbanov leg. • 1 ♀ (TNU 10188), Crimea, Simferopol Distr., nr Perevalnoye Vil., western slope of the Dolgorukovskaya Yaila, Kizil-Koba (= Krasnaya) Cave, 9.XI.2014, A.A. Nadolny leg. • 1 ♀ (TNU 10225), Crimea, Simferopol Distr., central part of the Dolgorukovskaya Yaila, Sliyanie Cave, 23.VII.2017, I.S. Turbanov leg. • 1 ♀ (TNU 10182), Crimea, Simferopol Distr., eastern part of Dolgorukovskaya Yaila, Vostotshny Potok Cave, 22.II.2014, I.S. Turbanov leg. • 2 ♀♀ (TNU 10198), Crimea, Simferopol Distr., eastern part of Dolgorukovskaya Yaila, Partizanskaya Cave, 5.IV.2014, I.S. Turbanov leg. • 5 ♂♂ 8 ♀♀ (TNU 10192), Crimea, nr Alushta, south-eastern slope of Karabi Yaila, Tuakskaya (= Ful-Koba) Cave, 8.V.2012, I.S. Turbanov leg.

Distribution. East Mediterranean: Greece, Turkey, Ukraine, the south part of European Russia, Georgia, Azerbaijan, Iran. Crimea lies at the northernmost limit of the species range (Kovblyuk and Kastrygina 2015; Nentwig et al. 2024).

Records from the Crimean caves. Map (Fig. 17B – orange circle). Known from the Crimean caves of Sevastopol in the west to Karabi Yaila in the east: Kay-Kobasy, Tshernoretshenskaya, Baidar-Tshokrak, Skelskaya, Zemlyanitshnaya, Kristalnaya, Villyaburunskaya, Ayu-Teshik, Avantyura, Paskhalnaya, Binbash-Koba, Kizil-Koba, Sliyanie, Vostotshny Potok, Partizanskaya, Tisovaya, and Tuakskaya (type locality of *P. khobarum*) (Novikov 1912; Lebedinsky 1914; Charitonov 1947a; present data).

Ecology. A troglophile (Mammola et al. 2018). *Palliduphantes khobarum* is found everywhere in the mountains and on the southern coast of Crimea (Kovblyuk and Kastrygina 2015). One of the most widespread and common spiders in the Crimean caves, apparently capable of maintaining permanent populations in subterranean biotopes; can be classified as an eutroglophile.

Remarks. *Palliduphantes khobarum* was described based on the spider collection by Lebedinsky (1914). According to Charitonov (1947a, b), the reports of *Lepthyphantes monticola* (now, *Anguliphantes monticola*) for the Crimean caves (Novikov 1912; Lebedinsky 1914; Mokrzecki 1914; Charitonov 1932, 1939) in fact belong to *P. khobarum*. Yet, a number of researchers have erroneously mentioned *A. monticola* as occurring in Crimea (Mikhailov 1997, 2013; Kovblyuk 2004a, 2014). Later, *A. monticola* was excluded from the list of species of Crimea (Kovblyuk and Kastrygina 2015: 32).

Genus *Tenuiphantes* Saaristo & Tanasevitch, 1996

? *Tenuiphantes zimmermanni* (Bertkau, 1890)

? *Lepthyphantes zimmermanni* Bertkau, 1890: Evtushenko 2004: 67–68; Zagorodniuk and Vargovitsh 2004: 207.

? *Tenuiphantes zimmermanni* (Bertkau, 1890): Mikhailov 2013: 93; Kovblyuk 2014: 44; Kovblyuk and Kastrygina 2015: 34.

Distribution. West Palearctic polyzonal: from Portugal to the European part of Russia and from Scandinavia to Turkey (Kovblyuk and Kastrygina 2015; Nentwig et al. 2024).

Records from the Crimean caves. Map (Fig. 17B – pink circle). Troizkogo (= Kharkovskaya, ZUG) Cave in E part of Ai-Petri Yaila and Tisovaya Cave in central part of Karabi Yaila (Evtushenko 2004).

Ecology. A troglophile (Mammola et al. 2018). Mentioned from Crimea as a probable trogloxene (Evtushenko 2004).

Remarks. According to some publications (Mikhailov 2013; Kovblyuk 2014; Kovblyuk and Kastrygina 2015), the record of *T. zimmermanni* from Crimea is questionable and not supported by the collected material.

Genus *Troglohyphantes* Joseph, 1881

Troglohyphantes exspectatus sp. nov.

https://zoobank.org/1C70B3DF-8B98-4916-A04B-241A071463FB
Figs 1F, 11–14

Type material. ***Holotype*** • ♂ (ZMMU Ta-8257), Crimea, nr Sevastopol, SW part of Ai-Petri Yaila, Mortsheka Mt., Druzhba Cave, 3.X.2020, I.S. Turbanov leg. ***Paratypes*** • 1 ♀ (ZMMU Ta-8258), 4.V.2015 • 8 ♀♀ (ZMMU Ta-8259), 22.IX.2018 • 1 ♂ 1 ♀ (TNU 10289), 3.X.2020, same cave and collector as for the holotype.

Other material examined. • 3 juv. ♀♀ 4 subad. ♂♂ (TNU 10233), 22.IX.2018 • 9 ♀♀ 4 juv. (IT), 3.X.2020, same cave and collector as for the holotype.

Diagnosis. *Troglohyphantes exspectatus* sp. nov. is most similar to the Bulgarian endemic *T. drenskii* Deltshev, 1973 (the *salax* group sensu Deeleman-Reinhold 1978). Two species can be easily distinguished by the eyes (in *T. exspectatus* sp. nov. well developed, with black pigmentation around, see Fig. 11A, B vs strongly reduced, without pigmentation in *T. drenskii*, see Deltshev 1973: fig. 1) and the clypeus (in *T. exspectatus* sp. nov. without modifications vs concave, with modification in *T. drenskii*, see Deltshev 1973: fig. 1). Structures of male palps are almost identical in both species and differ in details of the cymbium (cf. Figs 11D, E, 12C, D and Deltshev 1973: figs 2, 4). Epigynes differ in the shape of scape: ventral max/min width ratio in *T. exspectatus* sp. nov. 1.9 and in *T. drenskii* 2.9 (cf. Fig. 11C and Deltshev 1973: fig. 7).

Description. Male (paratype). Total length 2.12. Carapace 0.98 long, 0.88 wide, yellow. Palps, chelicerae, and legs yellow. Basal chelicerae segment 0.52 long. Leg **I** length: femur 1.9, patella 0.3, tibia 2.18, metatarsus 2.15, tarsus 1.18, TLL 7.71. Leg **II** length: femur 1.85, patella 0.3, tibia 2.0, metatarsus 1.92, tarsus 1.05, TLL 7.12. Leg **III** length: femur 1.55, patella 0.28, tibia 1.48, metatarsus 1.5,

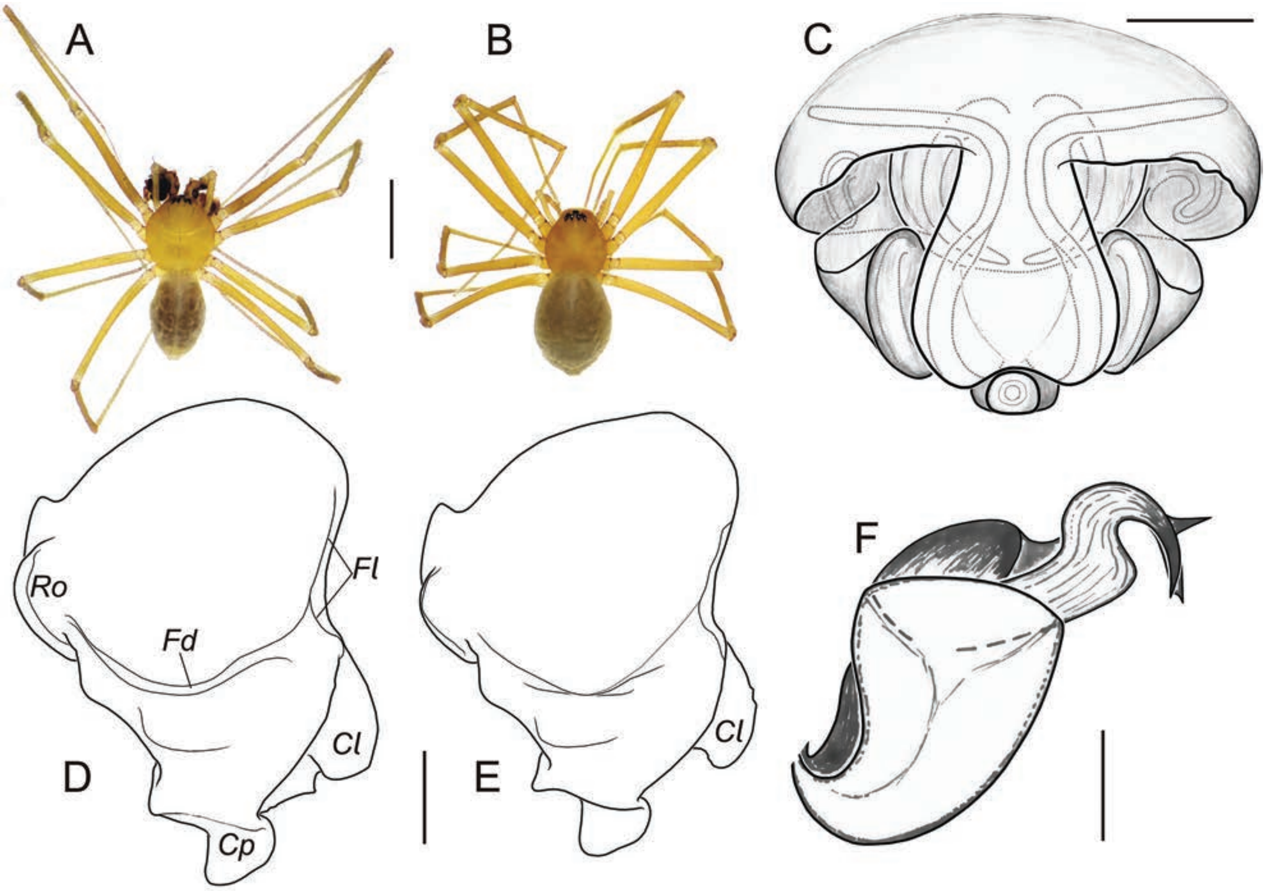

Figure 11. Habitus and copulatory organs of *Troglohyphantes exspectatus* sp. nov. from Druzhba Cave (paratypes): **A, B** male and female, dorsal view **C** epigyne, ventral view **D, E** cymbium, dorsal views **F** distal part of radix and lamella. Abbreviations: *Cl* – prolateral process, *Cp* – posterior process, *Fd* – dorsal furrow, *Fl* – prolateral furrow, *Ro* – rounded deflection. Scale bars: 1.0 mm (**A, B**); 0.1 mm (**C–F**).

tarsus 0.8, TLL 5.61. Leg IV length: femur 1.85, patella 0.28, tibia 1.9, metatarsus 1.88, tarsus 1.0, TLL 6.91. Leg I spination: femur one dorsal and one prolateral spine; tibia two dorsal, two prolateral and two retrolateral spines; metatarsus one dorsal spine. Leg II spination: femur one dorsal spine; tibia two dorsal and one retrolateral spine; metatarsus one dorsal spine. Leg III spination: femur one dorsal spine; tibia two dorsal spines; metatarsus one dorsal spine. Leg IV spination: femur no spine; tibia one dorsal spine; metatarsus no spine. Metatarsi IV without trichobothrium. TmI 0.14. Palp as in Figs 11D, E, 12A–K, 13A, B: cymbium has two processes (prolateral and posterior), two furrows (dorsal and prolateral), rounded deflection in anterior-retrolateral edge, with hollows and ridges in retrolaleral part; paracymbium with two shallow furrows closely situated to each other; suprategular apophysis with a ridge; F-shaped proximal part of radix (two lobes and one small apophysis); median membrane joined with the proximal part of radix dorsally; the distal part of radix with flat pointed terminal apophysis; lamella characteristica with two sclerotised branches, clearly distinct when palp is expanded; embolus with a serrate area dorsally and a keel on prolateral side; cymbium length/width ratio 1.3 (same ratio with and without apophyses). Eyes normal. Abdomen grey.

Female. Total length 1.92. Carapace 0.88 long, 0.78 wide. Basal chelicerae segment 0.6 long. Leg I length: femur 1.68, patella 0.29, tibia 1.82, metatarsus

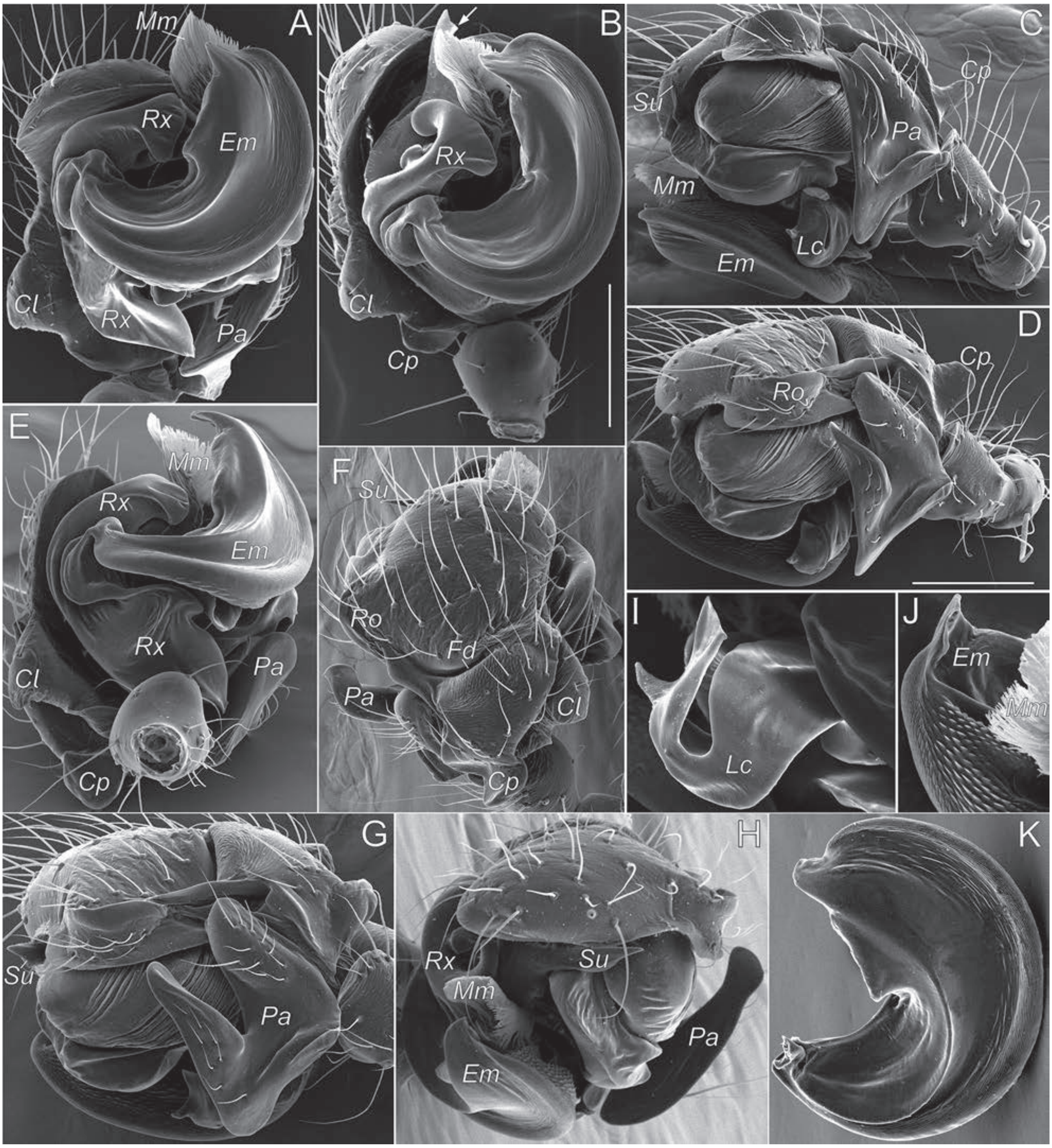

Figure 12. Male palps of *Troglohyphantes exspectatus* sp. nov. from Druzhba Cave (paratype): **A, B** palps, ventral in different aspects (arrow in B indicates ridge of *Su*) **C, D** palp, retrolateral views **E** palp, posterior view **F** palp, dorsal view **G** palp with focus on paracymbium, posterio-retrolateral view **H** palp, anterior view **I** lamella, posterior view **J** tip of embolus, dorsal view **K** embolus, ventral view. Abbreviations: *Cl* – prolateral cymbial process, *Cp* – posterior cymbial process, *Em* – embolus, *Fd* – dorsal furrow of cymbium, *Lc* – lamella, *Mm* – median membrane, *Pa* – paracymbium, *Ro* – rounded deflection of cymbium; *Rx* – radix, *Su* – suprategular apophysis. Scale bars: 0.2 mm (**B, D**); not scaled (**A, C, E–K**).

1.64, tarsus 0.98, TLL 6.41. Leg II length: femur 1.6, patella 0.29, tibia 1.66, metatarsus 1.51, tarsus 0.89, TLL 5.95. Leg III length: femur 1.35, patella 0.25, tibia 1.2, metatarsus 1.18, tarsus 0.68, TLL 4.66. Leg IV length: femur 1.6, patella 0.25, tibia 1.56, metatarsus 1.46, tarsus 0.81, TLL 5.68. Leg I spination: femur one dorsal and one prolateral spine; tibia one dorsal, one prolateral, one

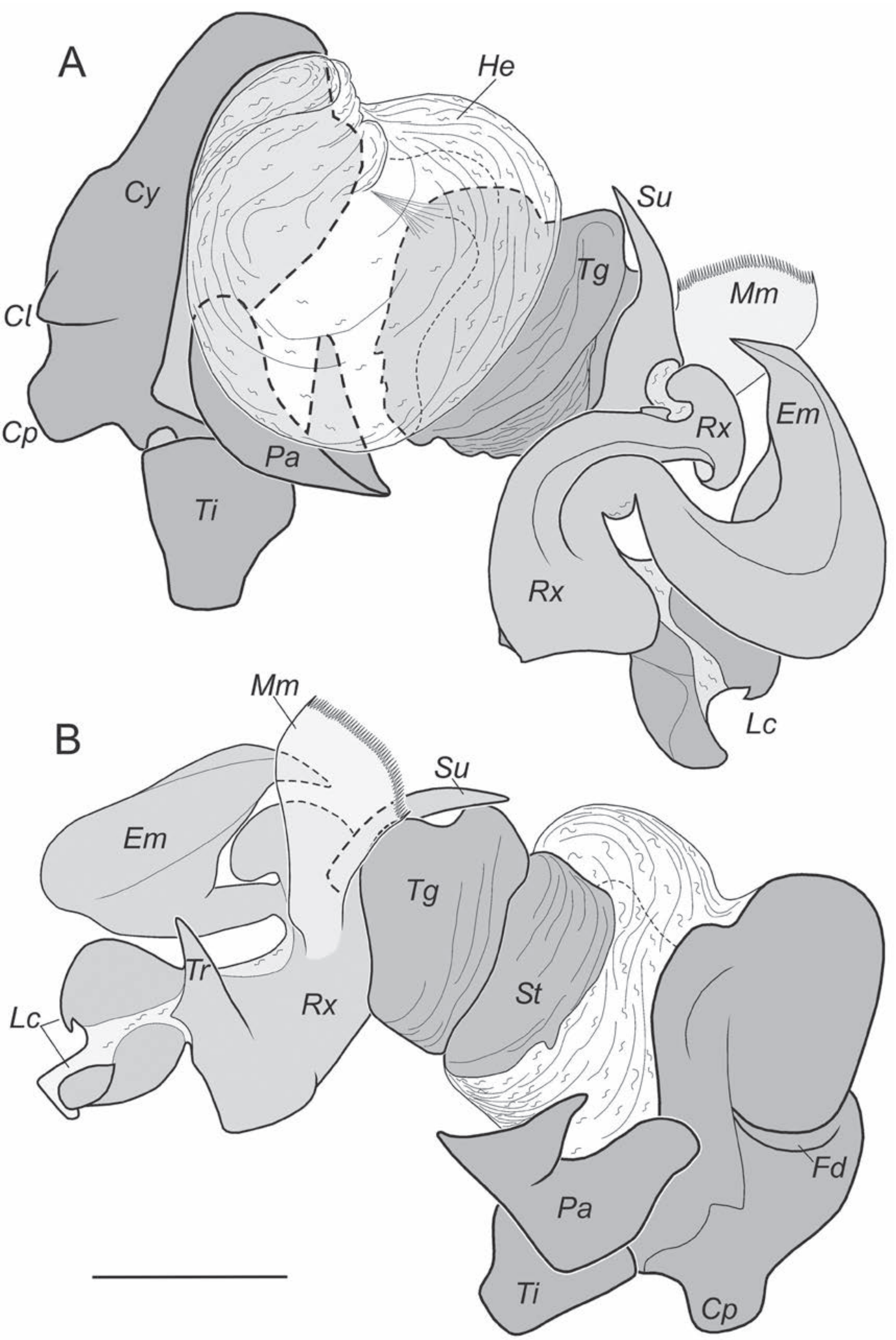

Figure 13. Palp with expanded bulbus of *Troglohyphantes exspectatus* sp. nov. from Druzhba Cave (paratype): **A, B** cymbium in prolateral and retrolateral positions. Abbreviations: *Cy* – cymbium, *Cl* – prolateral cymbial process, *Cp* – posterior cymbial process, *Em* – embolus, *Fd* – dorsal furrow of cymbium, *He* – haemathodoha, *Lc* – lamella characteristica, *Mm* – median membrane, *Pa* – paracymbium, *Rx* – radix, *Su* – suprategular apophysis, *St* – subtegulum, *Tg* – tegulum, *Ti* – tibia, *Tr* – terminal apophysis. Scale bar: 0.2 mm.

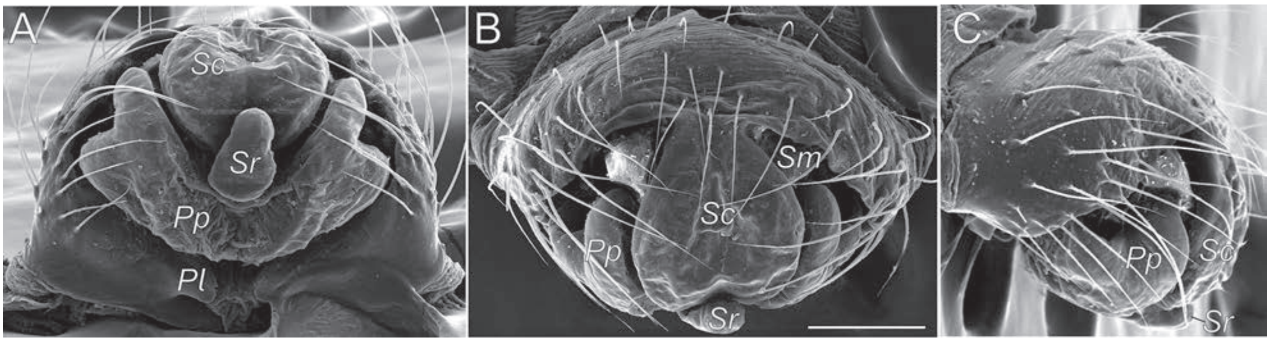

Figure 14. Epigyne of *Troglohyphantes exspectatus* sp. nov. from Druzhba Cave (paratype): **A–C** posterior, ventral, and lateral views. Abbreviations: *Pl* – posterior lobes, *Pp* – posterior plate, *Sc* – scape, *Sm* – median part of scape, *Sr* – stretcher. Scale bar: 0.1 mm.

retrolateral, and four ventral spines; metatarsus one dorsal spine. Leg II spination: femur one dorsal spine; tibia two dorsal, one retrolateral and two ventral spines; metatarsus two dorsal spines. Leg II spination: femur one dorsal spine; tibia two dorsal spines; metatarsus two dorsal spines. Leg IV spination: femur no spine; tibia two dorsal spines; metatarsus no spine. Metatarsi IV without trichobothrium. TmI 0.15. Epigyne as in Figs 11C, 14A–C: in ventral view scape resembling a shape of water drop with truncated anterior side; posterior plate in caudal view looks bifurcated, each branch with two rounded protrusions; posteriorly sides of epigyne folded and terminate with posterior lobes, directed towards each other. Body colouration as in male.

Remarks. The embolic and radix structure of the new species is similar to that of *T. adjaricus* Tanasevitch, 1987, *T. deelemanae* Tanasevitch, 1987, *T. lucifuga* (Simon, 1884), and other related species from the *orpheus* group (sensu Deeleman-Reinhold 1978 and Isaia et al. 2017), but can be distinguished by the pear-shape cymbium (in dorsal view), with two small apophyses in its proximal part (vs in *T. lucifuga* complex and *T. adjaricus* one or three apophyses, usually prolateral apophysis is large; in *T. deelemanae* with large prolateral apophysis, whose length is equal to width of middle part of cymbium). The shape of the lamella in the new species differs in detail from that of all the congeners. Some similarity can be found in new species and *T. cyrnaeus* Isaia, 2023 from the *salax* group (Isaia et al. 2023: fig. 2D). Both have S-shaped lamellae, but in *T. exspectatus* sp. nov. the end of the lamella is bifurcated with one branch pointed and the other flatted (Figs 11F, 12I). The epigyne of the new species is similar to those of *T. deelemanae* and *T. konradi* Brignoli, 1975 (see Isaia et al. 2011). Females of these species are distinguishable by the angle between lateral side of scape and edge of epigyne (in a new species sides are perpendicular to each other, with angle between side of scape and edge of epigyne ~ 70° vs subparallel in *T. deelemanae*) and the eye development (well developed in the new species, but reduced in *T. konradi*). Also, *T. exspectatus* sp. nov. has the epigyne similar to that of some species of the *salax* group (sensu Deeleman-Reinhold 1978; *T. strandi* Absolon & Kratochvil, 1932, *T. fallax* Deeleman-Reinhold, 1978, *T. lesserti* Kratochvil, 1935 – all of them have reduced eyes) and the embolus similar to those of the members of the *polyophthalmus* group (*T. inermis* Deeleman-Reinhold, 1978 is distinguishable by the shapes of the lamella and cymbium).

Variation. Males (*n* = 2): carapace width 0.83–0.88; femur I length 1.81–1.9. Females (n = 9): carapace width 0.77–0.85; femur I length 1.67–1.9.

Distribution and records from the Crimean caves. Map (Fig. 17B – yellow circle). Only known from the type locality: Druzhba Cave on Mortsheka Mt. in the SW part of Ai-Petri Yaila.

Ecology. Given that *T. exspectatus* sp. nov. has the well-developed eyes but permanently occurs and reproduces in Druzhba Cave (we have recorded individuals at all developmental stages), it can be classified as an eutroglophile.

Etymology. From the Latin *exspectatus*, meaning expected, due to the fact that we have not come across adult males of this species for a long time, but only females, subadult males, and juveniles.

Family Lycosidae Sundevall, 1833
Genus *Alopecosa* Simon, 1885

Alopecosa farinosa (Herman, 1879)

Material examined. • 1 ♂ (TNU 10199/2), Crimea, nr Sevastopol, western part of Ai-Petri Yaila, Karadagh Forest, Kristalnaya (= Maksimovitcha) Cave, 1.V.2013, I.S. Turbanov leg.

Distribution. Transpalaearctic polyzonal (Kovblyuk and Kastrygina 2015; Nentwig et al. 2024).

Records from the Crimean caves. Map (Fig. 17A – grey circle). Kristalnaya Cave on the western part of Ai-Petri Yaila.

Ecology. *Alopecosa farinosa* is distributed throughout Crimea and is a common species in the mountains (Kovblyuk and Kastrygina 2015). This species has never been previously recorded in caves. Clearly, *A. farinosa* is an accidental species in caves, hence can be classified as a trogloxene species.

Family Nesticidae Simon,1894
Genus *Aituaria* Esyunin & Efimik, 1998

Aituaria borutzkyi (Reimoser, 1930)
Figs 2B, 15, 16

Material examined. • 3 ♀♀ (TNU 10226), Crimea, Bakhchisarai Distr., nr Khodzha-Sala Vil., steep southern slope of Baba-Dagh Plateau (= Mangup-Kale Gorodishche), Mangupskaya I (= MK-1) Cave, 28.IV.2017, I.S. Turbanov leg. • 10 ♀♀ (TNU 10237/1), same cave, 3.V.2018, I.S. Turbanov leg. • 3 ♀♀ (TNU 10266), same cave, 6–8.V.2017, O.L. Makarova, K.V. Makarov leg. • 1 ♂ (TNU 10236/1), same cave, 11.VI.2018, I.S. Turbanov, A.A. Nadolny leg. • 1 ♂ 1 ♀ (TNU 10273), same cave, 2.X.2020, I.S. Turbanov, A.A. Turbanova leg.

Comparative material. • 1 ♂ (TNU 10274), southern part of Simferopol, indoors; 27.VI.2011; A.A. Nadolny leg.

Distribution. Minor Asia (Turkey), the west Caucasus (Abkhazia) and Crimea (Nadolny and Kovblyuk 2007).

Records from the Crimean caves. Map (Fig. 17B – black circle). Mangupskaya I Cave on a steep southern slope of Baba-Dagh Plateau (present data).

Ecology. A troglophile and synanthropic species (Nadolny and Kovblyuk 2007; Mammola et al. 2018; present data). In Crimea, *A. borutzkyi* has been found in anthropogenic biotopes of Simferopol and Fersmanovo Vil. (Nadolny

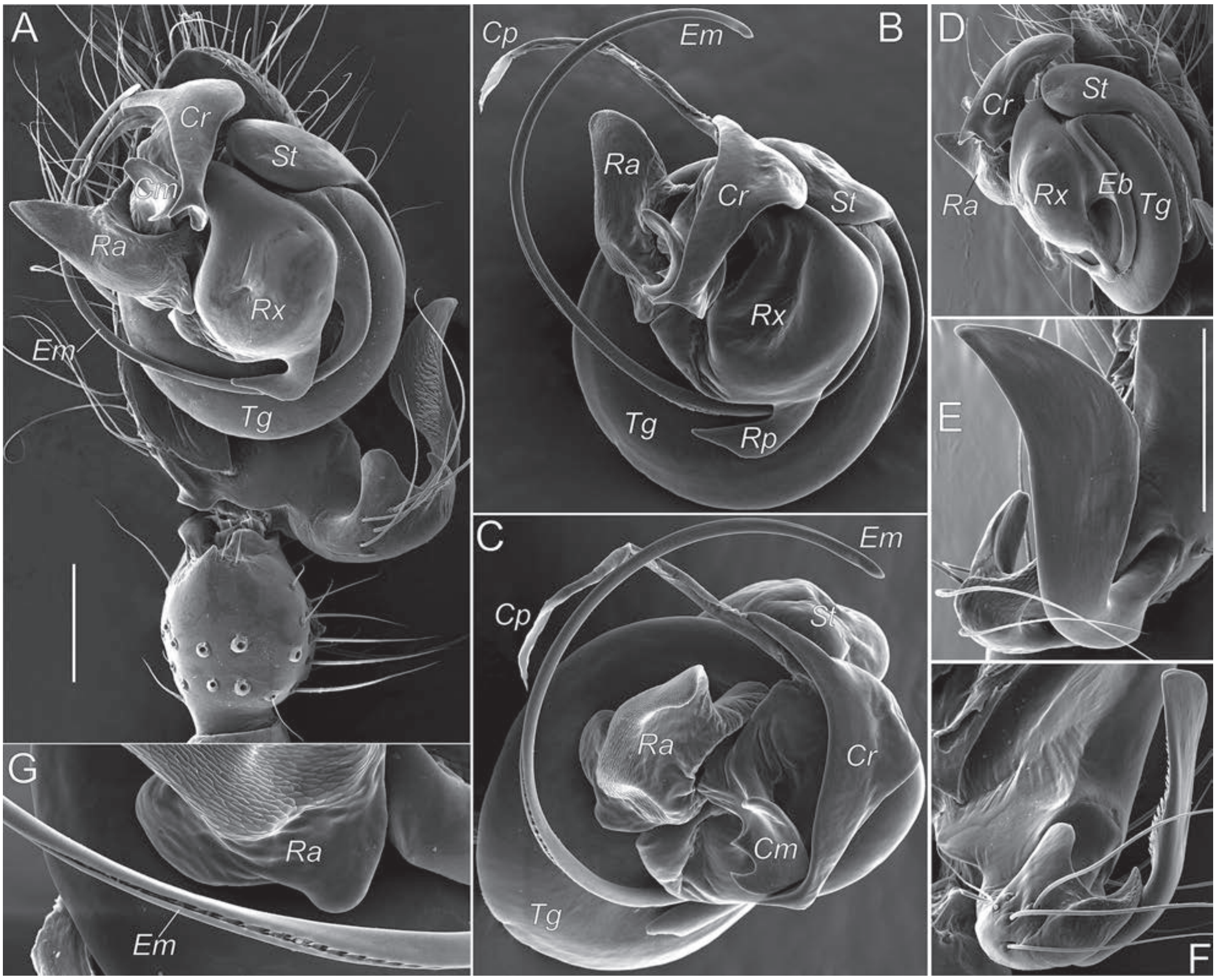

Figure 15. Male palp of *Aituaria borutzkyi* from Mangupskaya I Cave: **A** palp, ventral view; **B–D** bulbus, ventral, anterior, and retrolateral views **E, F** paracymbium, dorso-retrolateral and ventro-retrolateral views **G** fragment of embolus with a furrow, prolateral view. Abbreviations: *Cm* – median process of the conductor, *Cp* – prolateral process of the conductor, *Cr* – retrolateral process of the conductor, *Eb* – embolic base, *Em* – embolus, *Ra* – radical apophysis, *Rp* – radical process, *Rx* – radix, *St* – subtegulum, *Tg* – tegulum. Scale bars: 0.2 mm (**A, E**); not scaled (**B–D, F, G**).

and Kovblyuk 2007, present data). During the present study, it was found only in Mangupskaya I Cave on Baba-Dagh Plateau. On this plateau there was the city of Dori (= Doros), the capital of the medieval late Byzantine Orthodox Principality of Theodoro (13th – mid-15th centuries), where some of currently known caves were used for economic and religious purposes. After the siege and capture of Dori in 1475 by Ottoman troops, the Turkish fortress of Mangup-Kale was built on the plateau and existed there until 1774. In our opinion, under the influence of long-term human activity on Baba-Dagh Plateau, special conditions were created for the colonisation of caves by troglophilous species, which could have been unintentionally introduced to Crimea by active trade between the medieval Principality of Theodoro and/or the Turkish fortress of Mangup-Kale and medieval states of the west Caucasus and the Ottoman Empire (Herzen and Makhneva-Chernets 2006), the native range of *A. borutzkyi* lays (Nadolny and Kovblyuk 2007). Therefore, in Crimea *A. borutzkyi* seems to be an accidentally introduced facultative synanthrope, locally established in suitable subterranean biotope as a subtroglophile.

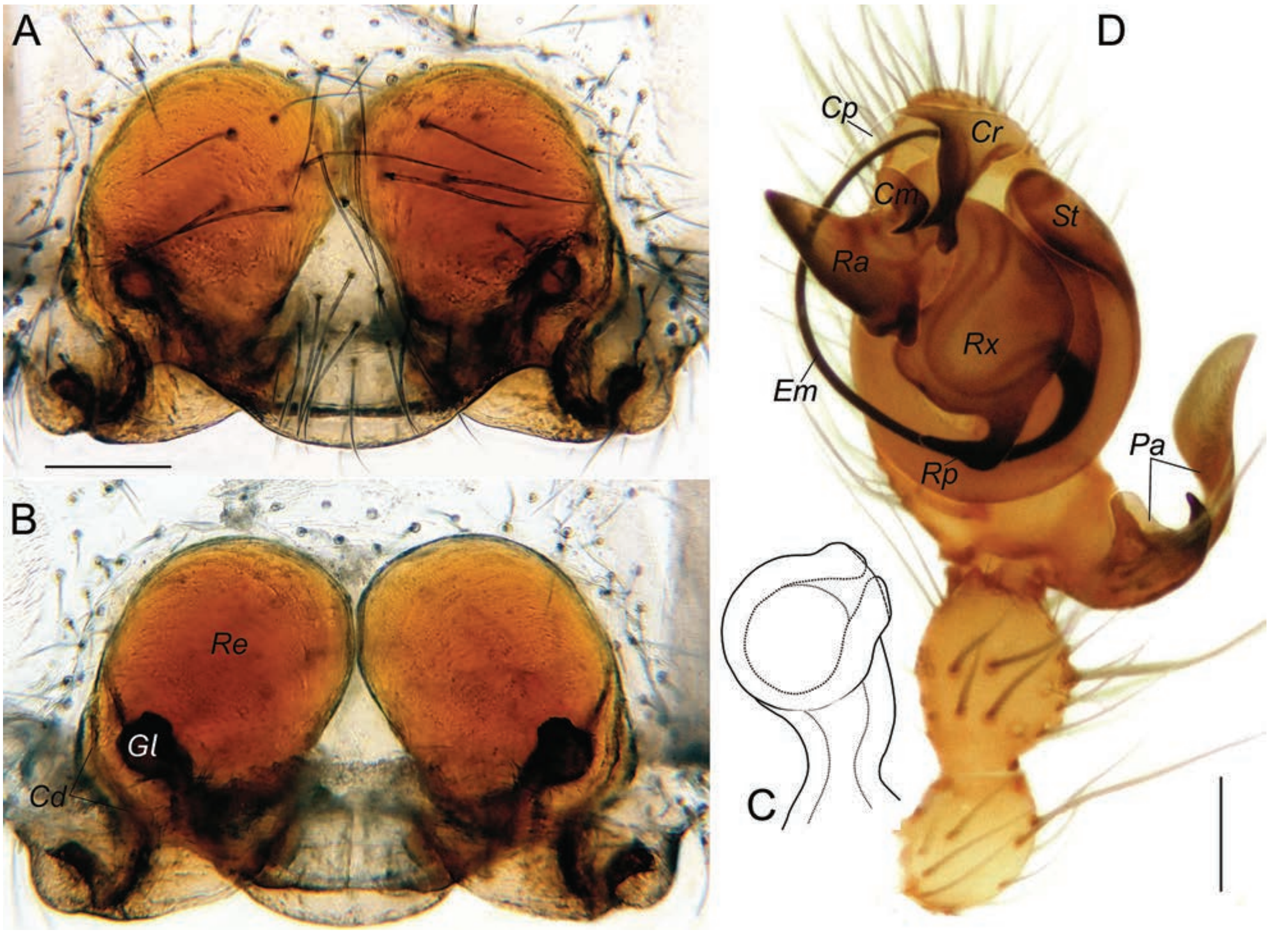

Figure 16. Female and male copulatory organs of *Aituaria borutzkyi* from Mangupskaya I Cave: **A, B** epigyne, ventral and dorsal views **C** club-like gland, dorsal view **D** male palp, ventral view. Abbreviations: *Cd* – copulatory duct, *Cm* – median process of the conductor, *Cp* – prolateral process of the conductor, *Cr* – retrolateral process of the conductor, *Em* – embolus, *Gl* – club-like gland, *Pa* – paracymbium, *Ra* – radical apophysis, *Re* – receptacle, *Rp* – radical process, *Rx* – radix, *St* – subtegulum. Scale bars: 0.2 mm (**A, B, D**); not scaled (**C**).

Additional diagnostic details. The complex structure of copulatory organs in *Aituaria* members has been discussed and illustrated (Marusik et al. 2017; Fomichev et al. 2022). Here we give SEM micrographs of the male palp of *A. borutzkyi* to show their details (Fig. 15A–G): the paracymbium bears three apophyses, of which the dorsal and distal apophyses are covered with triangular scales (Fig. 15A, E, F); the rounded anterior part of subtegulum is prominent in ventral view, the rest of it is hidden behind the tegulum (Fig. 15A); the tegulum is discoidal; the radix pear-shaped with a pointed posterior process; the triangular radical apophysis has a scaly surface (Fig. 15A, C, G); the conductor consists of three parts: median process with two pointed and one rounded outgrowths, the relatively massive retrolateral process that is bifurcated on its ventral side, and the long, narrow and transparent prolateral process (Fig. 15B, C); the connection between embolus and tegulum forms a sharp bend on the anterio-retrolateral side of the bulb (Fig. 15D); the embolus with a furrow almost along its entire length (Fig. 15C, G). For the female of *A. borutzkyi*: the epigyne has a rounded edge and is oval, with poorly sclerotised receptacles; the spherical, club-like gland is heavily sclerotised (Fig. 16A, B); the copulatory openings situate near the epigynal edge, entering the receptacles laterally (Fig. 16B).

A recent review (Fomichev et al. 2022) considered four species of *Aituaria*, of which only two have been found in Crimea, including its subterranean habitats: viz., *A. borutzkyi* and *A. pontica*. Males of these species are easily separable by the embolic shape: the narrow embolus in *A. borutzkyi* and wide in *A. pontica*; also, all other apophysis differ in their shapes (cf. Fomichev et al. 2022: figs 25, 27). The females differ in detailed structures of the epigyne (cf. Fig. 16A–C and Marusik et al. 2017: figs 18, 19): *A. pontica* has a more bended edge of the epigynal plate compared to that in *A. borutzkyi*; the stem and head in the club-shaped gland are of equal width in *A. pontica*, while the head is wider than the stem in *A. borutzkyi*.

Aituaria pontica **(Spassky, 1932)**
Fig. 2A

Aituaria pontica (Spassky, 1932): Nadolny and Turbanov 2014: 569; Kovblyuk and Kastrygina 2015: 42; Turbanov et al. 2016b: 1284; Esyunin 2017: 243; Turbanov and Nadolny 2017: 114–115.

Material examined. • 2 ♂♂, 1 ♀, 5 juv. (TNU), Crimea, nr Sevastopol, Khomutovaya Gorge, Maksimova Datsha, abandoned aqueduct carved into an unnamed cave-spring, 11.III.2014, I.S. Turbanov leg.

Distribution. It is found in natural habitats in Krasnodar Territory, Russia. Also, reported from Ukraine and Russia (the Urals) as a synanthropic species (Nadolny and Turbanov 2014; Esyunin 2017).

Records from the Crimean caves. Map (Fig. 17B – grey circle). Abandoned aqueduct carved into an unnamed cave-spring of Maksimova Datsha nr Sevastopol (Nadolny and Turbanov 2014).

Ecology. A troglophile and synanthropic species (Esyunin 2017). In Crimea, the species has been found only in an abandoned aqueduct in Sevastopol, which was made by enlarging a cave spring (Nadolny and Turbanov 2014). Maksimova Datsha was the site with intensive agricultural and other economic activities carried out in the second half of the 19th and early 20th centuries, where ornamental/cultivated plants were introduced mainly from the west Caucasus (Chikin 2005). In our opinion, this was a pathway for spreading alien species to Crimea, including *A. pontica*. Therefore, in Crimea this species is an accidentally introduced facultative synanthrope, locally established in suitable subterranean biotope as a subtroglophile.

Family Pholcidae C.L. Koch, 1850
Genus *Pholcus* Walckenaer, 1805

Pholcus phalangioides **(Fuessling, 1775)**

Pholcus phalangioides (Fuessling, 1775): Charitonov 1947a: 47; Charitonov 1947b: 1; Birstein 1963: 128; Tyshchenko 1971: 23; Kovblyuk 2004a: 238; Kovblyuk 2014: 44; Turbanov et al. 2016b: 1283.

Pholcus phalangoides [sic!] (Fuessling, 1775): Evtushenko 2004: 66, 68.

Pholcus phalangoidaes [sic!] (Fuessling, 1775): Zagorodniuk and Vargovitsh 2004: 207.

Material examined. • 1 ♀ (TNU 10193/1), Crimea, nr Sevastopol, Khomutovaya Gorge, Maksimova Datsha, abandoned aqueduct carved into an unnamed cave-spring, 11.III.2014, I.S. Turbanov leg. • 1 ♂ (TNU 10190/3), same cave, 23.V.2015, A.A. Nadolny leg. • 1 ♂ (TNU), Crimea, Bakhchisarai Distr., nr Khodzha-Sala Vil., steep southern slope of Baba-Dagh Plateau (= Mangup-Kale Gorodishche), Mangupskaya I (= MK-1) Cave, 2.VI.2021, I.S. Turbanov leg.

Distribution. Cosmopolite (Kovblyuk and Kastrygina 2015; Nentwig et al. 2024).

Records from the Crimean caves. Map (Fig. 17A – pink circle). Small unnamed cave (= ?Malaya Cave) in Nizhnie Limeny (now Goluboi Zaliv, Yalta) and abandoned aqueduct of Maksimova Datsha nr Sevastopol; Mangupskaya I (= MK-1) Cave in Bakhchisarai Distr. (Charitonov 1947a; present data).

Ecology. A troglophile and synanthropic species (Mammola et al. 2018; Nentwig et al. 2024). *Pholcus phalangioides* usually is found in anthropogenic biotopes and less frequently in caves (Huber 2011). In Crimea, this species is also mainly synanthropic (Kovblyuk et al. 2016), except for few findings in caves (Charitonov 1947a; present data), which are somehow associated with human economic activity. In particular, in the abandoned aqueduct in Sevastopol, which was made by enlarging a cave spring, and where intensive agricultural and other economic activities were carried out in the second half of the 19th and early 20th centuries (Chikin 2005). Small unnamed cave in Nizhnie Limeny (Charitonov 1947a) is another site from where *P. phalangioides* has been recorded. That site is situated on Koshka Mt. containing the ruins of a medieval Genoese fortification (shelter) from the 13–15th centuries, Limena-Kale (Myts 1991). Therefore, in Crimea, this species can be classified as a facultative synanthrope, established as a subtroglophile in suitable subterranean biotopes.

Family Tetragnathidae Menge, 1866
Genus *Meta* C.L. Koch, 1836

Meta bourneti Simon, 1922
Fig. 2E–G

Meta bourneti Simon, 1922: Spassky 1936: 535; Charitonov 1936: 201; Charitonov 1939: 197; Charitonov 1947a: 44–45; Charitonov 1947b: 1; Birstein 1963: 128; Tyshchenko 1971: 190; Mikhailov 1997: 108; Amelichev et al. 2004: 136; Evtushenko 2004: 66, 68; Zagorodniuk and Vargovitsh 2004: 207; Kovblyuk 2004a: 244; Mikhailov 2013: 101; Kovblyuk 2014: 44–45, fig. 23; Kovblyuk and Kastrygina 2015: 56; Turbanov et al. 2016b: 1283; Prokopov and Turbanov 2017: 101; Turbanov et al. 2019a: 218; Samokhin et al. 2019: 247.
Meta sp.: Turbanov et al. 2019b: 41.

Material examined. • 1 ♀ (TNU 10265), Crimea, Bakhchisarai Distr., nr Khodzha-Sala Vil., steep southern slope of Baba-Dagh Plateau (= Mangup-Kale Gorodishche), Mangupskaya I (= MK-1) Cave, 6–8.V.2017, O.L. Makarova, K.V. Makarov leg. • 2 ♂♂ (TNU 10191/2) • 2 ♀♀ (IT), same cave, 2.X.2020, I.S. Turbanov, A.A. Turbanova leg. • 1 ♂, 1 ♀, 4 juv. (IT), same cave, 2.VI.2021, I.S. Turbanov leg. • 1 ♂ (TNU 10179), Crimea, Sevastopol, nr Balaklava, Aya Cape Mt. Range, Mt. Kala-Fatlar, Gnomov Cave, 9.X.2016, A.A. Nadolny leg. • 1 ♂ 1 ♀ (IT), Crimea, Sevastopol, nr Balaklava, Aya Cape Mt. Range, Kala-Fatlar Mt., Gekkonovaya Cave,

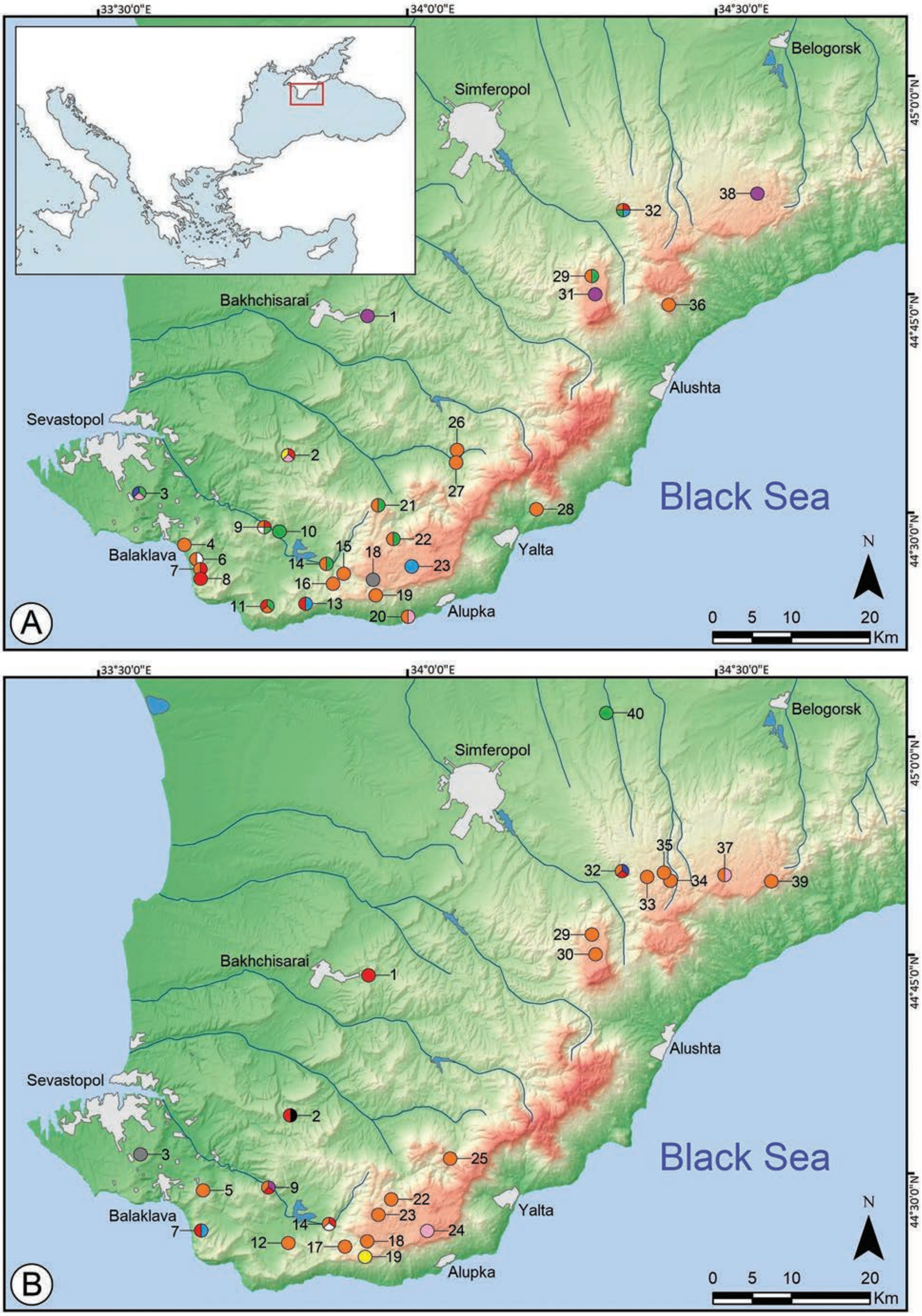
33°30'0"E
34°0'0"E
34°30'0"E
45°0'0"N
44°45'0"N
44°30'0"N
Belogorsk
Simferopol
Bakhchisarai
Alushta
Sevastopol
Balaklava
Yalta
Alupka
Black Sea
N
0 5 10 20
Km
A
1
2
3
4
6
7
8
9
10
11
13
14
15
16
18
19
20
21
22
23
26
27
28
29
31
32
36
38
B
1
2
3
5
7
9
12
14
17
18
19
22
23
24
25
29
30
32
33
34
35
37
39
40

28.XII.2012, I.S. Turbanov leg. • 1 ♀ (TNU 10229) • 3 juv. (IT), Crimea, nr Sevastopol, Tshernaya River canyon, Tshernoretshenskaya Cave, 5.V.2017, I.S. Turbanov leg. • 1 ♂ (TNU 10231/1), same cave, 3.III.2018, A.A. Nadolny leg. • 1 ♀ (TNU 10287/3) • 2 ♀♀ 3 juv. (IT), same cave, 3.VI.2021, I.S. Turbanov, A.A. Nadolny leg. • 1 ♀ (TNU 10191/2), Crimea, nr Sevastopol, northeastern slope of Baidarskaya Yaila, Baidarskaya Valley, nr Kizilovoye Vil., Mamut-Tshokrak Cave, 1–2.VI.2013, I.S. Turbanov leg. • 1 ♂ (TNU 10228), same cave, 25.VI.2017, I.S. Turbanov leg. • 2 ♀♀ (TNU 10181/1), Crimea, nr Sevastopol, western part of Ai-Petri Yaila, northeastern slope of Kilse-Burun Mt., unnamed cave, 14.IV.2014; I.S. Turbanov leg • 1 ♂, 1 ♀ (IT), Crimea, Simferopol Distr., nr Perevalnoye Vil., western slope of Dolgorukovskaya Yaila, Kizil-Koba (= Krasnaya) Cave, 18.XII.2019, I.S. Turbanov leg.

Distribution. West Palearctic nemoral-subtropical: from Portugal to Georgia and from Britain to North Africa (Kovblyuk and Kastrygina 2015; Nentwig et al. 2024).

Records from the Crimean caves. Map (Fig. 17A – red circle). Caves in the south-western and central parts of the Crimean Mountains: Mangupskaya I, Gnomov, Gekkonovaya, Tshernoretshenskaya, Mamut-Tshokrak, unnamed cave on the northeastern slope of Kilse-Burun Mt. and Kizil-Koba (Spassky 1936; Charitonov 1947a; Evtushenko 2004; Turbanov et al. 2019a, b; present data).

Ecology. A troglophile (Mammola et al. 2018). In Crimea, *M. bourneti* has been recorded only from caves, and hence is classified as a eutroglophile. There are data on the life cycle of *M. bourneti*, according to which the first instars of its postembryonic development may occur outside of caves (Mammola and Isaia 2014). However, we have repeatedly recorded juvenile specimens of different instars in Mangupskaya I and Tshernoretshenskaya caves, including those found at 50–100 meters from the entrances, and this suggests that in Crimea the life cycle of *M. bourneti* is completely restricted to caves.

Remarks. The reference of *Meta* sp. for the caves of Cape Aya (Turbanov et al. 2019b) refers to the material from Gnomov and Gekkonovaya caves used in present data.

Figure 17. Distributions of cave-dwelling spiders in Crimea (including data from references and this work): **A** *Tegenaria lapicidinarum* (purple circle), *T. parietina* (blue circle), *T. taurica* (orange circle), *Amaurobius erberi* (yellow circle), *Alopecosa farinosa* (grey circle), *Pholcus phalangioides* (pink circle), *Meta bourneti* (red circle), *Metellina segmentata* (pale blue circle), *M. merianae* (green circle), *Steatoda triangulosa* (white circle) **B** *Bisetifer gruzin* (blue circle), *B. tactus* sp. nov. (purple circle), *Caviphantes dobrogicus* (green circle), *Lepthyphantes leprosus* (red circle), *Megalepthyphantes nebulosus* (pale blue circle), *M. pseudocollinus* (white circle), *Palliduphantes khobarum* (orange circle), ? *Tenuiphantes zimmermanni* (pink circle), *Troglohyphantes exspectatus* sp. nov. (yellow circle), *Aituaria pontica* (grey circle), *A. borutzkyi* (black circle). The numbering of the caves is common for both maps: 1 – in unnamed cave near the city of Bakhchisarai; 2 – Mangupskaya I (= MK-1) Cave; 3 – abandoned aqueduct carved into an unnamed cave-spring in area of the Maksimova Datsha; 4 – Asketi I Cave; 5 – Kay-Kobasy Cave; 6 – Izumrudnaya Cave; 7 – Gekkonovaya Cave; 8 – Gnomov Cave; 9 – Tshernoretshenskaya Cave; 10 – Azis-Koba (= Kara-Koba) Cave; 11 – Mamut-Tshokrak Cave; 12 – Baidar-Tshokrak Cave; 13 – unnamed cave on northeastern slope of Mt. Kilse-Burun; 14 – Skelskaya Cave; 15 – Rodnikovskaya Cave; 16 – Koryta (= Kuznetsova) Cave; 17 – Zemlyanitshnaya Cave; 18 – Kristalnaya (= Maksimovitcha) Cave; 19 – Druzhba Cave; 20 – unnamed cave (= ?Malaya Cave) in Nizhnie Limeny (now Goluboi Zaliv); 21 – Daniltsha-Koba Cave; 22 – Ayu-Teshik Cave; 23 – Villyaburunskaya Cave; 24 – Troizkogo (= Kharkovskaya, ZUG) Cave; 25 – Avantyura Cave; 26 – Kaply-Kayanskaya (= Khaplu-Khoba) Cave; 27 – Ayu-Koba Cave; 28 – grotto in Massandra; 29 – Binbash-Koba Cave; 30 – Paskhalnaya Cave; 31 – Alushtinskaya Cave; 32 – Kizil-Koba (= Krasnaya) Cave; 33 – Sliyanie Cave; 34 – Vostotshny Potok Cave; 35 – Partizanskaya Cave; 36 – grotto on Mt. Yuznaya Demerdzhi; 37 – Tisovaya Cave; 38 – Karani-Koba Cave; 39 – Tuakskaya (= Ful-Koba) Cave; 40 – Tavrida Cave.

Genus *Metellina* Chamberlin & Ivie, 1941

Metellina merianae (Scopoli, 1763)

Fig. 2C, D

Meta merianae (Scopoli, 1763): Spassky 1927: 4; Charitonov 1932: 123; Charitonov 1939: 197; Charitonov 1947a: 45–46; Charitonov 1947b: 1; Birstein 1963: 128; Tyshchenko 1971: 23.

Metellina merianae (Scopoli, 1763): Amelichev et al. 2004: 136; Evtushenko 2004: 66, 68; Kovblyuk 2004a: 245; Zagorodniuk and Vargovitsh 2004: 207; Turbanov et al. 2016b: 1283; Prokopov and Turbanov 2017: 101; Samokhin et al. 2019: 247; Turbanov et al. 2019a: 218.

Material examined. • 5 ♀♀ (TNU 10193/2), Crimea, nr Sevastopol, Khomutovaya Gorge, Maksimova Datsha, abandoned aqueduct carved into an unnamed cave-spring, 11.III.2014, I.S. Turbanov leg. • 1 ♀ (TNU 10190/2), same cave, 23.V.2015, A.A. Nadolny leg. • 1♀ (TNU 10287/4), Crimea, nr Sevastopol, canyon of the Tshernaya River, Tshernoretshenskaya Cave, 3.VI.2021, I.S. Turbanov, A.A. Nadolny leg. • 1 ♀ (TNU 10184), Crimea, nr Sevastopol, northeastern slope of Baidarskaya Yaila, Baidarskaya Valley, nr Kizilovoye Vil., Mamut-Tshokrak Cave, 10.VIII.2010, I.S. Turbanov leg. • 1 ♂ 1 ♀ (TNU 10191/1), same cave; 1–2.VI.2013, I.S. Turbanov leg. • 1 ♀ (TNU 10238/2), Crimea, nr Sevastopol, northwestern slope of Ai-Petri Yaila, Baidarskaya Valley, nr Rodnikovskoye Vil., entrance to Skelskaya Cave, 25.IX.2018, I.S. Turbanov, A.A. Turbanova leg. • 1 ♀ (IT), same cave, 27.XII.2019, I.S. Turbanov leg. • 2 ♂♂ 6 ♀♀ (IT), same cave, 1.VI.2021, I.S. Turbanov, A.A. Turbanova leg. • 1 ♀ (TNU 10261/2), Crimea, Bakhchisarai Distr., northern part of Ai-Petri Yaila, Ayu-Teshik Mt., Ayu-Teshik Cave, 8.V.2015, I.S. Turbanov leg. • 1 ♂ 1 ♀ (TNU 10258), same cave, 16.VII.2017, O.V. Kukushkin leg • 4 ♂♂ (TNU 10195/2), Crimea, Simferopol Distr., northern part of Tshatyr-Dagh Yaila, Binbash-Koba Cave, 12.II.2015, I.S. Turbanov leg.

Distribution. West and Central Palaearctic polyzonal: from Portugal to the Altai Mts and from Scandinavia to Iran (Kovblyuk and Kastrygina 2015; Nentwig et al. 2024).

Records from the Crimean caves. Map (Fig. 17A – green circle). Caves of the southwestern and central parts of the Crimean Mountains: Tshernoretshenskaya, Azis-Koba (= Kara-Koba), Mamut-Tshokrak, Skelskaya, Ayu-Teshik, Daniltsha-Koba, Binbash-Koba, and Kizil-Koba, as well as abandoned aqueduct of Maksimova Datsha nr Sevastopol (Spassky 1927; Charitonov 1947a; Samokhin et al. 2019; Turbanov et al. 2019a; present data).

Ecology. A troglophile (Mammola et al. 2018). In Crimea, the species inhabits broad-leaved forests of northern macro-slopes of the mountains (Kovblyuk and Kastrygina 2015). In the Crimean caves, *M. merianae* can be classified as a subtroglophile.

Metellina segmentata (Clerck, 1757)

Material examined. • 1 ♀ (TNU 10181/2), Crimea, nr Sevastopol, the western part of Ai-Petri Yaila, the northeastern slope of Kilse-Burun Mt., unnamed cave, 14.IV.2014; I.S. Turbanov leg. • 1 ♀ (TNU 10194), Crimea, Bakhchisarai Distr., the central part of Ai-Petri Yaila, Vorontsovsky Forest, Rutsheinaya Cave, 8–9.II.2014, I.S. Turbanov leg. • 1 ♂ (TNU 10178), Crimea, Simferopol Distr., nr Perevalnoye Vil., the western slope of Dolgorukovskaya Yaila, Kizil-Koba (= Krasnaya) Cave, 8–9.XI.2014, A.A. Nadolny leg.

Distribution. Transpalaearctic polyzonal (Kovblyuk and Kastrygina 2015; Nentwig et al. 2024).

Records from the Crimean caves. Map (Fig. 17A – pale blue circle). Unnamed cave on the northeastern slope of Kilse-Burun Mt., Rutsheinaya Cave on Ai-Petri Yaila and Kizil-Koba Cave on the western slope of Dolgorukovskaya Yaila (present data).

Ecology. In Crimea, *M. segmentata* is common in the mountainous forest part of the Peninsula (Kovblyuk and Kastrygina 2015). There is an indication of this species as a trogloxene in Tshudesnitsa Cave in Perm Oblast of Russia (Pankov et al. 2009). In the Crimean caves, *M. segmentata* can be classified as a trogloxene.

Family Theridiidae Sundevall, 1833

Genus *Steatoda* Sundevall, 1833

Steatoda triangulosa (Walckenaer, 1802)

Material examined. • 1 ♀ (TNU 10259/2), Crimea, Sevastopol, nr Balaklava, Aya Cape Mt. Range, Kala-Fatlar Mt., Izumrudnaya Cave, 20.III.2016, O.V. Kukushkin leg. • 1 ♀ (TNU 10287/5), Crimea, nr Sevastopol, Tshernaya River canyon, entrance to Tshernoretshenskaya Cave, 3.VI.2021, I.S. Turbanov, A.A. Nadolny leg.

Distribution. Cosmopolite (Kovblyuk and Kastrygina 2015; Nentwig et al. 2024).

Records from the Crimean caves. Map (Fig. 17A – white circle). Izumrudnaya Cave on Kala-Fatlar Mt. of the Aya Cape Mt. Range and Tshernoretshenskaya Cave nr Sevastopol (present data).

Ecology. A troglophile and synanthropic species (Nentwig et al. 2024). In Crimea, it has been recorded everywhere as a synanthropic, except for the southern coast where it occurs in natural habitats (Kovblyuk and Kastrygina 2015). In the Crimean caves, the ecological association of *S. triangulosa* remains unclear. Since we have collected only two specimens from the entrances of Tshernoretshenskaya and Izumrudnaya caves, it is likely to be a subtroglophile.

Discussion

A total of 20 spider species in eight families have been discovered in the Crimean caves. Of these species, four have Crimean caves as their type locality: viz., *Tegenaria taurica* and *Palliduphantes khobarum* (see Charitonov 1947a), *Bisetifer tactus* sp. nov., and *Troglohyphantes exspectatus* sp. nov. The dubious record of ?*Tenuiphantes zimmermani* (Evtushenko 2004; Zagorodniuk and Vargovitsh 2004) is not taken into account, as it requires confirmation.

According to the literature-derived and present data, spiders have been recorded in 40 caves of the Crimean Mountains (see Fig. 17), accounting for just 2.5% of all the known karst cavities (Amelichev et al. 2014). The highest spider diversity was recorded in Tshernoretshenskaya and Kizil-Koba Caves, each with seven species (Fig. 17).

Based on the study of local populations, cave spiders in Crimea are classified into four ecological groups:

1. Troglobionts – a single species, *Bisetifer tactus* sp. nov. It has clear troglomorphic features, such as the almost completely reduced eyes. This is only the second true troglobiont spider species with reduced eyes from the caves of the former USSR; the first was *Iberina* (?) *ljovuschkini* Pichka, 1965 found in Shakalya Cave (the West Caucasus, Russia) (Pichka 1965), currently considered a nomen dubium (Růžička 2022);
2. Eutroglophiles – six species, *Tegenaria taurica*, *Bisetifer gruzin*, *Caviphantes dobrogicus*, *Palliduphantes khobarum*, *Troglohyphantes exspectatus* sp. nov., and *Meta bourneti*. They do not possess noticeable troglomorphic features, but in Crimea they are confined to caves only and/or are capable of maintaining stable subterranean populations;
3. Subtroglophiles – nine species. They can be subdivided into three groups: (i) native subtroglophilous species: *Tegenaria lapicidinarum*, *Lepthyphantes leprosus*, *Megalepthyphantes nebulosus*, *Metellina merianae*, and *Steatoda triangulosa*, which are known from both caves and epigeic habitats, repeatedly reported by other researchers as troglophiles; (ii) cosmopolitan subtroglophilous species: *Tegenaria parietina* and *Pholcus phalangioides*, which in Crimea are not a native but rather facultative synanthropic species, because they occur in the caves that have been used for economic human activities; (iii) subtroglophiles unintentionally introduced: *Aituaria borutzkyi* and *A. pontica*, locally established as facultative synanthropes in caves that were used for economic human activities;
4. Trogloxenes – four species, *Amaurobius erberi*, *Megalepthyphantes pseudocollinus*, *Alopecosa farinosa*, and *Metellina segmentata*. They accidentally appear in caves, since their life cycles are not associated with subterranean biotopes; they have not been reported for subterranean biotopes previously, or indicated by other researchers as trogloxenes in other parts of their ranges.

In his review, Charitonov (1947a) characterised the araneofauna of the Crimean caves as "*Tegenaria–Lephthyphantes*" (under the name *Lephthyphantes* was meant *Palliduphantes khobarum*) and contrasted it with the araneofauna of Caucasus caves, which he termed "*Nesticus–Troglohyphantes*" (under the name *Nesticus* were meant various members of the family Nesticidae). As another important feature, he considered the Crimean cave araneofauna conflicted with the data on other arthropod groups (because no troglobiont spiders were found), and only further study of the Crimean caves would be able to change this situation or give an opportunity to explain it correctly. Thus, based on the review of the cave biota of the former USSR (Turbanov 2016a, b, c) and taking into account more recent taxonomic works (Golovatch et al. 2017; Vinarski and Palatov 2019; Sendra et al. 2020; Turbanov and Kolesnikov 2020, 2021; Marin et al. 2022), the Crimean caves have most likely acted as glacial refugia for many of troglo- and stygomorphic invertebrates, as suggested by more than 50 reported species, including mainly crustaceans, pseudoscorpions, millipedes, diplurans, springtails, and beetles. Yet, Kovblyuk (2014) pointed out the low species diversity and lack of endemics of the araneofauna of the Crimean caves. As an explanation, he suggested that the ancient cave fauna became extinct during marine transgressions and karst flooding, and that the modern cave fauna consists of species that have colonised the peninsula relatively recently. Based on the new data, it seems possible to partially answer the questions raised by Charitonov (1947a) and Kovblyuk (2014) and thereby in general provide a possible reconstruction of the genesis of the araneofauna of the Crimean caves.

The bulk, 80%, of the spider species considered are widespread, with cosmopolitan, Holarctic, trans-Palaearctic, West and Central Palaearctic, East European or East Mediterranean ranges: *Aituaria borutzkyi*, *A. pontica*, *Alopecosa farinosa*, *Caviphantes dobrogicus*, *Tegenaria lapicidinarum*, *T. parietina*, *Amaurobius erberi*, *Lepthyphantes leprosus*, *Meta bourneti*, *Megalepthyphantes nebulosus*, *M. pseudocollinus*, *Metellina merianae*, *M. segmentata*, *Palliduphantes khobarum*, *Pholcus phalangioides*, *Steatoda triangulosa*. At present, we have no data for these species to establish the chronology of their colonisation across Crimea. It is possible that the scenario indeed conforms to Kovblyuk's (2014) speculation that most species colonised Crimea during the multiple Pleistocene-Holocene regressions of the Black Sea basin, when shelf zoogeographic corridors between Crimea, the Caucasus and the Balkans opened up. However, we believe that four synanthropic species – *Aituaria borutzkyi*, *A. pontica*, *Tegenaria parietina*, and *Pholcus phalangioides* – entered the Crimean caves during historical times Further considerations on the history of the cave araneofauna will be based on analysing the distribution of species with restricted ranges: viz., the three Crimean endemics, *Tegenaria taurica*, *Bisetifer tactus* sp. nov., and *Troglohyphantes exspectatus* sp. nov., and the Crimean-Caucasian subendemic *Bisetifer gruzin*.

The genesis of cave habitats is known to occur simultaneously with the formation of the caves themselves (Prokopov and Turbanov 2017). The recent relief of the Crimean Mountains was formed in the late Pliocene and Pleistocene periods (Muratov and Nikolaev 1940; Muratov 1954; Vakhrushev 2010), which determined the predominantly Pleistocene age of the Crimean karst (Dublyansky 1966, 1977; Vakhrushev 2010; Klimchouk et al. 2009, 2012; Amelichev et al. 2016). It is assumed that global climate changes associated with glacial periods and interglacials initiated colonisation of karst cavities (Jeannel 1959; Vandel 1964). Most likely, the terrestrial troglobiont fauna could have originated from forest litter dwellers. Cold periods, the development of ice shield, even locally, could have led a number of species to shelter in karst cavities, where the temperature regime was more stable (Jeannel 1965). Presumably the ancestral forms of the eutroglophilic spiders *Tegenaria taurica* and *Troglohyphantes exspectatus* sp. nov. and the troglobiont spider *Bisetifer tactus* sp. nov. were more widely distributed.

The species that are most morphologically related to *Tegenaria taurica* have relatively large ranges in the Western Palaearctic: *T. ferruginea* (Panzer, 1804), *T. lapicidinarum*, and *T. parietina* (Nentwig et al. 2024). The current distribution of *T. taurica* in the Crimean Mountains is limited to the caves of the western and central karst massifs (see Fig. 17A – orange circle), which finally lost their geological and hydrological connections with each other in the late Pleistocene (Klimchouk 2009). This seems to indicate that, under the influence of global climate change, there has been a relatively recent (the late Pleistocene – early Holocene) simultaneous penetration of ancestral epigeic species in these isolated karst massifs. Furthermore, the caves of Montenegro on the Balkan Peninsula harbour a local endemic eutroglophile *T. gordani* Komnenov, 2020, which is morphologically very close to *T. taurica* (see Komnenov 2020). Their close relationships and restricted distribution (both are local endemics) are likely to reflect similar scenarios of their origin from a common widespread ancestor at the same time (late Pleistocene).

The genus *Bisetifer* has the Crimean-Caucasian range (Tanasevitch et al. 2015). In the Caucasus, both *Bisetifer* species inhabit humid epigeic microbiotopes (Tanasevitch 1987; Tanasevitch et al. 2015). The common to Crimea and the Caucasus, *B. gruzin* occurs only in the Crimean caves, which, in our opinion, could indicate its recent (probably the early Holocene) zoogeographic connections. Yet, due to the drier climate of Crimea in the late Holocene, this species appears to have used caves as more mesophilic habitats, while its epigeic populations may have become extinct.

According to Isaia et al. (2017), the large genus *Troglohyphantes* has an ancient Mediterranean origin and some of its species occur in epigeic habitats. Thus, *T. exspectatus* sp. nov. is morphologically closest to the Balkan local endemic troglobiont *T. drenskii*, as well as to the Caucasian troglophile *T. deelemanae* and the epigeic *T. adjaricus*, which may indicate the ancient (Pleistocene) Eastern Mediterranean biogeographical connections in this genus.

Both newly described species, *B. tactus* sp. nov. and *T. exspectatus* sp. nov., have narrow distribution and are known only from their type localities. The microclimatic conditions of the caves where the new species were discovered seems to be unique for surviving some species, making these caves a kind of Pleistocene refugia.

Bisetifer tactus sp. nov. is described from the small horizontal Tshernoretshenskaya Cave (length 87 m) situated in the central part of the Tshernaya River canyon, the south-western Crimea (see Fig. 18). This is the only known cave in the canyon with stable microclimatic conditions – high relative humidity and a very static annual temperature in the range from 10.5 °C to 12.4 °C (present data). Such uniquely stable conditions are possible due to a small entrance and the presence of a permanent small watercourse (see Fig. 18B). All other caves of the Tshernaya River Canyon differ from Tshernoretshenskaya Cave in having large entrances, shorter lengths, lacking watercourses, and higher seasonal fluctuations in relative air humidity and temperatures: e.g., in Tomenko Cave from 2 °C to 21 °C, Azis-Koba (= Kara-Koba) Cave from 4 °C to 17 °C (present data).

Troglohyphantes exspectatus sp. nov. is described from the small vertical Druzhba Cave (depth 45 m), which is located in the southern cliffs of Mortsheka Mt., the west part of Ai-Petri Yaila, the south-western Crimea (see Fig. 19). This is the only cave in the area at hand with stable microclimatic conditions: a high relative humidity and very static annual temperature ranging from 9.7 °C to 12.5 °C (present data). These unique conditions are possible due to cave structure as well: the small entrance and the cave's position on cliffs of the southern macroslope, which contributes to the warm climatic conditions of the site. In comparison, the horizontal Honey Cave is nearby on the same slope but due to its huge entrance, it experiences seasonal fluctuations in relative humidity and temperature from 2.3 °C to 12.2 °C (present data). There are several vertical caves on the plateau of Mortsheka Mt., near Druzhba Cave. They also have relatively stable humidity, but because of the remoteness from the

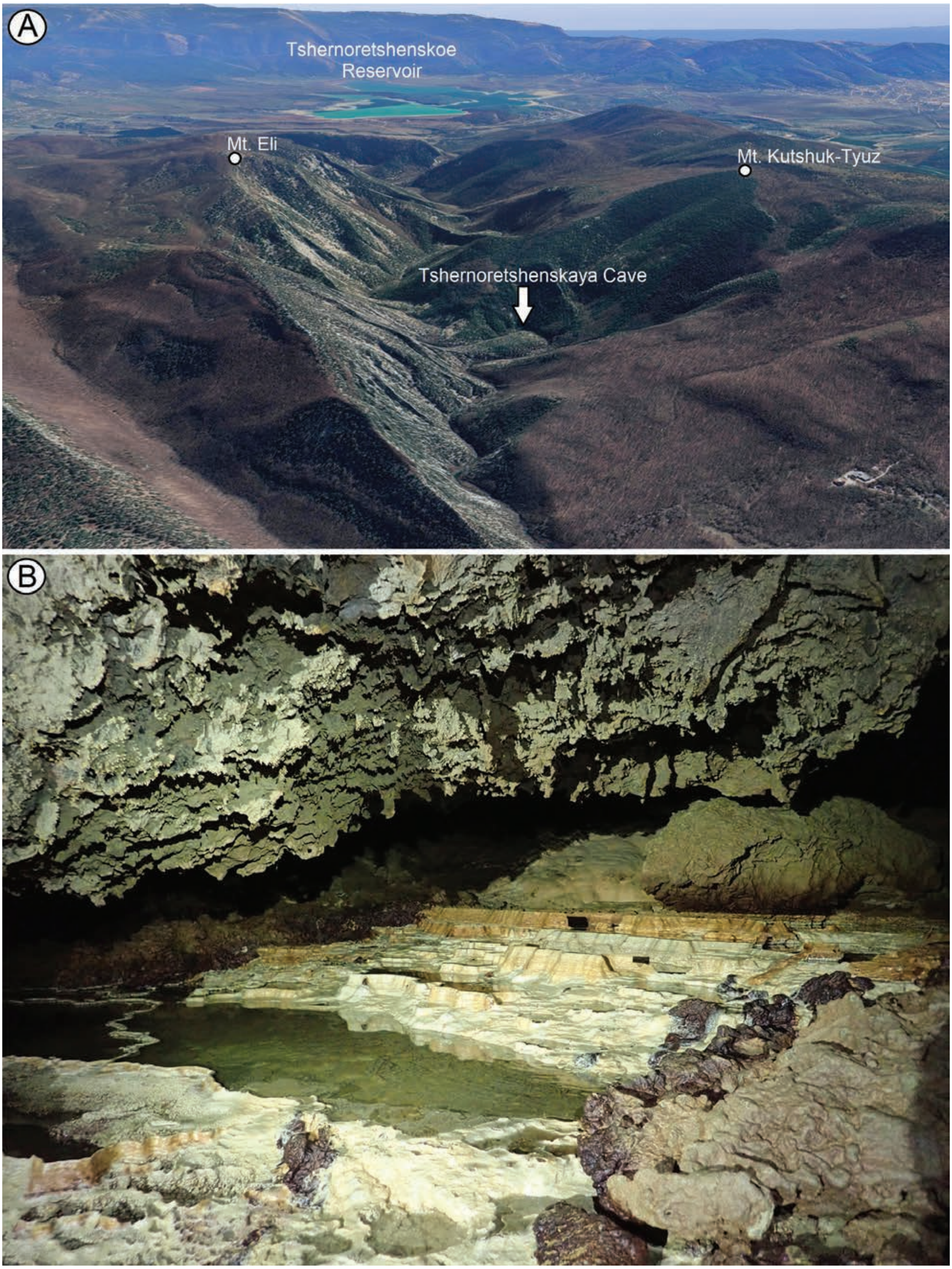

Figure 18. Location and biotope of the type locality of *Bisetifer tactus* sp. nov.: **A** map with type locality showing the entrance of Tshernoretshenskaya Cave (from Google Earth Pro) **B** biotope inhabited by the new species in Tshernoretshenskaya Cave (photographs by IST).

Figure 19. Location and biotope of the type locality of *Troglohyphantes exspectatus* sp. nov. **A** map with type locality showing the entrance of Druzhba Cave (from Google Earth Pro) **B** biotope inhabited by the new species in Druzhba Cave (photographs by Yu.S. Balakhtinova).

well-warmed edge of the southern cliff, the temperature inside them is lower: e.g., Akvalangistitsheskaya Cave, depth 80 m, temperatures range from 5.9 °C to 7.0 °C (present data). Thus, it seems possible to characterise *B. tactus* sp. nov. and *T. exspectatus* sp. nov. as stenobiont species inhabiting at relatively high humidity and rather static and comparatively high temperatures. The caves in which they occur are probably a refuge for Pleistocene thermophilic fauna.

Acknowledgments

The authors express their sincere gratitude to: Kirill G. Mikhailov (ZMMU, Moscow, Russia) and Mykola M. Kovblyuk (TNU, Simferopol, Crimea) for the possibility of deposit types and examined materials in the museum collections under their care; Olga L. Makarova, Kirill V. Makarov (Moscow, Russia), Oleg V. Kukushkin (Feodosia – Sevastopol, Crimea) and Sergey V. Arefyev (Sevastopol, Crimea) for providing spiders collected in the Crimean caves; Grigoriy A. Prokopov (Simferopol, Crimea) for providing photos of spiders and Yulia S. Balakhtinova (Yalta – Sevastopol, Crimea) for providing photo of Druzhba Cave; Alexandr G. Koval (St Petersburg, Russia) for editing and commenting on an early draft; Dmitri V. Logunov (St Petersburg, Russia and Manchester, United Kingdom) for editing the English of the first draft; Miquel A. Arnedo (Barcelona, Spain), Martina Pavlek (Zagreb, Croatia) and Christo Deltshev (Sofia, Bulgaria) for manuscript review and valuable remarks that significantly improved this publication.

Additional information

Conflict of interest

The authors have declared that no competing interests exist.

Ethical statement

No ethical statement was reported.

Funding

The research was performed in the framework of the state assignment of the Ministry of Education and Science of the Russian Federation: Anton A. Nadolny (No. 124022400148-4) and Ilya S. Turbanov (No. 124032500016-4).

Author contributions

Conceptualization: AAN, IST. Investigation: AAN, IST. Writing – original draft: AAN, IST.

Author ORCIDs

Anton A. Nadolny https://orcid.org/0000-0001-5555-1721
Ilya S. Turbanov https://orcid.org/0000-0001-9441-2791

Data availability

All of the data that support the findings of this study are available in the main text.

References

Amelichev G, Shkvyrya M, Nedrya Y (2004) Description of the caves of Mountain Crimea. In: Zagorodniuk I (Ed.) The Cave Fauna of Ukraine. Kiev, 131–143. [in Ukrainian]

Amelichev GN, Klimchouk AB, Tokarev SV, Memetova EI (2014) The Cadaster of karst caverns of the Crimea: past, present and future. Geopolitics and ecogeodynamics of regions 10(1): 345–351. [in Ukrainian]

Amelichev GN, Timokhina EI, Tokarev SV (2016) Towards identifying hypogene karst on the main ridge of the Crimean Mountains. Proceedings of the XXXV Plenum of the Geomorphological Commission of the Russian Academy of Sciences “Theory and

Methods of Recent Geomorphology". Vol. 1. October 3–8, 2016, Simferopol, 159–165. [in Russian with English summary]

Birstein JA (1963) Some results of research of the subterranean fauna of Crimea. Proceedings of the Complex Karst Expedition of the USSR Academy of Sciences. Issue 1. USSR Academy of Sciences, Kiev, 123–134. [in Russian]

Bolzern A, Burckhardt D, Hanggi A (2013) Phylogeny and taxonomy of European funnel-web spiders of the *Tegenaria-Malthonica* complex (Araneae: Agelenidae) based upon morphological and molecular data. Zoological Journal of the Linnean Society 168: 723–848. https://doi.org/10.1111/zoj.12040

Brignoli PM (1980) Secondo contributo alla conoscenza dei ragni cavernicoli della Jugoslavia (Araneae). Revue Suisse Zoologie 87(1): 183–192. https://doi.org/10.5962/bhl.part.85542

Charitonov DE (1932) Catalog of Russian spiders. Publishing House of the Academy of Sciences of the USSR, Leningrad, 206 pp. [Appendix to vol. 32 of the Annuaire du Musée Zoologique de l'Académie des Sciences] [In Russian]

Charitonov DE (1936) An addition to the catalogue of Russian spiders. Scientific notes of the Perm Institute 2(1): 167–225. [In Russian with German summary]

Charitonov DE (1939) About cave spiders of Abkhazia. Materials for the fauna of Abkhazia. Publishing House of the Georgian Branch of the Academy of Sciences of the USSR, Tbilisi, 197–211.

Charitonov DE (1947a) Contribution to the fauna of spiders Crimean caves. Speleological Bulletin Natural History Institute at M. Gorky State University, Molotov 1: 43–54. [In Russian, with English summary]

Charitonov DE (1947b) To the fauna of spiders of the Crimean caves. Abstracts of reports of the karst-speleological conference. Natural Science Institute, Molotov, 1–2. [In Russian]

Chikin AM (2005) Maksimova Datsha. Biblex, Sevastopol, 152 pp. [In Russian]

Deeleman-Reinhold CL (1978) Revision of the cave-dwelling and related spiders of the genus *Troglohyphantes* Joseph (Linyphiidae), with special reference to the Yugoslav species. Opera Academia Scientiarum et Artium Slovenica (Classis IV), Ljubljana 23(6): 1–221.

Deli OF, Kovtun OA, Pronin KK (2017) Preliminary data on the species composition of spiders (Araneae) from the catacombs in the city of Odessa, Ukraine. Materials of the II All-Russia Youth Conference "Biospeleological studies in Russia and neighbouring states", Moscow, December 1–2, 2017. Filigran, Yaroslavl, 25–29. [in Russian with English summary]

Deltshev C (1973) A new *Troglohyphantes* from Bulgarian caves (Araneae, Linyphiidae). International Journal of Speleology 5: 103–109. https://doi.org/10.5038/1827-806X.5.2.1

Dublyansky VN (1966) Age of the deep karst cavities of the Mountain Crimea. Peshchery 6(7): 70–81. [in Russian]

Dublyansky VN (1977) Karst Caves and Mines of the Mountain Crimea (Genesis, Sediments, Hydrogeological Significance). Nauka, Leningrad, 183 pp. [in Russian]

Dumitrescu M, Miller F (1962) *Lessertiella dobrogica* n. gen. n. sp. araignée endémique de la grotte "Peștera Liliecilor dela Gura Dobrogei" (Aranea). Časopis Československé Společnosti Entomologické 59: 165–173.

Esyunin SL (2017) New data on *Aituaria pontica* (Spassky, 1932) (Aranei: Nesticidae). Arthropoda Selecta 26(3): 241–243. https://doi.org/10.15298/arthsel.26.3.05

Esyunin SL, Farzalieva GSh (2001) Redescription of *Tegenaria taurica* Charitonov, 1947 (Aranei: Agelenidae). Arthropoda Selecta 10(3): 261–263.

Evtushenko K (2004) Spiders (Aranei). In: Zagorodniuk I (Ed.) The Cave Fauna of Ukraine. Kiev, 64–68. [in Ukrainian]

Fomichev AA, Ballarin F, Marusik YM (2022) A new genus of the family Nesticidae (Arachnida: Aranei) from the Caucasus. Arthropoda Selecta 31(1): 99–110. https://doi.org/10.15298/arthsel.31.1.12

Golovatch SI, Turbanov IS, VandenSpiegel D (2017) Contributions to the cave millipede fauna of the Crimean Peninsula (Diplopoda), with the description of a new species. Arthropoda Selecta 26(2): 103–111. https://doi.org/10.15298/arthsel.26.2.02

Herzen AG, Makhneva-Chernets OA (2006) Cave towns of Crimea. Guide. Sevastopol, Bybleks, 192 pp. [in Russian]

Huber BA (2011) Revision and cladistic analysis of *Pholcus* and closely related taxa (Araneae, Pholcidae). Bonner Zoologische Monographien 58: 1–509.

Isaia M, Paschetta M, Lana E, Pantini P, Schonhofer AL, Christian E, Badino G (2011) Subterranean arachnids of the Western Italian Alps (Arachnida: Araneae, Opiliones, Palpigradi, Pseudoscorpiones). Monografie del Museo di Scienze Naturali, Torino, 47: 1–325.

Isaia M, Mammola S, Mazzuca P, Arnedo MA, Pantini P (2017) Advances in the systematics of the spider genus *Troglohyphantes* (Araneae, Linyphiidae). Systematics and Biodiversity 15(4): 307–326. https://doi.org/10.1080/14772000.2016.1254304

Isaia M, Mammola S, Arnedo MA (2023) A relict subterranean spider (Araneae: Linyphiidae: *Troglohyphantes*) reveals a unique component of the biogeography of Corsica. Insect Systematics and Diversity 7(3): 1–16. https://doi.org/10.1093/isd/ixad008

Jeannel R (1959) Situation geographique et peuplement des cavernes. Annales de spéléologie 14: 333–338.

Jeannel R (1965) Le genèse du peuplement des milieux souterrains. Revue d'ècologie et biologie du sol 2: 1–22.

Klimchouk AB (2009) Epikarst: hydrogeology, morphogenesis, and evolution. Simferopol, Sonat. 112 pp. [in Russian]

Klimchouk AB, Amelichev GN, Tymokhina EI (2009) Karst features of the south-west part of the Piedmont Crimea from the standpoint of the theory of hypogene speleogenesis. Speleology and Karstology 2: 35–53. [in Russian with English summary]

Klimchouk AB, Tymokhina EI, Amelichev GM, Dublyansky YuV, Staubwasser M (2012) Age of the relief of the Inner range of the Mountainous Crimea according to the U/T h dating of the calcite deposit s of karst cavities. Reports of the National Academy of Sciences of Ukraine 7: 88–96. [in Russian with English summary]

Komnenov M (2020) Subterranean spiders (Arachnida, Araneae) of Montenegro. The Montenegrin Academy of Sciences and Arts, Proceedings of the Section of Natural Sciences 23: 119–169.

Kovblyuk NM (2002) On the issue of endemism of Crimean spiders (Arachnida, Aranei). Reserves of the Crimea. Biodiversity in priority areas: 5 years after Gurzuf. Materials of the II scientific conference, Simferopol, April 25–26, 2002. CSMU, Simferopol, 103–109. [in Russian]

Kovblyuk NM (2004a) Catalog of spiders (Arachnida: Aranei) of the Crimea. Questions of development of the Crimea. Scientific and Practical Discussion and Analytical Collection, 15 (Problems of Inventory of the Crimean Biota), Tavria-Plus, Simferopol, 211–262. [in Russian]

Kovblyuk NM (2004b) Redescription and synonymy of *Tegenaria lapicidinarum* (Aranei, Agelenidae). Vestnik Zoologii 38(3): 43–51. [in Russian with English summary]

Kovblyuk NM (2004c) A survey of spider species with Crimeo-Caucasian disjunct ranges (Arachnida, Araneae). In: F Samu and Cs Szinetar (Eds) European Arachnology 2002. Plant Protection Institute & Berzsenyi College, Budapest, 251–258.

Kovblyuk NM (2007) New data on the spiders (Aranei) of the Crimea. Problems and perspectives of general entomology. Abstracts of the XIII-th Congress of Russian Entomological Society, Krasnodar, September 9–15, 2007. Krasnodar, 152–153.

Kovblyuk NM (2010) Diversity and endemism of spiders (Arachnida: Araneae) of the Crimean Peninsula, Ukraine. Book of abstracts of the 18th International Congress of Arachnology, Siedlce, 11–17 July 2010, University of Podlasie & International Society of Arachnology, Siedlce, 224–226.

Kovblyuk NM (2014) Spiders (Arachnida, Aranei) of Crimea: faunogenesis and hypothesis of Pontida. Ukrainska Entomofaunistyka 5(2): 29–53. [In Russian, with English summary]

Kovblyuk MM, Kastrygina ZA (2015) Updated catalogue of the spiders (Arachnida, Aranei) of the Crimea. Ukrainska Entomofaunistyka 6(2): 1–81. [In Russian, with English summary]

Kovblyuk MM, Gnelitsa VA, Nadolny AA, Kastrygina ZA, Kukushkin OV (2016). Spiders (Arachnida: Aranei) of the Karadag Nature Reserve (Crimea). Ekosistemy 3: 3–288. [In Russian]

Lebedinsky Ya (1904) To the fauna of the Crimean caves. Continuation. Notes of the Novorossiysk Society of Naturalists 25(2): 75–88. [2 pls.] [In Russian]

Lebedinsky Ya (1914) To the fauna of the Crimean caves 40 (1): 113–128. [2 pls.] [In Russian]

Mammola S, Isaia M (2014) Niche differentiation in *Meta bourneti* and *M. menardi* (Araneae, Tetragnathidae) with notes on the life history. International Journal of Speleology 43(3): 343–353. https://doi.org/10.5038/1827-806X.43.3.11

Mammola S, Cardoso P, Ribera C, Pavlek M, Isaia M (2018) A synthesis on cave-dwelling spiders in Europe. Journal of Zoological Systematics and Evolutionary Research 56(1): 301–316. https://doi.org/10.1111/jzs.12201

Marin IN, Turbanov IS, Prokopov GA, Palatov DM (2022) A new species of the genus *Niphargus* Schiödte, 1849 (Crustacea: Amphipoda: Niphargidae) from groundwater habitats of the Tarkhankut Upland, Crimean Peninsula. Diversity 14(12): 1010. https://doi.org/10.3390/d14121010

Marusik YM, Fedoriak MM, Koponen S, Prokopenko EV, Voloshyn VL (2017) Taxonomic notes on two species of Nesticidae (Arachnida: Araneae) in the Ukraine, with the first description of the male of *Carpathonesticus eriashvilii*. Arachnology 17(6): 302–308. https://doi.org/10.13156/arac.2017.17.6.302

Mikhailov KG (1997) Catalogue of the spiders of the territories of the former Soviet Union (Arachnida, Aranei). Zoological Museum of the Moscow State University, Moscow, 416 pp.

Mikhailov KG (1998) Catalogue of the spiders (Arachnida, Aranei) of the territories of the former Soviet Union. Addendum 1. KMK Scientific Press Ltd, Moscow, 50 pp.

Mikhailov KG (2013) The spiders (Arachnida: Aranei) of Russia and adjacent countries: a non-annotated checklist. Arthropoda Selecta, Supplement 3. KMK Scientific Press, Moscow, 262 pp.

Mkheidze TS (1997) Spiders of Georgia (systematics, ecology, zoogeographic review). Tbilisi University, Tbilisi, 390 pp. [in Georgian]

Mokrzecki SA (1914) Crimean fauna. In: Bumber KYu et al. (Eds) Crimea. Guidebook. Printing house of the Tauride provincial zemstvo, Simferopol, 73–103. [In Russian]

Muratov MV (1954) About Miocene and Pliocene history of development of the Crimean Peninsula. Bulletin of the Moscow Society of Naturalists. Department of Geology 29(1): 4–20. [in Russian]

Muratov MV, Nikolaev NI (1940) Quaternary history and development of relief of the Mountain Crimea. Scientific Notes of Moscow State University 48: 65–73 [in Russian]

Myts VL (1991) Fortifications of Taurica X–XV centuries. Naukova Dumka, Kyiv, 162 pp.

Nadolny AA, Kovblyuk MM (2007) *Carpathonesticus borutzkyi*, the first record of Nesticidae from the Crimea (Aranei: Nesticidae). Arthropoda Selecta 15(4): 291–294.

Nadolny AA, Turbanov IS (2014) The first record of *Aituaria pontica* (Aranei, Nesticidae) in the Crimea. Vestnik Zoologii 48(6): 569.

Nentwig W, Blick T, Bosmans R, Gloor D, Hänggi A, Kropf C (2024) Spiders of Europe. https://www.araneae.nmbe.ch [accessed 21 July 2024]

Novikov MM (1912) Skelskaya stalactite cave and its fauna. Notes of the Crimean Society of Naturalists and Nature Lovers 1: 97–109. [In Russian]

Pankov NN, Starova OS, Pankova NV (2009) The invertebrate animals of the Perm Region caves: fauna, ecological structure, horology, and seasonal dynamics. Peshchery (Caves): Collection of scientific transactions, Perm, 31: 144–155. [In Russian, with English summary]

Pichka VE (1965) On the spider fauna of the caves in the West Transcaucasia. Zoologicheskiy Zhurnal 44: 1190–1196. [In Russian, with English summary]

Polchaninova NYu, Prokopenko EV (2013) Catalogue of the spiders (Arachnida, Aranei) of Left-Bank Ukraine. Arthropoda Selecta, Supplement 2. KMK Scientific Press, Moscow, 268 pp.

Prokopov GA, Turbanov IS (2017) To the question of speleofauna formation in the Crimean Peninsula. Materials of the II All-Russia Youth Conference “Biospeleological studies in Russia and neighbouring states”, Moscow, December 1–2, 2017. Filigran, Yaroslavl, 99–106. [in Russian with English summary]

Růžička V (2022) A review of the spider genus *Iberina* (Araneae, Hahniidae). Zootaxa 5133(4): 555–566. https://doi.org/10.11646/zootaxa.5133.4.6

Samokhin GV, Turbanov IS (2019) Skelskaya Cave. In: Shelepin AL et al. (Eds) Atlas of caves of Russia. Russian Geographical Society, Russian Union of Speleologists. Moscow, 230–233. [in Russian]

Samokhin GV, Shelepin AL, Turbanov IS (2019) Kizil-Koba Cave (Krasnaya) In: Shelepin AL et al. (Eds) Atlas of caves of Russia. Russian Geographical Society, Russian Union of Speleologists. Moscow, 242–253. [in Russian]

Sendra A, Antić D, Barranco P, Borko Š, Christian E. Delić T, Fadrique F, Faille A, Galli L, Gasparo F, Georgiev D, Giachino PM, Kováč L, Lukić M, Marcia P, Miculinić K, Nicolosi G, Palero F, Paragamian K, Pérez T, Polak S, Prieto CE, Turbanov I, Vailati D, Reboleira ASPS (2020) Flourishing in subterranean ecosystems: Euro-Mediterranean Plusiocampinae and tachycampoids (Diplura, Campodeidae). European Journal of Taxonomy 591: 1–138. https://doi.org/10.5852/ejt.2020.728.1181

Sket B (2008) Can we agree on an ecological classification of subterranean animals? Journal of Natural History 42(21–22): 1549–1563. https://doi.org/10.1080/00222930801995762

Spassky SA (1927) Materials for the spider fauna of the Tauride Province. Proceedings of the Don Institute of Agriculture and Land Reclamation, Novocherkassk 7: 66–80. [in Russian with French summary]

Spassky SA (1936) New species and genera of spiders for the USSR. Proceedings of the Zoological Institute of the Academy of Sciences of the USSR, 3: 533–536. [in Russian]

Tanasevitch AV (1987) The linyphiid spiders of the Caucasus, USSR (Arachnida: Araneae: Linyphiidae). Senckenbergiana Biologica 67: 297–383.

Tanasevitch AV, Ponomarev AV, Chumachenko YuA (2015) Notes on the spider genus *Bisetifer* Tanasevitch, 1987 (Aranei: Linyphiidae), with the description of a new species. Arthropoda Selecta 24(4): 445–450. https://doi.org/10.15298/arthsel.24.4.08

Turbanov IS, Kolesnikov VB (2020) Two new cave-dwelling species of the false scorpion genus *Pseudoblothrus* Beier, 1931 (Arachnida: Pseudoscorpiones: Syarinidae) from the Crimean Peninsula. Arthropoda Selecta 29(10): 28–50. https://doi.org/10.15298/arthsel.29.1.03

Turbanov IS, Kolesnikov VB (2021) Three new hypogean species of the false scorpions genus *Ephippiochthonius* Beier, 1930 (Arachnida: Pseudoscorpiones: Chthoniidae) from the Crimean Peninsula. Arthropoda Selecta 30(2): 193–204. https://doi.org/10.15298/arthsel.30.2.06

Turbanov IS, Nadolny AA (2017) Some data on the species composition of spiders (Aranei) in caves of the Western Caucasus. Materials of the II All-Russia Youth Conference “Biospeleological studies in Russia and neighbouring states”, Moscow, December 1–2, 2017. Filigran, Yaroslavl, 113–117. [in Russian with English summary]

Turbanov IS, Palatov DM, Golovatch SI (2016a) The present state of the art of biospeleology in Russia and the countries of the former Soviet Union: a review of the cave (endogean) invertebrate fauna. 1. Introduction—Crustacea. Zoologicheskiy Zhurnal 95(10): 1136–1159. [In Russian, with English summary] https://doi.org/10.7868/S0044513416110064

Turbanov IS, Palatov DM, Golovatch SI (2016b) The present state of the art of biospeleology in Russia and the countries of the former Soviet Union: a review of the cave (endogean) invertebrate fauna. 2. Arachnida – Acknowledgments. Zoologicheskiy Zhurnal 95(11): 1283–1304. [In Russian, with English summary] https://doi.org/10.7868/S0044513416100093

Turbanov IS, Palatov DM, Golovatch SI (2016c) The present state of the art of biospeleology in Russia and the countries of the former Soviet Union: a review of the cave (endogean) invertebrate fauna. 3. References. Zoologicheskiy Zhurnal 95(12): 1399–1426. [In Russian, with English summary] https://doi.org/10.7868/S0044513416120187

Turbanov IS, Kebets SN, Amelichev GN (2019a) Mamut-Tshokrak Cave. In: Shelepin AL et al. (Eds) Atlas of caves of Russia. Russian Geographical Society, Russian Union of Speleologists. Moscow, 217–222. [in Russian]

Turbanov IS, Kukushkin OV, Vargovitsh RS (2019b) Amphibians and reptiles in the subterranean cavities of the Crimean Mountains. Russian Journal of Herpetology 26(1): 29–53. https://doi.org/10.30906/1026-2296-2019-26-1-29-53

Turbanov IS, Nadolny AA, Turbanova AA (2021) To the study of arthropods of Tavrida Cave, Crimea. Invertebrate Zoology 18(2): 177–185. https://doi.org/10.15298/invertzool.18.2.08

Tyshchenko VP (1971) Key to spiders in the European part of the USSR. Keys to the fauna of the USSR, published by the Zoological Institute of the Academy of Sciences of the USSR. Issue 109. Nauka, Leningrad, 281 pp. [In Russian]

Vakhrushev BO (2010) Crimean Mountains. In: Stetsyuk VV (Ed.) Relief of Ukraine: textbook. Slovo, Kyiv, 432–485. [in Ukrainian]

Vandel A (1964) Biospéologie. La Biologie des Animaux Cavernicoles. Paris, Gauthier-Villars, 679 pp.

Vinarski MV, Palatov DM (2019) A survey of the *Belgrandiella*-like gastropods of the northern Black Sea region (Mollusca, Gastropoda, Hydrobiidae s. l.): morphological variability and morphospecies. Zoologicheskiy Zhurnal 98(9): 988–1002. https://doi.org/10.1134/S0044513419070122

WSC (2024) World Spider Catalog. Version 25.5. Natural History Museum Bern. https://doi.org/10.24436/2 [accessed on 21 July 2024]

Zagorodniuk I, Vargovitsh R (2004) Checklist of cave fauna of Ukraine. In: Zagorodniuk I (Ed.) The cave fauna of Ukraine. Kiev, 191–216. [in Ukrainian]

ZooKeys 1230: 81–97 (2025)
DOI: 10.3897/zookeys.1230.141900

Research Article

New records of leaf-miner flies (Diptera, Agromyzidae) from Morocco

Mourad Doukale Daief[1], Michael von Tschirnhaus[2], Kawtar Kettani[1]

1 *Laboratory of Ecology, Systematics and Conservation of Biodiversity (LESCB), URL-CNRST N°18, FS, Abdelmalek Essaadi University, Tetouan, Morocco*
2 *Faculty of Biology, Biological Collection, University of Bielefeld, P.O. Box 100 131, 33501 Bielefeld, Germany*
Corresponding author: Mourad Doukale Daief (mouraddoukale@gmail.com)

Abstract

New records are provided of the family Agromyzidae (leaf-miner flies) from Morocco. Thirty agromyzid species are newly recorded, seven of these in Agromyzinae: *Agromyza* (*Agromyza anthracina*, *A. conjuncta*, *A. mobilis*, *A. myosotidis*, *A. nigrescens*), *Hexomyza* (*H. simples*), and *Ophiomyia* (*O. pinguis*). The other 23 new records are in Phytomyzinae: *Amauromyza* (*Cephalomyza*) *karli*, *Calycomyza flavomaculata*, *C. solidaginis*, *Cerodontha* (*Butomomyza*) *eucaricis*, *C.* (*Dizygomyza*) *luctuosa*, *C.* (*Icteromyza*) *geniculata*, *Chromatomyia centaurii*, *Liriomyza amoena*, *L. brassicae*, *L. strigata*, *Phytoliriomyza arctica*, *P. perpusilla*, *P. pteridii*, *Phytomyza anemones*, *Ph. clematidis*, *Ph. crassiseta*, *Ph. notata*, *Ph. plantaginis*, *Ph. rufipes*, *Ph. vitalbae*, *Pseudonapomyza confusa*, *Ps. palavae*, and *Ps. vota*. The genus *Calycomyza* Hendel is newly reported from the country. The present study is based on recent entomological surveys and has increased the total number of agromyzid species in Morocco to 92. Information on the distribution and ecology of each species is provided.

Key words: Agromyzidae, faunistics, flies, Moroccan fauna

Academic editor: Owen Lonsdale
Received: 15 November 2024
Accepted: 14 January 2025
Published: 5 March 2025

ZooBank: https://zoobank.org/57CCF242-9E56-4623-A6A1-B9D04706C71D

Citation: Doukale Daief M, von Tschirnhaus M, Kettani K (2025) New records of leaf-miner flies (Diptera, Agromyzidae) from Morocco. ZooKeys 1230: 81–97. https://doi.org/10.3897/zookeys.1230.141900

Introduction

The family Agromyzidae, or leaf-miner flies (Diptera, Acalyptratae), is widely distributed in the Palaearctic Region, in which it comprises more than 1,303 species (von Tschirnhaus and Groll 2024a, 2024b). Of these, 984 species are recorded from Europe (Černý, pers. comm. to MvT, 24.ix.2024). They are small to medium-sized acalyptratae flies (0.8–6.5 mm), with variable colour, from black to yellow. They are considered as the third largest of Acalyptratae families which possess entirely phytophagous larvae that develop in a wide range of hosts in the plant kingdom (Hering 1957, 1966; Spencer 1972, 1990). They inhabit a wide variety of habitats in forests, high mountains, arctic tundra and all types of lowlands, wetlands, and marine coasts. They play a major role in agricultural entomology and are therefore of economic interest (Spencer 1973), as larvae of many species are known to damage crop plants (Dempewolf 2004; Lonsdale et al. 2023). This family of Diptera is also of significant ecological importance (Spencer 1973). The larvae of most species are monophagous or oligophagous, but polyphagy is the exception. They attack different parts of plants such as leaves, stems, sometimes the roots, flower heads, seeds and the young xylem of shrubs and trees, erroneously addressed by authors as the cambium. After host plant identification, the form of the leaf-mine can be useful to identify the species that caused the damage (Černý et al. 2018).

In Morocco, the first record of the family Agromyzidae was reported by Becker and Stein (1913) who found *Amauromyza morionella* [at that time included in the genus *Agromyza*] at Tangier. After the 1930s, new records were added by Séguy's study of the Diptera of Morocco. He reported seven species for the country (Séguy 1936, 1953) with a few other records by Hendel (1931–1936) and Kozlowsky and Rungs (1932). Only three species have been described from Morocco after 1936. These are *Aulagromyza cydoniae* [described by Hendel (1936) in combination with *Phytagromyza*], *Aulagromyza atlantidis* [described by Spencer (1967) in combination with *Paraphytomyza*], and *Cerodontha* (*Icteromyza*) *rozkosnyi* described by Černý (2007). It was not until the 1960s that more records were made with Spencer's (1967, 1973) studies on the Agromyzidae of Morocco and whose contribution had slightly improved the knowledge of these flies by adding 17 species to the Moroccan fauna. After that, few further records have been added by foreign researchers such as Griffiths (1974, 1967), Geipert et al. (1994), Maarouf (2003), and Hanafi and Schnitzler (2004). The most important contribution to the improvement of our knowledge of Moroccan Agromyzidae was made recently by Černý through his many studies (Černý 2007, 2009, 2010, 2012, 2013, 2019; Černý and Merz 2006, 2007; Černý and von Tschirnhaus 2014; Černý et al. 2020). Those articles provided a further 20 species to the country. Beyond that, our knowledge of Moroccan agromyzid fauna is still poor and many gaps remain for this diverse family of Diptera. Many regions of Morocco were still unexplored such as the Rif region in northern Morocco. Indeed, only 62 species of Agromyzidae are listed so far in the catalogue of the Diptera of Morocco compiled by Kettani et al. (2022). Of these, only seven species were recorded from the Rif.

The aim of this study is to present new faunistic records, in particular from some regions which have not previously been explored as an attempt to fill gaps in our knowledge of Moroccan leaf-miners.

The distribution of the species given in this study was mainly gathered from the literature provided by Papp and Černý in their four volumes (Papp and Černý 2015, 2016, 2017, 2020 [as 2019]), Černý et al. 2020; Lonsdale 2021, Lonsdale et al. 2023, and using the file cards and bibliography for world Agromyzidae in von Tschirnhaus and Groll (2024a, 2024b).

Materials and methods

The specimens examined in the present study were collected by MD and to a large extent by KK and her students. Insects were captured by sweep net and by Malaise trap at different localities throughout Morocco from 2012 to 2023. Of the 140 sites surveyed, 38 were home to the agromyzid species mentioned in this article. The sites are mainly in the Rif and Atlas Mountains region (Fig. 1) where a variety of habitats including forests, grasslands, riverbanks, and wetlands were prospected. Table 1 summarizes the main geographical cartographic data and types of habitats of the prospected sites.

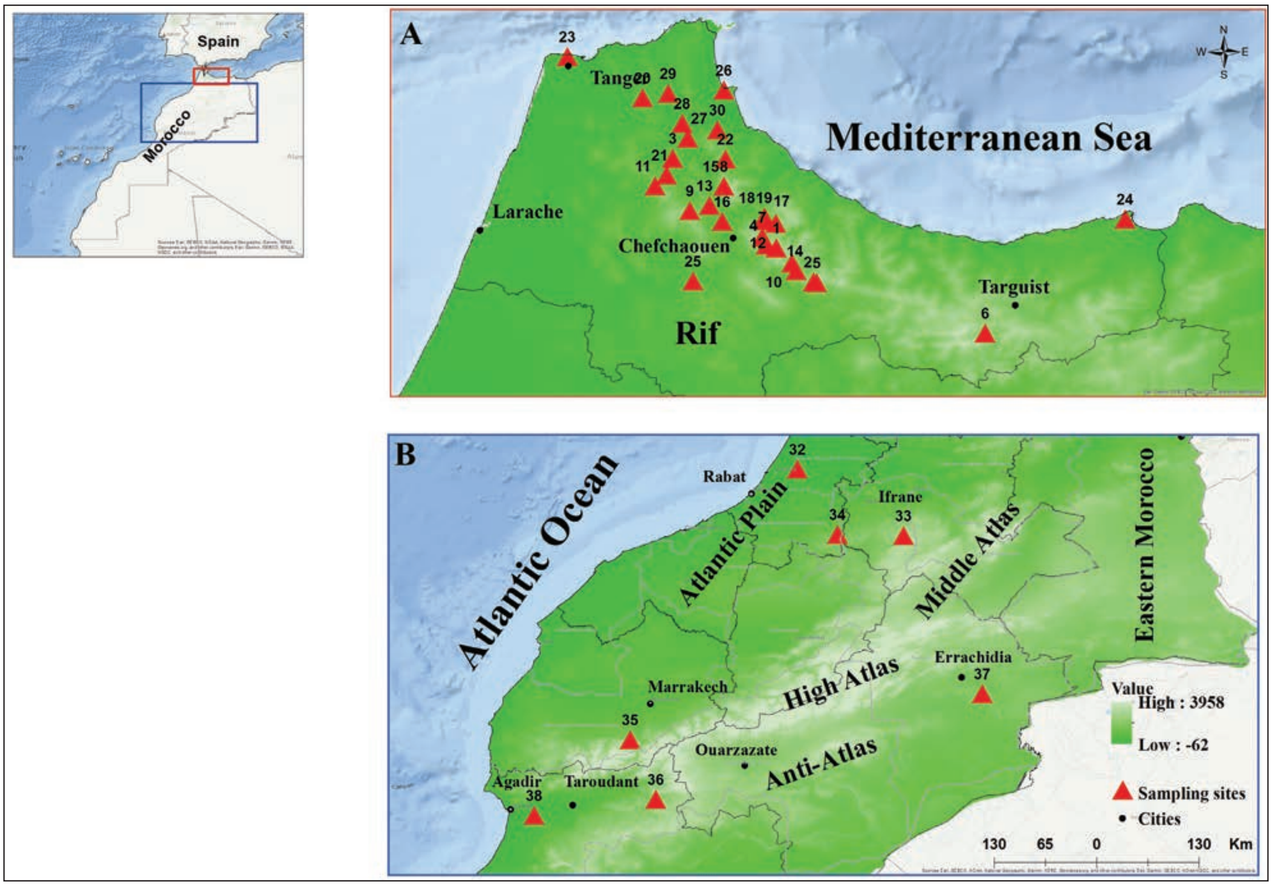

Figure 1. Location of the studied sites in Morocco **A** the Rif at the north of Morocco **B** central Morocco with Atlantic Plain and Atlas Mountains.

The Rif region consists of a mountainous domain overlooking the Mediterranean Sea at the north of Morocco. The climate is mainly of the Mediterranean type and is characterized by high levels of precipitation and is considered very rich and diverse in vegetation cover (Benabid 1982; Valdés Castrillón et al. 2002). It integrates five bioclimatic stages: per-humid and humid which are mainly restricted to the high mountain summits, while the subhumid, semi-arid and arid parts are more widespread in the rest of the Rif. The Atlas region consists of mountain massifs located in the centre and further south of Morocco, made up of three large mountain ranges: High Atlas, Middle Atlas and Anti-Atlas with high summits incised by deep valleys. The bioclimates of this area include perhumid, humid, sub-humid, semi-arid and arid zones with more than 800 mm of annual precipitation on the highest peaks (HCEFLCD 2017) which have favoured a great diversity of vegetation such as *Tetraclinis articulata*, *Argania spinosa*, *Quercus suber*, *Quercus faginea*, *Quercus ilex*, *Cedrus atlantica*, and *Juniperus thurifera* (Mokhtari et al. 2014).

Most specimens captured in the field were stored in 70% ethanol until identification. Each specimen was examined in detail before and after its genitalia were mounted. The genitalia, cut off from the rest of the abdomen, were cleared in 10% KOH at 80 °C for 8 or 10 min and then transferred into 10% acetic acid for ~ 5 min, and finally placed in a droplet of glycerine. The genitalia are firmly embedded in glycerine on glass-slides which were sealed by resistant nail varnish to protect them from dust and from drying out. All species have been identified based on the male genitalia. The second author confirmed and validated all the species identifications by checking all photographs.

Table 1. Localities with respective biogeographical areas, coordinates and altitudes of the studied sites.

Code of locality	Biogeographic area, locality, collecting site (protected area)	Geographic coordinates	Altitude (m)	Habitat
1	Rif, Talassemtane, Maison forestière (NPTL)	35°8'6.11"N, 5°8'18.06"W	1696	Fir forest
2	Rif, Chefchaouen, Bab Tariouant	35°01'7.68"N, 5°0'35.999"W	1429	Oak forest (*Quercus pyrenaica*)
3	Rif, Tarzout, Riba (PNPB)	35°15'755"N, 5°99'691"W	1421	Mixed forest
4	Rif, Talassemtane, Place Espagna (NPTL)	35°05'938"N, 5°08'956"W	1386	Fir forest
5	Rif, El Anasser, Dayat El Anasser	35°00'59.8"N, 4°59'59.77"W	1383	Around pond
6	Rif, Targuist, Beni Bounsar	34°50'36"N, 4°25'23"W	1340	Cedar forest
7	Rif, Afeska, Oued Afeska (NPTL)	35°10'18.4"N, 5°11'10.5"W	1293	Banks of mountain stream
8	Rif, Jbel Kelti, Oued Tanina	35°20'45.50"N, 5°19'01.70"W	1195	Banks of mountain stream
9	Rif, Bouhachem, Amsemlil (PNPB)	35°15'44.424"N, 5°26'0.276"W	1059	Edges of mountain peat bog
10	Rif, Ametrasse, Oued Ametrasse	35°05'01"N, 5°05'03"W	841	Riverbank
11	Rif, Tazia, Dayat Tazia	35°20'52"N, 5°33'12"W	720	Edges of pond
12	Rif, Akchour, Chellal Kbir (NPTL)	35°13'8"N, 5°8'19"W	680	Banks of waterfall
13	Rif, Bni Hassan, Triwa	35°16'50.7"N, 5°22'01.6"W	654	Meadow
14	Rif, Bni Darkoul, Oued Souk Lhad	35°3'26"N, 5°4'10"W	613	Riverbank
15	Rif, Chefchaouen, Bni Ahmed	35°20'45.50"N, 5°19'01.70"W	590	Agricultural field
16	Rif, Tazrout, Adrou (PNPB)	35°13'32.30"N, 5°19'24.35"W	556	Mixed forest
17	Rif, Akchour, Pont de Dieu (NPTL)	35°13'42"N, 5°10'31"W	536	Riverbank
18	Rif, Akchour, Chellal Sghir (NPTL)	35°14'21"N, 5°10'37"W	424	Banks of waterfall
19	Rif, Talembote, Oued Talembote (NPTL)	35°14'20.586"N, 5°10'42.037"W	405	Riverbank
20	Rif, Fahs-Anjra, Rmel	35°38'57.4"N, 5°35'41.4"W	372	Riverbank
21	Rif, El Hamma, Masjid El Hamma	35°23'6"N, 5°30'46"W	330	Matorral dominated by cork oak trees
22	Rif, Tétouan, Oued Raouz	35°26'23.03"N, 5°18'41.70"W	265	Matorral dominated by pine trees
23	Rif, Rmilat, Parc Perdicaris	35°47'26.675"N, 5°51'12.938"W	223	Urban park
24	Rif, Oulad Sidi Mansour, Oued Tassikeste	35°14'05"N, 3°56'37"W	144	Riverbank
25	Rif, Souk El Had, Oued El Koub	35°1'17.88"N, 5°25'19.98"W	124	Riverbank
26	Rif, M'Diq, Koudiat Taifour	35°40'28.706"N, 5°19'1.841"W	100	Pine forest
27	Rif, Ben Karrich, Oued Mhajrate	35°30'39"N, 5°26'27"W	67	Riverbank
28	Rif, Tétouan, Khemis Anjra	35°33'42.453"N, 5°27'34.246"W	63	Riverbank
29	Rif, Tétouan, Oued Khemis	35°39'51.00"N, 5°30'29.00"W	61	Riverbank
30	Rif, Kitane, Oued Zarka	35°32'24.72"N, 5°20'23.58"W	49	Riverbank
31	Eastern Morocco, Taourirt, El Aïoun Sidi Mellouk	34°35'25.336"N, 2°31'4.263"W	589	Agricultural field
32	Atlantic Plain, Sidi Yahya Gharb, forest of Sidi Yahya Gharb	34°18'16"N, 6°18'38"W	20	Eucalyptus forest
33	Middle Atlas, Ifrane, Lac Zarouka (NPIF)	33°32'36.163"N, 5°5'45.277"W	1615	Edges of mountain lake
34	Middle Atlas, Ifrane, Zaouiet Ifrane (NPIF)	33°33'32.884"N, 5°51'0.31"W	1535	Cedar forest
35	High Atlas, Al Haouz, Amizmiz (NPTB)	31°12'54.93"N, 8°13'6.14"W	991	Mixed forest
36	Anti-Atlas, Taroudant, Taliouine	30°31'56"N, 7°55'27"W	928	Agricultural field
37	Anti-Atlas, Errachidia, Aoufous	31°44'31.607"N, 4°11'54.896"W	906	Agricultural field
38	Anti-Atlas, Agadir Idaoutanane, Vallée du Paradis	30°21'6.84"N, 9°18'46.8"W	587	Riverbank

Specimens are housed in the Laboratory of Ecology, Systematics and Conservation of the Biodiversity (**LESCB**) in the Faculty of Sciences of Tetouan in the personal collection of Mourad DOUKALE DAIEF.

The following abbreviations are used for the material examined:

NPIF	National Park of Ifrane
NPTB	National Park of Toubkal
NPTL	National Park of Talassemtane
PNPB	Project of Natural Park of Bouhachem

Results

Subfamily Agromyzinae

Agromyza anthracina Meigen, 1830

Material examined. Morocco. • 1 ♂; Rif, M'Diq, Koudiat Taifour; 3 Apr. 2018; K. Kettani leg.; sweep net; LESCB-R18/21.

Distribution. Palaearctic species, widespread in Europe. First record from Morocco.

Habitat. Collected in pine forest (*Pinus pinaster*).

Agromyza conjuncta Spencer, 1966

Material examined. Morocco. • 2 ♂♂; Rif, Souk El Had, Oued El Koub; 23 Apr. 2018; K. Kettani leg.; sweep net; LESCB-R18/23. • 1 ♂; Rif, Bni Hassan, Triwa; 8 May 2018; K. Kettani leg.; sweep net; LESCB-R18/25. • 1 ♂; Rif, Tazrout, Riba (PNPB); 29 Apr.–22 May 2019; K. Kettani leg.; Malaise trap; LESCB-R19/28.

Distribution. Great Britain, Greece (Crete), Hungary, Romania, Serbia, Italy (Sicily), Slovakia and Spain. First record from Morocco.

Habitat. This species has a large distribution in the Rif Region across a wide altitudinal range (124–1421 m). It was found on the banks of wetlands bordered by *Erica arborea*, *Pistacia lentiscus*, and *Rubus ulmifolius*, in a meadow dotted by Asteraceae and Poaceae and in a mixed oak forest (*Quercus suber*, *Quercus canariensis*).

Agromyza mobilis Meigen, 1830

Material examined. Morocco. • 1 ♂; Rif, Akchour, Chellal Sghir (NPTL); 7 June–14 July 2017; K. Kettani leg.; Malaise trap; LESCB-R19/29.

Distribution. Andorra, Belgium, Czech Republic, Denmark, Estonia, Finland, France (including Corsica), Germany, Great Britain, Greece (Dodecanese, Rhodes), Hungary, Italy, Japan, Latvia, Lithuania, Netherlands, Norway, Poland, Portugal, Russia, Slovakia, Spain, Sweden, Switzerland, Turkey, Ukraine, and Yugoslavia. First record from Morocco.

Habitat. Banks of waterfall lined by *Pistacia lentiscus*, *Nerium oleander*, *Ficus carica*, *Mentha* sp., and *Thuya* sp.

Agromyza myosotidis Kaltenbach, 1864

Material examined. Morocco. • 1 ♂; Rif, El Hamma, Masjid El Hamma; 6–21 June 2016; K. Kettani leg.; Malaise trap; LESCB-R16/10.

Distribution. Belgium, Bulgaria, Czech Republic, Denmark, Finland, Germany, Great Britain, Hungary, Kashmir, Malta, Poland, Spain incl. Canary Islands, Sweden, Switzerland, Turkey and Ukraine. First record from Morocco.

Habitat. Collected in maquis composed of *Quercus coccifera*, *Olea europaea*, *Fraxinus angustifolia*, *Phillyrea angustifolia*, *Dittrichia viscosa*, *Pistacia lentiscus*, and *Erica arborea*.

Agromyza nigrescens Hendel, 1920

Material examined. Morocco. • 1 ♂; Rif, Rmilat, Parc Perdicaris; 16 May 2015; K. Kettani leg.; sweep net; LESCB-R15/06.

Distribution. Austria, Belgium, Croatia, Czech Republic, Denmark, Estonia, Finland, Germany, Great Britain, Hungary, Iraq, Italy, Japan, Kyrgyzstan, Lithuania, Malta, Norway, Poland, Romania, Russia, Serbia, Slovenia, Spain incl. Canary Islands, Sweden, Switzerland, and Turkey. First record from Morocco.

Habitat. This species was collected in the forest of Perdicaris Park, at an altitude of 223 m. The habitat is a preserved forest with significant natural and replanted vegetation such as *Olea europaea*, *Cupressus macrocarpa*, *Quercus canariensis*, *Pittosporum undulatum*, *Quercus suber*, *Quercus lusitanica*, and *Acacia longifolia*.

Hexomyza simplex (Loew, 1869)

Material examined. Morocco. • 1 ♂; Anti-Atlas, Errachidia, Aoufous; 26 Sept. 2022; S. Fekrani leg.; sweep net; LESCB-AA22/42.

Distribution. This Holarctic species is known from Albania, Austria, Great Britain, Denmark, Finland, France, Germany, Greece, Hungary, Israel, Italy, Netherlands, Poland, Turkey, Ukraine and in the USA from California, Connecticut, Hawaii, Iowa, Massachusetts, Michigan, and New Jersey. First record from Morocco.

Habitat. This species was found at medium altitude in agricultural fields in arid areas in the south of Morocco.

Ophiomyia pinguis (Fallén, 1820)

Material examined. Morocco. • 8 ♂♂, 7 ♀♀; Rif, Tazrout, Adrou (PNPB); 14 July–15 Aug. 2013; K. Kettani leg.; Malaise trap; LESCB-R13/02. • 1 ♂; Rif, Kitane, Oued Zarka; 2 Dec. 2017; K. Kettani leg.; sweep net; LESCB-R17/19.

Distribution. Recorded from Austria, Belgium, Great Britain, Bulgaria, China, Croatia, Czech Republic, Denmark, Egypt, Finland, France, Germany, Greece, Hungary, Israel, Italy, Kashmir, Kyrgyzstan, Lithuania, Netherlands, Norway, Poland, Romania, Russia, Slovakia, Spain, Sweden, Switzerland, Tajikistan, Turkey, Ukraine, Uzbekistan, and Yugoslavia. First record from Morocco.

Habitat. This species was collected in a mixed forest (*Quercus suber*, *Pinus pinaster*) and on the banks of a lowland stream (Oued Zarka) bordered by *Nerium oleander*.

Subfamily Phytomyzinae

Amauromyza (*Cephalomyza*) *karli* (Hendel, 1927)

Material examined. Morocco. • 1 ♂, Rif, Kitane Oued Zarka; 2 Dec. 2017; K. Kettani leg.; sweep net; LESCB-R17/20.

Distribution. Recorded from **Canada:** AB, BC*, MB, NS*, ON, QC, SK*. **USA:** MD*. Europe: Austria, Croatia, Czech Republic, Great Britain, Finland, France, Germany, Greece, Hungary, Korea, Netherlands, Poland, Romania, Russia, Serbia, Slovakia, Spain, Sweden, Switzerland, and Ukraine. China. Mongolia, South Korea. First record from Morocco.

Habitat. This species was collected in one site at low altitude (49 m) on the banks of a lowland stream (Oued Zarka) bordered by *Nerium oleander*.

Calycomyza flavomaculata (Spencer, 1960)

Material examined. Morocco. • 1 ♂; Rif, Akchour, Chellal Kbir (NPTL); 25 Apr.–6 June 2016; K. Kettani leg.; Malaise trap; LESCB-R16/12.

Distribution. Croatia, Greece, and Spain. First record from Morocco.

Habitat. Collected on the banks of the Akchour waterfall, lined by *Pistacia lentiscus*, *Nerium oleander*, *Ficus carica*, *Mentha* sp., and *Thuya* sp.

Calycomyza solidaginis (Kaltenbach, 1869)

Material examined. Morocco. • 1 ♂; Rif, Jbel Kelti, Oued Tanina; 6 June 2021; L. Zouhair leg.; sweep net; LESCB-R21/38.

Distribution. China, Germany, Hungary, Lithuania, Poland, Sweden, Switzerland, Yemen, and **Canada:** AB, NB, NS, ON, QC, YT. **USA:** widespread outside of AK and HI. First record from Morocco.

Habitat. Collected on the banks of a mountain river bordered by *Pistacia lentiscus*, *Juniperus oxycedrus*, *Tetraclinis articulata* and crossing a mixed forest dominated by *Quercus suber*, *Pinus pinaster*, and *Pinus halepensis*. A wide variety of shrubs and herbaceous plant species (*Prunus lusitanica*, *Stachys fontqueri*, *Paeonia coriacea*, *Eryngium caespitiferum*, *Eryngium triquetrum*, *Digitalis laciniata*, *Ptilostemon rhiphaeus*, *Ruscus hypophyllum*, *Astragalus armatus*, *Merendera filifolia*, *Viola* sp.) occupy the undergrowth.

Cerodontha (*Butomomyza*) *eucaricis* Nowakowski, 1967

Material examined. Morocco. • 1 ♂; Anti-Atlas, Taroudant, Taliouine; 2 Dec. 2017; Y. Fekrani leg.; sweep net; LESCB-AA17/14.

Distribution. It is known from Belgium, Great Britain, Canada, Czech Republic, Denmark, Finland, France, Germany, Greece, Hungary, Japan, Lithuania, Poland, Slovakia, Sweden, and Switzerland. First record from Morocco.

Habitat. It was collected in an agricultural field bordered by *Carex acuta* and *Carex nigra* in an arid area.

***Cerodontha* (*Dizygomyza*) *luctuosa* (Meigen, 1830)**

Material examined. Morocco. • 1 ♂, 1 ♀; Rif, El Anasser, Dayat El Anasser; 22 Mar. 2019; K. Kettani leg.; sweep net; LESCB-R19/30.

Distribution. Species known from Alaska, Albania, Austria, Belarus, Belgium, Canada, Great Britain, Bulgaria, Byelorussia, Czech Republic, Denmark, Finland, France, Germany, Greece, Hungary, Iraq, Ireland, Israel, Italy including Sicily, Latvia, Lithuania, Netherlands, Norway, Poland, Portugal, Romania, Russia, Slovakia, Spain, Sweden, Switzerland, Tunisia, Uzbekistan, Yugoslavia, and USA (Oklahoma). First record from Morocco.

Habitat. This species was collected in high altitude on the edge of a pond bordered by *Quercus pyrenaica*.

***Cerodontha* (*Icteromyza*) *geniculata* (Fallén, 1823)**

Material examined. Morocco. • 1 ♂; Middle Atlas, Ifrane, Lac Zarouka (NPIF); 13 Oct. 2023; M. Doukale leg.; sweep net; LESCB-MA23/46.

Distribution. A widespread species. It has been recorded from Albania, Austria, Belarus, Great Britain, Bulgaria, Czech Republic, Denmark, Estonia, Finland, France, Germany, Greece, Hungary, Italy, Latvia, Lithuania, and Macedonia. First record from Morocco.

Habitat. This species was collected on the edge of a mountain lake lined by *Eriophorum latifolium*, *Populus alba*, *Carex* sp., *Juncus bufonius*, *Schoenoplectus lacustris*, *Typha latifolia*, and *Salix* sp.

***Chromatomyia centaurii* Spencer, 1990**

Material examined. Morocco. • 1 ♂; Rif, Akchour, Pont de Dieu (NPTL); 1 July 2019; M. Nourti leg.; sweep net; LESCB-R19/32.

Distribution. Known from Great Britain, Germany, Greece, Hungary, Ireland, Lithuania, and Poland. First record from Morocco.

Habitat. This species was found near running water (Akchour) lined by *Nerium oleander*, *Erica* sp., and *Cistus* sp.

***Liriomyza amoena* (Meigen, 1830)**

Material examined. Morocco. • 3 ♂♂, 2 ♀♀; Rif, Khemis Anjra, Oued Khemis; 16 Sep. 2012; K. Kettani leg.; sweep net; LESCB-R12/01.

Distribution. The species is recorded from Austria, Belgium, Great Britain, Bulgaria, Czech Republic, Denmark, Finland, France, Germany, Greece, Ireland, Italy, Japan, Latvia, Lithuania, Moldavia, Netherlands, Poland, Portugal (Madeira Island), Romania, Russia, Serbia, Slovakia, Slovenia, Spain, Sweden, Turkey, and in the Oriental Region (India). First record from Morocco.

Habitat. Collected on the bank of a lowland river bordered by *Nerium oleander*, *Phragmites australis*, *Tamarix africana*, *Rubus ulmifolius*, and *Juncus acutus*.

Liriomyza brassicae **(Riley, 1884)**

Material examined. Morocco. • 1 ♂; Rif, Souk El Had, Oued El Koub; 23 Apr. 2018; K. Kettani leg.; sweep net; LESCB-R18/24.

Distribution. Wide distribution as an agricultural pest, including in the Afrotropical Region: Cape Verde Islands, Ethiopia, Kenya, Mozambique, Namibia, Oman, Senegal, Spain (Canary Islands), South Africa, Yemen, and Zimbabwe. In the Palaearctic Region including Egypt, France (Corsica), Germany, Iraq, Japan, Malta, Poland, Portugal, Romania, Saudi Arabia, Spain, and Turkey. First record from Morocco.

Habitat. The male was captured on the banks of a river bordered by *Erica arborea*, *Pistacia lentiscus* and *Rubus ulmifolius*.

Liriomyza strigata **(Meigen, 1830)**

Material examined. Morocco. • 2 ♂♂; Anti-Atlas, Agadir Idaoutanane, Vallée du Paradis; 4 Dec. 2017; Y. Fekrani leg.; sweep net; LESCB-AA17/15.

Distribution. Ubiquitous polyphagous species. It is recorded from Albania, Belarus, Belgium, Bosnia-Herzegovina, Great Britain, Czech Republic, Denmark, Estonia, Finland, France, Germany, Greece, Hungary, Iraq, Ireland, Italy, Kazakhstan, Kyrgyz Republic, Lithuania, Netherlands, Portugal (Madeira Isl.), Norway, Poland, Romania, Russia, Slovakia, Spain, Sweden, Switzerland, Turkey, Ukraine, and Uzbekistan. First record from Morocco.

Habitat. This species was collected on the sandy riverbank in an arid region.

Phytoliriomyza arctica **(Lundbeck, 1901)**

Material examined. Morocco. • 1 ♂; Rif, Chefchaouen, Bni Ahmed; 10 May 2021; K. Kettani leg.; sweep net; LESCB-R21/39.

Distribution. Known from Brazil, Chile, Greenland, North America. Europe. Iran, South Korea, Taiwan, and Sri Lanka. First record from Morocco.

Habitat. It was collected in a *Cannabis* cultivation field with *Cannabis sativa* and *Cannabis indica*.

Phytoliriomyza perpusilla **(Meigen, 1830)**

Material examined. Morocco. • 1 ♂; High Atlas, Al Haouz, Amizmiz (NPTB); 26 Mar. 2017; Y. Fekrani leg.; sweep net; LESCB-HA17/16.

Distribution. Known from Albania, Austria, Great Britain, Bulgaria, Cape Verde Islands, Czech Republic, Estonia, Finland, France, Germany, Greece, Hungary, Italy including Sardinia, Japan, Lesotho, Lithuania, Malta, Nepal, Netherlands, Norway, Oman, Poland, Portugal incl. Azores Islands, Romania, Russia (Yakutia), Serbia, Spain (Canary Islands), South Africa, Sweden, Switzerland, Taiwan, Tunisia, Turkey, and Yemen. First record from Morocco.

Habitat. Collected in a pine forest (*Pinus pinaster*) with herbaceous plants composed of *Trifolium* spp.

Phytoliriomyza pteridii Spencer, 1973

Material examined. Morocco. • 1 ♂; Rif, Fahs-Anjra, Rmel; 27 Feb. 2020; M. Nourti leg.; sweep net; LESCB-R20/36.

Distribution. The species is known from Andorra, Great Britain, Bulgaria, Croatia, France, Germany, Hungary, Ireland, Italy, Montenegro, Poland, Portugal, Scotland, Slovakia, Slovenia, Switzerland, and Yugoslavia. First record from Morocco.

Habitat. It was collected at 372 m in a scrubland with rocky soil of a clay-calcareous habitat crossed by a small stream and bordered by vegetation mainly composed of *Pistacia lentiscus*, *Carlina racemosa*, *Conyza canadensis*, *Erica arborea*, and *Cistus monspeliensis*. On a nearby field, fruit trees such as *Olea europaea* and *Ficus carica* were growing.

Phytomyza anemones Hering, 1925

Material examined. Morocco. • 2 ♂♂, 1 ♀; Rif, Chefchaouen, Bab Tariouant; 31 May 2015; K. Kettani leg.; sweep net; LESCB-R15/07.

Distribution. Denmark, Finland, France, Germany, Great Britain, Greece, Hungary, Ireland, Italy, Lithuania, Malta, Netherlands, Poland, Spain (Mallorca), Sweden, and Yugoslavia. First record from Morocco.

Habitat. Collected in an oak forest at high altitude (*Quercus pyrenaica*).

Phytomyza clematidis Kaltenbach, 1859

Material examined. Morocco. • 1 ♂; Rif, Tazia, Dayat Tazia; 12 May 2015; K. Kettani leg.; sweep net; LESCB-R15/05.

Distribution. Recorded from Andorra, Austria, Cyprus, Czech Republic, France incl. Corsica, Germany, Great Britain, Greece, Hungary, Israel, Italy, Lithuania, Maltese Islands, Netherlands, Norway, Portugal, Spain incl. Balearic and Canary Islands, Slovakia, Switzerland, and Turkey. First record from Morocco.

Habitat. Collected on the edge of a pond surrounded by cork oak forest.

Phytomyza crassiseta Zetterstedt, 1860

Material examined. Morocco. • 2 ♂♂; Rif, Bni Darkoul, Oued Souk Lhad; 30 Apr. 2016; F.Z. Bahid leg.; sweep net; LESCB-R16/08. • 6 ♂♂, 4 ♀♀;

Rif, Ametrasse, Oued Ametrasse; 30 Apr. 2016; F.Z. Bahid leg.; sweep net; LESCB-R16/09. • 1 ♂, 1 ♀; Rif, Tétouan, Oued Raouz; 18 May 2018; A. Adghir leg.; sweep net; LESCB-R18/26. • 5 ♂♂, 1 ♀♀; Rif, Tazrout, Riba (PNPB); 29 Apr.–22 May 2019; K. Kettani leg.; Malaise trap; LESCB-R19/31. • 4 ♂♂; Rif, Akchour, Pont de Dieu (NPTL); 1 July 2019; M. Nourti leg.; sweep net; LESCB-R19/33. • 1 ♂, 1 ♀; Rif, Oulad Sidi Mansour, Oued Tassikeste; 16 May 2023; K. Kettani leg.; sweep net; LESCB-R23/47.

Distribution. Known from Albania, Andorra, Austria, Belarus, Bulgaria, Croatia, Czech Republic, Denmark, Estonia, Finland, France, Germany, Great Britain, Greece, Hungary, Ireland, Italy, Latvia, Liechtenstein, Lithuania, Montenegro, Netherlands, Norway, Poland, Portugal, Romania, Slovakia, Spain incl. Canary Islands, Sweden, Switzerland. Canada. ON*, QC. USA: CA, ID, IN*, MA, MD, ME, NC, NJ*, NY, PA, VA, WA, WV. Argentina, Chile. Japan, Turkey, and Russia. First record from Morocco.

Habitat. This species has a wide distribution in the Rif across a wide altitudinal range (144–1421 m). It was mainly caught at the banks of rivers bordered by *Nerium oleander*, *Rubus ulmifolius*, *Erica* sp., and *Cistus* sp. It was also found in a mixed forest of *Quercus faginea*, *Quercus suber*, and *Pinus pinaster* at 1421 m altitude.

Phytomyza notata Meigen, 1830

Material examined. Morocco. • 6 ♂♂, 4 ♀♀; Rif, Talassemtane, Maison forestière (NPTL); 7 June–17 July 2014; K. Kettani leg.; Malaise trap; LESCB-R14/04.

Distribution. This species was reported from Belarus, Bulgaria, Czech Republic, Denmark, Finland, France, Germany, Great Britain, Hungary, Italy, Lativia, Lithuania, Poland, Romania, Russia, Serbia, Slovakia, Spain, Sweden, and Switzerland. First record from Morocco.

Habitat. This species was captured in a fir forest (*Abies marocana*) at an altitude of 1696 m in Jbel Talassemtane.

Phytomyza plantaginis Robineau-Desvoidy, 1851

Material examined. Morocco. • 1 ♂, 2 ♀♀; Rif, Ametrasse, Oued Ametrasse; 30 Apr. 2016; F.Z. Bahid leg.; sweep net; LESCB-R16/11. • 6 ♂♂, 3 ♀♀; Rif, Talassemtane, Place Espagna (NPTL); 16 Apr. 2018; K. Kettani leg.; sweep net; LESCB-R18/22. • 1 ♂; Rif, Bouhachem, Amsemlil (PNPB); 1 July 2019; K. Kettani leg.; sweep net; LESCB-R19/34. • 2 ♂♂; Atlantic Plain, Sidi Yahya Gharb, forest of Sidi Yahya Gharb; 4 May 2020; M. Doukale leg.; sweep net; LESCB-AP20/35. • 2 ♂♂; Rif, Talembote, Oued Talembote (NPTL); 1 July 2018; K. Kettani leg.; sweep net; LESCB-R18/27. • 1 ♂, 1 ♀; Rif, Tétouan, Khemis Anjra; 27 Mar. 2021; L. Zouhair leg.; sweep net; LESCB-R21/37. • 1 ♂; Rif, Talassemtane, Maison forestière (NPTL); 10 June 2021; K. Menouar & L. Zouhair leg.; sweep net; LESCB-R21/41. • 3 ♂♂; Rif, Afeska, Oued Afeska (NPTL); 10 June 2021; K. Menouar & L. Zouhair leg.; sweep net; LESCB-R21/40.

Distribution. It is recorded from Canada: BC*, ON, QC. USA: Widespread, including HI. Bermuda*. Widespread in Europe, recorded from almost every country including Azores, Canary Islands, Cyprus, Italy, Portugal including Madeira. In the Palaearctic, recorded also from Algeria, Egypt, Iran, Israel, Japan, Kyrgyzstan, Russia, Tunisia, Turkey, and Uzbekistan. It is recorded also from South Africa, Australia, New Zealand, Taiwan, and Thailand. First record from Morocco.

Habitat. This species exhibits a large distribution in the Rif Region of northern Morocco across a wide altitudinal range (11–1683 m) and inhabits a large variety of habitats such as the edge of wetlands (river, peat bog), mixed forest dominated by oak (*Quercus suber*, *Quercus canariensis*), fir (*Abies marocana*), and cedar (*Cedrus atlantica*) at high altitudes and some other vegetation such *Tetraclinis articulata*, *Eucalyptus globulus*, *Scolymus maculatus*, and *Carlina corymbosa*.

Phytomyza rufipes Meigen, 1830

Material examined. Morocco. • 2 ♂♂, 1 ♀; Rif, Ben Karrich, Oued Mhajrate; 20 July–13 Sep. 2016; K. Kettani leg.; Malaise trap; LESCB-R16/13.

Distribution. It is recorded from Albania, Austria, Belgium, Canada, Croatia (Dalmatia), Czech Republic, Denmark, Egypt, Estonia, Finland, France, Germany, Great Britain, Greece, Iceland, Iraq, Ireland, Italy, Latvia, Lithuania, Netherlands, Norway, Poland, Portugal (Madeira), Russia, Slovakia, Spain (mainland, Canary Islands), Sweden, Switzerland, Turkey, and United Kingdom (Yugoslavia). In the Nearctic Region: Canada (New Brunswick, Newfoundland), USA (California). In the Neotropical Region: Argentina, Colombia. First record from Morocco.

Habitat. Collected on a riverbank bordered by *Armoracia rusticana*, *Alliaria petiolata*, *Brassica oleracea*, *Diplotaxis* sp., and *Myagrum perfoliatum* and ground vegetation in a pine forest.

Phytomyza vitalbae Kaltenbach, 1872

Material examined. Morocco. • 1 ♂; Rif, Targuist, Bni Bounsar; 1–30 Apr. 2022; K. Kettani leg.; Malaise trap; LESCB-R22/44.

Distribution. The species is very widely distributed, being known from Andorra, Austria, Belgium, Bulgaria, Canada, China, Croatia, Cyprus, Czech Republic, Denmark, Estonia, Finland, France incl. Corsica, Germany, Great Britain, Greece, Hungary, Ireland, Italy, Montenegro, Nepal, Netherlands, New Zealand, Poland, Romania, Russia (Yakutia), Serbia, South Africa, Spain incl. Canary Islands, Sweden, Switzerland. First record from Morocco.

Habitat. Collected in cedar forest (*Cedrus atlantica*).

Pseudonapomyza confusa Zlobin, 1993

Material examined. Morocco. • 2 ♂♂; Middle Atlas, Ifrane, Zaouiet Ifrane (PNIF); 2 Apr. 2017; Y. Fekrani leg.; sweep net; LESCB-MA17/17. • 1 ♂; Anti-Atlas, Errachidia, Aoufous; 26 Sep. 2022; S. Fekrani leg.; sweep net; LESCB-AA22/43. • 1 ♂; Eastern Morocco, Taourirt, El Aïoun Sidi Mellouk; 9 Jul. 2023; M. Doukale leg.; sweep net; LESCB-EM23/45.

Distribution. It is recorded from Cape Verde Islands, Greece (Crete), Madagascar, and Namibia. First record from Morocco.

Habitat. This species was found at medium altitude in agricultural fields in arid areas in Eastern Morocco as well as in the Anti-Atlas. It was also captured at high altitude in cedar forest (*Cedrus atlantica*) in the Middle Atlas.

Pseudonapomyza palavae Černý, 1998

Material examined. Morocco. • 1 ♂; Eastern Morocco, Taourirt, El Aïoun Sidi Mellouk; 9 July 2023; M. Doukale leg.; sweep net; LESCB-EM24/48.

Distribution. It is recorded from Czech Republic and Hungary. First record from Morocco.

Habitat. This species was found at medium altitude in agricultural fields in arid areas in the Eastern Morocco.

Pseudonapomyza vota Spencer, 1973

Material examined. Morocco. • 1 ♂; Rif, Tazrout, Adrou (PNPB); 14 Jul.–15 Aug. 2013; K. Kettani leg.; Malaise trap; LESCB-R13/03. • 2 ♂♂; Rif, Akchour, Chellal Sghir (NPTL); 7 June–14 July 2017; K. Kettani leg.; Malaise trap; LESCB-R17/18.

Distribution. This species is known from Croatia, Cyprus, France, Greece, Hungary, Italy, Malta, Portugal, Serbia, Spain, Switzerland, and Turkey. First record from Morocco.

Habitat. Collected in an oak-dominated forest and on the banks of a waterfall lined by *Pistacia lentiscus*, *Nerium oleander*, *Ficus carica*, *Mentha* sp., and *Thuya* sp.

Discussion

This article presents additions to the Moroccan fauna represented by 30 new records of leaf-miner flies, bringing the total number of Agromyzidae currently known for Morocco to 92 species. This faunal assemblage is subdivided into 11 genera, three genera in Agromyzinae, in which *Agromyza* (*A. anthracina*, *A. conjuncta*, *A. mobilis*, *A. myosotidis*, *A. nigrescens*) dominates in the Rif region and was found in various habitats. The second genus, *Hexomyza* (*H. simplex*) is quite rare, with only one species found in the Atlas region in an agricultural field. The third genus is *Ophiomyia* with the single species *O. pinguis* and 16 individuals present only in the Rif region in various habitats (forest and riverbank). The eight genera in Phytomyzinae are widely distributed across Morocco. *Calycomyza* is newly reported from the country, represented by two species (*C. flavomaculata* and *C. solidaginis*) found in the Rif region on riverbanks at a significant altitude of 1463 m. *Phytomyza* was the prevalent genus in the Rif region and the most diversified with seven species (*Ph. anemones*, *Ph. clematidis*, *Ph. crassiseta*, *Ph. notata*, *Ph. plantaginis*, *Ph. rufipes*, *Ph. vitalbae*). Some other genera were less diversified such as *Cerodontha* (*C.* (*Butomomyza*) *eucaricis*, *C.* (*Dizygomyza*) *luctuosa*, *C.* (*Icteromyza*) *geniculata*), *Liriomyza* (*L. amoena*, *L. brassicae*, *L. strigata*), *Phytoliriomyza* (*P. arctica*, *P. perpusilla*, *P. pteridii*), and *Pseudonapomyza* (*Ps. confusa*, *Ps. palavae*, and *Ps. vota*). The other two genera were less diversified and were found in forest habitats such as *Amauromyza* (*A.* (*Cephalomyza*) *karli*) and *Chromatomyia* (*C. centaurii*). Most obtained species belonged into *Phytomyza* (23,4%) with *Phytomyza crassiseta* being the most frequent species (38.8%). *Agromyza nigrescens* has a wide distribution in Europe.

These numbers, however, cannot be considered final because further collecting in unexplored areas will undoubtedly bring new additions to the Moroccan fauna

Acknowledgements

We are grateful to the Water and Forests National Agency of Morocco for providing permits for the entomological surveys.

Additional information

Conflict of interest

The authors have declared that no competing interests exist.

Ethical statement

No ethical statement was reported.

Funding

No funding was reported.

Author contributions

Writing - original draft: MD. Writing - review and editing: MT, KK.

Author ORCIDs

Mourad Doukale Daief https://orcid.org/0009-0000-6946-2244
Michael von Tschirnhaus https://orcid.org/0000-0002-1903-4767
Kawtar Kettani https://orcid.org/0000-0003-2361-3996

Data availability

All of the data that support the findings of this study are available in the main text.

References

Becker T, Stein P (1913) Dipteren aus Marokko. Annuaire du Musée zoologique de l'Académie impériale de Sciences de St.-Petersbourg 18: 62–95.

Benabid A (1982) Étude phytoécologique, biogéographique et dynamique des associations et séries sylvatiques du Rif occidental (Maroc). Thèse de Doctorat Es. Sc. Nat. Faculté de St. Jérôme Marseille III, France, 165 pp.

Černý M (2007) New faunistic records of Agromyzidae (Diptera) from Andorra including descriptions of three new species. Boletín de la Sociedad entomológica aragonesa, Zaragoza 41: 43–51.

Černý M (2009) New faunistic data on the Agromyzidae (Diptera) from the West Palaearctic Region. Klapalekiana, Praha 45(1–2): 9–21.

Černý M (2010) Agromyzidae: 185 + 233 - In: Borges PAV, Costa A, Cunha R, Gabriel R, Gonçalves V, Martins AF, Melo I, Parente M, Raposeiro P, Rodrigues P, Santos RS, Silva L, Vieira P, Vieira V (Eds): Listagem dos organismos terrestres e marinhos dos Açores. / A list of the terrestrial and marine biota from the Azores. Princípia, Cascais [ISBN 978-989-8131-75-1], Parede, Portugal, 429 pp.

Černý M (2012) The fauna of Agromyzidae (Diptera) in the Gemer region (Central Slovakia), with descriptions of three new species from Slovakia. Časopis slezského zemského Muzea Opava (A), Opava 61: 49–76.

Černý M (2013) Additional records of Agromyzidae (Diptera) from the West Palaearctic Region. Časopis slezského zemského Muzea Opava (A), Opava 62: 281–288.

Černý M (2019) Additional new records of Agromyzidae (Diptera) from the Palaearctic Region. Acta Musei Silesiae, Scientiae naturales 67(2018): 117–137. https://doi.org/10.2478/cszma-2018-0010

Černý M, Merz B (2006) New records of Agromyzidae (Diptera) from Palaearctic Region. Mitteilungen der schweizerischen entomologischen Gesellschaft, Zürich 79(1): 77–106. http://doi.org/10.2478/cszma-2018-0010

Černý M, Merz B (2007) New records of Agromyzidae (Diptera) from the West Palaearctic Region, with an updated checklist for Switzerland. Mitteilungen der schweizerischen entomologischen Gesellschaft, Zürich 80(1/2): 107–121.

Černý M, von Tschirnhaus M (2014) New records of Agromyzidae (Diptera) from the Afrotropical Region, with a checklist. Acta Musei Silesiae, Scientiae naturales, Opava 63(2): 159–176. https://doi.org/10.2478/cszma-2014-0017

Černý M, Andrade R, Gonçalves AR, von Tschirnhaus M (2018) New records of Agromyzidae (Diptera) from Portugal, with an updated checklist. Acta Musei Silesiae, Scientiae naturales 67: 7–57. https://doi.org/10.2478/cszma-2018-0002

Černý M, von Tschirnhaus M, Winqvist K (2020) First records of Palaearctic Agromyzidae (Diptera) from 40 countries and major islands. Acta Musei Silesiae, Scientiae naturales, Opava 69(3): 193–229. https://doi.org/10.2478/cszma-2020-0017

Dempewolf M (2004) Arthropods of Economic Importance – Agromyzidae of the World (CD-ROM). ETI. University of Amsterdam, Amsterdam. https://nlbif.eti.uva.nl/bis/agromyzidae.p

Geipert S, Kroschel J, Sauerborn J (1994) Incidence of *Phytomyza orobanchia* Kalt. (Diptera: Agromyzidae) in northern Morocco and perspectives for a biological control of Orobanche spp. Results of a field survey. In: Fifth Arab Congress of Plant Protection, 27th November – 2nd December 1994, Fès, Morocco, 235 pp

Griffiths GCD (1967) Revision of the *Phytomyza syngenesiae* group (Diptera, Agromyzidae), including species hitherto known as "*Phytomyza atricornis* Meigen". Stuttgarter Beiträge zur Naturkunde 177: 1–28.

Griffiths GCD (1974) Studies on boreal Agromyzidae (Diptera). V. On the genus *Chromatomyia* Hardy, with revision of Caprifoliaceae-mining species. Quaestiones entomologicae, Edmonton 10(1): 35–69. https://biostor.org/reference/194955

Hanafi A, Schnitzler WH (2004) Integrated production and protection in greenhouse tomato in Morocco. Acta Horticulturae, ISHS (International Society for Horticultural Science), Leuven, Belgium 659: 323–330. https://doi.org/10.17660/ActaHortic.2004.659.38

HCEFLCD [Haut-Commissariat aux Eaux et Forêts et à la Lutte Contre la Desertification] (2017) Plan d'Aménagement et de Gestion du Parc National de Toubkal. Mission I – Diagnostic: analyse du périmetre d'intervention et du territoire environnant. Mai 2017, 305 pp.

Hendel F (1936) Fam. Agromyzidae. In: Frey R, von O. Duda B, Hendel Fr, Lackschewitz P, Schmitz H, Storå R, Villeneuve J (Eds) Die Dipterenfauna der Kanarischen Inseln und ihre Probleme. Mit - Commentationes biologicae, Helsingfors und Berlin 6(1): 120–124.

Hendel FG (1931–36) 59. Agromyzidae. In: Lindner E (Ed.) Die Fliegen der palaearktischen Region 6(2): xi + 570 pp. [pls i–xvi + 16 pp]

Hering EM (1957) Minierfliegen in Lebermoosen (Dipt. Agromyzidae) = (Leaf miner flies in liverworts (Dipt. Agromyzidae)). Mitteilungen der deutschen entomologischen Gesellschaft, Berlin 16: 48–51. https://doi.org/10.1002/mmnd.4820160311

Hering EM (1966) Minierfliegen in Lebermoosen II (Dipt. Agromyzidae) = (Leaf miner flies in liverworts II (Dipt. Agromyzidae)). Deutsche entomologische Zeitschrift (neue Folge), Berlin 13(I/III): 231–235.

Kettani K, Ebejer MJ, Ackland DM, Bächli G, Barraclough D, Barták M, Carles-Tolrá M, Černý M, Cerretti P, Chandler P, Dakki M, Daugeron C, De Jong H, Dils J, Disney H, Droz B, Evenhuis N, Gatt P, Graciolli G, Grichanov IY, Haenni JP, Hauser M, Himmi O, Macgowan I, Mathieu B, Mouna M, Munari L, Nartshuk EP, Negrobov OP, Oosterbroek P, Pape T, Pont AC, Popov GV, Rognes K, Skuhravá M, Skuhravý V, Speight M, Tomasovic G, Trari B, Tschorsnig HP, Vala JC, von Tschirnhaus M, Wagner R, Whitmore D, Woźnica AJ, Zatwarnicki T, Zwick P: Catalogue of the Diptera (Insecta) of Morocco - an annotated checklist, with distributions and a bibliography. ZooKeys 1094: 279–283. [466 pp] https://doi.org/10.3897/zookeys.1094.62644

Kozlowsky S, Rungs C (1932) Sur quelques insectes ennemis des plantes maraîchères au Maroc. Bulletin de la Société des Sciences naturelles du Maroc, Rabat 12(1–3): 66–68.

Lonsdale O (2021) Manual of North American Agromyzidae (Diptera, Schizophora), with revision of the fauna of the “Delmarva” states. ZooKeys 1051: 1–481. https://doi.org/10.3897/zookeys.1051.64603

Lonsdale O, Murphy ST, Scheffer SJ (2023) Agromyzidae (Diptera) Plant Pests. Pensoft Publishers, Sofia, i + 110 pp. https://doi.org/10.3897/ab.e108410

Maarouf A (2003) Diptères Cyclorrhaphes et Brachycères nouveaux pour le Maroc. L’entomologiste 59(1–2): 41–47.

Mokhtari N, Mrabet R, Lebailly P, Bock L (2014) Spatialisation des bioclimats, de l’aridité et des étages de végétation du Maroc. Revue marocaine des Sciences agronomiques et vétérinaires 2(1): 50–66.

Papp L, Černý M (2015) Agromyzidae (Diptera) of Hungary. Volume 1. Agromyzinae - Pars Ltd, Nagykovácsi, Hungary, 416 pp. https://doi.org/10.18655/Agromyzidae.Vol.1

Papp L, Černý M (2016) Agromyzidae (Diptera) of Hungary. Volume 2. Phytomyzinae I - Pars Ltd, Nagykovácsi, Hungary, 385 pp. https://doi.org/10.18655/Agromyzidae.Vol.2

Papp L, Černý M (2017) Agromyzidae (Diptera) of Hungary. Volume 3. Phytomyzinae II - Pars Ltd, Nagykovácsi, Hungary, 427 pp. https://doi.org/10.18655/Agromyzidae.Vol.3

Papp L, Černý M (2020) [as 2019]: Agromyzidae (Diptera) of Hungary. Volume 4. Phytomyzinae III - Pars Ltd, Nagykováksi, Hungary, 708 pp.

Séguy E (1936) Un nouveau Muscide nuisible à l’orge au Maroc. Liste des Diptères vivant sur les Hordeum. Bulletin de la Société des sciences naturelles du Maroc 16: 3–5.

Séguy E (1953) Diptères du Maroc. Encyclopédie entomologique. Série B II. Memoires et notes. (1947–1953) 11: 77–92.

Spencer KA (1967) Some Agromyzidae (Diptera) from Morocco. Entomologist’s Monthly Magazine 103: 126–130.

Spencer KA (1972) Diptera, Family Agromyzidae - Handbooks for the Identification of British Insects, Royal Entomological Society of London, London 10(5g): 1–136.

Spencer KA (1973) Agromyzidae (Diptera) of economic importance. Series entomologica, Volume 9. W. Junk B.V., The Hague, xi + 418 pp. https://doi.org/10.1007/978-94-017-0683-4

Spencer KA (1990) Host Specialization in the World Agromyzidae (Diptera). In: Spencer KA (Ed.): Series entomologica 45: - Kluwer Academic Publishers, continued as Springer Science + Business Media Netherlands, Dordrecht, XII + 444. https://doi.org/10.1007/978-94-009-1874-0

Valdés Castrillón B, Rejdali M, Achhal el Kadmiri A, Jury JL, Montserrat JM (2002) Catalogue des plantes vasculaires du nord du Maroc, incluant des clés d'identification. Vol. 1. CSIC, Centre Mixt del Consejo superior de Investigationes Cientificas, Madrid, Biblioteca de Ciencias, Vol. 39479, X + 491 pp.

von Tschirnhaus M, Groll E (2024a) World Agromyzidae Online. https://sdei.senckenberg.de/tschirnhaus-agromyzidae

von Tschirnhaus M, Groll E (2024b) World Bibliography of Agromyzidae and Chloropidae Online. https://sdei.senckenberg.de/tschirnhaus-bibliography

ZooKeys 1230: 99–154 (2025)
DOI: 10.3897/zookeys.1230.136906

Research Article

From 153-year-old records to contemporary discoveries: land snail (Mollusca, Gastropoda) diversity in Penang Hill, Malaysia

Soo-Mun Goh[1], Dulipat Jasrul[1], Mei-Yi Lee[2], Jaap J. Vermeulen[3], Thor-Seng Liew[1]

1 *Institute for Tropical Biology and Conservation, Universiti Malaysia Sabah, Kota Kinabalu, Malaysia*
2 *School of Biological Science, Universiti Sains Malaysia, Penang, Malaysia*
3 *jk.artandscience, Lauwerbes 8, 2318 AT, Leiden, Netherlands*
Corresponding author: Thor-Seng Liew (thorseng@ums.edu.my)

Abstract

This study highlights the diversity of land snails in Penang Hill, a non-limestone hill in Peninsular Malaysia. A systematic survey of land snails in Penang Hill was conducted, inventoried, and compared with those specimens collected by Stoliczka (1872, 1873) in 1869. Based on the 33 sampling plots established in this study, the differences in species composition along the elevation gradient (75 m to 770 m a.s.l.) and between three different habitats on Penang Hill were examined: disturbed forests with anthropogenic activities, undisturbed forests, and orchards with various crops. A total of 54 species were recorded from the sampling plots and random observations, of which only 20 overlapped with Stoliczka's list; 34 were new records for Penang Hill, and 12 previously recorded species were not found in this study. Most of the new records were micro-snails smaller than 5 mm. Species richness was highest in disturbed forests and showed no correlation with elevation. There was no clear grouping of plots by species composition across habitat types, except for those in orchards. Indicator species analysis revealed strong associations between a few land snail species and disturbed forests and orchards. The number of species in Penang Hill increased from 32 to 66, with species richness comparable to the high numbers usually found in limestone habitats and higher mountains in Malaysia.

Key words: Bukit Bendera, Gastropoda, Island, Malay Peninsula, Pulau Pinang, semi-slugs, slugs

OPEN ACCESS

Academic editor: Martin Haase
Received: 23 September 2024
Accepted: 27 November 2024
Published: 5 March 2025

ZooBank: https://zoobank.org/0FBF41B0-1D35-4A31-9653-B1F475FBDF80

Citation: Goh S-M, Jasrul D, Lee M-Y, Vermeulen JJ, Liew T-S (2025) From 153-year-old records to contemporary discoveries: land snail (Mollusca, Gastropoda) diversity in Penang Hill, Malaysia. ZooKeys 1230: 99–154. https://doi.org/10.3897/zookeys.1230.136906

Introduction

The history of land snail research in Peninsular Malaysia began during the establishment of the Straits Settlements in 1826, which at that time consisted of Penang Island, Singapore, and Malacca. The first land snail species described from the Malay Peninsula islands was *Quantula striata* (Gray, 1834) from Singapore, while *Dyakia mackensiana* (Souleyet, 1841) was described from the Malay Peninsula mainland in Malacca (Gray 1834; Souleyet 1841). Since then, more land snail species have been described from these areas: another 15 species from the Malay Peninsula mainland (Souleyet 1841, 1842; Sowerby 1842; Pfeiffer 1855a, 1855b, 1857); six species from Penang Island (Benson 1851a, 1851b, 1852a, 1861; Souleyet 1852; Pfeiffer 1856); and another six species from

Singapore (Sowerby 1843; Adams and Adams 1851; Pfeiffer 1851, 1853, 1855c; Benson 1852b). Most of the species described in the above literature were from non-systematic sampling. The first detailed land snail inventory study was conducted by Stoliczka, who explored the northwestern part of Penang Island, mainly Penang Hill, for 16 days in 1869, and recorded a total of 32 species. He also described 19 new species from Penang Hill, which was close to the total number of species described in the previous three decades in this region.

Despite the earlier works, all of which were from non-limestone areas, most later land snail inventory studies have largely focused on limestone hills, with little attention paid to non-limestone areas (de Morgan 1885a, 1885b; van Benthem Jutting 1950, 1952, 1954, 1960; Davison 1991; Clements et al. 2008; Liew et al. 2008; Foon et al. 2017; Phung et al. 2018; Foon and Marzuki 2023). For the studies conducted in non-limestone areas, most were based on opportunistic sampling that may not be sufficient to capture the true extent of land snail diversity, and comparative analysis could not be done (Chan 1998a, 1998b). Moreover, valuable information from these scattered inventory studies is often buried in the taxonomic literature (von Möllendorff 1886, 1891; Collinge 1902; Sykes 1903).

Land snail populations occur in low densities in non-limestone areas (Schilthuizen et al. 2003). This gives the impression that lowlands in non-limestone areas have very low land snail diversity (Liew et al. 2008). To date, most of the previous records of land snails in non-limestone areas are from former British colonial hill stations, namely Maxwell Hill (i.e., Bukit Larut), the Highlands of Telom Valley (i.e., Cameron Highlands), and Penang Hill, and from recent studies, namely Lojing Highlands and Temengor Forest Reserve (Stoliczka 1872, 1873; van Benthem Jutting 1949; Davison 1995; Liew 2010).

Stoliczka's work remains a historical benchmark for the study of land snails in non-limestone areas. In the last 150 years, climate and habitat changes have likely affected land snail populations on Penang Hill, hence a contemporary study with systematic sampling is necessary. In particular, the presence of a small pocket of lower montane habitats at the top of the Penang Hills, due to the Massenerhebung effect (at ca 600–800 m a.s.l.), deserves attention, as such habitats that are normally found at higher elevations on the mainland have a smaller geographical extent on tropical islands. Furthermore, the habitat around Penang has changed significantly due to land use and the increase in tourism activities. To provide a comparison with the historical data collected by Stoliczka in the late 19th century, we conducted a systematic survey of land snails on Penang Hill and compared the inventory with previously published lists by Stoliczka (1872, 1873). We then examined the land snail assemblages in three habitats on Penang Hill, namely disturbed forests with anthropogenic activities, undisturbed forests, and orchards with different crops. Finally, we investigated whether there are differences in land snail composition along the elevation gradient of Penang Hill.

Materials and methods

Study sites and sampling design

A total of 33 standard plots were established for systematic sampling (Table 1, Fig. 1). Three habitat types with different degrees of habitat degradation: (1) forest with almost no anthropogenic activities (hereafter "Undisturbed Forest");

Table 1. Details of the 33 standard sampling plots and six random sampling locations, and the number of species and specimens recorded for each of the plots and sites.

Plot number	Location description	Plot	Elevation (m a.s.l.)	Habitat type	Latitude (dd), Longitude (dd)	Number of land snails species	Total number of specimens
Penang.Plot.01	Penang Hill. The Habitat. Research Trail.	Standard Sampling	720	Undisturbed Forest	5.42484, 100.26695	9	23
Penang.Plot.02	Penang Hill. The Habitat. Research Trail.	Standard Sampling	720	Undisturbed Forest	5.42371, 100.26494	2	3
Penang.Plot.03	Penang Hill. The Habitat. Research Trail.	Standard Sampling	750	Undisturbed Forest	5.42262, 100.26455	7	10
Penang.Plot.04	Penang Hill. The Habitat. Habitat nature trail.	Standard Sampling	770	Disturbed Forest	5.42318, 100.26683	10	55
Penang.Plot.05	Penang Hill. The Habitat. Habitat nature trail.	Standard Sampling	770	Disturbed Forest	5.42286, 100.26531	13	39
Penang.Plot.06	Penang Hill. The Habitat. Research Trail.	Standard Sampling	750	Undisturbed Forest	5.42471, 100.26749	10	41
Penang.Plot.07	Penang Hill. The Habitat. Habitat nature trail.	Standard Sampling	760	Disturbed Forest	5.42105, 100.26428	14	79
Penang.Plot.08	Penang Hill. The Habitat. Habitat nature trail.	Standard Sampling	760	Disturbed Forest	5.42238, 100.26484	9	28
Penang.Plot.09	Penang Hill. Moon Gate Station 5 trail.	Standard Sampling	410	Disturbed Forest	5.4216, 100.28575	1	1
Penang.Plot.10	Penang Hill. Moon Gate Station 5 trail.	Standard Sampling	250	Disturbed Forest	5.4305, 100.29133	4	7
Penang.Plot.11	Penang Hill. Moon Gate Station 5 trail.	Standard Sampling	110	Disturbed Forest	5.43411, 100.29213	9	34
Penang.Plot.12	Penang Hill. Botanical garden.	Standard Sampling	85	Undisturbed Forest	5.43967, 100.28605	7	14
Penang.Plot.13	Penang Hill. Teluk Bahang- Balik Pulau. Lam durian farm.	Standard Sampling	290	Orchard	5.41988, 100.22592	5	15
Penang.Plot.14	Penang Hill. Teluk Bahang- Balik Pulau. Tropical Fruit Farm.	Standard Sampling	260	Orchard	5.41484, 100.21877	4	26
Penang.Plot.15	Penang Hill. Teluk Bahang- Balik Pulau. Tropical Fruit Farm.	Standard Sampling	250	Orchard	5.41605, 100.22006	9	37
Penang.Plot.16	Penang Hill. Teluk Bahang. Taman Rimba Teluk Bahang. Trail. Simpang 6.	Standard Sampling	120	Undisturbed Forest	5.44297, 100.22122	10	22
Penang.Plot.17	Penang Hill. Teluk Bahang-Balik Pulau. Entrance of a durian farm, near Boulder Valley. Old rubber tree.	Standard Sampling	180	Orchard	5.418, 100.21598	9	19
Penang.Plot.18	Penang Hill. Teluk Bahang. Taman Rimba Teluk Bahang. Trail. Stesen 3.	Standard Sampling	150	Undisturbed Forest	5.44209, 100.2218	4	8
Penang.Plot.19	Penang Hill. Teluk Bahang- Balik Pulau. Lam durian farm.	Standard Sampling	280	Orchard	5.42186, 100.22632	5	17
Penang.Plot.20	Penang Hill. Teluk Bahang- Balik Pulau. Bukit Kerajaan ForestReserve next to Lam durian farm.	Standard Sampling	330	Undisturbed Forest	5.41992, 100.22654	4	4
Penang.Plot.21	Penang Hill. Air Itam. Forest near farm.	Standard Sampling	340	Disturbed Forest	5.39087, 100.26371	4	6
Penang.Plot.22	Penang Hill. Trail to Western hill. Junction to Teluk Bahang from Penang Hill.	Standard Sampling	760	Undisturbed Forest	5.42231, 100.2494	3	3
Penang.Plot.23	Penang Hill. Trail to Western hill. Km 3.6.	Standard Sampling	750	Undisturbed Forest	5.42035, 100.25171	6	16
Penang.Plot.24	Penang Hill. Air Itam. Forest near Dam.	Standard Sampling	380	Undisturbed Forest	5.3904, 100.2612	11	30
Penang.Plot.25	Penang Hill. Air Itam. Forest near Dam.	Standard Sampling	290	Undisturbed Forest	5.39003, 100.2575	8	32
Penang.Plot.26	Penang Hill. Air Itam. Forest near Dam.	Standard Sampling	290	Undisturbed Forest	5.39772, 100.2612	7	19
Penang.Plot.27	Penang Hill. Trail from Viaduct to Claremont, after shelter.	Standard Sampling	500	Undisturbed Forest	5.42051, 100.27242	8	12

Plot number	Location description	Plot	Elevation (m a.s.l.)	Habitat type	Latitude (dd), Longitude (dd)	Number of land snails species	Total number of specimens
Penang.Plot.28	Penang Hill. Trail - Moniot Road East.	Standard Sampling	530	Undisturbed Forest	5.42406, 100.2746	11	29
Penang.Plot.29	Penang Hill. Botanical garden.	Standard Sampling	75	Disturbed Forest	5.44009, 100.28661	15	38
Penang.Plot.30	Penang Hill. Western hill to Teluk Bahang Trail Stetion 4	Standard Sampling	570	Undisturbed Forest	5.42111, 100.24208	1	1
Penang.Plot.31	Penang Hill. Western hill to Teluk Bahang Trail Stetion 7	Standard Sampling	490	Undisturbed Forest	5.42919, 100.23344	1	1
Penang.Plot.32	Penang Hill. Moniot Trail	Standard Sampling	695	Undisturbed Forest	5.41655, 100.25743	6	10
Penang.Plot.33	Penang Hill. By Path H	Standard Sampling	610	Disturbed Forest	5.42106, 100.27014	16	90
Penang.Random1	Penang Hill. Path B.	Random Sampling	730	Disturbed Forest	5.42162, 100.26749	8	15
Penang.Random2	Penang Hill. Plaza.	Random Sampling	740	Disturbed Forest	5.4247, 100.2689	1	1
Penang.Random3	Penang Hill. Air Itam Farm. Batu Panay road.	Random Sampling	270	Orchard	5.38914, 100.2664	1	5
Penang.Random4	Penang Hill. The Habitat. Research Trail.	Random Sampling	740	Undisturbed Forest	5.42299, 100.26458	1	1
Penang.Random5	Penang Hill. Bukit Laksamana	Random Sampling	710	Undisturbed Forest	5.42399, 100.23627	1	1
Penang.Random6	Penang Hill. Along Jalan Tunku Yahya Petra	Random Sampling	730	Disturbed Forest	5.422586082, 100.266207	3	11

(2) moderately degraded habitat - disturbed forest with signs of anthropogenic activities such as man-made physical structures and altered vegetation structures (hereafter "Disturbed Forest"); and (3) highly degraded habitat – forest has been replaced by farmland and orchard (hereafter "Orchard"). The plots in disturbed and undisturbed forest can be divided into two altitudinal zones, lowland forest (< 600 m a.s.l.) and lower montane forest (> 600 m a.s.l.). Furthermore, any land snails found outside the standard sampling plots at six random locations were also collected for the species inventory list.

Research permits were obtained from Penang Forestry Department – JPNPP/600-9/1 Jld.3(47), Forestry Department Peninsular Malaysia – JH/100 Jld.34(8), Penang Botanic Gardens – JTB/pp/02/03/032 Jld.5(7), and Penang Water Supply Corporation – PBAPP/CAD/SC/#EXT/1/05/14(6).

Land snail sampling and identification

Each standard plot, an area of 20 m × 20 m, was searched by two persons for one hour, and a total of 5 litres of soil and leaf litter was collected. The sampling was conducted on the following dates: 4–7 Sept 2022, 21–26 Oct 2022, 2–6 Feb 2023, and on 20 Jun 2023. Afterwards, the snails were cleaned and preserved, and the micro-snails (species smaller than 5 mm) were extracted from the soil and leaf litter samples (Foon et al. 2017). After that, the species were identified by comparing the material with illustrations and description in the literature. Where a species could not be identified with certainty, a working morphospecies name (for example, "sp.", or "Penang sp. 1") was used after the genus name. All authorities are provided in the checklist. All specimens were catalogued in the BORNEENSIS Mollusca collection database and were deposited in the BORNEENSIS collection of Institute for Tropical Biology and Conservation, Universiti Malaysia Sabah: BOR/MOL 15081 – BOR/MOL 15164, BOR/MOL 15195 – BOR/MOL 15201, BOR/MOL 15217 – BOR/MOL 15250, BOR/MOL 15268 – BOR/MOL 15305, BOR/MOL 15412 – BOR/MOL 15486, BOR/MOL 15539 – BOR/MOL 15566, BOR/MOL 15726 – BOR/MOL 15773.

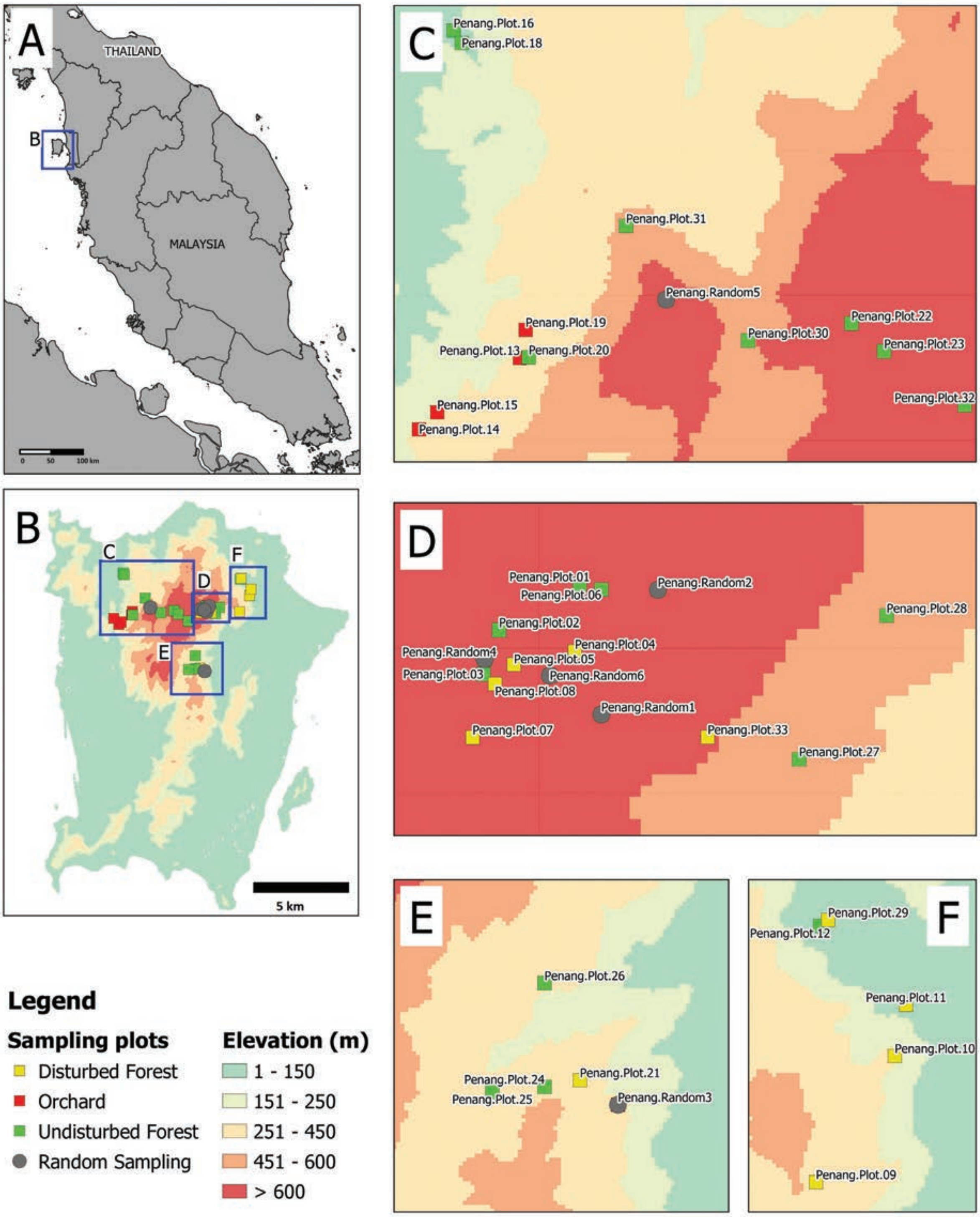

Figure 1. The locations sampling plots and locations on Penang Hill. The details of each of the 33 standard plots and the six random locations are given in Table 1 **A** the location of Penang in Malaysia **B** an overview of sampling plots and locations at Penang Hill **C–F** the detailed distribution of the sampling plots and locations of the three habitat types at different elevations of this study.

Data analysis

For the compilation of the species list, the data from the standard sampling plots and random sites were combined with the records of Stoliczka (1872, 1873). We also checked all the snail photos uploaded by citizen naturalists at iNaturalist. We filtered the records for the geographical extent of Penang Hill, and for Mollusca (https://www.inaturalist.org/observations?captive=false&nelat=5.474271882208513&nelng=100.29576600820225&photos&place_id=any&subview=table&swlat=5.364899735652405&swlng=100.17491639882725&verifiable=any&iconic_taxa=Mollusca). After compiling the list, we checked the status of each species, alien or native. We also gathered distribution data for each species to assess the likelihood that it is endemic to Penang Hill.

For the other biodiversity analysis, only the data from the standard sampling plots were used. The number of species (species richness) and the number of specimens of each species (abundance) were tabulated for each standard sampling plot. The sampling completeness and the estimate of total species richness based on the data from the standard sampling plots were determined using the iNEXT package in R.

For comparison of species richness and fauna composition among plots of different habitat types, we test the hypothesis that there are no differences in species richness among the three habitat types and the species richness is not correlated with elevation. As the normality of species richness and homogeneity of variance between habitat types did not violate the test assumptions, we tested the hypothesis by using a one-way ANCOVA. The response variable is species richness of the plots, with the habitat types as different groups and elevation as a cofounding factor. To investigate whether fauna composition is determined by habitat types and/or elevation, we conducted two analyses to identify underlying patterns of land snail composition. First, we conducted a cluster analysis based on absence and presence data (Jaccard index) of the 50 species in the 33 plots. Then we performed non-metric multidimensional scaling (NMDS) based on the absence/presence data (Jaccard's distance). NMDS analysis is a dimensionality reduction technique used to visualise and explore similarities, while cluster analysis is used to identify natural groupings based on similarity of land snail composition. Finally, we conducted an indicator species analysis (package "indicspecies") to identify species significantly associated with each of the three habitat types (Cáceres and Legendre 2009). All analyses were done with R.

Results

Sampling completeness and inventory of land snails

Our samples yielded 54 land snail species, with a total of 803 specimens. Altogether, 50 species were found in the 33 standard sampling plots, while the remaining four species were found in random and opportunistic sampling locations. Of these 54 land snail species, 34 represent new records compared to the lists of Stoliczka (1872, 1873). We did not recover 12 species recorded previously by Stoliczka, although one of these species (*Meghimatium pictum*) has recently been recorded a few times by citizen naturalists (https://www.inaturalist.org/observations/102000427). Since the work of Stoliszca, the total number of recorded land snail species from Penang has increased from 32 species to 66 species (Table 2). Among the 34 species additional to Stoliczka's list, 19 species are micro-snails (species smaller than 5 mm). They belong to the genera *Kaliella* (6 species), *Microcystina* (5 species), *Philalanka* (2 species), *Diplommatina* (2 species), *Charopa* (2 species), and one species each of *Ditropopsis* and *Paralaoma*. The remaining seven species are commonly found garden snails and slugs, namely, *Allopeas clavulinum*, *Laevicaulis alte*, *Lissachatina fulica*, *Macrochlamys indica*, *Macrochlamys tersa*, *Parmarion martensi*, and *Subulina octona*. These species are identified as alien species.

The land snail diversity across the sampling plots shows several patterns. Among the 33 plots, nine contained between 10 and 16 species, while 14 plots had 5–9 species, seven plots had 2–4 species, and three plots had only one species. Four species emerged as the most common, being found in more than half of the sampling plots: *Pseudoplecta bijuga* (recorded in 22 plots), *Cyclophorus malayanus* (found in 17 plots), *Macrochlamys* Penang sp. 1 (present in 17 plots), and *Microcystina* Penang sp. 1 (observed in 17 plots). The latter two were not recorded by Stoliczka.

In contrast, 28 species displayed limited distributions, being found in not more than three sampling plots (10% of the 33 plots). Among these species, 18 were singleton species; they were found in a single plot only. Additionally, five species were found in only two plots, and five species were recorded in just three plots. Altogether ten of the 34 species not recorded by Stolizka were singleton species. The sampling coverage for the 33 plots was determined to be 92.3%, with 50 observed species (Fig. 2). Based on species richness estimates with rarefied and extrapolated samples, the further extrapolation resulted in the expectation of 94 species.

Species richness and composition among plots of different habitat types

Disturbed forest seems to have the highest species richness per plot: undisturbed forest (mean ± s.d.: 6.4 ± 3.3 species), disturbed forest (9.5 ± 5.1 species), and orchards (6.4 ± 2.4 species), but it is not statistically significantly different (F = 2.206, df = 2.29, p = 0.128). Elevation did not have a confounding effect (F = 0.079, df = 1.29, p = 0.780).

Cluster analysis based on the absence/presence of 50 species in the 33 plots did not show a general pattern of clustering of plots with respect to elevation (Fig. 3). The plots in the different types of orchards showed some similarity in terms of species composition, and plot 29 in the small forest patch in the botanical garden was clustered with other plots in orchards (cluster 2 in Fig. 3). There is also no clear indication that the plots in disturbed and undisturbed forests differ in terms of species composition (cluster 1 and cluster 3 in Fig. 3).

To further investigate species composition between plots, we used NMDS to visualise and reduce the dimensionality of Jaccard's distance matrices based on absence/presence data (Fig. 4). The stress value of 0.17 indicates that the NMDS plot is a fair representation of the data among plots. However, similar to the cluster analysis, there are no clear patterns for species composition in the plots of different habitat types and of different elevations, with the exception of plots in orchards.

Table 2. Comparison of the species list between the previous study by Stoliczka (1872, 1873) and this study.

Family	Species	Stoliczka (1872, 1873)	This study
Alycaeidae	*Alycaeus gibbosulus* Stoliczka, 1872	1	0
Cyclophoridae	*Cyclophorus malayanus* (Benson, 1852)	1	1
Cyclophoridae	*Cyclophorus perdix borneensis* (Metcalfe, 1854)	1	1
Cyclophoridae	*Cyclotus solutus* (Stoliczka, 1872)	1	0
Cyclophoridae	*Ditropopsis* sp.	0	1
Cyclophoridae	*Lagocheilus* Penang sp. 2	0	1
Cyclophoridae	*Lagocheilus trochoides* (Stoliczka, 1872)	1	1
Cyclophoridae	*Lagocheilus striolatus* Stoliczka, 1872	1	1
Cyclophoridae	*Opisthoporus penangensis* (Stoliczka, 1872)	1	1
Diplommatinidae	*Diplommatina* Penang sp. 1	0	1
Diplommatinidae	*Diplommatina crosseana* Godwin-Austen & Nevill, 1879	0	1
Pupinidae	*Coptocheilus sectilabris* (A. Gould, 1844)	1	1
Pupinidae	*Pupina aureola* Stoliczka, 1872	1	1
Pupinidae	*Rhaphaulus lorraine* L. Pfeiffer, 1856	0	1
Achatinidae	*Allopeas clavulinum* (Potiez & Michaud, 1838)	0	1
Achatinidae	*Allopeas gracile* (T. Hutton, 1834)	1	1
Achatinidae	*Lissachatina fulica* (Bowdich, 1822)	0	1
Achatinidae	*Paropeas tchehelense* (de Morgan, 1885)	0	1
Achatinidae	*Subulina octona* (Bruguière, 1792)	0	1
Philomycidae	*Meghimatium pictum* (Stoliczka, 1873)	1	0
Clausiliidae	*Oospira penangensis* (Stoliczka, 1873)	1	1
Clausiliidae	*Phaedusa filicostata* (Stoliczka, 1873)	1	0
Ariophantidae	*Hemiplecta cymatium* (L. Pfeiffer, 1856)	1	1
Ariophantidae	*Microcystina* Penang sp. 1	0	1
Ariophantidae	*Microcystina* Penang sp. 2	0	1
Ariophantidae	*Microcystina* Penang sp. 4	0	1
Ariophantidae	*Microcystina* Penang sp. 5	0	1
Ariophantidae	*Microcystina* Penang sp. 6	0	1
Ariophantidae	*Parmarion martensi* Simroth, 1893	0	1
Ariophantidae	*Tanychlamys indica* Godwin-Austen, 1883	0	1
Ariophantidae	*Tanychlamys* Penang sp. 1	0	1
Ariophantidae	*Tanychlamys* Penang sp. 2	0	1
Ariophantidae	*Tanychlamys stephoides* Stoliczka, 1873	1	1
Ariophantidae	*Tanychlamys tersa* (Issel, 1874)	0	1
Helicarionidae	*Helicarion permolle* Stoliczka, 1873	1	1
Camaenidae	*Amphidromus atricallosus* (A. Gould, 1843)	1	0
Camaenidae	*Amphidromus perversus* (Linnaeus, 1758)	1	0
Camaenidae	*Bradybaena similaris* (A. Férussac, 1821)	1	1
Camaenidae	*Trichochloritis penangensis* (Stoliczka, 1873)	1	1
Charopidae	*Charopa perlata* van Benthem Jutting, 1959	0	1
Charopidae	*Charopa* Penang sp. 2	0	1
Charopidae	*Philalanka carinifera* (Stoliczka, 1873)	1	1
Charopidae	*Philalanka* Penang sp. 2	0	1
Charopidae	*Philalanka kusana* (Aldrich, 1889)	0	1
Punctidae	*Paralaoma* sp.	0	1
Gastrocoptidae	*Gastrocopta palmira* (Stoliczka, 1873)	1	0
Valloniidae	*Pupisoma orcella* (Stoliczka, 1873)	1	0
Streptaxidae	*Gulella bicolor* (T. Hutton, 1834)	1	0
Chronidae	*Kaliella barrakporensis* (Pfeiffer, 1852)	0	1
Chronidae	*Kaliella* Penang sp. 1	0	1
Chronidae	*Kaliella* Penang sp. 2	0	1
Chronidae	*Kaliella* Penang sp. 4	0	1
Chronidae	*Kaliella* Penang sp. 5	0	1
Chronidae	*Kaliella* scandens (Cox, 1872)	0	1
Microcystidae	*Microcystis palmicola* Stoliczka, 1873	1	0

Family	Species	Stoliczka (1872, 1873)	This study
Chronidae	*Vitrinopsis* sp.	0	1
Chronidae	*Vitrinopsis nucleata* (Stoliczka, 1873)	1	1
Dyakiidae	*Quantula striata* (J. E. Gray, 1834)	0	1
Dyakiidae	*Pseudoplecta bijuga* (Stoliczka, 1873)	1	1
Trochomorphidae	*Videna castra* (Benson, 1852)	1	1
Trochomorphidae	*Videna cantoriana* (W. H. Benson, 1861)	1	0
Trochomorphidae	*Videna timorensis* (E. von Martens, 1867)	1	1
Rathouisiidae	*Atopos tourannensis* (Souleyet, 1852)	1	1
Rathouisiidae	*Atopos punctata* Collinge, 1902	0	1
Veronicellidae	*Laevicaulis alte* (A. Férussac, 1822)	0	1
Veronicellidae	*Semperula birmanica* (Theobald, 1864)	1	0

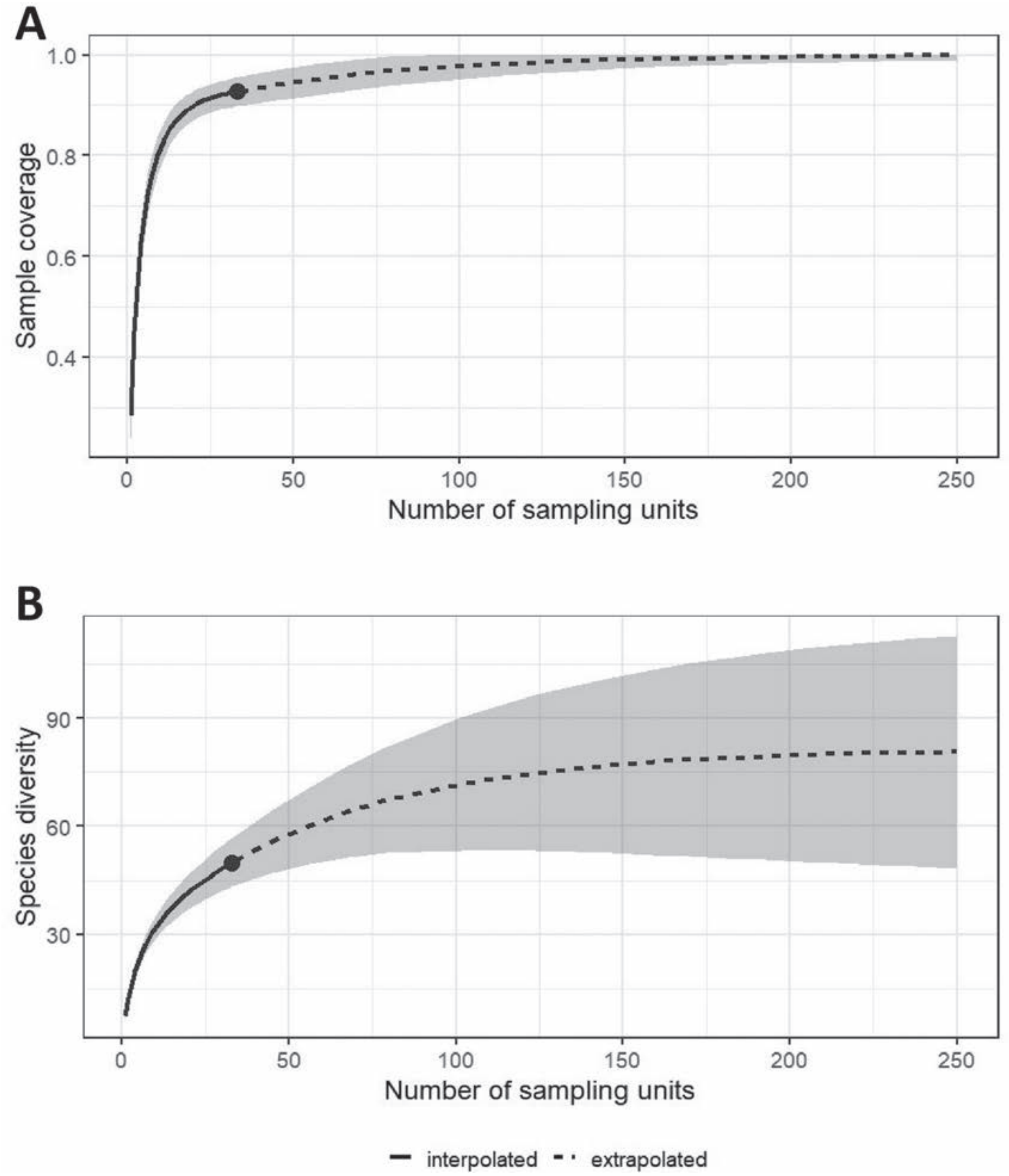

Figure 2. The sample completeness curve based on the 33 standard plots (black dot, i.e., sampling units). Plots of sample coverage for interpolated (solid line) and extrapolated sampling plots (dashed line). The 95% confidence intervals (shaded areas) were obtained by a bootstrap method based on 1000 replications. Each of the two curves was extrapolated to up to 250 plots **A** sampling coverage **B** species diversity (richness) estimated based on the extrapolated samples.

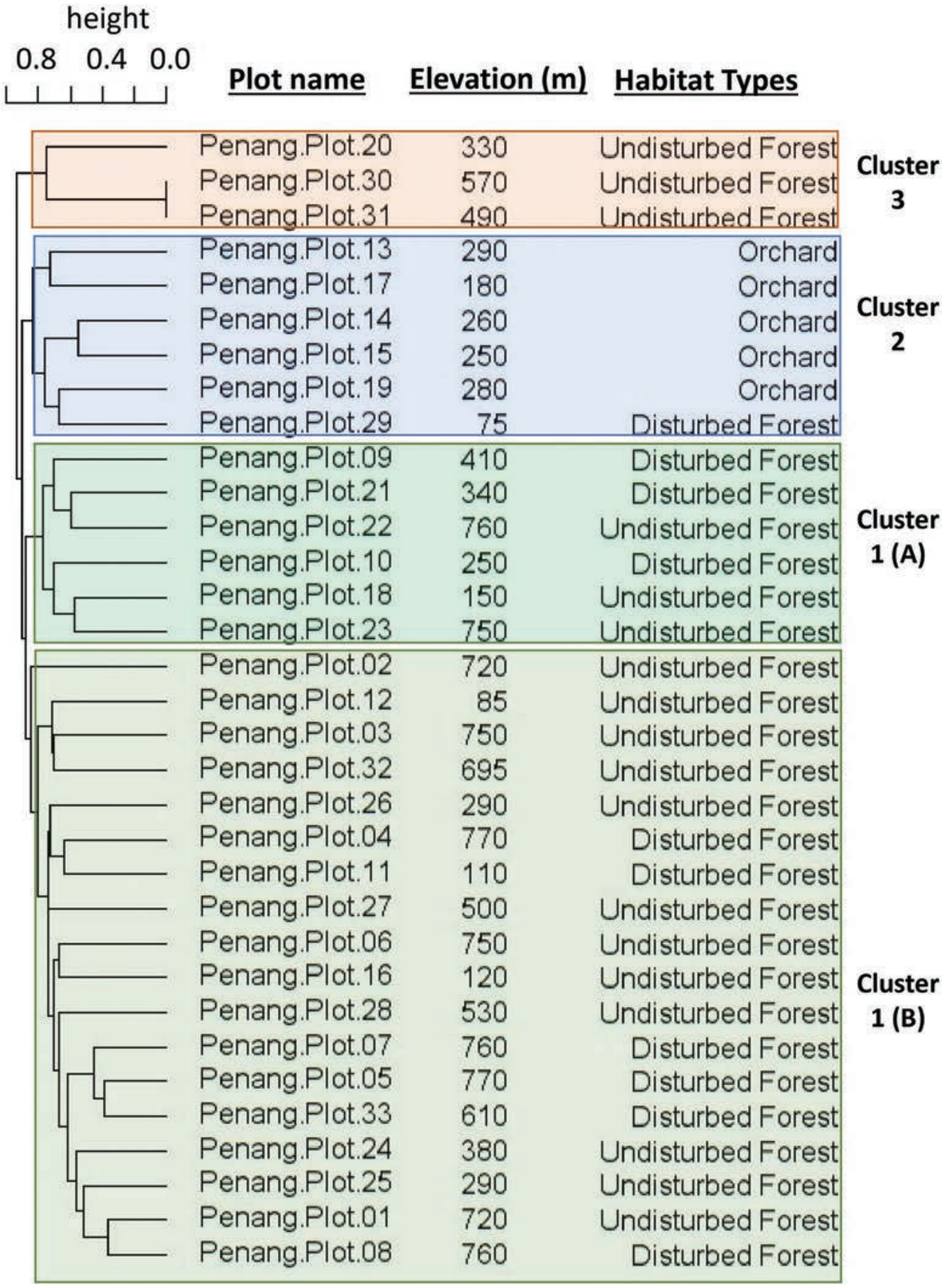

Figure 3. Cluster analysis based on Jaccard dissimilarity of absence and presence data of land snail species composition in 33 standard plots in Penang Hill, Penang Island, Peninsular Malaysia. Three main clusters were identified: Cluster 1, comprising two sub-clusters in which almost all plots in undisturbed and disturbed forests were grouped; Cluster 2, comprising all plots in orchards and one plot in a disturbed forest patch in the botanical garden; and Cluster 3, comprising three undisturbed plots.

The indicator species analysis revealed strong associations between certain land snail species and specific habitat types. *Helicarion permolle* (value = 0.52, p = 0.024) and *Lissachatina fulica* (value = 0.618, p = 0.008) were found to be closely linked to disturbed forest areas, signifying their preference for such habitats. On the other hand, *Allopeas gracile* (value = 0.731, p = 0.002), *Kaliella*

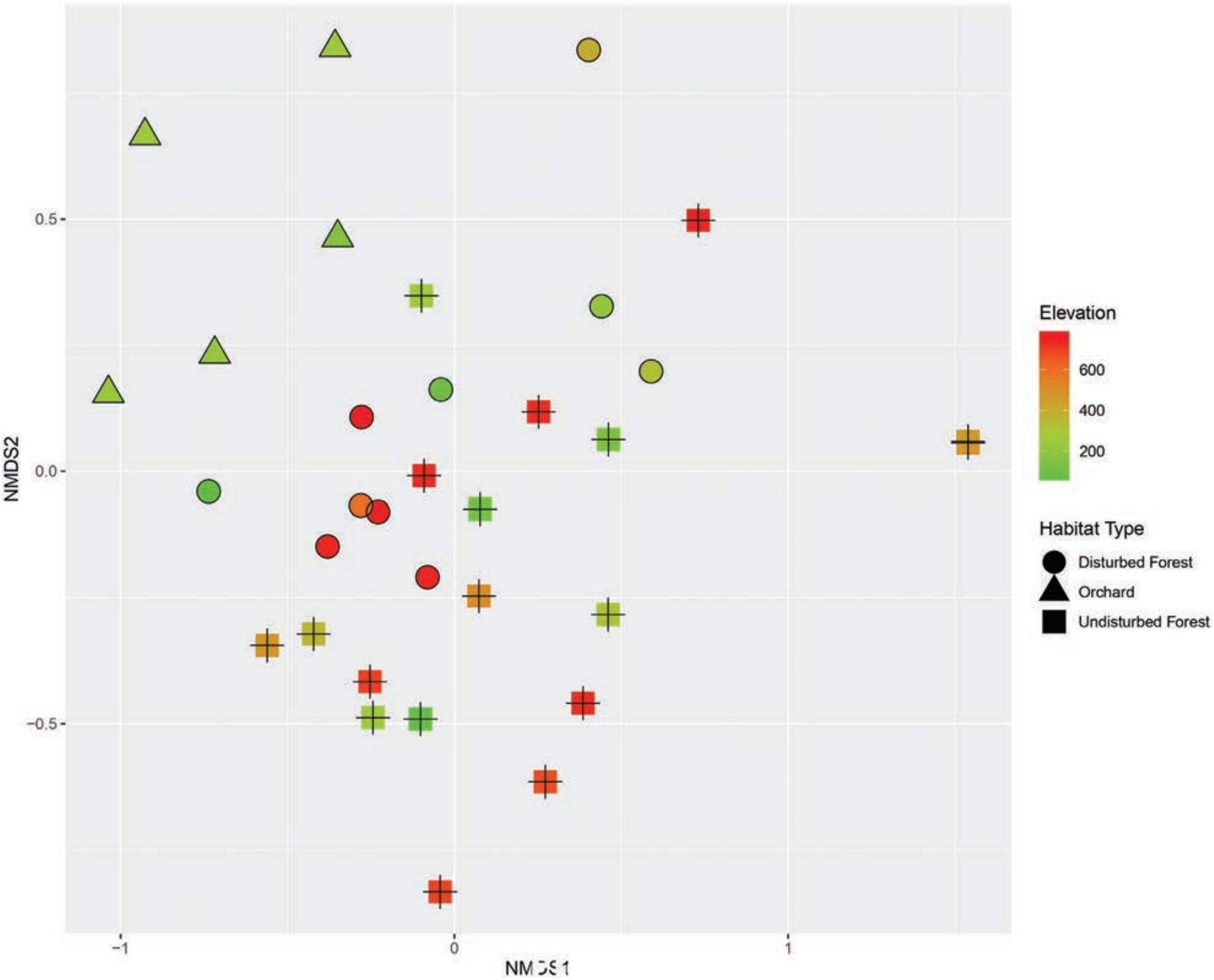

Figure 4. Non-metric multidimensional scaling (NMDS) ordination of land snail communities between the 33 standard plots based on Jaccard's distance (stress value 0.19). Different symbols represent different habitat types. The colour of the symbols indicates the elevation of the plots.

scandens (value = 0.567, p = 0.016), and *Charopa* Penang sp. 2 (value = 0.567, p = 0.014) exhibited strong affiliations with orchards, indicating their specific affinity for these modified landscapes.

Checklist

Class Gastropoda Cuvier, 1795,
Subclass Caenogastropoda Cox, 1960
Superfamily Cyclophoroidea J. E. Gray, 1847
Family Alycaeidae W. T. Blanford, 1864
Genus *Alycaeus* J. E. Gray, 1850

Alycaeus gibbosulus Stoliczka, 1872

Remark. Old record from the base of Penang Hill by Stoliczka (1872).

Family Cyclophoridae J. E. Gray, 1847
Genus *Cyclophorus* Montfort, 1810

Cyclophorus malayanus (W. H. Benson, 1852)
Figs 5A, 19A

Material examined. Malaysia • Penang Hill, The Habitat, Research trail, Plot.01; 5.4248°N, 100.2669°E; 720 m a.s.l.; 5 Sept. 2022; T.S. Liew, J. Dulipat, S.M. Goh leg.; BOR/MOL 15163 • Penang Hill, The Habitat, Habitat nature trail, Plot.04; 5.4231°N, 100.2668°E; 770 m a.s.l.; 5 Sept. 2022; T.S. Liew, J. Dulipat, S.M. Goh leg.; BOR/MOL 15119 • Penang Hill, The Habitat, Habitat nature trail, Plot.05; 5.4228°N, 100.2653°E; 770 m a.s.l.; 5 Sept. 2022; T.S. Liew, J. Dulipat, S.M. Goh leg.; BOR/MOL 15126 • Penang Hill, The Habitat, Research trail, Plot.06; 5.4247°N, 100.2674°E; 750 m a.s.l.; 5 Sept. 2022; T.S. Liew, J. Dulipat, S.M. Goh, M.Y. Lee, M.Y. Wua leg.; BOR/MOL 15140 • Penang Hill, The Habitat, Habitat nature trail, Plot.08; 5.4223°N, 100.2648°E; 760 m a.s.l.; 6 Sept. 2022; J. Dulipat, S.M. Goh, M.Y. Lee leg.; BOR/MOL 15099 • Penang Hill, Moon Gate Station 5 trail, Plot.11; 5.4341°N, 100.2921°E; 110 m a.s.l.; 7 Sept. 2022; T.S. Liew, J. Dulipat, S.M. Goh leg.; BOR/MOL 15100 • same data as for preceding; BOR/MOL 15101 • same data as for preceding; BOR/MOL 15152 • Penang Hill, Botanical garden, Plot.12; 5.4396°N, 100.2860°E; 85 m a.s.l.; 4 Sept. 2022; T.S. Liew, J. Dulipat, S.M. Goh leg.; BOR/MOL 15091 • Penang Hill, Teluk Bahang, Taman Rimba Teluk Bahang, Trail, Simpang 6, Plot.16; 5.4429°N, 100.2212°E; 120 m a.s.l.; 21 Oct. 2022; T.S. Liew, J. Dulipat, M.Y. Lee leg.; BOR/MOL 15221 • same data as for preceding; BOR/MOL 15273 • Penang Hill, Teluk Bahang-Balik Pulau, Entrance of a durian farm, near Boulder Valley, Old rubber tree, Plot.17; 5.418°N, 100.2159°E; 180 m a.s.l.; 22 Oct. 2022; T.S. Liew, J. Dulipat leg.; BOR/MOL 15222 • same data as for preceding; BOR/MOL 15278 • Penang Hill, Teluk Bahang- Balik Pulau, Bukit Kerajaan ForestReserve next to Lam durian farm, Plot.20; 5.4199°N, 100.2265°E; 330 m a.s.l.; 23 Oct. 2022; T.S. Liew, J. Dulipat, M.Y. Lee leg.; BOR/MOL 15281 • Penang Hill, Air Itam, Forest near Dam, Plot.24; 5.3904°N, 100.2612°E; 380 m a.s.l.; 24 Oct. 2022; T.S. Liew, J. Dulipat leg.; BOR/MOL 15219 • same data as for preceding; BOR/MOL 15232 • same data as for preceding; BOR/MOL 15289 • Penang Hill, Air Itam, Forest near Dam, Plot.25; 5.3900°N, 100.2575°E; 290 m a.s.l.; 25 Oct. 2022; T.S. Liew, J. Dulipat leg.; BOR/MOL 15295 • Penang Hill, Air Itam, Forest near Dam, Plot.26; 5.3977°N, 100.2612°E; 290 m a.s.l.; 25 Oct. 2022; T.S. Liew, J. Dulipat leg.; BOR/MOL 15240 • same data as for preceding; BOR/MOL 15296 • Penang Hill, Trail - Moniot Road East, Plot.28; 5.4240°N, 100.2746°E; 530 m a.s.l.; 26 Oct. 2022; T.S. Liew, J. Dulipat leg.; BOR/MOL 15298 • Penang Hill, Botanical garden, Plot.29; 5.4400°N, 100.2866°E; 75 m a.s.l.; 2 Feb. 2023; T.S. Liew, M.Y. Lee, A. Yusni leg.; BOR/MOL 15729 • same data as for preceding; BOR/MOL 15766 • Penang Hill, Moniot trail, Plot.32; 5.4165°N, 100.2574°E; 695 m a.s.l.; 4 Feb. 2023; T.S. Liew, A. Yusni leg.; BOR/MOL 15769 • Penang Hill, By Path H, Plot.33; 5.4210°N, 100.2701°E; 610 m a.s.l.; 4 Feb. 2023; T.S. Liew, A. Yusni leg.; BOR/MOL 15730 • Penang Hill, Path B, Random1. PathB; 5.4216°N, 100.2674°E; 730 m a.s.l.; 4 Sept. 2022; T.S. Liew, J. Dulipat leg.; BOR/MOL 15103 • same data as for preceding; BOR/MOL 15107 • same data as for preceding; BOR/MOL 15149.

Figure 5. **A** *Cyclophorus malayanus* (W. H. Benson, 1852) BOR/MOL 15149 **B** *Cyclophorus perdix borneensis* (Metcalfe, 1854) BOR/MOL 15726 **C** *Ditropopsis* sp. BOR/MOL 15747 **D** *Lagocheilus* Penang sp. 2 BOR/MOL 15429 **E** *Lagocheilus trochoides* (Stoliczka, 1872) BOR/MOL 15739 **F** *Lagocheilus striolatus* Stoliczka, 1872 BOR/MOL 15200. Scale bars: 10 mm (**A, B**); 1 mm (**C**); 5 mm (**D–F**).

Remarks. One of the most common large land snails at Penang Hill, with a shell width of up to 45 mm. It is also known from other localities in the northern part of Peninsular Malaysia. This species can be found in Perak as well (Foon et al. 2017).

Cyclophorus perdix perdix (Broderip & G. B. Sowerby I, 1830)

Figs 5B, 19B

Material examined. Malaysia • Penang Hill, The Habitat, Research trail, Plot.03; 5.4226°N, 100.2645°E; 750 m a.s.l.; 5 Sept. 2022; T.S. Liew, J. Dulipat, S.M. Goh leg.; BOR/MOL 15157 • Penang Hill, The Habitat, Habitat nature trail, Plot.04; 5.4231°N, 100.2668°E; 770 m a.s.l.; 5 Sept. 2022; T.S. Liew, J. Dulipat, S.M. Goh leg.; BOR/MOL 15127 • same data as for preceding; BOR/MOL 15118 • Penang Hill, The Habitat, Habitat nature trail, Plot.05; 5.4228°N, 100.2653°E; 770 m a.s.l.; 5 Sept. 2022; T.S. Liew, J. Dulipat, S.M. Goh leg.; BOR/MOL 15135 • Penang Hill, The Habitat, Research trail, Plot.06; 5.4247°N, 100.2674°E; 750 m a.s.l.; 5 Sep . 2022; T.S. Liew, J. Dulipat, S.M. Goh, M.Y. Lee, M.Y. Wua leg.; BOR/MOL 15141 • Penang Hill, Teluk Bahang, Taman Rimba Teluk Bahang, Trail Stesen 3, Plot.18; 5.4420°N, 100.2218°E; 150 m a.s.l.; 22 Oct. 2022; T.S. Liew, J. Dulipat leg.; BOR/MOL 15282 • Penang Hill, Trail - Moniot Road East, Plot.28; 5.4240°N, 100.2746°E; 530 m a.s.l.; 26 Oct. 2022; T.S. Liew, J. Dulipat leg.; BOR/MOL 15299 • Penang Hill, Moniot trail, Plot.32; 5.4165°N, 100.2574°E; 695 m a.s.l.; 4 Feb. 2023; T.S. Liew, A. Yusni leg.; BOR/MOL 15728 • Penang Hill, By Path H, Plot.33; 5.4210°N, 100.2701°E; 610 m a.s.l.; 4 Feb. 2023; T.S. Liew, A. Yusni leg.; BOR/MOL 15726 • Penang Hill, Path B, Random1. PathB; 5.4216°N, 100.2674°E; 730 m a.s.l.; 4 Sept. 2022; T.S. Liew, J. Dulipat leg.; BOR/MOL 15102.

Remarks. Less common than *Cyclophorus malayanus* on Penang Hill, it was found to occur sympatrically with *Cyclophorus malayanus* in this study. This species can also be found in Perak (Foon et al. 2017).

Genus *Cyclotus* Swainson, 1840

Cyclotus solutus (Stoliczka, 1872)

Remarks. This species is common in Perak (Foon et al. 2017) and was recorded by Stoliczka (1872) at the base of Penang Hill. However, it was not recorded in this study.

Genus *Ditropopsis* E. A. Smith, 1897

Ditropopsis sp.

Fig. 5C

Materials examined. Malaysia • Penang Hill, Moniot trail, Plot.32; 5.4165°N, 100.2574°E; 695 m a.s.l.; 4 Feb. 2023; T.S. Liew, A. Yusni leg.; BOR/MOL 15747.

Remarks. New record for Penang Hill. So far, only one *Ditropopsis* species has been recorded from Peninsular Malaysia (Maassen 2001), namely

Ditropopsis cavernae (Sykes, 1903), which is distinctly different from the species found on Penang Hill. This genus was not recorded in previous systematic inventory studies in Peninsular Malaysia (Liew 2010; Foon et al. 2017; Foon and Marzuki 2023). The species from Penang Hill is similar to *Ditropopsis constricta* Vermeulen, Liew & Schilthuizen, 2015 in terms of size, shape, and shell sculpture but differs by having a detached protoconch.

Genus *Lagocheilus* W. T. Blanford, 1864

Lagocheilus Penang sp. 2
Fig. 5D

Material examined. Malaysia • Penang Hill, The Habitat, Habitat nature trail, Plot.04; 5.4231°N, 100.2668°E; 770 m a.s.l.; 5 Sept. 2022; T.S. Liew, J. Dulipat, S.M. Goh leg.; BOR/MOL 15430 • Penang Hill, The Habitat, Habitat nature trail, Plot.05; 5.4228°N, 100.2653°E; 770 m a.s.l.; 5 Sept. 2022; T.S. Liew, J. Dulipat, S.M. Goh leg.; BOR/MOL 15428 • Penang Hill, Moon Gate Station 5 trail, Plot.11; 5.4341°N, 100.2921°E; 110 m a.s.l.; 7 Sept. 2022; T.S. Liew, J. Dulipat, S.M. Goh leg.; BOR/MOL 15427 • Penang Hill, Teluk Bahang, Taman Rimba Teluk Bahang, Trail, Simpang 6, Plot.16; 5.4429°N, 100.2212°E; 120 m a.s.l.; 21 Oct. 2022; T.S. Liew, J. Dulipat, M.Y. Lee leg.; BOR/MOL 15541• Penang Hill, Teluk Bahang-Balik Pulau, Entrance of a durian farm, near Boulder Valley, Old rubber tree, Plot.17; 5.418°N, 100.2159°E; 180 m a.s.l.; 22 Oct. 2022; T.S. Liew, J. Dulipat leg.; BOR/MOL 15429.

Remarks. This is a new record for Penang Hill. This species differs from *L. trochoides* by having more, less prominent spiral ribs, and from *L. striolatus* by having more spiral ribs. It also differs from *L. garelli* (Souleyet, 1852), which was previously recorded and described from Penang, by having more rapidly expanding whorl size.

Lagocheilus trochoides (Stoliczka, 1872)
Figs 5E, 19C

Material examined. Malaysia • Penang Hill, The Habitat, Research trail, Plot.01; 5.4248°N, 100.2669°E; 720 m a.s.l.; 5 Sept. 2022; T.S. Liew, J. Dulipat, S.M. Goh leg.; BOR/MOL 15081 • Penang Hill, The Habitat, Habitat nature trail, Plot.05; 5.4228°N, 100.2653°E; 770 m a.s.l.; 5 Sept. 2022; T.S. Liew, J. Dulipat, S.M. Goh leg.; BOR/MOL 15134 • Penang Hill, The Habitat, Research trail, Plot.06; 5.4247°N, 100.2674°E; 750 m a.s.l.; 5 Sept. 2022; T.S. Liew, J. Dulipat, S.M. Goh, M.Y. Lee, M.Y. Wua leg.; BOR/MOL 15084 • same data as for preceding; BOR/MOL 15085 • same data as for preceding; BOR/MOL 15139 • Penang Hill, The Habitat, Habitat nature trail, Plot.07; 5.4210°N, 100.2642°E; 760 m a.s.l.; 6 Sept. 2022; T.S. Liew, J. Dulipat, S.M. Goh, M.Y. Lee leg.; BOR/MOL 15143 • Penang Hill, The Habitat, Habitat nature trail, Plot.08; 5.4223°N, 100.2648°E; 760 m a.s.l.; 6 Sept. 2022; J. Dulipat, S.M. Goh, M.Y. Lee leg.; BOR/MOL 15156 • Penang Hill, Teluk Bahang, Taman Rimba Teluk Bahang, Trail, Simpang 6, Plot.16; 5.4429°N, 100.2212°E; 120 m a.s.l.; 21 Oct. 2022; T.S. Liew, J. Dulipat, M.Y. Lee leg.; BOR/MOL 15540 •

Penang Hill, Teluk Bahang- Balik Pulau, Bukit Kerajaan ForestReserve next to Lam durian farm, Plot.20; 5.4199°N, 100.2265°E; 330 m a.s.l.; 23 Oct. 2022; T.S. Liew, J. Dulipat, M.Y. Lee leg.; BOR/MOL 15425 • Penang Hill, Air Itam, Forest near Dam, Plot.24; 5.3904°N, 100.2612°E; 380 m a.s.l.; 24 Oct. 2022; T.S. Liew, J. Dulipat leg.; BOR/MOL 15287 • Penang Hill, Trail from Viaduct to Claremont, after shelter, Plot.27; 5.4205°N, 100.2724°E; 500 m a.s.l.; 26 Oct. 2022; T.S. Liew, J. Dulipat leg.; BOR/MOL 15426 • Penang Hill, Botanical garden, Plot.29; 5.4400°N, 100.2866°E; 75 m a.s.l.; 2 Feb. 2023; T.S. Liew, M.Y. Lee, A. Yusni leg.; BOR/MOL 15738 • Penang Hill, By Path H, Plot.33; 5.4210°N, 100.2701°E; 610 m a.s.l.; 4 Feb. 2023; T.S. Liew, A. Yusni leg.; BOR/MOL 15737.

Remark. This species is more common than *L. striolatus* at Penang Hill.

Lagocheilus striolatus Stoliczka, 1872

Fig. 5F

Material examined. MALAYSIA • Penang Hill, The Habitat, Habitat nature trail, Plot.04; 5.4231°N, 100.2668°E; 770 m a.s.l.; 5 Sept. 2022; T.S. Liew, J. Dulipat, S.M. Goh leg.; BOR/MOL 15200.

Remark. A rare species on Penang Hill.

Genus *Opisthoporus* W. H. Benson, 1851

Opisthoporus penangensis Stoliczka, 1872

Fig. 6A

Material examined. MALAYSIA • Penang Hill, Teluk Bahang, Taman Rimba Teluk Bahang, Trail, Simpang 6, Plot.16; 5.4429°N, 100.2212°E; 120 m a.s.l.; 21 Oct. 2022; T.S. Liew, J. Dulipat, M.Y. Lee leg.; BOR/MOL 15275.

Remarks. Originally described from base of Penang Hill (Stoliczka 1872) and recorded in only one plot of this study. This species has also been recorded in the northern part of Peninsular Malaysia and southern Thailand (Maassen 2001; Foon et al. 2017).

Family Diplommatinidae L. Pfeiffer, 1856

Genus *Diplommatina* W. H. Benson, 1849

Diplommatina Penang sp. 1

Fig. 6B

Material examined. MALAYSIA • Penang Hill, Moon Gate Station 5 trail, Plot.10; 5.4305°N, 100.2913°E; 250 m a.s.l.; 7 Sept. 2022; T.S. Liew, J. Dulipat, S.M. Goh leg.; BOR/MOL 15442 • Penang Hill, Trail to Western hill, Km 3.6, Plot.23; 5.4203°N, 100.2517°E; 750 m a.s.l.; 24 Oct. 2022; T.S. Liew, J. Dulipat, M.Y. Lee leg.; BOR/MOL 15542.

Remarks. This is a new record for Penang Hill. Based on the only shell fragments collected, it is likely *Diplommatina ventriculus*, which was originally described from Perak (von Möllendorff 1891).

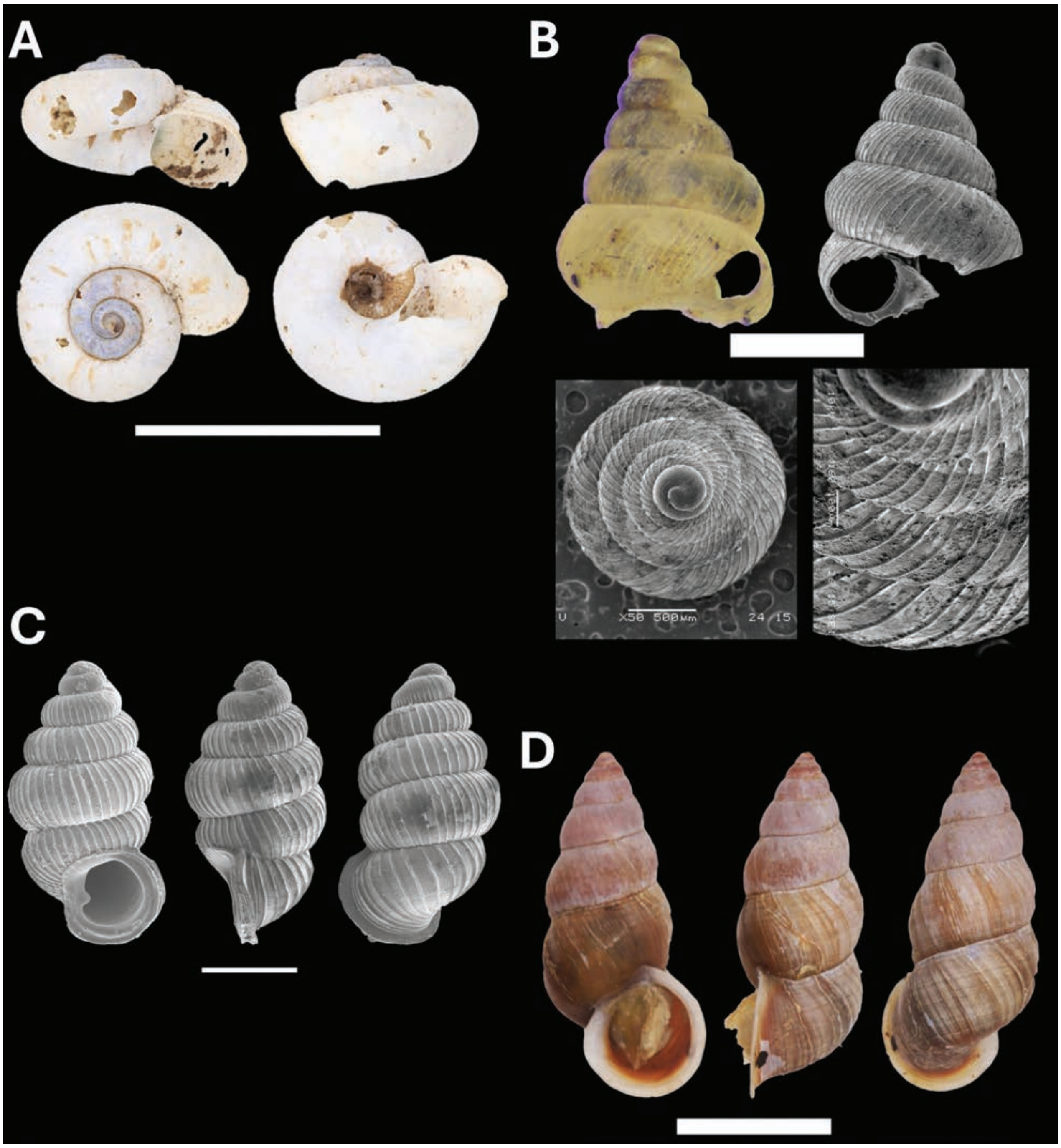

Figure 6. A *Opisthoporus penangensis* Stoliczka, 1872 BOR/MOL 15275 **B** *Diplommatina* Penang sp. 1 BOR/MOL 15442 **C** *Diplommatina crosseana* Godwin-Austen & Nevill, 1879 BOR/MOL 15543 **D** *Coptocheilus sectilabris* (A. Gould, 1844) BOR/MOL 15270. Scale bars: 10 mm (**A, D**); 0.5 mm (**B, C**).

Diplommatina crosseana Godwin-Austen & Nevill, 1879
Fig. 6C

Material examined. Malaysia • Penang Hill, Botanical garden, Plot.12; 5.4396°N, 100.2860°E; 85 m a.s.l.; 4 Sept. 2022; T.S. Liew, J. Dulipat, S.M. Goh leg.; BOR/MOL 15443 • Penang Hill, Teluk Bahang, Taman Rimba Teluk Bahang, Trail, Simpang 6, Plot.16; 5.4429°N, 100.2212°E; 120 m a.s.l.; 21 Oct. 2022; T.S. Liew, J. Dulipat, M.Y. Lee leg.; BOR/MOL 15543 • Penang Hill, Teluk Bahang, Taman

Rimba Teluk Bahang, Trail Stesen 3, Plot.18; 5.4420°N, 100.2218°E; 150 m a.s.l.; 22 Oct. 2022; T.S. Liew, J. Dulipat leg.; BOR/MOL 15444 • Penang Hill, Air Itam, Forest near farm, Plot.21; 5.3908°N, 100.2637°E; 340 m a.s.l.; 23 Oct. 2022; T.S. Liew, J. Dulipat leg.; BOR/MOL 15544.

Remark. New record for Penang Hill. Previously known only from Perak (Maassen 2001; Foon et al. 2017).

Family Pupinidae L. Pfeiffer, 1853
Genus *Coptocheilus* A. Gould, 1862

***Coptocheilus sectilabris* (A. Gould, 1844)**
Figs 6E, 19D

Material examined. Malaysia • Penang Hill, The Habitat, Research trail, Random4.; 5.4229°N, 100.2645°E; 740 m a.s.l.; 27 Oct. 2022; M.Y. Lee leg.; BOR/MOL 15270.

Remarks. So far, all the records were found at the top of Penang Hill, specifically around the Habitat, but it is very rare elsewhere on Penang Hill. It is a widespread species in Indochina and Peninsular Malaysia (Maassen 2001; Tumpeesuwan and Panha 2008; Foon et al. 2017).

Genus *Pupina* Vignard, 1829

***Pupina aureola* Stoliczka, 1872**
Figs 7A, 19E

Material examined. Malaysia • Penang Hill, Moon Gate Station 5 trail, Plot.10; 5.4305°N, 100.2913°E; 250 m a.s.l.; 7 Sept. 2022; T.S. Liew, J. Dulipat, S.M. Goh leg.; BOR/MOL 15124 • Penang Hill, Moon Gate Station 5 trail, Plot.11; 5.4341°N, 100.2921°E; 110 m a.s.l.; 7 Sept. 2022; T.S. Liew, J. Dulipat, S.M. Goh leg.; BOR/MOL 15094 • Penang Hill, Trail - Moniot Road East, Plot.28; 5.4240°N, 100.2746°E; 530 m a.s.l.; 26 Oct. 2022; T.S. Liew, J. Dulipat leg.; BOR/MOL 15225.

Remark. This species is also recorded from the northern part of Peninsular Malaysia and southern Thailand (Maassen 2001; Jirapatrasilp et al. 2022).

Genus *Rhaphaulus* L. Pfeiffer, 1856

***Rhaphaulus lorraini* L. Pfeiffer, 1856**
Figs 7B, 19F

Material examined. Malaysia • Penang Hill, Trail to Western hill, Km 3.6, Plot.23; 5.4203°N, 100.2517°E; 750 m a.s.l.; 24 Oct. 2022; T.S. Liew, J. Dulipat, M.Y. Lee leg.; BOR/MOL 15226 • same data as for preceding; BOR/MOL 15285.

Remarks. This species was described from Penang Hill (Pfeiffer 1856) but was not recorded by Stoliczka (1872, 1873). It is a widespread species in Malaysia and southern Thailand (Laidlaw 1928; Pall-Gergely et al. 2014; Jirapatrasilp et al. 2022).

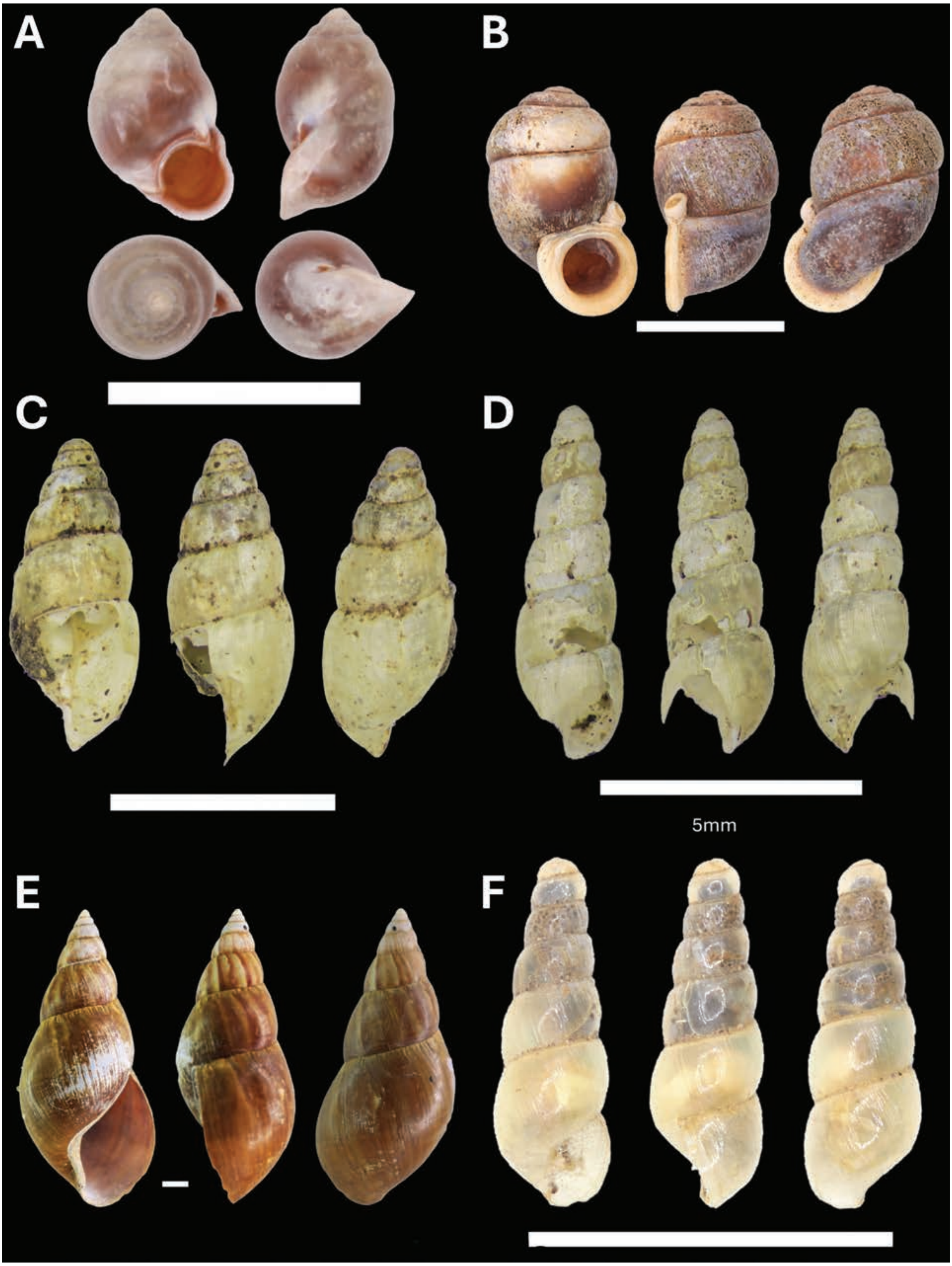

Figure 7. **A** *Pupina aureola* Stoliczka, 1872 BOR/MOL 15225 **B** *Rhaphaulus lorraini* L. Pfeiffer, 1856 BOR/MOL 15285 **C** *Allopeas clavulinum* (Potiez & Michaud, 1838) BOR/MOL 15419 **D** *Allopeas gracile* (T. Hutton, 1834) BOR/MOL 15547 **E** *Lissachatina fulica* (Bowdich, 1822) BOR/MOL 15195 **F** *Subulina octona* (Bruguière, 1789) BOR/MOL 15545. Scale bars: 5 mm (**A–C, D, F**); 10 mm (**E**).

Subclass Heterobranchia
Informal group Pulmonata Cuvier, in de Blainville 1814
Superfamily Achatinoidea Swainson, 1840
Family Achatinidae Swainson, 1840
Genus *Allopeas* H. B. Baker, 1935

***Allopeas clavulinum* (Potiez & Michaud, 1838)**
Fig. 7C

Material examined. Malaysia • Penang Hill, The Habitat, Habitat nature trail, Plot.05; 5.4228°N, 100.2653°E; 770 m a.s.l.; 5 Sept. 2022; T.S. Liew, J. Dulipat, S.M. Goh leg.; BOR/MOL 15416 • Penang Hill, The Habitat, Habitat nature trail, Plot.07; 5.4210°N, 100.2642°E; 760 m a.s.l.; 6 Sept. 2022; T.S. Liew, J. Dulipat, S.M. Goh, M.Y. Lee leg.; BOR/MOL 15418 • Penang Hill, Moon Gate Station 5 trail, Plot.11; 5.4341°N, 100.2921°E; 110 m a.s.l.; 7 Sept. 2022; T.S. Liew, J. Dulipat, S.M. Goh leg.; BOR/MOL 15420 • Penang Hill, Teluk Bahang-Balik Pulau, Entrance of a durian farm, near Boulder Valley, Old rubber tree, Plot.17; 5.418°N, 100.2159°E; 180 m a.s.l.; 22 Oct. 2022; T.S. Liew, J. Dulipat leg.; BOR/MOL 15415 • Penang Hill, Teluk Bahang- Balik Pulau, Lam durian farm, Plot.19; 5.4218°N, 100.2263°E; 280 m a.s.l.; 23 Oct. 2022; T.S. Liew, J. Dulipat, M.Y. Lee leg.; BOR/MOL 15419 • same data as for preceding; BOR/MOL 15421 • Penang Hill, Air Itam, Forest near Dam, Plot.24; 5.3904°N, 100.2612°E; 380 m a.s.l.; 24 Oct. 2022; T.S. Liew, J. Dulipat leg.; BOR/MOL 15417 • Penang Hill, Botanical garden, Plot.29; 5.4400°N, 100.2866°E; 75 m a.s.l.; 2 Feb. 2023; T.S. Liew, M.Y. Lee, A. Yusni leg.; BOR/MOL 15750 • Penang Hill, By Path H, Plot.33; 5.4210°N, 100.2701°E; 610 m a.s.l.; 4 Feb. 2023; T.S. Liew, A. Yusni leg.; BOR/MOL 15751.

Remark. New record for Penang Hill. It is possibly an introduced species and is widespread in Malaysia (Foon et al. 2017).

***Allopeas gracile* (T. Hutton, 1834)**
Fig. 7D

Material examined. Malaysia • Penang Hill, The Habitat, Research trail, Plot.06; 5.4247°N, 100.2674°E; 750 m a.s.l.; 5 Sept. 2022; T.S. Liew, J. Dulipat, S.M. Goh, M.Y. Lee, M.Y. Wua leg.; BOR/MOL 15414 • Penang Hill, Teluk Bahang- Balik Pulau, Lam durian farm, Plot.13; 5.4198°N, 100.2259°E; 290 m a.s.l.; 21 Oct. 2022; T.S. Liew, J. Dulipat, M.Y. Lee leg.; BOR/MOL 15546 • Penang Hill, Teluk Bahang- Balik Pulau, Tropical fruit farm, Plot.14; 5.4148°N, 100.2187°E; 260 m a.s.l.; 21 Oct. 2022; T.S. Liew, J. Dulipat, M.Y. Lee leg.; BOR/MOL 15547 • Penang Hill, Teluk Bahang- Balik Pulau, Tropical fruit farm, Plot.15; 5.4160°N, 100.2200°E; 250 m a.s.l.; 21 Oct. 2022; T.S. Liew, J. Dulipat, M.Y. Lee leg.; BOR/MOL 15548 • Penang Hill, Teluk Bahang- Balik Pulau, Lam durian farm, Plot.19; 5.4218°N, 100.2263°E; 280 m a.s.l.; 23 Oct. 2022; T.S. Liew, J. Dulipat, M.Y. Lee leg.; BOR/MOL 15284 • Penang Hill, Botanical garden, Plot.29; 5.4400°N, 100.2866°E; 75 m a.s.l.; 2 Feb. 2023; T.S. Liew, M.Y. Lee, A. Yusni leg.; BOR/MOL 15749.

Remarks. More common in disturbed habitats on Penang Hill. It is possibly an introduced species and is widespread in Malaysia (Foon et al. 2017).

Genus *Lissachatina* Bequaert, 1950

Lissachatina fulica (Bowdich, 1822)

Figs 7E, 20A

Material examined. Malaysia • Penang Hill, The Habitat, Habitat nature trail, Plot.04; 5.4231°N, 100.2668°E; 770 m a.s.l.; 5 Sept. 2022; T.S. Liew, J. Dulipat, S.M. Goh leg.; BOR/MOL 15486 • Penang Hill, The Habitat, Habitat nature trail, Plot.05; 5.4228°N, 100.2653°E; 770 m a.s.l.; 5 Sept. 2022; T.S. Liew, J. Dulipat, S.M. Goh leg.; BOR/MOL 15131 • same data as for preceding; BOR/MOL 15195 • Penang Hill, The Habitat, Habitat nature trail, Plot.07; 5.4210°N, 100.2642°E; 760 m a.s.l.; 6 Sept. 2022; T.S. Liew, J. Dulipat, S.M. Goh, M.Y. Lee leg.; BOR/MOL 15088 • same data as for preceding; MOL 15147 • same data as for preceding; BOR/MOL 15423 • Penang Hill, Teluk Bahang- Balik Pulau, Lam durian farm, Plot.13; 5.4198°N, 100.2259°E; 290 m a.s.l.; 21 Oct. 2022; T.S. Liew, J. Dulipat, M.Y. Lee leg.; BOR/MOL 15271 • Penang Hill, Teluk Bahang- Balik Pulau, Tropical fruit farm, Plot.15; 5.4160°N, 100.2200°E; 250 m a.s.l.; 21 Oct. 2022; T.S. Liew, J. Dulipat, M.Y. Lee leg.; BOR/MOL 15272 • Penang Hill, Teluk Bahang-Balik Pulau, Entrance of a durian farm, near Boulder Valley, Old rubber tree, Plot.17; 5.418°N, 100.2159°E; 180 m a.s.l.; 22 Oct. 2022; T.S. Liew, J. Dulipat leg.; BOR/MOL 15412 • Penang Hill, Teluk Bahang- Balik Pulau, Lam durian farm, Plot.19; 5.4218°N, 100.2263°E; 280 m a.s.l.; 23 Oct. 2022; T.S. Liew, J. Dulipat, M.Y. Lee leg.; BOR/MOL 15230 • same data as for preceding; BOR/MOL 15283 • Penang Hill, Botanical garden, Plot.29; 5.4400°N, 100.2866°E; 75 m a.s.l.; 2 Feb. 2023; T.S. Liew, M.Y. Lee, A. Yusni leg.; BOR/MOL 15731 • Penang Hill, By Path H, Plot.33; 5.4210°N, 100.2701°E; 610 m a.s.l.; 4 Feb. 2023; T.S. Liew, A. Yusni leg.; BOR/MOL 15727.

Remarks. New record for Penang Hill. This species was likely introduced to Malaysia as earlier as 1911 in Kedah, and 1922 in Penang (South 1926; Berry and Chan 1968). A widespread introduced species in Malaysia.

Genus *Paropeas* Pilsbry, 1906

Paropeas tchehelense (de Morgan, 1885)

Fig. 8B

Material examined. Malaysia • Penang Hill, The Habitat, Research trail, Plot.01; 5.4248°N, 100.2669°E; 720 m a.s.l.; 5 Sept. 2022; T.S. Liew, J. Dulipat, S.M. Goh leg.; BOR/MOL 15162 • Penang Hill, The Habitat, Habitat nature trail, Plot.08; 5.4223°N, 100.2648°E; 760 m a.s.l.; 6 Sept. 2022; J. Dulipat, S.M. Goh, M.Y. Lee leg.; BOR/MOL 15097.

Remark. New record from Penang Hill. This species is also recorded from the mainland of Peninsular Malaysia and southern Thailand (Maassen 2001; Foon et al. 2017).

Genus *Subulina* H. Beck, 1837

Subulina octona (Bruguière, 1789)
Fig. 7F

Material examined. Malaysia • Penang Hill, Teluk Bahang- Balik Pulau, Lam durian farm, Plot.19; 5.4218°N, 100.2263°E; 280 m a.s.l.; 23 Oct. 2022; T.S. Liew, J. Dulipat, M.Y. Lee leg.; BOR/MOL 15422 • Penang Hill, Trail to Western hill, Junction to Teluk Bahang from Penang Hill, Plot.22; 5.4223°N, 100.2494°E; 760 m a.s.l.; 24 Oct. 2022; T.S. Liew, J, Dulipat, M.Y. Lee leg.; BOR/MOL 15545 • Penang Hill, Botanical garden, Plot.29; 5.4400°N, 100.2866°E; 75 m a.s.l.; 2 Feb. 2023; T.S. Liew, M.Y. Lee, A. Yusni leg.; BOR/MOL 15748.

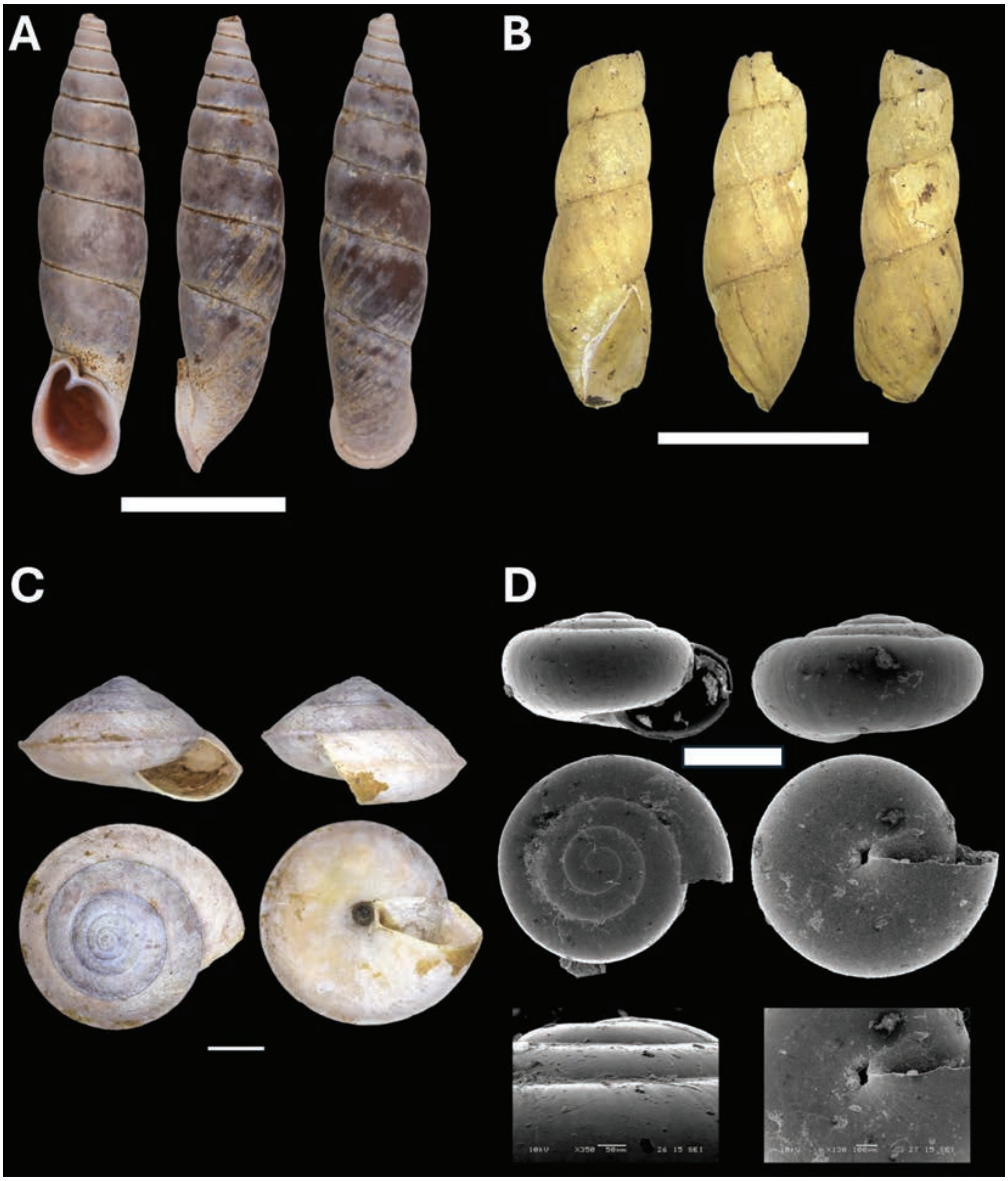

Figure 8. **A** *Oospira penangensis* (Stoliczka, 1873) BOR/MOL 15243 **B** *Prosopeas tchehelense* (de Morgan, 1885) BOR/MOL 15162 **C** *Hemiplecta cymatium* (L. Pfeiffer, 1856) BOR/MOL 15736 **D** *Microcystina* Penang sp. 1 BOR/MOL 15754. Scale bars: 10 mm (**A–C**); 0.5 mm (**D**).

Remarks. New record from Penang Hill. This species is also recorded from the mainland of Peninsular Malaysia (Maassen 2001; Foon et al. 2017).

Superfamily Arionoidea Gray, 1840
Family Philomycidae Gray, 1847
Genus *Meghimatium* van Hasselt, 1823

***Meghimatium pictum* (Stoliczka, 1873)**
Fig. 22E

Remarks. This species was previously described by Stoliczka (1873) from the base of the hill in the north, at ca 100 feet above sea level. It was not found during the sampling of this study. However, this species was recently photographed on Penang Hill (Fig. 22E). It is thought to be a widespread species found from East Asia to Indochina (Tsai et al. 2011 Inkhavilay et al. 2019; Ito et al. 2023).

Superfamily Clausilioidea J. E. Gray, 1855
Family Clausiliidae J. E. Gray, 1855
Genus *Oospira* W. T. Blanford, 1872

***Oospira penangensis* (Stoliczka, 1873)**
Figs 8A, 20B

Material examined. Malaysia • Penang Hill, Air Itam, Forest near Dam, Plot.24; 5.3904°N, 100.2612°E; 380 m a.s.l.; 24 Oct. 2022; T.S. Liew, J. Dulipat leg.; BOR/MOL 15223 • Penang Hill, Air Itam, Forest near Dam, Plot.25; 5.3900°N, 100.2575°E; 290 m a.s.l.; 25 Oct. 2022; T.S. Liew, J. Dulipat leg.; BOR/MOL 15224 • Penang Hill, Trail - Moniot Road East, Plot.28; 5.4240°N, 100.2746°E; 530 m a.s.l.; 26 Oct. 2022; T.S. Liew, J. Dulipat leg.; BOR/MOL 15243.

Remark. This species was described and recorded by Stoliczka (1873) from Penang Hill, and it can also be found in Perak (Maassen 2001).

Genus *Phaedusa* H. Adams & A. Adams, 1855

***Phaedusa filicostata* (Stoliczka, 1873)**

Remark. Previously described and recorded by Stoliczka (1873) from Penang Hill but not found in this study.

Superfamily Helicarionoidea Bourguignat, 1877
Family Ariophantidae Godwin-Austen, 1883
Genus *Hemiplecta* Albers, 1850

***Hemiplecta cymatium* (L. Pfeiffer, 1856)**
Figs 8C, 20C

Material examined. Malaysia • Penang Hill, The Habitat, Research trail, Plot.01; 5.4248°N, 100.2669°E; 720 m a.s.l.; 5 Sept. 2022; T.S. Liew, J. Dulipat, S.M.

Goh leg.; BOR/MOL 15161 • Penang Hill, The Habitat, Research trail, Plot.02; 5.4237°N, 100.2649°E; 720 m a.s.l.; 5 Sept. 2022; T.S. Liew, J. Dulipat, S.M. Goh leg.; BOR/MOL 15158 • Penang Hill, The Habitat, Habitat nature trail, Plot.05; 5.4228°N, 100.2653°E; 770 m a.s.l.; 5 Sept. 2022; T.S. Liew, J. Dulipat, S.M. Goh leg.; BOR/MOL 15136 • Penang Hill, The Habitat, Research trail, Plot.06; 5.4247°N, 100.2674°E; 750 m a.s.l.; 5 Sept. 2022; T.S. Liew, J. Dulipat, S.M. Goh, M.Y. Lee, M.Y. Wua leg.; BOR/MOL 15137 • Penang Hill, The Habitat, Habitat nature trail, Plot.07; 5.4210°N, 100.2642°E; 760 m a.s.l.; 6 Sept. 2022; T.S. Liew, J. Dulipat, S.M. Goh, M.Y. Lee leg.; BOR/MOL 15087 • same data as for preceding; BOR/MOL 15105 • same data as for preceding; BOR/MOL 15142 • Penang Hill, The Habitat, Habitat nature trail, Plot.08; 5.4223°N, 100.2648°E; 760 m a.s.l.; 6 Sept. 2022; J. Dulipat, S.M. Goh, M.Y. Lee leg.; BOR/MOL 15096 • Penang Hill, Botanical garden, Plot.12; 5.4396°N, 100.2860°E; 85 m a.s.l.; 4 Sept. 2022; T.S. Liew, J. Dulipat, S.M. Goh leg.; BOR/MOL 15092 • Penang Hill, Teluk Bahang, Taman Rimba Teluk Bahang, Trail, Simpang 6, Plot.16; 5.4429°N, 100.2212°E; 120 m a.s.l.; 21 Oct. 2022; T.S. Liew, J. Dulipat, M.Y. Lee leg.; BOR/MOL 15269 • Penang Hill, Teluk Bahang-Balik Pulau, Entrance of a durian farm, near Boulder Valley, Old rubber tree, Plot.17; 5.418°N, 100.2159°E; 180 m a.s.l.; 22 Oct. 2022; T.S. Liew, J. Dulipat leg.; BOR/MOL 15277 • Penang Hill, Air Itam, Forest near Dam, Plot.24; 5.3904°N, 100.2612°E; 380 m a.s.l.; 24 Oct. 2022; T.S. Liew, J. Dulipat leg.; BOR/MOL 15220 • same data as for preceding; BOR/MOL 15290 • Penang Hill, Air Itam, Forest near Dam, Plot.25; 5.3900°N, 100.2575°E; 290 m a.s.l.; 25 Oct. 2022; T.S. Liew, J. Dulipat leg.; BOR/MOL 15294 • Penang Hill, Botanical garden, Plot.29; 5.4400°N, 100.2866°E; 75 m a.s.l.; 2 Feb. 2023; T.S. Liew, M.Y. Lee, A. Yusni leg.; BOR/MOL 15736 • Penang Hill, By Path H, Plot.33; 5.4210°N, 100.2701°E; 610 m a.s.l.; 4 Feb. 2023; T.S. Liew, A. Yusni leg.; BOR/MOL 15735 • Penang Hill, Path B, Random1. PathB; 5.4216°N, 100.2674°E; 730 m a.s.l.; 4 Sept. 2022; T.S. Liew, J. Dulipat leg.; BOR/MOL 15104 • same data as for preceding; BOR/MOL 15148.

Remarks. One of the most common large land snails at Penang Hill, with a shell width of up to 40 mm. It is also known from other localities in Peninsular Malaysia. This species can also be found in Perak (Maassen 2001; Foon et al. 2017).

Genus *Microcystina* Mörch, 1872

Microcystina Penang sp. 1

Fig. 8D

Material examined. Malaysia • Penang Hill, The Habitat, Habitat nature trail, Plot.05; 5.4228°N, 100.2653°E; 770 m a.s.l.; 5 Sept. 2022; T.S. Liew, J. Dulipat, S.M. Goh leg.; BOR/MOL 15453 • Penang Hill, The Habitat, Research trail, Plot.06; 5.4247°N, 100.2674°E; 750 m a.s.l.; 5 Sept. 2022; T.S. Liew, J. Dulipat, S.M. Goh, M.Y. Lee, M.Y. Wua leg.; BOR/MOL 15455 • Penang Hill, The Habitat, Habitat nature trail, Plot.07; 5.4210°N, 100.2642°E; 760 m a.s.l.; 6 Sept. 2022; T.S. Liew, J. Dulipat, S.M. Goh, M.Y. Lee leg.; BOR/MOL 15448 • Penang Hill, The Habitat, Habitat nature trail, Plot.08; 5.4223°N, 100.2648°E; 760 m a.s.l.; 6 Sept. 2022; J. Dulipat, S.M. Goh, M.Y. Lee leg.; BOR/MOL 15450 • Penang Hill, Moon

Gate Station 5 trail, Plot.09; 5.4216°N, 100.2857°E; 410 m a.s.l.; 7 Sept. 2022; T.S. Liew, J. Dulipat, S.M. Goh leg.; BOR/MOL 15445 • Penang Hill, Moon Gate Station 5 trail, Plot.10; 5.4305°N, 100.2913°E; 250 m a.s.l.; 7 Sept. 2022; T.S. Liew, J. Dulipat, S.M. Goh leg.; BOR/MOL 15451 • Penang Hill, Moon Gate Station 5 trail, Plot.11; 5.4341°N, 100.2921°E; 110 m a.s.l.; 7 Sept. 2022; T.S. Liew, J. Dulipat, S.M. Goh leg.; BOR/MOL 15449 • Penang Hill, Teluk Bahang- Balik Pulau, Lam durian farm, Plot.13; 5.4198°N, 100.2259°E; 290 m a.s.l.; 21 Oct. 2022; T.S. Liew, J. Dulipat, M.Y. Lee leg.; BOR/MOL 15558 • Penang Hill, Teluk Bahang, Taman Rimba Teluk Bahang, Trail, Simpang 6, Plot.16; 5.4429°N, 100.2212°E; 120 m a.s.l.; 21 Oct. 2022; T.S. Liew, J. Dulipat, M.Y. Lee leg.; BOR/MOL 15557 • Penang Hill, Teluk Bahang-Balik Pulau, Entrance of a durian farm, near Boulder Valley, Old rubber tree, Plot.17; 5.418°N, 100.2159°E; 180 m a.s.l.; 22 Oct. 2022; T.S. Liew, J. Dulipat leg.; BOR/MOL 15447 • Penang Hill, Teluk Bahang, Taman Rimba Teluk Bahang, Trail Stesen 3, Plot.18; 5.4420°N, 100.2218°E; 150 m a.s.l.; 22 Oct. 2022; T.S. Liew, J. Dulipat leg.; BOR/MOL 15452 • Penang Hill, Air Itam, Forest near farm, Plot.21; 5.3908°N, 100.2637°E; 340 m a.s.l.; 23 Oct. 2022; T.S. Liew, J. Dulipat leg.; BOR/MOL 15555 • Penang Hill, Trail to Western hill, Junction to Teluk Bahang from Penang Hill, Plot.22; 5.4223°N, 100.2494°E; 760 m a.s.l.; 24 Oct. 2022; T.S. Liew, J, Dulipat, M.Y. Lee leg.; BOR/MOL 15556 • Penang Hill, Trail to Western hill, Km 3.6, Plot.23; 5.4203°N, 100.2517°E; 750 m a.s.l.; 24 Oct. 2022; T.S. Liew, J. Dulipat, M.Y. Lee leg.; BOR/MOL 15554 • Penang Hill, Air Itam, Forest near Dam, Plot.26; 5.3977°N, 100.2612°E; 290 m a.s.l.; 25 Oct. 2022; T.S. Liew, J. Dulipat leg.; BOR/MOL 15454 • Penang Hill, Trail - Moniot Road East, Plot.28; 5.4240°N, 100.2746°E; 530 m a.s.l.; 26 Oct. 2022; T.S. Liew, J. Dulipat leg.; BOR/MOL 15446 • Penang Hill, By Path H, Plot.33; 5.4210°N, 100.2701°E; 610 m a.s.l.; 4 Feb. 2023; T.S. Liew, A. Yusni leg.; BOR/MOL 15754.

Remarks. This is a new record for Penang Hill of a widespread species. The shell has a slightly raised spire with a height less than half of the last whorl height. The upper shell, including the apical and subsequent whorls, shows growth lines, while the lower shell exhibits faint spiral lines.

Microcystina **Penang sp. 2**

Fig. 9A

Material examined. Malaysia • Penang Hill, The Habitat, Research trail, Plot.01; 5.4248°N, 100.2669°E; 720 m a.s.l.; 5 Sept. 2022; T.S. Liew, J. Dulipat, S.M. Goh leg.; BOR/MOL 15456 • Penang Hill, The Habitat, Habitat nature trail, Plot.07; 5.4210°N, 100.2642°E; 760 m a.s.l.; 6 Sept. 2022; T.S. Liew, J. Dulipat, S.M. Goh, M.Y. Lee leg.; BOR/MOL 15458 • Penang Hill, Air Itam, Forest near Dam, Plot.25; 5.3900°N, 100.2575°E; 290 m a.s.l.; 25 Oct. 2022; T.S. Liew, J. Dulipat leg.; BOR/MOL 15459 • Penang Hill, Trail - Moniot Road East, Plot.28; 5.4240°N, 100.2746°E; 530 m a.s.l.; 26 Oct. 2022; T.S. Liew, J. Dulipat leg.; BOR/MOL 15457 • Penang Hill, By Path H, Plot.33; 5.4210°N, 100.2701°E; 610 m a.s.l.; 4 Feb. 2023; T.S. Liew, A. Yusni leg.; BOR/MOL 15763.

Remarks. This is a new record for Penang Hill. The shell spire is highly raised, with a height more than half of the last whorl height. This species has the most convex shell compared to other *Microcystina* species from Penang

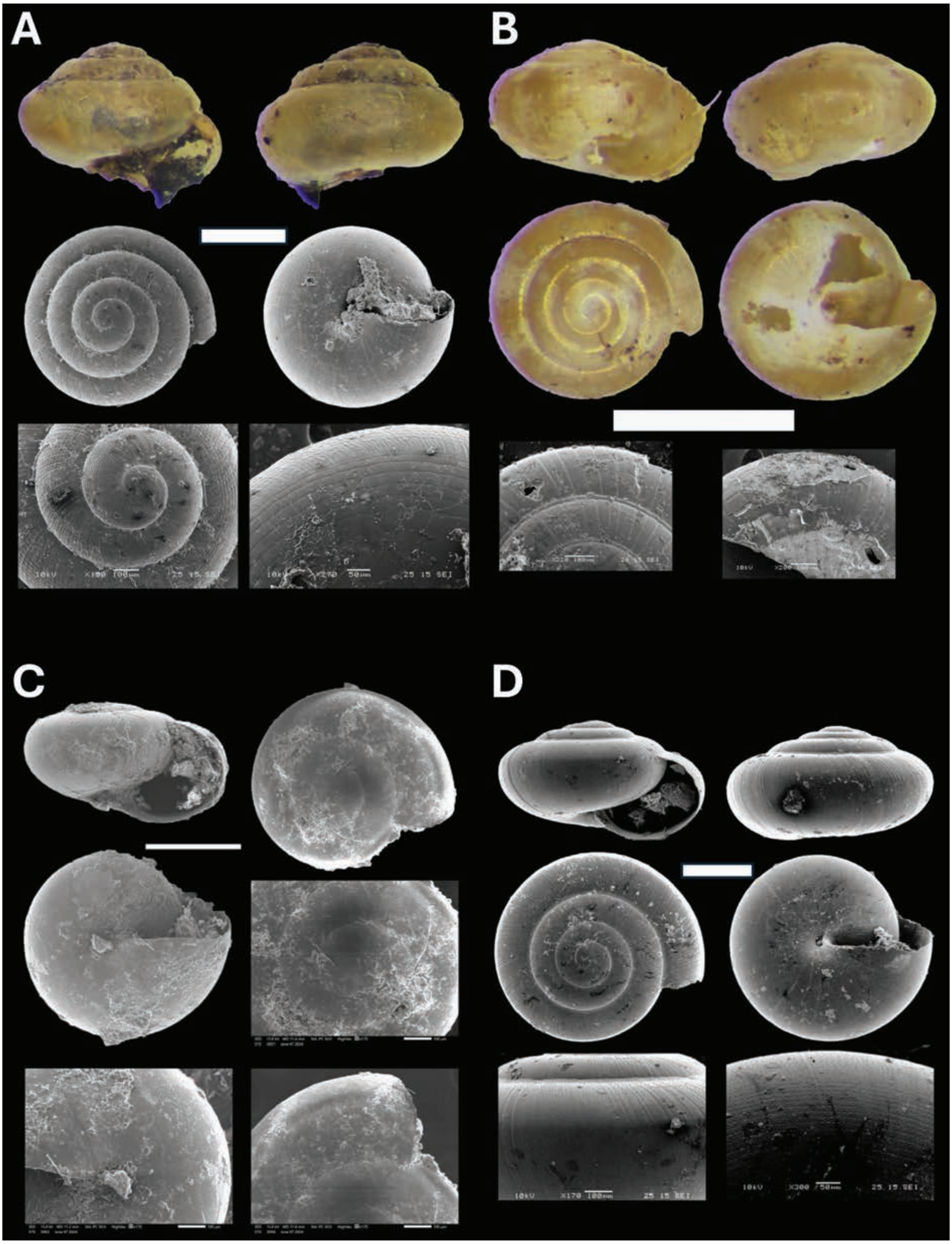

Figure 9. A *Microcystina* Penang sp. 2 BOR/MOL 15458 **B** *Microcystina* Penang sp. 4 BOR/MOL 15755 **C** *Microcystina* Penang sp. 5 BOR/MOL 15762 **D** *Microcystina* Penang sp. 6 BOR/MOL 15756. Scale bar: 0.5 mm.

Hill. On the upper shell, the apical whorls have elevated spiral ribs that continue onto subsequent whorls, which are crossed by radial ribs forming granule-like sculptures. Below the shell, there are spaced grooves with spiral lines at the periphery, which reduce towards the umbilicus.

Microcystina Penang sp. 4

Fig. 9B

Material examined. Malaysia • Penang Hill, The Habitat, Research trail, Plot.03; 5.4226°N, 100.2645°E; 750 m a.s.l.; 5 Sept. 2022; T.S. Liew, J. Dulipat, S.M. Goh leg.; BOR/MOL 15462 • Penang Hill, Botanical garden, Plot.12; 5.4396°N, 100.2860°E; 85 m a.s.l.; 4 Sept. 2022; T.S. Liew, J. Dulipat, S.M. Goh leg.; BOR/MOL 15463 • Penang Hill, Moniot trail, Plot.32; 5.4165°N, 100.2574°E; 695 m a.s.l.; 4 Feb. 2023; T.S. Liew, A. Yusni leg.;BOR/MOL 15755.

Remarks. This is a new record for Penang Hill. The shell spire is moderately raised, with a height less than half of the last whorl height. On the upper shell, the apical whorls are smooth, and subsequent whorls have regularly spaced deep radial grooves. This species has the most prominent radial grooves compared to other *Microcystina* species from Penang Hill. Below the shell, there are regularly spaced, deep, radial grooves that continue from the upper shell.

Microcystina Penang sp. 5

Fig. 9C

Material examined. Malaysia • Penang Hill, Air Itam, Forest near Dam, Plot.26; 5.3977°N, 100.2612°E; 290 m a.s.l.; 25 Oct. 2022; T.S. Liew, J. Dulipat leg.; BOR/MOL 15464 • Penang Hill, By Path H, Plot.33; 5.4210°N, 100.2701°E; 610 m a.s.l.; 4 Feb. 2023; T.S. Liew, A. Yusni leg.; BOR/MOL 15762.

Remarks. This is a new record for Penang Hill. The shell spire is hardly raised, with a height less than half of the last whorl height. On the upper shell, there are densely spirally arranged pits on the apical and subsequent whorls. This species is unique among the *Microcystina* species from Penang Hill in having densely spirally arranged pits on the whorls near the periphery. Below the shell, there are densely spirally arranged pits that continue from the upper shell and fade away towards the umbilicus.

Microcystina Penang sp. 6

Fig. 9D

Material examined. Malaysia • Penang Hill, Teluk Bahang- Balik Pulau, Lam durian farm, Plot.13; 5.4198°N, 100.2259°E; 290 m a.s.l.; 21 Oct. 2022; T.S. Liew, J. Dulipat, M.Y. Lee leg.; BOR/MOL 15559 • Penang Hill, Botanical garden, Plot.29; 5.4400°N, 100.2866°E; 75 m a.s.l.; 2 Feb. 2023; T.S. Liew, M.Y. Lee, A. Yusni leg.; BOR/MOL 15756.

Remarks. This is a new record for Penang Hill. The shell spire is slightly raised, and the shell whorls are more rapidly expanded compared to other *Microcystina* species from Penang Hill. On the upper shell, there are densely spirally arranged pits on the apical whorls, transitioning to densely placed spiral grooves on the subsequent whorls, which become more densely placed towards the periphery. Below the shell, there are densely placed spiral grooves that continue from the upper shell and fade away towards the umbilicus.

Genus *Parmarion* P. Fischer, 1855

Parmarion martensi Simroth, 1893

Figs 10A, 20D

Material examined. Malaysia • Penang Hill, Teluk Bahang- Balik Pulau, Tropical fruit farm, Plot.15; 5.4160°N, 100.2200°E; 250 m a.s.l.; 21 Oct. 2022; T.S. Liew, J. Dulipat, M.Y. Lee leg.; BOR/MOL 15229 • same data as for preceding; BOR/MOL 15239.

Remark. This is a new record for Penang Hill. This species is widespread in Malaysia and might have been introduced to this location (Maassen 2001).

Genus *Tanychlamys* W. H. Benson, 1834

Tanychlamys indica (Godwin Austen, 1883)

Figs 10B, 20E

Material examined. Malaysia • Penang Hill, Along Jalan Tunku Yahya Petra, Random6.; 5.4225°N, 100.2662°E; 730 m a.s.l.; 20 Jun. 2023; T.S. Liew leg.; BOR/MOL 15771.

Remarks. This is a new record for Penang Hill. This species is widespread in Malaysia and might have been introduced to this location (Maassen 2001).

Tanychlamys Penang sp. 1

Figs 10C, 20F

Material examined. Malaysia • Penang Hill, The Habitat, Research trail, Plot.01; 5.4248°N, 100.2669°E; 720 m a.s.l.; 5 Sept. 2022; T.S. Liew, J. Dulipat, S.M. Goh leg.; BOR/MOL 15160 • Penang Hill, The Habitat, Research trail, Plot.03; 5.4226°N, 100.2645°E; 750 m a.s.l.; 5 Sept. 2022; T.S. Liew, J. Dulipat, S.M. Goh leg.;, BOR/MOL 15198 • Penang Hill, The Habitat, Habitat nature trail, Plot.04; 5.4231°N, 100.2668°E; 770 m a.s.l.; 5 Sept. 2022; T.S. Liew, J. Dulipat, S.M. Goh leg.; BOR/MOL 15130 • Penang Hill, The Habitat, Habitat nature trail, Plot.05; 5.4228°N, 100.2653°E; 770 m a.s.l.; 5 Sept. 2022; T.S. Liew, J. Dulipat, S.M. Goh leg.; BOR/MOL 15132 • Penang Hill, The Habitat, Habitat nature trail, Plot.07; 5.4210°N, 100.2642°E; 760 m a.s.l.; 6 Sept. 2022; T.S. Liew, J. Dulipat, S.M. Goh, M.Y. Lee leg.; BOR/MOL 15145 • Penang Hill, The Habitat, Habitat nature trail, Plot.08; 5.4223°N, 100.2648°E; 760 m a.s.l.; 6 Sept. 2022; J. Dulipat, S.M. Goh, M.Y. Lee leg.; BOR/MOL 15098 • same data as for preceding; BOR/MOL 15154 • Penang Hill, Moon Gate Station 5 trail, Plot.11; 5.4341°N, 100.2921°E; 110 m a.s.l.; 7 Sept. 2022; T.S. Liew, J. Dulipat, S.M. Goh leg.; BOR/MOL 15153 • Penang Hill, Botanical garden, Plot.12; 5.4396°N, 100.2860°E; 85 m a.s.l.; 4 Sept. 2022; T.S. Liew, J. Dulipat, S.M. Goh leg.; BOR/MOL 15413 • Penang Hill, Teluk Bahang- Balik Pulau, Tropical fruit farm, Plot.14; 5.4148°N, 100.2187°E; 260 m a.s.l.; 21 Oct. 2022; T.S. Liew, J. Dulipat, M.Y. Lee leg.; BOR/MOL 15247 • Penang Hill, Teluk Bahang- Balik Pulau, Tropical fruit farm, Plot.15; 5.4160°N, 100.2200°E; 250 m a.s.l.; 21 Oct. 2022; T.S. Liew, J. Dulipat, M.Y. Lee leg.; BOR/MOL 15302 • Penang Hill, Air Itam, Forest near farm, Plot.21; 5.3908°N, 100.2637°E; 340

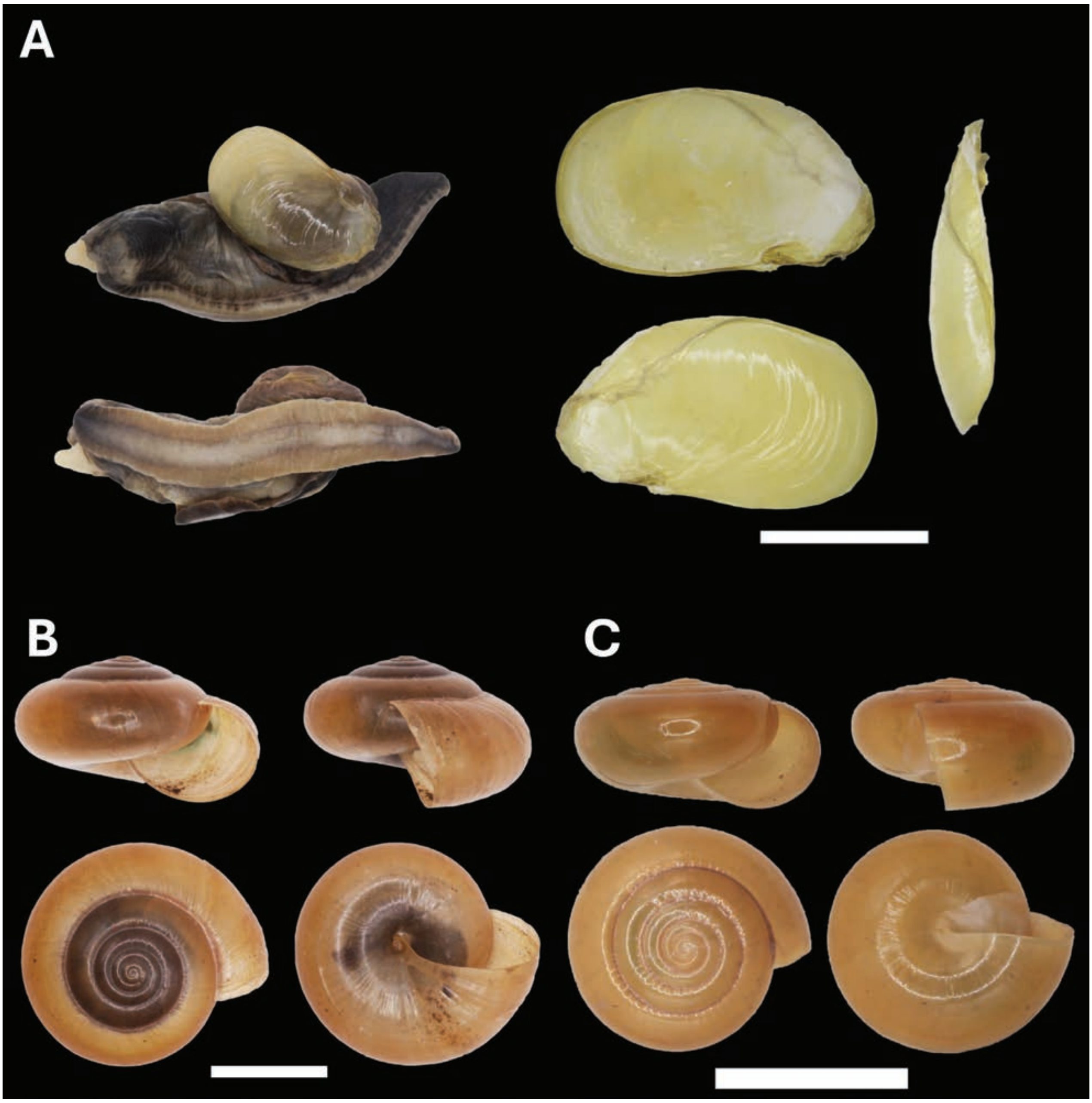

Figure 10. A *Parmarion martensi* Simroth, 1893 BOR/MOL 15239 **B** Tanychlamys indica (Godwin Austen, 1883) BOR/MOL 15771 **C** *Tanychlamys* Penang sp. 1 BOR/MOL 15151. Scale bar: 10 mm.

m a.s.l.; 23 Oct. 2022; T.S. Liew, J. Dulipat leg.; BOR/MOL 15248 • Penang Hill, Trail to Western hill, Km 3.6, Plot.23; 5.4203°N, 100.2517°E; 750 m a.s.l.; 24 Oct. 2022; T.S. Liew, J. Dulipat, M.Y. Lee leg.; BOR/MOL 15549 • Penang Hill, Air Itam, Forest near Dam, Plot.24; 5.3904°N, 100.2612°E; 380 m a.s.l.; 24 Oct. 2022; T.S. Liew, J. Dulipat leg.; BOR/MOL 15244 • same data as for preceding; BOR/MOL 15303 • Penang Hill, Air Itam, Forest near Dam, Plot.25; 5.3900°N, 100.2575°E; 290 m a.s.l.; 25 Oct. 2022; T.S. Liew, J. Dulipat leg.; BOR/MOL 15249 • Penang Hill, Air Itam, Forest near Dam, Plot.26; 5.3977°N, 100.2612°E; 290 m a.s.l.; 25 Oct. 2022; T.S. Liew, J. Dulipat leg.; BOR/MOL 15245 • same data as for preceding; BOR/MOL 15304 • Penang Hill, Trail from Viaduct to Claremont, after shelter, Plot.27; 5.4205°N, 100.2724°E; 500 m a.s.l.; 26 Oct. 2022; T.S. Liew, J. Dulipat leg.; BOR/MOL 15305 • Penang Hill, By Path H, Plot.33; 5.4210°N, 100.2701°E;

610 m a.s.l.; 4 Feb. 2023; T.S. Liew, A. Yusni leg.; BOR/MOL 15740 • Penang Hill, Path B, Random1. PathB; 5.4216°N, 100.2674°E; 730 m a.s.l.; 4 Sept. 2022; T.S. Liew, J. Dulipat leg.; • same data as for preceding; BOR/MOL 15151.

Remark. This is a new record for Penang Hill. It is one of the most common large land snails found there.

Tanychlamys **Penang sp. 2**

Figs 11A, 21A

Material examined. Malaysia • Penang Hill, The Habitat, Research trail, Plot.03; 5.4226°N, 100.2645°E; 750 m a.s.l.; 5 Sept. 2022; T.S. Liew, J. Dulipat, S.M. Goh leg.; BOR/MOL 15424 • Penang Hill, Teluk Bahang- Balik Pulau, Bukit Kerajaan ForestReserve next to Lam durian farm, Plot.20; 5.4199°N, 100.2265°E; 330 m a.s.l.; 23 Oct. 2022; T.S. Liew, J. Dulipat, M.Y. Lee leg.; BOR/MOL 15552 • Penang Hill, Air Itam, Forest near farm, Plot.21; 5.3908°N, 100.2637°E; 340 m a.s.l.; 23 Oct. 2022; T.S. Liew, J. Dulipat leg.; BOR/MOL 15550 • Penang Hill, Trail to Western hill, Junction to Teluk Bahang from Penang Hill, Plot.22; 5.4223°N, 100.2494°E; 760 m a.s.l.; 24 Oct. 2022; T.S. Liew, J, Dulipat, M.Y. Lee leg.; BOR/MOL 15551 • Penang Hill, Western hill to Teluk Bahang Trail Stetion 4, Plot.30; 5.4211°N, 100.2420°E; 570 m a.s.l.; 3 Feb. 2023; T.S. Liew, M.Y. Lee, A. Yusni leg.; BOR/MOL 15759 • Penang Hill, Western hill to Teluk Bahang Trail Stetion 7, Plot.31; 5.4291°N, 100.2334°E; 490 m a.s.l.; 3 Feb. 2023; T.S. Liew, M.Y. Lee, A. Yusni leg.; BOR/MOL 15757.

Remark. This is a new record for Penang Hill.

Tanychlamys stephoides **(Stoliczka, 1873)**

Fig. 11B

Material examined. Malaysia • Penang Hill, The Habitat, Research trail, Plot.01; 5.4248°N, 100.2669°E; 720 m a.s.l.; 5 Sept. 2022; T.S. Liew, J. Dulipat, S.M. Goh leg.; BOR/MOL 15164.

Remark. This species was previously described by Stoliczka (1873) from Penang Hill.

Tanychlamys tersa **(Issel, 1874)**

Figs 11C, 21B

Material examined. Malaysia • Penang Hill, Teluk Bahang- Balik Pulau, Tropical fruit farm, Plot.14; 5.4148°N, 100.2187°E; 260 m a.s.l.; 21 Oct. 2022; T.S. Liew, J. Dulipat, M.Y. Lee leg.; BOR/MOL 15553 • Penang Hill, Teluk Bahang- Balik Pulau, Tropical fruit farm, Plot.15; 5.4160°N, 100.2200°E; 250 m a.s.l.; 21 Oct. 2022; T.S. Liew, J. Dulipat, M.Y. Lee leg.; BOR/MOL 15246 • Penang Hill, Air Itam, Forest near Dam, Plot.24; 5.3904°N, 100.2612°E; 380 m a.s.l.; 24 Oct. 2022; T.S. Liew, J. Dulipat leg.; BOR/MOL 15250 • Penang Hill, Botanical garden, Plot.29; 5.4400°N, 100.2866°E; 75 m a.s.l.; 2 Feb. 2023; T.S. Liew, M.Y. Lee, A. Yusni leg.; BOR/MOL 15758.

Remarks. This is a new record for Penang Hill. This species is widespread in Malaysia and might have been introduced to this location (Maassen 2001).

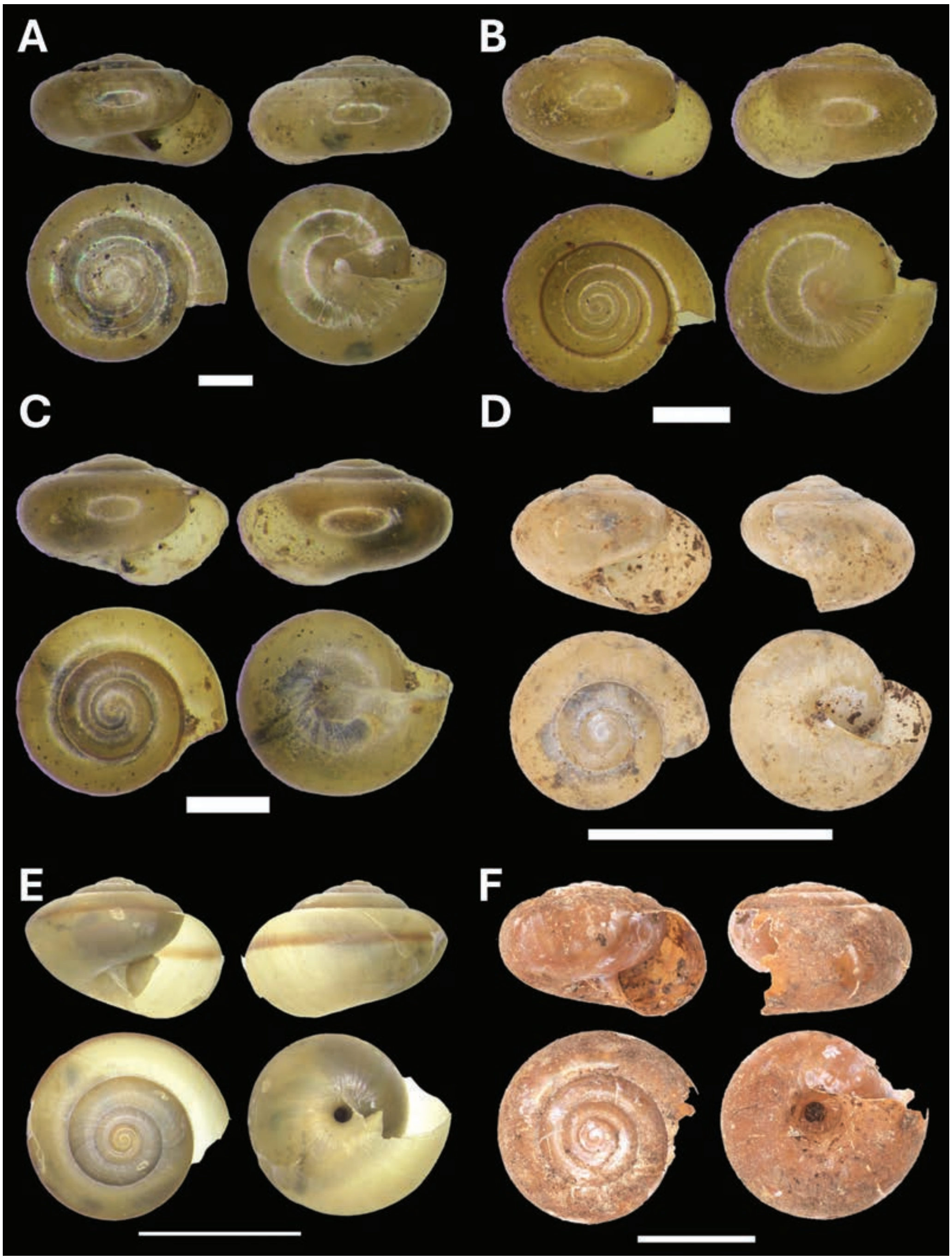

Figure 11. A *Tanychlamys* Penang sp. 2 BOR/MOL 15759 **B** *Tanychlamys stephoides* (Stoliczka, 1873) BOR/MOL 15164 **C** *Tanychlamys tersa* (Issel, 1874) BOR/MOL 15533 **D** *Helicarion permolle* Stoliczka, 1873 BOR/MOL 15741 **E** *Bradybaena similaris* (A. Férussac, 1821) BOR/MOL 15772 **F** *Trichochloritis penangensis* (Stoliczka, 1873) BOR/MOL 15291. Scale bars: 1 mm (**A–C**); 10 mm (**D–F**).

Family Helicarionidae Bourguignat, 1877
Genus *Helicarion* A. Férussac, 1821

Helicarion permolle Stoliczka, 1873
Figs 11D, 21C

Material examined. Malaysia • Penang Hill, The Habitat, Habitat nature trail, Plot.04; 5.4231°N, 100.2668°E; 770 m a.s.l.; 5 Sept. 2022; T.S. Liew, J. Dulipat, S.M. Goh leg.; BOR/MOL 15117 • same data as for preceding; BOR/MOL 15480 • Penang Hill, The Habitat, Habitat nature trail, Plot.05; 5.4228°N, 100.2653°E; 770 m a.s.l.; 5 Sept. 2022; T.S. Liew, J. Dulipat, S.M. Goh leg.; BOR/MOL 15196 • Penang Hill, The Habitat, Habitat nature trail, Plot.07; 5.4210°N, 100.2642°E; 760 m a.s.l.; 6 Sept. 2022; T.S. Liew, J. Dulipat, S.M. Goh, M.Y. Lee leg.; BOR/MOL 15144 • Penang Hill, Botanical garden, Plot.12; 5.4396°N, 100.2860°E; 85 m a.s.l.; 4 Sept. 2022; T.S. Liew, J. Dulipat, S.M. Goh leg.; BOR/MOL 15121 • Penang Hill, Trail from Viaduct to Claremont, after shelter, Plot.27; 5.4205°N, 100.2724°E; 500 m a.s.l.; 26 Oct. 2022; T.S. Liew, J. Dulipat leg.; BOR/MOL 15235 • Penang Hill, Botanical garden, Plot.29; 5.4400°N, 100.2866°E; 75 m a.s.l.; 2 Feb. 2023; T.S. Liew, M.Y. Lee, A. Yusni leg.; BOR/MOL 15742 • same data as for preceding; BOR/MOL 15768 • Penang Hill, By Path H, Plot.33; 5.4210°N, 100.2701°E; 610 m a.s.l.; 4 Feb. 2023; T.S. Liew, A. Yusni leg.; BOR/MOL 15741 • Penang Hill, Path B, Random1. PathB; 5.4216°N, 100.2674°E; 730 m a.s.l.; 4 Sept. 2022; T.S. Liew, J. Dulipat leg.; BOR/MOL 15109.

Remarks. This species was previously described by Stoliczka (1873), and it is one of the most common semi-slugs from Penang Hill. It was listed as taxon inquirendum on MolluscaBase (2024) [https://molluscabase.org/aphia.php?p=taxdetails&id=1337679]. We suggest that this is a valid species as the specimens fit the description in Stoliczka (1873).

Superfamily Helicoidea Rafinesque, 1815
Family Camaenidae Pilsbry, 1895
Genus *Amphidromus* Albers, 1850

Amphidromus atricallosus (A. Gould, 1843)

Remark. This species was previously described by Stoliczka (1873) from Penang Hill but was not found during the sampling of this study.

Amphidromus perversus (Linnaeus, 1758)

Remarks. This species was previously described by Stoliczka (1873) from Penang Hill. However, it was not found during the sampling of this study.

Genus *Bradybaena* H. Beck, 1837

Bradybaena similaris (A. Férussac, 1821)

Figs 11E, 21D

Material examined. Malaysia • Penang Hill, Along Jalan Tunku Yahya Petra, Random6.; 5.4225°N, 100.2662°E; 730 m a.s.l.; 20 Jun. 2023; T.S. Liew leg.; BOR/MOL 15772.

Remarks. This species was found by Stoliczka (1873) from Penang Hill. It is an introduced species and, as noted by Stoliczka (1873), it was only found in cocoa and palm plantations at the foothills and was not encountered in the forest. Similar observations were also made in this study.

Genus *Trichochloritis* Pilsbry, 1891

Trichochloritis penangensis (Stoliczka, 1873)

Fig. 11F

Material examined. Malaysia • Penang Hill, Air Itam, Forest near Dam, Plot.24; 5.3904°N, 100.2612°E; 380 m a.s.l.; 24 Oct. 2022; T.S. Liew, J. Dulipat leg.; BOR/MOL 15291.

Remarks. This species was previously described by Stoliczka (1873) from Penang Hill. It can also be found in Perak (Maassen 2001; Foon et al. 2017).

Superfamily Punctoidea E. S. Morse, 1864
Family Charopidae F. W. Hutton, 1884
Genus *Charopa* E. von Martens, 1860

Charopa perlata van Benthem Jutting, 1959

Fig. 12A

Material examined. Malaysia • Penang Hill, Moon Gate Station 5 trail, Plot.11; 5.4341°N, 100.2921°E; 110 m a.s.l.; 7 Sept. 2022; T.S. Liew, J. Dulipat, S.M. Goh leg.; BOR/MOL 15482 • Penang Hill, Teluk Bahang, Taman Rimba Teluk Bahang, Trail, Simpang 6, Plot.16; 5.4429°N, 100.2212°E; 120 m a.s.l.; 21 Oct. 2022; T.S. Liew, J. Dulipat, M.Y. Lee leg.; BOR/MOL 15560 • Penang Hill, Botanical garden, Plot.29; 5.4400°N, 100.2866°E; 75 m a.s.l.; 2 Feb. 2023; T.S. Liew, M.Y. Lee, A. Yusni leg.; BOR/MOL 15753.

Remarks. This is a new record for Penang Hill. The shell characters match the description of the species originally described from Sumatra (van Benthem Jutting 1959).

Charopa Penang sp. 2

Fig. 12B

Material examined. Malaysia • Penang Hill, The Habitat, Research trail, Plot.06; 5.4247°N, 100.2674°E; 750 m a.s.l.; 5 Sept. 2022; T.S. Liew, J. Dulipat, S.M. Goh, M.Y. Lee, M.Y. Wua leg.; BOR/MOL 15483 • Penang Hill, Teluk Bahang- Balik Pulau, Lam durian farm, Plot.13; 5.4198°N, 100.2259°E; 290 m a.s.l.; 21 Oct. 2022; T.S. Liew, J. Dulipat, M.Y. Lee leg.; BOR/MOL 15562 • Penang Hill, Teluk Bahang- Balik Pulau, Tropical fruit farm, Plot.15; 5.4160°N, 100.2200°E; 250 m a.s.l.; 21 Oct. 2022; T.S. Liew, J. Dulipat, M.Y. Lee leg.; BOR/MOL 15561 • Penang Hill, Teluk Bahang-Balik Pulau, Entrance of a durian farm, near Boulder Valley, Old rubber tree, Plot.17; 5.418°N, 100.2159°E; 180 m a.s.l.; 22 Oct. 2022; T.S. Liew, J. Dulipat leg.; BOR/MOL 15484 • Penang Hill, By Path H, Plot.33; 5.4210°N, 100.2701°E; 610 m a.s.l.; 4 Feb. 2023; T.S. Liew, A. Yusni leg.; BOR/MOL 15761.

Remarks. This is a new record for Penang Hill. The shell spire is moderately raised. Teleoconch with densely spirally arranged pits above periphery, transitioning to densely placed spiral grooves on the subsequent whorls, which become more densely placed towards the periphery. Below periphery with densely placed spiral grooves that continue from the upper shell and fade away

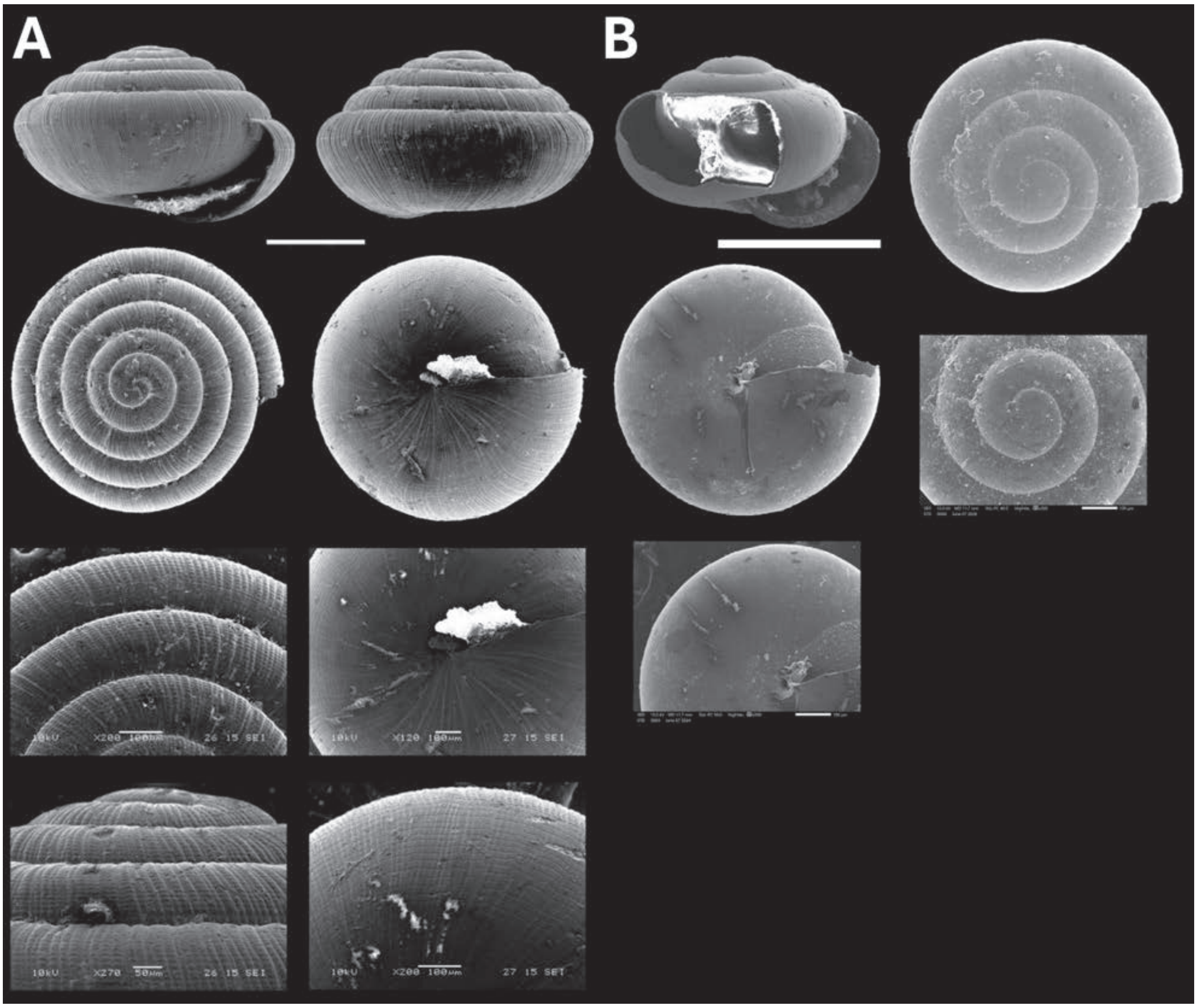

Figure 12. A *Charopa perlata* van Benthem Jutting, 1959 BOR/MOL 15560 **B** *Charopa* Penang sp. 2 BOR/MOL 15561. Scale bar: 0.5 mm.

towards the umbilicus. The shell sculptures of this species are similar to *Microcystina* Penang sp. 6, but it differs by having a smaller shell size, only half the size of *Microcystina* Penang sp. 6.

Genus *Philalanka* Godwin-Austen, 1898

Philalanka carinifera (Stoliczka, 1873)

Fig. 13A

Material examined. Malaysia • Penang Hill, The Habitat, Research trail, Plot.01; 5.4248°N, 100.2669°E; 720 m a.s.l.; 5 Sept. 2022; T.S. Liew, J. Dulipat, S.M. Goh leg.; BOR/MOL 15434 • Penang Hill, The Habitat, Habitat nature trail, Plot.05; 5.4228°N, 100.2653°E; 770 m a.s.l.; 5 Sept. 2022; T.S. Liew, J. Dulipat, S.M. Goh leg.; BOR/MOL 15435 • Penang Hill, The Habitat, Habitat nature trail, Plot.07; 5.4210°N, 100.2642°E; 760 m a.s.l.; 6 Sept. 2022; T.S. Liew, J. Dulipat, S.M. Goh, M.Y. Lee leg.; BOR/MOL 15433 • Penang Hill, The Habitat, Habitat nature trail, Plot.08; 5.4223°N, 100.2648°E; 760 m a.s.l.; 6 Sept. 2022; J. Dulipat, S.M. Goh, M.Y. Lee leg.; BOR/MOL 15437 • Penang Hill, Air Itam, Forest near Dam, Plot.24; 5.3904°N, 100.2612°E; 380 m a.s.l.; 24 Oct. 2022; T.S. Liew, J. Dulipat leg.; BOR/MOL 15436 • Penang Hill, Air Itam, Forest near Dam, Plot.25; 5.3900°N, 100.2575°E; 290 m a.s.l.; 25 Oct. 2022; T.S. Liew, J. Dulipat leg.; BOR/MOL 15440 • Penang Hill, Air Itam, Forest near Dam, Plot.26; 5.3977°N, 100.2612°E; 290 m a.s.l.; 25 Oct. 2022; T.S. Liew, J. Dulipat leg.; BOR/MOL 15438 • Penang Hill, Trail from Viaduct to Claremont, after shelter, Plot.27; 5.4205°N, 100.2724°E; 500 m a.s.l.; 26 Oct. 2022; T.S. Liew, J. Dulipat leg.; BOR/MOL 15441 • Penang Hill, Trail - Moniot Road East, Plot.28; 5.4240°N, 100.2746°E; 530 m a.s.l.; 26 Oct. 2022; T.S. Liew, J. Dulipat leg.; BOR/MOL 15439 • Penang Hill, Botanical garden, Plot.29; 5.4400°N, 100.2866°E; 75 m a.s.l.; 2 Feb. 2023; T.S. Liew, M.Y. Lee, A. Yusni leg.; BOR/MOL 15746 • Penang Hill, By Path H, Plot.33; 5.4210°N, 100.2701°E; 610 m a.s.l.; 4 Feb. 2023; T.S. Liew, A. Yusni leg.; BOR/MOL 15745 • same data as for preceding; BOR/MOL 15764.

Remarks. This species was previously described by Stoliczka (1873) from Penang Hill. It differs from the other two *Philalanka* species by having three spiral ribs on the penultimate whorls.

Philalanka Penang sp. 2

Fig. 13B

Material examined. Malaysia • Penang Hill, Teluk Bahang, Taman Rimba Teluk Bahang, Trail, Simpang 6, Plot.16; 5.4429°N, 100.2212°E; 120 m a.s.l.; 21 Oct. 2022; T.S. Liew, J. Dulipat, M.Y. Lee leg.; BOR/MOL 15539.

Remarks. This is a new record for Penang Hill. This species differs from the other two *Philalanka* species by having more than seven spiral ribs on the penultimate whorls.

Philalanka kusana (Aldrich, 1889)

Fig. 13C

Material examined. Malaysia • Penang Hill, By Path H, Plot.33; 5.4210°N, 100.2701°E; 610 m a.s.l.; 4 Feb. 2023; T.S. Liew, A. Yusni leg.; BOR/MOL 15760.

Remarks. This is a new record for Penang Hill. This species differs from the other two *Philalanka* species by having no more than two spiral ribs on the penultimate whorls.

Family Punctidae E. S. Morse, 1864
Genus *Paralaoma* Iredale, 1913

Paralaoma sp.

Fig. 13D

Material examined. Malaysia • Penang Hill, Air Itam, Forest near Dam, Plot.26; 5.3977°N, 100.2612°E; 290 m a.s.l.; 25 Oct. 2022; T.S. Liew, J. Dulipat leg.; BOR/MOL 15481.

Remark. This is a new record for Penang Hill.

Superfamily Pupilloidea W. Turton, 1831
Family Gastrocoptidae Pilsbry, 1918
Genus *Gastrocopta* Wollaston, 1878

Gastrocopta palmira (Stoliczka, 1873)

Remark. Previously described and recorded by Stoliczka (1873) from Penang Hill, but not found in this study.

Family Valloniidae E. S. Morse, 1864
Genus *Pupisoma* Stoliczka, 1873

Pupisoma orcella (Stoliczka, 1873)

Remark. Previous described and recorded by Stoliczka (1873) from the base of Penang Hill but not found in this study.

Superfamily Streptaxoidea J. E. Gray, 1860
Family Streptaxidae J. E. Gray, 1860
Genus *Gulella* L. Pfeiffer, 1856

Gulella bicolor (T. Hutton, 1834)

Remark. Previously recorded by Stoliczka (1873) from the base of Penang Hill but not found in this study.

Superfamily Trochomorphoidea Mörch, 1864
Family Chronidae Thiele, 1931
Genus *Kaliella* W. T. Blanford, 1863

Kaliella barrakporensis (Reeve, 1852)

Fig. 14A

Material examined. Malaysia • Penang Hill, Botanical garden, Plot.29; 5.4400°N, 100.2866°E; 75 m a.s.l.; 2 Feb. 2023; T.S. Liew, M.Y. Lee, A. Yusni leg.; BOR/MOL 15739.

Remarks. This is a new record for Penang Hill. It is a widespread species in Malaysia (Vermeulen et al. 2015; Foon et al. 2017; Foon and Marzuki 2023).

Kaliella Penang sp. 1

Fig. 14B

Material examined. Malaysia • Penang Hill, The Habitat, Habitat nature trail, Plot.05; 5.4228°N, 100.2653°E; 770 m a.s.l.; 5 Sept. 2022; T.S. Liew, J. Dulipat, S.M. Goh leg.; BOR/MOL 15466 • Penang Hill, The Habitat, Habitat nature trail, Plot.07; 5.4210°N, 100.2642°E; 760 m a.s.l.; 6 Sept. 2022; T.S. Liew, J. Dulipat, S.M. Goh, M.Y. Lee leg.; BOR/MOL 15465.

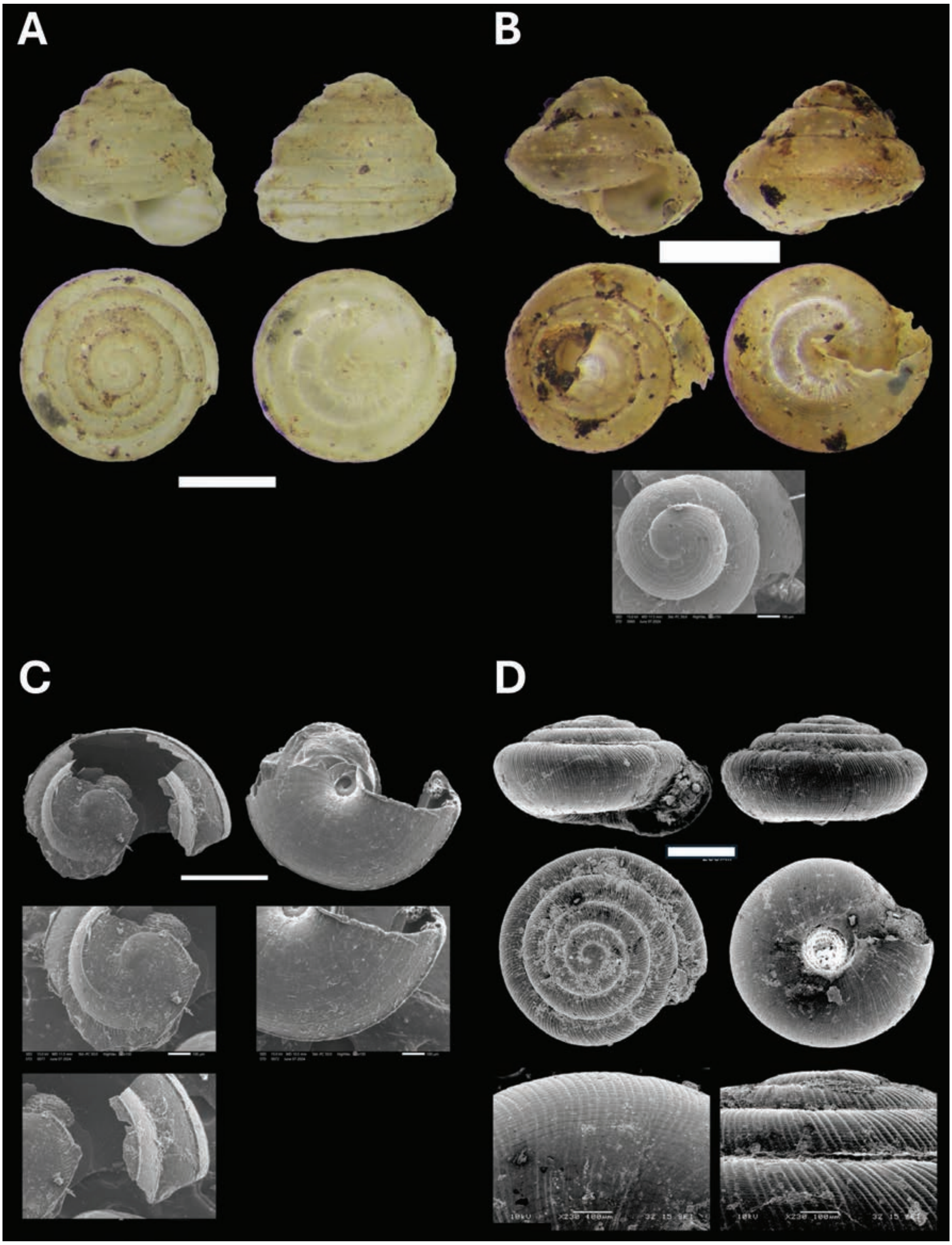

Figure 13. A *Philalanka carinifera* (Stoliczka, 1873) BOR/MOL 15436 **B** *Philalanka* Penang sp. 2 BOR/MOL 15539 **C** *Philalanka kusana* (Aldrich, 1889) BOR/MOL 15760 **D** *Paralaoma* sp. BOR/MOL 15481. Scale bars: 1 mm (**A**); 0.5 mm (**B–D**).

Remarks. This is a new record for Penang Hill. The shell periphery is angular with a spiral thread visible above the suture of the penultimate whorl. Above the shell, the apical whorls are unknown, followed by regularly placed shallow radial ribs on the subsequent whorls. Below the shell, there are densely spaced spiral grooves at the periphery, which reduce towards the umbilicus.

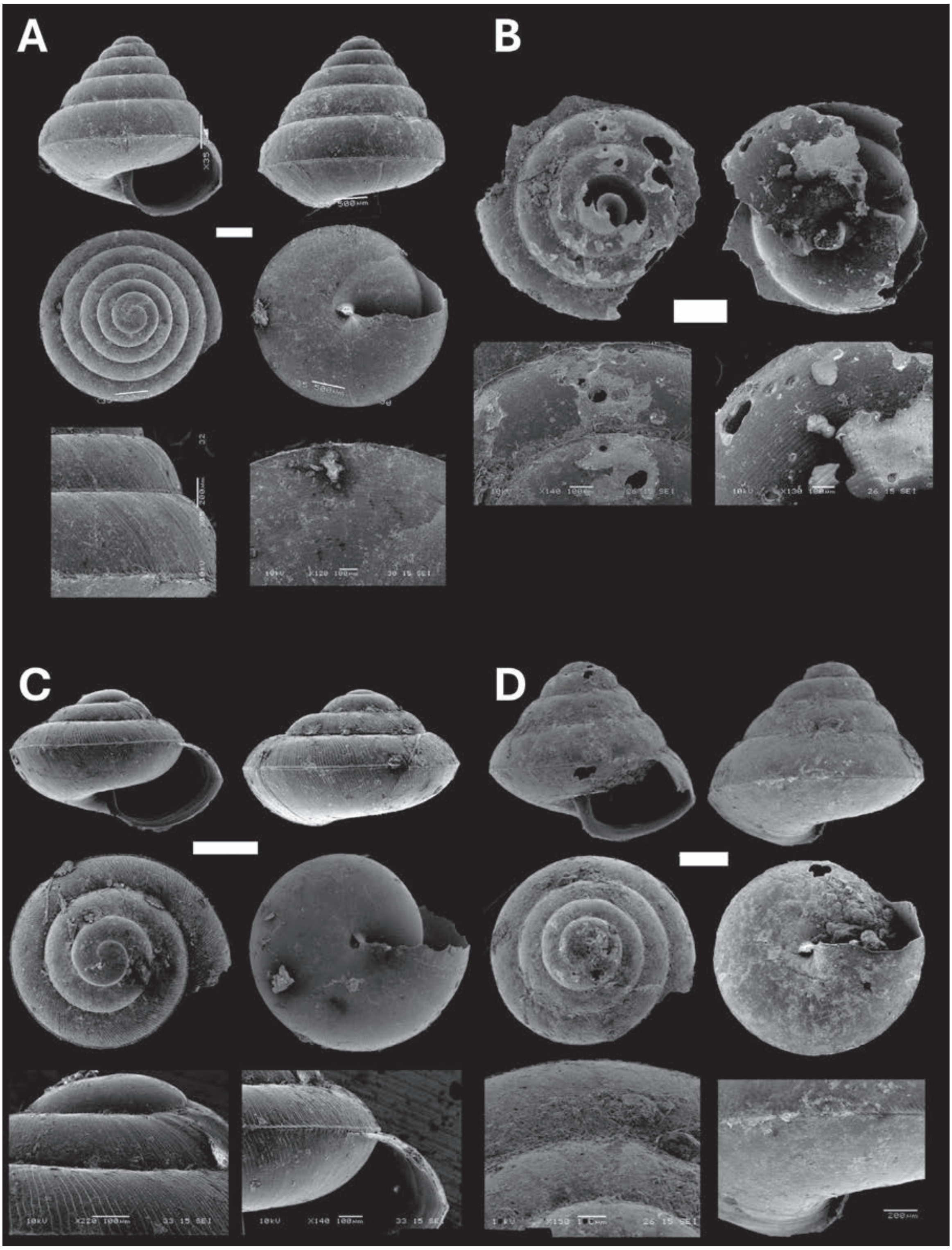

Figure 14. A *Kaliella barrakporensis* (Reeve, 1852) BOR/MOL 15739 **B** *Kaliella* Penang sp. 1 BOR/MOL 15465 **C** *Kaliella* Penang sp. 2 BOR/MOL 15467 **D** *Kaliella* Penang sp. 4 BOR/MOL 15474. Scale bar: 0.5 mm.

Kaliella Penang sp. 2

Fig. 14C

Material examined. Malaysia • Penang Hill, The Habitat, Habitat nature trail, Plot.07; 5.4210°N, 100.2642°E; 760 m a.s.l.; 6 Sept. 2022; T.S. Liew, J. Dulipat, S.M. Goh, M.Y. Lee leg.; BOR/MOL 15468 • Penang Hill, The Habitat, Habitat nature trail, Plot.08; 5.4223°N, 100.2648°E; 760 m a.s.l.; 6 Sept. 2022; J. Dulipat, S.M. Goh, M.Y. Lee leg.; BOR/MOL 15469 • Penang Hill, Trail to Western hill, Km 3.6, Plot.23; 5.4203°N, 100.2517°E; 750 m a.s.l.; 24 Oct. 2022; T.S. Liew, J. Dulipat, M.Y. Lee leg.; BOR/MOL 15563 • Penang Hill, Trail - Moniot Road East, Plot.28; 5.4240°N, 100.2746°E; 530 m a.s.l.; 26 Oct. 2022; T.S. Liew, J. Dulipat leg.; BOR/MOL 15467 • Penang Hill, Moniot trail, Plot.32; 5.4165°N, 100.2574°E; 695 m a.s.l.; 4 Feb. 2023; T.S. Liew, A. Yusni leg.; BOR/MOL 15752.

Remarks. This is a new record for Penang Hill. The shell is convex discus-shaped. The shell periphery is angular with a spiral thread. Above the shell, the apical whorls have shallow spiral ribs crossed by growth lines, transitioning to regularly placed prominent radial ribs on the subsequent whorls. Below the shell, radial ribs continue from above at the periphery, transitioning to spaced spiral grooves which reduce towards the umbilicus.

Kaliella **Penang sp. 4**

Fig. 14D

Material examined. Malaysia • Penang Hill, The Habitat, Research trail, Plot.03; 5.4226°N, 100.2645°E; 750 m a.s.l.; 5 Sept. 2022; T.S. Liew, J. Dulipat, S.M. Goh leg.; BOR/MOL 15473 • Penang Hill, The Habitat, Research trail, Plot.06; 5.4247°N, 100.2674°E; 750 m a.s.l.; 5 Sept. 2022; T.S. Liew, J. Dulipat, S.M. Goh, M.Y. Lee, M.Y. Wua leg.; BOR/MOL 15474 • Penang Hill, The Habitat, Habitat nature trail, Plot.07; 5.4210°N, 100.2642°E; 760 m a.s.l.; 6 Sept. 2022; T.S. Liew, J. Dulipat, S.M. Goh, M.Y. Lee leg.; BOR/MOL 15470 • Penang Hill, Air Itam, Forest near Dam, Plot.25; 5.3900°N, 100.2575°E; 290 m a.s.l.; 25 Oct. 2022; T.S. Liew, J. Dulipat leg.; BOR/MOL 15471 • Penang Hill, Trail - Moniot Road East, Plot.28; 5.4240°N, 100.2746°E; 530 m a.s.l.; 26 Oct. 2022; T.S. Liew, J. Dulipat leg.; BOR/MOL 15472.

Remarks. This is a new record for Penang Hill. The shell is conical in shape with an angular periphery adorned with a spiral thread. Teleoconch with elevated radial ribs above periphery that transition to densely placed fine spiral ribs on the subsequent whorls, crossed by irregular growth lines. Below periphery with less densely spaced spiral grooves at the periphery, which diminish towards the umbilicus.

Kaliella **Penang sp. 5**

Fig. 15A

Material examined. Malaysia • Penang Hill, Teluk Bahang- Balik Pulau, Tropical fruit farm, Plot.15; 5.4160°N, 100.2200°E; 250 m a.s.l.; 21 Oct. 2022; T.S. Liew, J. Dulipat, M.Y. Lee leg.; BOR/MOL 15564.

Remarks. This is a new record for Penang Hill. The shell is flat conical with an angular periphery adorned with a visible spiral thread above the suture of the penultimate whorl. Teleoconch with elevated radial ribs above periphery that transition to densely placed radial ribs on the subsequent whorls. Below periphery with dense radial ribs continuing from above and transitioning to spaced spiral grooves that diminish towards the umbilicus.

Kaliella scandens **(J. C. Cox, 1872)**

Fig. 15B

Material examined. Malaysia • Penang Hill, Teluk Bahang- Balik Pulau, Tropical fruit farm, Plot.14; 5.4148°N, 100.2187°E; 260 m a.s.l.; 21 Oct. 2022; T.S. Liew, J. Dulipat, M.Y. Lee leg.; BOR/MOL 15566 • Penang Hill, Teluk Bahang- Balik Pulau, Tropical fruit farm, Plot.15; 5.4160°N, 100.2200°E; 250 m a.s.l.; 21 Oct. 2022; T.S. Liew, J. Dulipat, M.Y. Lee leg.; BOR/MOL 15565 • Penang Hill, Teluk Bahang- Balik Pulau, Lam durian farm, Plot.19; 5.4218°N, 100.2263°E; 280 m a.s.l.; 23 Oct. 2022; T.S. Liew, J. Dulipat, M.Y. Lee leg.; BOR/MOL 15476 • Penang Hill, Trail from Viaduct to Claremont, after shelter, Plot.27; 5.4205°N, 100.2724°E; 500 m a.s.l.; 26 Oct. 2022; T.S. Liew, J. Dulipat leg.; BOR/MOL 15475 • Penang Hill, Botanical garden, Plot.29; 5.4400°N, 100.2866°E; 75 m a.s.l.; 2 Feb. 2023; T.S. Liew, M.Y. Lee, A. Yusni leg.; BOR/MOL 15744 • same data as for preceding; BOR/MOL 15765.

Remarks. This is a new record for Penang Hill. This species is widespread, found from Sundaland to Australia and the Pacific Islands (Vermeulen et al. 2015).

Family Microcystidae Thiele, 1931
Genus *Microcystis* H. Beck, 1838

Microcystis palmicola **Stoliczka, 1873**

Remark. This species was previously described by Stoliczka (1873) from the base of Penang Hill but was not found during the sampling of this study.

Genus *Vitrinopsis* C. Semper, 1873

Vitrinopsis **sp.**

Figs 16A, 21E

Material examined. Malaysia • Penang Hill, The Habitat, Habitat nature trail, Plot.07; 5.4210°N, 100.2642°E; 760 m a.s.l.; 6 Sept. 2022; T.S. Liew, J. Dulipat, S.M. Goh, M.Y. Lee leg.; BOR/MOL 15120 • Penang Hill, Path B, Random1. PathB; 5.4216°N, 100.2674°E; 730 m a.s.l.; 4 Sept. 2022; T.S. Liew, J. Dulipat leg.; BOR/MOL 15108.

Remarks. This is a new record for Penang Hill. This species differs from *Vitrinopsis nucleata* by having fewer than two whorls on the shell.

Vitrinopsis nucleata **(Stoliczka, 1873)**

Figs 16B, 21F

Material examined. Malaysia • Penang Hill, The Habitat, Habitat nature trail, Plot.04; 5.4231°N, 100.2668°E; 770 m a.s.l.; 5 Sept. 2022; T.S. Liew, J. Dulipat, S.M. Goh leg.; BOR/MOL 15115 • Penang Hill, The Habitat, Research trail, Plot.06; 5.4247°N, 100.2674°E; 750 m a.s.l.; 5 Sept. 2022; T.S. Liew, J. Dulipat, S.M. Goh, M.Y. Lee, M.Y. Wua leg.; BOR/MOL 15479 • Penang Hill, Moon Gate Station 5 trail, Plot.11; 5.4341°N, 100.2921°E; 110 m a.s.l.; 7 Sept. 2022; T.S. Liew, J. Dulipat, S.M. Goh leg.; BOR/MOL 15122 • same data as for preceding;

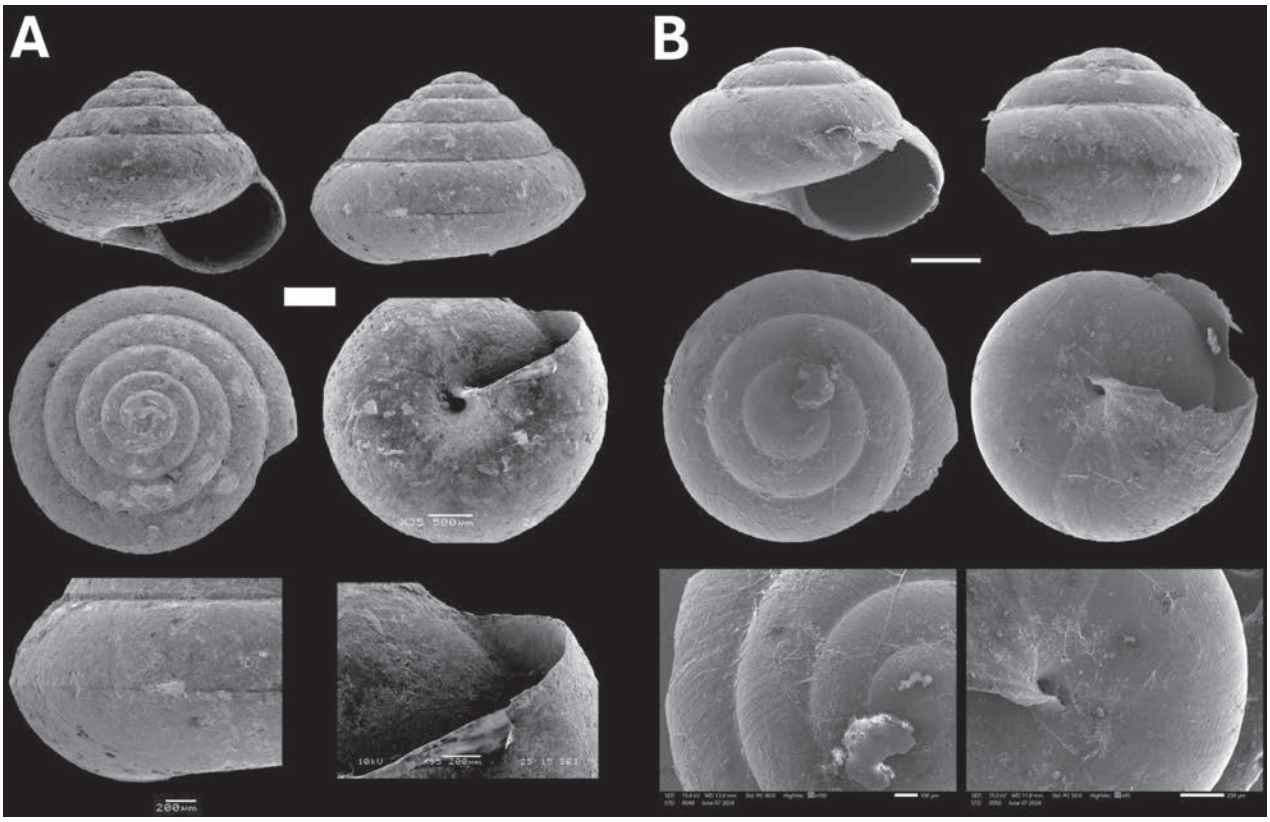

Figure 15. A *Kaliella* Penang sp. 5 BOR/MOL 15564 **B** *Kaliella scandens* (J. C. Cox, 1872) BOR/MOL 15476. Scale bar: 0.5 mm.

BOR/MOL 15477 • Penang Hill, Air Itam, Forest near Dam, Plot.24; 5.3904°N, 100.2612°E; 380 m a.s.l.; 24 Oct. 2022; T.S. Liew, J. Dulipat leg.; BOR/MOL 15242 • same data as for preceding; BOR/MOL 15292 • Penang Hill, Air Itam, Forest near Dam, Plot.26; 5.3977°N, 100.2612°E; 290 m a.s.l.; 25 Oct. 2022; T.S. Liew, J. Dulipat leg.; BOR/MOL 15478 • Penang Hill, Trail from Viaduct to Claremont, after shelter, Plot.27; 5.4205°N, 100.2724°E; 500 m a.s.l.; 26 Oct. 2022; T.S. Liew, J. Dulipat leg.; BOR/MOL 15238 • Penang Hill, Trail - Moniot Road East, Plot.28; 5.4240°N, 100.2746°E; 530 m a.s.l.; 26 Oct. 2022; T.S. Liew, J. Dulipat leg.; BOR/MOL 15233 • Penang Hill, By Path H, Plot.33; 5.4210°N, 100.2701°E; 610 m a.s.l.; 4 Feb. 2023; T.S. Liew, A. Yusni leg.; BOR/MOL 15743.

Remark. This species was described and recorded by Stoliczka (1873) from Penang Hill, and it can also be found in Perak (Maassen 2001; Foon et al. 2017).

Family Dyakiidae Gude & B. B. Woodward, 1921

Genus *Quantula* H. B. Baker, 1941

Quantula striata (J. E. Gray, 1834)

Fig. 17A

Material examined. Malaysia • Penang Hill, Botanical garden, Plot.29; 5.4400°N, 100.2866°E; 75 m a.s.l.; 2 Feb. 2023; T.S. Liew, M.Y. Lee, A. Yusni leg.; BOR/MOL 15732 • same data as for preceding; BOR/MOL 15767 • Penang Hill, Air Itam Farm, Batu Panay road, Random3. Farm; 5.3891°N, 100.2664°E; 270 m a.s.l.; 23 Oct. 2022; T.S. Liew, J. Dulipat leg.; BOR/MOL 15301.

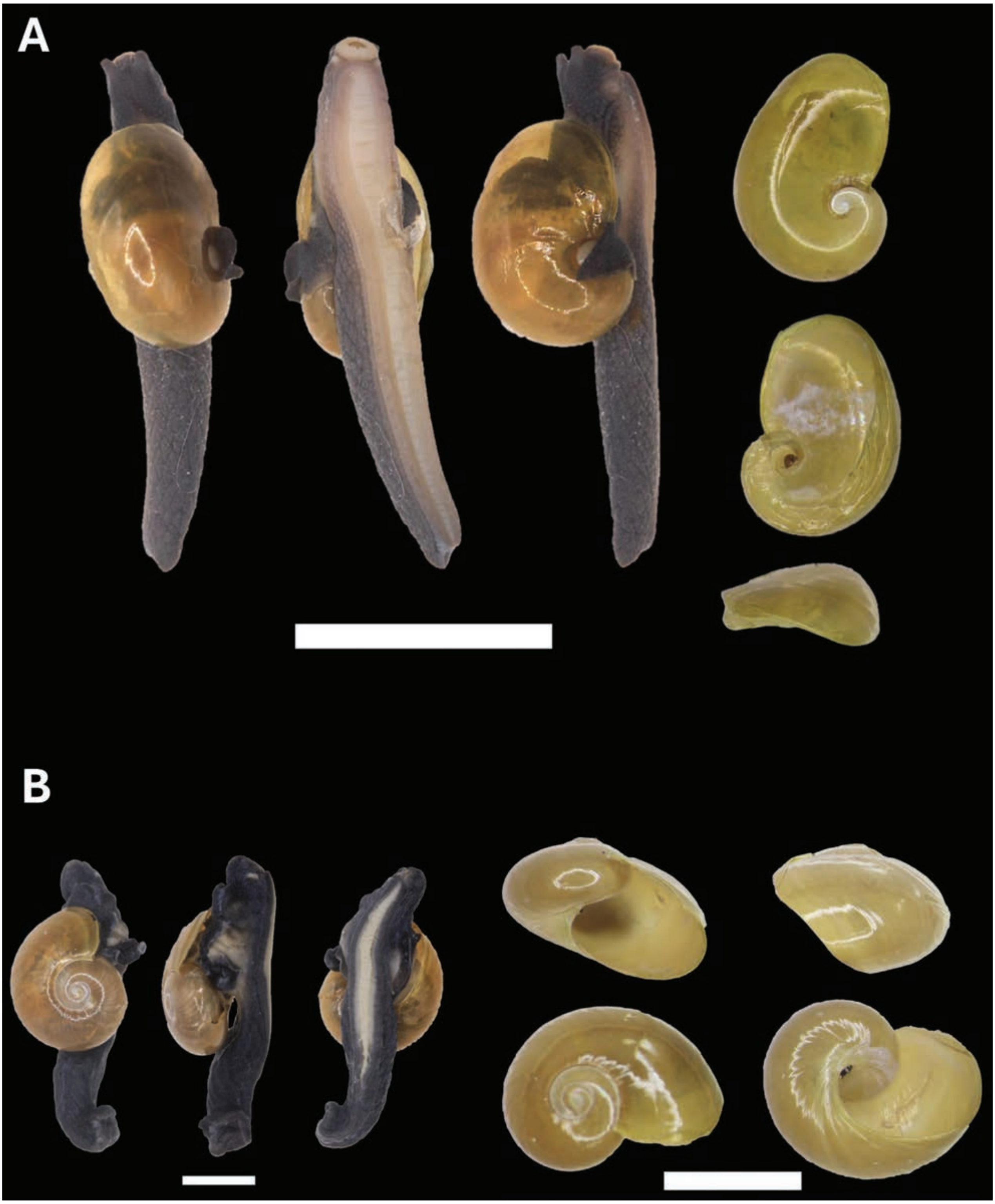

Figure 16. A *Vitrinopsis* sp. BOR/MOL 15108 **B** *Vitrinopsis nucleata* (Stoliczka, 1873) BOR/MOL 15238 & BOR/MOL 15233. Scale bar: 10 mm.

Remarks. One of the most common large land snails at vegetable farms of Penang Hill with a shell width of up to 28 mm. It is also known from other localities in Peninsular Malaysia, Sundaland, and the Philippines (Maassen 2001; Foon et al. 2017).

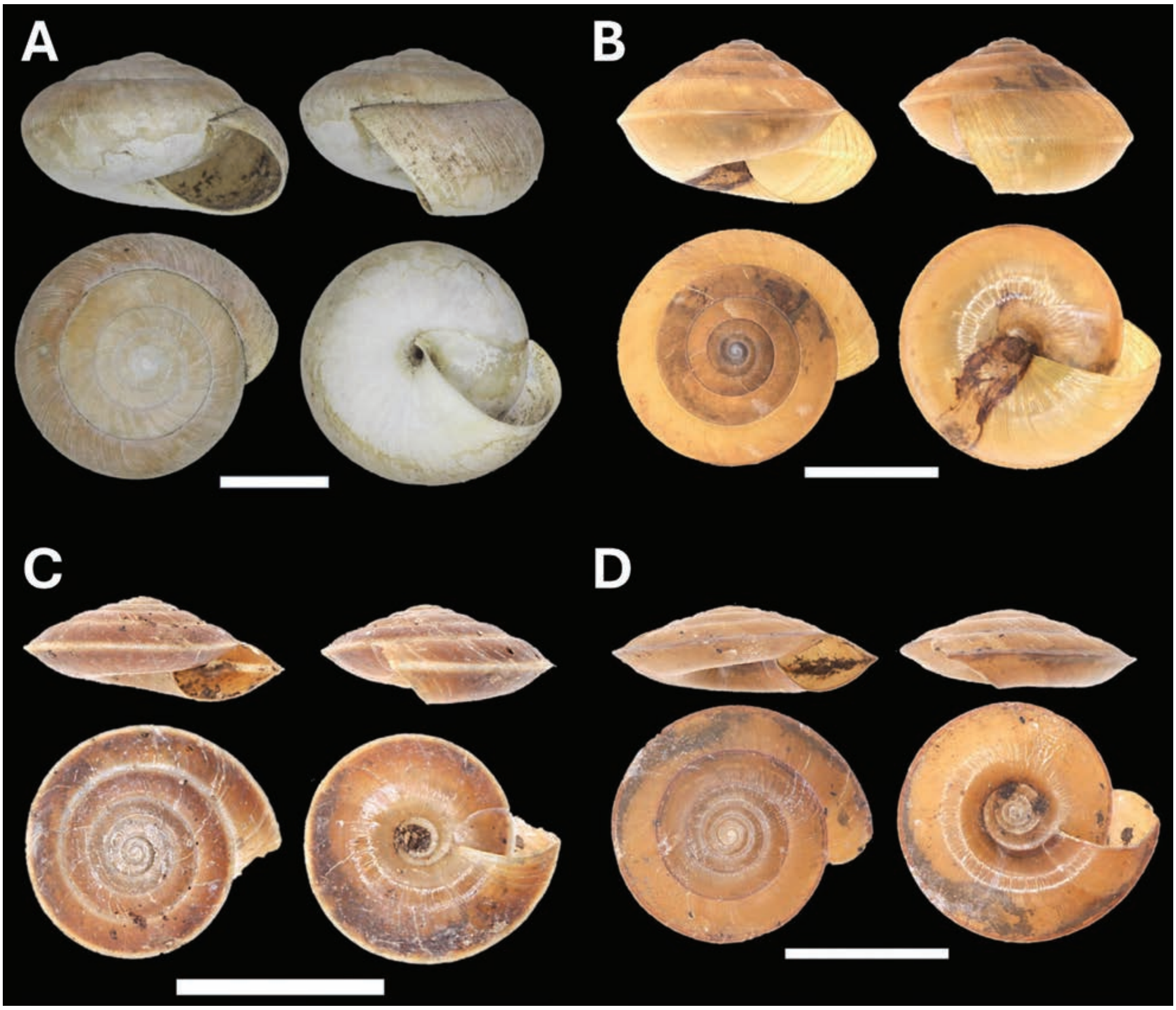

Figure 17. A *Quantula striata* (J. E. Gray, 1834) BOR/MOL 15732 **B** *Pseudoplecta bijuga* (Stoliczka, 1873) BOR/MOL 15734 **C** *Videna castra* (Benson, 1852) BOR/MOL 15279 **D** *Videna timorensis* (E. von Martens, 1867) BOR/MOL 15129. Scale bar: 10 mm.

Genus *Pseudoplecta* Laidlaw, 1932

Pseudoplecta bijuga (Stoliczka, 1873)
Figs 17B, 22A

Material examined. Malaysia • Penang Hill, The Habitat, Research trail, Plot.01; 5.4248°N, 100.2669°E; 720 m a.s.l.; 5 Sept. 2022; T.S. Liew, J. Dulipat, S.M. Goh leg.; BOR/MOL 15114 • same data as for preceding; BOR/MOL 15114 • same data as for preceding; BOR/MOL 15159 • Penang Hill, The Habitat, Research trail, Plot.02; 5.4237°N, 100.2649°E; 720 m a.s.l.; 5 Sept. 2022; T.S. Liew, J. Dulipat, S.M. Goh leg.; BOR/MOL 15113 • same data as for preceding; BOR/MOL 15197 • Penang Hill, The Habitat, Research trail, Plot.03; 5.4226°N, 100.2645°E; 750 m a.s.l.; 5 Sept. 2022; T.S. Liew, J. Dulipat, S.M. Goh leg.; BOR/MOL 15106 • Penang Hill, The Habitat, Habitat nature trail, Plot.04; 5.4231°N, 100.2668°E; 770 m a.s.l.; 5 Sept. 2022; T.S. Liew, J. Dulipat, S.M. Goh leg.; BOR/MOL 15116 • same data as for preceding; BOR/MOL 15128 • Penang Hill, The Habitat, Habitat nature trail, Plot.05; 5.4228°N, 100.2653°E; 770 m a.s.l.; 5 Sept. 2022; T.S. Liew, J. Dulipat, S.M. Goh leg.; BOR/MOL 15125 • same data as for preceding; BOR/MOL 15133 • Penang Hill, The Habitat, Research trail, Plot.06; 5.4247°N, 100.2674°E; 750 m a.s.l.; 5 Sept. 2022; T.S. Liew, J. Dulipat, S.M. Goh, M.Y. Lee, M.Y. Wua leg.; BOR/MOL 15082 • same data as for preceding; BOR/MOL 15083 • same data as for preceding; BOR/MOL 15138 • Penang Hill, The Habitat, Habitat nature trail, Plot.07; 5.4210°N, 100.2642°E; 760 m a.s.l.; 6 Sept. 2022; T.S. Liew, J. Dulipat, S.M. Goh, M.Y. Lee leg.; BOR/MOL 15086 • same data as for preceding; BOR/MOL 15089 • same data as for preceding; BOR/MOL 15146 • same data as for preceding; BOR/MOL 15431 • Penang Hill, The Habitat, Habitat nature trail, Plot.08; 5.4223°N, 100.2648°E; 760 m a.s.l.; 6 Sept. 2022; J. Dulipat, S.M. Goh, M.Y. Lee leg.; BOR/MOL 15095 • same data as for preceding; BOR/MOL 15155 • Penang Hill, Moon Gate Station 5 trail, Plot.10; 5.4305°N, 100.2913°E; 250 m a.s.l.; 7 Sept. 2022; T.S. Liew, J. Dulipat, S.M. Goh leg.; BOR/MOL 15123 • Penang Hill, Moon Gate Station 5 trail, Plot.11; 5.4341°N, 100.2921°E; 110 m a.s.l.; 7 Sept. 2022; T.S. Liew, J. Dulipat, S.M. Goh leg.; BOR/MOL 15093 • Penang Hill, Botanical garden, Plot.12; 5.4396°N, 100.2860°E; 85 m a.s.l.; 4 Sept. 2022; T.S. Liew, J. Dulipat, S.M. Goh leg.; BOR/MOL 15090 • Penang Hill, Teluk Bahang- Balik Pulau, Tropical fruit farm, Plot.15; 5.4160°N, 100.2200°E; 250 m a.s.l.; 21 Oct. 2022; T.S. Liew, J. Dulipat, M.Y. Lee leg.; BOR/MOL 15276 • Penang Hill, Teluk Bahang, Taman Rimba Teluk Bahang, Trail, Simpang 6, Plot.16; 5.4429°N, 100.2212°E; 120 m a.s.l.; 21 Oct. 2022; T.S. Liew, J. Dulipat, M.Y. Lee leg.; BOR/MOL 15268 • same data as for preceding; BOR/MOL 15274 • Penang Hill, Teluk Bahang, Taman Rimba Teluk Bahang, Trail Stesen 3, Plot.18; 5.4420°N, 100.2218°E; 150 m a.s.l.; 22 Oct. 2022; T.S. Liew, J. Dulipat leg.; BOR/MOL 15236 • same data as for preceding; BOR/MOL 15280 • Penang Hill, Teluk Bahang- Balik Pulau, Bukit Kerajaan ForestReserve next to Lam durian farm, Plot.20; 5.4199°N, 100.2265°E; 330 m a.s.l.; 23 Oct. 2022; T.S. Liew, J. Dulipat, M.Y. Lee leg.; BOR/MOL 15217 • Penang Hill, Trail to Western hill, Km 3.6, Plot.23; 5.4203°N, 100.2517°E; 750 m a.s.l.; 24 Oct. 2022; T.S. Liew, J. Dulipat, M.Y. Lee leg.; BOR/MOL 15218 • same data as for preceding; BOR/MOL 15286 • Penang Hill, Air Itam, Forest near Dam, Plot.24; 5.3904°N, 100.2612°E; 380 m a.s.l.; 24 Oct. 2022; T.S. Liew, J. Dulipat leg.; BOR/MOL 15241 • same data as for preceding; BOR/MOL 15288 • Penang Hill, Air Itam, Forest near Dam, Plot.25; 5.3900°N, 100.2575°E; 290 m a.s.l.; 25 Oct. 2022; T.S. Liew, J. Dulipat leg.; BOR/MOL 15237 • same data as for preceding; BOR/MOL 15293 • same data as for preceding; BOR/MOL 15432 • Penang Hill, Trail from Viaduct to Claremont, after shelter, Plot.27; 5.4205°N, 100.2724°E; 500 m a.s.l.; 26 Oct. 2022; T.S. Liew, J. Dulipat leg.; BOR/MOL 15234 • same data as for preceding; BOR/MOL 15297 • Penang Hill, Trail - Moniot Road East, Plot.28; 5.4240°N, 100.2746°E; 530 m a.s.l.; 26 Oct. 2022; T.S. Liew, J. Dulipat leg.; BOR/MOL 15231 • same data as for preceding; BOR/MOL 15300 • Penang Hill, Moniot trail, Plot.32; 5.4165°N, 100.2574°E; 695 m a.s.l.; 4 Feb. 2023; T.S. Liew, A. Yusni leg.; BOR/MOL 15733 • Penang Hill, By Path H, Plot.33; 5.4210°N, 100.2701°E; 610 m a.s.l.; 4 Feb. 2023; T.S. Liew, A. Yusni leg.; BOR/MOL 15734 • Penang Hill, Path B, Random1. PathB; 5.4216°N, 100.2674°E; 730 m a.s.l.; 4 Sept. 2022; T.S. Liew, J. Dulipat leg.; BOR/MOL 15150 • Penang Hill, Bukit Laksamana, Random5.; 5.4239°N, 100.2362°E; 710 m a.s.l.; 3 Feb. 2023; T.S. Liew, M.Y. Lee, A. Yusni leg.; BOR/MOL 15770.

Remark. One of the most common large land snails at Penang Hill, with a shell width of up to 22 mm. It is also known from other localities in Peninsular Malaysia and Thailand (Maassen 2001; Foon et al. 2017).

Family Trochomorphidae Möllendorff, 1890
Genus *Videna* H. Adams & A. Adams, 1855

Videna castra (Benson, 1852)
Fig. 17C

Material examined. Malaysia • Penang Hill, Teluk Bahang-Balik Pulau, Entrance of a durian farm, near Boulder Valley, Old rubber tree, Plot.17; 5.418°N, 100.2159°E; 180 m a.s.l.; 22 Oct. 2022; T.S. Liew, J. Dulipat leg.; BOR/MOL 15279.

Remarks. This species was also previously recorded by Stoliczka (1873). It is similar to *Videna cantoriana* but has more regularly expanded whorls. This species is also recorded from mainland Peninsular Malaysia, India, and Thailand (Maassen 2001; Foon et al. 2017).

Videna cantoriana (W. H. Benson, 1861)

Remarks. This species was previously recorded and described from Penang Hill (at ca 2000 feet a.s.l.) by Stoliczka (1873). It was not found in this study.

Videna timorensis (E. von Martens, 1867)
Fig. 17D

Material examined. Malaysia • Penang Hill, The Habitat, Habitat nature trail, Plot.04; 5.4231°N, 100.2668°E; 770 m a.s.l.; 5 Sept. 2022; T.S. Liew, J. Dulipat, S.M. Goh leg.; BOR/MOL 15129.

Remarks. This species was also previously recorded by Stoliczka (1873). It differs from the other two *Videna* species of Penang Hill by having a wider, more open umbilicus, approximately one-third of the shell width.

Superfamily Veronicelloidea J. E. Gray, 1840
Family Rathouisiidae Heude, 1885
Genus *Atopos* Simroth, 1891

Atopos tourannensis (Souleyet, 1852)
Figs 18A, 22B

Material examined. Malaysia • Penang Hill, Teluk Bahang-Balik Pulau, Entrance of a durian farm, near Boulder Valley, Old rubber tree, Plot.17; 5.418°N, 100.2159°E; 180 m a.s.l.; 22 Oct. 2022; T.S. Liew, J. Dulipat leg.; BOR/MOL 15227.

Remarks. This is a new record for Penang Hill. This species differs from *Atopos punctata* by having a black mantle with white areas at both ends (head and tail) of the mantle.

Atopos punctata Collinge, 1902

Figs 18B, 22C

Material examined. Malaysia • Penang Hill, Trail from Viaduct to Claremont, after shelter, Plot.27; 5.4205°N, 100.2724°E; 500 m a.s.l.; 26 Oct. 2022; T.S. Liew, J. Dulipat leg.; BOR/MOL 15228.

Remarks. This species was also previously recorded by Stoliczka (1873). It differs from *Atopos tourannensis* by having a brown mantle.

Family Veronicellidae J. E. Gray, 1840

Genus *Laevicaulis* Simroth, 1913

Laevicaulis alte (A. Férussac, 1822)

Figs 18C, 22D

Material examined. Malaysia • Penang Hill, Path B, Random1. PathB; 5.4216°N, 100.2674°E; 730 m a.s.l.; 4 Sept. 2022; T.S. Liew, J. Dulipat leg.; BOR/MOL 15111 • Penang Hill, Plaza, Random2. Plaza; 5.4247°N, 100.2689°E; 740 m a.s.l.; 6 Sept. 2022; T.S. Liew, J. Dulipat leg.; BOR/MOL 15112 • Penang Hill, Along Jalan Tunku Yahya Petra, Random6.; 5.4225°N, 100.2662°E; 730 m a.s.l.; 20 Jun. 2023; T.S. Liew leg.; BOR/MOL 15773.

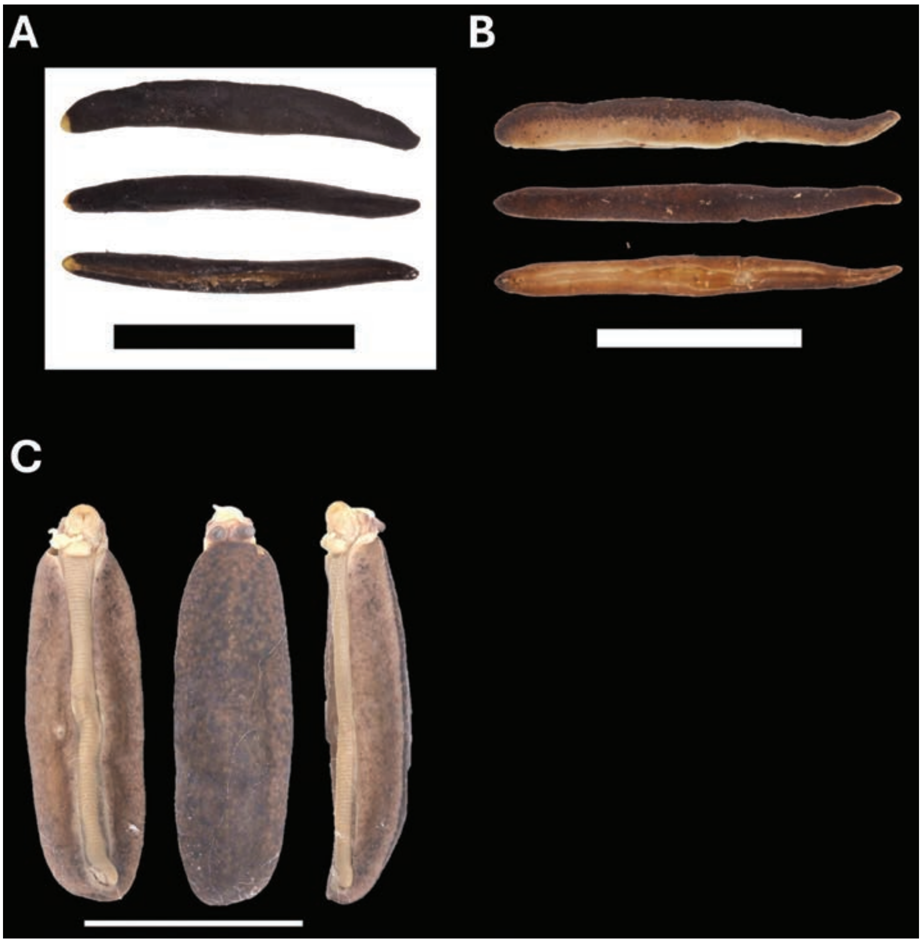

Figure 18. A *Atopos tourannensis* (Souleyet, 1852) BOR/MOL 15227 **B** *Atopos punctata* Collinge, 1902 BOR/MOL 15228 **C** *Laevicaulis alte* (A. Férussac, 1822) BOR/MOL 15773. Scale bar: 10 mm.

Remarks. This is a new record for Penang Hill. So far, this species has only been found in human-altered habitats. The most reliable method for determining species identity involves detailed anatomical examination. However, as this specimen is a juvenile, some identifying features may not be fully developed. Based on the available evidence, we tentatively identify it as *L. alte*.

Genus *Semperula* Grimpe & Hoffmann, 1924

Semperula birmanica (Theobald, 1864)

Remark. Old record by Stoliczka (1873).

Discussion

Sampling completeness and inventory of land snails

Our work has led to a significant increase of the number of recorded species from Penang Hill since Stoliczka (1872, 1873): 34 new records of 66 species recorded. Many of the new records are micro-snails from genera such as *Kaliella*, *Microcystina*, *Diplommatina*, *Charopa*, *Ditropopsis*, *Paralaoma*, and *Philalanka*. This discovery can be attributed to our greatly improved collecting techniques. Others are singletons, and the fact that they have not been collected before may be due to the patchiness of their distribution.

The species richness estimates by iNEXT suggested that the species richness of Penang Hill is 94 species. This indicates that, while our systematic sampling design is effective in capturing a substantial proportion of the land snail diversity in the area, considerably more sampling effort will be needed to obtain a complete overview of the land snail community at Penang Hill. The number of species recorded in Penang Hill increased from 32 to 66, demonstrating a high species richness compared to that typically found in limestone habitats (e.g., Foon et al. 2017; Foon and Marzuki 2023) or in very high mountains for non-limestone areas (e.g., 82 species on Mount Kinabalu (Malaysia) at 4095 m a.s.l. and 66 species on Mount Tambuyukon (Malaysia) at 2579 m a.s.l. in Liew et al. 2010). By comparing the historical records with those species found in this study, seven of the newly recorded species are found to be alien species: these are not micro-snails which could have been missed by Stoliczka (1872, 1873). Almost all the species were found in the disturbed forests and orchards, and on a few occasions recorded along the trails in undisturbed forest. This observation aligns with the findings by Cowie (1998), who noted that non-indigenous land snails and slugs are generally associated with disturbed, low- and mid-elevation habitats. This could suggest the possibility that these species were introduced after the sampling made by Stoliczka in 1869. Another possibly introduced species is *Macrochlamys* Penang sp. 1, which is relatively large, and currently one of the most common snail species (found in 17 of the 33 sampled plots) that, if it would have been present in Stoliczka's time, would not have been overlooked by him. Unlike the confirmed alien species that are affiliated with disturbed habitats, this species can be found in disturbed and undisturbed habitats, which raises concerns about their potential impact on the native ecosystem.

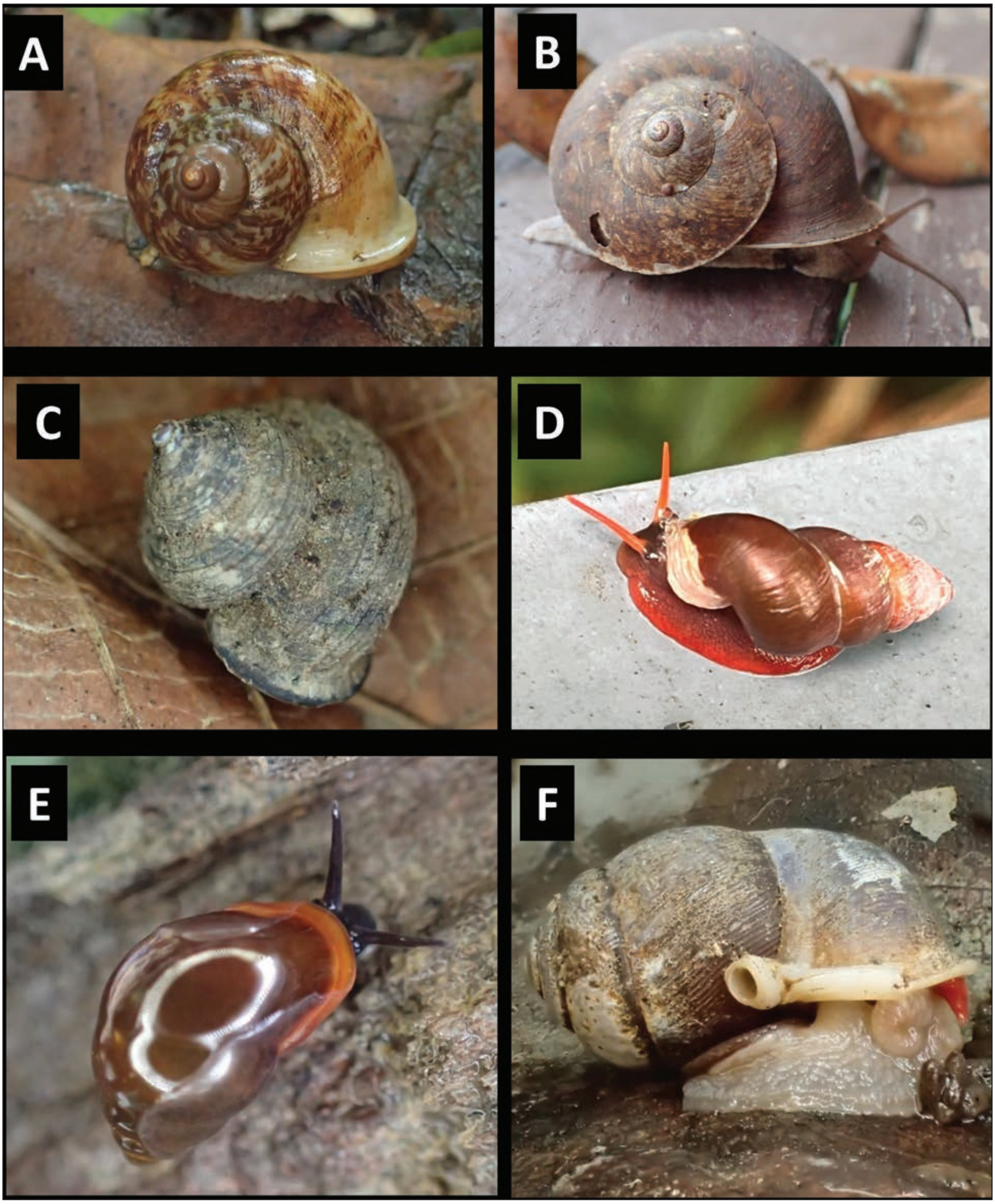

Figure 19. A *Cyclophorus malayanus* (W. H. Benson, 1852) **B** *Cyclophorus perdix borneensis* (Metcalfe, 1854) **C** *Lagocheilus trochoides* (Stoliczka, 1872) **D** *Coptocheilus sectilabris* (A. Gould, 1844), photo credit Mei Yi Lee **E** *Pupina aureola* Stoliczka, 1872 **F** *Rhaphaulus lorraini* L. Pfeiffer, 1856.

Species diversity and composition among plots of different habitat types

The habitat types (undisturbed forest, disturbed forest, and orchards) do exhibit differences in species richness, though it is not statistically significant. Orchards and undisturbed forest have a similar number of species, but with

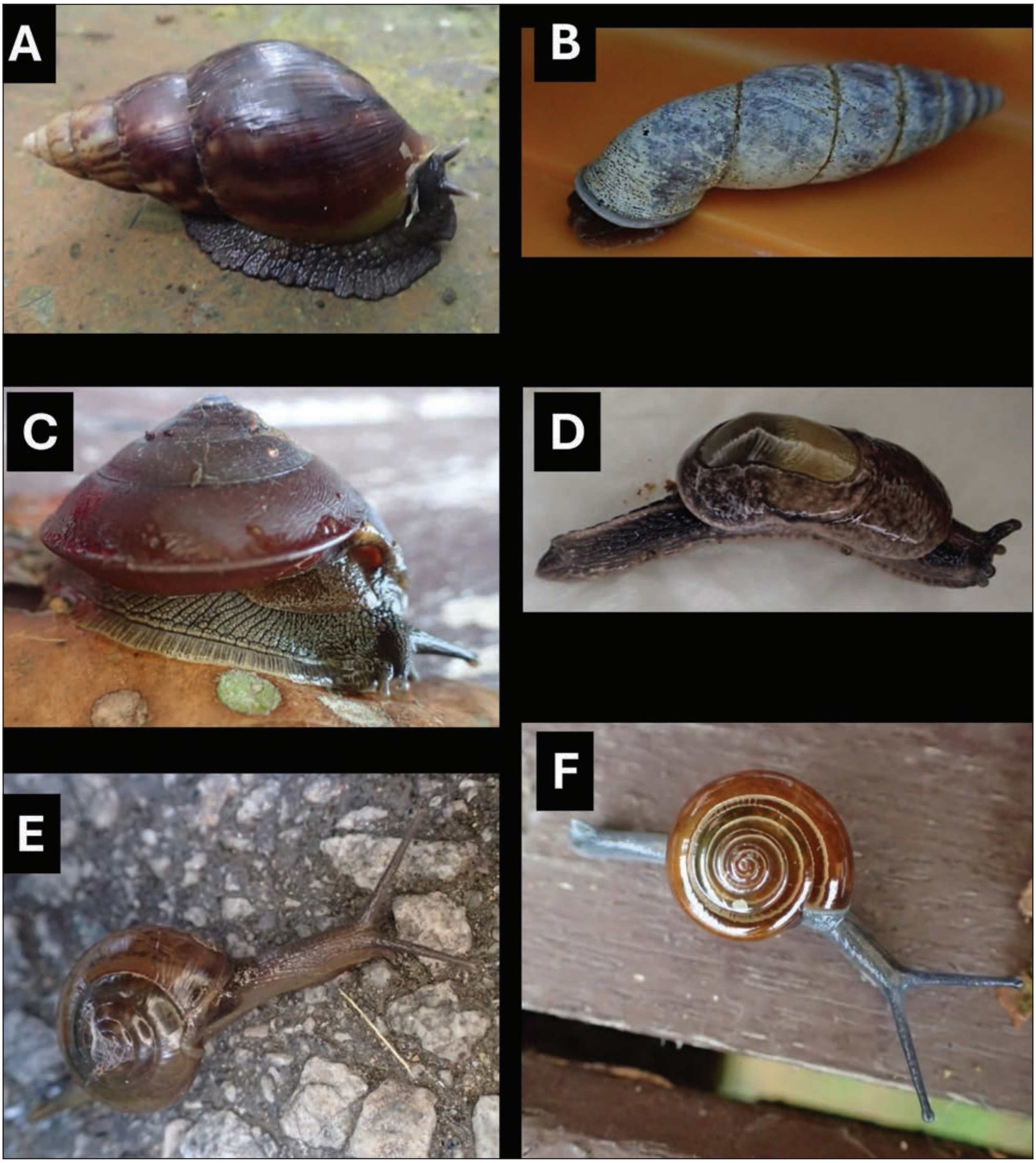

Figure 20. A *Lissachatina fulica* (Bowdich, 1822) **B** *Oospira penangensis* (Stoliczka, 1873) **C** *Hemiplecta cymatium* (L. Pfeiffer, 1856) **D** *Parmarion martensi* Simroth, 1893 **E** *Tanychlamys indica* (Godwin Austen, 1883) **F** *Tanychlamys* Penang sp. 1.

different species composition, revealed by the cluster analysis and NMDS. Disturbed habitats seem to have higher numbers of species and could be due to the mid-disturbance effect on species richness (Čiliak et al. 2024). The intermediate levels of disturbance, such as man-made structures and modified vegetation with ornamental plants, in the disturbed forest plots seemed to create favourable conditions for non-native species while the remaining original vegetation and forest can support the native species: both conditions contribute to greater diversity of land snail species.

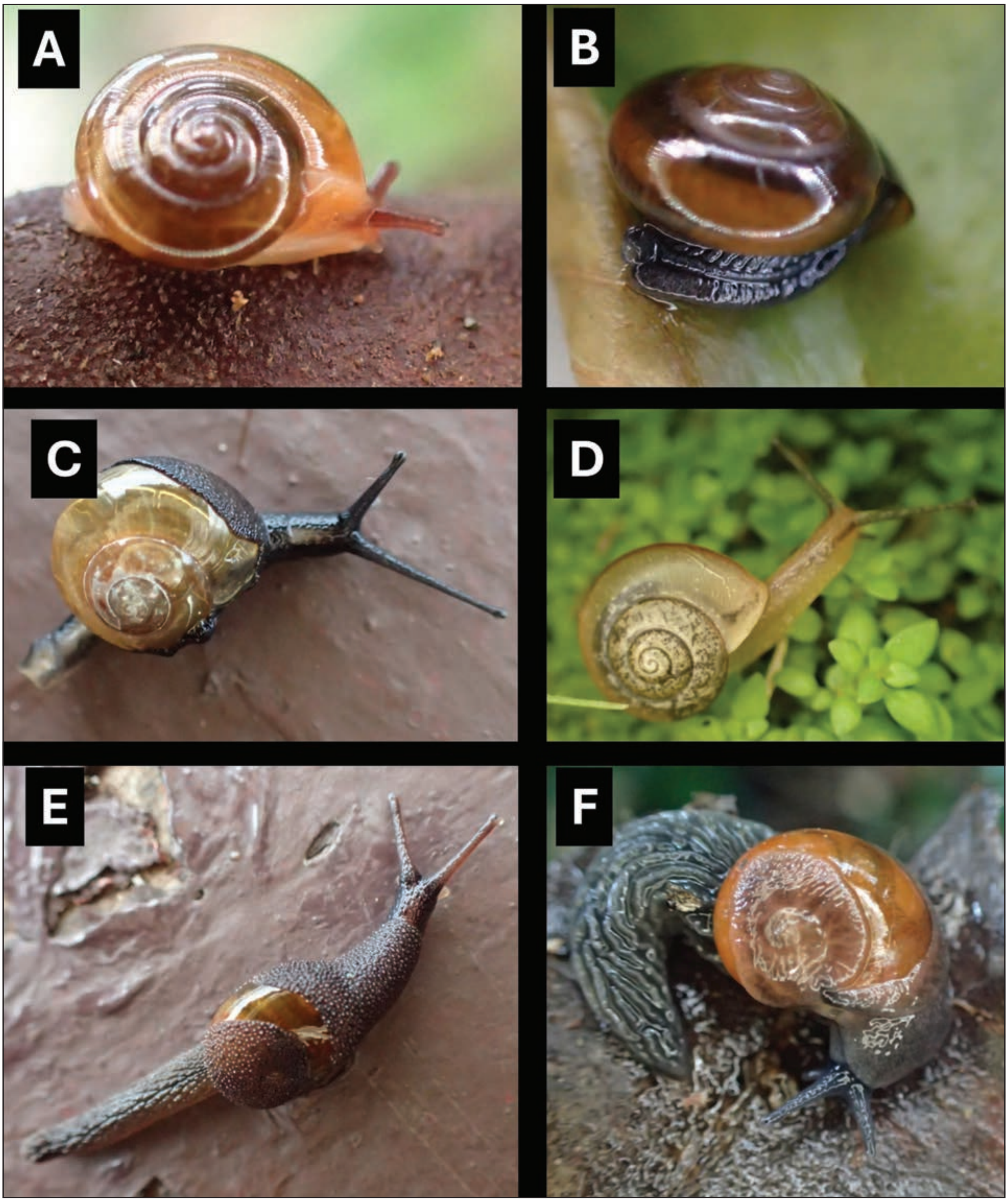

Figure 21. A *Tanychlamys* Penang sp. 2 **B** *Tanychlamys tersa* (Issel, 1874) **C** *Helicarion permolle* Stoliczka, 1873 **D** *Bradybaena similaris* (A. Férussac, 1821) **E** *Vitrinopsis* sp. **F** *Vitrinopsis nucleata* (Stoliczka, 1873).

While there were no clear patterns of grouping based on elevation or habitat types, the plots in orchards exhibited some similarity in terms of species composition. We found five species have strong associations to disturbed forest areas and orchards, while most of the other species do not show clear preferences for a certain habitat. This observation suggests that human-modified landscapes, such as orchards, might create specific microhabitats that support a particular group of land snail species.

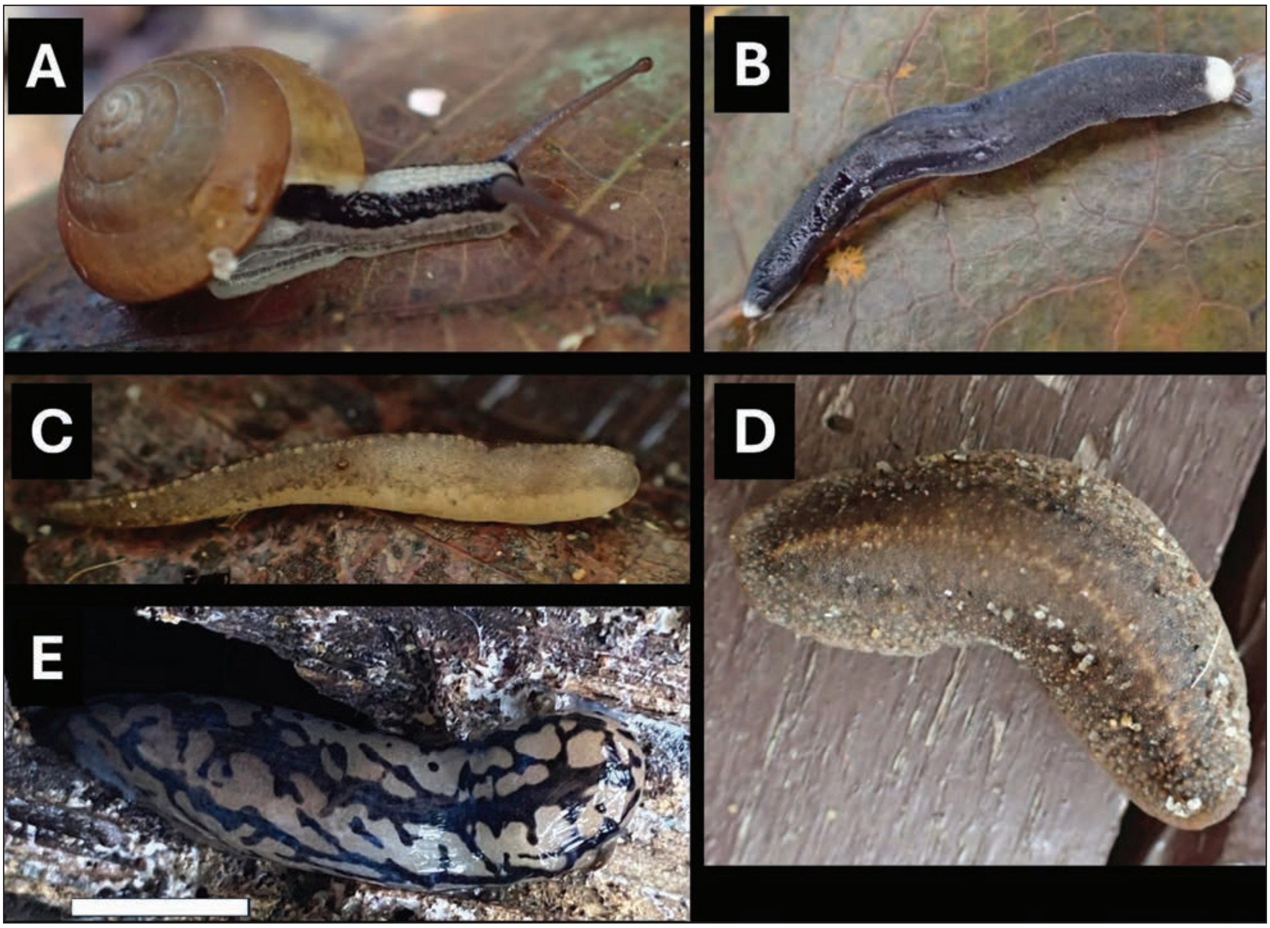

Figure 22. **A** *Pseudoplecta bijuga* (Stoliczka, 1873) **B** *Atopos tourannensis* (Souleyet, 1852) **C** *Atopos punctata* Collinge, 1902 **D** *Laevicaulis alte* (A. Férussac, 1822) **E** *Meghimatium pictum* (Stoliczka, 1873), photo credit Xin Wei Ooi.

Conclusions

Overall, this study significantly increases our knowledge of land snail diversity in non-limestone areas of Peninsular Malaysia. Additionally, the material collected in this study are valuable for future taxonomic research in this region, given that Penang Hill is the type locality for 19 species newly described by Stoliczka (1872, 1873). Penang Hill remains one of the most important historical sites for biodiversity research and continues to harbour a rich biodiversity.

Acknowledgements

We would like to thank various agencies for granting permission to carry out this work, namely the Forestry Department Pulau Pinang (JPNPP/600-9/1 Jld.3(47)); Forestry Department of Peninsular Malaysia (JH/100 Jld.34(8)); Department of Botanical Garden Pulau Pinang (JTB/pp/02/03/032 Jld.5(7)); and Perbadanan Bekalan Air Pulau Pinang (PBAPP/CAD/SC/#EXT/1/05/14(6)). We thank Ethan Pang (The Habitat Foundation) for facilitating our work at Penang Hill, Ashraft Yusni (Universiti Malaysia Sabah) for assistance during sampling, and Xin-Wei Ooi (The Habitat Penang Hill) for sharing information about the slug. We are also grateful to Noor Haliza Binti Hasan (Universiti Malaysia Sabah) for supporting part of the laboratory work. Additionally, we thank Martin Haase, Jonathan Ablett, and Ayu Savitri Nurinsiyah for their constructive comments, which improved an earlier version of the manuscript.

Additional information

Conflict of interest

The authors have declared that no competing interests exist.

Ethical statement

No ethical statement was reported.

Funding

This research was supported by The Habitat Foundation Grant 2022.

Author contributions

Conceptualization: TSL. Data curation: SMG, DJ, TSL. Formal analysis: SMG, TSL. Funding acquisition: TSL. Investigation: DJ, MYL, SMG, TSL. Methodology: JJJV, TSL. Project administration: TSL. Resources: TSL. Supervision: TSL. Visualization: SMG, TSL. Writing - original draft: SMG, TSL. Writing - review and editing: MYL, JJJV, TSL, DJ, SMG.

Author ORCIDs

Mei-Yi Lee https://orcid.org/0009-0005-8200-3508
Thor-Seng Liew https://orcid.org/0000-0002-9437-5924

Data availability

All of the data that support the findings of this study are available in the main text or Supplementary Information.

References

Adams H, Adams A (1851) On two new genera of Mollusca. The Annals and Magazine of Natural History Ser. 2 7: 63–64. https://www.biodiversitylibrary.org/item/48970#page/81/mode/1up

Benson WH (1851a) Geographical notices, and characters of fourteen new species of Cyclostoma, from the East Indies. Annals and Magazine of Natural History Ser. 2, 8(45): 184–195. https://doi.org/10.1080/03745486109496203

Benson WH (1851b) Descriptive characters of two species of the genus *Pterocyclos*, discovered by Dr. Bland. Annals and Magazine of Natural History Ser. 2, 8: 195–197. https://doi.org/10.1080/03745486109496204

Benson WH (1852a) Notes on the genus *Cyclostoma*; and characters of some new species from India, Borneo, and Natal. Annals and Magazine of Natural History Ser. 2 10: 268–272. https://doi.org/10.1080/03745485609495694

Benson WH (1852b) Notice of an Australian *Diplommatina*; and characters of new East Indian Helicidae from Darjiling and Singapore. Annals and Magazine of Natural History Ser. 2, 10: 348–351. https://doi.org/10.1080/03745485609495711

Benson WH (1861) Characters of a gigantic Helix from southern India, and of other species from northern India, the Malayan Coast, and the Andaman Islands. Annals and

Magazine of Natural History. Ser. 3, 7(38): 81–85. https://www.biodiversitylibrary.org/item/65735#page/99/mode/1up

Berry AJ, Chan LC (1968) Reproductive condition and tentacle extirpation in Malayan *Achatina fulica* (Pulmonata). Australian Journal of Zoology 16(5): 849–855. https://doi.org/10.1071/ZO9680849

Cáceres MD, Legendre P (2009) Associations between species and groups of sites: indices and statistical inference. Ecology 90(12): 3566–3574. https://doi.org/10.1890/08-1823.1

Chan SY (1998a) A brief collecting trip to Perak, West Malaysia. part one. The Papustyla 12(1): 4–5.

Chan SY (1998b) A brief collecting trip to Perak, West Malaysia. part two. The Papustyla 12(2): 1–2.

Čiliak M, Čejka T, Tej B, Oboňa J, Manko P (2024) Species richness patterns and community structure of land snail communities along an urban-rural gradient in river floodplains. Urban Ecosystems 27(3): 953–963. https://doi.org/10.1007/s11252-023-01501-1

Clements R, Ng PK, Lu XX, Ambu S, Schilthuizen M, Bradshaw CJ (2008) Using biogeographical patterns of endemic land snails to improve conservation planning for limestone karsts. Biological conservation 141(11): 2751–2764. https://doi.org/10.1016/j.biocon.2008.08.011

Collinge WE (1902) On the non-operculate land and freshwater Molluscs collected by the members of the “Skeat-Expedition” in the Malay Peninsula, 1899–1900. The Journal of Malacology 9: 71–95. https://www.biodiversitylibrary.org/item/89648#page/253/mode/1up

Cowie RH (1998) Patterns of introduction of non-indigenous non-marine snails and slugs in the Hawaiian Islands. Biodiversity & Conservation 7: 349–368. https://doi.org/10.1023/A:1008881712635

Davison GWH (1991) A conservation assessment of limestone hills in the Kinta Valley. Final report – MNS Project 1/90, Malayan Nature Society, Kuala Lumpur, 202 pp.

Davison GWH (1995) The terrestrial molluscan fauna of Temengor Forest Reserve, Hulu Perak, Malaysia. Malayan Nature Journal 48: 233–248.

de Morgan J (1885a) Quelques espèces nouvelles de mollusques terrestres recueillis dans la peninsula Malaise. Le Naturaliste 7: 68–70. https://www.biodiversitylibrary.org/item/105819#page/83/mode/1up

de Morgan J (1885b) Mollusques terrestes et fiuviatiles de Royaume de Perak et des pais voisins (presque’Ile Malaise). Bulletin de la Société zoologique de France 10: 353–429. https://doi.org/10.5962/bhl.part.14301

Foon JK, Marzuki ME (2023) A checklist of land snails (Mollusca, Gastropoda) of Batu Caves, Selangor, Malaysia. Malayan Nature Journal 75(1): 133–148.

Foon JK, Clements GR, Liew TS (2017) Diversity and biogeography of land snails (Mollusca, Gastropoda) in the limestone hills of Perak, Peninsular Malaysia. ZooKeys 682: 1–94. https://doi.org/10.3897/zookeys.682.12999

Gray JE (1834) [Several shells, which … referred to a genus to be separated from Helix under the name of Nanina.]. Proceedings of the Zoological Society of London 2: 58–59. https://www.biodiversitylibrary.org/item/96158#page/70/mode/1up

Inkhavilay K, Sutcharit C, Bantaowong U, Chanabun R, Siriwut W, Srisonchai R, Pholyotha A, Jirapatrasilp P, Panha S (2019) Annotated checklist of the terrestrial molluscs from Laos (Mollusca, Gastropoda). ZooKeys 834: 1–166. https://doi.org/10.3897/zookeys.834.28800

Ito S, Yamazaki D, Kameda Y, Kagawa O, Ye B, Saito T, Kimura K, Do VT, Chiba S, Hirano T (2023) Taxonomic insights and evolutionary history in East Asian terrestrial slugs of the genus *Meghimatium*. Molecular Phylogenetics and Evolution 182: 107730. https://doi.org/10.1016/j.ympev.2023.107730

Jirapatrasilp P, Sutcharit C, Panha S (2022) Annotated checklist of the operculated land snails from Thailand (Mollusca, Gastropoda, Caenogastropoda): the family Pupinidae, with descriptions of several new species and subspecies, and notes on classification of *Pupina* Vignard, 1829 and *Pupinella* Gray, 1850 from mainland Southeast Asia. ZooKeys 1119: 1–115. https://doi.org/10.3897/zookeys.1119.85400

Laidlaw FF (1928) A list of the Land and Fresh-water Mollusca of the Malay Peninsula with notes. Journal of the Malayan Branch of the Royal Asiatic Society 6: 25–37. http://www.jstor.org/stable/41559818

Liew TS (2010) The land snail fauna of the Lojing Highlands (Mollusca: Gastropoda). In: Omar IC, Hamzah Z (Eds) Conservation Lojing Highlands for Sustainable Development. Universiti Malaysia Kelantan, 98–104. https://doi.org/10.13140/RG.2.1.4311.5364

Liew TS, Schilthuizen M, bin Lakim M (2010) The determinants of land snail diversity along a tropical elevational gradient: insularity, geometry and niches. Journal of Biogeography 37(6): 1071–1078. https://doi.org/10.1111/j.1365-2699.2009.02243.x

Liew TS, Clements R, Schilthuizen M (2008) Sampling micromolluscs in tropical forests: one size does not fit all. Zoosymposia 1: 271–280. https://doi.org/10.11646/zoosymposia.1.1.16

Maassen WJM (2001) A preliminary checklist of the non-marine molluscs of West Malaysia. De Kreukel (extra edition 2001) 2001: 1–155.

MolluscaBase (2024) MolluscaBase. https://doi.org/10.14284/448 [accessed 22 September 2024]

Pall-Gergely B, Hunyadi A, Maassen WJ (2014) Review on *Rhaphaulus* L. Pfeiffer 1856 and Streptaulus Benson 1857 species with description of *Rh. tonkinensis* n. sp. from Vietnam (Gastropoda: Pupinidae). Journal of Conchology 41(5): 565–573. https://conchsoc.org/sites/default/files/jconch/41/5/2014-41504.pdf

Pfeiffer L (1851) Uebersicht der Gattung Pterocyclos Bens. Zeitschrift für Malakozoologie 8(1): 1–10. https://www.biodiversitylibrary.org/page/16300501

Pfeiffer L (1853) Diagnosen neuer Heliceen. Zeitschrift für Malakozoologie. Cassel (Theodor Fischer) 10(4): 51–58 [31 März 1853]; 10(10): 145–151 [30 November 1853]. https://www.biodiversitylibrary.org/page/16300951

Pfeiffer L (1855a) Descriptions of twenty-three species of Helicea, from the collection of H. Cuming, Esq. Proceedings of the zoological Society of London 22(269)["1854"]: 145–150. https://www.biodiversitylibrary.org/item/96679#page/449/mode/1up

Pfeiffer L (1855b) ["1854"] Descriptions of fifty-seven new species of Helicea, from Mr. Cuming's collection. Proceedings of the Zoological Society of London 22(277): 286–288; 22(278): 289–298 [8 May 1855]. https://www.biodiversitylibrary.org/item/96679#page/616/mode/1up

Pfeiffer L (1855c) A monograph of the genera *Realia* and *Hydrocena*. Proceedings of the Zoological Society of London 22(278)["1854"]: 304; 22(279)["1854"]: 305–309 [8. May 1855]. https://www.biodiversitylibrary.org/item/96679#page/635/mode/1up

Pfeiffer L (1856) Descriptions of twenty-five new species of land-shells, from the collection of H. Cuming, Esq. Proceedings of the zoological Society of London 24(302): 32; 24(303): 33–36. https://www.biodiversitylibrary.org/page/12860555

Pfeiffer L (1857) Descriptions of thirty-three new species of land-shells, from the collection of H. Cuming, Esq. Proceedings of the zoological Society of London 24(325) ["1856"]: 385–392. https://www.biodiversitylibrary.org/page/12860951

Phung CC, Yong YZ, Mat Said MA, Liew TS (2018) Land snail fauna in Gunung Kuang Limestone Hill, Perak, Malaysia and its conservation implications (Mollusca, Gastropoda). ZooKeys 769: 1–11. https://doi.org/10.3897/zookeys.769.25571

Schilthuizen M, Chai HN, Kimsin TE, Vermeulen JJ (2003) Abundance and diversity of land-snails (Mollusca: Gastropoda) on limestone hills in Borneo. Raffles Bulletin of Zoology 51(1): 35–42. https://lkcnhm.nus.edu.sg/wp-content/uploads/sites/11/app/uploads/2017/06/51rbz035-042.pdf

Souleyet M (1841) Description de deux espèces nouvelles des genres Hélice et Cyclostome. Revue Zoologique par la Société Cuvierrenne 4: 347. https://www.biodiversitylibrary.org/item/19646#page/355/mode/1up

Souleyet LFA (1842) Description de quelques coquilles terrestres appartenant aux genres Cyclostome, Hélice, etc. Revue Zoologique par la Société Cuvierienne. (1842): 101–102. https://www.biodiversitylibrary.org/item/51063#page/111/mode/1up

Souleyet LFA (1852) Tome Deuxième. Mollusques. In: Eydoux F, Souleyet LFA (1841–1852). Voyage autour du monde exécuté pendant les années 1836 et 1837 sur la corvette La Bonite. Zoologie. Arthus Bertrand, Paris, 664 pp. https://www.biodiversitylibrary.org/page/28264738

South FW (1926) The giant snail (*Achatina fulica*, Fer.) in Malaya. Malayan Agricultural Journal 14: 231–240.

Sowerby GBI (1842) Descriptions of new species of shells belonging to the genus *Cyclostoma*, collected by Mr. H. Cuming in the Philippine Islands. Proceedings of the Zoological Society of London 1842: 80–84. https://biodiversitylibrary.org/page/30679842

Sowerby GBI (1843) Descriptions of new species of shells belonging to the genus *Cyclostoma*. Proceedings of the Zoological Society of London 11: 29–31 [October 1843], 59–66 [November 1843]. https://www.biodiversitylibrary.org/page/30680007

Stoliczka F (1872) On the land shells of Penang Island, with descriptions of the animals and anatomical notes; part first, Cyclostomacea. Journal of the Asiatic Society of Bengal 41: 261–271. https://www.biodiversitylibrary.org/item/114229#page/271/mode/1up

Stoliczka F (1873) On the land shells of Penang Island, with descriptions of the animals and anatomical notes; part second, Helicacea. Journal of the Asiatic Society of Bengal 42: 11–38. https://www.biodiversitylibrary.org/page/35546163#page/25/mode/1up

Sykes ER (1903) On the land operculate Mollusca collected during the "Skeat Expedition" to the Malay Peninsula in 1899–1900. Proceedings of the Zoological Society of London 1903(1): 194–199. https://www.biodiversitylibrary.org/page/31598794#page/258/mode/1up

Tsai CL, Lu CC, Kao HW (2011) Morphology and molecular phylogeny of the east and southeast Asian *Meghimatium* slugs (Gastropoda: Pulmonata: Philomycidae) and description of a new species. Zootaxa 2890(1): 1–19. https://doi.org/10.11646/zootaxa.2890.1.1

Tumpeesuwan S, Panha S (2008) First Record of the Genus *Schistoloma* Kobelt, 1902 (Prosobranchia: Pupinidae) in Thailand. Tropical Natural History 8(1): 65–67. https://www.thaiscience.info/journals/Article/NHCU/10439781.pdf

van Benthem Jutting WSS (1949) On a collection of non-marine Mollusca from Malaya in the Raffles Museum, Singapore, with an appendix on cave shells. Bulletin of the Raffles Museum Singapore 19: 50–77. https://lkcnhm.nus.edu.sg/app/uploads/2017/06/19brm050-077.pdf

van Benthem Jutting WSS (1950) The Malayan species of *Boysidia*, *Paraboysidia*, *Hypselostoma* and *Gyliotrachela* (Gastropoda, Pulmonata, Vertiginidae). Bulletin of the Raffles Museum 21: 5–47. https://lkcnhm.nus.edu.sg/app/uploads/2017/06/21brm005-047.pdf

van Benthem Jutting WSS (1952) The Malayan species of *Opisthostoma* (Gastropoda, Prosobranchia, Cyclophoridae), with a catalogue of all the species hitherto described. Bulletin of the Raffles Museum 24: 5–62. https://lkcnhm.nus.edu.sg/app/uploads/2017/06/24brm005-062.pdf

van Benthem Jutting WSS (1954) The Malayan Streptaxidae of the genera *Discartemon* and *Oophana*. Bulletin of the Raffles Museum 25: 71–106. https://lkcnhm.nus.edu.sg/app/uploads/2017/06/25brm071-106.pdf

van Benthem Jutting WSS (1959) Catalogue of the non-marine Mollusca of Sumatra and of its satellite islands. Beaufortia 7(83): 41–191. https://repository.naturalis.nl/pub/504682

van Benthem Jutting WSS (1960) Non-marine Mollusca of the limestone hills in Malaya. Proceedings of Centenary and Bicentenary Congress of Biology, 63–68. https://natuurtijdschriften.nl/pub/596402/BAST1960024001002.pdf

Vermeulen JJ, Liew, TS, Schilthuizen M (2015) Additions to the knowledge of the land snails of Sabah (Malaysia, Borneo), including 48 new species. ZooKeys 531: 1–139. https://doi.org/10.3897/zookeys.531.6097

von Möllendorff OF (1886) The land shells of Perak. Journal of the Asiatic Society of Bengal 55: 299–316. https://www.biodiversitylibrary.org/item/110098#page/337/mode/1up

von Möllendorff OF (1891) On the land and freshwater shells of Perak. Proceedings of the Zoological Society of London 59(3): 330–348. https://doi.org/10.1111/j.1096-3642.1891.tb01757.x

Supplementary material 1

Species plot data matrix for the 33 standard sampling sites at Penang Hill (plot locations, habitat types, and elevation details in Table 1)

Author: Thor-Seng Liew

Data type: csv

Link: https://doi.org/10.3897/zookeys.1230.136906.suppl1

ZooKeys 1230: 155–194 (2025)
DOI: 10.3897/zookeys.1230.133585

Research Article

New species and new records of families, genera and species of land snails (Mollusca, Gastropoda) from French Guiana

Olivier Gargominy[1], Benoît Fontaine[2], Sandrine Tercerie[1], Dario Zuccon[3]

1 *PatriNat (OFB-MNHN-CNRS-IRD), Muséum national d'Histoire naturelle - CP41, 36 rue Geoffroy Saint-Hilaire 75005 Paris, France*
2 *PatriNat (OFB-MNHN-CNRS-IRD), CESCO (MNHN-CNRS-SU), Muséum national d'Histoire naturelle - 3 allée des crapauds - Bat 135 - 43, rue Buffon 75005 Paris, France*
3 *Institut de Systématique, Évolution, Biodiversité (ISYEB), Muséum national d'Histoire naturelle, CNRS, Sorbonne Université, EPHE, Université des Antilles, CP 50, 57 rue Cuvier, 75005 Paris, France*
Corresponding author: Olivier Gargominy (olivier.gargominy@mnhn.fr)

Abstract

This paper presents an investigation of material collected during four intensive collecting trips of land snails in French Guiana from 1995 to 2020 and deposited in the French National Museum of Natural History collections. This material forms the basis of the following novelties: four families are reported for the first time from French Guiana: Diplommatinidae, Cystopeltidae, Thysanophoridae and Strobilopsidae; three native species: *Lyroconus plagioptycha* (Helicoidea, Thysanophoridae), *Pupisoma macneilli* (Pupilloidea, Valloniidae) and *Strobilops morsei* (Pupilloidea, Strobilopsidae) and one introduced species *Diplosolenodes occidentalis* (Veronicelloidea, Veronicellidae) are reported for the first time from French Guiana; five new species are described: *Adelopoma quasimodo* Gargominy, **sp. nov.** (Cyclophoroidea, Diplommatinidae), *Lilloiconcha galbao* Gargominy, **sp. nov.** (Punctoidea, Cystopeltidae), *Protoglyptus bernicolae* Gargominy, **sp. nov.** (Orthalicoidea, Bulimulidae), *Pseudosubulina santi* Gargominy, **sp. nov.** (Testacelloidea, Spiraxidae), and *Happia decaensi* Gargominy, **sp. nov.** (Scolodontoidea, Scolodontidae). Finally, *Drymaeus surinamensis* Vernhout, 1914, **syn. nov.** is considered as a new synonym of *Mesembrinus lusorius* (L. Pfeiffer, 1855), and *Drymaeus arcuatostriatus* (L. Pfeiffer, 1855) is proposed as the new identification of *Drymaeus meesi* sensu Tillier, 1980 non Breure, 1976.

Résumé

Cet article présente une étude du matériel collecté lors de quatre missions de collecte intensive d'escargots terrestres en Guyane française de 1995 à 2020, dont le matériel est déposé dans les collections du Muséum national d'Histoire naturelle. Ce matériel a permis de révéler les nouveautés suivantes: quatre familles sont signalées pour la première fois de Guyane française: Diplommatinidae, Cystopeltidae, Thysanophoridae et Strobilopsidae ; trois espèces indigènes: *Lyroconus plagioptycha* (Helicoidea, Thysanophoridae), *Pupisoma macneilli* (Pupilloidea, Valloniidae) et *Strobilops morsei* (Pupilloidea, Strobilopsidae) et une espèce introduite *Diplosolenodes occidentalis* (Veronicelloidea, Veronicellidae) sont signalées pour la première fois de Guyane française ; cinq nouvelles espèces sont décrites: *Adelopoma quasimodo* Gargominy, **sp. nov.** (Cyclophoroidea, Diplommatinidae), *Lilloiconcha galbao* Gargominy, **sp. nov.** (Punctoidea, Cystopeltidae), *Protoglyptus bernicolae* Gargominy, **sp. nov.** (Orthalicoidea, Bulimulidae), *Pseudosubulina santi* Gargominy, **sp. nov.** (Testacelloidea, Spiraxidae) et *Happia decaensi* Gargominy, **sp. nov.** (Scolodontoidea, Scolodontidae). Enfin, *Drymaeus surinamensis* Vernhout,

Academic editor: Eike Neubert
Received: 31 July 2024
Accepted: 25 November 2024
Published: 6 March 2025

ZooBank: https://zoobank.org/9BD7CC64-BD60-4B9E-B1D1-8F23B26F5FC6

Citation: Gargominy O, Fontaine B, Tercerie S, Zuccon D (2025) New species and new records of families, genera and species of land snails (Mollusca, Gastropoda) from French Guiana. ZooKeys 1230: 155–194. https://doi.org/10.3897/zookeys.1230.133585

1914, **syn. nov.** est considéré comme un nouveau synonyme de *Mesembrinus lusorius* (L. Pfeiffer, 1855), et *Drymaeus arcuatostriatus* (L. Pfeiffer, 1855) est proposé comme une nouvelle identification de *Drymaeus meesi* sensu Tillier, 1980 non Breure, 1976.

Key words: Hidden diversity, Mitaraka, Nouragues, rainforest, Saül, Trinité

Introduction

French Guiana remains a real field of adventure and discovery for malacologists: access to sites is generally very difficult, land snails are very rare, and very few people make field collections. The very low visible abundance of land snails in the Guianan forest, already observed by early collectors (Drouët 1859), has been confirmed: one can spend whole days in the forest without seeing a single living snail. In a comprehensive revision published in 1980 (Tillier 1980), only 52 species were recorded from the territory of French Guiana. However, large tracts of the forest interior had never been surveyed, and very few minute species were documented, suggesting that the inventory was far from complete.

In this context, in order to fill the gaps in the knowledge of this fauna, surveys (years 1997, 1999, 2015, 2018, 2019, 2020) have been conducted in remote areas of French Guiana in order to inventory the molluscan diversity. They included massive sieving of leaf-litter and revealed a neglected small to minute mollusc fauna (e.g., Gargominy and Ripken 1998; Gargominy and Fontaine 2015; Gargominy et al. 2022). The purpose of this article is to present some of the results of these surveys, including revision of the taxonomy of species collected, except for the Subulininae and the micro Scolodontidae, both of which need a specific paper. Four families previously unknown from French Guiana are documented and five species new to science are described. Material for molecular studies and COI sequences are provided for the first time from the area, although molecular studies are not possible due to lack of comparative material.

Finally, we discuss the reasons this fauna is so poorly known, including the lack of prospecting in French Guiana and neighbouring countries, the rarity of snails, and their patchy distribution in a seemingly homogeneous rainforest.

Material and methods

Studied material

Studied material comes from four main collecting events (Fig. 1):

1. Survey at the Réserve Naturelle Nationale des Nouragues organized by the Muséum national d’Histoire naturelle (**MNHN**) and the Centre National de la Recherche Scientifique (**CNRS**). The scientific station (ca 130 m a.s.l.) is situated at the foot of an inselberg in the Balenfois Mountains (482 m) on the watershed dividing Comté and Approuagues catchments. Molluscs were sampled between 1 and 20 November 1997 (GBIF dataset) and in June 1999 (GBIF dataset) by the first author (OG) and Theo Ripken. Some

material has already been the subject of publications and descriptions of new species (Muratov and Gargominy 2011; Gargominy and Muratov 2012).

2. 'Our Planet Reviewed' Mitaraka 2015 Survey (GBIF dataset), co-organized by the MNHN and the NGO Pro-Natura International (**PNI**) (Touroult et al. 2018). The expedition was conducted in the Mitaraka Mountains, a largely unknown and uninhabited area in the south-westernmost corner of French Guiana, directly bordering Suriname and Brazil. It forms part of the Maroni river catchment and of the Tumuc-Humac mountain chain, extending east in the Amapá region (Brazil) and west in southern Suriname. Molluscs were sampled between 1 and 24 March 2015 by the first (OG) and second (BF) authors (see report Gargominy and Fontaine 2015).
3. Atlas de la Biodiversité Communale (ABC) of Saül, initiated in 2018 and organized by the Parc Amazonien de Guyane (PAG) with financial support from the Office Français de la Biodiversité (OFB). Saül is a small village situated in the middle of French Guiana at an altitude of 200 m a.s.l. from where Mont Galbao (717 m) can be reached in a day's walk. Saül and Mont Galbao are situated on the watershed between the Mana and Maroni river catchments. Molluscs were sampled between 16 and 29 November 2018 by the three first authors and Sébastien Sant (PAG), and between 14 and 26 February 2020 by the first (OG) and second (BF) authors, Sébastien Sant (PAG), and Ahmed Abdou (MNHN) (GBIF dataset). The first results were published in Gargominy et al. (2022).
4. Survey at the Réserve naturelle nationale de La Trinité organized by the Office national des Forêts (ONF). This reserve comprises an isolated mountain range with inselbergs (478 m) on the watershed dividing the Maroni and Sinnamary catchments. Molluscs were sampled between 8 and 18 April 2019 by the second (BF) and third (ST) authors (GBIF dataset).

Additional material comes from donations, in particular Thibaud Decaëns and Sébastien Cally from Itoupé (DIADEMA project) on the watershed dividing the Maroni and Camopi/Oyapock catchments.

All the studied material is deposited in the Mollusc collection of the MNHN. Each lot can be traced with its inventory number, MNHN-IM-20XX-XXXX, in the collection database of the MNHN at the following address: https://science.mnhn.fr/institution/mnhn/collection/im/item/search?lang=en_US.

Sampling methods

Extensive sieving of leaf litter was conducted in all four field trips. This technique is the only way to approach species inventory completeness, because many species are either small or rare, and many are both. Leaf litter is processed at the collection site using a Winkler sieve (1 cm mesh), with the coarse material checked for snails (empty shells and live animals) and discarded. The remaining material is processed as quickly as possible at the base camp to collect live animals: it is passed through 5 mm, 2 mm, and 0.6 mm sieves. The two larger fractions are carefully examined with the naked eye and the third is sorted under a dissecting microscope. Material passing through the 0.6 mm sieve is discarded. Live molluscs are drowned overnight or prepared with the niku-nuki method (Fukuda et al. 2008) mainly for the smaller ones and fixed in 96% ethanol.

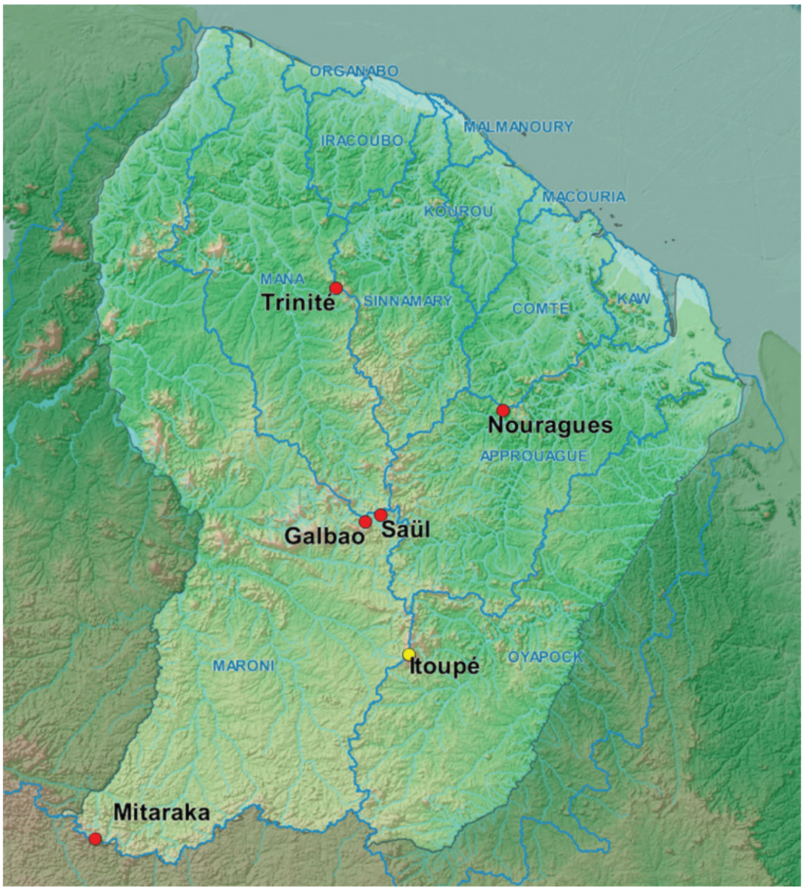

Figure 1. Location of the four main collecting events providing material for this study (Nouragues, Mitaraka, Saül/Galbao, and Trinité, red dots). Itoupé is the type locality for *Happia decaensi* sp. nov. (yellow dot). Main river basins are represented.

DNA barcoding

Total genomic DNA was extracted using the Macherey-Nagel NucleoSpin 96 Tissue Kit and following the manufacturer's protocol, in combination with the epMotion 5075 robot (Eppendorf). We amplified the 658 bp barcode portion of the mitochondrial cytochrome oxidase I (COI) with primers LCO1490 and HCO2198 (Folmer et al. 1994). Newly obtained sequences were deposited in GenBank and BOLD (Barcode of Life Datasystem).

Abbreviations

AA	Ahmed Abdou
BF	Benoît Fontaine
FMNH	Field Museum of Natural History, Chicago, USA
MNHN	Muséum national d'Histoire naturelle, Paris, France
NHMUK	Natural History Museum, London, United Kingdom
OG	Olivier Gargominy
ONF	Office national des Forêts
PAG	Parc amazonien de Guyane
RN	Réserve Naturelle
ST	Sandrine Tercerie
TR	Theo E. J. Ripken

Systematics

Class Gastropoda Cuvier, 1795
Subclass Caenogastropoda Cox, 1960
Order Architaenioglossa Haller, 1890
Superfamily Cyclophoroidea Gray, 1847
Family Neocyclotidae Kobelt & Möllendorff, 1897
Subfamily Amphicyclotinae Kobelt & Möllendorff, 1897
Genus *Cyclopedus* Gargominy & Muratov, 2012

Cyclopedus anselini Gargominy & Muratov, 2012
Fig. 2

Cyclopedus anselini Gargominy & Muratov, 2012: 785, fig. 2.

Link. https://molluscabase.org/aphia.php?p=taxdetails&id=1477355.

Type locality. French Guiana, Régina, Réserve naturelle des Nouragues, Montagnes Balenfois, field station.

Type material. ***Holotype***. French Guiana • 1 dry specimen; Régina, RN des Nouragues, carré N10 du km^2 layonné (N10); 4.08845°N, 52.67269°W; alt. 140 m; 11 Nov. 1997; TR, OG leg.; leaf litter on lateritic soil in a natural forest gap; MNHN-IM-2000-25066. ***Paratypes*** (3). French Guiana • 1 dry specimen; same data as the holotype; MNHN-IM-2000-25067 • 1 dry specimen; Régina, RN des Nouragues, carré M12 du km^2 layonné (N7); 4.08699°N, 52.67381°W; alt. 140 m; 08 Nov. 1997; TR, OG leg.; forêt primaire, grand plateau; MNHN-IM-2000-25138 • 1 dry specimen; Régina, RN des Nouragues, carré N15 du km^2 layonné (N14); 4.08372°N, 52.67503°W; alt. 155 m; 15 Nov. 1997; TR, OG leg.; forêt primaire, pied d'arbre à contrefort (code N-15-138); MNHN-IM-2000-25139.

Other material examined. French Guiana • 42 dry specimens; Régina, RN des Nouragues, carré M12 du km^2 layonné (N7); 4.08699°N, 52.67381°W; alt. 140 m; 08 Nov. 1997; TR, OG leg.; forêt primaire, grand plateau; MNHN-IM-2018-14184• 2 dry specimens; Régina, RN des Nouragues, carré N10 du km^2 layonné (N10); 4.08845°N, 52.67269°W; alt. 140 m; 11 Nov. 1997; TR, OG leg.; forêt primaire, chablis; MNHN-IM-2018-14183 • 2 dry specimens; Régina, RN des Nouragues, carré N13 du km^2 layonné (NB5); 4.08603°N, 52.67353°W; alt. 170 m; 03 Jun. 1999-29 Jun. 1999; TR, OG leg.; MNHN-IM-2018-14292 • 4 95% ethanol specimen; Saül, Mont Galbao (SAUL47); 3.60183°N, 53.27239°W; alt. 650 m; 27 Nov. 2018; OG, SS, ST, BF (PAG & MNHN) leg.; DZ brulée et cambrouse à l'est; GenBank: PQ629106; Bold: DREAL124-23; MNHN-IM-2013-75859; GenBank: PQ629100; Bold: DREAL123-23; MNHN-IM-2013-75860; GenBank: PQ629099; Bold: DREAL122-23; MNHN-IM-2013-75861; GenBank: PQ629094; Bold: DREAL121-23; MNHN-IM-2013-75862 • 2 dry specimens; Saül, same data as preceding; MNHN-IM-2012-21975 • 3 dry specimens; Saül, Cascades du Mont Galbao, face nord-est (SAUL64); 3.60376°N, 53.26121°W; alt. 320 m; 19 Feb. 2020; BF, AA, OG (PAG & MNHN) leg.; Bordure de cambrouse; MNHN-IM-2018-14064 • 2 95% ethanol specimens; Saül, Mont Galbao face nord-est (SAUL65); 3.59681°N, 53.26257°W; alt. 503 m; 20 Feb. 2020; BF, AA, OG (PAG & MNHN) leg.; Cambrouse et lianes en forêt; MNHN-IM-2013-76396 • 2 dry specimens; Saül, Mont Galbao face nord-est (SAUL66); 3.59995°N, 53.26697°W; alt. 382 m; 20 Feb. 2020; BF, AA, OG (PAG & MNHN) leg.; MNHN-IM-2018-14139 • 2 dry specimens; Saül, Mont Galbao face

Figure 2. *Cyclopedus anselini* from Mont Galbao (MNHN-IM-2013-75862).

nord-est (SAUL68); 3.60018°N, 53.25877°W; alt. 251 m; 21 Feb. 2020; BF, AA, OG (PAG & MNHN) leg.; Bord de cambrouse, sous lianes; MNHN-IM-2018-14029 • 2 dry specimens; Mana, Réserve de la Trinité, layon inselberg 120m (pente inselberg) (TRI21); 4.61157°N, 53.40833°W; alt. 180 m; 15 Apr. 2019; BF, ST (MNHN/ONF) leg.; pied de rochers granitiques; MNHN-IM-2014-7310.

Remarks. Mont Galbao and Montagnes de la Trinité represent two new records for this species previously only known from its type locality in Nouragues (Gargominy and Muratov 2012), suggesting a broader distribution probably extending outside French Guiana.

The first living specimens are reported here. The body is totally white but the area around and below the eyes is lightly pink; two quite distinct black eyes at the outer base of the tentacles; tentacle slightly conical, with the outer third pale pink (Fig. 2). From the four sequenced specimens (all from the same locality) we recovered two haplotypes differing by one synonymous mutation only.

Family Diplommatinidae L. Pfeiffer, 1847

Genus *Adelopoma* Doering, 1885

Adelopoma quasimodo Gargominy, sp. nov.

https://zoobank.org/5EDCF9CB-1E0B-46BB-8983-577469F12790

Figs 3–5

Type locality. French Guiana, Saül, northeastern foothills of Bœuf Mort mountain.

Type material. ***Holotype*.** French Guiana • 1 dry specimen; Saül, Versant nord de Bœuf Mort, le long du sentier de Grand Bœuf Mort (SAUL44); 3.64098°N, 53.21863°W; alt. 300 m; 24 Nov. 2018; OG, SS, ST, BF (PAG & MNHN) leg.; Pied d'arbre à contreforts; MNHN-IM-2012-21233. ***Paratypes*** (7). French Guiana • 1 95% ethanol specimen; same data as the holotype; GenBank: PQ629098; Bold: DREAL176-23; MNHN-IM-2013-75603 • 1 95% ethanol specimen; Saül, Versant nord-

Figure 3. *Adelopoma quasimodo* sp. nov., holotype MNHN-IM-2012-21233. Scale bar: 2 mm.

est de Bœuf Mort, le long du sentier de Grand Bœuf Mort (SAUL37); 3.63555°N, 53.21035°W; alt. 340 m; 21 Nov. 2018; OG, SS, ST, BF (PAG & MNHN) leg.; Autour d'un arbre à contreforts; GenBank: PQ629107; Bold: DREAL373-23; MNHN-IM-2013-75648 • 1 95% ethanol specimen and 4 dry specimens; same data as preceding; MNHN-IM-2013-75652 and MNHN-IM-2012-21955 respectively.

Other material examined. French Guiana • 9 dry specimens; Saül, Cascades du Mont Galbao, face nord-est (SAUL64); 3.60376°N, 53.26121°W; alt. 320 m; 19 Feb. 2020; BF, AA, OG (PAG & MNHN) leg.; Bordure de cambrouse; MNHN-IM-2018-14065 • 13 dry specimens; Saül, Mont Galbao face nord-est (SAUL65); 3.59681°N, 53.26257°W; alt. 503 m; 20 Feb. 2020; BF, AA, OG (PAG & MNHN) leg.; Cambrouse et lianes en forêt; MNHN-IM-2018-14047 • 1 95% ethanol specimen; same data as preceding; MNHN-IM-2013-76395 • 1 dry specimen; Saül, Mont Galbao face nord-est (SAUL66); 3.59995°N, 53.26697°W; alt. 382 m; 20 Feb. 2020; BF, AA, OG (PAG & MNHN) leg.; MNHN-IM-2018-14143 • 1 95% ethanol specimen; same data as preceding; MNHN-IM-2013-76473 • 5 dry specimens; Saül, Mont Galbao face nord-est (SAUL68); 3.60018°N, 53.25877°W; alt.

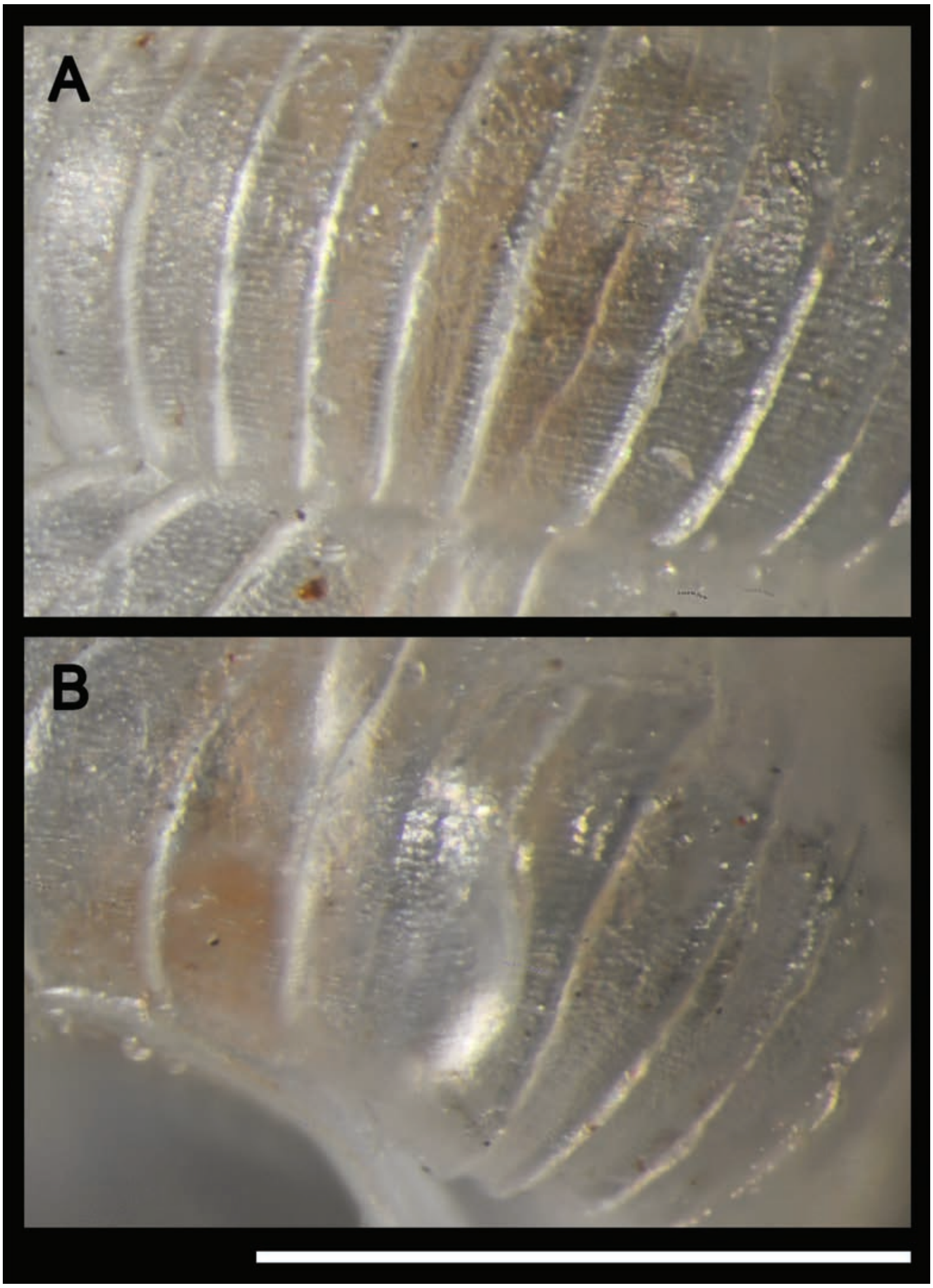

Figure 4. *Adelopoma quasimodo* sp. nov., holotype MNHN-IM-2012-21233: **A** detail of antepenultimate whorl showing spiral microsculpture **B** detail of the bulge of body whorl showing denticle inside the shell by transparency. Scale bar: 0.5 mm.

251 m; 21 Feb. 2020; BF, AA, OG (PAG & MNHN) leg.; Bord de cambrouse, sous lianes; MNHN-IM-2018-14032 • 1 95% ethanol specimen; same data as preceding; MNHN-IM-2013-76384.

Diagnosis. An *Adelopoma* species of minute size, more ovate than conical, densely ribbed, and with a deep suture.

Description. Holotype: Shell minute (height 2.0 mm, diameter 1.1 mm), sinistral, thin, elongate, conical in first whorls then cylindrical; colour white, subtranslucent. Whorls 5.2, inflated, strongly rounded, separated by a deep suture. Protoconch 1.5 whorls, smooth; protoconch/teleoconch transition distinct be-

Figure 5. *Adelopoma quasimodo* sp. nov., paratype MNHN-IM-2013-75652 crawling on a dead leaf with two faeces on its shell.

cause of change in sculpture; surface of teleoconch with lamellate axial ribs (27 on body whorl) and distinct minute spiral striae between the ribs. Body whorl rounded, ventrolaterally with a distinct bulge through which an inner, palatal, crescent-shaped denticle can be seen. Aperture almost circular; upper insertion of the peristome not descending; peristome continuous but the upper part largely merged to the preceding whorl, double, weakly expanded and thickened; there is a columellar lamella at the bottom of the columella, which can be fully seen only by looking through the aperture (also indistinctly visible in frontal view in the aperture); perforate, umbilicus marked by the continuation of the axial ribs. Operculum unknown.

Paratypes: Operculum ~ 0.5 mm, corneous, concave, almost completely circular in shape, completely transparent and whitish. Body (5) colourless and transparent; except for the ca two first whorls where the light brown odd caesura can be seen by transparency. Eyes black, quite minute, at the base of the tentacles. Tentacles ~ 0.2 mm long, cylindrical, extending upward.

Etymology. The species is named after Quasimodo, the hunchback character of Victor Hugo's novel Notre-Dame de Paris, and refers to the bulge on the body whorl. It also reminds one of the catastrophic event of the fire at Notre-Dame de Paris cathedral on 15 April 2019, which occurred during the Trinité collecting trip. Treated as a noun in apposition.

Distribution. This species is only known from Saül, on the northeastern foothills of both Bœuf Mort and Galbao mountains.

Habitat. Primary forest, under leaf litter on alkaline soils.

Remarks. This species shares with *Adelopoma peruvianum* Hausdorf & Munoz, 2004 the distinct bulge on the body whorl, the presence of a columellar lamella and the distinct perforation which are distinctive characteristics of *A. peruvianum* according to the original description (Hausdorf and Munoz 2004).

It differs from that species, together with *Adelopoma brasiliense* Morretes, 1954 (unfortunately not mentioned in Hausdorf and Munoz (2004) but the holotype was illustrated by Simone (2006: 46) later) in being smaller, more cylindrical and less conical, the sutures deeper, and with a higher rib density. Hausdorf and Munoz (2004) mentioned that the columellar denticle has been overlooked in other species; the presence of the distinct bulge on the body whorl might also have been ignored because it is hardly visible even if fully developed as in *A. quasimodo*. Thus the whole genus would need a revision over its large distribution.

We obtained two COI sequences differing by nine mutations. Both are related to one sequence of *Adelopoma tucma* (Döring, 1884) from Argentina, type species of the genus (*p*-distance 6.1–6.4%, GenBank HM753341; Webster et al. 2012).

The genus *Adelopoma* is known from Mexico to Peru, northern Argentina (Tucumán), south-eastern Brazil, Venezuela, and Trinidad (Torre et al. 1942; Hausdorf and Munoz 2004; Martins and Simone 2014). Its occurrence in French Guiana is not surprising, but its scarcity is remarkable as it is only known from foothills around Saül, on slopes oriented east-northeast on alkaline complexes. However, it is probable that it has been overlooked and that its range in French Guiana is larger than the Saül area.

Subclass Heterobranchia Burmeister, 1837
Infraclass Euthyneura
Subterclass Tectipleura Schrödl, Jörger, Klussmann- Kolb & N. G. Wilson, 2011
Superorder Eupulmonata Haszprunar & Huber, 1990
Order Stylommatophora A. Schmidt, 1855
Suborder Helicina Rafinesque, 1815
Superfamily Punctoidea Morse, 1864
Family Cystopeltidae Cockerell, 1891
Genus *Lilloiconcha* Weyrauch, 1965

***Lilloiconcha galbao* Gargominy, sp. nov.**
https://zoobank.org/CA9FA418-C36E-4AF2-92B5-01A754807284
Figs 6, 7

Type locality. French Guiana, Saül, Mont Galbao.

Type material. ***Holotype***. French Guiana • 1 dried specimen; Saül, Mont Galbao (SAUL47); 3.60183°N, 53.27239°W; alt. 650 m; 27 Nov. 2018; OG, SS, ST, BF (PAG & MNHN) leg.; DZ brulée et cambrouse à l'est; MNHN-IM-2013-75668. ***Paratypes*** (20). French Guiana • 1 95% ethanol specimen; same data as the holotype; GenBank: PQ629092; Bold: DREAL909-23; MNHN-IM-2013-75966 • 3 95% ethanol specimens; same data as the holotype; MNHN-IM-2013-75667 • 1 dry specimen; same data as the holotype; MNHN-IM-2012-21986 • 4 dry adult specimens; same data as the holotype; MNHN-IM-2018-896 • 11 dry juvenile specimens; same data as the holotype; MNHN-IM-2018-897.

Diagnosis. A *Lilloiconcha* species with more than five whorls, as high as large, with a small umbilicus and strong ribs.

Description. Holotype: Shell minute (height 2.2 mm, diameter 2.6 mm), dextral, globose, dome-shaped to gibbous, thin; colour corneous; whorls 5.4, inflated, rounded, separated by a deep suture; spire coiling regularly increasing. Protoconch two whorls, smooth; protoconch/teleoconch transition distinct because

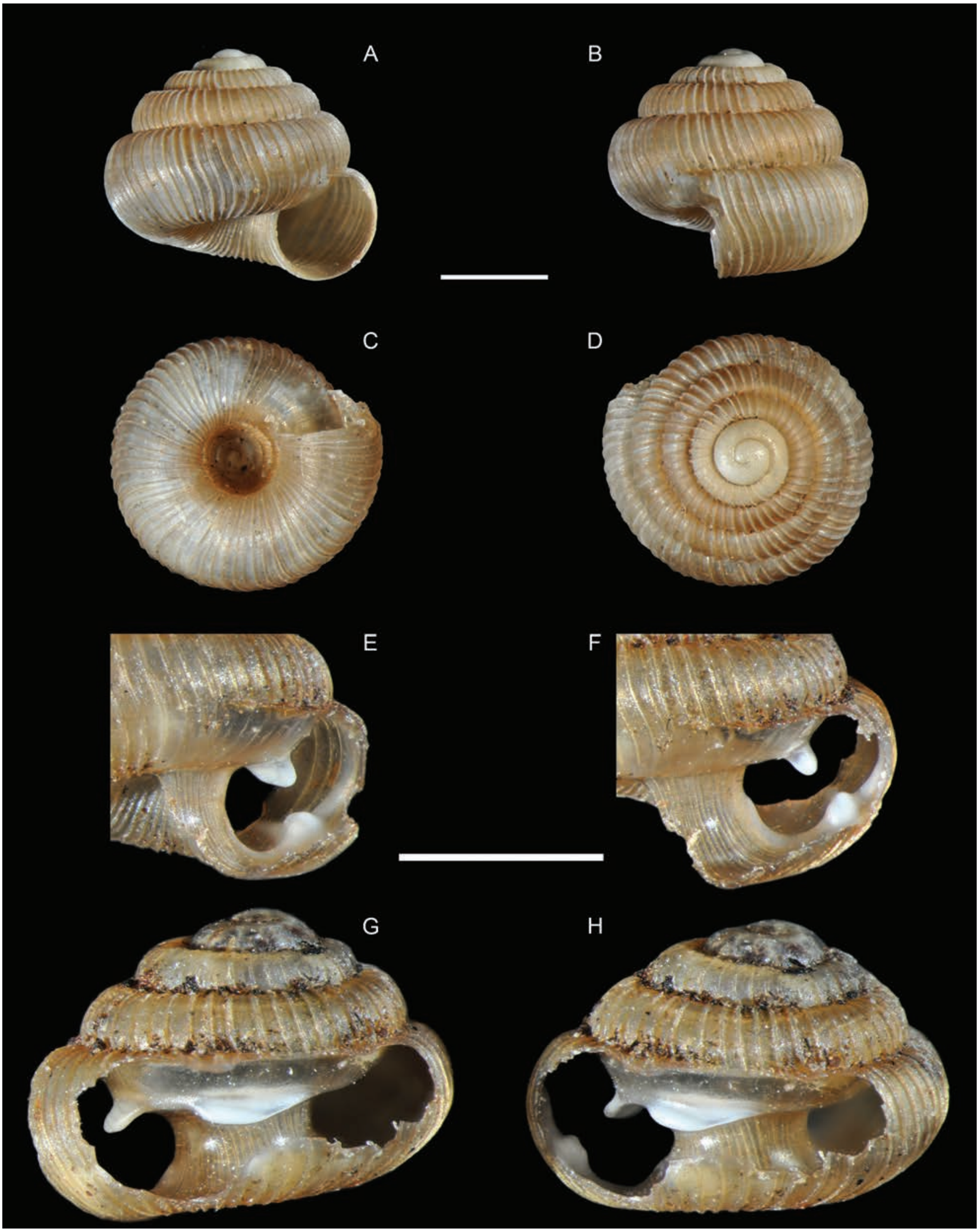

Figure 6. *Lilloiconcha galbao* sp. nov.: **A–D** holotype MNHN-IM-2013-75668 **E–H**, paratype MNHN-IM-2012-21986, details of dentition inside the body whorl after the shell has been broken. Scale bars: 1 mm.

of change in sculpture; teleoconch sculpture of regular radial ribs, 60 on the body whorl, and a reticulate pattern consisting of fine growth-striae and dense microscopical spiral threads between the ribs. Body whorl rounded. Aperture almost

Figure 7. *Lilloiconcha galbao* sp. nov., holotype MNHN-IM-2013-75668 crawling on a dead leaf.

circular; upper insertion of the peristome not descending towards the aperture; suture impressed. Peristome simple, sharp, neither expanded nor thickened. Umbilicus U-shaped, almost cylindrical, contained 3.8× in the shell greater diameter.

Animal greyish, sole paler; tail without distinct caudal pit, not distinctly truncated; ocular tentacles long and gracile, inflated at the tip; eyes black, small, on the upper front of the tentacles (Fig. 7).

Paratypes: Juveniles have internal lamellae which are dissolved (not present) in adult specimens (more than 4.5–5 whorls, as the holotype): a longitudinal lamella in the middle of the parietal wall formed by up to three (one or two in subadult specimens) elongate, high (~ 40% of the aperture diameter) teeth separated by gaps of half their length, covering ~ 1/8 whorl in length; at the opposite palatal side of each parietal tooth, there is a transversal lamella, extending from the outermost side of the aperture towards half of the columellar wall, principally thickened in front of its corresponding parietal tooth and extending a little bit inside along the whorl. In early juveniles this palatal lamella is reduced to a simple denticle. The lamellar complex reduces the aperture diameter to half its value.

Etymology. The species is named after the type locality, Mont Galbao; treated as a noun in apposition.

Distribution. This species is only known from its type locality, Mont Galbao.

Habitat. Primary forest, under leaf litter on alkaline soils.

Remarks. This species is attributed to genus *Lilloiconcha* Weyrauch, 1965 based on the conchological characters given by Weyrauch (1965), who established the name for a single species which usually has basal and parietal denticles in juvenile stages, *Austrodiscus superbus tucumanus* Hylton Scott, 1963 (see Schileyko 2001; Hausdorf 2005; Miquel et al. 2007). The anatomy of the new species is not known: the only adult specimen is the holotype and its body is dried and contracted inside the shell, thus not available for anatomy without cracking the shell. However, it would not help much for generic attribution as the anatomy of the type species of *Lilloiconcha* and its related genera (for example *Radioconus* Baker, 1927, type species *Helix bactriola* Guppy, 1868) are not known, as indicated by Hausdorf (2005).

We provide the COI sequence of one paratype which relates to the congeneric *Lilloiconcha superba* from Brazil (*p*-distance 12.5%, GenBank MN792606; Salvador et al. 2020).

The presence of *Lilloiconcha* in French Guiana is not surprising regarding the distribution of the widespread *Lilloiconcha gordurasensis* (Thiele, 1927) (Hausdorf 2005). However, the distribution of the genus in French Guiana seems to be limited to the mountainous habitats of the Galbao range, as it has never been collected on the Mitaraka, Trinité, or Nouragues mountains despite intensive collecting. The new species represents the first record of the superfamily Punctoidea and of the family Cystopeltidae in French Guiana.

Infraorder Helicoidei

Superfamily Helicoidea Rafinesque, 1815

Family Thysanophoridae Pilsbry, 1926

Genus *Lyroconus* H.B. Baker, 1927

Lyroconus plagioptycha (Shuttleworth, 1854)

Figs 8, 9

Helix plagioptycha Shuttleworth, 1854: 37.
Thysanophora plagioptycha (Shuttleworth, 1854)— Pilsbry (1920): 94, figs 2, 3.
Lyroconus plagioptycha (Shuttleworth, 1854)— Schileyko (2006): 1896.

Link. https://molluscabase.org/aphia.php?p=taxdetails&id=1065439.

Material examined. French Guiana • 1 dry specimen; Régina, Montagne Favard (Montagne de Kaw), ca 200 m sur le chemin W depuis la fin de la route (dégrad) D6 (COT03); 4.5°N, 52.05722°W; 20 Oct. 1997; TR, OG leg.; Petit ruisseau, forêt; MNHN-IM-2012-21187 • 1 dry specimen; Remire-Montjoly, Lotissement DDE, 1.4 km sur la route des plages (D1) après le carrefour de Dégrad des Cannes, Montagne du Mahury (COT06); 4.86056°N, 52.25917°W; alt. 15 m; 21 Oct. 1997; TR, OG leg.; culture de bananes et papayes; MNHN-IM-2012-23924 • 3 dry specimens; Roura, Crique Sourou, Rte forestière de Nancibo (COT10); 4.67273°N, 52.42825°W; alt. 10 m; 23 Oct. 1997; TR, OG leg.; ripisylve, sol alluvial; MNHN-IM-2022-2131 • 1 dry specimen; Saint-Laurent-du-Maroni, Rte du Plateau des cascades, plateau des mines, 3.7 km après la D11 (COT27); 5.38569°N, 54.06283°W; 28 Oct. 1997; TR, OG leg.; reste de forêt sur une route bordée de parcelles conquises sur la forêt; MNHN-IM-2022-2130 • 1 dry specimen; Sinnamary, Petit Saut, 1.4 km avant le rond-point "barrage du Petit Saut" (COT30); 5.06111°N, 52.99778°W; 28 Oct. 1997; TR, OG leg.; forêt dense, fond de talweg; MNHN-IM-2022-2137 • 24 dry specimens; Saül (SAUL25); 3.61274°N, 53.21626°W; alt. 174 m; 17 Nov. 2018; OG, SS, ST, BF (PAG & MNHN) leg.; Pied d'arbre à con-

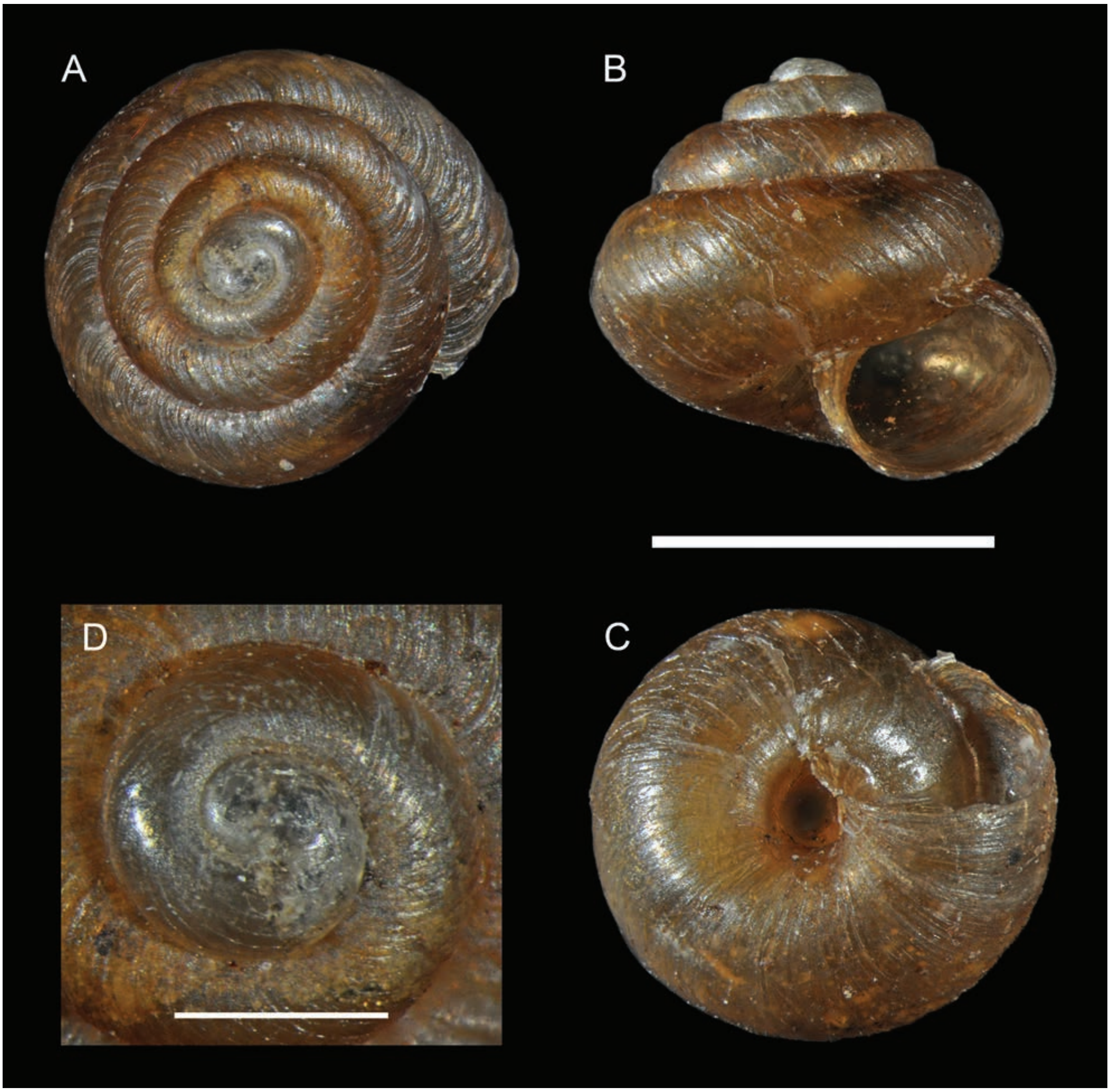

Figure 8. *Lyroconus plagioptycha*, Saül, MNHN-IM-2012-21932. Scale bars: 2 mm (**A–C**); 0.5 mm (**D**).

trefort; MNHN-IM-2012-21932 • 5 95% ethanol specimens; Saül (SAUL25); 3.61274°N, 53.21626°W; alt. 174 m; 17 Nov. 2018; OG, SS, ST, BF (PAG & MNHN) leg.; Pied d'arbre à contrefort; MNHN-IM-2013-75621 • 2 dry specimens; Saül (SAUL37); 3.63555°N, 53.21035°W; alt. 276 m; 21 Nov. 2018; OG, SS, ST, BF (PAG & MNHN) leg.; Autour d'un arbre à contreforts; MNHN-IM-2012-21956 • 2 95% ethanol specimens; Saül (SAUL37); 3.63555°N, 53.21035°W; alt. 276 m; 21 Nov. 2018; OG, SS, ST, BF (PAG & MNHN) leg.; Autour d'un arbre à contreforts; MNHN-IM-2013-75655 • 4 dry specimens; Saül, Versant nord de Bœuf Mort, le long du sentier de Grand Bœuf Mort (SAUL44); 3.64098°N, 53.21863°W; alt. 300 m; 24 Nov. 2018; OG, SS, ST, BF (PAG & MNHN) leg.; Pied d'arbre à contreforts; MNHN-IM-2012-21965 • 1 95% ethanol specimen; Saül, Cascades au pied du Galbao (SAUL49); 3.60254°N, 53.26051°W; alt. 220 m; 29 Nov. 2018; OG, SS, ST, BF (PAG & MNHN) leg.; Chaos rocheux; GenBank: PQ629103; Bold: DREAL353-23; MNHN-

Figure 9. *Lyroconus plagioptycha* from the southern ridge of Bœuf Mort, Saül.

IM-2013-75961 • 1 dry specimen; Saül, Cascades au pied du Galbao (SAUL49); 3.60254°N, 53.26051°W; alt. 220 m; 29 Nov. 2018; OG, SS, ST, BF (PAG & MNHN) leg.; Chaos rocheux; MNHN-IM-2018-677 • 1 95% ethanol specimen; Mana, Layon C vers 1900m (TRI19); 4.583°N, 53.40587°W; alt. 50 m; 14 Apr. 2019; BF, ST (MNHN/ONF) leg.; forêt de lianes; GenBank: PQ629104; Bold: DREAL358-23; MNHN-IM-2013-75993 • 1 95% ethanol specimen; Mana, cambrouse layon C à environ 1300 m du camp Aya (TRI20); 4.58417°N, 53.4054°W; alt. 80 m; 14 Apr. 2019; BF, ST (MNHN/ONF) leg.; Cambrouse; MNHN-IM-2013-75819 • 3 dry specimens; same data as preceding; MNHN-IM-2014-7922 • 2 dry specimens; Mana, Layon inselberg 120m (pente inselberg) (TRI21); 4.61157°N, 53.40833°W; alt. 180 m; 15 Apr. 2019; BF, ST (MNHN/ONF) leg.; pied de rochers granitiques; MNHN-IM-2014-7923 • 1 95% ethanol specimen; Mana, Réserve naturelle de La Trinité, Layon C à environ 1600m du camp Aya (TRI31); 4.58421°N, 53.40542°W; alt. 67 m; 18 Apr. 2019; BF, ST (MNHN/ONF) leg.; Cambrouse; GenBank: PQ629101; Bold: DREAL364-23; MNHN-IM-2013-75992 • 1 95% ethanol specimen; Mana, Réserve naturelle de La Trinité, Layon C à environ 1600m du camp Aya (TRI31); 4.58421°N, 53.40542°W; alt. 67 m; 18 Apr. 2019; BF, ST (MNHN/ONF) leg.; Cambrouse; MNHN-IM-2013-75820 • 12 dry specimens; Mana, Réserve naturelle de La Trinité, Layon C à environ 1600m du camp Aya (TRI31); 4.58421°N, 53.40542°W; alt. 67 m; 18 Apr. 2019; BF, ST (MNHN/ONF) leg.; Cambrouse; MNHN-IM-2014-7924 • 2 dry specimens; Saül, Chemin des Monts la Fumée (SAUL63); 3.63119°N, 53.20586°W; alt. 177 m; 18 Feb. 2020; BF, AA, OG (PAG & MNHN) leg.; Pied d'arbre à contrefort; MNHN-IM-2018-14083 • 1 dry specimen; Saül, Cascades du Mont Galbao, face nord-est (SAUL64); 3.60376°N, 53.26121°W; alt. 320 m; 19 Feb. 2020; BF, AA, OG (PAG & MNHN) leg.; Bordure de cambrouse; MNHN-IM-2018-14067 • 3 dry specimens; Saül, Mont Galbao face nord-est (SAUL65); 3.59681°N, 53.26257°W; alt. 503 m; 20 Feb. 2020; BF, AA, OG (PAG & MNHN) leg.; Cambrouse et lianes en forêt; MNHN-IM-2018-14051 • 1 95% ethanol specimen; Saül, Mont Galbao face nord-est (SAUL65); 3.59681°N, 53.26257°W; alt. 503 m; 20 Feb. 2020; BF, AA, OG (PAG & MNHN) leg.; Cambrouse et lianes en forêt; MNHN-IM-2013-76405 • 1 dry specimen; Saül (SAUL70); 3.60864°N, 53.21492°W; alt. 212 m; 23 Feb. 2020; BF, AA, OG (PAG & MNHN) leg.; MNHN-IM-2018-14120.

Remarks. All specimens collected in French Guiana are consistent with the diagnosis by Pilsbry (1920) and the illustration of syntype NMBE 18878 figured in Neubert and Gosteli (2003: pl. 20 fig. 4).

Lyroconus plagioptycha (type locality Puerto Rico) is a widespread species in Greater Antilles and Central America from Florida to Venezuela (https://www.gbif.org/species/5190501), and was recently recorded in northeastern Brazil (Salvador et al. 2021). It was reported from Suriname as early as 1960 (Altena 1960). Until now it has never been recorded from French Guiana and this is the first record of the family Thysanophoridae in this territory.

In French Guiana, the species is known from 10 to 500 m a.s.l. both on coastal areas (e.g., Saint-Laurent, Cayenne, Kaw mountain) as well as in the interior in Saül and Trinité.

Two haplotypes were recovered, one from Mana and the other from Saül. Despite their large genetic difference (*p*-distance 2.7%), the specimens appear identical in morphology.

Infraorder Orthalicoidei
Superfamily Orthalicoidea Martens, 1860
Family Bulimulidae Tryon, 1867
Subfamily Bulimulinae Tryon, 1867
Genus *Protoglyptus* Pilsbry, 1897

Protoglyptus bernicolae Gargominy, sp. nov.

https://zoobank.org/4794633F-BE95-4418-9B93-C93A29D6C6FB
Figs 10, 11

Type locality. French Guiana, Saül, Mont Galbao.

Type material. ***Holotype***. French Guiana • 1 95% ethanol specimen (shell separated); Saül, Mont Galbao (SAUL47); 3.60183°N, 53.27239°W; alt. 650 m; 27 Nov. 2018; OG, SS, ST, BF (PAG & MNHN) leg.; DZ brulée et cambrouse à l'est; GenBank: PQ629105; Bold: DREAL855-23; MNHN-IM-2013-75865. ***Paratypes*** (14). French Guiana • 2 95% ethanol specimens; Saül, Mont Galbao, same data as the holotype; GenBank: PQ629096; Bold: DREAL1376-23; MNHN-IM-2013-75863; GenBank: PQ629093; Bold: DREAL856-23; MNHN-IM-2013-75864 • 1 dry specimen; Saül, Mont Galbao, same data as the holotype; MNHN-IM-2012-21977 • 4 dry specimens; Saül, Mont Galbao face nord-est (SAUL65); 3.59681°N, 53.26257°W; alt. 503 m; 20 Feb. 2020; BF, AA, OG (PAG & MNHN) leg.; Cambrouse et lianes en forêt; MNHN-IM-2018-14041 • 4 95% ethanol specimens; Saül, Mont Galbao, same data as preceding; MNHN-IM-2013-76397• 3 95% ethanol specimen; Mana, Réserve de la Trinité, cambrouse layon C à environ 1300 m du camp Aya

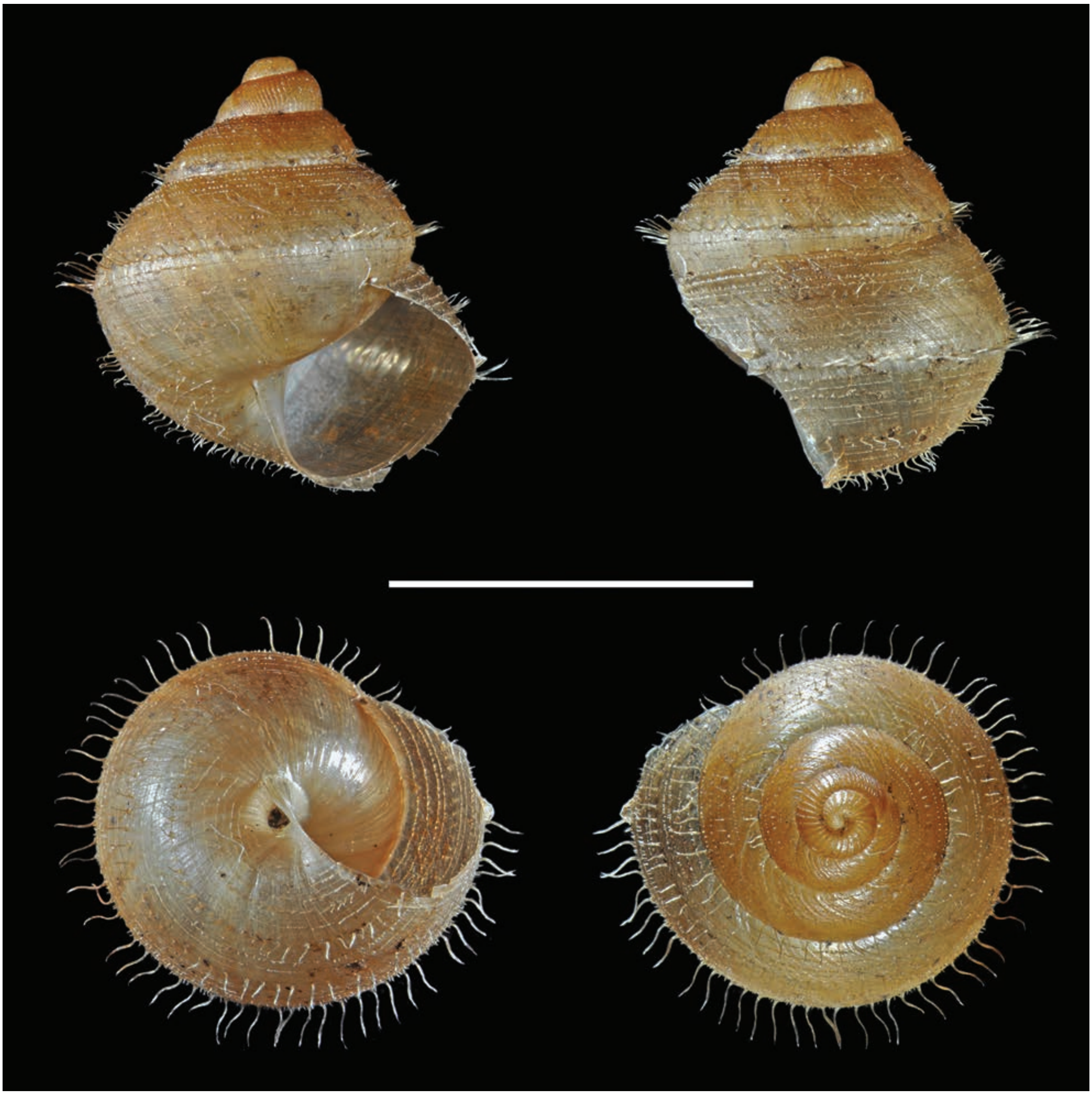

Figure 10. *Protoglyptus bernicolae* sp. nov., holotype MNHN-IM-2013-75865. Scale bar: 5 mm.

(TRI20); 4.58417°N, 53.4054°W; alt. 80 m; 14 Apr. 2019; BF, ST (MNHN/ONF) leg.; Cambrouse; GenBank: PQ629097; Bold: DREAL859-23; MNHN-IM-2013-75989; GenBank: PQ629102; Bold: DREAL858-23; MNHN-IM-2013-75990; GenBank: PQ629111; Bold: DREAL857-23; MNHN-IM-2013-75991.

Other material examined. French Guiana • 4 dry specimens; Mana, Réserve de la Trinité, cambrouse layon C à environ 1300 m du camp Aya (TRI20); 4.58417°N, 53.4054°W; alt. 80 m; 14 Apr. 2019; BF, ST (MNHN/ONF) leg.; Cambrouse; MNHN-IM-2014-7920 • 5 dry juvenile specimens; Mana, Réserve naturelle de La Trinité, Layon C à environ 1600 m du camp Aya (TRI31); 4.58421°N, 53.40542°W; alt. 67 m; 18 Apr. 2019; BF, ST (MNHN/ONF) leg.; Cambrouse; MNHN-IM-2014-7921.

Diagnosis. A *Protoglyptus* species with whorls slightly keeled at the periphery and spiral rows of long setae mainly placed on this keel.

Figure 11. *Protoglyptus bernicolae* sp. nov.: holotype MNHN-IM-2013-75865 alive.

Description. Holotype. Shell of medium size (height 6.0 mm, diameter 5.5 mm), dextral, thin, shiny, medium-spired, conical; colour uniformly brownish, almost subtranslucent. Whorls 4.5, slightly inflated with shallow suture, slightly keeled at the periphery; last whorl descending more rapidly below the periphery of the preceding. Protoconch one whorl, with sculpture consisting of oblique radial ribs, interstices ~ 3× as wide as the ribs, with very fine spiral striae in between the riblets; protoconch/teleoconch transition distinct because of change in sculpture; surface of teleoconch with sculpture consisting, on the upper part of the whorl, of 6–10 fine spiral rows of periostracal scales expanding to long setae at the periphery of the whorl and shorter setae at the middle of its upper part; on the lower part, ~ 16 fine spiral rows of periostracal scales expanding to shorter setae on three rows; this spiral sculpture on the lower part of the whorl totally disappearing from the aperture into the interior of the shell. Peristome not formed, simple; aperture oblique, prosocline, crescent-like. Umbilicus very small, punctiform, partially covered by the columellar wall.

Body pale grey, whitish around the head; head brownish, similar to the colour of the shell; upper tentacles elongated, inflated at the tip; eyes black, small, situated on the upper part of the tentacles; lower tentacles with whitish tips. Inner mantle with small white patches visible through the transparency of the shell (Fig. 11).

Etymology. The species is named after Bernard and Nicole Gargominy, parents of the first author, in recognition of the unswerving taste for nature they have transmitted. The species name is a contraction of both first names declined in the feminine genitive as it ends with Nicole.

Distribution. This species is only known from French Guiana: Mont Galbao and Réserve de la Trinité.

Habitat. In leaf litter of vegetation dominated by *Lasiacis* species ("cambrouses").

Remarks. No fully adult specimens have been found. The holotype is the more subadult specimen and the aperture description is thus not informative. The structure of the protoconch immediately places the species as belonging to genus *Protoglyptus*. *Protoglyptus longiseta* (S. Moricand, 1846) described from Bahia Province, Brazil (Moricand 1846: 156, pl. 5 figs 18–20) shares the long setae but is larger, as large as tall, has more convex whorls, and setae of equal length all over the teleoconch.

This species seems to be restricted to vegetation dominated by *Lasiacis* species (Poaceae) locally called "cambrouses".

The six COI sequences (four haplotypes) form two groups, from Saül and Trinité, respectively, differing by 2.1–2.7% (*p*-distance).

Subfamily Peltellinae Gray, 1855

Genus *Drymaeus* Albers, 1850

Drymaeus arcuatostriatus (L. Pfeiffer, 1855)

Figs 12, 13

Bulimus arcuatostriatus L. Pfeiffer, 1855: 95: "Peru" "Long. 30, lat. 13 mill." (Cuming coll.).

Drymaeus (*Drymaeus*) *arcuatostriatus* (L. Pfeiffer, 1855)—Breure and Ablett 2014: 23, fig. 41A–C (lectotype NHMUK1975455, dimensions H 27.6, D 15.6, W 6.5)

"*Drymaeus meesi* Breure, 1976"—Tillier 1980: 75, pl. 4 fig. 1, text-figs 60, 61.

Link. https://molluscabase.org/aphia.php?p=taxdetails&id=1364218.

Material examined. French Guiana • 1 dry specimen; Saül, Arbre à contreforts au niveau du belvédère de Saül, crête sud de Bœuf Mort (SAUL20); 3.62593°N, 53.21714°W; alt. 297 m; 16 Nov. 2018; OG, SS, ST, BF (PAG & MNHN) leg.; MNHN-IM-2012-21920 • 1 dry specimen; Saül (SAUL12); 3.61951°N, 53.20751°W; 08 Jul. 1999; TR, OG leg.; MNHN-IM-2012-21547 • 1 dry specimen; Saül (SAUL12); 3.61951°N, 53.20751°W; 08 Jul. 1999; TR, OG leg.; MNHN-IM-2013-21248.

Remarks. The specimen illustrated by Tillier (1980: pl. 4 fig. 1) and Massemin et al. (2009: pl. 6A) identified as *Drymaeus meesi* Breure, 1976 conchologically differs greatly from the holotype RMNH.MOL.55077 of *Drymaeus glaucostomus meesi* Breure, 1976 (Breure 1976: pl. 1). Tillier (1980: 77) already stated that his species should be more related to *Drymaeus strigatus* (G.B. Sowerby I (1838: fig. 95, original illustration) (Breure and Ablett 2014: fig. 30A–C, possible syntype NHMUK 20090168) rather than to *Drymaeus glaucostomus* and consequently elevated the taxon to species level. Indeed *Drymaeus strigatus*, together with the synonymised *Bulimus musivus* L. Pfeiffer, 1855 (Richardson 1995; Breure and Ablett 2014: fig. 29J–L, lectotype NHMUK 1975292), *Bulimus saccatus* L. Pfeiffer, 1855 (Breure and Ablett 2014: fig. 30D–F, lectotype NHMUK 1975207), as well as *Drymaeus schunkei* F. Haas (1949: 237, fig. 50b; Holotype FMNH 30040), all described from Peru, share the same global shape,

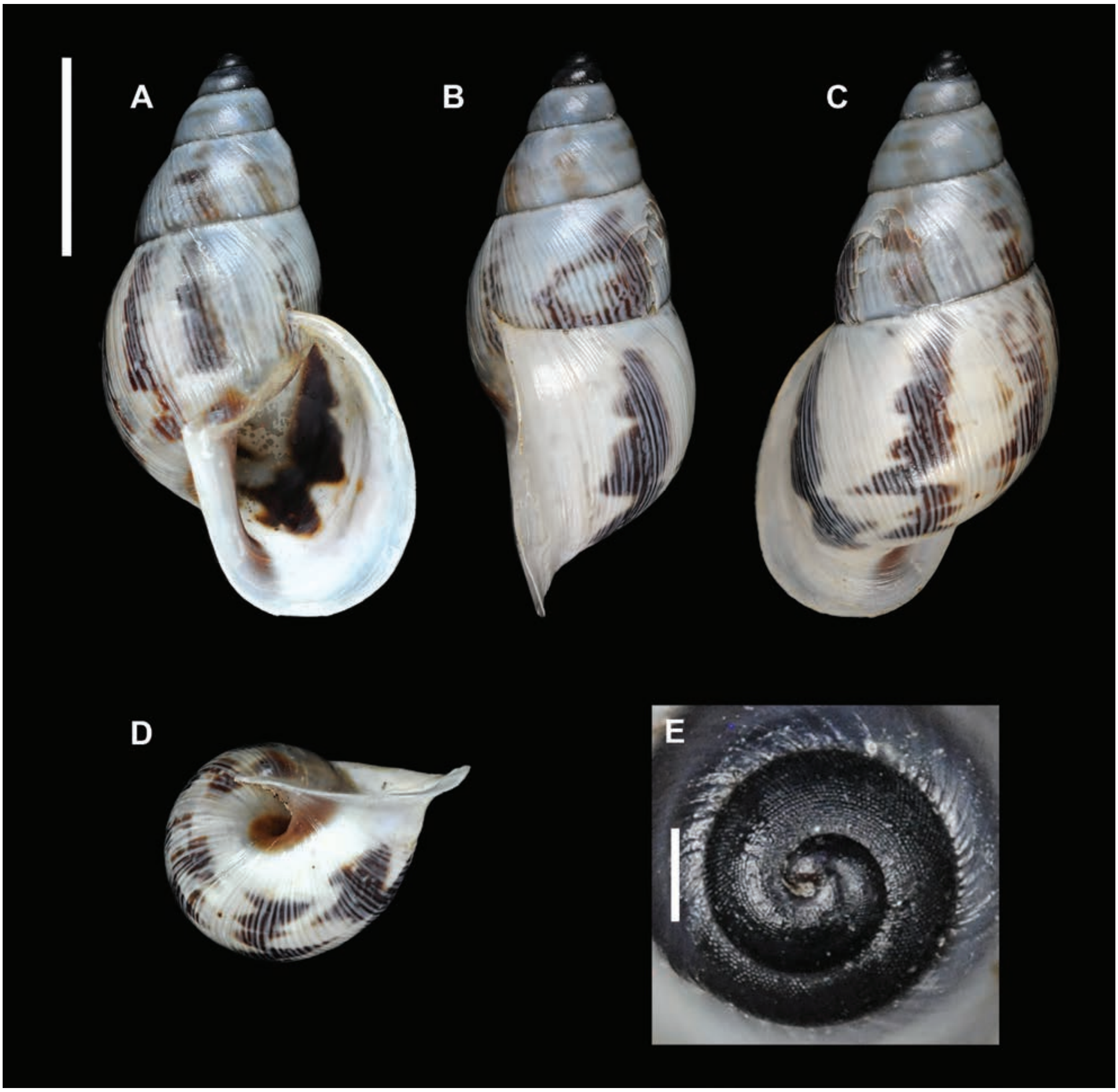

Figure 12. *Drymaeus arcuatostriatus*, Saül, MNHN-IM-2012-21547. Scale bars: 10 mm (**A–D**); 1 mm (**E**).

chromatic pattern, and expanded aperture with the French Guianan species. However, they lack two characters that are shared between the French Guiana species and *Drymaeus arcuatostriatus*, i.e., the distinctive impressed radial white calcareous ribbing and the dark early whorls. Thus, we tentatively identify the French Guiana species previously known as "*Drymaeus meesi*" sensu Tillier (1980) as *Drymaeus arcuatostriatus* L. Pfeiffer, 1855.

The species is to be considered within the *Drymaeus* (*Drymaeus*) *expansus* (L. Pfeiffer, 1848) species complex as defined by Breure and Borrero (2019), although the latter does not share the black early whorls.

A living specimen (Fig. 13, https://www.inaturalist.org/observations/74538163) shows a yellow body, mostly on the sole and the head, whitish otherwise; longitudinal black lines extend from the bottom of the optical tentacle to the aperture. The optical tentacles are conical and elongated.

Figure 13. *Drymaeus arcuatostriatus*, Saül. Photograph by S. Sant (https://www.inaturalist.org/observations/74538163).

Genus *Mesembrinus* Albers, 1850

Mesembrinus lusorius (L. Pfeiffer, 1855)
Fig. 14

Bulimus lusorius L. Pfeiffer, 1855: 291; Breure (1979): 121, lectotype designation.
Drymaeus (*Mesembrinus*) *lusorius*—Breure and Eskens (1981): 77, pl. 7 fig. 12.
Mesembrinus lusorius—Simone (2006): 145, fig. 487.
Drymaeus surinamensis Vernhout, 1914: 13, pl. 1 fig. 3. syn. nov.
Mesembrinus surinamensis (Vernhout, 1914)—MolluscaBase, "new comb. herein, based on the ranking of *Mesembrinus* by Salvador et al. (2023)" [https://molluscabase.org/aphia.php?p=taxdetails&id=1713521]

Link. https://molluscabase.org/aphia.php?p=taxdetails&id=1713485.

Material examined. French Guiana • 1 dry specimen; Apatou; 1931–1932; BOUGE leg.; MNHN-IM-2023-4121 • 1 95% ethanol specimen; Régina, RN des Nouragues, carré F15 du km^2 layonné (NB7); 4.08755°N, 52.68241°W; alt. 150 m; 03 Jun. 1999–29 Jun. 1999; TR, OG leg.; MNHN-IM-2013-87076 • 1 dry specimen; Régina, RN des Nouragues, carré N19 du km^2 layonné (N11); 4.08083°N, 52.67617°W; alt. 90 m; 12 Nov. 1997; TR, OG leg.; forêt primaire, bord de pinotière; MNHN-IM-2023-4120 • 2 dry specimens; Saül, Mont Galbao face nord-est (SAUL66); 3.59995°N, 53.26697°W; alt. 382 m; 20 Feb. 2020; BF, AA, OG (PAG & MNHN) leg.; MNHN-IM-2018-14136 • 1 dry specimen; Saül, Camp Galbao (SAUL46); 3.6015°N, 53.27498°W; alt. 628 m; 26 Nov. 2018; OG, SS, ST, BF

Figure 14. *Mesembrinus lusorius*, juvenile specimen on Mont Galbao, Saül, 630 m a.s.l., MNHN-IM-2013-75878.

(PAG & MNHN) leg.; Bord de crique; MNHN-IM-2018-684 • 1 95% ethanol specimen; Saül, Camp Galbao (SAUL46); 3.6015°N, 53.27498°W; alt. 628 m; 26 Nov. 2018; OG, SS, ST, BF (PAG & MNHN) leg.; Bord de crique; MNHN-IM-2013-75878.

Remarks. *Bulimus lusorius* L. Pfeiffer, 1855 was described from the "Banks of Amazon, Brazils" (Pfeiffer 1855). The lectotype NHMUK 1975543 illustrated in Breure and Ablett (2014: fig. 17A–C) and the specimen illustrated by Simone (2006: fig. 487) are morphologically similar to the syntype of *Drymaeus surinamensis* described by Vernhout (1914) (RMNH.MOL.335814) and with all specimens identified as this species from French Guiana where it is the commonest species of its genus s.l. Thus, we suggest that *Drymaeus surinamensis* Vernhout, 1914 is a junior synonym of *Bulimus lusorius* L. Pfeiffer, 1855 until further investigations, in particular molecular data, are carried out.

Described as a subgenus of *Drymaeus*, *Mesembrinus* has been elevated to genus rank by Salvador et al. (2023).

Specimen A of Simone (2006: fig. 453, NMW.1955.158) as well as specimen RMNH.MOL.266069, both identified as *Drymaeus germaini* (Ancey, 1892), might also belong to the species.

Infraorder Pupilloidei
Superfamily Pupilloidea W. Turton, 1831
Family Strobilopsidae Wenz, 1915
Genus *Strobilops* Pilsbry, 1893

Strobilops morsei (Dall, 1885)
Figs 15, 16

Strobila labyrinthica var. *morsei* Dall, 1885: 263.
Strobilops morsei—Pilsbry (1927–1935): 39, pl. 6 figs 4, 6 [type], pl. 6 fig. 5.
Strobila labyrinthica morsei—Baker (1925): 3; Altena (1975): 36.

Figure 15. *Strobilops morsei* from Mitaraka, MNHN-IM-2012-21265. Scale bar: 2 mm.

Figure 16. *Strobilops morsei* from Mitaraka, MNHN-IM-2012-21266.

Link. https://molluscabase.org/aphia.php?p=taxdetails&id=1497894.

Material examined. French Guiana • 1 95% ethanol specimen; Maripasoula, Massif du Mitaraka, Sommet en Cloche (mitaraka02); 2.22804°N, 54.467°W; alt. 599 m; 12 Mar. 2015; OG, BF leg.; inselberg avec bromeliacées; GenBank: PQ629108; Bold: DREAL1035-23; MNHN-IM-2013-77374 • 1 95% ethanol specimen; Maripasoula, Massif du Mitaraka, Sommet en Cloche (mitaraka34); 2.2316°N, 54.46109°W; alt. 339 m; 22 Mar. 2015; OG, BF leg.; bord de ruisseau avec rochers; GenBank: PQ629095; Bold: DREAL1036-23; MNHN-IM-2013-77375 • 3+1 dry specimens; same data as preceding; MNHN-IM-2012-21268, MNHN-IM-2012-21266 • 5+1 dry specimens; Maripasoula, Massif du Mitaraka, Sommet en Cloche (mitaraka36); 2.22847°N, 54.46721°W; alt. 586 m; 24 Mar. 2015; OG leg.; Forêt sommitale; MNHN-IM-2012-21267 and MNHN-IM-2012-21265.

Remarks. This species was described from Venezuela (Dall 1885) and reported from Surinam as early as 1975 (Altena 1975). The studied material represents the first record of the family Strobilopsidae in French Guiana (Gargominy and Fontaine 2015).

In French Guiana, *Strobilops morsei* is only known from the Mitaraka Mountains between 340 and 600 m a.s.l.

The two COI sequences (same haplotype) are related to some *Strobilops labyrinthicus* from Canada (*p*-distance 7.2–8.1%).

Family Valloniidae Morse, 1864
Genus *Pupisoma* Stoliczka, 1873

Pupisoma macneilli (G.H. Clapp, 1918)

Thysanophora macneilli G.H. Clapp, 1918: 74, pl. 8 fig. 1.
Pupisoma macneilli (G.H. Clapp, 1918)— Hausdorf (2007: 1497, figs 9, 10, 14).

Link. http://molluscabase.org/aphia.php?p=taxdetails&id=1299519.

Material examined. French Guiana • 25 dry specimens; Cayenne, Ilet la Mère (carré J14 de l'Institut Pasteur) (GUY34); 4.89102°N, 52.18392°W; alt. 10 m; 28 Nov. 1997; TR, OG leg.; forêt anciennement dégradée, pied d'un fromager; MNHN-IM-2018-14186 • 2 dry specimens; Régina, RN des Nouragues, carré J12 du km^2 layonné (N3); 4.0883°N, 52.67675°W; alt. 80 m; 04 Nov. 1997; TR, OG leg.; forêt primaire, pied d'arbre à contrefort (code J-12-22); MNHN-IM-2018-14216 • 1 dry specimen; Régina, RN des Nouragues, carré E19 du km^2 layonné (N9); 4.08487°N, 52.68361°W; alt. 110 m; 10 Nov. 1997; TR, OG leg.; forêt primaire, fond de talweg; MNHN-IM-2018-14197 • 1 dry specimen; Régina, RN des Nouragues, carré I14 du km^2 layonné (N19); 4.08712°N, 52.67874°W; alt. 70 m; 19 Nov. 1997; TR, OG leg.; fond de vallée, pied d'arbre à contrefort (code I-14-187); MNHN-IM-2018-14199 • 1 dry specimen; Saül, Arbre à contreforts au niveau du belvédère de Saül, crête sud de Bœuf Mort (SAUL20); 3.62593°N, 53.21714°W; alt. 297 m; 16 Nov. 2018; OG, SS, ST, BF (PAG & MNHN) leg.; MNHN-IM-2012-21926 • 4 95% ethanol specimens; Saül, Sommet Mont Galbao (SAUL48); 3.60427°N, 53.28153°W; alt. 701 m; 28 Nov. 2018; OG, SS, ST, BF (PAG & MNHN) leg.; MNHN-IM-2013-75677 • 3 dry specimens; Saül, Bœuf mort (SAUL52); 3.63691°N, 53.21442°W; alt. 380 m; 15 Feb. 2020; BF, AA, OG (PAG & MNHN) leg.; Pied d'arbre à contrefort sous lianes et cambrouse à *Guadua*; MNHN-IM-2018-14154 • 9 dry specimens; Saül, Sommet Bœuf Mort (SAUL53); 3.63546°N, 53.21453°W; alt. 400 m; 15 Feb. 2020; BF, AA, OG (PAG & MNHN) leg.; Pied d'arbre à contrefort; MNHN-IM-2018-14128 • 9 dry specimens; Saül, Mont Galbao face nord-est (SAUL65); 3.59681°N, 53.26257°W; alt. 503 m; 20 Feb. 2020; BF, AA, OG (PAG & MNHN) leg.; Cambrouse et lianes en forêt; MNHN-IM-2018-14052 • 1 dry specimen; Saül, Mont Galbao face nord-est (SAUL68); 3.60018°N, 53.25877°W; alt. 251 m; 21 Feb. 2020; BF, AA, OG (PAG & MNHN) leg.; Bord de cambrouse, sous lianes; MNHN-IM-2018-14033 • 1 95% ethanol specimens; Mana, roche bénitier, 200m avant abri arca (sommet inselberg) (TRI12); 4.62154°N, 53.40515°W; alt. 429 m; 12 Apr. 2019; BF, ST (MNHN/ONF) leg.; Forêt en pied de falaise granitique; MNHN-IM-2013-75760 • 1 dry specimen; Mana, Layon A 1350 m du camp Aya (TRI15); 4.59933°N, 53.42685°W; alt. 129 m; 13 Apr. 2019; BF, ST (MNHN/ONF) leg.; Forêt de plateau; MNHN-IM-2013-75761.

Remarks. We revised all *Pupisoma* species we collected in French Guiana according to Hausdorf (2007), which allowed us to recognize *Pupisoma macneilli* as a new record for French Guiana, in addition to the previously known *Pupisoma dioscoricola* (C.B. Adams, 1845).

Infraorder Succineoidei
Superfamily Testacelloidea Gray, 1840
Family Spiraxidae H.B. Baker, 1939
Subfamily Spiraxinae H.B. Baker, 1939
Genus *Pseudosubulina* Strebel & Pfeffer, 1882

Pseudosubulina santi Gargominy, sp. nov.

https://zoobank.org/7EE76DD9-3553-4A00-8BFD-0C6B808A447B
Figs 17, 18

Type locality. French Guiana, in the vicinity of Saül village, southern foothill of Bœuf Mort mountain.

Type material. ***Holotype*.** French Guiana • 1 dry specimen; Saül, Arbre à contreforts au niveau du belvédère de Saül, crête sud de Bœuf Mort (SAUL20); 3.62593°N, 53.21714°W; alt. 297 m; 16 Nov. 2018; OG, SS, ST, BF (PAG & MNHN) leg.; MNHN-IM-2012-21923. ***Paratypes*** (8). French Guiana • 2 95% ethanol specimens; Saül, Bananeraie, Crique gros fossé (SAUL51); 3.6288°N, 53.21246°W; alt. 201 m; 14 Feb. 2020; BF, AA, OG (PAG & MNHN) leg.; Cambrouse à *Guadua*; MNHN-IM-2013-76444; MNHN-IM-2013-76882 (both tentatively barcoded without success) • 6 dry specimens; same data as preceding; MNHN-IM-2018-14018.

Other material examined. French Guiana • 1 95% ethanol specimens; Saül, Bœuf Mort (SAUL54); 3.63966°N, 53.21413°W; alt. 350 m; 15 Feb. 2020; BF, AA, OG (PAG & MNHN) leg.; MNHN-IM-2013-76486 (tentatively barcoded without success) • 1 95% ethanol specimen; Saül, Crête au sud de crique cochon (SAUL58); 3.61427°N, 53.19857°W; alt. 127 m; 16 Feb. 2020; BF, AA, OG (PAG & MNHN) leg.; Pied d’arbre à contrefort et écorces mortes au sol; MNHN-IM-2013-76456 (tentatively barcoded without success) • 1 95% ethanol specimens; Saül, Abattis en arrière du village (SAUL60); 3.62609°N, 53.21105°W; alt. 162 m; 17 Feb. 2020; BF, AA, OG (PAG & MNHN) leg.; Forêt bordant le village; MNHN-IM-2013-76488 (tentatively barcoded without success) • 2 dry specimens; same data as preceding; MNHN-IM-2018-14165 • 2 dry specimens; Saül, Mont Galbao (SAUL47); 3.60183°N, 53.27239°W; alt. 650 m; 27 Nov. 2018; OG, SS, ST, BF (PAG & MNHN) leg.; DZ brulée et cambrouse à l’est; MNHN-IM-2012-21982 • 1 dry specimen; Saül, Cascades du Mont Galbao, face nord-est (SAUL64); 3.60376°N, 53.26121°W; alt. 320 m; 19 Feb. 2020; BF, AA, OG (PAG & MNHN) leg.; Bordure de cambrouse; MNHN-IM-2018-14063 • 1 dry specimen; Saül, Mont Galbao face nord-est (SAUL65); 3.59681°N, 53.26257°W; alt. 503 m; 20 Feb. 2020; BF, AA, OG (PAG & MNHN) leg.; Cambrouse et lianes en forêt; MNHN-IM-2018-14042.

Diagnosis. A *Pseudosubulina* of normal size characterised by its absence of sculpture on the shell where only growth lines are visible.

Figure 17. *Pseudosubulina santi* sp. nov. holotype MNHN-IM-2012-21923. Scale bar: 10 mm.

Figure 18. *Pseudosubulina santi* sp. nov. from Saül, paratype MNHN-IM-2013-76882.

Description. Holotype. Shell of normal size for the genus (height 13.1 mm, major diameter 2.9 mm), dextral, slender, turreted with straight outline, glossy, rather thin, semi-translucent, white. Whorls 13, rounded, slightly flattened at the periphery, with a rather deep straight crenulated suture all the way to the aperture. Protoconch smooth, protoconch/teleoconch transition indistinct. Surface of teleoconch with very fine and numerous growth lines. Aperture elongated, orthocline, with slightly more than 90° columellar-basal angle, cut by penultimate whorl. Peristome simple, with sharp margin, not reflected except at columellar edge; reflection of columellar edge more developed in its upper part. Umbilicus tiny, partially covered by columellar edge.

Etymology. The species is named after Sébastien Sant, a good friend and experienced botanist and naturalist who helped us so much during our field trip in Saül.

Distribution. This species is only known from French Guiana in the vicinity of Saül village, including the southern foothill of Mont Galbao.

Habitat. Primary forest, under leaf litter on granitic or lateritic soil.

Remarks. Paratype (MNHN-IM-2013-76882) has the body white; first ~ 7 whorls darker because of dark hepatopancreas; tentacles elongated, white, a little darker at the tip; eyes not distinctly visible (Fig. 18).

Four specimens were barcoded without success.

Pseudosubulina santi sp. nov. is the third species of the genus recorded from French Guiana. Although it is known only from Saül area, it is not rare there: it is recorded in the vicinity of the village as well as on Mont Galbao, i.e., at altitudes between 125 and 650 m a.s.l.

Pseudosubulina santi sp. nov. is found in syntopy with *Pseudosubulina theoripkeni* Gargominy & Muratov, 2012.

Pseudosubulina theoripkeni **Gargominy & Muratov, 2012**

Fig. 19

Pseudosubulina theoripkeni Gargominy & Muratov, 2012: 786, figs 3, 4.

Link. https://molluscabase.org/aphia.php?p=taxdetails&id=1477357.

Type locality. French Guiana, Régina, Réserve naturelle des Nouragues, Montagnes Balenfois, field station.

Type material. ***Holotype*.** French Guiana • Régina, RN des Nouragues, carré G17 du km^2 layonné (N1); 4.08524°N, 52.68179°W; alt. 75 m; 03 Nov. 1997; TR, OG leg.; forêt primaire, bord de ruisseau, bloc granitique; MNHN-IM-2000-25068. ***Paratypes*** (8). French Guiana 1 95% ethanol specimen and 1 dry specimen; same data as the holotype; MNHN-IM-2000-25069 and MNHN-IM-2000-25070 respectively • 5 dry specimens; Régina, RN des Nouragues, carré M12 du km^2 layonné (N7); 4.08699°N, 52.67381°W; alt. 140 m; 08 Nov. 1997; TR, OG leg.; forêt primaire, grand plateau; MNHN-IM-2000-25071 • 1 dry specimen; Régina, RN des Nouragues, carré N15 du km^2 layonné (N14); 4.08372°N, 52.67503°W; alt. 155 m; 15 Nov. 1997; TR, OG leg.; forêt primaire, pied d'arbre à contrefort (code N-15-138); MNHN-IM-2000-25072.

Other material examined. French Guiana • 1 dry specimen; Roura, Route de Cacao (Boulanger), 5.3 km après embranchement N2, 700 m après la scierie (COT13); 4.56548°N, 52.41922°W; alt. 100 m; 23 Oct. 1997; TR, OG leg.; Une parcelle brûlée et forêt adjacente; MNHN-IM-2018-14056 • 1 dry specimen; Régina, RN des Nouragues, carré L14 du km^2 layonné (N2); 4.08564°N, 52.67651°W; alt. 110 m; 04 Nov. 1997; TR, OG leg.; forêt primaire, forêt de lianes; MNHN-IM-2018-14180 • 3 dry specimens; Régina, RN des Nouragues, carré M12 du km^2 layonné (N7); 4.08699°N, 52.67381°W; alt. 140 m; 08 Nov. 1997; TR, OG leg.; forêt primaire, grand plateau; MNHN-IM-2018-14057 • 1 dry specimen; Régina, RN des Nouragues, carré E19 du km^2 layonné (N9); 4.08487°N, 52.68361°W; alt. 110 m; 10 Nov. 1997; TR, OG leg.; forêt primaire, fond de talweg; MNHN-IM-2018-14182 • 7 dry specimens; Régina, RN des Nouragues, carré N10 du km^2 layonné (N10); 4.08845°N, 52.67269°W; alt. 140 m; 11 Nov. 1997; TR, OG leg.; forêt primaire, chablis; MNHN-IM-2018-14055 • 2 dry specimens; Régina, RN des Nouragues, carré N15 du km^2 layonné (N14); 4.08372°N, 52.67503°W; alt. 155 m; 15 Nov. 1997; TR, OG leg.; forêt primaire, pied d'arbre à contrefort (code N-15-138); MNHN-IM-2018-14181 • 1 dry specimen; Régina, RN des Nouragues, carré N13 du km^2 layonné (NB5); 4.08603°N, 52.67353°W; alt. 170 m; 03 Jun. 1999–29 Jun. 1999; TR, OG leg.; MNHN-IM-2018-14295 • 1 dry specimen; Maripasoula, Mont Itoupé (Itoupé600); 3.02314°N, 53.09533°W; alt. 600 m; 06 Jan. 2016–17 Jan. 2016; Thibaud Decaëns, Sébastien Cally leg.; MNHN-IM-2012-21480 • 1 95% ethanol specimen; Maripasoula, Mont Itoupé (Itoupé600); 3.02314°N, 53.09533°W; alt. 600 m; 06 Jan. 2016–17 Jan. 2016; Thibaud Decaëns, Sébastien Cally leg.; MNHN-IM-2012-21482 • 2 95% ethanol specimens; Saül, Arbre à contreforts au niveau du belvédère de Saül (SAUL20); 3.62593°N, 53.21714°W; alt. 297 m; 16 Nov. 2018; OG, SS, ST, BF (PAG & MNHN) leg.; MNHN-IM-2013-75869; MNHN-IM-2013-75870 • 5 95% ethanol specimens; same data as preceding; MNHN-IM-2013-75597 • 14 dry specimens; same data as preceding; MNHN-IM-2012-21922 • 1 95% ethanol specimen; Saül, Versant nord de Bœuf Mort, le long du sentier de Grand Bœuf

Figure 19. *Pseudosubulina theoripkeni* from Saül, southern foothills of Bœuf Mort, MNHN-IM-2013-75869.

Mort (SAUL44); 3.64098°N, 53.21863°W; alt. 300 m; 24 Nov. 2018; OG, SS, ST, BF (PAG & MNHN) leg.; Pied d'arbre à contreforts; MNHN-IM-2013-75604 • 8 dry specimens; Saül, Mont Galbao (SAUL47); 3.60183°N, 53.27239°W; alt. 650 m; 27 Nov. 2018; OG, SS, ST, BF (PAG & MNHN) leg.; DZ brulée et cambrouse à l'est; MNHN-IM-2012-21981 • 2 95% ethanol specimens; Saül, Sommet Bœuf Mort (SAUL53); 3.63546°N, 53.21453°W; alt. 400 m; 15 Feb. 2020; BF, AA, OG (PAG & MNHN) leg.; Pied d'arbre à contrefort; MNHN-IM-2013-77069 and MNHN-IM-2013-77070 • 5 dry specimens; same data as preceding; MNHN-IM-2018-14125 • 2 95% ethanol specimens; Saül, Chemin des Monts la Fumée (SAUL63); 3.63119°N, 53.20586°W; alt. 177 m; 18 Feb. 2020; BF, AA, OG (PAG & MNHN) leg.; Pied d'arbre à contrefort; MNHN-IM-2013-76420 • 1 95% ethanol specimen; Saül, Mont Galbao face nord-est (SAUL65); 3.59681°N, 53.26257°W; alt. 503 m; 20 Feb. 2020; BF, AA, OG (PAG & MNHN) leg.; Cambrouse et lianes en forêt; MNHN-IM-2013-76401 • 2 dry specimens; Saül, Mont Galbao face nord-est (SAUL66); 3.59995°N, 53.26697°W; alt. 382 m; 20 Feb. 2020; BF, AA, OG (PAG & MNHN) leg.; MNHN-IM-2018-14141 • 1 dry specimen; Saül, Piste Limonade (SAUL71); 3.58813°N, 53.21204°W; alt. 170 m; 24 Feb. 2020; BF, AA, OG (PAG & MNHN) leg.; Bord de cambrouse; MNHN-IM-2018-14172 • 1 dry specimen; Mana (TRI05); 4.59397°N, 53.4146°W; alt. 94 m; 09 Apr. 2019; BF, ST (MNHN/ONF) leg.; MNHN-IM-2014-7865 • 1 dry specimen; Mana, Abri Arca (sommet inselberg) (TRI10); 4.62181°N, 53.40359°W; alt. 429 m; 11 Apr. 2019; BF, ST (MNHN/ONF) leg.; grotte; MNHN-IM-2014-7866.

Description of external body. Body white, first ~ 8 whorls darker because of dark hepatopancreas; tentacles almost cylindrical but a little larger at the base, with thickening, pale brownish tip; eyes not distinctly visible (Fig. 19).

Distribution. Roura, Saül (including Mont Galbao), Itoupé, and Montagnes de la Trinité are new records for this species previously only known from its type locality in Nouragues (Gargominy and Muratov 2012), suggesting a much broader distribution probably extending outside French Guiana.

Remarks. The first living specimens ever found are reported here; they were barcoded without success.

Suborder Scolodontina
Superfamily Scolodontoidea H.B. Baker, 1925
Family Scolodontidae H.B. Baker, 1925
Genus *Happia* Bourguignat, 1890

Happia decaensi Gargominy, sp. nov.

https://zoobank.org/DA2519E0-8142-4AD2-8081-572CDC0C4833
Fig. 20

Type locality. French Guiana, Camopi, Mont Itoupé.

Type material. ***Holotype***. French Guiana • 1 95% ethanol specimen (shell separated); Camopi, Mont Itoupé; 3.02696°N, 53.07902°W; alt. 800 m; 06 Jan. 2016–17 Jan. 2016; Thibaud Decaëns, Sébastien Cally leg.; MNHN-IM-2013-75995. ***Paratypes*** (7). French Guiana • 4 dry specimens; Régina, RN des Nouragues, carré J12 du km^2 layonné (N3); 4.0883°N, 52.67675°W; alt. 80 m; 04 Nov. 1997; TR, OG leg.; forêt primaire, pied d'arbre à contrefort (code J-12-22); MNHN-IM-2018-14023, MNHN-IM-2018-14429, MNHN-IM-2018-14430, MNHN-IM-2018-14431 • 1 dry specimen; Régina, RN des Nouragues, carré G12 du km^2 layonné (N16); 4.09011°N, 52.67922°W; alt. 80 m; 16 Nov. 1997; TR, OG leg.; forêt primaire, bord de Crique Couac (rive droite); MNHN-IM-2018-14024 • 2 dry specimens; Régina, RN des Nouragues, carré I17 du km^2 layonné (N17); 4.08535°N, 52.67996°W; alt. 73 m; 17 Nov. 1997; TR, OG leg.; confluence crique Nouragues et crique Moteur, forêt primaire, accumulation de bois pourri; MNHN-IM-2018-14022, MNHN-IM-2018-14428.

Diagnosis. A large *Happia* species with relatively high whorls, strong indentation on the upper sutural margin, largely umbilicated.

Description. Holotype. Shell small (height 2.8 mm, greater diameter 5.6 mm), dextral, totally depressed, thin; colour pale corneous; whorls 3.8, inflated, rounded, slightly flattened on the upper part, overlapping the preceding, separated by a marked suture; spire planispiral, coiling rapidly increasing. Protoconch 1.7 whorl, with ~ 10 delicate spiral threads hardly visible due to periostracal erosion, also visible from adapical view; protoconch/teleoconch transition distinct, particularly from adapical view; teleoconch smooth (but see remarks below), with sigmoid, prominent, closely spaced growth wrinkles with irregular levels of shell calcification underneath, radial on umbilical part of whorls, strongly rounded backwards near upper suture. Body whorl rounded, strongly flattened above periphery up to a small bulge above the suture. Aperture prosocline, strongly sigmoid with an acute and deep (1 mm) incision in parietal angle, basally circular. Peristome simple, sharp. Umbilicus very large, almost half of the greater diameter, conical with flat protoconch entirely visible.

Etymology. The species is named after Thibaud Decaëns who provided the holotype and only living specimen, a good friend and experienced earthworm expert.

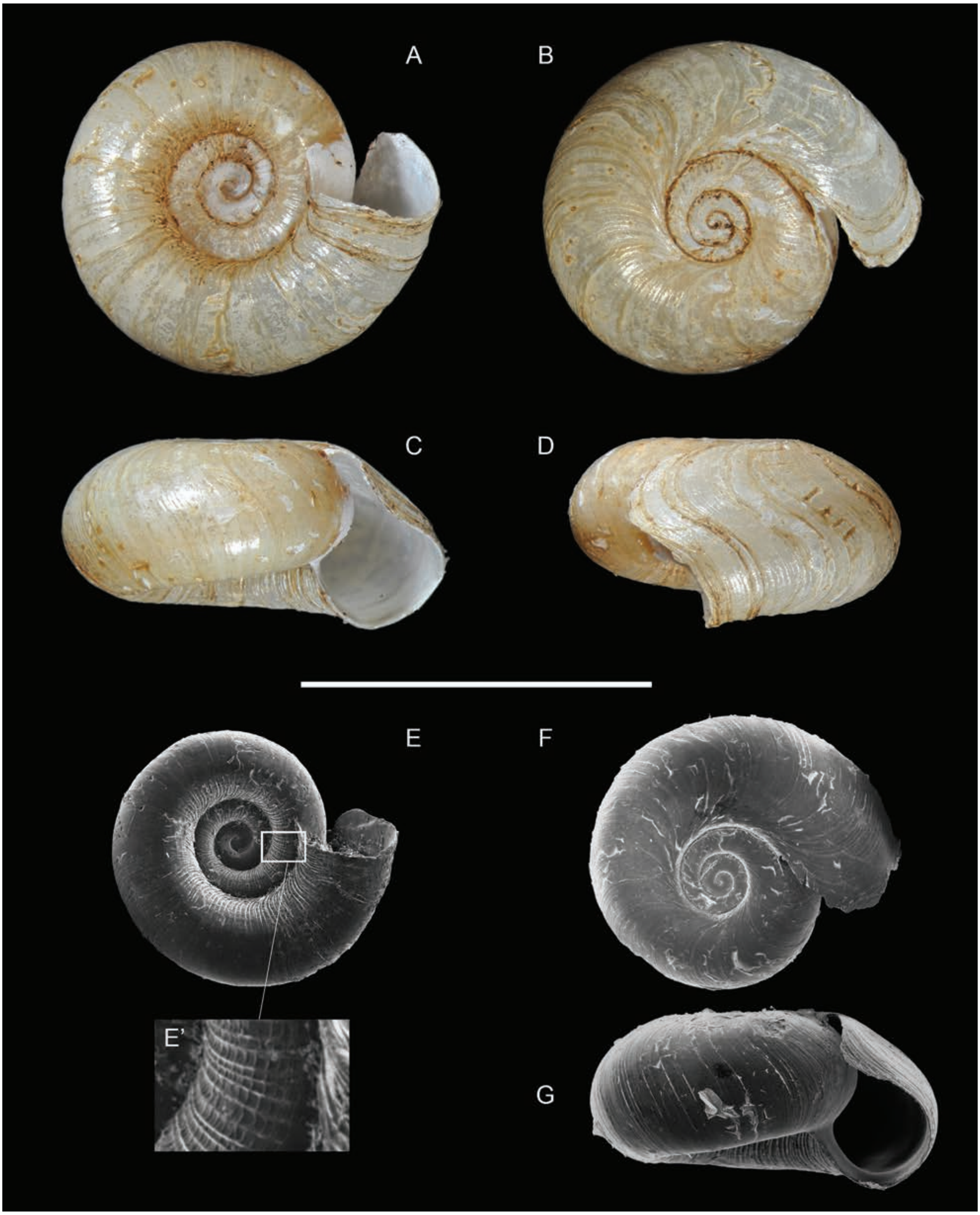

Figure 20. *Happia decaensi* sp. nov.: **A–D** holotype MNHN-IM-2013-75995 **E** paratype MNHN-IM-2018-14429 **F** paratype MNHN-IM-2018-14430 **G** paratype MNHN-IM-2018-14431. Scale bar: 5 mm.

Distribution. This species is known from French Guiana only, Nouragues and Itoupé.

Habitat. Leaf litter of tropical rain forest, from 80 (Nouragues) to 800 m (Itoupé) a.s.l.

Remarks. The holotype was barcoded, without success.

The paratype MNHN-IM-2018-14022 is a juvenile (2.7 whorls) and distinctly shows the spiral rows of minute papillae on the protoconch; this spiral micro-sculpture is also visible on the complete teleoconch which argues for its attribution to genus *Happia* (Baker 1925: pl. 8 fig. 35; Roosen and Breure 2024). Paratype MNHN-IM-2018-14429 (3.7 whorls) also shows this spiral micro-sculpture on the umbilical part of the teleoconch whorls, thus appearing reticulate when crossed with the marked growth lines (Fig. 20E').

Referring to Roosen and Breure (2024), the new species is the largest of the genus. The type species *Happia ammonoceras* (L. Pfeiffer, 1855) (syntype NHMUK 20210342) from Colombia is smaller, flatter, the body whorl more inflated. *Drepanostomella pinchoti* Pilsbry, 1930 (holotype ANSP152648) described from Panama and recorded from Venezuela (Thompson 1957) is smaller with the umbilicus only 1/3 of the diameter. When compared to a juvenile of the new species (of the same size), it is more discoid and flatter.

This new species represents the first record of the genus *Happia* in French Guiana.

Order Systellommatophora Pilsbry, 1948
Superfamily Veronicelloidea J. E. Gray, 1840
Family Veronicellidae J. E. Gray, 1840
Genus *Diplosolenodes* Thomé, 1975

Diplosolenodes occidentalis (Guilding, 1825)
Fig. 21

Onchidium occidentale Guilding, 1825: 323.

Link. https://molluscabase.org/aphia.php?p=taxdetails&id=1064168.

Material examined. French Guiana • 2 95% ethanol specimens; Saül, Dans le village sur la piste (SAUL22); 3.62386°N, 53.21075°W; alt. 173 m; 16 Nov. 2018; OG, SS, ST, BF (PAG & MNHN) leg.; GenBank: PQ629109; Bold: DREAL580-23; MNHN-IM-2013-75891; GenBank: PQ629110; Bold: DREAL579-23; MNHN-IM-2013-75892.

Remarks. These two specimens were collected at night on a track within the village of Saül and nowhere outside the village, which argues for a human introduction rather than a natural occurrence. Identification is based on the COI sequences. The same haplotype recovered from two specimens matches with a Suriname specimen (*p*-distance 99.83%, GenBank KM489511; Gomes, S.R., Barr, N. and Robinson, D., 2015, unpubl.).

Discussion

The French Guiana land gastropod fauna (81 species) is surprisingly not diverse when compared to other groups from the same area: 15,100 species of insects (Brûlé and Touroult 2014) revised to 19,151 ten years later (TAXREF 2024), 476 species of spiders (Vedel et al. 2013; TAXREF 2024), and 134 species of amphibians (Lescure et al. 2022). This paper exemplifies the fact that this fauna is very poorly known, with each single collecting trip revealing new records, species new to science, or even new family records for the territory.

Figure 21. *Diplosolenodes occidentalis* from Saül village, MNHN-IM-2013-75891.

Total number of extant species

There are currently 81 known land gastropod species in French Guiana, including 13 introduced or cryptogenic ones (this paper, TAXREF 2024). Among these 68 native species, eight (11.8%) have been described since 2010, a pattern reminiscent of that observed in Brazil, with 7% of the ~ 700 known species having been described after 2005 (Salvador 2019). Perhaps fuelled by an awareness of this unexpected richness, and by the recent use of leaf-litter sieving to reveal minute and rare species, there has been a renewed interest for the malacofauna of this region since the beginning of the 21st century. However, even large species may still be discovered, as shown by the example of *Pseudosubulina santi*, a relatively large (1 cm) species new to science, discovered with the naked eye in a banana plantation just outside the village of Saül, i.e., in an easily reachable area. These knowledge gaps are also shown by another example from the same area, the discovery of a previously unmentioned large introduced species, *Diplosolenodes occidentalis*. Since the 1997 collecting trips in Nouragues, each collection campaign has brought its share of discoveries, including species new to science (e.g., this paper; Gargominy and Muratov 2012), and there is no doubt that any new collecting trip by experienced collectors would reveal new records and new species. Another indication of our lack of knowledge is the fact that the MNHN collections harbour several old specimens of unrecorded species, in particular 27 specimens of an Urocoptidae (possibly genus *Macroceramus*) labelled “Guyane franc, M Etienne, 1877” (MNHN-IM-2018-945) which needs confirmation. However, the most important reservoir of new species definitely consists of a micro-fauna of Scolodontidae, living in forest litter and observed as early as 1998 (Gargominy and Ripken 1998); these species are a few millimetres in size, have translucent shells and yellowish, pinkish, or purple bodies. In this context, it would be very hazardous to assess the expected total number of land snail species in French Guiana.

Under-surveyed areas

The logistical difficulties to reach the forested interior of French Guiana, together with the low abundance of most species, account for the fact that apart from the coastal zone, French Guiana is very poorly known. Fig. 22 shows that the vast majority of the French Guianan territory has never been visited by malacologists. This is especially striking when localities of large, conspicuous species such as *Sultana sultana* or *Solaropsis undata*, which are often collected or photographed by non-malacologist naturalists, are removed from the map: outside the coastal zone, the only places where numerous small species have been collected are Nouragues, Saül, Trinité, and Mitaraka, i.e., places where experienced malacologists have made extensive collections with litter sieving.

Range of known species

Some recently described (*Cyclopedus anselini*, *Happia decaensi*, *Pseudosubulina theoripkeni*) or recorded species (*Lyroconus plagioptycha*, *Pupisoma macneilli*) appear to be potentially widespread in French Guiana, suggesting they have been overlooked by previous collectors. Recent collecting events have added four new families to French Guiana (this paper; Gargominy and Muratov 2012).

Conversely, many species are only known from their type localities, such as *Adelopoma quasimodo*, *Lilloiconcha galbao*, and *Pseudosubulina santi* only known around Saül, or *Strobilops morsei* which is only known from Mitaraka. However, the vast majority of French Guiana has never been searched for land snails, it is therefore premature to draw any conclusions about the real range of these species.

Genetics

Whenever possible, we have endeavoured to collect live specimens and extract DNA to obtain COI sequences (total of 126 specimens belonging to ~ 29 species). However, apart from introduced species (Veronicellidae, Subulininae), these sequences could not be analysed using phylogenetic trees, since there are very few available published genetic data for South American species. Thus, supplementary field work targeting live specimens for genetic material and massive sequencing is needed to complete our knowledge.

Shelf life and turbo-taxonomy

The situation is similar for another soil invertebrate taxon, earthworms (Order Crassiclitellata), of which 42 described species are known from French Guiana (TAXREF 2024), including 18 described in 2024 (Decaëns et al. 2024). As with the terrestrial molluscs, a large proportion of the diversity of earthworms is still

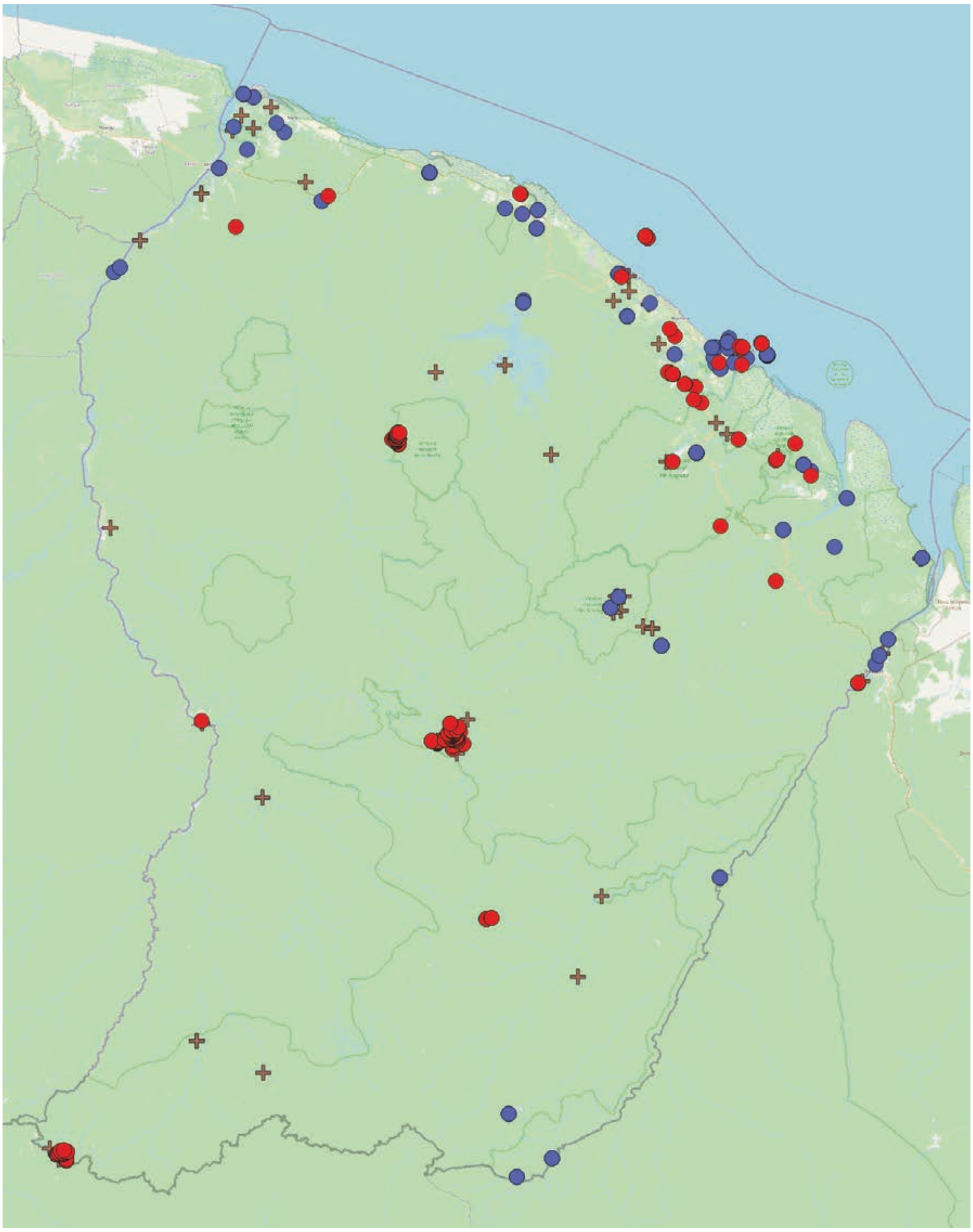

Figure 22. Map of sample localities for land snails in French Guiana: pre-2000 samples (blue dots), post-1999 samples (red dots), and opportunistic large (mostly single) species samples (plus symbol; *Angustipes carceralis*, *Bulimulus eyriesii*, *Euglandina striata*, *Labyrinthus* spp., *Lissachatina immaculata*, *Megalobulimus oblongus*, *Neocyclotus* spp., Orthalicidae, *Solaropsis undata*).

unknown, since a recent study using DNA barcoding has revealed an unsuspected diversity, with 119 putative species (Maggia et al. 2021).

All described species in this paper are mainly based on material collected in Saül, a shelf life of 6 years, with the exception of *Happia decaensi* collected as early as 1997, a shelf life of 27 years. This is less than the 21 years of shelf life between discovery and description of 600 species randomly taken from among the 16,994 species described in 2007, fungi, plants, and animals together (Fontaine et al. 2012a). However, our collections have revealed a great diversity of Scolodontidae, with probably at least fifteen species that are new to science. We may have to wait a few years before they are described, since the taxonomic workforce is sparse, and relies heavily on non-professional taxonomists (none of the authors of the present paper is a professional taxonomist sensu Fontaine et al. 2012b). In conclusion, if we are to reduce the length of the shelf life, integrative and turbo-taxonomy is needed, particularly for diversified groups such as scolodontids.

Acknowledgements

We thank Charles Dominique and Jean-Marie Betsch for inviting OG and Theo Ripken to the 1997 and 1999 Nouragues field trips through the “Programme pluri-formation” (MNHN). The Mitaraka expedition was part of the “Our Planet Reviewed” French Guiana-2015 initiative organised by the Muséum national d’Histoire naturelle (Paris) and the NGO Pro-Natura International, and funded by the European Regional Development Fund (ERDF), the Conseil Régional de Guyane, the Conseil Général de Guyane, the Direction de l’Environnement, de l’Aménagement et du Logement and by the Ministère de l’Éducation nationale, de l’Enseignement Supérieur et de la Recherche (authorization number APA-973-1). It was conducted in collaboration with the Parc amazonien de Guyane. Greatest thanks to Olivier Pascal for this tremendous organisation, and to Serge Fernandez for helping in the field.

The Saül expeditions were conducted in the framework of Atlas de la Biodiversité Communale (ABC) of Saül organized by the Parc amazonien de Guyane (convention n°2020-PNC-02) with financial support from Office français de la biodiversité (OFB). We especially thank Audrey Thonnel and the local team of the PAG at Saül, in particular Sébastien Sant. Ahmed Abdou took part in the second field session in Saül and was a great help.

The Trinité field trip was organized by Luc Ackermann (Office National des Forêts), with funding from Office National des Forêts (ONF) and DEAL Guyane.

We thank Thibaud Decaëns and Sébastien Cally for material collected during DIADEMA project on Mont Itoupé allowed by Parc Amazonien de Guyane (financial support provided by an Investissement d’Avenir grant of the Agence Nationale de la Recherche CEBA, ANR-10-LABX-25-01) (authorization number TREL1820249A/51).

Jon Ablett was very helpful with types of the British Museum. We thank the malacological team at MNHN for determined support: Nicolas Puillandre, Philippe Bouchet, Virginie Héros, Philippe Maestrati, Pierre Lozouet, and Barbara Buge. Finally, the first author thanks Theo Ripken for sparking the malacological light during the first 1997 and 1999 expeditions to Nouragues.

Additional information

Conflict of interest

The authors have declared that no competing interests exist.

Ethical statement

No ethical statement was reported.

Funding

This work was in part supported by 'Service de Systématique Moléculaire' (UMS 2700 2AD, MNHN, CNRS).

Author contributions

OG, BF and ST did the field work. DZ did the molecular analyses. OG described the new species, proposed some taxonomic modifications and wrote the first draft of the manuscript and all the authors reviewed and amended the manuscript.

Author ORCIDs

Olivier Gargominy https://orcid.org/0000-0001-7807-944X
Benoît Fontaine https://orcid.org/0000-0002-1017-5643
Sandrine Tercerie https://orcid.org/0000-0002-4341-062X
Dario Zuccon https://orcid.org/0000-0001-8236-5924

Data availability

All of the data that support the findings of this study are available in the main text.

References

Altena CO, van Regteren (1960) On a small collection of land Mollusca from Suriname. Basteria 24: 48–51.

Altena CO, van Regteren (1975) Land Gastropoda of Suriname, with the description of a new species of *Nesopupa*. Basteria 39: 29–50.

Baker HB (1925) The Mollusca collected by the University of Michigan-Williamson Expedition in Venezuela. Part III: Pupillidae to Oleacinidae. Occasional Papers of the Museum of Zoology University of Michigan 156: 1–57 [figs 58–61, pls 51–11].

Breure ASH (1976) Notes on Bulimulidae (Gastropoda, Euthyneura), 4). Some Bulimulidea from French Guyana and Surinam, with notes on their anatomy. Zoologische Mededelingen 50: 107–115.

Breure ASH (1979) Systematics, phylogeny and zoogeography of Bulimulinae (Mollusca). Zoologische Mededelingen 168: 1–125.

Breure ASH, Ablett JD (2014) Annotated type catalogue of the Bulimulidae (Mollusca, Gastropoda, Orthalicoidea) in the Natural History Museum, London. ZooKeys 392: 1–367. https://doi.org/10.3897/zookeys.392.6328

Breure ASH, Borrero FJ (2019) A review of *Stenostylus* Pilsbry, 1898 and *Drymaeus* Albers, 1850 (Mollusca: Gastropoda: Orthalicoidea: Bulimulidae) from Colombia, with description of new species. Folia Conchyliologica 52: 1–79.

Breure ASH, Eskens AAC (1981) Notes on and descriptions of Bulimulidae (Mollusca, Gastropoda), 2. Zoologische Verhandelingen (Leiden) 186: 3–111.

Brûlé S, Touroult J (2014) Insects of French Guiana: a baseline for diversity and taxonomic effort. ZooKeys 434: 111–130. https://doi.org/10.3897/zookeys.434.7582

Dall W (1885) Notes on some Floridan Land and Fresh-water Shells with a Revision of the Auriculacea of the Eastern United States. Proceedings of the United States National Museum 8: 255–289. https://doi.org/10.5479/si.00963801.8-519.255

Decaëns T, Carolina Bartz ML, Feijoo-Martínez A, Goulpeau A, Lapied E, Marchán DF, Maggia M-E, Papuga G, James SW (2024) Earthworms (Oligochaeta, Clitellata) of the Mitaraka range (French Guiana): commented checklist with description of one genus and eighteen species new to science. Zoosystema 46: 195–244. https://doi.org/10.5252/zoosystema2024v46a9

Drouët H (1859) Essai sur les Mollusques terrestres et fluviatiles de la Guyane française. J.-B. Baillière, libraire de l'Académie de Médecine, Paris, 116 pp. https://doi.org/10.5962/bhl.title.13112

Folmer O, Black M, Hoeh W, Lutz R, Vrijenhoek R (1994) DNA primers for amplification of mitochondrial cytochrome c oxidase subunit I from diverse metazoan invertebrates. Molecular Marine Biology and Biotechnology 3: 294–299.

Fontaine B, Perrard A, Bouchet P (2012a) 21 years of shelf life between discovery and description of new species. Current Biology 22: R943–944. https://doi.org/10.1016/j.cub.2012.10.029

Fontaine B, van Achterberg K, Alonso-Zarazaga MA, Araujo R, Asche M, Aspoeck H, Aspoeck U, Audisio P, Aukema B, Bailly N, Balsamo M, Bank RA, Belfiore C, Bogdanowicz W, Boxshall G, Burckhardt D, Chylarecki P, Deharveng L, Dubois A, Enghoff H, Fochetti R, Fontaine C, Gargominy O, Gomez Lopez MS, Goujet D, Harvey MS, Heller K-G, van Helsdingen P, Hoch H, De Jong Y, Karsholt O, Los W, Magowski W, Massard JA, McInnes SJ, Mendes LF, Mey E, Michelsen V, Minelli A, Nafria JMN, van Nieukerken EJ, Pape T, De Prins W, Ramos M, Ricci C, Roselaar C, Rota E, Segers H, Timm T, van Tol J, Bouchet P (2012b) New Species in the Old World: Europe as a Frontier in Biodiversity Exploration, a Test Bed for 21st Century Taxonomy. PLoS ONE 7: e36881, 36881–36887. https://doi.org/10.1371/journal.pone.0036881

Fukuda H, Haga T, Tatara Y (2008) Niku-nuki: a useful method for anatomical and DNA studies on shell-bearing. Zoosymposia 1: 15–38. https://doi.org/10.11646/zoosymposia.1.1.5

Gargominy O, Fontaine B (2015) Mollusques terrestres et aquatiques. In: Pascal O, Touroult J, Bouchet P (Eds) Expédition La Planète Revisitée Guyane 2014–15, synthèse des premiers résultats. Muséum national d'Histoire naturelle; Pro-Natura International, Paris, 54–60.

Gargominy O, Muratov IV (2012) New taxa of land snails from French Guiana. Zoosystema 34: 783–792. https://doi.org/10.5252/z2012n4a7

Gargominy O, Ripken T (1998) Conservation d'une biodiversité reconnue mais méconnue: le cas des mollusques continentaux en Guyane. Journal d'agriculture traditionnelle et de botanique appliquée 40: 261–277. https://doi.org/10.3406/jatba.1998.3673

Gargominy O, Fontaine B, Tercerie S, Abdou A, Sant S (2022) Les mollusques continentaux de Saül (Guyane). Bilan des missions 2018–2020 de l'Atlas de la biodiversité communale. Les Cahiers scientifiques du Parc amazonien de Guyane 7: 83–99.

Hausdorf B (2005) The genus *Lilloiconcha* in Colombia (Gastropoda: Charopidae). Journal of Natural History 39: 2795–2808. https://doi.org/10.1080/00222930500145057

Hausdorf B (2007) Revision of the American *Pupisoma* species (Gastropoda: Pupilloidea). Journal of Natural History 41: 1481–1511. https://doi.org/10.1080/00222930701401069

Hausdorf B, Munoz SG (2004) *Adelopoma peruvianum* new species from northern Peru (Gastropoda: Diplommatinidae). Journal of Conchology 38: 369–372. https://doi.org/10.5962/p.408152

Lescure J, Dewynter M, Frétey T, Ineich I, Ohler AM, Vidal N, Massary J-Cd (2022) Liste taxinomique de l'herpétofaune dans l'outre-mer français: VII. Les Amphibiens de la Guyane française. Bulletin de la Société Herpétologique de France 181: 1–17.

Maggia M-E, Decaëns T, Lapied E, Dupont L, Roy V, Schimann H, Orivel J, Murienne J, Baraloto C, Cottenie K, Steinke D (2021) At each site its diversity: DNA barcoding reveals remarkable earthworm diversity in neotropical rainforests of French Guiana. Applied Soil Ecology 164: 103932. https://doi.org/10.1016/j.apsoil.2021.103932

Martins CM, Simone LRL (2014) A new species of *Adelopoma* from São Paulo Urban Park, Brazil (Caenogastropoda, Diplommatinidae). Journal of Conchology 41: 765–773.

Massemin D, Lamy D, Pointier JP, Gargominy O (2009) Coquillages et escargots de Guyane. Biotope, Collection Parthénope, Mèze, 456 pp.

Miquel SE, Ramirez R, Thome JW (2007) Biodiversidad y taxonomía de micromoluscos Punctoidea del sur de Brasil, con la descripción de una nueva especie de *Radiodiscus* de la Mata Atlántica (Mollusca, Gastropoda, Pulmonata). Revista del Museo Argentino de Ciencias Naturales 9: 205–230. https://doi.org/10.22179/REVMACN.9.308

Moricand S (1846) Troisième supplément au mémoire sur les coquilles terrestres et fluviatiles de la province de Bahia, envoyées par. M.J. Blanchet. Mémoires de la Société de Physique et d'Histoire naturelle de Genève 11: 147–160.

Muratov IV, Gargominy O (2011) Taxonomic position of the land snail *Bulimus demerarensis* L. Pfeiffer 1861 (Gastropoda, Pulmonata, Bulimulidae). Journal of Conchology 40: 611–615.

Neubert E, Gosteli M (2003) The molluscan species described by Robert James Shuttleworth. I. Gastropoda: Pulmonata. Contributions to Natural History, Scientific papers from the Natural History Museum Bern 1: 1–123.

Pfeiffer L (1855) Descriptions of fifty-seven new species of Helicea, from Mr. Cuming's collection. Proceedings of the Zoological Society of London 22: 286–298. https://doi.org/10.1111/j.1469-7998.1854.tb07277.x

Pilsbry HA (1920) Review of the *Thysanophora plagioptycha* group. The Nautilus 33: 93–96.

Richardson CL (1995) Bulimulidae: catalog of species. Tryonia 28: i–iii, 1–458.

Roosen MT, Breure ASH (2024) Revision of the genera of Scolodontidae, part 1: disentangling *Happia* Bourguignat, 1890 from *Austroselenites* Kobelt, 1905, *Drepanostomella* Bourguignat, 1890, *Hirtudiscus* Hylton Scott, 1973, *Luteostriatella* gen. nov., and *Systrophiella* H.B. Baker, 1925. Journal of Conchology 45: 91–110. https://doi.org/10.61733/jconch/4511

Salvador RB (2019) Land snail diversity in Brazil. Strombus 25: 10–20.

Salvador RB, Brook FJ, Shepherd LD, Kennedy M (2020) Molecular phylogenetic analysis of Punctoidea (Gastropoda, Stylommatophora). Zoosystematics and Evolution 96: 397–410. https://doi.org/10.3897/zse.96.53660

Salvador RB, Charles L, Simone LRL, Maestrati P (2021) First record of Thysanophoridae from Brazil (Gastropoda, Stylommatophora). Check List 17: 1113–1116. https://doi.org/10.15560/17.4.1113

Salvador RB, Silva FS, Cavallari DC, Kohler F, Slapcinsky J, Breure ASH (2023) Molecular phylogeny of the Orthalicoidea land snails: Further support and surprises. PLoS ONE 18: e0288533. https://doi.org/10.1371/journal.pone.0288533

Schileyko AA (2001) Treatise on Recent terrestrial pulmonate molluscs. Part 7. Endodontidae, Thyrophorellidae, Charopidae. Ruthenica Supplement 2: 879–1034.

Schileyko AA (2006) Treatise on Recent terrestrial pulmonate molluscs. Part 13. Helicidae, Pleurodontidae, Polygyridae, Ammonitellidae, Oreohelicidae, Thysanophoridae. Ruthenica Supplement 2: 1765–1906.

Simone LRL (2006) Land and Freshwater Molluscs of Brazil. Editora Grafíca Bernardi, FAPESP, São Paulo, 390 pp.

TAXREF (2024) TAXREF v17.0, référentiel taxonomique pour la France. Archive de téléchargement contenant 8 fichiers générés le 10 janvier 2024. PatriNat (OFB-MNHN-CNRS-IRD), Muséum national d'Histoire naturelle. https://doi.org/10.15468/vqueam

Thompson FG (1957) A collection of mollusks from northern Venezuela. Occasional Papers of the Museum of Zoology University of Michigan 591: 1–10 [14 figs, 12 pls].

Tillier S (1980) Gastéropodes terrestres et fluviatiles de Guyane française. Mémoires du Muséum national d'Histoire naturelle (A)118: 1–188.

Torre C de la, Bartsch P, Morrison JP (1942) The cyclophorid operculate land Mollusks of America. United States National Museum Bulletin 181: 1–291.

Touroult J, Pollet M, Pascal O (2018) Overview of Mitaraka survey: research frame, study site and field protocols. Zoosystema 40: 327–365. https://doi.org/10.5252/zoosystema2018v40a13

Vedel V, Rheims C, Murienne J, Brescovit AD (2013) Biodiversity baseline of the French Guiana spider fauna. Springerplus 2:361: 1–19. https://doi.org/10.1186/2193-1801-2-361

Vernhout JH (1914) The non-marine molluscs of Surinam. Notes from the Leyden Museum 36: 1–46 [pls. 41–42].

Webster NB, Van Dooren TJM, Schilthuizen M (2012) Phylogenetic reconstruction and shell evolution of the Diplommatinidae (Gastropoda: Caenogastropoda). Molecular Phylogenetics and Evolution 63: 625–638. https://doi.org/10.1016/j.ympev.2012.02.004

Weyrauch WK (1965) Neue und verkannte Endodontiden aus Südamerika. Archiv für Molluskenkunde 94: 121–134.

ZooKeys 1230: 195–212 (2025)
DOI: 10.3897/zookeys.1230.135523

Research Article

Lost for more than a century: the rediscovery of *Alsodes vittatus* (Philippi, 1902) (Anura, Alsodidae), one of the rarest and most elusive amphibians from Chile

Claudio Correa[1], Edvin Riveros-Riffo[2], Juan P. Donoso[1]

1 *Laboratorio de Sistemática y Conservación de Herpetozoos (SyCoH), Departamento de Zoología, Facultad de Ciencias Naturales y Oceanográficas, Universidad de Concepción, Barrio Universitario S/N, Concepción, Chile*
2 *Magíster(c) en Ciencias Biológicas mención Biodiversidad y Conservación, Instituto de Biología, Facultad de Ciencias, Universidad de Valparaíso, Valparaíso, Chile*
Corresponding author: Claudio Correa (ccorreaq@udec.cl)

Abstract

The legacy of the 19th-century naturalist Rudolph Philippi to the taxonomy of Chilean amphibians has been controversial since most of the species he described in 1902 have been questioned or invalidated. Here, we describe the rediscovery of *Alsodes vittatus*, a species that was not observed for 130 years after being collected, in three places very close to the type locality in the Andean foothills of the La Araucanía Region, Chile. The species was identified phenotypically by the vertebral line of some individuals, which turned out to be an intrapopulationally polymorphic trait. A phylogenetic analysis with mitochondrial genes, including most of the species of the genus, showed that the discovered populations of *A. vittatus* are paraphyletic with respect to the only individual of *A. neuquensis* included. We also describe populations from another area where *A. vittatus* was searched in the past, which we assigned here to *A. igneus* due to its geographic location and phylogenetic and phenotypic affinity. All these populations are part of two well-supported clades, but their relationships with nearby species (e.g., *A. norae* and *A. barrioi*) remain uncertain. These results ratify that the diversity and phylogenetic relationships of the genus in the Chilean Andes, particularly in the La Araucanía Region, are not yet well established. We discuss the possibility that *A. vittatus* and *A. neuquensis*, known until now only in Argentina, are the same species, and suggest downgrading the conservation status of *A. vittatus* from Critically Endangered to Endangered, considering the information from the new localities discovered.

Key words: *Alsodes igneus*, *Alsodes neuquensis*, *Alsodes verrucosus*, Andean foothills, Chilean amphibians, conservation category, Rudolph Philippi, taxonomy

Academic editor: Uri García-Vázquez
Received: 26 August 2024
Accepted: 13 December 2024
Published: 6 March 2025

ZooBank: https://zoobank.org/FBB90869-BDDD-4807-B4AD-935F95C74129

Citation: Correa C, Riveros-Riffo E, Donoso JP (2025) Lost for more than a century: the rediscovery of *Alsodes vittatus* (Philippi, 1902) (Anura, Alsodidae), one of the rarest and most elusive amphibians from Chile. ZooKeys 1230: 195–212. https://doi.org/10.3897/zookeys.1230.135523

Introduction

Rudolph Amandus Philippi (1808–1904), of German origin, was one of the most important naturalists of Chile during the 19th century (Kabat and Coan 2017). Philippi contributed enormously to the development of natural sciences in Chile in areas as diverse as zoology, botany, paleontology and geology. This work resulted in more than 450 publications (Taylor and Muñoz-Schick 1994), made during the more than five decades that he remained active. One of the most important positions he held was as director of the Museo Nacional de Historia Natural (MNHN) in Santiago, where he contributed to organizing and increasing the collections.

One of Philippi's most enduring legacies is the extensive number of species of plants, animals, and fungi that he described, including more than 3300 species of plants (Muñoz-Schick et al. 2012), 2500 recent and fossil mollusks (Coan and Kabat 2017), and 800 species of insects (Camousseight 2005). It has been argued that the vast number of species that Philippi recognized is due to his adherence to the typological species concept prevailing at that time, differentiating many taxa by minimal phenotypic differences (Cei 1958; Castro et al. 2006). This is one of the main reasons Philippi's contributions to the current taxonomy of many groups have been critically reviewed. Despite the criticism and progress in taxonomy over the last century, his contribution to the knowledge of Chile's biota is undeniable. A century after his death, 1670 of the species he described were still considered valid, most of them plants (Castro et al. 2006). Among the animals, amphibians, phasmids (order Phasmatodea) and earwigs (Dermaptera) stand out, whose diversity as of 2006 included more than 10% of the species originally described by Philippi.

The revisions of the herpetozoans of Chile, which he carried out at a very late age, exemplify his taxonomic approach, by recognizing an excessively high number of species in comparison to previous studies. Thus, Philippi indicated that there were 45 species of snakes (Philippi 1899) and ~80 species of amphibians in Chile (Philippi 1902, *Suplemento a los batraquios chilenos descritos en la Historia Física i Política de Chile de don Claudio Gay*, in short, the "Suplemento"). Both works were critically reviewed: Donoso-Barros and Cárdenas (1965) focused on snakes, while Cei (1958) focused on amphibians. In the case of snakes, Philippi's proposal proved to be totally unfounded, but in the case of amphibians, most species were considered synonymous or *incertae sedis* and only one (*Telmatobius laevis*) was considered valid by Cei (1958).

Subsequent studies revalidated some of the Philippi's amphibian species, thanks to the collection of material from type localities (e.g., *Heminectes rufus* Philippi, 1902, currently *Rhinoderma rufum*; Formas et al. 1975) or by the discovery of new populations that fit their descriptions (e.g., *Bufo venustus* Philippi, 1899, currently *Telmatobufo venustus*; Formas and Veloso 1982). Thus, a century after its publication, six species of amphibians described or redescribed by Philippi (1902) were recognized as valid (14.6% of the 41 species recognized at that time in Chile; Castro et al. 2006), although the magnitude of his contribution should be reevaluated, considering the taxonomic changes of the last two decades.

Among those six species are two of the genus *Alsodes*, whose taxonomic status is more controversial. *Alsodes verrucosus* (Philippi, 1902), originally described as *Borborocoetus verrucosus*, has a very vague type locality (the Andes of Cautín Province). It was first rediscovered in Argentina (Vellard 1947), and later, the population of Puyehue National Park, Chile (200 km south of the type locality) was assigned to this species without any explanation (Formas and Vera 1983). The type material of this species is probably lost (Formas 1995). The second species, *A. vittatus* (Philippi, 1902), has a more complex history. Roberto Donoso-Barros recovered from the MNHN some of the types used by Philippi to make his descriptions, including one of the three syntypes of *Cystignathus vittatus* (its original designation). However, Donoso-Barros (1976) considered that this specimen corresponded to *Eupsophus vertebralis* Grandison, 1961, so he proposed the new combination *Eupsophus vittatus*. This name appeared in several publications as referring to specimens of *Eupsophus* until Formas (1989a) demonstrated that the syntype recovered by Donoso-Barros corresponded to an *Alsodes*.

Unlike *A. verrucosus*, Philippi indicated a more precise type locality for *C. vittatus*, Hacienda San Ignacio de Pemehue (but see Material and methods), the collector (entomologist Philibert Germain) and the year in which he received the specimens (1894). Furthermore, the original drawing of the species was later found and published by Cei (1958). Despite all this information, there have been no sightings of the species after its description, and all more recent attempts (1995–2002) to find it have failed (Formas 1989a; IUCN SSC Amphibian Specialist Group 2016).

Recently, Correa et al. (2023) reconstructed the route that Philibert Germain possibly followed inside the Hacienda San Ignacio de Pemehue in late 1893, where he collected specimens of *Telmatobufo venustus* (Fig. 1B). The description of *A. vittatus* (Philippi 1902) specifies the same locality, collector and date as *T. venustus*, so we assumed that both species were collected at some point along that route, which served to guide our explorations.

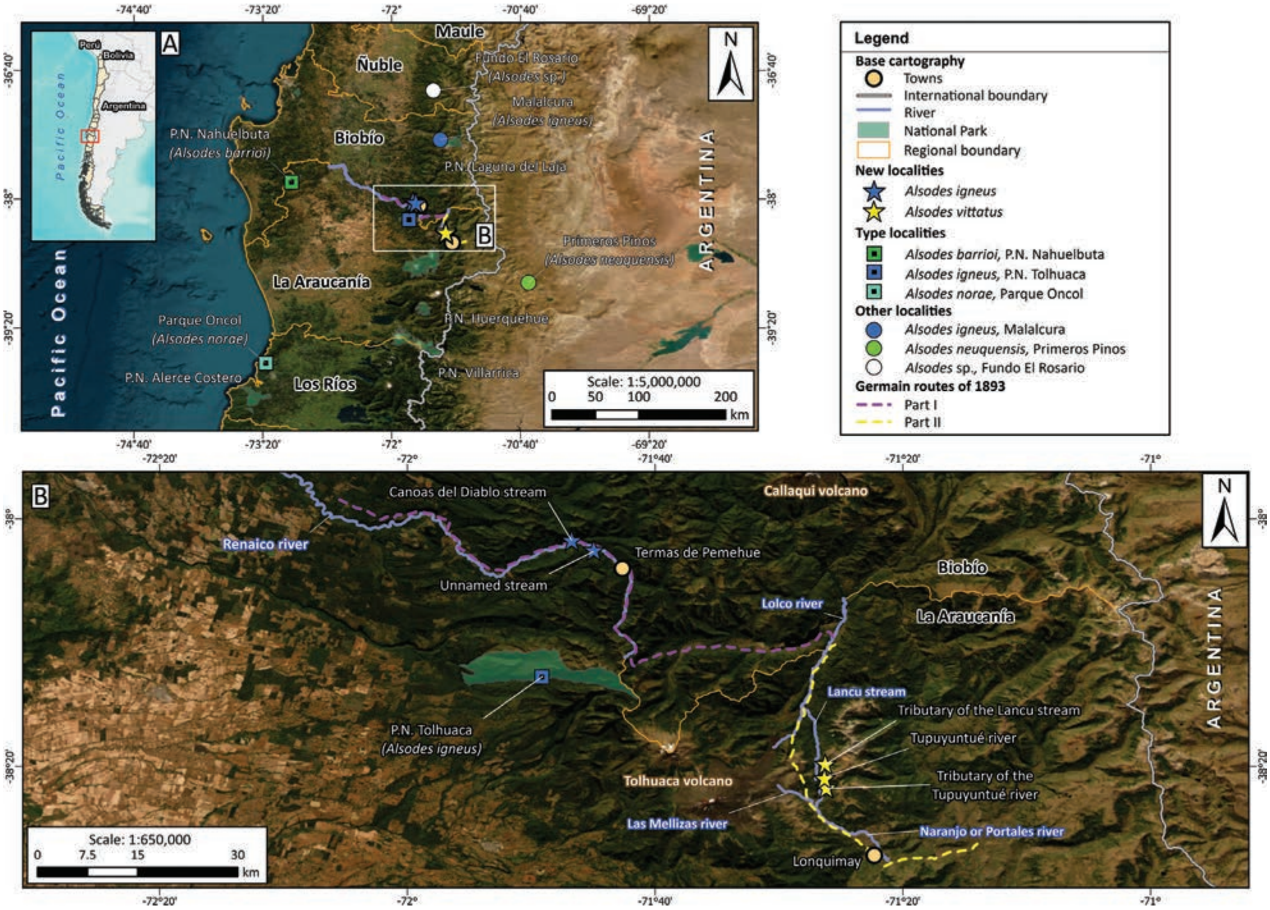

Figure 1. Location of the newly discovered populations of *Alsodes igneus* and *A. vittatus*, geographically and phylogenetically close species, and the reconstructed routes that Philibert Germain followed within the Hacienda San Ignacio de Pemehue in 1893 **A** populations of *Alsodes* between 36°40' and 40°S included in the phylogenetic analysis, including the new populations of *A. igneus* and *A. vittatus* described in this study **B** detail of map **A** showing the location of the newly discovered populations of *A. igneus* and *A. vittatus* (stars) and the routes (dashed lines) followed by Philibert Germain through the Hacienda San Ignacio de Pemehue according to Correa et al. (2023).

In this study, we report the discovery of five localities of *Alsodes* located along or around the reconstructed route of Germain, three of which we assign to *A. vittatus* based on external morphological characteristics of adults and juveniles. We briefly describe these populations and investigate their phylogenetic relationships in the context of all the geographically closest species of the genus. Furthermore, we discuss the possible implications of this phylogenetic hypothesis for the taxonomy of *A. vittatus* and reevaluate the conservation category of this species, considering the information from the new localities discovered.

Material and methods

Explored areas

The type locality of *A. vittatus* (and *T. venustus*), Hacienda San Ignacio de Pemehue, was a huge *hacienda* (estate) located in the Andean zone of what is currently the southern end of the Biobío Region and the northern end of La Araucanía Region in Chile (~38°–38°30'S) (see the map in Klubock 2022). Philibert Germain described his journey through the estate in December 1893 (Germain 1894), which was reconstructed by Correa et al. (2023) (Fig. 1B). Germain (1894) indicated that he began his journey at the northwest end of the *hacienda*, where the landowner's house was located, and then continued east along the north bank of the Renaico River. Currently, the public road runs along the southern bank of the Renaico River, whose valley initially runs approximately from west to east and, after passing the town of Termas de Pemehue, turns south. In 2015 and 2016 we explored some tributaries of the Renaico River along the road to Termas de Pemehue. In 2023 and 2024, we explored part of the final section of the reconstructed route of Germain's journey (yellow dashed line on map in Fig. 1B). We departed from Lonquimay town towards the northwest, entering the valley of the Naranjo or Portales River, which has two tributaries, Las Mellizas and Tupuyuntué rivers. Finally, we followed the course of the Tupuyuntué River to the north, until we reached the valley of the Lancu stream (tributary of the Lolco River) in the adjacent sub-basin, located to the north.

Samples and DNA extraction

We collected and/or sampled different numbers of specimens at different stages of development from five new localities (see details in Results). DNA was extracted from different types of tissue depending on the stage of development and whether the specimen was collected: thigh muscle or tongue for adults and juveniles, tail muscle for tadpoles, and buccal mucosa for one uncollected juvenile individual (unnamed stream). The buccal mucosa was obtained with a Copan 516CS01 swab and immediately dried with silica gel; the individual was released at the same capture site. The DNA was extracted with a commercial kit (Promega ReliaPrep™ gDNA Tissue Miniprep System) following the manufacturer's instructions.

PCR protocols and phylogenetic analysis

We obtained two mitochondrial fragments—one that extends between the 12S and 16S ribosomal genes (12S-16S), including the intervening tRNA-Val, and part of the cytochrome *b* (cytb)—to examine the phylogenetic affinities of the new populations. PCR protocols and primers to obtain these fragments are found in Correa et al. (2006), Correa et al. (2008) and Correa et al. (2013). We analyzed these two fragments together (concatenated) by Bayesian inference (BI), including one or a few specimens of most species of the genus (extracted from Faivovich et al. 2005; Blotto et al. 2013; Charrier et al. 2015; Correa et al. 2020). The BI analysis was performed with the program MrBayes v. 3.2.7a (Ronquist et al. 2012), applying independently to the fragment 12S-16S and to each codon position of cytochrome *b* the model-jumping option to explore the space of all General Time Reversible sub-models, plus gamma and proportion of invariable sites parameters. The analysis consisted of four independent chains run for 20 million generations, sampled every 1000 generations, conservatively discarding the first 25% of generations as burn-in after observing the stationarity of ln-likelihoods of trees in Tracer v. 1.7.1 (Rambaut et al. 2018). Convergence and mixing of chains were assessed by examining the average standard deviation of split frequencies (ASDSF), and expected sampling sizes (ESS) and the Potential Scale Reduction Factor (PSRF) for all parameters. The consensus tree was rooted with one specimen of *Eupsophus calcaratus* (Günther, 1881), a representative of the sister genus to *Alsodes* (Blotto et al. 2013).

Morphological descriptions

We described some external morphological characteristics of the collected adults and juveniles which were compared with those described for the geographically closest species from the Andean foothills—*A. igneus* Cuevas & Formas, 2005, *A. verrucosus* (Philippi, 1902), and *A. vittatus* (Philippi, 1902; Formas 1989a). Special emphasis was given to characters used in the diagnosis of these species, such as coloration patterns, shape of snout, interdigital membranes and other characteristics of the foot, and to their variation.

Results

New localities and sampled specimens

We discovered five new localities of *Alsodes* along or near the route followed by Philibert Germain through the former Hacienda San Ignacio de Pemehue (Fig. 1B, Table 1). Two of these localities correspond to small water courses that flow north (Canoas del Diablo) and south of the Renaico River (unnamed stream). The first point is very close to a locality of *Eupsophus nodosus* (Duméril & Bibron, 1841) (*Alsodes nodosus*?) by Webb and Greer (1969). Both streams are located in an area dominated by temperate deciduous *Nothofagus* forest, although along the banks of the Renaico River the original vegetation has been partially eliminated or modified by human activities, or it has been replaced by forest plantations. The Canoas del Diablo stream has a steep slope, with a bed mainly made up of large rocks, and is surrounded by native forest. During two-night visits in spring 2015, several juveniles and numerous tadpoles were observed, and three juveniles were collected (Fig. 2A). The unnamed stream has a lower slope, with few rocks in its bed, and is located in an intervened area where native forest persists mainly along its bed. There, during the last of three-night visits made in the summer of 2016, only one small juvenile was

Table 1. New localities described in this study and specimens collected in each one. Altitudes according to Google Earth Pro. The specimen codes that appear in the Bayesian phylogenetic tree (Fig. 4) and in the text are indicated in parentheses.

Species	Locality	Latitude, Longitude	Altitude (m a.s.l.)	Collected/sampled specimens
Alsodes igneus	Canoas del Diablo stream	38°01'45"S, 71°46'44"W	631	Three juveniles (Pem1j-Pem3j)
Alsodes igneus	Unnamed stream	38°02'27"S, 71°44'57"W	674	One juvenile (not collected) (AS1j)
Alsodes vittatus	Tributary of the Lancu stream	38°19'49"S, 71°26'15"W	1491	One juvenile (AEL2j) and one adult female (AEL2h)
Alsodes vittatus	Tupuyuntué River	38°20'59"S, 71°26'19"W	1610	Two adult males (RTp1m and RTp2m), two juveniles and two tadpoles
Alsodes vittatus	Tributary of the Tupuyuntué River	38°21'44"S, 71°26'11"W	1421	Three tadpoles (ART1l)

observed on the leaf litter at the edge of the stream (Fig. 2B). The other three localities are situated at a higher altitude, in a temperate forest area where deciduous and resinous trees (*Araucaria araucana*) are mixed. The tributary of the Lancu stream has a gentle slope, a mainly rocky bed, and is situated in a sparse forest with signs of human intervention. There, we explored at night ~250 m along the stream, and only found one adult female and one juvenile; we did not observe any tadpole. In contrast, in the Tupuyuntué River, we observed several adults, numerous juveniles and innumerable tadpoles at night, but only a few specimens were collected (Table 1). The river in the explored sector is rather a stream with a very slight slope, surrounded by a clearly intervened forest (Fig. 2F). Finally, we explored, during the day, a small section of a tributary of the Tupuyuntué River in an area almost completely cleared by human occupation, where we observed numerous tadpoles. In none of these last localities did we observe other species of amphibians. We observed a few adult individuals of *Eupsophus* sp. only in the two tributary streams of the Renaico River.

Description of the new populations of *Alsodes igneus*

According to the phylogenetic analysis, geographic location (Fig. 1A), and some morphological similarities, the populations from the tributaries of the Renaico River were assigned to *A. igneus*. Here, we describe the external morphology of the two largest specimens of the three collected in the Canoas del Diablo stream, and the coloration pattern of the small juvenile from the unnamed stream. The largest specimen (SVL = 42.5 mm) from Canoas del Diablo can be considered a subadult male because it has patches of spines on the chest and poorly developed spines on fingers 1 and 2 of the hand (not cornified) (Fig. 2A). It has the canthus rostralis and postocular fold (supratympanic fold) well-developed, short and rounded snout in dorsal and lateral view, smooth skin with small granulations on the dorsal surface of body and limbs, ventral surface of thighs with numerous small tubercles, toes with reduced lateral fringes and poorly developed interdigital membranes. Another smaller juvenile (SVL = 34.5 mm) is morphologically similar to the previous one but has a less developed canthus rostralis and postocular fold, and lacks spines on the chest and fingers. Both specimens in life had a light brown background color with a continuous dark brown spot on the anterior part of the back. This spot included a triangle that converges towards the back, with its base between the eyes, which is flanked on both sides by elongated, lighter scapular spots (Fig. 2A, B). Additionally, they

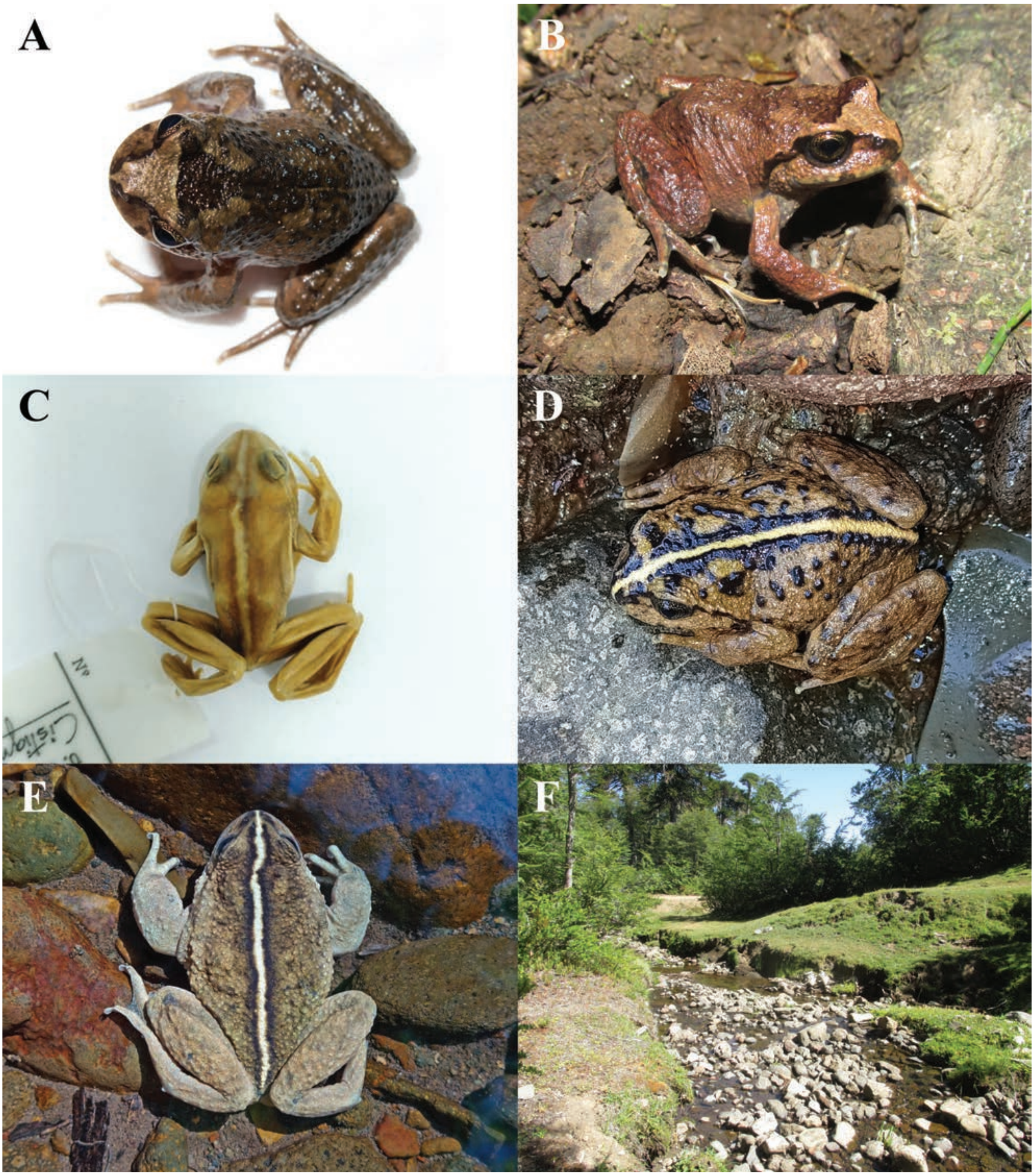

Figure 2. Individuals of *Alsodes igneus* and *A. vittatus* from the new populations, syntype of *A. vittatus* and environment of one of the new localities. The individual code used in the phylogenetic analysis is indicated in parentheses in Table 1 **A** subadult male from Canoas del Diablo stream (Pem1j) **B** juvenile from the unnamed stream (not collected) (AS1j) **C** syntype of *A. vittatus*, Zoological Collection of the Museo de Concepción (MZUC), labeled as the holotype of *"Cistignathus" vittatus*, without collection number **D** juvenile from the tributary of the Lancu stream (AEL1j) **E** adult male from Tupuyuntué River underwater (RTp1m) **F** Tupuyuntué River at the point where tadpoles and juveniles of *A. vittatus* were observed.

had other small, irregular dark spots scattered over the back and limbs and a lighter triangle on the head. This lighter triangle was delimited by the base of the dark dorsal triangle and two dark bands extending from the tip of the snout to the eyes, beneath the canthus rostralis. The belly was whitish with small, diffuse brown spots, and the iris was black with golden reticulations. The smaller juvenile (SVL = 32 mm) from the unnamed stream is similar to the previous two but has a reddish-brown color (Fig. 2B). The lateral band on the head extends beyond the eye to near the base of the arm, and its belly is leaden, speckled with small, pale yellowish spots. Therefore, similarities in coloration patterns, as well as in the development of the lateral fringes of the toes and interdigital membranes, reinforce the idea that the new populations can be assigned to *A. igneus* (Cuevas and Formas 2005).

Description of the new populations of *Alsodes vittatus*

The new populations of *A. vittatus* were assigned to this species due to their proximity to the route followed by the original collector (Germain) through the type locality (Fig. 1B), as well as the presence of the species' most conspicuous characteristic, the vertebral line (Figs 2, 3). The external morphology, color patterns and variation of adult and juvenile specimens from two of three of the discovered localities are described here and compared with the original descriptions of *A. vittatus* and *A. verrucosus* (Philippi 1902). The two specimens from the tributary of the Lancu stream—a juvenile (AEL1j, Fig. 2D) and an adult female (AEL2h)—show that *A. vittatus* exhibits variation in coloration patterns and a polymorphism in the presence/absence of the vertebral line. The juvenile has a well-defined yellowish vertebral band bordered by black. The dorsal background color is brown, with numerous granulations on the back and limbs, most of which are pigmented black. The ventral surface is pinkish-brown (greyish on the abdomen), with diffuse yellowish reticulations. The ventral surface of the thighs has numerous small, densely arranged granulations. The snout is slightly pointed in dorsal view and slightly truncated in lateral view. The toes are fringed, and the interdigital membranes are poorly developed. The color pattern of the female differs markedly: the vertebral line is absent, the dorsal background color is light brown, and the skin is smooth with irregular dark brown spots on the back. The largest dorsal spot anteriorly has an inverted triangular shape, with one of its vertices pointing backwards and the opposite side located between the eyes. There are numerous small granulations scattered over the dorsal surface. The ventral color is whitish with a slight pinkish tint, particularly under the thighs, where the ventral surface has numerous, dense, small granulations. The snout is short, rounded in dorsal view, and truncated in lateral view. The canthus rostralis is poorly developed, while the postocular fold is thick and extends to the base of the arm. The toes have well-developed lateral fringes and more extensive interdigital membranes than those of the juvenile.

The two adult males from the Tupuyuntué River (RTp1m and RTp2m; Fig. 3A) exhibit the secondary sexual characteristics that define the genus (Fig. 3B) and confirm the polymorphism of the vertebral line within the species. They also extend the range of variation in the species' coloration patterns: male RTp1m is light brown with light yellow and green tints, while male RTp2m is olive brown. We also observed a female of similar size and coloration to male RTp2m (not collected; Fig. 3D). In both males, the dorsal coloration is darker with very diffuse dark spots; however, male RTp1m has a darker color around the vertebral line. Both males have numerous granulations on the dorsal surface and skin folds on the sides, which are more developed in male RTp2m. They both

Figure 3. Some morphological characteristics of *Alsodes vittatus* **A** two adult males from the Tupuyuntué River showing the polymorphisms of vertebral line and coloration patterns (left, RTp1m; right, RTp2m) **B** secondary sexual characters (thickened forearms, patches of spines on chest and spines on fingers 1 and 2) of the male RTp2m **C** plantar view of the right foot of the same male **D** adult female from the Tupuyuntué River underwater (not collected) **E** juvenile from the Tupuyuntué River underwater (SVL = ~40 mm).

possess a rounded snout in dorsal and lateral view, a slightly accentuated canthus rostralis, and a well-developed postocular fold. They have toes with lateral fringes and well-developed interdigital membranes, although these are emarginate (Fig. 3C). Both individuals have black irises with golden reticulations.

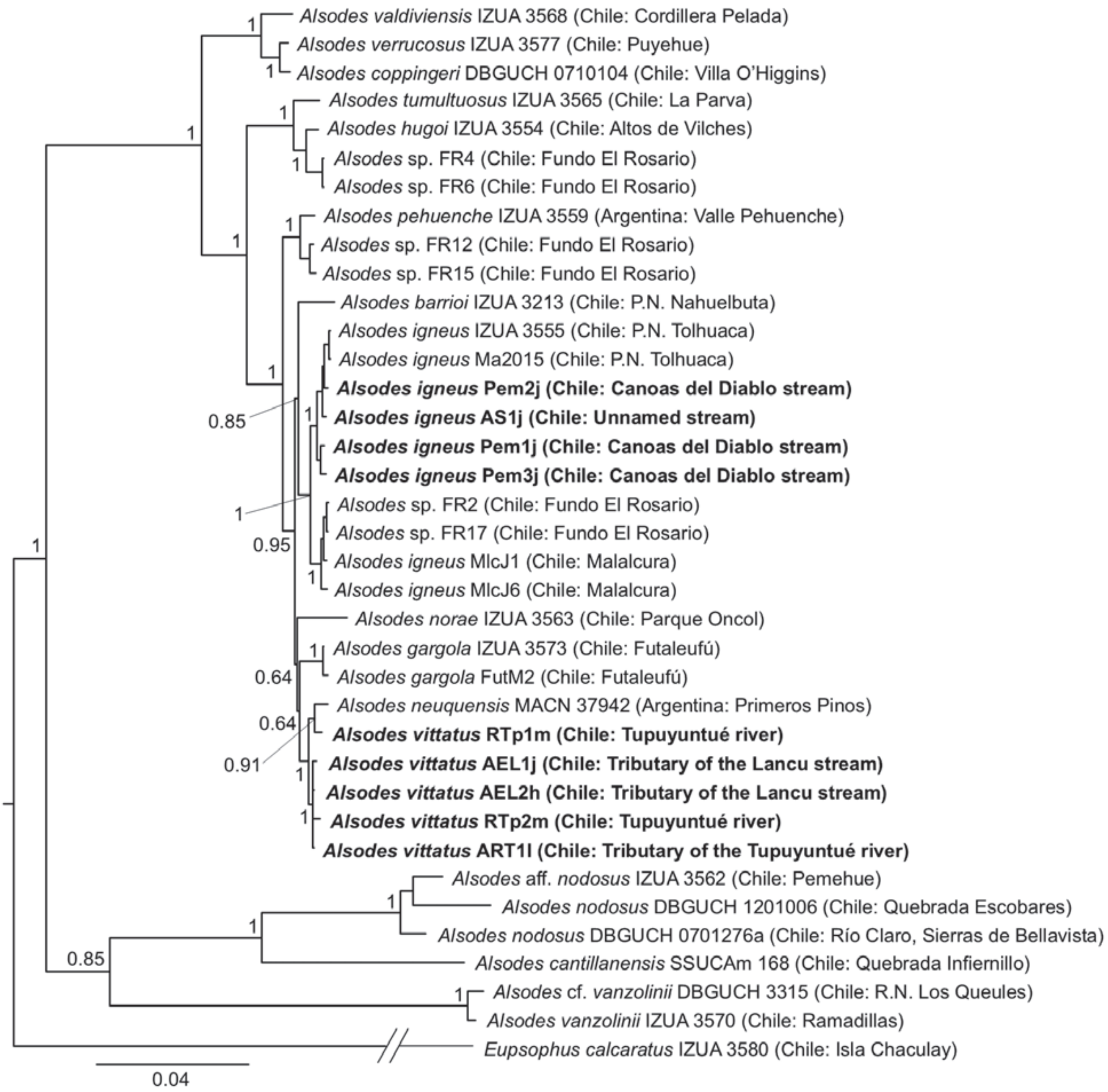

Figure 4. Bayesian consensus tree (50% majority-rule) of the two concatenated mitochondrial fragments, showing the relationships of the new populations within the genus *Alsodes*. Individuals from the new populations are highlighted in bold (see details of the codes in Table 1). Numbers next to the nodes correspond to posterior probabilities and the scale bar below the tree represents the expected substitutions per site along the branches.

Apart from the vertebral line, there are few external features in the original description of *A. vittatus* that can be compared with those of the newly collected specimens. In fact, there is a significant difference in the coloration pattern. According to Philippi (1902), "the upper part of the body" of *A. vittatus* "is more or less intense black". Most of the individuals that we observed do not fit this description, as the dorsal coloration of the juvenile AEL1j and adult individuals ranges from olive brown to pale brown, with either indistinct or well-marked dark spots. In the existing syntype (Fig. 2C), the only dark area preserved is that bordering the vertebral line. One possibility is that the specimens described by Philippi were already darkened due to fixation in alcohol, as he mentions this detail (the specimens we collected darkened when preserved in ethanol). However, we observed several juveniles (~35–40 mm) in the Tupuyuntué River exhibiting dark brown dorsal coloration and a vertebral line, which align with the size reported by Philippi for the species ("trunk length 41 mm"; Fig. 3E). Therefore, Philippi's description may have been based on subadult individuals with such coloration. The greatest coincidence is observed in the coloration of the palms and soles, which Philippi described as blackish. All the individuals we captured exhibit darker ventral surfaces on the feet and hands (Fig. 3C). Additionally, the geographic location of the new populations coincides with the area where *A. verrucosus* was described; however, there are few external morphological characteristics for comparison in this case. According to Philippi (1902), this species lacks the vertebral line but is blackish above and reddish-brown below. While there is no coincidence in color, some individuals observed in the Tupuyuntué River (e.g., male RTp2m) have "the back densely covered with soft warts" (although small), as described by Philippi for this species. Therefore, it cannot be ruled out that Philippi's description pertains to specimens similar to those observed in the Tupuyuntué River, although darker. However, the resolution of the taxonomic status of *A. verrucosus* is beyond the scope of this study.

Phylogenetic relationships and taxonomic issues

The sequences obtained in this study were deposited in GenBank (fragment 12S-16S: PQ800373–PQ800387; cytb: PQ800388–PQ800401). We obtained final alignments of 2001 nucleotide sites for the fragment 12S-16S and of 953 for the cytb. The cytb alignment was almost complete due to a few slightly shorter sequences and because the only available *A. neuquensis* sequence is only 385 base pairs long (Faivovich et al. 2005; only 361 sites from this species were aligned). Our phylogenetic reconstruction is congruent with previous hypotheses, identifying two main clades within the genus with high support. One clade comprises *A. cantillanensis* Charrier, Correa, Castro & Méndez, 2015, *A. nodosus*, and *A. vanzolinii* (Donoso-Barros, 1974), while the other includes all remaining species (e.g., Blotto et al. 2013; Charrier et al. 2015; Correa et al. 2020). Within the latter clade, several groupings have been consistently recovered in these studies. One such grouping includes species known from the Coastal Mountains of Chile and the Andean foothills of Chile and Argentina between 37°15' and 39°45'S (*A. barrioi* Veloso, Díaz, Iturra & Penna, 1981, *A. igneus*, *A. neuquensis*, and *A. norae* Cuevas, 2008), as well as *A. gargola* Gallardo, 1970, which extends further south between 40°25' and 44°25'S, mainly in Argentina and marginally in Chile (Mella-Romero et al. 2022). All populations described here are included within this clade, but they are related to different nominal species. The two populations located on either side of the Renaico River are closely related to the known populations of *A. igneus* and are geographically situated between them. Furthermore, the specimens are phenotypically similar to *A. igneus* (see above), leading us to assign them to that species. On the other hand, populations identified as *A. vittatus* based on morphology and geographical location are closely related to *A. neuquensis*. In fact, a specimen from the Tupuyuntué River (the male with the vertebral line, Figs 2E, 3A) is more related to *A. neuquensis* than to another male specimen from the same population. In this case, we did not make a taxonomic decision due to the lack of additional material for *A. neuquensis* for morphological comparisons and a more complete molecular phylogenetic analysis. However, we emphasize the great morphological similarity between the male from Tupuyuntué related to *A. neuquensis* and a specimen from the vicinity of Primeros Pinos (east of the type locality of *A. neuquensis*), which also exhibits a vertebral line that was identified by Cei (1987) and Lavilla and Cei (2001) as *A. verrucosus* (see color photo in this last source). Consequently, Cei (1987) assumed that *A. neuquensis* (as *A. gargola neuquensis*) and *A. verrucosus* coexist in Primeros Pinos. More recent observations allow us to interpret the coexistence of these two species in that place as a polymorphism of presence/absence of the vertebral line in *A. neuquensis* (Carmen Úbeda, personal communication). Therefore, the absence of reciprocal monophyly (at least of mitochondrial DNA) and morphological affinity (coloration patterns and polymorphism of the vertebral line) between *A. vittatus* and *A. neuquensis* indicate that it is necessary to evaluate the possible conspecificity of these two species. Finally, it is necessary to emphasize that the relationships among the lineages made up of *A. barrioi*, *A. norae*, *A. gargola*, *A. igneus* and *A. vittatus* + *A. neuquensis* are not well resolved (low support values) as observed in previous studies (e.g., Blotto et al. 2013; Charrier et al. 2015).

Discussion

More than 120 years after its publication, Philippi’s “Suplemento” continues to have a significant influence on the current taxonomy of Chilean amphibians. Editorial issues (such as the non-publication of the figures), museological problems (the loss of most of the types), and taxonomic challenges (e.g., numerous species that are not currently recognizable) (Formas 1995) led to the near-complete dismissal of this work (Cei 1958). However, later discoveries confirmed the validity of some of the described species. The rediscovery of *A. vittatus*, after 130 years since the collection of the type specimens, demonstrates that Philippi’s taxonomic legacy has not yet been fully dimensioned.

The data and material available for *A. vittatus* are exceptional among the amphibian species described by Philippi. Firstly, it is one of the few species in the “Suplemento” that has a precisely defined type locality, as well as the name of the collector and year of collection. Although, in this case, the type locality turned out to be extraordinarily broad, a detailed investigation of this information and other historical documents enabled the identification of the route followed by Germain in 1893 (Fig. 1B; see details in Correa et al. 2023) and so a more specific area where the species was finally found. Secondly, the most conspicuous external characteristic originally described for *A. vittatus*—”a white or yellow band, which runs from the tip of the snout to the anus” (from which its name is derived; Lavilla 2021)—is clearly observed in Philippi’s original drawing, which was published later (Cei 1958). This characteristic facilitated its unambiguous identification in the field. Thirdly, *A. vittatus* is one of the few amphibian species described by Philippi (1902) for which a type specimen has survived, specifically one of the three original syntypes. The careful examination of this specimen (Fig. 2C) allowed Formas (1989a) to definitively clarify that the species belongs to the genus *Alsodes*. All this information together provides a stronger evidential basis to support the validity of *A. vittatus* compared to other taxa from the same area described by Philippi (1902) that would be congeneric (e.g., *Borborocoetus verrucosus* and *B. andinus*).

As previously mentioned, the most distinctive external feature of *A. vittatus* is its vertebral line, observable in the only remaining syntype, as well as in some recently collected specimens. However, our molecular data reveal that this line represents an intraspecific polymorphism, which we verified in two newly described populations, despite the low number of individuals observed. The polymorphism of presence/absence of the vertebral line has been documented in several species of *Alsodes* (e.g., *A. gargola*, Gallardo 1970; *A. hugoi* Cuevas & Formas, 2001; Correa et al. 2018; *A. verrucosus* from Puyehue, Chile, Charrier 2019, and from Pucará, Lake Lácar, Argentina; Cei 1980; *A. neuquensis*, Carmen Úbeda, personal communication), as well as in other genera inhabiting Chile, such as *Eupsophus* (notably within the species of the *vertebralis* group; Formas 1989b) and *Pleurodema* (e.g., *P. thaul* (Schneider, 1799), Cei and Capurro 1957). Therefore, despite the importance that Philippi gave to this feature in the description of the species, our observations allow us to rule it out as a diagnostic character.

Another distinctive feature of the description of *A. vittatus*, evident in the original drawing, is the more or less intense black color of the upper part of the body. We observed juvenile individuals with dark brown coloration and a vertical line very similar to that depicted in the drawing (Fig. 3E) and with a size similar to the SVL reported by Philippi (1902) for the species (41 mm). This suggests that the description may have been based on immature specimens with that coloration. In addition to these dark-colored juveniles, we observed adults (males and females) and juveniles with different color patterns coexisting in two locations, but despite the low number of individuals observed, we did not find an association between certain colorations and developmental stage and/or sex. We also did not observe whether individuals changed color or whether coloration was associated with certain microhabitat characteristics (for example, lighter or darker substrates), so we interpret the variation in coloration as intra- and interpopulation polymorphism. However, we cannot rule out the possibility of ontogenetic variation and that the different color patterns are transient responses to thermoregulatory requirements or strategies for camouflage in environments with different degrees of illumination, as has been described in other anurans (e.g., Kang et al. 2016, Park et al. 2023).

From a phylogenetic perspective, all the new populations described here are grouped with *A. barrioi*, *A. igneus*, *A. gargola*, *A. neuquensis* and *A. norae*, a clade recognized since Blotto et al. (2013), which makes biogeographical sense. Although the relationships among these species remain unsolved, the populations along the road to the Termas de Pemehue locality are more closely related to *A. igneus*, while the populations of *A. vittatus* are grouped with *A. neuquensis*, in both cases with high support. In the first one, the taxonomic decision seems uncontroversial, but the second poses a more complex situation. The specimens from the populations that we identify as *A. vittatus* are paraphyletic with respect to the only specimen of *A. neuquensis* included in the analysis. Although this may be due in part to using only mitochondrial evidence and a shorter fragment of cytochrome *b* from *A. neuquensis*, the high morphological similarity between the male with vertebral line from Tupuyuntué River (Figs 2E, 3A) and the specimen from the vicinity of Primeros Pinos (identified as *A. verrucosus* by Cei 1987; Lavilla and Cei 2001) is evident. Therefore, morphological similarity, shared vertebral line polymorphism, lack of reciprocal mitochondrial monophyly, and geographic proximity suggest that *A. vittatus* and *A. neuquensis* could be the same species.

The IUCN lists *A. vittatus* as Data Deficient, recognizing that it has not been observed again in more than 100 years and that there is no population, ecological, distributional, or threat information available for this species. However, the official classification system of the Government of Chile, made official by Supreme Decree No. 42/2011 of the Ministry of the Environment, considers it Critically Endangered due to its reduced distribution, restricted to the type locality, and the deterioration of its habitat due to agricultural and forestry activity. The latter is an observation by Formas (1989a) referring to the area of the Termas de Pemehue, where according to our data, only *A. igneus* is found, so the current Chilean categorization refers to this taxon. Therefore, it is necessary to review whether the available information from the newly discovered populations of *A. vittatus* is sufficient to reevaluate its conservation category under the criteria of IUCN.

The maximum distance between the new three localities of *A. vittatus* is ~3.5 km in a straight line (Fig. 1), but they are located in the headwaters of two different hydrographic sub-basins. Two of these localities are directly hydrographically connected, so according to the IUCN guidelines, they could be considered only two localities. The three original localities are arranged in a line with a north-south direction, so it is difficult to estimate the extent of occurrence; however, due to their distances, the area of occupancy can be approximated to be 8 km^2. Applying criterion B, this falls within the limits to classify it as Critically Endangered, but the condition of a severely fragmented range, or number of localities equal to one can be ruled out (condition a). There is also no indication that the range, population numbers, or abundance are fluctuating extremely (condition c), but our observations suggest that criterion b can be applied cautiously.

The new populations are found in montane forests dominated by *Nothofagus* and *Araucaria araucana*. Satellite images show that the forest is continuous only in the highest parts of these mountain systems (at the sources of the valleys) and highly fragmented in the lower parts of the valleys (such as Naranjo or Portales River). We were able to confirm that there is timber exploitation and livestock activity throughout the entire valley, and the presence of introduced salmonids (trout) in the highest flow rivers throughout the area. Two other recognized threats in the area are forest fires and the presence of *Didymosphenia geminata* (didymo) in some Andean water systems (reported in state reports). In addition, testimonies from local residents indicate that summers are becoming increasingly hotter in the area, with less snow accumulation in winter. This suggests that climate change could constitute an additional threat. Therefore, considering all these factors, we infer a continuing decline in habitat quality and recommend evaluating this species as Endangered based on the B2ab(iii) criterion.

In summary, the rediscovery of *A. vittatus* shows that there are still aspects of Philippi's work that need to be revised. Furthermore, it confirms the limited biogeographic knowledge of amphibians in this area of the Andes, particularly concerning *Alsodes*, as the new populations were found in an extensive region where there were no previous records of the genus (compare with Correa et al. 2018). Findings like these demonstrate that a greater exploration effort, guided by rigorous historical research, is required to continue revealing the diversity and distribution patterns of Chile's amphibians.

Acknowledgements

We would like to thank Pablo Rojas (Canoas del Diablo stream), David Espinoza and Felipe Durán (unnamed stream) for their valuable assistance in the field and Catherine Pardo for her help with mapping. We acknowledge the capture permits 4394/2022 and 3917/2023 granted by the SAG. Finally, we thank the Mapuche Pehuenche community of Lonquimay for allowing us to conduct this study in their territory.

Additional information

Conflict of interest

The authors have declared that no competing interests exist.

Ethical statement

This study had the bioethical approval of the ethics, bioethics and biosafety committee of the Vicerrectoría de Investigación y Desarrollo (VRID) of the Universidad de Concepción (CEBB 197-2022).

Funding

Field work in the Pemehue area (2015–2016) was funded by Fondecyt Project PAI 79130032 (C. Correa).

Author contributions

Conceptualization: CC. Formal analysis: CC. Investigation: JPD, ERR, CC. Resources: ERR, CC. Writing - original draft: CC. Writing - review and editing: ERR, JPD.

Author ORCIDs

Claudio Correa https://orcid.org/0000-0002-2081-3565

Data availability

All of the data that support the findings of this study are available in the main text.

References

Blotto BL, Nuñez JJ, Basso NG, Úbeda CA, Wheeler WC, Faivovich J (2013) Phylogenetic relationships of a Patagonian frog radiation, the *Alsodes* + *Eupsophus* clade (Anura: Alsodidae), with comments on the supposed paraphyly of *Eupsophus*. Cladistics 29(2): 113–131. https://doi.org/10.1111/j.1096-0031.2012.00417.x

Camousseight A (2005) La contribución entomológica de R.A. Philippi entre 1859 y 1875 y el estado actual de sus especies. Boletín del Museo Nacional de Historia Natural, Chile 54: 81–106. html https://doi.org/10.54830/bmnhn.v54.2005.283

Castro SA, Camousseight A, Muñoz-Schick M, Jaksic FM (2006) Rodulfo Amando Philippi, el naturalista de mayor aporte al conocimiento taxonómico de la diversidad biológica de Chile. Revista Chilena de Historia Natural 79(1): 133–143. https://doi.org/10.4067/S0716-078X2006000100011

Cei JM (1958) Las láminas originales del suplemento a los batraquios chilenos de Philippi: primera impresión y comentarios. Investigaciones Zoológicas Chilenas 4: 265–288.

Cei JM (1980) Amphibians of Argentina. Monitore Zoologico Italiano (N.S.) Monografia 2: [XII +] 609.

Cei JM (1987) Additional notes to "Amphibians of Argentina": an update, 1980–1986. Monitore Zoologico Italiano - Italian Journal of Zoology 21(3): 209–272. https://www.tandfonline.com/doi/abs/10.1080/00269786.1987.10736530

Cei JM, Capurro LF (1957) La distribución de los patrones de coloración en *Pleurodema bibroni* en relación con la distribución geográfica y el hábitat. Investigaciones Zoológicas Chilenas 3(8–10): 156–161.

Charrier A (2019) Guía de Campo: Anfibios de los Bosques de la Zona Centro Sur y Patagonia de Chile. Ed. Corporación Chilena de la Madera, Chile, 300 pp. https://fundacionphilippi.cl/wp-content/uploads/2020/03/Anfibios-de-los-bosques-de-la-zona-centro-sur-y-patagonia-de-Chile.pdf

Charrier A, Correa C, Castro C, Méndez MA (2015) A new species of *Alsodes* (Anura: Alsodidae) from Altos de Cantillana, central Chile. Zootaxa 3915: 540–550. https://doi.org/10.11646/zootaxa.3915.4.5

Coan EV, Kabat AR (2017) The Malacological Contributions of Rudolph Amandus Philippi (1808–1904). Malacologia 60(1–2): 31–322. https://doi.org/10.4002/040.060.0108

Correa C, Veloso A, Iturra P, Méndez MA (2006) Phylogenetic relationships of Chilean leptodactylids: a molecular approach based on mitochondrial genes 12S and 16S. Revista Chilena de Historia Natural 79(4): 435–450. https://doi.org/10.4067/S0716-078X2006000400003

Correa C, Lobos G, Pastenes L, Méndez MA (2008) Invasive *Pleurodema thaul* (Anura, Leiuperidae) from Robinson Crusoe Island: molecular identification of its geographic origin and comments on the phylogeographic structure of this species in mainland Chile. Herpetological Journal 18(2): 77–82.

Correa C, Pastenes L, Iturra P, Calderón P, Vásquez D, Lam N, Salinas H, Méndez MA (2013) Confirmation of the presence of *Alsodes pehuenche* Cei, 1976 (Anura, Cycloramphidae) in Chile: morphological, chromosomal and molecular evidence. Gayana 77(2): 117–123. https://doi.org/10.4067/S0717-65382013000200006

Correa C, Zepeda P, Lagos N, Salinas H, Palma RE, Vásquez D (2018) New populations of two threatened species of *Alsodes* (Anura, Alsodidae) reveal the scarce biogeographic knowledge of the genus in the Andes of central Chile. Zoosystematics and Evolution 94(2): 349–358. https://doi.org/10.3897/zse.94.25189

Correa C, Morales J, Schussler C, Ortiz JC (2020) An enigmatic population of *Alsodes* (Anura, Alsodidae) from the Andes of central Chile with three species-level mitochondrial lineages. Mitochondrial DNA Part A 31(1): 25–34. https://doi.org/10.1080/24701394.2019.1704744

Correa C, Osses JI, Morales JA, Ortiz JC (2023) Geographic distribution of the rare and endangered *Telmatobufo venustus* (Philippi, 1899) (Anura, Calyptocephalellidae), with the description of a new locality and comments on the type locality. Herpetozoa 36: 335–343. https://doi.org/10.3897/herpetozoa.36.e107328

Cuevas CC, Formas JR (2005) A new frog of the genus *Alsodes* (Leptodactylidae) from the Tolhuaca National Park, Andes Range, southern Chile. Amphibia-Reptilia 26(1): 39–48. https://doi.org/10.1163/1568538053693288

Donoso-Barros R (1976) *Eupsophus vittatus* Philippi: revalidación de una buena especie. Archivos de Biología y Medicina Experimentales 10(1–3): R49–50.

Donoso-Barros R, Cárdenas S (1965) Los tipos de serpiente de Rodulfo Amando Philippi, en el Museo de Historia Natural de Santiago de Chile. Anais do Segundo Congresso Latino-Americano de Zoologia 2: 225–234.

Faivovich J, Haddad CFB, Garcia PCA, Frost DR, Campbell JA, Wheeler WC (2005) Systematic review of the frog family Hylidae, with special reference to Hylinae: Phylogenetic analysis and taxonomic revision. Bulletin of the American Museum of Natural History 294: 1–240. https://doi.org/10.1206/0003-0090(2005)294[0001:SROTFF]2.0.CO;2

Formas JR (1989a) Sinonimia e identidad de la rana austral chilena *Eupsophus vittatus* (Philippi, 1902) (Anura, Leptodactylidae). Boletín de la Sociedad de Biología de Concepción 60: 123–127.

Formas JR (1989b) A new species of *Eupsophus* (Amphibia: Anura: Leptodactylidae) from Southern Chile. Proceedings of the Biological Society of Washington 102(3): 568–576.

Formas JR (1995) Anfibios. In: Simonetti JA, Arroyo MTK, Spotorno AE, Lozada E (Eds) Diversidad biológica de Chile. Comisión Nacional de Investigación Científica y Tecnológica, Santiago, 314–325.

Formas JR, Veloso A (1982) Taxonomy of *Bufo venustus* Philippi, 1899 (Anura: Leptodactylidae) from Central Chile. Proceedings of the Biological Society of Washington 95(4): 688–693.

Formas JR, Vera MI (1983) Karyological Relationships among Frogs of the Genus *Alsodes*, with Description of the Karyotypes of *A. vanzolinii* and *A. verrucosus*. Copeia 1983(4): 1104–1107. https://doi.org/10.2307/1445121

Formas R, Pugín E, Jorquera B (1975) La identidad del batracio chileno *Heminectes rufus* Philippi 1902. Physis 34(89): 147–157.

Gallardo JM (1970) A propósito de los Telmatobiinae (Anura, Leptodactylidae) patagónicos. Neotropica 16(50): 73–85.

Germain P (1894) Apuntes sobre los insectos de Chile. Anales de la Universidad de Chile 87: 59–76. https://anales.uchile.cl/index.php/ANUC/article/view/20781

IUCN SSC Amphibian Specialist Group (2016) *Alsodes vittatus*. The IUCN Red List of Threatened Species 2016: e.T56322A79811780. https://doi.org/10.2305/IUCN.UK.2016-1.RLTS.T56322A79811780.en [Accessed on 24 August 2024]

Kabat AR, Coan EV (2017) The Life and Work of Rudolph Amandus Philippi (1808–1904). Malacologia 60(1–2): 1–30. https://doi.org/10.4002/040.060.0103

Kang C, Kim YE, Jang Y (2016) Colour and pattern change against visually heterogeneous backgrounds in the tree frog *Hyla japonica*. Scientific Reports 6: 22601. https://doi.org/10.1038/srep22601

Klubock TM (2022) Ránquil. Rural Rebellion, Political Violence, and Historical Memory in Chile. Yale University Press, 352 pp. https://www.jstor.org/stable/j.ctv240df24

Lavilla EO (2021) Etimologías de los anfibios de Chile. Boletín Chileno de Herpetología 8: 36–54. http://www.boletindeherpetologia.com/uploads/3/2/2/9/32291217/4._lavilla2021.pdf

Lavilla EO, Cei JM (2001) Amphibians of Argentina. A Second Update, 1987–2000. Monografie di Museo Regionale di Scienze Naturali, Torino 28: 1–177.

Mella-Romero J, Mella J, Muñoz C, Correa C (2022) Range extension of Catedral spiny-chest frog, *Alsodes gargola* Gallardo, 1970: a record in an unknown road of the Chilean Patagonia. Gayana 86(1): 22–29. https://doi.org/10.4067/S0717-65382022000100022

Muñoz-Schick M, Morales V, Moreira-Muñoz A (2012) La colección de tipos de plantas vasculares del Herbario Nacional de Chile (SGO): análisis histórico, temporal y espacial. Gayana Botánica 69(1): 123–135. https://doi.org/10.4067/S0717-66432012000100012

Park C, No S, Yoo S, Oh D, Hwang Y, Kim Y, Kang C (2023) Testing multiple hypotheses on the colour change of treefrogs in response to various external conditions. Scientific Reports 13: 4203. https://doi.org/10.1038/s41598-023-31262-y

Philippi RA (1899) Sobre las serpientes de Chile. Anales de la Universidad de Chile 104: 715–723. https://www.revistas.uchile.cl/index.php/ANUC/article/view/21463/22760

Philippi RA (1902) Suplemento a los Batraquios chilenos descritos en la Historia Física i Política de Chile de don Claudio Gay. Librería Alemana de José Ivens, Santiago, Chile, [Xi +] 161 pp. https://doi.org/10.5962/bhl.title.104403

Rambaut A, Drummond AJ, Xie D, Baele G, Suchard MA (2018) Posterior summarization in Bayesian phylogenetics using Tracer 1.7. Systematic Biology 67(5): 901–904. https://doi.org/10.1093/sysbio/syy032

Ronquist F, Teslenko M, van der Mark P, Ayres DL, Darling A, Höhna S, Larget B, Liu L, Suchard MA, Huelsenbeck JP (2012) MrBayes 3.2: efficient Bayesian phylogenetic inference and model choice across a large model space. Systematic Biology 61(3): 539–542. https://doi.org/10.1093/sysbio/sys029

Taylor CM, Muñoz-Schick M (1994) The Botanical Works of Philippi, Father and Son, in Chile. Annals of the Missouri Botanical Garden 81(4): 743–748. https://doi.org/10.2307/2399918

Vellard J (1947) Dos batracios interesantes de la región de Bariloche. Acta Zoológica Lilloana 4: 145–153.

Webb RG, Greer JK (1969) Amphibians and reptiles from Malleco Province. Publications of the Museum, Michigan State University, Biological Series 4(6): 193–226.

ZooKeys 1230: 213–229 (2025)
DOI: 10.3897/zookeys.1230.139837

Review Article

Comparison of muscle structure and transcriptome analysis of eyed-side muscle and blind-side muscle in *Cynoglossus semilaevis* (Osteichthyes, Cynoglossidae)

Zhenming Lü[1], Yuzhen Wang[2], Jing Yu[1], Yijing Yang[1], An Xu[1], Li Gong[1], Jing Liu[1], Fenghui Li[1], Liqin Liu[1]

1 *National Engineering Laboratory of Marine Germplasm Resources Exploration and Utilization, College of Marine Sciences and Technology, Zhejiang Ocean University, Zhoushan 316022, China*
2 *National Engineering Research Center for Facilitated Marine Aquaculture, Zhejiang Ocean University, Zhoushan 316022, China*
Corresponding author: Liqin Liu (liulq@zjou.edu.cn)

Academic editor: Maria Elina Bichuette
Received: 22 October 2024
Accepted: 11 December 2024
Published: 6 March 2025

ZooBank: https://zoobank.org/18E36063-48E3-4426-B162-0904DC7BF407

Citation: Lü Z, Wang Y, Yu J, Yang Y, Xu A, Gong L, Liu J, Li F, Liu L (2025) Comparison of muscle structure and transcriptome analysis of eyed-side muscle and blind-side muscle in *Cynoglossus semilaevis* (Osteichthyes, Cynoglossidae). ZooKeys 1230: 213–229. https://doi.org/10.3897/zookeys.1230.139837

Abstract

Cynoglossus semilaevis (Osteichthyes, Cynoglossidae) is one of the most significant commercial marine fish species in China and has evolved a specialized asymmetrical body axis. In addition, *C. semilaevis* displays different muscle thickness between the eyed side and the blind side. However, the mechanisms underlying the muscle development difference between the two sides in *C. semilaevis* are unclear. In this study, we generated the first comparative investigation on the structure of muscle cells, and transcriptome analysis between the eyed-side muscle (ESM) and blind-side muscle (BSM) in *C. semilaevis*. Histological assays showed the obvious mosaic appearance of muscles on both the eyed side and blind side. However, the number of new muscle cells in ESM was significantly more than that in the BSM group. Comparative analyses of RNA-seq data showed that 1177 differentially expressed genes (DEGs) were identified between ESM and BSM groups, including 291 up-regulated and 886 down-regulated genes. The expression levels of myosin family genes (actin, myosin-binding protein C, titin, troponin, tnnil, and astrotactin-2) were significantly higher in ESM and might be a candidate regulator of muscle filament assembly in *C. semilaevis*. Murine double minute 2 (Mdm2) and cyclin A2 (ccna2) were also up-regulated in ESM, which indicates that the muscle development difference between ESM and BSM in *C. semilaevis* might be owing to the variation in myofibroblast proliferation. In addition, KEGG pathway enrichment analyses suggested that the glycolysis/gluconeogenesis pathway may be involved in the muscle development of *C. semilaevis*. Taken together, this study may provide useful information to understand the molecular mechanism of muscle development in flatfishes.

Key words: *Cynoglossus semilaevis*, differentially expressed genes, flatfishes, gluconeogenesis, glycolysis, muscle development, regulatory mechanism, transcriptome analysis

Introduction

External asymmetry is common in flatfishes, though rare in vertebrates. However, the asymmetry of flatfishes is astonishing because the flatfish larvae are perfectly symmetrical (Janvier 2008). The transformation of symmetrical larvae into asymmetrical juvenile is completed by the process of metamorphosis, in which the entire head structure is rapidly remodeled, involving the migration of one eye to the opposite side of the head (Schreiber 2006). After metamorphosis, the adult flatfish have a pigmented 'eyed' (dorsal) side and a non-pigmented 'blind' (ventral) side. In addition to eye-sidedness, another characteristic of postembryonic asymmetry is the presence of a much larger muscle thickness on the eyed side of adult individuals compared to the blind side in flatfishes (Hagen et al. 2008; Lü et al. 2021). In fish, muscle accounts for approximately 50%-70% of the body weight, and is the main consumed product (Valente et al. 2013). Its development influenced fish meat production and aquaculture development. Therefore, understanding the underlying mechanisms controlling fish muscle development of flatfishes is not only crucial to the aquaculture industry, but also provides insights for understanding the molecular mechanism of the asymmetrical body axis.

Muscle development in fish is different from that of mammals in which hypertrophic and hyperplasic growth continues throughout much of the life cycle (Johnston 1999; Veggetti et al. 1999). It is a polygenic and complex biological process that is influenced by a series of genes and signaling pathways (Ahammad et al. 2019; Rescan 2019; Chen et al. 2023; Yao et al. 2024). There have been many studies investigating how these genes and signaling pathways affect muscle development and growth in fish. For example, genes in the growth hormone-insulin-like growth factor-I (GH/IGF) axis have been identified as key genes in regulating muscle growth and development in Atlantic salmon (*Salmo salar*) (Johnston et al. 2003), and the glycolysis/gluconeogenesis pathway could influence the growth of starry flounder (*Platichthys stellatus*) and *C. semilaevis* (Osteichthyes, Cynoglossidae) (Wang et al. 2021). Zhang et al. (2021) observed the critical genes related to PI3K/Akt and mTOR signaling pathways to be involved in muscle development in grass carp (*Ctenopharyngodon idella*). Therefore, it is of great importance to identify muscle development-related genes and regulative pathways and analyze the molecular mechanisms responsible for fish muscle development.

Recently, with the development of high-throughput sequencing, RNA sequencing (RNA-seq) has provided a rapid and effective way of whole transcriptome analysis to characterize the differentially expressed genes (DEGs) and pathways related to muscle development of fish (Lu et al. 2020; Mohindra et al. 2022; Li et al. 2024a; Luo et al. 2024). For example, in Chinese longsnout catfish (*Leiocassis longirostris*) muscle tissue, 580 DEGs were identified in fish with different growth rates through RNA-seq. And some genes related to feeding behavior (pyruvate kinase and fatty acid-binding protein) were speculated to be the key genes in regulating muscle growth (Li et al. 2024b). In a study on rice flower carp (*Cyprinus carpio*),403 DEGs were identified in muscle tissue from different-sized individuals through RNA-seq. And some genes involved in promoting muscle contraction (such as gamma-actin, cytoplasmic beta actin, calcium/calmodulin-dependent kinase 2a), and the ubiquitin-proteasome pathway were thought to be related to fish growth (Li et al. 2022). These results indicated that RNA-seq could be an effective tool to identify the candidate genes related to fish growth.

Cynoglossus semilaevis belongs to the Cynoglossidae family and is an important economic marine fish species (Meng et al. 2018). Similar to other flatfishes, *C. semilaevis* also has a flat and asymmetrical body axis, and the muscle thickness on the 'eyed' side is greater than on the 'blind' side. So it is an ideal species for studying muscle development. However, previous studies have mainly focused on muscle development differences in females and males of *C. semilaevis* (Wang et al. 2021; Shi et al. 2023; Wang et al. 2023; Mai et al. 2024); muscle development on the different sides ('eyed' side and 'blind' side) of the one individual has not been reported. Here, we selected the eyed and blind side muscles in *C. semilaevis* (from the same individual) for muscle tissue structure and comparative transcriptome analysis. The results will not only help to provide potential candidate genes for muscle development but also reveal the regulatory mechanism of the asymmetrical body axis of *C. semilaevis*.

Materials and methods

Sample collection and preparation

Cynoglossus semilaevis used in this study were obtained from a commercial fish farm in Daishan (Zhoushan, China). Five fish (at 2.5 months post-fertilization (mpf), length 5–6 cm) were randomly chosen for this study. All fish sampled were anesthetized with tricaine methanesulfonate (MS-222, 150 mg/L) for subsequent sampling.

The muscle tissue pieces (length 1.5 cm) were dissected out of fish samples at the level of the anal opening and then fixed in 4% paraformaldehyde (PFA) for morphological observation.

Meanwhile, the eyed-side muscle (ESM) and blind-side muscle (BSM) from the same individual were collected for RNA-seq. All samples were frozen in liquid nitrogen, and stored at –80 °C for analysis.

Muscle histological assay and muscle thickness measurement

The fixed muscle tissues were dehydrated through a series of graded ethanol and embedded in paraffin wax. Transverse serial wax sections, 4 μm thick, were cut transversely to the long body axis and stained with hematoxylin-eosin (H&E). Sections were mounted on a glass slide with a cover slip and neutral resin, and photographed under light microscopy with a 40× objective lens (Nikon Ni-U, Tokyo, Japan).

Three pictures were taken of each sample, and the muscle thickness in the picture was measured. A vertical dotted line was drawn from the spine toward the epidermis as shown in Fig. 1A. The distance was specified as the subscapularis muscle thickness value. The muscle thickness from two sides was analyzed in all samples. Morphological data of muscle thickness was shown by the mean of three pictures.

RNA extraction, cDNA library construction, and sequencing

Total RNA was extracted using the TRIzol Reagent kit (Invitrogen, Carlsbad, CA, USA) according to the manufacturer's protocols (Rio et al. 2010). RNA quality and integrity were evaluated using an Agilent 2100 Bioanalyzer (Agilent Technologies, CA, USA). Then, total RNA was subjected to next-generation sequencing using the DNBSEQ-T7 platform at the Novogene Bioinformatics Technology Co., Ltd. (Tianjin, China). The cDNA libraries of three ESM and three BSM groups were sequenced using the DNBSEQ-T7 platform with 150 bp paired-end reads.

Data processing and bioinformatics analysis

Raw sequencing reads of six transcriptome datasets were cleaned by removing the adaptors and low-quality reads using Trimmomatic (v. 0.36) (Bolger et al. 2014). The obtained clean data were then quality-controlled by calculating the values of GC-content, Q20, and Q30 values. After quality control of each sample, the clean data were aligned to the reference gene of *C. semilaevis* (https://www.ncbi.nlm.nih.gov/datasets/genome/GCF_000523025.1/) using HISAT2 (v. 2.0.5) (Mortazavi et al. 2008)

Analysis of DEGs

The gene expression levels were calculated by fragments per kilobase of transcript per million reads (FPKMs) mapped (Mortazavi et al. 2008). Differentially expressed genes (DEGs) were identified utilizing the DESeq2 R package, with a significance *P*- value ≤ 0.05 and |log2 (FoldChange)| ≥ 1 (Love et al. 2014). Furthermore, the R package was utilized to perform the analysis and visualization of volcanic diagrams and heat maps of DEGs. Next, these identified DEGs were subjected to functional enrichment analysis, including gene ontology (GO) enrichment analysis and Kyoto Encyclopedia of Genes and Genomes (KEGG) pathway analyses via the R package clusterProfiler (v. 3.8.1) (Yu et al. 2012). GO terms and KEGG pathways with a $P \leq 0.05$ were considered significantly enriched.

Analysis of DAS

Alternative Splicing (AS) was conducted using rMATs (v. 4.1.0) software, including SE, MXE, A5SS, A3SS, and RI for each sample (Shen et al. 2014). For each AS event, rMATS calculated the percentage of exon inclusion (IncLevel) for each sample across the biological triplicates and detected differential IncLevel (IncLevel Difference) between the two groups. The differential alternative splicing (DAS) events were screened and categorized using summary.py in rMATS based on an IncLevelDifference absolute value greater than 0.1 and false discovery rate (FDR)<0.05.

Data validation by real-time PCR

To evaluate the reliability of the RNA-seq data, 9 DEGs were randomly chosen for RT-qPCR. 18S rRNA was chosen as the internal control. Total RNA was extracted as described above. The cDNA was synthesized from 1 μg of total RNA using an M-MLV reverse transcriptase (RNase H^-) (TaKaRa Bio Inc., Japan). Primers were designed using Primer 5.0 software (Suppl. material 1). RT-qPCR experiments in a total volume of 12.5 μ contained 0.6 μL of cDNA, 0.25 μL of each primer, 6.25 μL of SYBR Green mix, and 5.15 μL of ddH_2O. The amplification program was 95 °C for 2 min, 40 cycles at 95 °C for 5 s, 60 °C for 30 s, 72 °C for 3s. The expression level of genes was calculated using the $2^{-\Delta\Delta Ct}$ method, and each sample was performed in triplicate (Livak and Schmittgen 2001).

Statistical analysis

All data are shown as the mean ± standard error (SE). Statistical analysis was performed with SPSS 26.0 (SPSS, USA). One-way analysis of variance (ANOVA) was used to compare if there were differences between samples. Significant difference was obtained at $p < 0.05$, which was indicated by an asterisk (*).

Results

Muscle structure and thickness in eyed side and blind side of *C. semilaevis*

Transverse sections of *C. semilaevis* are shown in Fig. 1A. The muscle cells were arranged neatly, showed an obvious mosaic appearance, and the cell lines were visible. New muscle cell neogenesis (colored dark in Fig. 1A) is produced in the middle parts of the myotomes, neighboring to the horizontal septum, and extends to the end ventrally, which results in a mosaic appearance. In the same visual field, the number of new muscle cells in the ESM was significantly more than that in the BSM (Fig. 1A). Furthermore, the muscle thickness in the ESM (15.30 mm) was significantly greater than that in the BSM (13.33 mm) (Fig. 1B, $P < 0.05$). These results suggest that the mosaic hyperplastic growth of muscle cells may result in differences in muscle development and growth.

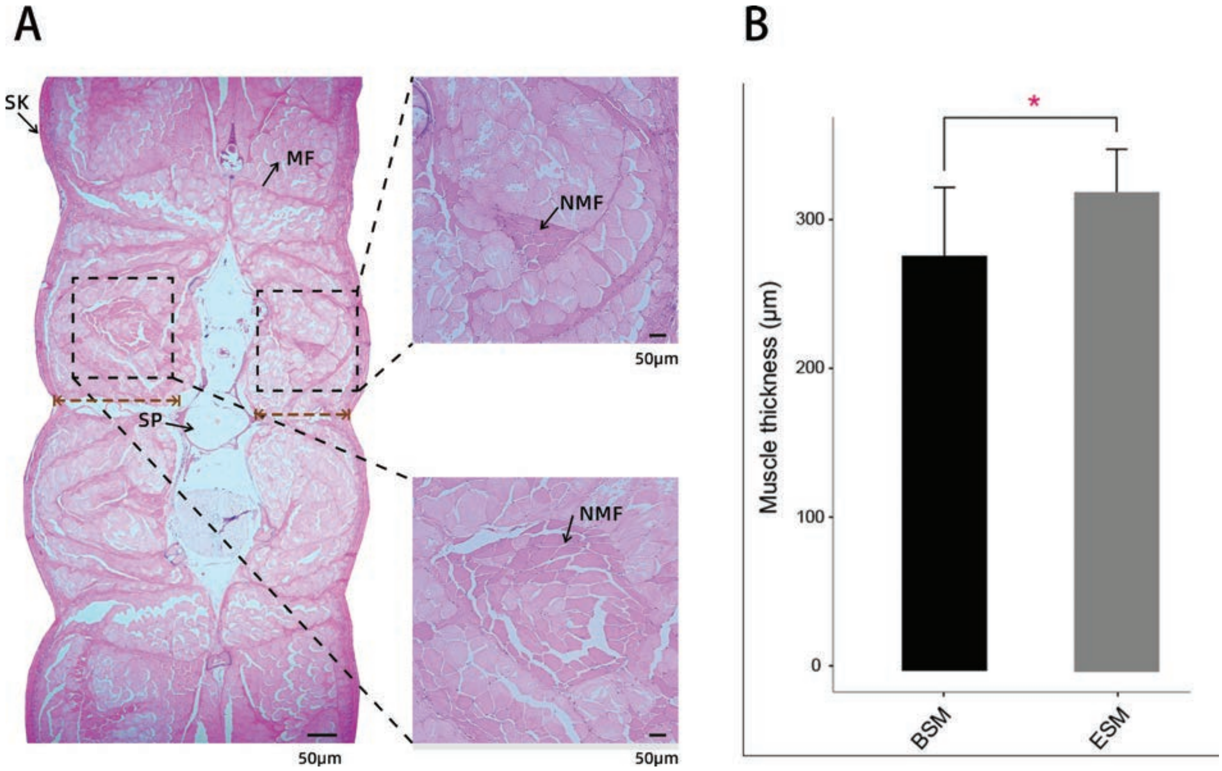

Figure 1. A histological transverse section of muscle tissue stained with haematoxylin and eosin in *C. semilaevis*. The arrow demonstrates the position of small new fibers. SK: skin; SC: Spinal cord; N: notochord; P: permysium; scale bar = 50 μm **B** the muscle thickness of ESM and BSM. Data was shown as mean ± standard error (SE) (*N* = 5), "*" indicates significant difference ($p < 0.05$).

Summary statistics of transcriptome sequencing

In this study, we constructed a total of six cDNA libraries from two groups, each replicated three times, with an average of 51.89 and 48.06 Mb raw reads for ESM and BSM, respectively. After quality filtering and assessment, an average of 50.52 million and 46.38 million clean reads were yielded, respectively. The GC percentage ranged from 51.77% to 52.62%, with Q20 > 98.38%, Q30 > 94.53%, and no more than 0.02% error rate (Table 1). In addition, over 94% of the clean reads (94.12% - 94.69%) were mapped to the reference genome of *C. semilaevis*. These results indicated that the sequencing data were reliable and could be used for subsequent analysis (Table 1). All raw data obtained in this study were submitted to the NCBI Sequence Read Archive database under the project (PRJNA1196394).

Identification and comparative analysis of the DEGs

In total, 1177 DEGs were identified by comparing the ESM vs BSM group (Suppl. material 1), of which 291 were up-regulated and 886 were downregulated (Fig. 2A). We constructed a clustered heatmap to depict the expression profile of DEGs between ESM vs BSM group. The clustered heatmap showed that the expression patterns within the two groups were mainly divided into main clades, indicating that some DEGs may perform the same or a similar function in a pathway (Fig. 2B).

Functional enrichment of DEGs

To explore the function of *C. semilaevis* muscle development-related genes and perform the potential functional annotation of DEGs, GO annotation and KEGG enrichment analyses were performed. The GO enrichment analysis showed that 1177 DEGs were enriched in 631 GO terms, and 43 terms were significantly enriched (Suppl. material 2). Fig. 3 shows the top 30 GO terms, of which 21 are associated with biological process (BP), two are related to cellular component (CC), and seven are related to molecular function (MF). These terms mainly affected peptidase inhibitor activity, peptidase regulator activity, carbohydrate metabolic process, endopeptidase inhibitor activity, etc.

KEGG enrichment analysis indicated that DEGs were annotated into 121 KEGG pathways and 19 pathways were significantly enriched (Suppl. material: Suppl. material 3). As shown in Fig. 4, the main significantly enriched pathways were “cell adhesion molecules”, “Tight junction”, “Amino sugar and nucleotide sugar metabolism”, “ECM-receptor interaction” pathways, etc. Among all the metabolic pathways, glycolysis/gluconeogenesis may be a key regulation pathway in skeletal muscle energy metabolism, including 12 DEGs.

Table 1. Sequencing statistics of six *C. semilaevis* muscle transcriptome sequencing samples.

Sample	Raw reads	Clean reads	Q20 (%)	Q30 (%)	GC (%)	Total mapped	Uniquely mapped
ESM1	48891078	47733506	98.38	95.69	49.8	45036059(94.35%)	42379887(88.78%)
ESM2	49458754	48288312	98.42	95.79	50.1	45664547(94.57%)	42834580(88.71%)
ESM3	57334764	55560808	98.37	95.66	50.22	52295278(94.12%)	48688909(87.63%)
BSM1	50618302	49421064	98.64	96.35	50.13	46563975(94.22%)	43617860(88.26%)
BSM2	47020094	44996010	98.8	96.78	49.8	42352606(94.13%)	39497453(87.78%)
BSM3	46550722	44732880	99.02	97.26	49.86	42358102(94.69%)	39536319(88.38%)

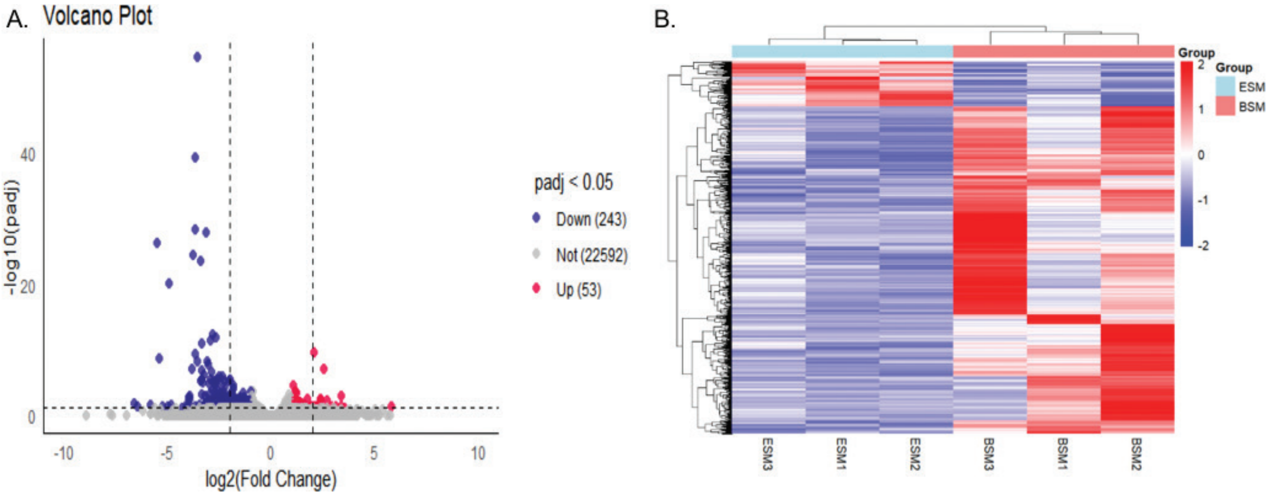

Figure 2. A volcano plot of DEGs between ESM and BSM groups (red dots represent up-regulated genes, blue dots represent down-regulated genes, and gray dots represent indistinguishable genes) **B** heatmap plot of DEGs in ESM and BSM groups of *C. semilaevis*. X-axis represents sample name. Y-axis represents the relative expression of DEGs. The different colors indicated changes in the relative expression of DEGs.

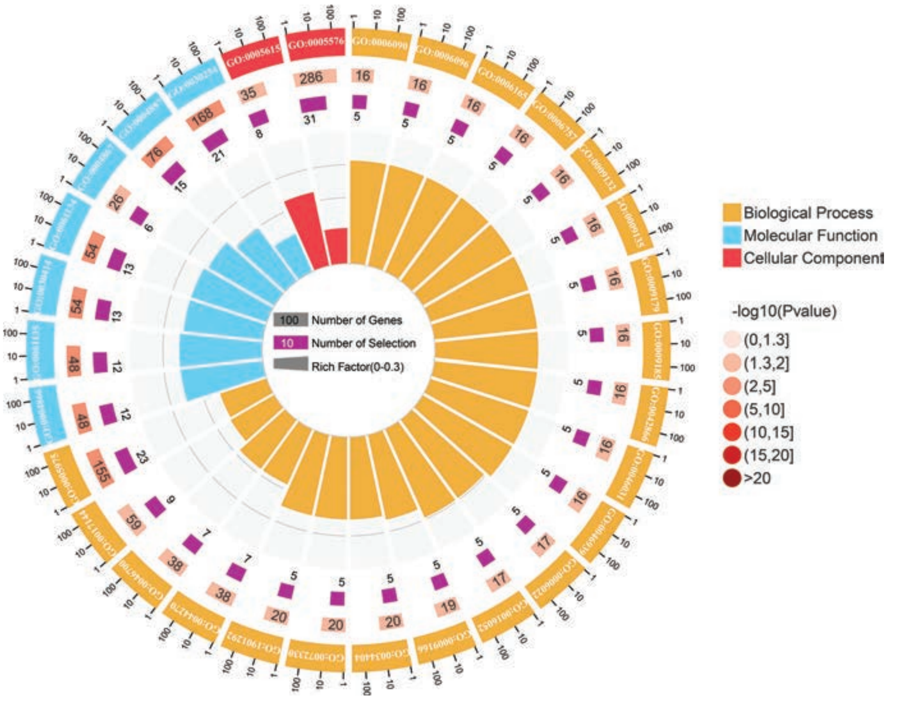

Figure 3. The top most significantly enriched GO terms (top 30) of DEGs between ESM and BSM groups in *C. semilaevis*.

Alternative splicing analysis

A total of 16728 AS genes were identified from ESM and BSM groups. The SE, A5SS, A3SS, MXE, and RI splicing types accounted for 71.71%, 6.79%, 12.27%, 5.39%, and 3.84% of all splicing events, respectively (Fig. 5A). After filtering (|IncLevelDifference| > 0.1 and FDR < 0.05), 167 differential AS (DAS) were identified between ESM and BSM. The SE, A5SS, A3SS, MXE, and RI splicing types accounted for 56.29%, 10.18%, 15.57%, 8.98%, and 8.98% of all splicing events, respectively (Fig. 5B).

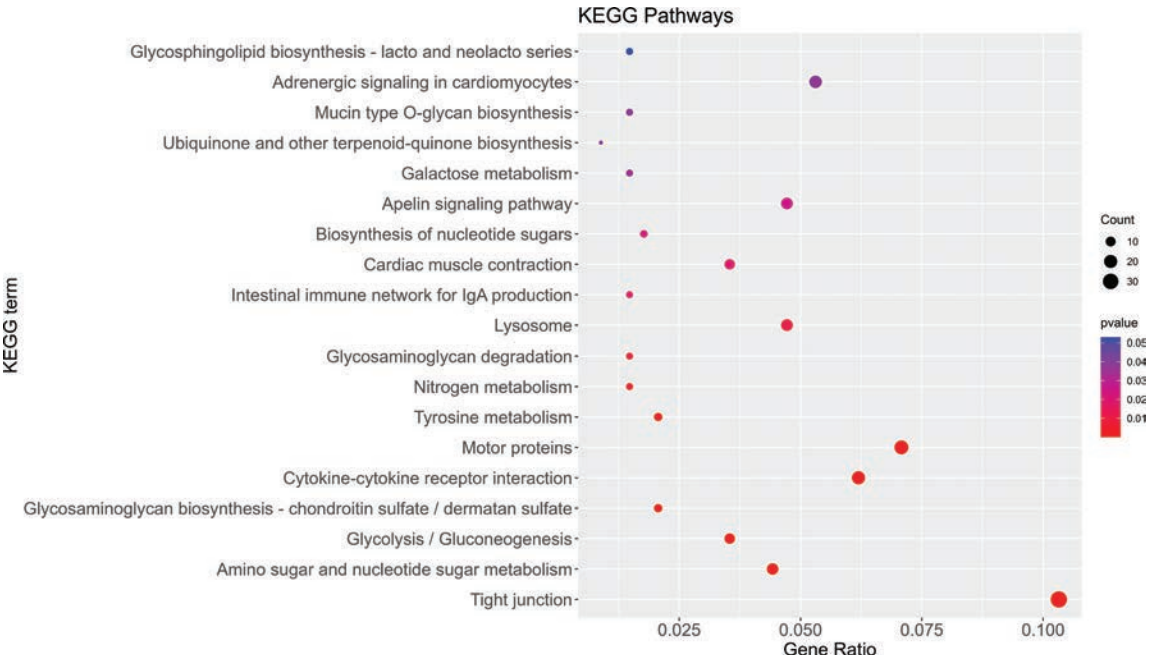

Figure 4. The top 20 enriched KEGG pathways of DEGs between ESM and BSM groups in *C. semilaevis*.

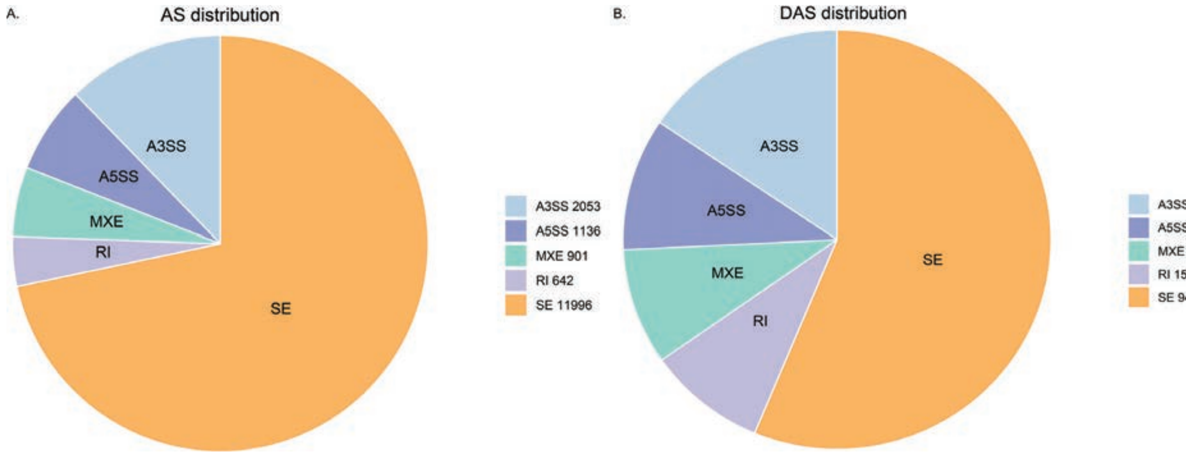

Figure 5. Type distribution of AS events (**A**) and DAS (**B**) in ESM and BSM of *C. semilaevis*.

Validation of the DEGs by qRT-PCR

Nine DEGs were randomly selected for qRT-PCR to verify the reliability of the results from the transcriptome sequencing. As shown in Fig. 6, the relative expression patterns of these genes revealed by qPCR were similar to the RNA-seq results, indicating that the RNA-seq results were reliable.

Discussion

Muscle morphology of eyed-side muscle and blind-side muscle in *C. semilaevis*

Muscle tissue is the most abundant tissue in the body mass and plays an important role in whole-body metabolism (Zhu et al. 2015). Teleost muscle usually grows in two ways: hypertrophy (increase in fiber size) and hyperplasia

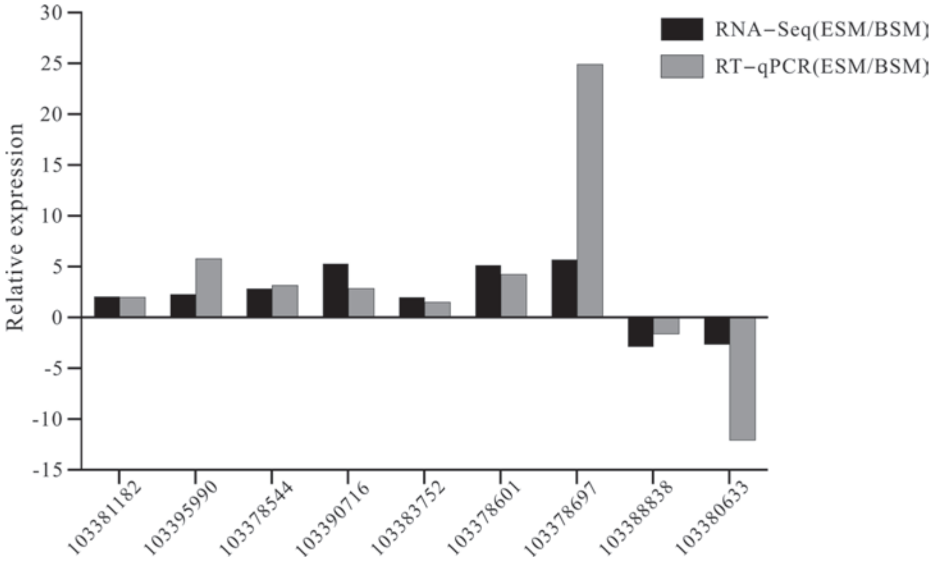

Figure 6. Validation of expression patterns of 9 genes from RNA-seq data by RT-qPCR with 18S gene as an internal control. The values represent the gene expression level of ESM compared with the BSM group.

(increase in the number of muscle fibers) (Rowlerson and Veggetti 2001). Hyperplasia continues until the fish body grows to a certain stage, after which hypertrophy mainly dominates muscle growth (Johnston et al. 2003). The relative timing of the main hyperplastic growth process concerning the life cycle varies between species (Rowlerson and Veggetti 2001). A previous study found that in the common sole (*Solea solea*), the first hyperplastic phase starts 12 days post-hatching, and the second hyperplastic phase was already underway at 2.5 months, and by 1 year, the hyperplastic growth of muscle had ceased (Veggetti et al. 1999). In this study, small new fibers were found between the already existing fibers located in the most dorsal and ventral areas of lateral muscle (Fig. 1), which indicated that muscle growth mainly relied on the recruitment of new muscle fibers (hyperplasia) during the juvenile stage of *C. semilaevis*. The same situation was also observed in other species including, European plaice (*Pleuronectes platessa*) (Brooks and Johnston 1993), turbot (*Scophthalmus maximus*) (Gibson and Johnston 1995), blackspot seabream (*Pagellus bogaraveo*) (Silva et al. 2009). Additionally, the muscle thickness in the ESM was significantly greater than that of the BSM, which may be caused by the hyperplastic growth of muscle fibers on the eyed side.

Transcriptome analysis of ESM and blind-side muscle in *C. semilaevis*

This is the first time that muscle transcriptome has been compared between the eyed side and blind side of *C. semilaevis* using transcriptome sequencing to investigate the potential mechanism of muscle development. In this study, a total of 26,550 unique transcripts were generated and 1177 DEGs were identified (Fig. 2). Among these DEGs, some genes are related to muscle development, for example, myosin family genes and ubiquitin family genes. Myosin family protein is the most abundant and important protein in muscle tissue, which participates in a variety of cellular processes, including cytokinesis, cell polarization, signal transduction, intracellular transport, etc. (Furst et al. 1989; Whiting et al.

1989; Hofmann et al. 2009; Hartman et al. 2011). Studies in salmonids, grass fish, and hybrid grouper indicate that myofibrillar component genes concern growth (Devlin et al. 2009; Sun et al. 2016; Lu et al. 2020). In the present study, several genes related to skeletal muscle myofibrillar components, such as actin, myosin-binding protein C (mybp-C), titin (ttn), troponin (tn), tnnil, myoglobin (mb), and astrotactin-2 (astn-2) were highly expressed in the ESM group. Elevated expression levels of these genes were also found in larger rainbow trout (Salem et al. 2012; Kocmarek et al. 2014). Tn, which is related to the calcium signaling pathway in muscle cells, was up-regulated in the BSM, suggesting that this gene controlling calcium homeostasis also regulates muscle growth in fish (Baar and Esser 1999). It's identical to the results in grass fish, which promote an increase in muscle tissue (Lu et al. 2020). In addition, mb was also found to be significantly up-regulated in ESM, which indicated that myoglobin directly facilitates aerobic exercise along with the growth of muscle through transporting the oxygen consumed during the process of respiration in muscle cell mitochondria (Wittenberg et al. 1975). However, we also observed up-regulation for different copies of myofibrillar components genes such as myosin light chain 4 (mlc4), myosin regulatory light chain 2 (myl2), troponin C (cTnC), alpha- actin (acta), troponin T-2C (tnt-2C) in ESM group, which were found in other fish (Kocmarek et al. 2014).

In addition, genes involved in the cell cycle (such as murine double minute 2 and cyclin A2) were also significantly up-regulated in the ESM. The organs' growth depends on an increase both in biomass of individual cells and cell number (Sablowski and Carnier Dornelas 2014). Usually, the increase in cell number is accomplished by cell division (cell cycle progression), which plays an important role in organism development (Goranov et al. 2009). Cyclins are important regulatory proteins, and which bind to cyclin-dependent kinases (CDKs) to regulate the cell cycle progression (Darzynkiewicz et al. 1996). In different animals, cyclin has been demonstrated to play a role in the cellular context of terminally differentiated muscle (Rao and Kohtz 1995). In this study, cyclin A2 was significantly up-regulated in ESM. Li et al. (2024a) showed that cyclin was involved in Yangtze sturgeon (*Acipenser dabryanus*) growth difference as a potential key hub gene through WGCNA analysis. Therefore, the results suggested that the upregulation of genes related to cell cycle might be another endogenous factor that is conducive to different muscle thicknesses between the eyed-side and blind-side muscle in *C. semilaevis*.

Muscle growth reflects the balance between protein synthesis and degradation. The ubiquitin Proteasome Pathway (UPP) is the main system for degrading unnecessary or damaged proteins (Lecker et al. 2006), and the E3-ubiquitin ligases are an important component of this system, which conjugate ubiquitin to the target protein, and then induce protein degradation (David et al. 2011). Furthermore, a large number of ubiquitin system genes is proven to be regulated in atrophying muscles (Lecker et al. 2006). In our study, 22 ubiquitin family genes were identified to be DEGs, 17 genes of which were up-regulated in BSM and 5 were up-regulated in ESM (Suppl. material 1). These results are in accordance with the finding that E3-ubiquitin ligases activate myogenesis in zebrafish. This suggests that ubiquitin system genes could affect muscle development through the ubiquitin-proteasome pathway to promote the degradation of protein in *C. semilaevis*.

Glycolysis is an important metabolic pathway in which glucose is converted into pyruvate producing ATP and NADH for cellular metabolic activity (Hers 1983;

Muirhead and Watson 1992). This pathway produces some important precursor metabolites, and also plays a vital role in muscle tissue (Wang et al. 2021). Several studies have shown that glycolysis promotes muscle growth in zebrafish, pigs, and chickens (Lametsch et al. 2006; Teltathum and Mekchay 2009; Wang et al. 2021). Regarding *C. semilaevis*, a previous study indicated that glycolysis/gluconeogenesis contributed to flatfish size dimorphism (Wang et al. 2021). In our study, two important genes in glycolysis (acetyl-CoA synthetase and glucose 6-phosphatase) were more highly expressed in eyed-side muscle tissue than in blind-side muscle tissue. These two DEGs, acs and g6pase, are the key enzymes playing important roles in the regulation of glycolytic/gluconeogenic pathways (Werve et al. 2011; James et al. 2016). The high expression levels of acs and g6pase in the ESM may contribute to the greater muscle thickness in the eyed side of *C. semilaevis*. However, the precise molecular mechanisms of glycolysis/gluconeogenesis and how they participate in muscle development in *C. semilaevis* require further study by the functional analysis of DEGs in this pathway.

Conclusions

In the present study, we found the difference in muscle thickness between the eyed side and blind side might be caused by the hyperplastic growth through histological assays. In addition, some DEGs related to muscle development (actin, myopic, titin, tn, tnnil, astn-2, Mdm2, and Ccna2) and the glycolysis/gluconeogenesis pathway were identified and proved to be involved in the muscle development of *C. semilaevis* through comparative transcriptome analysis. This study provides insights into the mechanism regulating muscle development in fish.

Acknowledgments

The authors would like to thank Zhoushan Blue Science Marine Biology Research Institute for providing the animals used in this study.

Additional information

Conflict of interest

The authors have declared that no competing interests exist.

Ethical statement

No ethical statement was reported.

Funding

This study was supported by “the Fundamental Research Funds for Zhejiang Provincial Universities and Research Institutes” (2024J005-2), and Natural Science Foundation of China (42171069).

Author contributions

Zhenming Lü and Liqin Liu planned and designed the research, and afforded the funding. Yuzhen Wang, Jing Yu, Yijing Yang, and An Xu collected samples, performed experiments, and analyzed the data. Yuzhen Wang and Liqin Liu wrote the original draft. Li Gong, Jing Liu, and Fenghui Li reviewed and edited the manuscript.

Author ORCIDs

Jing Yu https://orcid.org/0009-0004-4611-6102

Data availability

All of the data that support the findings of this study are available in the main text or Supplementary Information.

References

Ahammad AKS, Asaduzzaman, M, Ceyhun SB, Ceylan H, Asakawa S, Watabe S, Kinoshit S (2019) Multiple transcription factors mediating the expressional regulation of myosin heavy chain gene involved in the indeterminate muscle growth of fish. Gene 687: 308–318. https://doi.org/10.1016/j.gene.2018.11.040

Baar K, Esser K (1999) Phosphorylation of p70^{S6k} correlates with increased skeletal muscle mass following resistance exercise. American Journal of Physiology-Cell Physiology 276(1): C120-C127. https://doi.org/10.1152/ajpcell.1999.276.1.C120

Bolger AM, Lohse M, Usadel B (2014) Trimmomatic: A flexible trimmer for Illumina sequence data. Bioinformatics 30: 2114–2120. https://doi.org/10.1093/bioinformatics/btu170

Brooks S, Johnston IA (1993) Influence of development and rearing temperature on the distribution, ultrastructure and myosin sub-unit composition of myotomal muscle-fibre types in the plaice *Pleuronectes platessa*. Marine Biology 117: 501–513. https://doi.org/10.1007/BF00349326

Chen L, Pan YX, Cheng J, Zhu X, Chu WY, Meng YY, Bin SY, Zhang JS (2023) Characterization of myosin heavy chain (MYH) genes and their differential expression in white and red muscles of Chinese perch, *Siniperca chuatsi*. International Journal of Biological Macromolecules 250: 125907. https://doi.org/10.1016/j.ijbiomac.2023.125907

Darzynkiewicz Z, Gong J, Juan G, Ardelt B, Traganos F (1996) Cytometry of cyclin proteins. Cytometry 25(1): 1–13. https://doi.org/10.1002/(SICI)1097-0320(19960901)25:1<1::AID-CYTO1>3.0.CO;2-N

David Y, Ternette N, Edelmann MJ, Ziv T, Gayer B, Sertchook R (2011) E3 ligases determine ubiquitination site and conjugate type by enforcing specificity on E2 enzymes. Journal of Biological Chemistry 286(51): 44104–44115. https://doi.org/10.1074/jbc.M111.234559

Devlin RH, Sakhrani D, Tymchuck WE, Rise ML, Goh B (2009) Domestication and growth hormone transgenesis cause similar changes in gene expression in coho salmon (*Oncorhynchus kisutch*). PNAS: Proceedings of the National Academy of Sciences of the United States of America 106(9): 3047–3052. https://doi.org/10.1073/pnas.0809798106

Furst DO, Osborn M, Weber K (1989) Myogenesis in the mouse embryo: differential onset of expression of myogenic proteins and the involvement of titin in myofibril assembly. Journal of Cell Science 109(2): 517–527. https://doi.org/10.1083/jcb.109.2.517

Gibson S, Johnston IA (1995) Temperature and development in larvae of the turbot *Scophthalmus maximus*. Marine Biology 124: 15–22. https://doi.org/10.1007/BF00349142

Goranov AI, Cook M, Ricicova M, Ben-Ari G, Gonzalez C, Hansen C, Tyers M, Amon A (2009) The rate of cell growth is governed by cell cycle stage. Genes & Development 23(12): 1408–1422. https://doi.org/10.1101/gad.1777309

Hagen VL, Vieira A, Solberg C, Johnston IA (2008) Myotube production in fast myotomal muscle is switched-off at shorter body lengths in male than female Atlantic halibut *Hippoglossus hippoglossus* (L.) resulting in a lower final fibre number. Journal of Fish Biology 73: 139–152. https://doi.org/10.1111/j.1095-8649.2008.01917.x

Hartman MA, Finan D, Sivaramakrishnan S, Spudich JA (2011) Principles of unconventional myosin function and targeting. Annual Review of Cell and Developmental Biology 27: 133–155. https://doi.org/10.1146/annurev-cellbio-100809-151502

Hers HG (1983) The control of glycolysis and gluconeogenesis by protein phosphorylation. Philosophical Transactions Of The Royal Society B-biological Sciences 302(1108): 27–32. https://doi.org/10.1098/rstb.1983.0035

Hofmann WA, Richards TA, Lanerolle PD (2009) Ancient animal ancestry for nuclear myosin. Journal of Cell Science 122(Pt 5): 636–643. https://doi.org/10.1242/jcs.030205

James KL, Ríos-Hernández LA, Wofford NQ, Mouttaki H, Sieber JR, Sheik CS (2016) Pyrophosphate-dependent atp formation from acetyl coenzyme a in syntrophus aciditrophicus, a new twist on atp formation. mBio 7(4): 01208-16. https://doi.org/10.1128/mBio.01208-16

Janvier P (2008) Squint of the fossil flatfish. Nature 454: 169–170. https://doi.org/10.1038/454169a

Johnston IA (1999) Muscle development and growth: potential implications for flesh quality in fish. Aquaculture 177: 99–115. https://doi.org/10.1016/S0044-8486(99)00072-1

Johnston IA, Manthri S, Alderson R, Smart A, Campbell P, Nickell D, Robertson B, Paxton CGM, Burt ML (2003) Freshwater environment affects growth rate and muscle fibre recruitment in seawater stages of Atlantic salmon (*Salmo salar* L.). Journal of Experimental Biology 206: 1337–1351. https://doi.org/10.1242/jeb.00262

Kocmarek AL, Ferguson MM, Danzmann RG (2014) Differential gene expression in small and large rainbow trout derived from two seasonal spawning groups. BMC Genomics 15: 57–57. https://doi.org/10.1186/1471-2164-15-57

Lametsch R, Kristensen L, Larsen MR, Therkildsen M, Oksbjerg N, Ertbjerg N (2006) Changes in the muscle proteome after compensatory growth in pigs. Journal of Animal Science 84(4): 918–924. https://doi.org/10.2527/2006.844918x

Lecker S, Goldberg A, Mitch W (2006) Protein degradation by the ubiquitin-proteasome pathway in normal and disease states. Journal Of The American Society Of Nephrology 17(7): 1807–1819. https://doi.org/10.1681/ASN.2006010083

Li Z, Du XS, Wen LT, Li Y, Qin JQ, Chen Z, Huang Y, Wu X, Luo Y, Ye H (2022) Transcriptome analysis reveals the involvement of ubiquitin-proteasome pathway in the regulation of muscle growth of rice flower carp. Comparative Biochemistry and Physiology-Part D: Genomics and Proteomics 41: 100948. https://doi.org/10.1016/j.cbd.2021.100948

Li QZ, Wang J, Chen YY, Wu XY, Liu Y, Lai JS, Song MJ, Li FY, Li PP, He B, Wang B, Yan T, Gong Q (2024a) Comparison of muscle structure and transcriptome analysis reveals the mechanism of growth variation in Yangtze sturgeon (*Acipenser dabryanus*). Aquaculture 579: 740268. https://doi.org/10.1016/j.aquaculture.2023.740268

Li Y, Zou XX, Jin HH, Zhou B, Zhang L, Li Z, Ling LY, Liu F, Gao Y, Wang XY, Luo H, Chen KL, Ye H (2024b) Identification of genes related to growth from transcriptome profiles pf the muscle and liver of Chinese longsnout catfish (*Leiocassis longirostris*). Comparative Biochemistry and Physiology-Part D: Genomics and Proteomics 49: 101180. https://doi.org/10.1016/j.cbd.2023.101180

Livak KJ, Schmittgen TD (2001) Analysis of Relative Gene Expression Data Using Real-time Quantitative PCR and the 2(-Delta Delta C(T)) Methods. Methods 25(5): 402–408. https://doi.org/10.1006/meth.2001.1262

Love M, Huber W, Anders S (2014) Moderated estimation of fold change and dispersion for RNA-seq data with DESeq2. Genome Biology 15(12): 550. https://doi.org/10.1186/s13059-014-0550-8

Lu X, Chen HM, Qian XQ, Gui JF (2020) Transcriptome analysis of grass carp (*Ctenopharyngodon idella*) between fast and slow-growing fish. Comparative Biochemistry and Physiology-Part D 35: 100688. https://doi.org/10.1016/j.cbd.2020.100688

Lü ZM, Gong L, Ren YD, Chen YJ, Wang ZK, Liu LQ, Li HR, Chen XQ, Li ZZ, Luo HR, Jiang H, Zeng Y, Wang YF, Wang K, Zhang C, Jiang HF, Wan WT, Qin YL, Zhang JS, Zhu L, He SP, Mao BY, Wang W, Kong XY, Li YX (2021) Large-scale sequencing of flatfish genomes provides insights into the polyphyletic origin of their specialized body plan. Nature Genetics 53: 742–751. https://doi.org/10.1038/s41588-021-00836-9

Luo WW, Chi SC, Wang JR, Yu XM, Tong JG (2024) Comparative transcriptomic analyses of brain-liver-muscle in channel catfish (*Ictalurus punctatus*) with differential growth rate. Comparative Biochemistry and Physiology- Part D: Genomics and Proteomics 49: 101178. https://doi.org/10.1016/j.cbd.2023.101178

Mai JQ, Sun YQ, Li XH, Zhu Y, Xu WT, Chen ZF, Zhang Q, Wang JC, Wang N (2024) The potential role of hippo pathway effector yap1/yap1b in female-biased sexual size dimorphism of Chinese tongue sole (*Cynoglossus semilaevis*). Aquaculture 592: 741264. https://doi.org/10.1016/j.aquaculture.2024.741264

Meng L, Xu W, Zhu Y, Zhang N, Shao C, Liu Y, Chen S (2018) Molecular characterization and expression analysis of, strbp, in Chinese tongue sole (*Cynoglossus semilaevis*). Theriogenology 118: 225–232. https://doi.org/10.1016/j.theriogenology.2018.06.001

Mohindra V, Chowdhury LM, Chauhan N, Maurya RK, Jena JK (2022) Transcriptome analysis revealed hub genes for muscle growth in Indian major carp, *Catla catla* (Hamilton, 1822). Genomics 114: 110393. https://doi.org/10.1016/j.ygeno.2022.110393

Mortazavi A, Williams BA, Mccue K, Schaeffer L, Wold B (2008) Mapping and quantifying mammalian transcriptomes by RNA-Seq. Nature Methods 5: 621–628. https://doi.org/10.1038/nmeth.1226

Muirhead H, Watson H (1992) Glycolytic enzymes: from hexose to pyruvate. Current Opinion in Structural Biology 2(6): 870–876. https://doi.org/10.1016/0959-440X(92)90113-L

Rao SS, Kohtz DS (1995) Positive and negative regulation of D-type cyclin expression in skeletal myoblasts by basic fibroblast growth factor and transforming growth factor β: a role for cyclin D1 in control of myoblast differentiation. Journal of Biological Chemistry 270(8): 4093–4100. https://doi.org/10.1074/jbc.270.8.4093

Rescan PY (2019) Development of myofibres and associated connective tissues in fish axial muscle: Recent insights and future perspectives. Differentiation 106: 35–41. https://doi.org/10.1016/j.diff.2019.02.007

Rio DC, Ares MJ, Hannon GJ, Nilsen TW (2010) Purification of RNA using TRIzol (TRI reagent). Cold Spring Harbor Protocols, pdb-prot5439. https://doi.org/10.1101/pdb.prot5439

Rowlerson A, Veggetti A (2001) Cellular mechanisms of post-embryonic muscle growth in aquaculture species. In Fish Physiology 18: 103–140. https://doi.org/10.1016/S1546-5098(01)18006-4

Sablowski R, Carnier Dornelas M (2014) Interplay between cell growth and cell cycle in plants. Journal of Experimental Botany 65(10): 2703–2714. https://doi.org/10.1093/jxb/ert354

Salem M, Vallejo RL, Leeds TD, Palti Y, Liu S, Sabbagh A, RexroadIii CE, Yao J (2012) RNA-Seq identifies SNP markers for growth traits in rainbow trout. PLoS ONE 7: e36264. https://doi.org/10.1371/journal.pone.0036264

Schreiber AM (2006) Asymmetric craniofacial remodeling and lateralized behavior in larval flatfish. The Journal of Experimental Biology, 209: 610–621. https://doi.org/10.1242/jeb.02056

Shen SH, Park JW, Lu ZX, Lin L, Henry MD, Wu YN (2014) rMATS: robust and flexible detection of differential alternative splicing from replicate RNA-Seq data. Proceedings of the National Academy of Sciences of the United States of America 111(51): E5593–E5601. https://doi.org/10.1073/pnas.1419161111

Shi R, Li XH, Xu XW, Chen ZF, Zhu Y, Wang N (2023) Genome-wide analysis of BMP/GDF family and DAP-seq of YY1 suggest their roles in *Cynoglossus semilaevis* sexual size dimorphism. International Journal of Biological Macromolecules 253: 127201. https://doi.org/10.1016/j.ijbiomac.2023.127201

Silva P, Valente LMP, Olmedo M, Galante MH, Monteiro RaF, Rocha E (2009) Hyperplastic and hypertrophic growth of lateral muscle in blackspot seabream *Pagellus bogaraveo* from hatching to juvenile. Journal of Fish Biology 74: 37–53. https://doi.org/10.1111/j.1095-8649.2008.02122.x

Sun Y, Guo CY, Wang DD, Li XF, Xiao L, Zhang X, You X, Shi Q, Hu GJ, Fang C, Lin HR (2016) Transcriptome analysis reveals the molecular mechanisms underlying growth superiority in a novel grouper hybrid (*Epinephelus fuscogutatus*♀ × *E. lanceolatus*♂). BMC Genomics 17: 24. https://doi.org/10.1186/s12863-016-0328-y

Teltathum T, Mekchay S (2009) Proteome changes in Thai indigenous chicken muscle during growth period. International Journal of Biological Sciences 5(7): 679–685. https://doi.org/10.7150/ijbs.5.679

Valente LM, Moutou KA, Conceicao LE, Engrola S, Fernandes JMO, Johnston IA (2013) What determines growth potential and juvenile quality of farmed fish species? Reviews in Aquaculture 5(S1): S168-S193. https://doi.org/10.1111/raq.12020

Veggetti A, Rowlerson A, Radaelli G, Arrighi S, Domeneghini C (1999) Post-hatching development of the gut and lateral muscle in the sole. Journal of Fish Biology 55(sA): 44–65. https://doi.org/10.1111/j.1095-8649.1999.tb01045.x

Wang N, Tian YS, Zhang JJ, Li ZT, Cheng ML, Wu YP (2021) Involvement of glycolysis activation in flatfish sexual size dimorphism: Insights from transcriptomic analyses of *Platichthys stellatus* and *Cynoglossus semilaevis*. Comparative Biochemistry and Physiology - Part D: Genomics and Proteomics 39: 100832. https://doi.org/10.1016/j.cbd.2021.100832

Wang JL, Shi R, Yang Q, Chen ZF, Wang JC, Gong ZH, Chen SL, Wang N (2023) Characterization and potential function of 7-dehydrocholesterol reductase (dhcr7) and lathosterol 5-desaturase (sc5d) in *Cynoglossus semilaevis* sexual size dimorphism. Gene 853: 147089. https://doi.org/10.1016/j.gene.2022.147089

Werve GVD, Lange AJ, Newgard CB, Méchin MC, Li YZ (2011) New lessons in the regulation of glucose metabolism taught by the glucose 6-phosphatase system. European Journal of Biochemistry 267(6): 153–1549. https://doi.org/10.1046/j.1432-1327.2000.01160.x

Whiting A, Wardale J, Trinick J (1989) Does titin regulate the length of muscle thick filaments? Journal of Molecular Biology 201(1): 163–169. https://doi.org/10.1016/0022-2836(89)90381-1

Wittenberg BA, Wittenberg JB, Caldwell PRB (1975) Role of myoglobin in the oxygen supply to red skeletal muscle. Journal of Biological Chemistry 250(23): 9038–9043. https://doi.org/10.1016/S0021-9258(19)40690-X

Yao XL, Zheng J, Geletu TT, Zhao Y, Tang SJ, Zhao JL (2024) Genome-wide identification of igfbp genes and their different growth expression patterns of mandarin fish. Aquaculture Reports 35: 101971. https://doi.org/10.1016/j.aqrep.2024.101971

Yu G, Wang LG, Han Y, He QY (2012) ClusterProfiler: An R package for comparing biological themes among gene clusters. OMICS 16(5): 284–287. https://doi.org/10.1089/omi.2011.0118

Zhang L, Li XH, Yu YL, Zhang L, Dong LX, Gan JH, Mao T, Liu T, Peng J, He L (2021) Comparative analyses of liver transcriptomes reveal the effect of exercise on growth-, glucose metabolism-, and oxygen transport-related genes and signaling pathways in grass carp (*Ctenopharyngodon idella*). Comparative Biochemistry and Physiology Part A: Molecular & Integrative Physiology 262: 111081. https://doi.org/10.1016/j.cbpa.2021.111081

Zhu X, Chen D, Hu Y, Wu P, Wang K, Zhang J, Chu W, Zhang J (2015) The microRNA signature in response to nutrient restriction and refeeding in skeletal muscle of Chinese perch (*Siniperca chuatsi*). Marine Biotechnology 17: 180–189. https://doi.org/10.1007/s10126-014-9606-8

Supplementary material 1

Primer sequences used for RT-qPCR

Authors: Zhenming Lü, Yuzhen Wang, Jing Yu, Yijing Yang, An Xu, Li Gong, Jing Liu, Fenghui Li, Liqin Liu

Data type: xlsx

Link: https://doi.org/10.3897/zookeys.1230.139837.suppl1

Supplementary material 2

The catalogue of DEGs in in ESM and BSM groups of *C. semilaevis*

Authors: Zhenming Lü, Yuzhen Wang, Jing Yu, Yijing Yang, An Xu, Li Gong, Jing Liu, Fenghui Li, Liqin Liu

Data type: xlsx

Link: https://doi.org/10.3897/zookeys.1230.139837.suppl2

Supplementary material 3

The list of enriched GO annotations

Authors: Zhenming Lü, Yuzhen Wang, Jing Yu, Yijing Yang, An Xu, Li Gong, Jing Liu, Fenghui Li, Liqin Liu

Data type: xls

Link: https://doi.org/10.3897/zookeys.1230.139837.suppl3

Supplementary material 4

The list of enriched KEGG pathways

Authors: Zhenming Lü, Yuzhen Wang, Jing Yu, Yijing Yang, An Xu, Li Gong, Jing Liu, Fenghui Li, Liqin Liu

Data type: xls

Link: https://doi.org/10.3897/zookeys.1230.139837.suppl4

ZooKeys 1230: 231–245 (2025)
DOI: 10.3897/zookeys.1230.142418

Research Article

Four new species of *Pseudopoda* Jäger, 2000 (Araneae, Sparassidae, Heteropodinae) from China and Vietnam

He Zhang[1,2,3], Hailun Chen[3], Fan Zhang[4], Jie Liu[3], Peter Jäger[5], Qiangyong Fan[6], Lin Cheng[6], Changhao Hu[1,3,7]

1 *Guo Shoujing Innovation College, Xingtai University, Xingtai 054001, Hebei, China*
2 *Hebei Province Sweet Potato Breeding and Application Technology Innovation Center, Xingtai 054001, Hebei, China*
3 *Hubei Key Laboratory of Regional Development and Environmental Response, Faculty of Resources and Environmental Science, Hubei University, Wuhan 430062, Hubei, China*
4 *Hubei Key Laboratory of Resource Utilization and Quality Control of Characteristic Crops, College of Life Science and Technology, Hubei Engineering University, Xiaogan 432000, Hubei, China*
5 *Arachnology, Senckenberg Research Institute, Mertonstraße 17–21, 60325 Frankfurt am Main, Germany*
6 *Jiangxi Wuyi Mountain National Nature Reserve Administration, Shangrao 334599, Jiangxi, China*
7 *Hubei Broad Nature Technology Service Co. Ltd, Wuhan 430079, Hubei, China*
Corresponding author: Changhao Hu (changhaohu1998@gmail.com)

Abstract

Four new species of *Pseudopoda* Jäger, 2000 (Araneae, Sparassidae) are described based on material collected from China and Vietnam: *P. campylotropa* Zhang, Chen, Liu, Jäger & Hu, **sp. nov.** (♂♀) and *P. caoguii* Zhang, Chen, Liu, Jäger & Hu, **sp. nov.** (♀) from Yunnan Province of China; *P. yejiachangensis* Zhang, Chen, Liu, Jäger & Hu, **sp. nov.** (♂) from Jiangxi Province of China; and *P. ornithorhynchus* Zhang, Chen, Liu, Jäger & Hu, **sp. nov.** (♂) from Vinh Phuc Province of Vietnam.

Key words: Asia, biodiversity, huntsman spiders, morphology, taxonomy

Academic editor: Alireza Zamani
Received: 22 November 2024
Accepted: 8 January 2025
Published: 6 March 2025

ZooBank: https://zoobank.org/4CBCB13B-3A14-4788-A8A3-81D097994FCC

Citation: Zhang H, Chen H, Zhang F, Liu J, Jäger P, Fan Q, Cheng L, Hu C (2025) Four new species of *Pseudopoda* Jäger, 2000 (Araneae, Sparassidae, Heteropodinae) from China and Vietnam. ZooKeys 1230: 231–245. https://doi.org/10.3897/zookeys.1230.142418

Introduction

The spider genus *Pseudopoda* Jäger, 2000 is the largest genus within the family Sparassidae Bertkau, 1872, occurring in eastern, southern and southeastern Asia (Jäger et al. 2015) and currently comprising 264 species (World Spider Catalog 2025). Among them, 163 species are known in China, primarily distributed in southwestern regions, while only eight species have been recorded in Vietnam, primarily in northern areas (Jäger 2001; Jäger and Vedel 2005, 2007; Yang et al. 2009; Zhang et al. 2013a, 2013b; Logunov and Jäger 2015; Zhang et al. 2017; Jiang et al. 2018; Zhang et al. 2019; Yang et al. 2022; Zhang et al. 2023; Zhang et al. 2025).

Pseudopoda species primarily inhabit leaf litter and are less commonly found in the foliage or on tree trunks (Jäger et al. 2015). Most of these species are small-range endemics restricted to single mountains or forests (Zhang et al. 2023). Although the genus has been extensively studied, many new species are likely still undiscovered (Cao et al. 2016; Jiang et al. 2018; Zhang et al. 2023).

While examining Sparassidae collected from Yunnan and Jiangxi Provinces of China, as well as from Vinh Phuc Province of Vietnam, four new *Pseudopoda* species were identified. This study aims to provide diagnoses, morphological descriptions and photographic illustrations of these four new species.

Material and methods

The specimens examined in this study were preserved in absolute ethanol and deposited at the Center for Behavioural Ecology and Evolution (CBEE), College of Life Sciences, Hubei University, Wuhan and at Xingtai University (XTU), Xingtai. Specimens were examined using an Olympus SZX7 stereo microscope. Photographs were taken using a Leica M205C stereo microscope. The male palp was examined and photographed after dissection. The epigyne was examined after being cleared with Proteinase K. Eye diameters were taken at the widest point. Legs and palp measurements are given as: total length (femur, patella, tibia, metatarsus [absent in palp], tarsus). All measurements are in millimetres (mm). Spination follows Davies (1994). The terminologies used in text and figure legends follow Quan et al. (2014).

Abbreviations in text: **AB**, anterior bands; **ALE**, anterior lateral eyes; **AME**, anterior median eyes; **C**, conductor; **CA**, carapace; **CH**, clypeus height; **CO**, copulatory opening; **dRTA**, dorsal retrolateral tibial apophysis; **E**, embolus; **EF**, epigynal field; **EP**, embolic projection; **FD**, fertilization duct; **Fe**, femur; **FW**, first winding; **IDS**, internal duct system; **LL**, lateral lobes; **Mt**, metatarsus; **OS**, opisthosoma; **Pa**, patella; **PLE**, posterior lateral eyes; **PME**, posterior median eyes; **Pp**, palp; **RTA**, retrolateral tibial apophysis; **S**, spermathecae; **Sp**, spermophor; **ST**, subtegulum; **T**, tegulum; **Ti**, tibia; **vRTA**, ventral retrolateral tibial apophysis; **I, II, III, IV**, legs I to IV.

Taxonomy

Family Sparassidae Bertkau, 1872
Subfamily Heteropodinae Thorell, 1873

Genus *Pseudopoda* Jäger, 2000

Type species. *Pseudopoda prompta* (O. Pickard-Cambridge, 1885).

Diagnosis. See Zhang et al. (2023).

Distribution. East, South and Southeast Asia.

Pseudopoda campylotropa Zhang, Chen, Liu, Jäger & Hu, sp. nov.
https://zoobank.org/B043CE45-65A1-47E0-A081-A2A32A33F3FA
Figs 1–3, 11

Type material. ***Holotype*** male: China, • Yunnan Province: Zhaotong City, Weixin County, Houshan Forest Farm, 27°51'01"N, 105°00'48"E, alt. 1637 m, 25 April 2024, Caifu Tao leg. (CBEE, LJ2024002). ***Paratypes*:** • 3 males, 3 females, with same data as for holotype (CBEE, LJ2024003). 1 female, with same data as for holotype, except: 28 June 2020 (CBEE, LJ202005004).

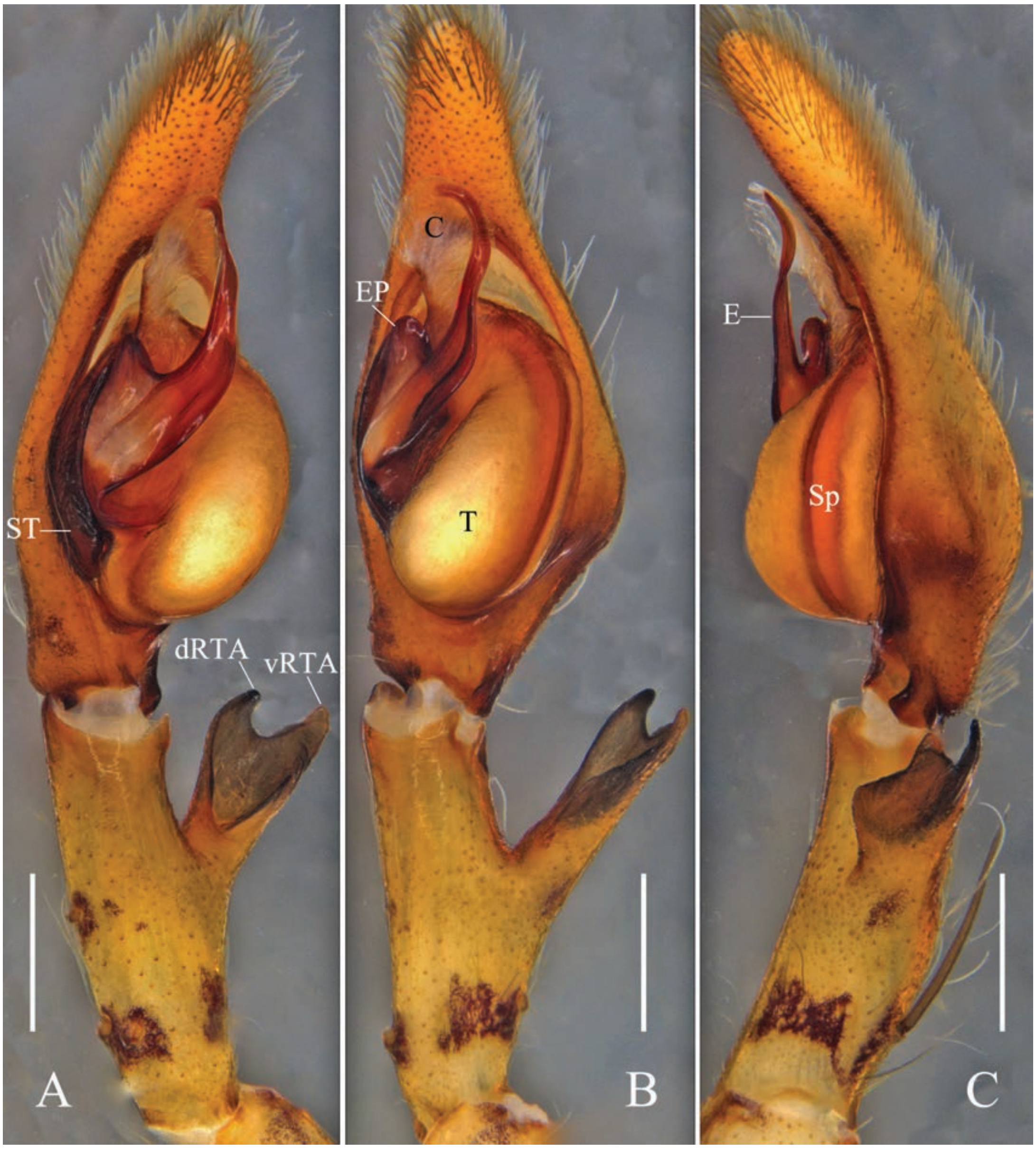

Figure 1. *Pseudopoda campylotropa* Zhang, Chen, Liu, Jäger & Hu, sp. nov., left male palp **A** prolateral **B** ventral **C** retrolateral. Abbreviations: C, conductor; dRTA, dorsal retrolateral tibial apophysis; E, embolus; EP, embolic projection; Sp, spermophor; ST, subtegulum; T, tegulum; vRTA, ventral retrolateral tibial apophysis. Scale bars: 0.5 mm.

Etymology. The specific name is derived from Greek 'campylo' meaning 'bend, turn', and 'trop' derived from 'trepein' meaning 'to turn', referring to the crook-shaped distal part of E in ventral view; adjective.

Diagnosis. Males of *P. campylotropa* Zhang, Chen, Liu, Jäger & Hu, sp. nov. resemble those of *P. explanata* Zhang, Jäger & Liu, 2023 (cf. figs 1A–C vs. figs 103A–C in Zhang et al. 2023) by having a sickle-shaped E, a broad, distad EP, and a medially arising RTA with broad elongated base and distal tips of dRTA and vRTA, but can be recognised by: 1) EP short and triangular with short and rounded tip, and 2) dRTA with rounded tip (vs. EP long and trapezoidal, dRTA with thin and acute tip in *P. explanata*). Females of *P. campylotropa* Zhang, Chen, Liu, Jäger & Hu, sp. nov. resemble those of *P. curva* Zhang, Jäger & Liu, 2023 and *P. shimenensis* Zhang, Jäger & Liu, 2023 (cf. figs 2A–C vs. figs 76A–C and

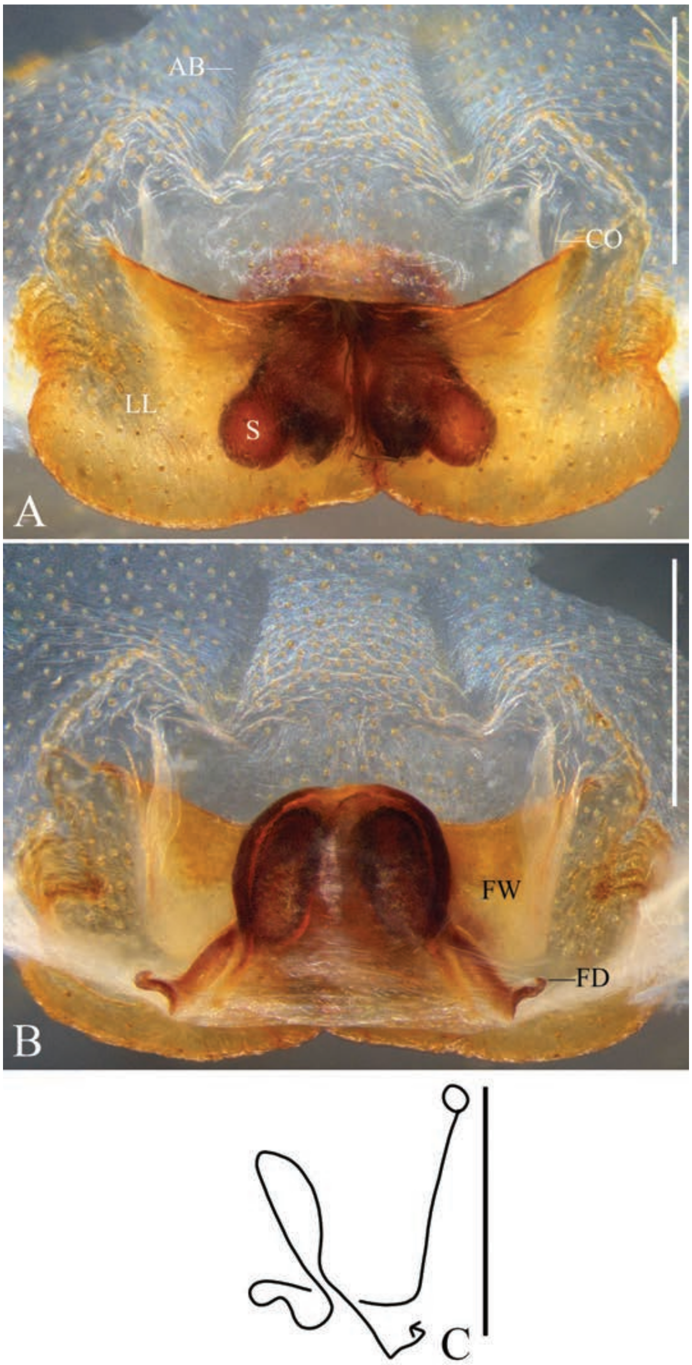

Figure 2. *Pseudopoda campylotropa* Zhang, Chen, Liu, Jäger & Hu, sp. nov., female **A** epigyne, ventral **B** vulva, dorsal **C** schematic course of internal duct system, dorsal. Abbreviations: AB, anterior bands; CO, copulatory opening; FD, fertilization duct; FW, first winding; LL, lateral lobes; S, spermathecae. Scale bars: 0.5 mm.

219A–C in Zhang et al. 2023) by having the epigyne distinctly wider than long with the anterior and posterior margins of LL almost straight, but can be distinguished from both species by: IDS with short sclerotized tubes with spherical end in ventral view (vs. IDS with long and curved tubes with rounded, but not spherical end in *P. curva* and *P. shimenensis*).

Description. Male (holotype): Measurements: Small-sized. Body length 7.8, CA length 4.0, width 3.8; OS length 3.7, width 2.2. Eyes: AME 0.20, ALE 0.30,

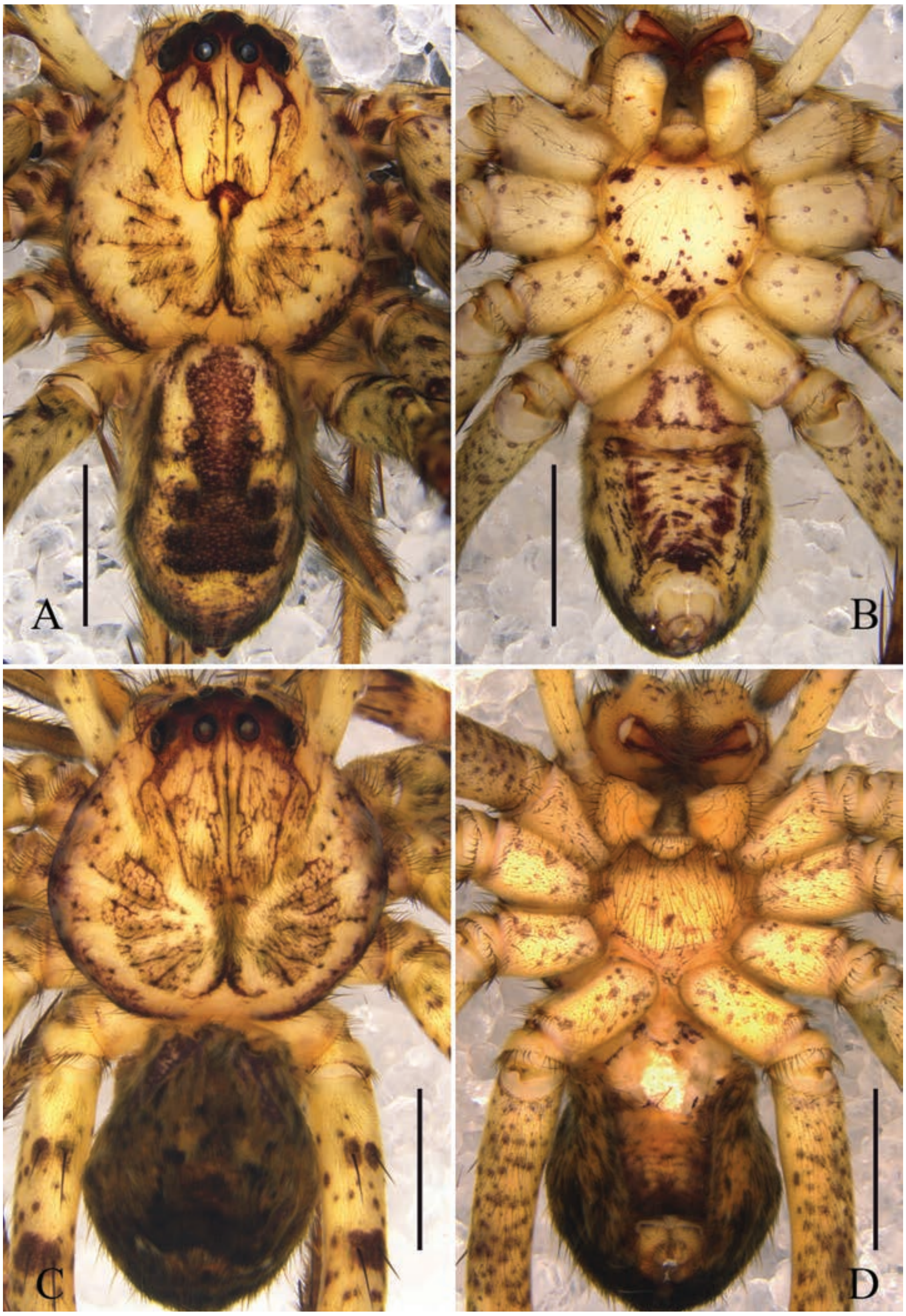

Figure 3. Habitus of *Pseudopoda campylotropa* Zhang, Chen, Liu, Jäger & Hu, sp. nov. **A, B** male (**A** dorsal **B** ventral) **C, D** female (**C** dorsal **D** ventral). Scale bars: 2 mm.

PME 0.24, PLE 0.25, AME–AME 0.18, AME–ALE 0.01, PME–PME 0.26, PME–PLE 0.32, AME–PME 0.24, ALE–PLE 0.27, CH AME 0.19, CH ALE 0.23. Spination: Pp 131, 101, 3110; Fe **I** 312, **II** 313, **III** 322, **IV** 331; Pa **I**–**II** 101, **IV** 000; Ti **I** 1218, **II** 121(10), **III** 2124, **IV** 2126; Mt **I** 2024, **II** 2026, **III** 2124, **IV** 3036. Measurements of palp and legs: Pp 6.1 (2.0, 0.6, 1.3, –, 2.2), **I** 23.4 (6.2, 1.7, 7.0, 6.3, 2.2), **II** 25.3 (6.7, 1.8, 7.4, 7.1, 2.3), **III** 18.7 (5.2, 1.4, 5.3, 5.2, 1.6), **IV** 21.0 (5.9, 1.5, 5.5, 6.2, 1.9). Leg formula: **II**-**I**-**IV**-**III**. Chelicerae with 3 promarginal, 4 retromarginal teeth, and c. 26 intermarginal denticles.

Palp (Figs 1A–C): as in diagnosis. C membranous, arising from T at 11:30 o'clock position; prolateral margin of C slightly sclerotized in basal half.

E slender and sickle-shaped in apical half, arising from 9 o'clock position of T. RTA arising medially from Ti; vRTA and dRTA with rounded tip.

Colouration (Figs 3A, B): CA yellow, with dark reddish-brown spots and lines, eye area reddish-brown, posterior margins dark brown. Fovea dark brown. Sternum and legs yellow, with dark reddish-brown spots. OS yellow, dorsum with distinct dark reddish-brown pattern of elongated heart-patch and three transversal fused chevrons, venter with some reddish-brown spots, some of them fused.

Female (paratype): Measurements: Small-sized. Body length 7.7, CA length 4.0, width 4.2; OS length 3.7, width 2.9. Eyes: AME 0.19, ALE 0.30, PME 0.27, PLE 0.24, AME–AME 0.18, AME–ALE 0.06, PME–PME 0.25, PME–PLE 0.32, AME–PME 0.26, ALE–PLE 0.28, CH AME 0.35, CH ALE 0.32. Spination: Pp 121, 101, 3130, 3020; Fe I 313, II 213, III 312, IV 311; Pa I–IV 101; Ti I 2227, II 111(10), III 2116, IV 2025; Mt I–II 2024, III 2124, IV 3034. Measurements of palp and legs: Pp 5.3 (1.6, 0.7, 1.3, –, 1.7), I 15.1 (4.4, 1.5, 4.2, 3.6, 1.4), II 16.4 (4.9, 1.5, 4.6, 3.9, 1.5), III 12.1 (3.7, 1.3, 3.3, 2.7, 1.1), IV 14.1 (4.4, 1.4, 3.5, 3.4, 1.4). Leg formula: II-I-IV-III. Chelicerae with 3 promarginal, 4 retromarginal teeth, and c. 26 intermarginal denticles.

Epigyne (Figs 2A–C): as in diagnosis. EF wider than long, AB indistinct. LL touching each other along the middle lines with a slight asymmetry, i.e. right LL larger than left one. Anterior margins of LL almost parallel to posterior part. FW membranous, with straight lateral margins. IDS with round cover of spermathecae, the latter sub-parallel and elongate. FD long and narrow, posteriorly diverging.

Colouration (Figs 3C, D): as in male, but OS generally darker.

Distribution. Known only from the type locality (Fig. 11).

Remarks. This species shares the same collecting locality with *P. taoi* Zhang, Jäger & Liu, 2023, but exhibits distinct differences in coloration and pattern (e.g., yellow habitus vs. reddish-brown habitus, and CA, sternum and legs with dark reddish-brown spots vs. without spots), which led us to consider them as different species. The colouration and patterns on the male and female habitus of *P. campylotropa* Zhang, Chen, Liu, Jäger & Hu, sp. nov. show strong support for our matching (cf. figs 3A–D vs. figs 241A, B in Zhang et al. 2023). Further research and collection of material of both sexes are needed to verify this taxonomic decision.

Pseudopoda caoguii Zhang, Chen, Liu, Jäger & Hu, sp. nov.

https://zoobank.org/47CC428F-E716-4D75-B3BE-E873DB46C27B
Figs 4, 5, 11

Type material. ***Holotype*** female: China, • Yunnan Province: Zhaotong City, Weixin County, Daxueshan Forest Farm, 27°52'48"N, 104°46'29"E, alt. 1560 m, 21 July 2024, Gui Cao leg. (CBEE, LJ2024001).

Etymology. The specific name is derived from the name of the collector; noun in genitive case.

Diagnosis. Females of *P. caoguii* Zhang, Chen, Liu, Jäger & Hu, sp. nov. resemble those of *P. langyaensis* Zhang, Jäger & Liu, 2023 (cf. figs 4A–C vs. figs 140A–C in Zhang et al. 2023) by having wide U-shaped anterior margins of LL and spherical S, but can be distinguished by: 1) the posterior margins of LL almost straight, 2) body colouration light yellowish-brown (vs. posterior margins of LL distinctly lobed and body colouration reddish-brown in *P. langyaensis*).

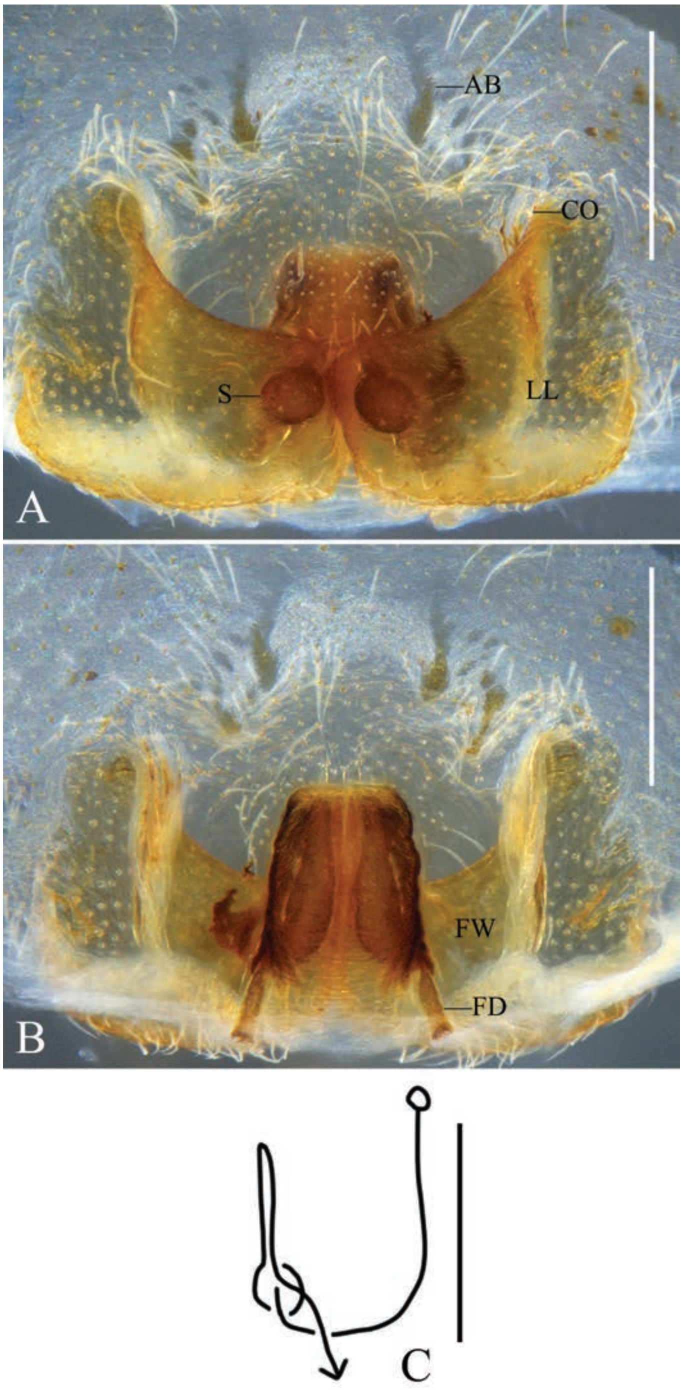

Figure 4. *Pseudopoda caoguii* Zhang, Chen, Liu, Jäger & Hu, sp. nov., female **A** epigyne, ventral **B** vulva, dorsal **C** schematic course of internal duct system, dorsal. Abbreviations: AB, anterior bands; CO, copulatory opening; FD, fertilization duct; FW, first winding; LL, lateral lobes; S, spermathecae. Scale bars: 0.5 mm.

Description. Female (holotype): Measurements: Medium-sized. Body length 12.6, CA length 4.8, width 4.3; OS length 7.3, width 4.1. Eyes: AME 0.18, ALE 0.22, PME 0.19, PLE 0.29, AME–AME 0.22, AME–ALE 0.14, PME–PME 0.32, PME–PLE 0.34, AME–PME 0.21, ALE–PLE 0.28, CH AME 0.36, CH ALE 0.35. Spination: Pp 121, 101, 3130, 3030; Fe I 313, II 323, III 322, IV 321; Pa I–II 101, III 001, IV 000; Ti I–II 2226, III–IV 2126; Mt I–II 2024, III 2124, IV 3036.

Figure 5. Habitus of female *Pseudopoda caoguii* Zhang, Chen, Liu, Jäger & Hu, sp. nov. **A** dorsal **B** ventral. Scale bars: 2 mm.

Measurements of palp and legs: Pp 7.2 (2.2, 1.0, 1.5, –, 2.5), I 22.9 (6.5, 1.8, 6.6, 5.8, 2.2), II 24.9 (7.2, 2.0, 7.1, 6.3, 2.3), III 17.6 (5.5, 1.8, 4.7, 4.1, 1.5), IV 19.5 (6.2, 1.5, 5.0, 4.9, 1.9). Leg formula: II-I-IV-III. Chelicerae with 3 promarginal, 4 retromarginal teeth, and c. 25 intermarginal denticles.

Epigyne (Figs 4A–C): as in diagnosis. EF wider than long, with distinct AB. LL touching each other along median line, anterior margins of LL forming a wide “U”. FW membranous, with straight lateral margins, covering whole IDS. FD short and narrow.

Colouration (Figs 5A, B): CA yellow, with black spots, median band of CA lighter than rest, fovea reddish-brown. Sternum light yellow. Legs yellow, with black spots. OS dorsally orange, with black marks, median band of OS lighter than rest; ventrally with a reddish-brown patch medially.

Male: Unknown.

Distribution. Known only from the type locality (Fig. 11).

Remarks. This species might potentially be conspecific with *P. taoi* Zhang, Jäger & Liu, 2023, given that the two localities are only about 20 kilometres apart. However, there are distinct somatic differences in the female compared to the male of *P. taoi*, including: 1) yellow to orange habitus vs. reddish-brown habitus, 2) OS dorsally with several dark regularly arranged spots vs. OS dorsally dark brown with some light spots, 3) OS ventrally with a reddish-brown patch in middle part behind epigastric furrow vs. OS ventrally without such distinct patch, 4) prosoma dorsally with distinct light median band without dark pattern inside and only few dark dots in lateral parts vs. median band with distinct dark pattern anterior, along and posterior of fovea and distinct dark pattern, partly fused in lateral parts (cf. figs 5A, B vs. figs 241A, B in Zhang et al. 2023). These differences indicate that the present material likely represents a different species than *P*. *taoi*. Moreover, *Pseudopoda* species have a very similar colouration pattern in both sexes and colour dimorphisms are almost absent. Further research and future findings are needed to resolve this ambiguity conclusively.

Pseudopoda yejiachangensis **Zhang, Chen, Liu, Jäger & Hu, sp. nov.**

https://zoobank.org/596F96F8-D9AB-4377-9B88-2864A8EAFA37
Figs 6, 7, 11

Type material. ***Holotype*** male: China, • Jiangxi Province: Shangrao City, Yanshan County, Jiangxi Wuyi Mountain National Nature Reserve, Yejiachang, 27°50'37"N, 117°44'00"E, alt. 889 m, 13 September 2024, Chenliang Li & Wanyu Li leg. (XTU, INS-R001).

Etymology. The specific name is derived from the type locality; adjective.

Diagnosis. Males of *P. yejiachangensis* Zhang, Chen, Liu, Jäger & Hu, sp. nov. resemble those of *P. shuqiangi* Jäger & Vedel, 2007, *P. lushanensis* (Wang, 1990), and *P. jiugongensis* Zhang, Jäger & Liu, 2023 (cf. figs 6A–D vs. figs 73–76 in Jäger and Vedel 2007, figs 4A–C, 5A–C in Quan et al. 2014, and figs 132A–C in Zhang et al. 2023) by having a similar long filiform E and similar simple RTA, but can be recognised from *P. shuqiangi* by: 1) subterminal E with a tiny tooth-shaped EP, and 2) width of RTA obviously thinner than Ti in venter view (vs. E without EP, width of RTA almost equal to Ti in *P. shuqiangi*); it can be recognised from *P. lushanensis* by: 1) E thin throughout its entire length, except embolic base, 2) subterminal E with a tiny tooth-shaped EP, and 3) RTA broad throughout its entire length, arising from Ti proximally (vs. both basal and proximal E broad, EP absent, and RTA finger-shaped, arising subdistally from Ti in *P. lushanensis*); it can be recognised from *P. jiugongensis* by: 1) E arising from T at 9 o'clock position, 2) subterminal E with a tiny tooth-shaped EP, and 3) RTA broad throughout its entire length, arising from Ti proximally (vs. E arising from T at 10:30 o'clock position, EP absent, and RTA finger-shaped with a blunt tip, arising medially from Ti in *P. jiugongensis*).

Description. Male (holotype): Measurements: Small-sized. Body length 8.3, CA length 3.7, width 3.6; OS length 4.5, width 2.7. Eyes: AME 0.17, ALE 0.29, PME 0.20, PLE 0.27, AME–AME 0.13, AME–ALE 0.06, PME–PME 0.25, PME–PLE 0.32, AME–PME 0.26, ALE–PLE 0.23, CH AME 0.31, CH ALE 0.30. Spination: Pp 131, 101, 3000; Fe I 523, II 323, III 322, IV 331; Pa I–II 001, III–IV 000; Ti I 1118, II 1116, III–IV 2126; Mt I–IV 2024. Measurements of palp and legs: Pp 5.7 (1.9, 0.8, 0.9, –, 2.1), I 18.1 (4.8, 1.3, 5.4, 4.9, 1.7), II 19.7 (5.7, 1.4, 5.7, 5.2, 1.7), III 14.9 (4.6, 1.2, 4.1, 3.8, 1.2), IV 17.2 (5.3, 1.1, 4.7, 4.6, 1.5). Leg formula: II-I-IV-III. Chelicerae with 3 promarginal, 4 retromarginal teeth, and c. 33 intermarginal denticles.

Palp (Figs 6A–D): as in diagnosis. T spherical. C long and membranous, arising from T in 12 o'clock position. E long and filiform, arising in 9 o'clock position from T; E running retrolaterally first, then distally, finally ventrally to distally; subterminal E with a tiny tooth-shaped EP. Length of RTA almost same as Ti.

Colouration (Figs 7A, B): CA yellow, with brown spots and dense cover of setae, both latter forming two lateral bands. Fovea dark. Sternum yellow. Legs yellow, with brown spots and spine patches. OS yellow, dorsum with dark brown margin and brown patches pairwise arranged, posteriorly fused, venter with some small brown spots and dark transversal patch posteriorly.

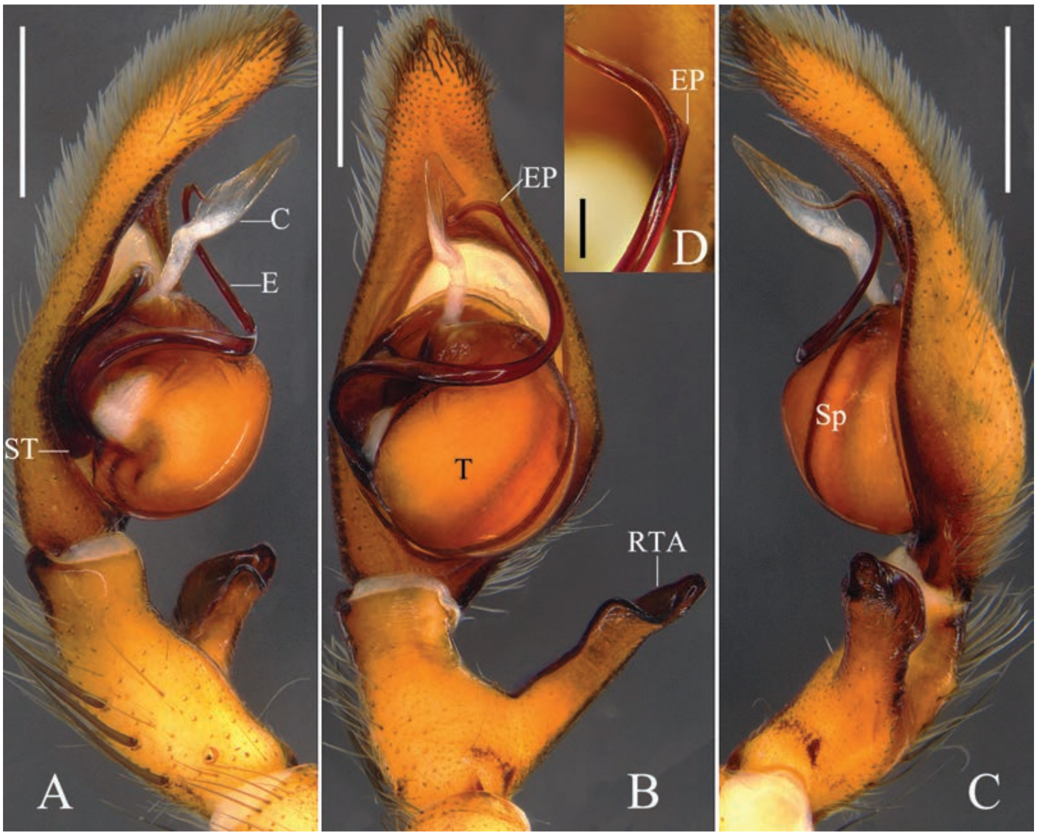

Figure 6. *Pseudopoda yejiachangensis* Zhang, Chen, Liu, Jäger & Hu, sp. nov., left male palp **A** prolateral **B** ventral **C** retrolateral **D** detail of EP. Abbreviations: C, conductor; E, embolus; EP, embolic projection; RTA, retrolateral tibial apophysis; Sp, spermophor; ST, subtegulum; T, tegulum. Scale bars: 0.5 mm (**A–C**); 0.1 mm (**D**).

Figure 7. Habitus of male *Pseudopoda yejiachangensis* Zhang, Chen, Liu, Jäger & Hu, sp. nov. **A** dorsal **B** ventral. Scale bars: 2 mm.

Female: Unknown.

Distribution. Known only from the type locality (Fig. 11).

Remarks. This species was collected from the same mountain range as *P. papilionacea* Zhang, Jäger & Liu, 2023. However, both sexes of *P. papilionacea* are known (Zhang et al. 2023). In addition, the nearest species of the genus, *P. longxiensis* Zhang, Jäger & Liu, 2023, is distributed about 150 km from this species (outside the endemic range of most *Pseudopoda* species, personal observation), and the distinct differences of habitus (e.g., CA with brown patterns and dense cover of setae vs. CA with black spots, without setae) (cf. figs 7A, B vs. figs 156A, B in Zhang et al. 2023) indicating that they are likely not conspecific. Further research and future findings are needed to resolve this ambiguity conclusively.

Pseudopoda ornithorhynchus **Zhang, Chen, Liu, Jäger & Hu, sp. nov.**

https://zoobank.org/9311A7A5-5244-431F-823E-DD90B3F4D1E5
Figs 8–11

Type material. ***Holotype*** male: Vietnam: • Vinh Phuc Province: Tam Dao National Park, Pitfall trap, 21°25'7"N, 105°37'24"E, alt. 80 m, 1–30 December 2007, Dinh Sac Pham leg. (CBEE, LJ201804699).

Etymology. The specific name is derived from Greek 'ornitho' meaning 'bird', and 'rhynchus' meaning 'beak', referring to the shape of the RTA; adjective.

Diagnosis. Males of *P. ornithorhynchus* Zhang, Chen, Liu, Jäger & Hu, sp. nov. resemble those of *P. yangtaiensis* Zhang, Jäger & Liu, 2023 (cf. figs 8A–C, 9A, B vs. figs 268A–C in Zhang et al. 2023) by having a bird's beak-shaped RTA, but can be recognised by: 1) E without basal protrusion, 2) EP short and digitiform, and 3)

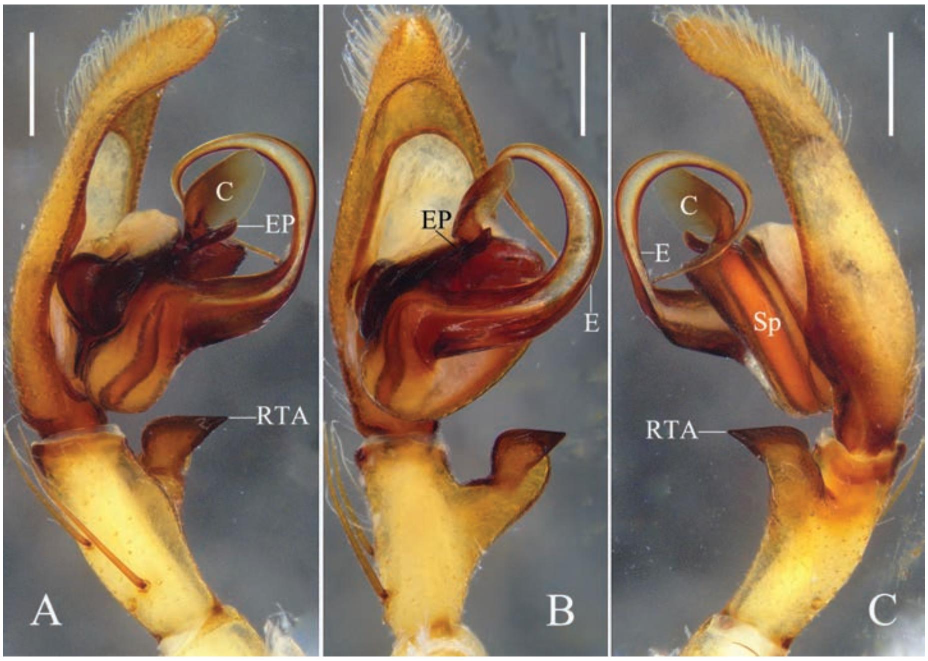

Figure 8. *Pseudopoda ornithorhynchus* Zhang, Chen, Liu, Jäger & Hu, sp. nov., left male palp **A** prolateral **B** ventral **C** retrolateral. Abbreviations: C, conductor; E, embolus; EP, embolic projection; RTA, retrolateral tibial apophysis; Sp, spermophor. Scale bars: 0.5 mm.

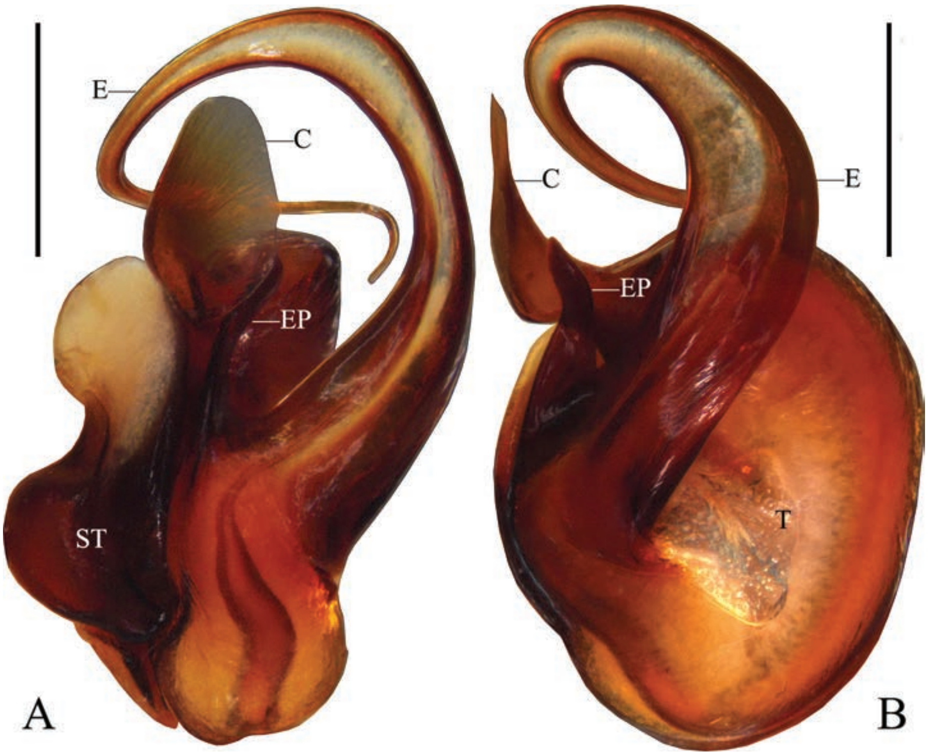

Figure 9. *Pseudopoda ornithorhynchus* Zhang, Chen, Liu, Jäger & Hu, sp. nov., left male palpal bulb **A** prolateral **B** ventral. Abbreviations: C, conductor; E, embolus; EP, embolic projection; ST, subtegulum; T, tegulum. Scale bars: 0.5 mm.

basal RTA columnar (vs. E with a basal prolateral protrusion, EP long and lamellar, arising from T at 1 o'clock position, basal RTA lamellar in *P. yangtaiensis*).

Description. Male (holotype): Measurements: Small-sized. Body length 7.6, CA length 3.8, width 3.2; OS length 3.6, width 2.3. Eyes: AME 0.15, ALE 0.29, PME 0.29, PLE 0.29, AME–AME 0.11, AME–ALE 0.04, PME–PME 0.12, PME–PLE 0.31, AME–PME 0.24, ALE–PLE 0.19, CH AME 0.43, CH ALE 0.32. Spination: Pp 131, 101, 3100; Fe **I** 323, **II** 313, **III** 323, **IV** 331; Pa **I**–**II** 101, **III** 001, **IV** 000; Ti **I** 2128, **II** 1116, **III**–**IV** 2126; Mt **I**–**III** 2024, **IV** 3036. Measurements of palp and legs: Pp 6.3 (2.0, 0.8, 1.1, –, 2.4), **I** 22.8 (6.2, 1.6, 6.7, 6.0, 2.3), **II** 23.6 (6.2, 1.5, 7.2, 6.4, 2.3), **III** 17.7 (5.2, 1.3, 5.0, 4.5, 1.7), **IV** 21.9 (6.3, 1.4, 5.7, 6.4, 2.1). Leg formula: **II**-**I**-**IV**-**III**. Chelicerae with 3 promarginal, 4 retromarginal teeth, and c. 28 intermarginal denticles.

Palp (Figs 8A–C, 9A, B): as in diagnosis. C slightly sclerotized throughout, arising from T at 11 o'clock position. E strongly elongated with one distal coil, with broad basal part and thin terminal part, arising from 8:30 o'clock position of T. EP digitiform. RTA arising medially from Ti, tip retrolaterad.

Colouration (Figs 10A, B): CA yellowish-brown with few dots. Fovea dark reddish-brown. Sternum and legs yellow, the latter with faint dots. OS yellow, dorsum with irregular brown markings, especially in the posterior half, i.e. transversal bars, venter with brown spots, with an inverted triangle brown marking anterior to spinnerets.

Female: Unknown.

Distribution. Known only from the type locality (Fig. 11).

Remarks. This species is located about 140 km from *P. anfracta* Zhang, Jäger & Liu, 2023 and *P. zhengi* Zhang, Jäger & Liu, 2023 (outside the endemic

Figure 10. Habitus of male *Pseudopoda ornithorhynchus* Zhang, Chen, Liu, Jäger & Hu, sp. nov. **A** dorsal **B** ventral. Scale bars: 2 mm.

Figure 11. Distribution map of the four new *Pseudopoda* species **1** *P. campylotropa* Zhang, Chen, Liu, Jäger & Hu, sp. nov. **2** *P. caoguii* Zhang, Chen, Liu, Jäger & Hu, sp. nov. **3** *P. yejiachangensis* Zhang, Chen, Liu, Jäger & Hu, sp. nov. **4** *P. ornithorhynchus* Zhang, Chen, Liu, Jäger & Hu, sp. nov.

range of most *Pseudopoda* species; personal observation, Zhang et al. 2023), and the unique character and colouration of the habitus (eye area as wide as head region, generally yellowish-brown in *P. ornithorhynchus* Zhang, Chen, Liu, Jäger & Hu, sp. nov. vs. the width of eye area almost two-thirds of head region, generally reddish-brown in the latter two known species) (cf. figs 10A, B vs.

figs 13A, B, 280A, B in Zhang et al. 2023) indicating that with the specimen described here is likely not conspecific with either *P. anfracta* or *P. zhengi*. Further research and future findings are needed to resolve this ambiguity conclusively.

Acknowledgments

We thank Caifu Tao (Zhaotong, China), Chenliang Li (Wuhan, China), Dinh Sac Pham (Vietnam National Museum of Nature, Vietnam), Gui Cao (Zhaotong, China), and Wanyu Li (Wuhan, China) for providing sparassid specimens. We also appreciate the valuable comments provided by the subject editor, Alireza Zamani, and the reviewer, Joseph Schubert (Melbourne, Australia), which greatly improved this manuscript.

Additional information

Conflict of interest

The authors have declared that no competing interests exist.

Ethical statement

No ethical statement was reported.

Funding

This study was supported in part by grants from National Natural Sciences Foundation of China (NSFC-32300378/32270495), the Science & Technology Fundamental Resources Investigation Program of China (2023FY100200).

Author contributions

Writing – original draft: HZ, PJ, CH. Writing – review and editing: HZ, HC, FZ, JL, PJ, QF, LC, CH.

Author ORCIDs

He Zhang https://orcid.org/0000-0002-1478-9837
Hailun Chen https://orcid.org/0009-0009-0879-6887
Jie Liu https://orcid.org/0000-0001-7744-9744
Peter Jäger https://orcid.org/0000-0003-1563-0147
Changhao Hu https://orcid.org/0009-0007-5591-3121

Data availability

All of the data that support the findings of this study are available in the main text.

References

Cao XW, Liu J, Chen J, Zheng G, Kuntner M, Agnarsson I (2016) Rapid dissemination of taxonomic discoveries based on DNA barcoding and morphology. Scientific Reports 6: 37066. https://doi.org/10.1038/srep37066

Davies VT (1994) The huntsman spiders *Heteropoda* Latreille and *Yiinthi* gen. nov. (Araneae: Heteropodidae) in Australia. Memoirs of the Queensland Museum 35(1): 75–122.

Jäger P (2001) Diversität der Riesenkrabbenspinnen im Himalaya – die Radiation zweier Gattungen in den Schneetropen (Araneae, Sparassidae, Heteropodinae). Courier Forschungsinstitut Senckenberg 232: 1–136.

Jäger P, Vedel V (2005) *Pseudopoda fissa* sp. nov. — first record of the genus from Vietnam (Araneae: Sparassidae). Zootaxa 837: 1–5. https://doi.org/10.11646/zootaxa.837.1.1

Jäger P, Vedel V (2007) Sparassidae of China 4. The genus *Pseudopoda* (Araneae: Sparassidae) in Yunnan Province. Zootaxa 1623: 1–38. https://doi.org/10.11646/zootaxa.1623.1.1

Jäger P, Li SQ, Krehenwinkel H (2015) Morphological and molecular taxonomic analysis of *Pseudopoda* Jäger, 2000 (Araneae: Sparassidae: Heteropodinae) in Sichuan Province, China. Zootaxa 3999(3): 363–392. https://doi.org/10.11646/zootaxa.3999.3.3

Jiang TY, Zhao QY, Li SQ (2018) Sixteen new species of the genus *Pseudopoda* Jäger, 2000 from China, Myanmar, and Thailand (Sparassidae, Heteropodinae). ZooKeys 791: 107–161. https://doi.org/10.3897/zookeys.791.28137

Logunov DV, Jäger P (2015) Spiders from Vietnam (Arachnida: Aranei): new species and records. Russian Entomological Journal 24(4): 343–363. https://doi.org/10.15298/rusentj.24.4.09

Quan D, Zhong Y, Liu J (2014) Four *Pseudopoda* species (Araneae: Sparassidae) from southern China. Zootaxa 3754(5): 555–571. https://doi.org/10.11646/zootaxa.3754.5.2

World Spider Catalog (2025) World Spider Catalog. Version 26. Natural History Museum Bern. http://wsc.nmbe.ch [accessed on 17 February 2025]

Yang ZZ, Chen YQ, Chen YL, Zhang YG (2009) Two new species of the genus *Pseudopoda* from Yunnan, China (Araneae: Sparassidae). Acta Arachnologica Sinica 18: 18–22.

Yang ZZ, Wu YY, Li ZM, Zhang BS (2022) Two new species of the genus *Pseudopoda* Jäger, 2000 and first description of the male of *Pseudopoda physematosa* (Araneae, Sparassidae) from Yunnan Province, China. Zootaxa 5188(4): 347–360. https://doi.org/10.11646/zootaxa.5188.4.3

Zhang BS, Zhang F, Zhang ZS (2013a) Four new species of the genus *Pseudopoda* Jäger, 2000 (Araneae, Sparassidae) from Yunnan province, China. Zootaxa 3702: 273–287. https://doi.org/10.11646/zootaxa.3702.3.5

Zhang F, Zhang BS, Zhang ZS (2013b) New species of *Pseudopoda* Jäger, 2000 from southern China (Araneae, Sparassidae). ZooKeys 361: 37–60. https://doi.org/10.3897/zookeys.361.6089

Zhang H, Jäger P, Liu J (2017) One new *Pseudopoda* species group (Araneae: Sparassidae) from Yunnan Province, China, with description of three new species. Zootaxa 4318(2): 271–294. https://doi.org/10.11646/zootaxa.4318.2.3

Zhang H, Jäger P, Liu J (2019) Establishing a new species group of *Pseudopoda* Jäger, 2000 with the description of two new species (Araneae, Sparassidae). ZooKeys 879: 91–115. https://doi.org/10.3897/zookeys.879.35110

Zhang H, Zhu Y, Zhong Y, Jäger P, Liu J (2023) A taxonomic revision of the spider genus *Pseudopoda* Jäger, 2000 (Araneae: Sparassidae) from East, South and Southeast Asia. Megataxa 9(1): 1–304. https://doi.org/10.11646/megataxa.9.1.1

Zhang JS, Pan TQ, Zhang H, Xing YQ, Yu H, Zhong Y (2025) Species delimitation of newly collected spiders of the genus *Pseudopoda* (Araneae, Sparassidae) from Honghe Hani and Yi Autonomous Prefecture, Yunnan, China: an integrated morphological and molecular approach. Zoosystematics and Evolution 101(1): 141–171. https://doi.org/10.3897/zse.101.136177

ZooKeys 1230: 247–286 (2025)
DOI: 10.3897/zookeys.1230.140159

Research Article

Revision of the Chinese species of the genus *Brachyponera* Emery, 1900 (Hymenoptera, Formicidae), with a key to the world species of the genus

Chao Chen[1,2], Yu Yu[3], Chuanhui Yi[2,4]

1 Kunming Natural History Museum of Zoology, Kunming Institute of Zoology, Chinese Academy of Sciences, Kunming, Yunnan Province 650221, China
2 Key Laboratory of Forest Disaster Warning and Control in Yunnan Province, College of Forestry, Southwest Forestry University, Kunming, Yunnan Province 650224, China
3 Huanglianshan National Nature Reserve, Lvchun, Yunnan Province 662599, China
4 Yunnan Institute of Biological Diversity, Southwest Forestry University, Kunming, Yunnan Province 650224, China
Corresponding author: Chuanhui Yi (ychuanh@126.com)

Abstract

The species of the ant genus *Brachyponera* Emery, 1900 are reviewed based on the morphological characters of the worker caste. *Brachyponera tianzun* (Terayama, 2009) is transferred to *Euponera* as *Euponera tianzun* (Terayama, 2009), **comb. nov.** Four new species, *B. paraarcuata* **sp. nov.**, *B. xui* **sp. nov.**, *B. candida* **sp. nov.**, and *B. myops* **sp. nov.**, are described from China based on the worker caste. Phylogenetic trees were constructed for eight known and four new species, and genetic distances were calculated. High-resolution images of *B. batak* (Yamane, 2007), *B. flavipes* (Yamane, 2007), *B. nakasujii* (Yashiro et al., 2010), *B. pilidorsalis* (Yamane, 2007), *B. wallacea* (Yamane, 2007), and *B. brevidorsa* Xu, 1994 are provided. Keys are provided to both the eight species groups and 23 known species of the world based on the worker caste.

Key words: High-resolution illustrations, new combination, new species, phylogenetics, Ponerinae, revision, taxonomy, Yunnan Province

Academic editor: Sebastian Salata
Received: 25 October 2024
Accepted: 17 January 2025
Published: 6 March 2025

ZooBank: https://zoobank.org/BDECAA4B-57ED-4DA9-B75F-4BA65C3FC37B

Citation: Chen C, Yu Y, Yi C (2025) Revision of the Chinese species of the genus *Brachyponera* Emery, 1900 (Hymenoptera, Formicidae), with a key to the world species of the genus. ZooKeys 1230: 247–286. https://doi.org/10.3897/zookeys.1230.140159

Introduction

The genus *Brachyponera* Emery, 1900, was initially established as a subgenus of *Euponera* Forel, 1891 with the type species *E.* (*B.*) *croceicornis* (Emery, 1900), and later elevated to the genus level (Bingham 1903). Subsequently, it was synonymized with the genus *Pachycondyla* F. Smith, 1858 (Snelling 1981) and placed within the tribe Ponerini (Bolton 2003). Since the 21st century, with the widespread application of molecular phylogenetic analysis, the subgenus *Brachyponera* has been reinstated as an independent genus and placed under the *Odontomachus* genus group of the tribe Ponerini (Schmidt 2013; Schmidt and Shattuck 2014).

Brachyponera workers have a small body size and are carnivorous or scavenging, typically choosing to construct their nests in decaying wood or soil (Wheeler 1933; Haskins and Haskins 1950; Wilson 1958; Ogata 1987; Matsuura 2002;

Matsuura et al. 2002; Kikuchi et al. 2007; Yamane 2007; Gotoh and Ito 2008). Two species of the genus known from Thailand are cave dwelling ants (*B*. *kumtongi* and *B*. *troglomorpha*). Ant crickets (*Myrmecophilus* Berthold, 1827) were found together with foraging workers of the species (Duanchay et al. 2024). *Brachyponera* is unusual among ponerines in that it displays a marked reproductive dimorphism between workers and queens, with the workers having completely lost their reproductive organs and queens having a large number of ovarioles (Ito and Ohkawara 1994; Gotoh and Ito 2008).

Brachyponera is widespread from Africa through southern Asia to Australia. It is the most species-rich in Southeast Asia (Duanchay et al. 2024). *Brachyponera chinensis* (Emery) was accidentally introduced to the southeastern United States and is now locally abundant (Nelder et al. 2006); it has also been introduced to New Zealand and Europe (Schmidt and Shattuck 2014; Menchetti et al. 2022; Duanchay et al. 2024). Currently, 20 valid species and five valid subspecies are recognized in the world (Bolton 2024). In this work, we focused only on the species level taxa due to their clear-cut criteria and data availability, while subspecies classification, which is more complex and variable, could introduce ambiguity and complicate our analysis.

Brachyponera sennaarensis (Mayr, 1862) is widely distributed in central to southern regions of Africa, representing the single species in Africa. The genus is represented by one species in Korea and Laos, two species in Australia and New Guinea, three species in Java, Sulawesi, Philippines, Sumatra, Malaysia, Japan, Myanmar, and Sri Lanka, four species in Vietnam and India, and five species in Thailand (Janicki et al. 2016). In China, five species have been recorded (Guénard et al. 2017). Currently, *B. brevidorsa* Xu, a species endemic to China, represents the only species within the genus described by a Chinese researcher (Xu 1994). The other taxon described as a member of *Brachyponera* was later transferred to the genus *Hypoponera* and is currently known as *H. mesoponeroides* (Dang et al. 2018).

It appears that the intergeneric transfers within Ponerini are still unresolved cases, as the results of our work revealed another species with a wrongly assigned genus. Terayama (2009) described *Pachycondyla tianzun* based on workers collected from Taiwan, China. Later, in 2014, Schmidt and Shattuck reinstated *Brachyponera* as a separate genus and reclassified *Pachycondyla tianzun* as a member of *Brachyponera*. Examining the original description of the species with photographs of the type specimen in the Institute of Agro-Environmental Research, Japan (https://www.naro.affrc.go.jp/archive/niaes/inventory/insect/inssys/hymlst.htm HYM-182), we have concluded the characterization of this species does not correspond with *Brachyponera*, but well agrees with *Euponera* in some important diagnostic characters separating the two genera. Therefore, in the present paper, *B. tianzun* is transferred to *Euponera* as a new combination. The species is redescribed below on the basis of the original description and photographs of the holotype specimen.

In this study, we review the Chinese species of *Brachyponera*, with descriptions of four new species from Yunnan, China, accompanied by high-resolution images and measurements of important morphological characters. We also provide a synoptic list of 23 extant species of the genus and a key to their determination. A key to species groups based on the worker caste is also provided.

Materials and methods

The ant specimens were obtained using sample-plots and search-collecting methods (e.g., Xu 2002). Sample plots were set up at the research site with different altitude gradients and included a variety of vegetation types within the survey area. Subsequently, the specimens were meticulously examined using an SDPTOP-SZM stereomicroscope. High-quality multifocus montage images were captured using a Keyence VHX-6000 ultra-depth microscopic three-dimensional microscope. To compare the worker morphology of the four new species, reference was made to the original descriptions of related species (Mayr 1862; Emery 1895; Karavaiev 1925). Sculptural and hair terminology follows Harris (1979) and Wilson (1955). The key was prepared using the examined specimens, images available on AntWeb (2024) and AntWiki (2024), and original descriptions of the species.

The investigated material is deposited in the following institutions:

KIZ	Kunming Natural History Museum of Zoology, Kunming Institute of Zoology, Chinese Academy of Sciences, Kunming, Yunnan Province, China.
SWFU	Insect Collection, Southwest Forestry University, Kunming, Yunnan Province, China.
GXNU	Insect Collection, Guangxi Normal University, Guilin, Guangxi, China.

Standard measurements and indices were employed as defined in Bolton (1975) and Lattke (2011), with the addition of mandible length and eye diameter as outlined below. Furthermore, alitrunk (mesosoma) length is substituted by Weber's Length in accordance with the methodology proposed by Xu and He (2015). Head lateral margin length, anterior head length, clypeal median lobe length, pronotum length and pronotum height were also measured (see Arimoto 2017). All measurements are expressed in millimeters.

HL	Head length: the straight-line length of the head in perfect full-face view, measured from the midpoint of the anterior clypeal margin to the midpoint of the posterior margin. In species where one or both of these margins are concave, the measurement is taken from the mid-point of a transverse line that spans the apices of the projecting portions.
HLL	Head lateral margin length: in full-face view, the head length measured from the mandible base to the nuchal carina.
HLA	Anterior head length: in full-face view, the head length measured from the mandible base to the anterior edge of the eye.
HW	Head width: the maximum width of the head in full-face view, excluding the eyes.
ML	Mandible length: the straight-line length of the mandible measured from the apex to the lateral base.
CML	Clypeal median lobe length: in full-face view, the straight-line length measured from the anterior margin of the clypeus to the anterior margin of the torulus.
SL	Scape length: the straight-line length of the antennal scape, excluding the basal constriction or neck.

ED	Eye diameter: the maximum diameter of the eye.
PrL	Pronotum length: in profile, the diagonal length of the pronotum, measured from the anterior margin of the pronotum excluding the collar to the posterior extremity of the pronotum.
PrH	Pronotum height: in profile, the maximum height of the pronotum, measured from the posterior base of the lateral margin of the pronotum to the highest point of the pronotum.
PrW	Pronotum width: the maximum width of the pronotum measured in dorsal view.
WL	Weber's length (= alitrunk length): the diagonal length of the mesosoma in lateral view, measured from the point at which the pronotum meets the cervical shield to the posterior basal angle of the metapleuron.
TL	Total length: the total outstretched length of the individual, from the mandibular apex to the gastral apex.
PL	Petiole length: the length of the petiole measured in lateral view from the anterior process to the posteriormost point of the tergite, where it surrounds the gastral articulation.
PH	Petiole height: the height of the petiole measured in lateral view from the apex of the ventral (subpetiolar) process vertically to a line intersecting the dorsal most point of the node.
DPW	Dorsal petiole width: the maximum width of the petiole in dorsal view.
CI	Cephalic Index = HW × 100 / HL.
SI	Scape index = SL × 100 / HW.
LPI	Lateral petiole index = PH × 100 / PL.
PDPI	Dorsal petiole index = DPW × 100 / PL.

Other abbreviations. w.: worker; **q.**: queen; **m.**: male; **var.**: variety; **subsp.**: subspecies.

DNA extraction of tissue fragments from ants was made using TSINGKE TSP202-50 Trelief® Hi-Pure Animal Genomic DNA Kit. The standard COI barcoding fragment (Hebert et al. 2003) was amplified using a cocktail of primers LCO1490 (GGTCAACAAATCATAAAGATATTGG) and HCO2198 (TAAACTTCAGGGTGACCAAAAAATCA) (Folmer et al. 1994). Amplification was performed with synthesized primers using TSINGKE Gold Mix (green), PCR reactions contained 47ul Gold Mix (green), 1 ul 10 μM Primer F, 1 ul 10 μM Primer R, with 1.0 μl of template DNA. PCR was performed using an initial denaturation step of 2 min at 98 °C, followed by 30 cycles of 10 s at 98 °C, 10 s at 50 °C and 10 s at 72 °C, and finishing with an extension of 5 min at 72 °C and pause at 4 °C. The amplified PCR products were subjected to agarose gel electrophoresis (2 μl sample + 6 μl bromophenol blue) at 300V for 12 min to obtain the identification gel graphs. The products were purified and sequenced by Tsingke Biotechnology (Beijing) Co., Ltd., using the same primers as in PCR. Sequences were edited and manually managed using SeqMan in Lasergene v. 7.1 (DNASTAR Inc., Madison, WI, USA) and MEGA 11 (Tamura et al. 2021). All new sequences were deposited in GenBank. *Hypoponera mesoponeroides* (Radchenko) and *Euponera sikorae* (Forel) were chosen as outgroups, and their sequences along with seven described *Brachyponera* species were obtained from GenBank (Table 1).

Table 1. Sequences used in this study.

Species	GenBank	Voucher/isolate	Length	AT%
Brachyponera brevidorsa	PQ863325	KIZ20231327	681	72.6
Brachyponera candida sp. nov.	PQ863326	KIZ20230168	677	70.9
Brachyponera chinensis	OM604749	MM21B056a1	658	71.6
Brachyponera croceicornis	PP069658	HP0159	659	69.8
Brachyponera luteipes	LC426718	Nago5	565	68
Brachyponera myops sp. nov.	PQ863327	KIZ20231049	676	72.2
Brachyponera nakasujii	MH370729	Bnak4	543	68.2
Brachyponera nigrita	GQ264596	63	565	71
Brachyponera obscurans	EF609940	CASENT0060572-D01	657	70
Brachyponera paraarcuata sp. nov.	PQ863328	KIZ20231657	680	69.8
Brachyponera sennaarensis	OR527449	RyadhLM2019	645	71.8
Brachyponera xui sp. nov.	PQ863329	KIZ20231023	679	72
Euponera sikorae	HQ925507	CASENT0152189-D01	635	70.1
Hypoponera mesoponeroides	LC349924	AD170525-04	558	74

Sequences were aligned using ClustalW (Thompson et al. 2002) with default parameters in MEGA 11 (Tamura et al. 2021) with default parameters. The genetic divergence (uncorrected p-distance) between species was calculated in MEGA 11 (Tamura et al. 2021). The best substitution model GTR+G+I was selected using the Akaike Information Criterion (AIC) in ModelFinder (Nei and Kumar 2000).

Evolutionary history was inferred by using the maximum likelihood method and the General Time Reversible model (Nei and Kumar 2000). The tree with the highest log likelihood (-3345.33) is shown. The percentage of trees in which the associated taxa clustered together is shown below the branches. Initial tree(s) for the heuristic search were obtained automatically by applying neighbor-joining and BioNJ algorithms to a matrix of pairwise distances estimated using the Maximum Composite Likelihood (MCL) approach and then selecting the topology with superior log likelihood value. A discrete Gamma distribution was used to model evolutionary rate differences among sites (5 categories (+G, parameter = 0.8794)). The rate variation model allowed for some sites to be evolutionarily invariable ([+I], 50.92% sites). The tree is drawn to scale, with branch lengths measured in the number of substitutions per site. This analysis involved 14 nucleotide sequences. There was a total of 668 positions in the final dataset. Evolutionary analyses were conducted in MEGA11 (Tamura et al. 2021), and nodal support was estimated by 1000 rapid bootstrap replicates. Bayesian inference phylogenies were inferred using MrBayes v. 3.2.7a (Ronquist et al. 2012) under the JC model (2 parallel runs, 2000000 generations), in which the initial 25% of sampled data were discarded as burn-in. Phylogenetic trees were edited with iTOL v. 5 (Letunic and Bork 2021).

Results

We obtained COI gene sequences of seven species of *Brachyponera* and two outgroups from GenBank (Table 1). We determined COI gene sequences de novo for the four new species and *B. brevidorsa* Xu, resulting in a total of 14 nucleotide sequences. The generated gene sequences were 668 bp in length. The topologies derived from Bayesian inference and maximum likelihood analyses were consistent (Fig. 1).

The 12 species of the genus *Brachyponera* were all grouped together and distinguished from the two outgroup species. *Brachyponera sennaarensis* and *B. xui* sp. nov. were located at the base of the tree. The genetic distance between *B. candida* sp. nov., *B. myops* sp. nov. and *B. brevidorsa* was relatively close, resulting in the three species grouping together. *B. paraarcuata* sp. nov. is a relatively derived species; the genetic distance between it and other species is greater than 0.13, and it is clustered with *B. obscurans* and *B. croceicornis*. *B. chinensis*, *B. luteipes* and *B. nakasujii* are grouped together (Table 2).

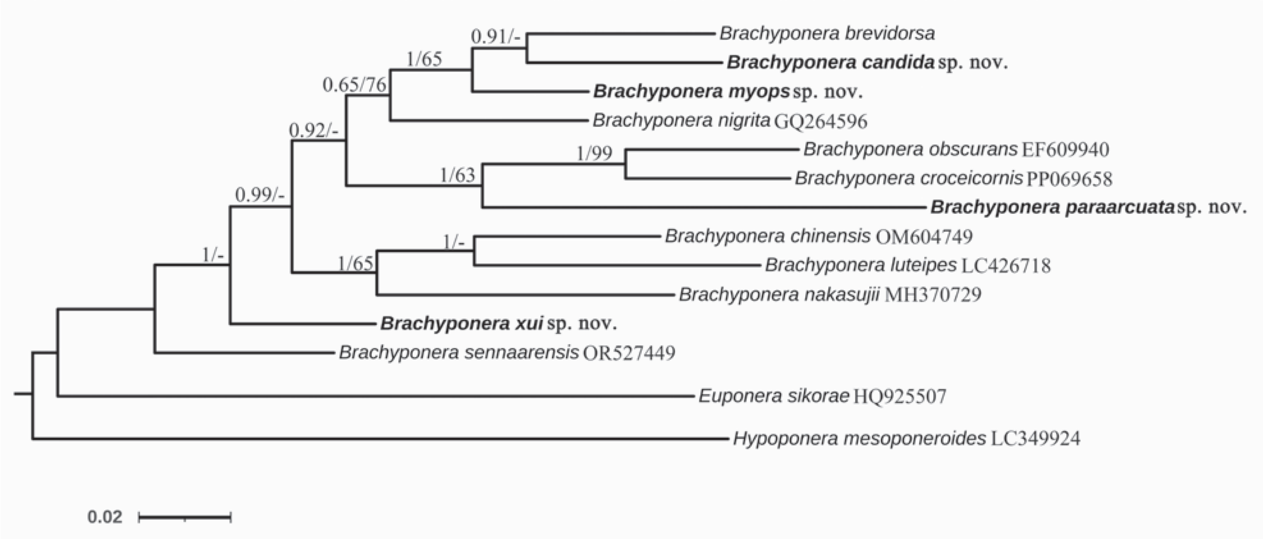

Figure 1. Phylogenetic tree inferred from Bayesian analysis based on the COI gene. Numbers before slashes indicate Bayesian posterior probabilities (only values above 0.6 are shown) and numbers after slashes indicate bootstrap support from maximum likelihood analysis (only values above 60 are shown).

Table 2. Estimates of evolutionary divergence between sequences.

		1	2	3	4	5	6	7	8	9	10	11	12	13
1	*B. chinensis*													
2	*B.croceicornis*	0.1398												
3	*B. luteipes*	0.0980	0.1385											
4	*B. nakasujii*	0.1154	0.1471	0.1258										
5	*B. nigrita*	0.1184	0.1487	0.1263	0.1194									
6	*B. obscurans*	0.1370	0.0700	0.1408	0.1517	0.1367								
7	*B. sennaarensis*	0.1226	0.1274	0.1389	0.1480	0.1197	0.1370							
8	*H. mesoponeroides*	0.1935	0.1989	0.1868	0.2182	0.1936	0.2043	0.1756						
9	*E. sikorae*	0.1874	0.1937	0.2163	0.2158	0.1939	0.2142	0.1680	0.2204					
10	*B. brevidorsa*	0.1079	0.1290	0.1303	0.1343	0.0957	0.1172	0.1163	0.1900	0.1827				
11	*B. candida* sp. nov.	0.1125	0.1214	0.1283	0.1407	0.0978	0.1157	0.1302	0.1989	0.1843	0.0793			
12	*B. myops* sp. nov.	0.1049	0.1184	0.1242	0.1173	0.0754	0.1111	0.1023	0.1935	0.1732	0.0704	0.0704		
13	*B. paraarcuata* sp. nov.	0.1565	0.1366	0.1670	0.1962	0.1507	0.1492	0.1519	0.2061	0.2000	0.1497	0.1482	0.1437	
14	*B. xui* sp. nov.	0.1003	0.1123	0.1059	0.1130	0.0896	0.1111	0.0946	0.1738	0.1843	0.1123	0.1123	0.0868	0.1452

Note: the number of base differences per site from between sequences is shown. Values represent the genetic distance between two different species. This analysis involved 14 nucleotide sequences. All ambiguous positions were removed for each sequence pair (pairwise deletion option). There was a total of 668 positions in the final dataset. Evolutionary analyses were conducted in MEGA11 (Tamura et al. 2021).

Key to species groups of *Brachyponera* based on workers

1 Lateral face of pronotum with transverse rugae .... ***atrata* group**
– Lateral face of pronotum smooth and shiny or only punctate **2**
2 In full-face view, head broader than long .... ***lutea* group (part)**
– In full-face view, head longer than broad **3**
3 In full-face view, eye small, with five ommatidia along longest axis (ED 0.07 mm) (China) .... ***kumtongi* group**
– In full-face view, eye moderately large, with more than nine ommatidia along longest axis (ED > 0.15 mm) **4**
4 In lateral view, propodeum densely transversely rugose; smooth area if any much restricted.. ***chinensis* group**
– In lateral view, propodeum smooth or only punctate **5**
5 In dorsal view, lateral margin of pronotum with well-defined edge; lateral slope of pronotum nearly vertical .... ***xui* group**
– In dorsal view, lateral margin of pronotum not well defined; lateral slope of pronotum convex...**6**
6 In lateral view, dorsal surface of propodeum continuously connected with declivity, forming complete circular arc **7**
– In lateral view, dorsal surface of propodeum clearly differentiated from declivity; posterodorsal corner of propodeum roundly angled..................**8**
7 Larger species, > 5 mm in total body length; antenna scape long, > 1/5 exceeds posterolateral corner; in lateral view, pronotum weakly convex.... .... ***arcuata* group**
– Smaller species, < 4 mm in total body length; antenna scape short, slightly exceeds posterolateral corner; in lateral view, pronotum relatively flat .... ***lutea* group (part)**
8 Larger species, > 4.5 mm in total body length; head width > 0.9 mm; flagellar segments 1 and 2 longer than broad; body color usually dark brown.... .... ***nigrita* group**
– Smaller species, < 4.5 mm in total body length; head width < 0.9 mm; flagellar segments 1 and 2 each as long as broad, or broader than long; body color usually yellowish brown to tan ....***obscurans* group**

Synoptic list of *Brachyponera*

Brachyponera atrata group

***Brachyponera atrata* (Karavaiev, 1925)** (Suppl. material 1: fig. S1)
Euponera (*Brachyponera*) *atrata* Karavaiev, 1925b: 126 (w.) Indonesia (Ambon I.).
***Brachyponera wallacea* (Yamane, 2007)** (Suppl. material 1: fig. S2)
Pachycondyla wallacea Yamane, 2007: 659, fig. 8 (w.q.) Indonesia (Lombok I.).
Brachyponera wallacei [sic]: Schmidt and Shattuck 2014: 81.

Brachyponera lutea group

***Brachyponera lutea* (Mayr, 1862)** (Suppl. material 1: fig. S3)
Ponera lutea Mayr, 1862: 721 (w.q.) Australia (New South Wales).

***Brachyponera sennaarensis* (Mayr, 1862)** (Suppl. material 1: figs S4, S5)
Ponera sennaarensis Mayr, 1862: 721 (w.) Sudan.
***Brachyponera brevidorsa* Xu, 1994** (Fig. 22)
Brachyponera brevidorsa Xu, 1994b: 183, figs 5, 6 (w.) China (Yunnan).
Brachyponera troglomorpha Duanchay & Jaitrong, 2024
Brachyponera troglomorpha Duanchay & Jaitrong, in Duanchay et al. 2024: 7, figs 2, 3C, 4 (w.) Thailand. Indomalaya.

***Brachyponera kumtongi* group**

***Brachyponera kumtongi* Duanchay & Jaitrong, 2024**
Brachyponera kumtongi Duanchay & Jaitrong, in Duanchay et al. 2024: 4, figs 1, 3B, 4 (w.) Thailand. Indomalaya.
***Brachyponera myops* Chen, Yu & Yi, sp. nov.** (Fig. 26). China (Yunnan).
Brachyponera chinensis group
***Brachyponera chinensis* (Emery, 1895)** (Fig. 24)
Ponera nigrita subsp. *chinensis* Emery, 1895 m: 460 (w.) China (Shanghai). Palearctic.
***Brachyponera nakasujii* (Yashiro et al., 2010)** (Suppl. material 1: fig. S6)
Pachycondyla nakasujii Yashiro et al., 2010: 44, figs 4, 5 (w.q.m.) Japan.

***Brachyponera xui* group**

***Brachyponera xui* Chen, Yu & Yi, sp. nov.** (Fig. 30). China (Yunnan).

***Brachyponera arcuata* group**

***Brachyponera arcuata* (Karavaiev, 1925)** (Suppl. material 1: figs S7, S8)
Euponera (*Brachyponera*) *luteipes* var. *arcuata* Karavaiev, 1925b: 125, figs 3c, 4 (w.q.m.) Indonesia (Java).
***Brachyponera paraarcuata* Chen, Yu & Yi, sp. nov.** (Fig. 29). China (Yunnan).

***Brachyponera nigrita* group**

***Brachyponera batak* (Yamane, 2007)** (Suppl. material 1: fig. S9)
Pachycondyla batak Yamane, 2007: 656, figs 3, 4, 12–16 (w.q.m.) Indonesia (Sumatra).
***Brachyponera candida* Chen, Yu & Yi, sp. nov.** (Fig. 23). China (Yunnan).
***Brachyponera flavipes* (Yamane, 2007)** (Suppl. material 1: fig. S10)
Pachycondyla flavipes Yamane, 2007: 658, fig. 5 (w.) Myanmar.
***Brachyponera nigrita* (Emery, 1895)** (Fig. 27)
Ponera nigrita Emery, 1895 m: 459 (w.) Myanmar.
***Brachyponera pilidorsalis* (Yamane, 2007)** (Suppl. material 1: fig. S11)
Pachycondyla pilidorsalis Yamane, 2007: 655, figs 7, 9–11 (w.q.) West Malasia.

***Brachyponera obscurans* group**

***Brachyponera christmasi* (Donisthorpe, 1935)** (Suppl. material 1: fig. S12)
Euponera (*Mesoponera*) *christmasi* Donisthorpe, 1935: 630 (w.) Christmas Island.

***Brachyponera croceicornis* (Emery, 1900)** (Suppl. material 1: fig. S13)
Euponera (*Brachyponera*) *luteipes* var. *croceicornis* Emery, 1900b: 315 (w.q.) New Guinea (Papua New Guinea).

***Brachyponera jerdonii* (Forel, 1900)** (Suppl. material 1: fig. S14)
Ponera jerdonii Forel, 1900f: 327 (w.) India (Maharashtra, West Bengal, Kerala, Assam).

***Brachyponera luteipes* (Mayr, 1862)** (Fig. 25)
Ponera luteipes Mayr, 1862: 722 (w.q.) India (Nicobar Is).

***Brachyponera obscurans* (Walker, 1859)** (Fig. 28)
Formica obscurans Walker, 1859: 372 (q.) Sri Lanka.

Key to *Brachyponera* species based on the worker caste

The distinction between the four species, *B. flavipes*, *B. batak*, *B. pilidorsalis*, and *B. nigrita* is principally based on Yamane (2007).

1 Lateral face of pronotum with transverse rugae (Fig. 2A, B)......................**2**
– Lateral face of pronotum smooth and shiny or only punctate (Fig. 2C, D)......................**3**
2 Dorsum of propodeal declivity with rugae only on upper part (Fig. 3A); in lateral view, propodeum with sparsely transverse rugae (Fig. 3C) (Maluku islands)...................... ***B. atrata* (Karavaiev)**
– Dorsum of propodeal declivity with rugae on middle and upper parts (Fig. 3B); in lateral view, propodeum with densely transverse rugae (Fig. 3D) (Sulawesi, Lombok, and Bali) .... ***B. wallacea* (Yamane)**
3 Eye small with 2–5 ommatidia along longest axis (ED 0.07 mm) (Fig. 4A, B)......................**4**
– Eye moderately large, with > 7 ommatidia along longest axis (ED > 0.10 mm) (Fig. 4C, D)......................**5**

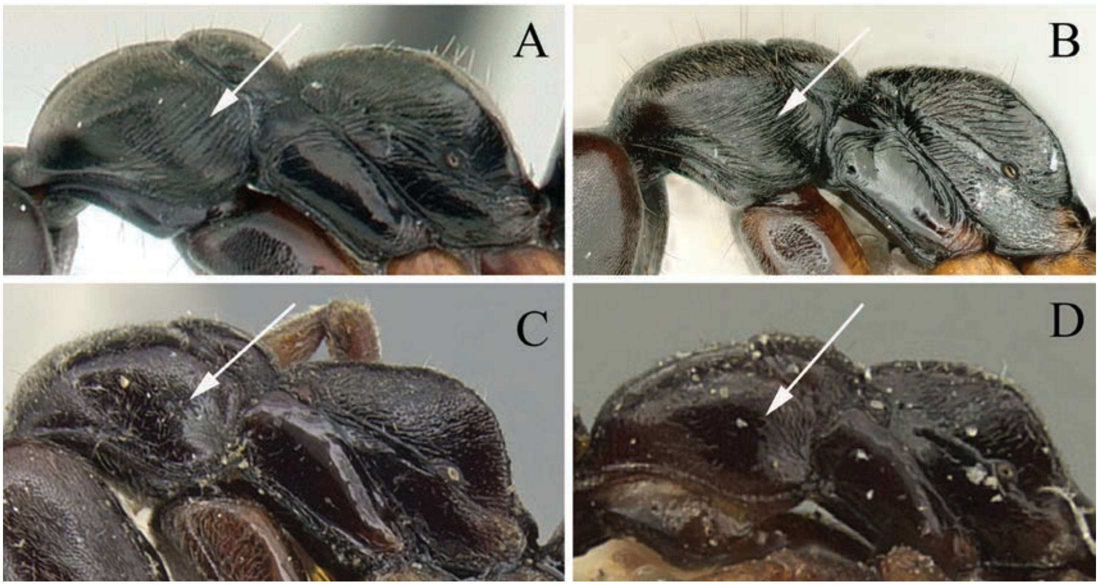

Figure 2. Mesosoma in profile showing sculpture of lateral face of pronotum **A** *Brachyponera atrata* (CASENT0178452) **B** *B. wallacea* (non-type) **C** *B. chinensis* (CASENT0903937, type) **D** *B. luteipes* (CASEN0915672, type). Photographers April Nobile (**A**), Chao Chen (**B**), Will Ericson (**C**), Harald Bruckner (**D**).

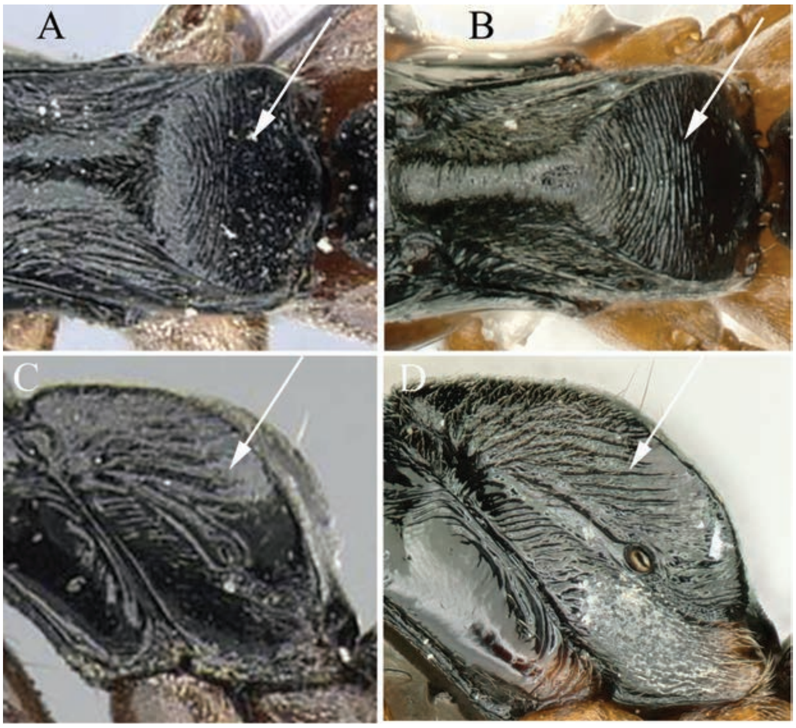

Figure 3. Mesosoma in dorsal view **A** *Brachyponera atrata* (CASENT0178452) **B** *B. wallacea* (non-type) Propodeum in lateral view **C** *Brachyponera atrata* (CASENT0178452) **D** *B. wallacea* (non-type). Photographers April Nobile (**A, C**), Chao Chen (**B, D**).

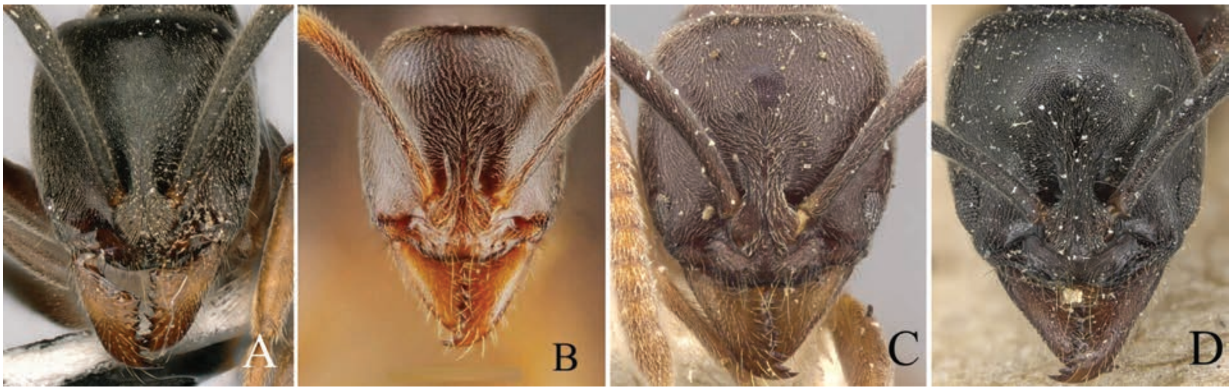

Figure 4. Head in full-face view showing size of eye **A** *Brachyponera myops* sp. nov. **B** *B. kumtongi* **C** *B. jerdonii* (CASENT0907282, type) **D** *B. nigrita* (CASENT0903936, type). Photographers Chao Chen (**A**), Duanchay et al. 2024 (**B**), Z. Liebermantype (**C**), Will Ericson (**D**).

4 Eye very small, present as a dot, with 2 or 3 ommatidia along longest axis (Fig. 4B); antennal segments 3 and 4 each as long as broad, or broader than long; body color reddish brown (Thailand)... .... ***B. kumtongi*** **Duanchay & Jaitrong**

– Eye relatively small, with 4 or 5 ommatidia along longest axis (Fig. 4A); antennal segments 3 and 4 each longer than broad; body color brownish black (China)...***B. myops*** **Chen, Yu & Yi, sp. nov.**

5 In full-face view, head broader than long, or almost as long as broad (Fig. 5A, B)...**6**

– In full-face view, head longer than broad (Fig. 5C, D)..................................**7**

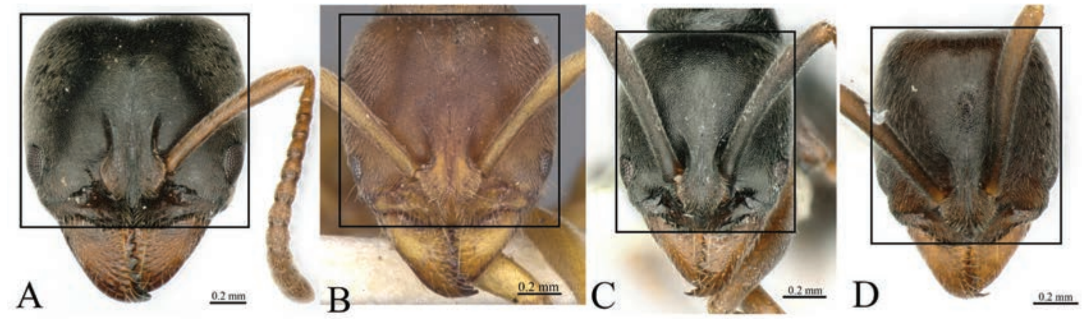

Figure 5. Shape of head in full-face view **A** *Brachyponera sennaarensis* **B** *B. lutea* (CASENT0902499, type) **C** *B. nakasujii* **D** *B. arcuata*. Photographers Chao Chen (**A, C, D**), Will Ericson (**B**).

6 Posterior margin of head in in full-face view strongly concave; scape long, slightly extending beyond posterolateral corner of head; eye large (Fig. 5A); body color dark brown (Fig. 6A) (Central to Southern Africa) .... ***B. sennaarensis*** **(Mayr)**

– Posterior margin of head in full-face view weakly concave; scape short, not reaching posterolateral corner of head; eye small (Fig. 5B); body color yellow brown (Fig. 6B) (Australia) .... ***B. lutea*** **(Mayr)**

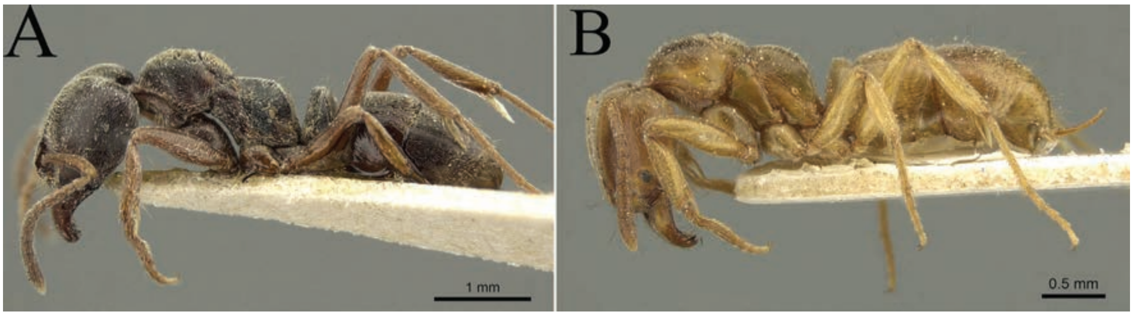

Figure 6. Body color in lateral view **A** *Brachyponera sennaarensis* (CASENT0915669, type) **B** *B. lutea* (CASENT0915668, type). Photographer Harald Bruckner (**A, B**)

7 In lateral view, propodeum densely transversely or irregularly rugose (Fig. 7A, B)..**8**

– In lateral view, propodeum smooth or only punctate (Fig. 7C, D) **9**

8 In dorsal view, petiolar node broader (PDPI 175) (Fig. 8A, B) (Japan)......... ....***B. nakasujii*** **(Yashiro et al.)**

– In dorsal view, petiolar node narrow (PDPI 130) (Fig. 8C, D) (China, North Korea, South Korea, Japan, Vietnam, Thailand, Nepal).........***B. chinensis*** **(Emery)**

9 In dorsal view, lateral margin of pronotum markedly edged; lateral face of pronotum nearly vertical (Fig. 9A) (China).....***B. xui*** **Chen, Yu & Yi, sp. nov.**

– In dorsal view, lateral margin of pronotum without well-defined edges; lateral faces of pronotum diverging downward, appearing more convex (Fig. 9B)..**10**

10 In lateral view, dorsal surface of propodeum continuously connected with declivity, forming complete circular arc (Fig. 10A)...................................**11**

– In lateral view, dorsal surface of propodeum and declivity separated by roundly-angled posterodorsal corner (Fig. 10B).......................................**14**

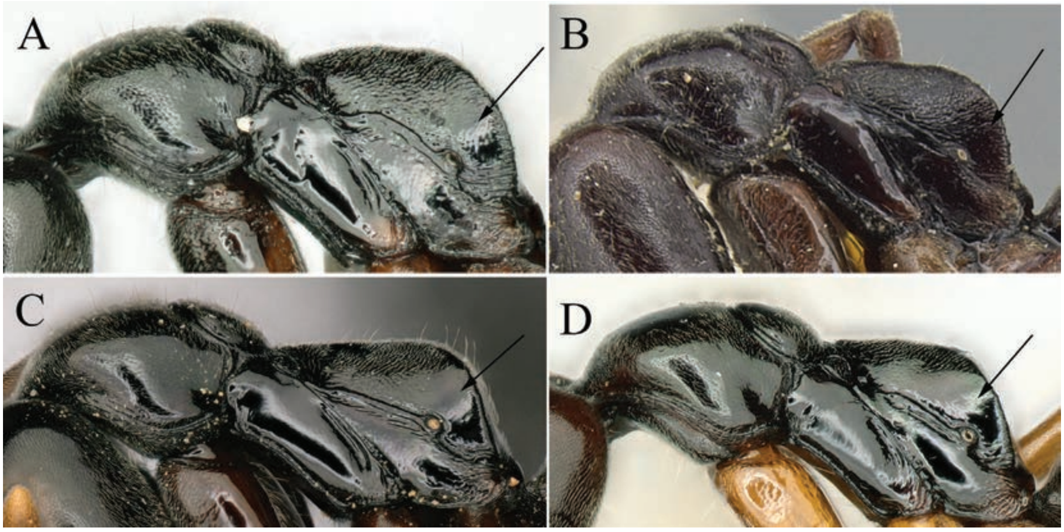

Figure 7. Mesosoma in profile showing sculpture of propodeum **A** *Brachyponera nakasujii* **B** *B. chinensis* (CASENT0903937, type) **C** *B. candida* sp. nov. **D** *B. flavipes*. Photographers Chao Chen (**A, C, D**), Will Ericson (**B**).

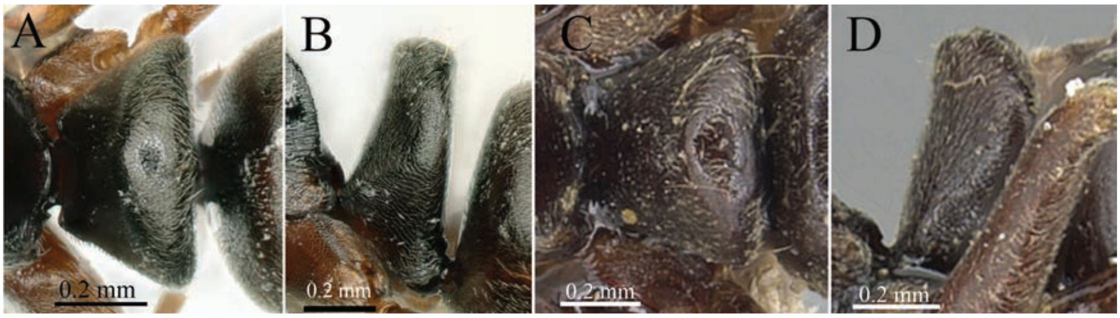

Figure 8. Petiole node in dorsal view and in lateral view **A**, **B** *Brachyponera nakasujii* (non-type) **C**, **D** *B. chinensis* (CASENT0903937, type). Photographers Chao Chen (**A, B**), Will Ericson (**C, D**).

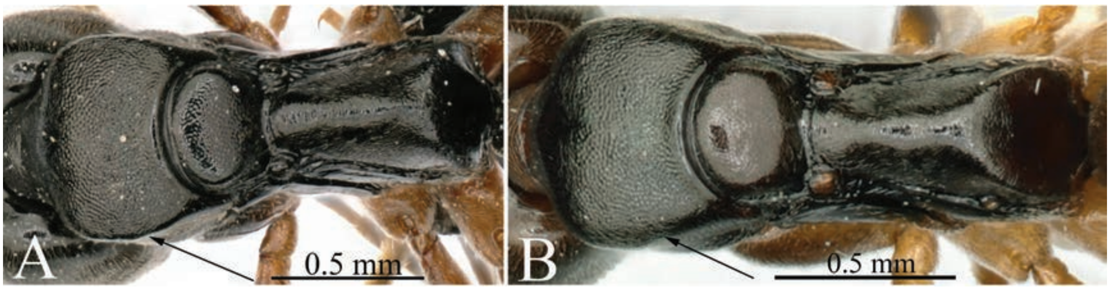

Figure 9. Mesosoma in dorsal view **A** *Brachyponera xui* sp. nov. **B** *B. batak*. Photographer Chao Chen (**A, B**).

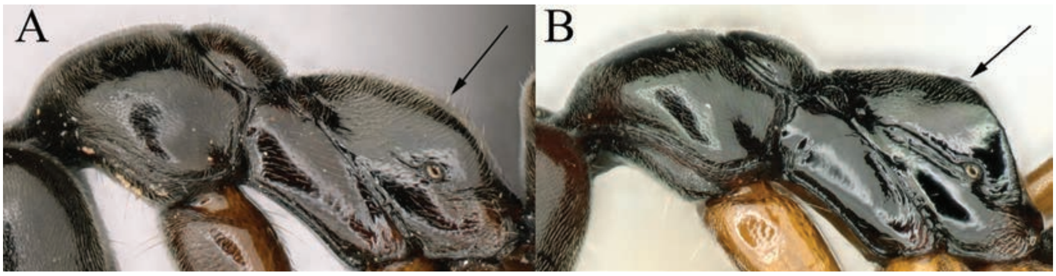

Figure 10. Shape of propodeum in lateral view **A** *Brachyponera paraarcuata* sp. nov. **B** *B. flavipes*. Photographer Chao Chen (**A, B**).

11 Smaller species; TL < 4 mm (Fig. 11A); HW < 0.80 mm............................**12**

– Larger species; TL > 5 mm (Fig. 11B); HW > 0.80 mm..............................**13**

12 Clypeal median lobe relatively long; frontal carina relatively long, reaching anterior to mid-length of head; body entirely yellowish brown (Thailand)... ***B. troglomorpha* Duanchay & Jaitrong**

– Clypeal median lobe relatively short; frontal carina relatively short, reaching level posterior margin of eye; body entirely black....... ***B. brevidorsa* Xu**

13 In full-face view, outline between mandibular base and anterior margin of eye (malar space) strongly convex (Fig. 12A); in lateral view, propodeal declivity rugose at margin; in posterior view propodeal declivity laterally weakly margined, transversely rugose except for median smooth area; rugae extending to posterior portion of lateral face of propodeum (Fig. 12B); body color brownish yellow (New Guinea, Java)......***B. arcuata* (Karavaiev)**

– In full-face view, outline between mandibular base and anterior margin of eye (malar space) nearly straight (Fig. 12C); in lateral view, propodeal declivity smooth at margin; in posterior view propodeal declivity smooth (Fig. 12D); body color black to brownish black (China) ....***B. paraarcuata* Chen, Yu & Yi, sp. nov.**

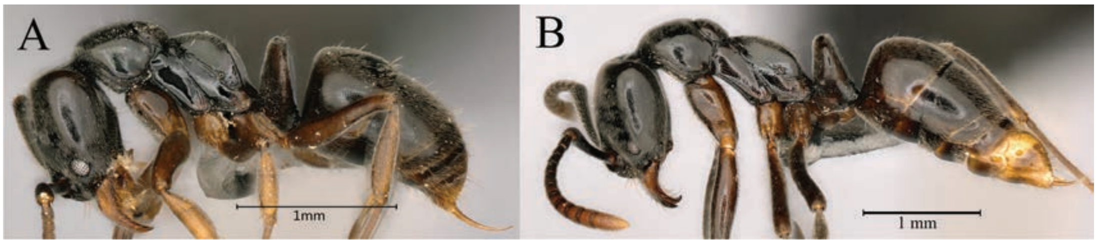

Figure 11. Habitus in lateral view, showing body length **A** *Brachyponera brevidorsa* **B** *B. paraarcuata* sp. nov. Photographer Chao Chen (**A, B**).

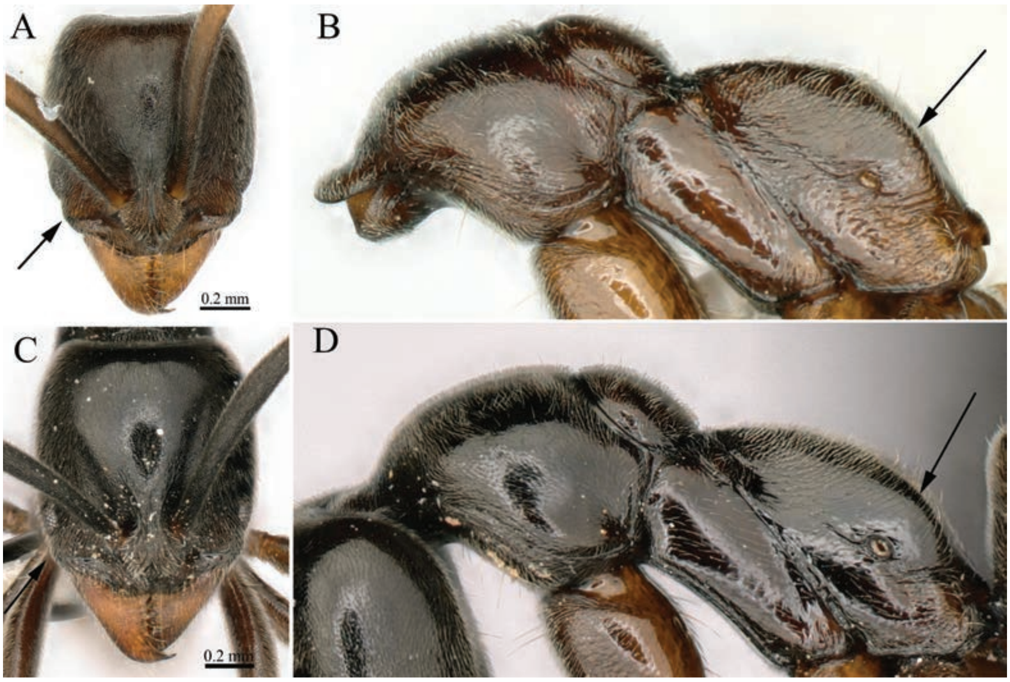

Figure 12. A, **C** head in full-face view **B**, **D** mesosoma in lateral view **A**, **B** *Brachyponera arcuate* (non-type from Java) **C**, **D** *B. paraarcuata* sp. nov. Photographer Chao Chen (**A–D**).

14 Large species, TL > 4.5 mm, HW > 0.9 mm; antennal segments 3 and 4 each longer than broad (Fig. 13A, B); body color usually dark brown......**15**

– Small-sized species, TL < 4.5 mm, HW < 0.9 mm; antennal segments 3 and 4 each as long as broad, or broader than long (Fig. 13C, D); body color usually yellowish brown to tan **19**

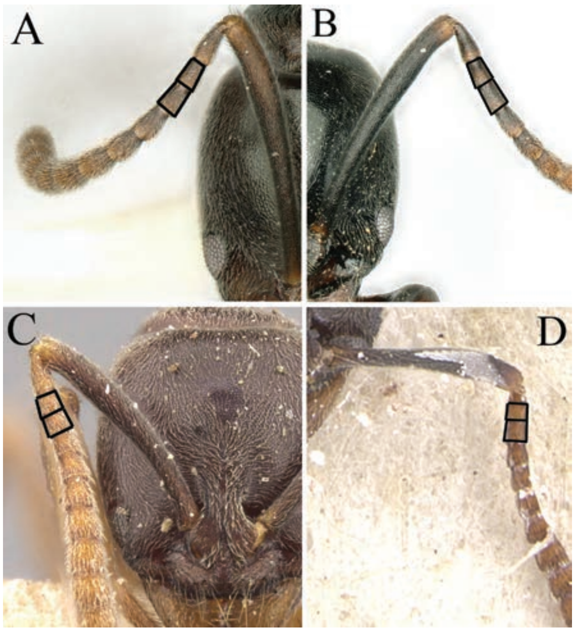

Figure 13. Shape of antennal segment in full-face view **A** *Brachyponera batak* (non-type) **B** *B. candida* sp. nov. **C** *B. jerdonii* (CASENT0907282, type) **D** *B. obscurans* (CASENT0902495, type). Photographers Chao Chen (**A, B**), Z. Liebermantype (**C**), Will Ericson (**D**).

15 Petiolar node thick (PL > 0.40 mm); in dorsal view, petiole long trapezoidal shape (Fig. 14A) (China) ....***B. candida* Chen, Yu & Yi, sp. nov.**

– Petiolar node thin (PL < 0.40 mm); in dorsal view, petiole semicircular or short trapezoid (Fig. 14B-D)..**16**

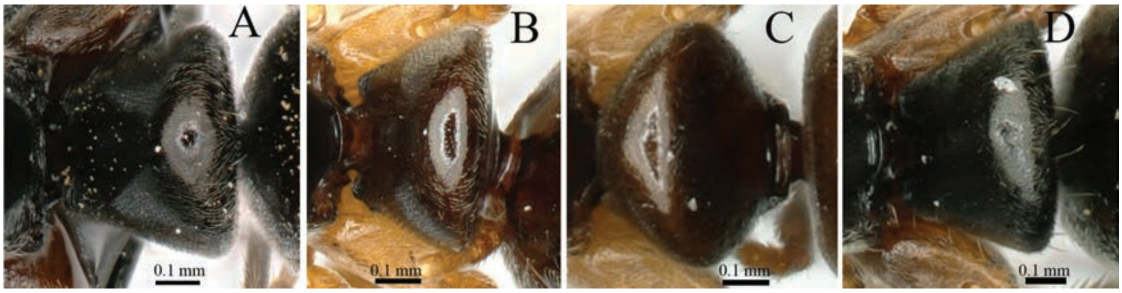

Figure 14. Petiolar node in dorsal view **A** *Brachyponera candida* sp. nov. **B** *B. flavipes* (paratype) **C** *B. batak*. (non-type) **D** *B. pilidorsalis* (non-type). Photographer Chao Chen (**A–D**).

16 Antennal scape shorter, surpassing posterior margin of head by < 1/4 of its length; legs yellowish brown to orangish, contrasting with jet black mesosoma (Fig. 15A) (Myanmar) ....***B. flavipes* (Yamane)**

– Antennal scape longer, surpassing posterior margin of head by > 1/4 of its total length; legs brown to dark brown, contrast with body color weaker (Fig. 15B)..**17**

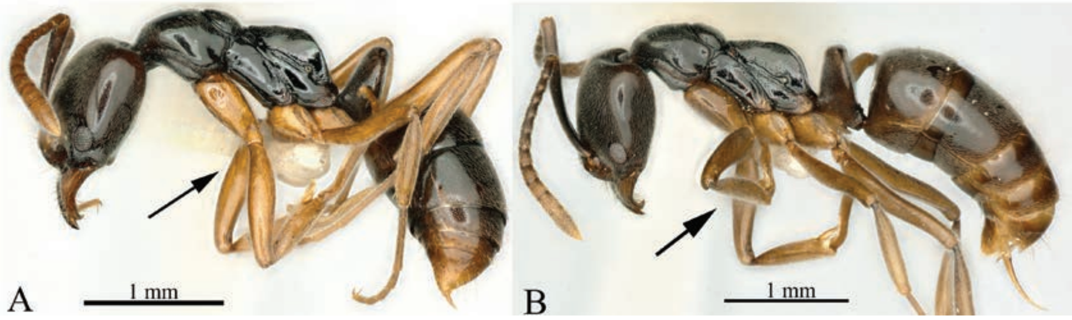

Figure 15. Legs color in lateral view **A** *Brachyponera flavipes* (paratype) **B** *B. batak* (non-type). Photographer Chao Chen (**A, B**).

17 Standing hairs on mesosomal dorsum absent or very few; standing hairs if any generally shorter than width of antennal segment 3 (Fig. 16A) (Sumatra)..***B. batak* (Yamane)**

– Mesosomal dorsum usually with > 10 standing hairs, some of which are as long as or longer than width of antennal segment 3 (Fig. 16B)..........**18**

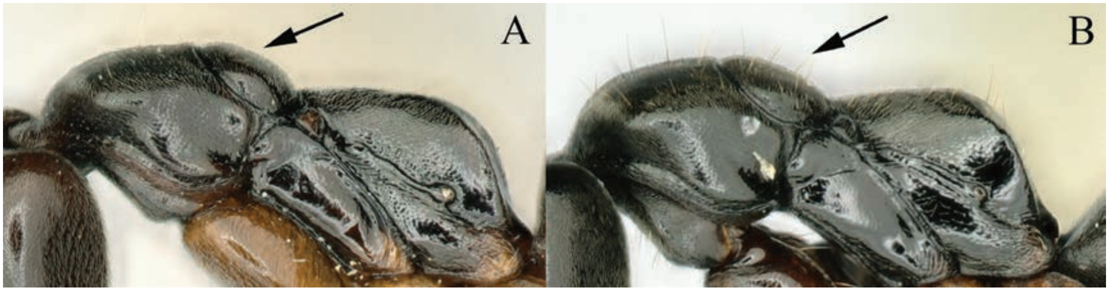

Figure 16. Mesosoma in lateral view **A** *Brachyponera batak* (non-type) **B** *B. pilidorsalis* (non-type from West Malaysia). Photographer Chao Chen (**A, B**).

18 Mesopleuron often with transverse groove; groove sometimes incomplete but at least scar visible (Fig. 17A); posterior faces of propodeum and petiole more strongly punctate (Fig. 17C); gastral tergite 1 usually with > 10 standing hairs (Fig. 17C) (Borneo; Malay Peninsula, Java).......***B. pilidorsalis* (Yamane)**

– Mesopleuron usually without such groove; groove if any vestigial (Fig. 17B); posterior face of propodeum medially and petiole entirely smooth or very weakly punctate (Fig. 17D); gastral tergite 1 with fewer standing hairs, the number, excluding those on posterior margin of tergite, being usually less than ten (Fig. 17D) (China, Philippines, Vietnam, Thailand, Myanmar, Sumatra, India, Nepal).. ***B. nigrita* (Emery)**

19 In dorsal view, gastral tergite 1 with densely sub-decumbent hairs (Fig. 18A, B) **20**

– In dorsal view, gastral tergite 1 with sparsely sub-decumbent hairs or fewer standing hairs (Fig. 18C, D) **21**

20 Eye small, with maximum width of scape accounting for 83% of the longest axis of eye; body color reddish brown (Fig. 19A) (Vietnam, Sri Lanka, India) ....***B. jerdonii* (Forel)**

– Eye moderately large, with maximum width of scape accounting for 65% of the longest axis of eye; body color tan (Fig. 19B) (Christmas Island)..... .... ***B. christmasi* (Donisthorpe)**

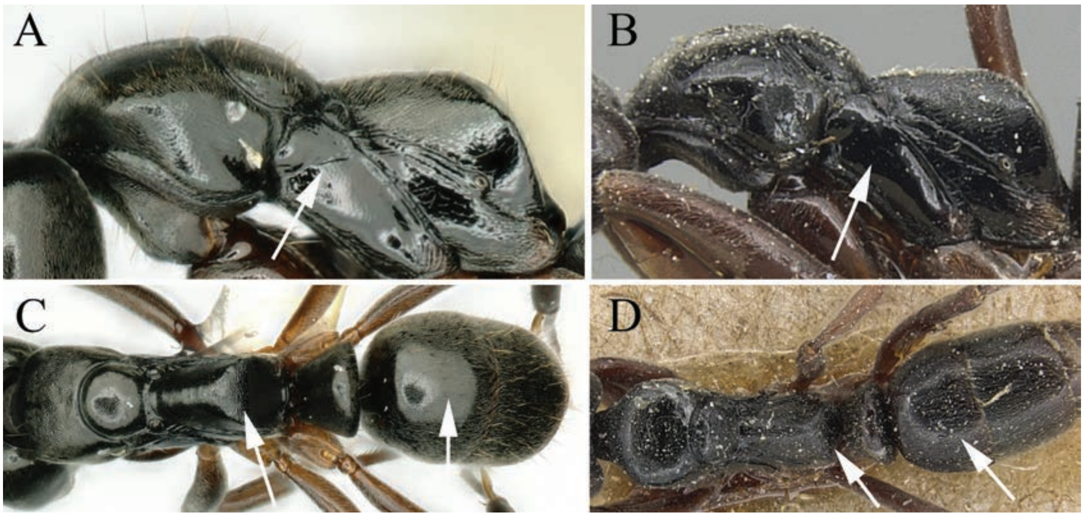

Figure 17. A, **B** mesosoma in lateral view **C**, **D** body in dorsal view **A**, **C** *Brachyponera pilidorsalis* (non-type from West Malaysia) **B**, **D** *B. nigrita* (CASENT0903936, type). Photographers Chao Chen (**A, C**), Will Ericson (**B, D**).

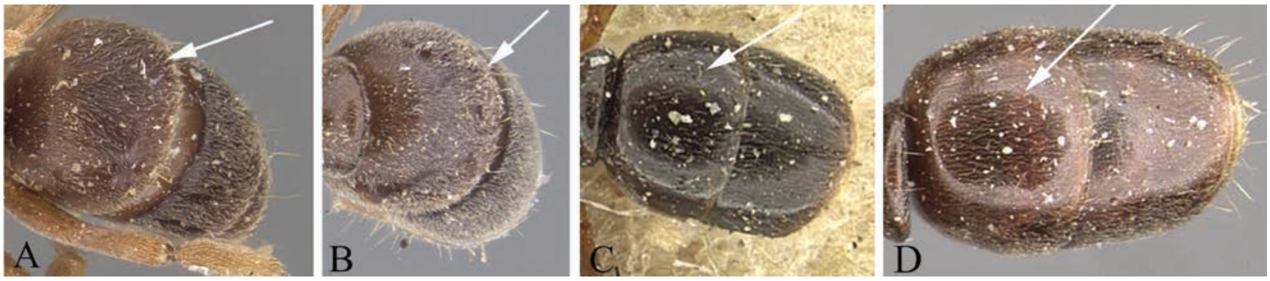

Figure 18. Gastral in dorsal view **A** *Brachyponera* jerdonii (CASENT0907282, type) **B** *B. christmasi* (CASENT0902496, type) **C** *B. luteipes* (CASENT0915672, type) **D** *B. croceicornis* (CASENT0907286, type). Photographers Z. Liebermantype (**A, D**), Will Ericson (**B**), Harald Bruckner (**C**).

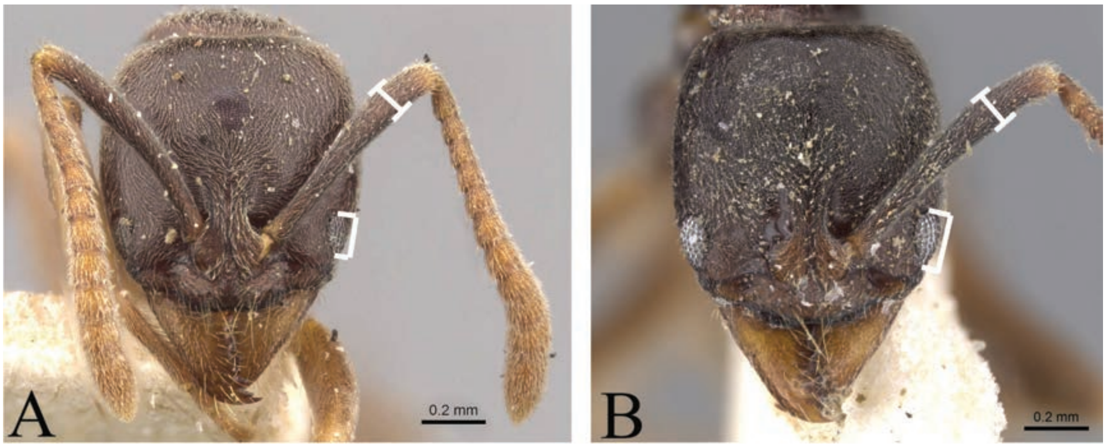

Figure 19. Head in full-face view **A** *Brachyponera jerdonii* (CASENT0907282, type) **B** *B. christmasi* (CASENT0902496, type). Photographers Z. Lieberman (**A**), Will Ericson (**B**).

21 In lateral view, dorsal surface of propodeum convex (Fig. 20A) (China, Vietnam, Laos, Thailand, Myanmar, India, Sri Lanka, Sumatra, Philippines, Borneo, Sulawesi, Java) .... ***B. luteipes*** **(Mayr)**

– In lateral view, dorsal surface of propodeum concave or almost straight (Fig. 20B, C) **22**

Figure 20. Mesosoma in lateral view **A** *Brachyponera luteipes* (CASENT0915672 type) **B** *B. croceicornis* (CASENT0907286, type) **C** *B. obscurans* (CASENT0902495, type). Photographers Harald Bruckner (**A**), Z. Lieberman (**B**), Will Ericson (**C**).

22 Upper part of propodeum with sparsely sub-decumbent hairs; body color reddish brown (Fig. 20B) (Australia, New Guinea)....***B. croceicornis* (Emery)**

– Upper part of propodeum with densely sub-decumbent hairs; body color dark brown (Fig. 20C) (China, Philippines, Borneo, Malaysia, Singapore, India, Sri Lanka) ....***B. obscurans* (Walker)**

Revision of the Chinese species of *Brachyponera*

***Brachyponera brevidorsa* Xu, 1994**

Fig. 21A-C

Brachyponera brevidorsa Xu, 1994b: 183, figs 5, 6 (w.). Type locality: China (Yunnan).

Type material. ***Holotype*** (worker). China: • Yunnan, Baoshan City, 1800 m, 11.x. 1991, Zhenghui Xu leg (SWFU), No. A91-1022. ***Paratypes*** (workers). China: • 11 workers; same collection data as for holotype.

Other material examined. 5 workers; China, • Yunnan, Lvchun City, 1515 m, 24 Jun. 2023, Chao Chen leg., No. KIZ20231057.1-KIZ20231057.5.

Measurements and indices. Worker (Fig. 21A–C): HL 0.84, HLL 0.77, HLA 0.11, HW 0.80, ML 0.46, CML 0.09, CI 95, SL 0.73, SI 92, ED 0.11, PrL 0.48, PrH 0.42, PrW 0.58, WL 1.16, TL 3.8, PL 0.26, PH 0.59, DPW 0.42, LPI 229, PDPI 165.

Diagnosis. The species can be separated from other Chinese members of the genus based on the combination of the following characters: smaller species, < 4 mm in total body length; antenna scape short, slightly exceeds posterolateral corner; clypeal median lobe relatively short; frontal carina relatively short, reaching level posterior margin of eye; in lateral view, pronotum relatively flat; propodeum low, dorsum slightly raised, obviously shorter than declivity, transition between declivity and dorsum is rounded; body entirely black.

Brief description. In full-face view, head longer than broad, roughly trapezoidal, posterolateral corners narrowly rounded. Mandible triangular with nine teeth. Antennae 12-segmented, scape slightly exceeds posterolateral corner, flagellar segments gradually become thicker and rod-shaped towards the end. Eye medium in size and located in front of lateral margin of head. In lateral view, promesonotal suture depressed, metanotal groove deeply impressed. Propodeum convex, mesonotum prominently elevated. Propodeum low, dorsum slightly raised, obviously shorter than declivity, transition between declivity and dorsum is rounded. Petiolar node nearly trapezoidal; subpetiolar process wedge-shaped. In dorsal view, propodeum anterior part narrower than posterior part. Petiolar node crescent-shaped. Head densely punctate. Pronotum with

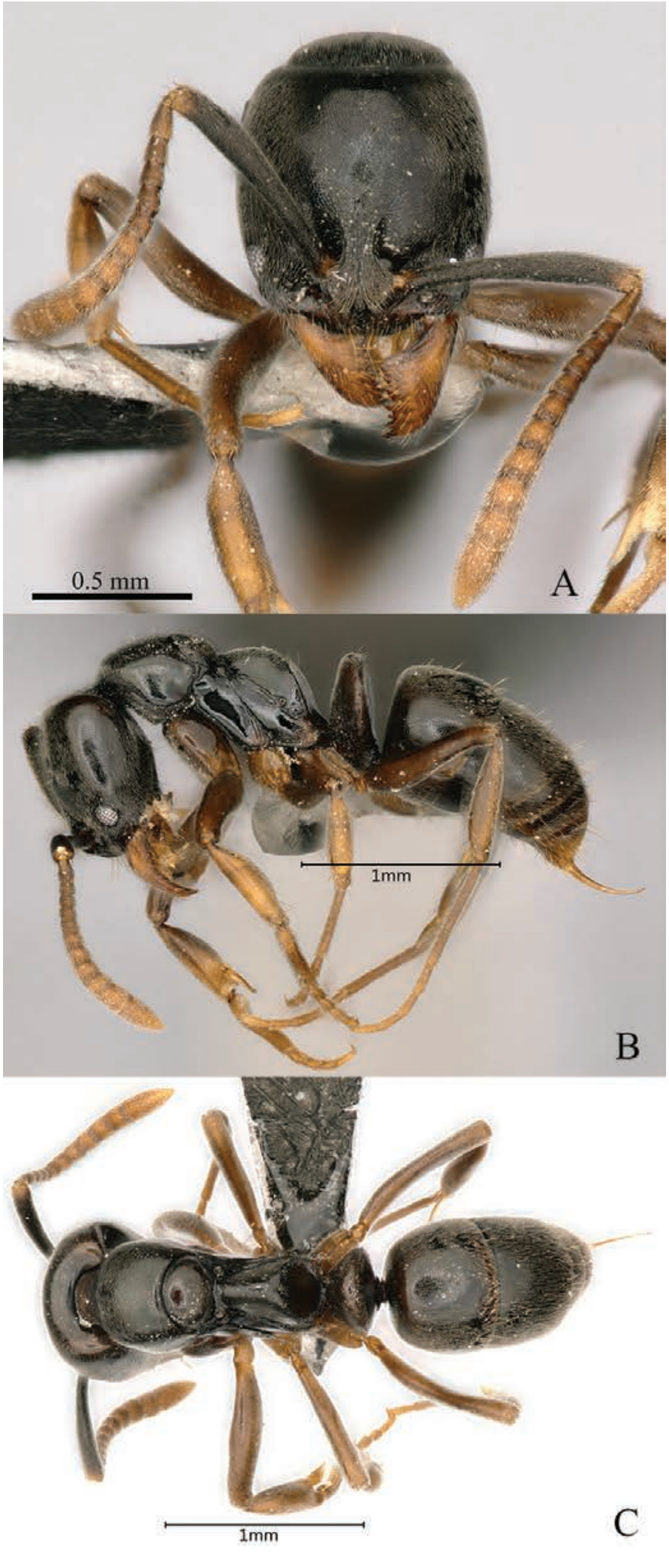

Figure 21. *Brachyponera brevidorsa* worker (non-type, No. KIZ20231057) **A** head in full-face view **B** body in lateral view **C** body in dorsal view. Photographer Chao Chen.

densely punctured. Propodeum lateral margin shiny; dorsum of mesonotum and propodeum shiny. dorsal surface of body with sparsely erect or suberect hairs and densely sub-decumbent hairs. Body color black, mandible, flagellum, legs, and end of gaster yellowish brown.

Brachyponera candida **Chen, Yu & Yi, sp. nov.**

https://zoobank.org/6CE2B706-123A-4270-89BB-4D3C03C122BA
Fig. 22A-C

Type material. ***Holotype***: worker, CHINA: • Yunnan Province, Honghe Hani and Yi Autonomous Prefecture, Lvchun County, Banpo Township, mohelongtang, 22.61721'N, 102.33585'E, 1263 m above sea level, from mixed coniferous-broad forest, 13.iv.2023, Chao Chen leg., No. KIZ20230168 (KIZ). ***Paratypes***: • 5 workers, same data as holotype (KIZ20230168A, KIZ20230168B deposited at SWFU; KIZ20230168C, KIZ20230168D, KIZ20230168E deposited at GXNU).

Non-type material examined. 16 workers, CHINA: • Yunnan Province, Honghe Hani and Yi Autonomous Prefecture, Lvchun County, Banpo Township, mohelongtang, 22.61721'N, 102.33585'E, 1263 m above sea level, from mixed coniferous-broad forest, 13.iv.2023, Chao Chen leg., No. KIZ20230168.1-KIZ20230168.16 (KIZ); • 1 worker, Honghe Hani and Yi Autonomous Prefecture, Lvchun County, Banpo Township, Erfu Village, 22.62882'N, 102.35430'E, 1497 m Monsoon evergreen broad-leaved forest, 13.iv.2023, Chao Chen leg., No. KIZ20230194 (KIZ); 1 worker, Honghe Hani and Yi Autonomous Prefecture, Lvchun County, Qimaba Township, Xiaoheijiang, 22.69476'N, 102.33646'E, 510 m Tropical seasonal rainforest, 13.iv.2023, Qiwei Shen leg., No. KIZ20230373 (KIZ); • 1 worker, Honghe Hani and Yi Autonomous Prefecture, Lvchun County, Banpo Township, Bayanhongdong, 22.63598'N, 102.34737'E, 1258 m Monsoon evergreen broad-leaved forest, 17.iv.2023, Huiping Zeng leg., No. KIZ20230502 (KIZ).

Measurements and indices. ***Holotype***: HL 1.07, HLL 0.97, HLA 0.12, HW 0.99, ML 0.52, CML 0.11, CI 93, SL 1.00, SI 101, ED 0.17, PrL 0.64, PrH 0.53, PrW 0.71, WL 1.63, TL 5.2, PL 0.43, PH 0.75, DPW 0.53, LPI 174, PDPI 123. ***Paratypes*** (*n* = 5): HL 1.04–1.11, HLL 0.92–0.97, HLA 0.11–0.19, HW 0.94–1.00, ML 0.50–0.58, CML 0.10–0.12, CI 88–95, SL 0.99–1.09, SI 101–114, ED 0.15–0.17, PrL 0.62–0.67, PrH 0.51–0.57, PrW 0.73–0.79, WL 1.62–1.70, TL 5.0–5.3, PL 0.44–0.47, PH 0.75–0.79, DPW 0.51–0.58, LPI 160–173, PDPI 113–126.

Diagnosis. The new species is similar to *B. pilidorsalis* (Yamane, 2007). However, it can be separated by relatively short scape that exceeds the posterolateral corner by 1/10 of its length (in *B. pilidorsalis* scape is longer, exceeding posterolateral corner with more than ¼ of its length); slightly shorter distance between anterior clypeal margin to anterior margin of torulus, CML 0.11 (relatively long in *B. pilidorsalis*, CML 0.15), dorsal length of propodeum longer than declivity, mesopleuron usually without a groove, dorsum of mesosoma with slightly short erect hairs (dorsal length of propodeum slightly longer than declivity, mesopleuron often with a transverse groove, dorsum of mesosoma with slightly long standing hairs in *B. pilidorsalis*).

Description. In full-face view, head longer than broad, roughly rectangular, posterior margin weakly concave, posterolateral corners narrowly rounded, lateral margins moderately convex. Mandible triangular with eight teeth, apical tooth largest, and with a basal mandibular pit. Clypeus transverse, center of anterior margin moderately concave. Frontal carina short, frontal lobes well developed, covering antennal socket, frontal region with central longitudinal ridge. Antennae 12-segmented, scape 1/10 exceeds posterolateral corner, flagellum gradually increases in size toward the end. Eye medium and maximum diameter consists of eleven ommatidia (ED 0.17 mm).

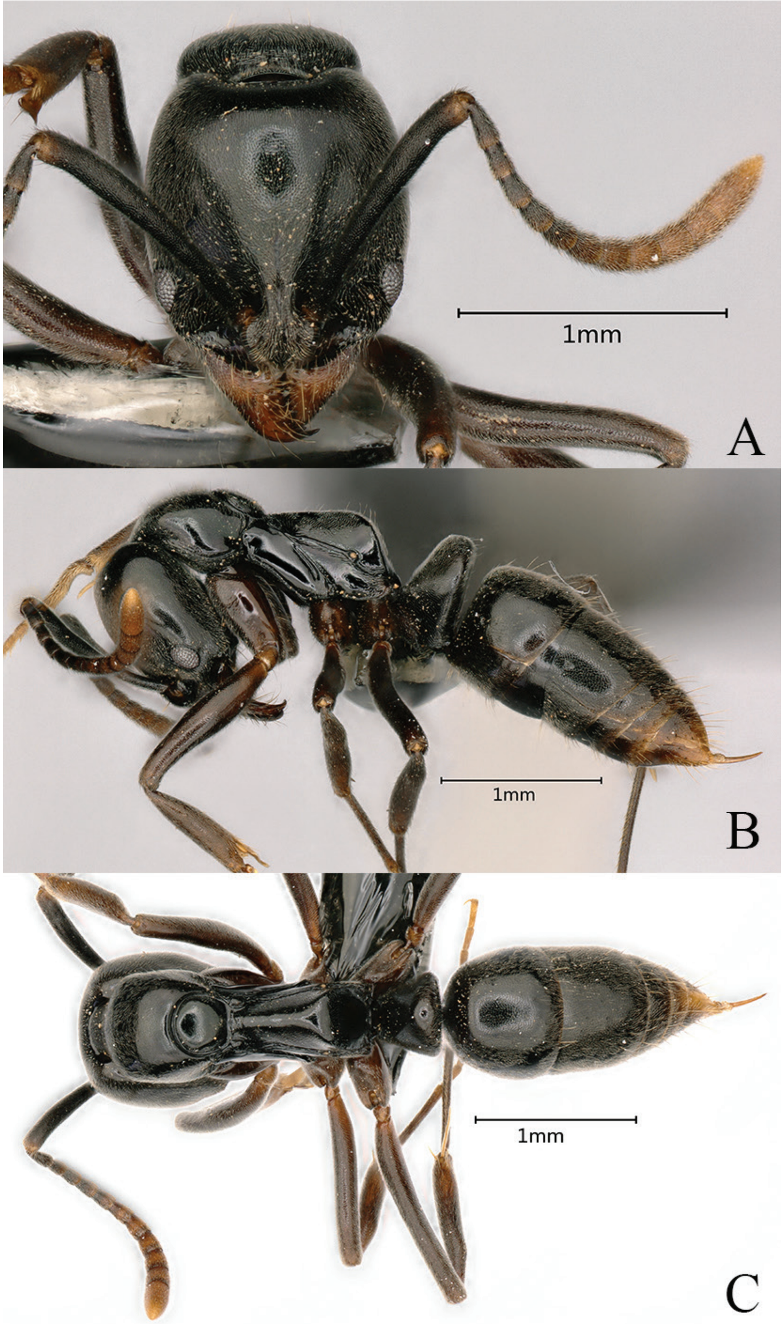

Figure 22. *Brachyponera candida* sp. nov. worker (holotype, No. KIZ20230168) **A** head in full-face view **B** body in lateral view **C** body in dorsal view. Photographer Chao Chen.

In lateral view, pronotum and mesonotum significantly higher than propodeum. Promesonotal suture seams evident, metanotal groove deeply impressed. Mesonotum moderately convex. Dorsal surface of propodeum nearly straight, with a length ~ 1.3× that of declivity, slope of declivity steep, nearly straight. Posterodorsal corner of propodeum broadly rounded. Propodeal spiracle rounded, with a groove between spiracle and metanotal groove. Metapleural bulla not visible. Petiolar node as high as propodeum, upright, thick (PDPI 123), nearly trapezoidal; anterior margin and dorsum moderately convex, posterior margin nearly straight; subpetiolar process forms a wedge. Prora absent. Gaster subconical, basal two intersegments contracted, apex with sting.

In dorsal view, pronotum widest in mesosoma, humeral corners bluntly rounded; lateral margins moderately convex. Anterior margin of mesonotum convex, posterior margin slightly straight. Propodeum nearly rectangular, gradually narrowing from bottom to the top, forming a ridge. Petiolar node trapezoidal, front narrow and gradually widening backwards; anterior margin flat, posterior margin moderately convex.

Dorsal surface of body with densely hairy punctation. Mesopleuron, metapleural and lower part of lateral side of petiolar node smooth and shiny. Dorsal surface of body with sparsely erect or suberect hairs and densely sub-decumbent hairs. Body color black, funiculus, mandible, and legs brownish black.

Ecological notes. The new species was collected in the Huanglianshan National Nature Reserve in Yunnan. The type series was collected from a nest in soil, which was built in a coniferous and broad-leaved mixed forest at an altitude of 1250 m. Sixteen workers of this new species were collected foraging on the forest floor. An additional 61 workers of this new species were collected in five sample plots. The forest types include tropical seasonal rainforest, monsoon evergreen broad-leaved forest, and mountain moss evergreen broad-leaved forest. The new species builds its nest in the soil. Workers were found foraging on the ground and tree trunks. The altitude of all sample plots is below 2000 m (Suppl. material 1: fig. S15).

Etymology. The new species name refers to its smooth and shiny body, with only a relatively small number of punctures.

***Brachyponera chinensis* (Emery, 1895)**

Fig. 23A-D

Ponera nigrita subsp. *chinensis* Emery, 1895 m: 460 (in text) (w.). Type locality: China (Shanghai). Indomalaya.

Type material. ***Holotype*** worker, from CHINA, • Shanghai, date and collector unknown (images of the holotype, CASENT0903937 available on AntWeb were examined).

Measurements and indices. Worker (Fig. 23A–D): HL 1.26, HLL 1.15, HLA 0.14, HW 1.16, ML 0.69, CML 0.19, CI 92, SL 0.99, SI 86, ED 0.23, PrL 0.71, PrH 0.57, PrW 0.77, WL 1.67, TL 5.0, PL 0.40, PH 0.60, DPW 0.58, LPI 150, PDPI 145.

Diagnosis. The species can be separated from other Chinese members of the genus based on the combination of the following characters: mandible base rough with fine puncta, tip smooth; antennae 12-segmented, scape slightly exceeds posterolateral corner; eye medium in size and located in front of lateral margin of head; in lateral view, propodeum densely transversely rugose; smooth area if any much restricted; dorsal of propodeum straight, declivity convex, the length is nearly equal.

Brief description. In full-face view, head longer than broad, roughly trapezoidal, posterolateral corners narrowly rounded. Mandible triangular with nine teeth. Antennae 12-segmented, scape slightly exceeds posterolateral corner, flagellar segments gradually become thicker and rod-shaped towards the end. Eye medium in size and located in front of lateral margin of head. In lateral view, metanotal groove deeply impressed. Dorsum of propodeum straight, declivity convex,

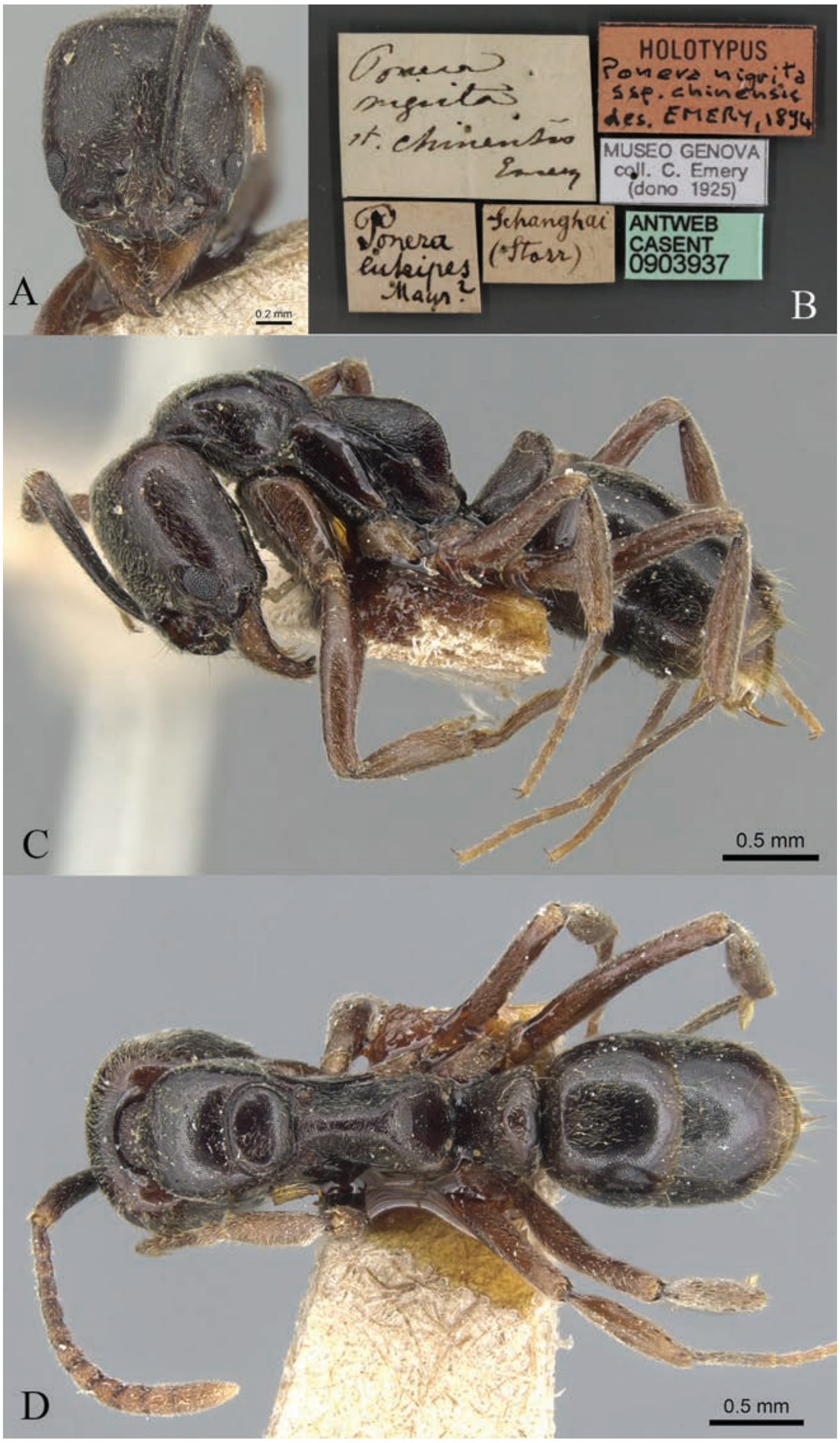

Figure 23. *Brachyponera chinensis* worker (CASENT0903937, type) **A** head in full-face view **B** label **C** body in lateral view **D** body in dorsal view. Photographer Will Ericson.

the length is nearly equal. Petiolar node nearly trapezoidal; subpetiolar process wedge-shaped. In dorsal view, pronotum anterior and lateral margins broad and round, posterior margin concave. Petiolar node crescent-shaped. Mandible base rough with fine puncta, tip smooth. Head and body densely and finely punctate; pronotum, petiolar node and gaster with fine, shiny puncta. Side plates of mesosoma smooth and shiny. Propodeum rough with dense, coarse puncta. Body black; mandible, antennae flagellum, legs, and end of gaster yellow brown.

Brachyponera luteipes **(Mayr, 1862)**

Fig. 24A-D

Ponera luteipes Mayr, 1862: 722 (w.q.), India (Nicobar Is).

Type material. Syntype workers and syntype queens (NHMW) from India, Nicobar Is, Milu I. (images of a syntype, CASENT0915672, available on AntWeb were examined).

Non-type material examined. • 13 workers, China: Yunnan Province, Honghe Hani and Yi Autonomous Prefecture, Lvchun County, Banpo Township, Daguyan, 22.61094'N, 102.28100'E, 367 m Tropical seasonal rainforest, 9.x.2023, Chao Chen leg., No. KIZ20231066.1- KIZ20231066.13(KIZ); • 20 workers, Honghe Hani and Yi Autonomous Prefecture, Lvchun County, Sanmeng Township, Laobianduan, 22.92752'N, 102.28553'E, 1749 m montane mossy evergreen broad-leaf forest, 16.x.2023, Chao Chen leg., No. KIZ20232340.1- KIZ20232340.20(KIZ); • 7 workers, Honghe Hani and Yi Autonomous Prefecture, Lvchun County, Qimaba Township, 22.80584'N, 102.22848'E, 745 m mixed coniferous and broad-leaved forest, 13.x.2023, Chao Chen leg., No. KIZ20232464.1- KIZ20232464.7(KIZ).

Measurements and indices. worker (Fig. 24A–D): HL 0.78, HLL 0.70, HLA 0.10, HW 0.71, ML 0.40, CML 0.08, CI 91, SL 0.65, SI 92, ED 0.11, PrL 0.45, PrH 0.32, PrW 0.50, WL 1.04, TL 3.0, PL 0.21, PH 0.44, DPW 0.39, LPI 211, PDPI 186.

Diagnosis. The species can be separated from other Chinese members of the genus based on the combination of the following characters: smaller species, < 4.5 mm in total body length; head width < 0.9 mm; flagellar segments 1 and 2 each as long as broad, or broader than long; dorsum of propodeum convex, declivity convex, the length is nearly equal; in lateral view, propodeum smooth or only punctate; in dorsal view, gastral tergite 1 with sparsely sub-decumbent hairs or fewer standing hairs.

Brief description. Head longer than wide, with broad rounded depression at posterior margin. Mandible triangular with nine teeth. Antennae 12-segmented, scape exceeds posterolateral corner, flagellar segments 1 and 2 as long as broad, or broader than long. Dorsum of propodeum convex, declivity convex, the length is nearly equal Mandible smooth, finely punctate. Head and body densely and finely punctate; pronotum and mesonotum puncta are rough; side plates of mesosoma smooth and shiny; Petiolar node and gaster finely punctate. Dorsal surface of head and body sparsely erected with abundant sub-decumbent hairs; scape and hind tibiae are densely covered in sub-decumbent hairs, lacking erected hairs. Body black; mandible, antennae flagellum, tibiae, tarsus, and end of gaster reddish brown.

Brachyponera myops **Chen, Yu & Yi, sp. nov.**

https://zoobank.org/C195D65F-5790-4B18-9705-577A18240D26

Fig. 25A–C

Type material. ***Holotype***: worker, China: • Yunnan Province, Honghe Hani and Yi Autonomous Prefecture, Lvchun County, Niukong Town, niaoliuyaozhai, 22.95837'N, 102.28872'E, 1515 m above sea level, *Eucalyptus* forest (plantation), 24.iv.2023, Chao Chen leg., No. KIZ20231049 (KIZ). ***Paratypes***: • 1 worker (KIZ20231049A), same data as holotype (SWFU); 4 workers (KIZ20230651, KIZ20230651A, KIZ20230651B, KIZ20230651C): Yunnan Province, Honghe

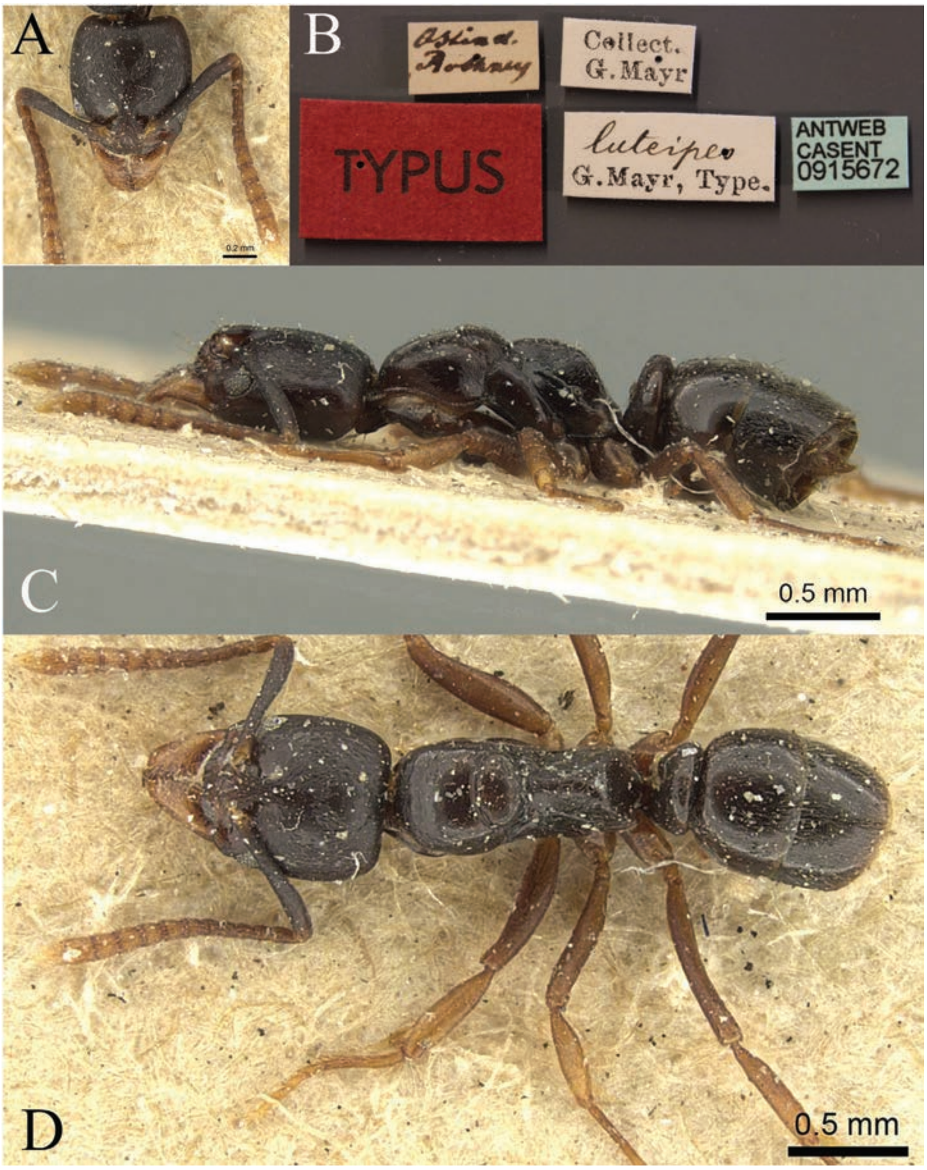

Figure 24. *Brachyponera luteipes* worker (CASENT0915672, type) **A** head in full-face view **B** label **C** body in lateral view **D** body in dorsal view. Photographer Harald Bruckner.

Hani and Yi Autonomous Prefecture, Lvchun County, Qimaba Township, Omo village, 22.68445'N, 102.29683'E, 1518 m above sea level, from monsoon evergreen broad-leaved forest, 18.iv.2023, Huiping Zeng leg.(GXNU).

Non-type material examined. • 4 workers, China: Yunnan Province, Honghe Hani and Yi Autonomous Prefecture, Lvchun County, Qimaba Township, Omo village, 22.68445'N, 102.29683'E, 1518 m above sea level, from monsoon evergreen broad-leaved forest, 18.iv.2023, Huiping Zeng leg., No. KIZ20230647, KIZ20230654.1- KIZ20230654.3 (KIZ); • 18 workers, Honghe Hani and Yi Autonomous Prefecture, Lvchun County, Niukong Township, niaoliuyaozhai, 22.95837'N, 102.28872'E, 1515 m above sea level, *Eucalyptus* forest (plantation), 24.iv.2023, Chao Chen leg., No. KIZ20231046.1-20231046.18 (KIZ).

Measurements and indices. ***Holotype***: HL 1.09, HLL 0.98, HLA 0.18, HW 1.00, ML 0.61, CML 0.13, CI 92, SL 1.04, SI 104, ED 0.07, PrL 0.65, PrH 0.57, PrW 0.72, WL 1.58, TL 5.0, PL 0.40, PH 0.75, DPW 0.50, LPI 188, PDPI 125. ***Paratype***

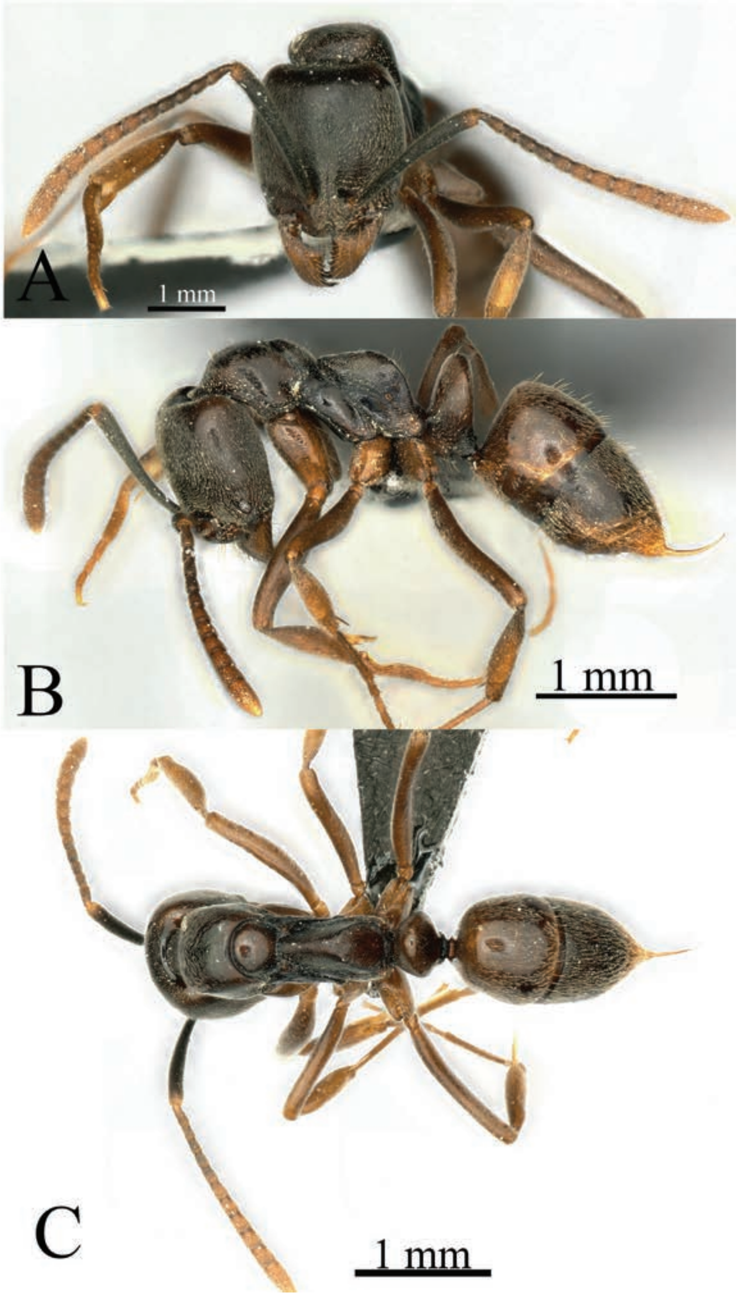

Figure 25. *Brachyponera myops* sp. nov. worker (holotype No. KIZ20231049) **A** head in full-face view **B** body in lateral view **C** body in dorsal view. Photographer Chao Chen.

(*n* = 5): HL 0.99–1.08, HLL 0.90–0.95, HLA 0.12–0.15, HW 0.90–0.98, ML 0.62–0.69, CML 0.10–0.14, CI 90–96, SL 0.98–1.1, SI 99–112, ED 0.06–0.07, PrL 0.62–0.68, PrH 0.50–0.57, PrW 0.74–0.79, WL 1.51–1.59, TL 4.9–5.3, PL 0.41–0.48, PH 0.71–0.76, DPW 0.45–0.48, LPI 148–185, PDPI 96–117.

Diagnosis. The new species is similar to *Brachyponera luteipes* (Mayr, 1862), but it differs in scape segments 3–7 longer than wide, small eye with maximum diameter consisting of five ommatidia (ED 0.07 mm), and inconspicuous or absent groove between spiracle and metanotal groove. In *B. luteipes*, scape segments 3–7 are subsquare, eye is moderately big with maximum diameter consisting of nine ommatidia (ED 0.13 mm), and groove between spiracle and metanotal groove is conspicuous.

Description. In full-face view, head longer than broad, roughly trapezoidal, posterior margin weakly concave, posterolateral corners narrowly rounded, lateral margins moderately convex. Mandible triangular with nine teeth, end tooth largest, and with a basal mandibular pit. Clypeus transverse, center of anterior margin moderately concave. Frontal carina short, frontal lobes well developed, covering antennal socket, frontal region with central longitudinal ridge. Antennae 12-segmented, scape exceeds posterolateral corner of head by 1/5 of its length, flagellar segments gradually increase in size toward the end. Eye small, and maximum diameter consists of five ommatidia (ED 0.07 mm).

In lateral view, anterior margin of pronotum forms a cervical shield extending forward. Pronotum and mesonotum significantly higher than propodeum. Promesonotal suture seams evident, metanotal groove deeply impressed. Mesonotum moderately convex. Dorsal surface of propodeum weakly convex, slightly longer than declivity, slope of declivity steep, nearly convex; posterodorsal corner of propodeum broadly rounded. Propodeal spiracle rounded, groove between spiracle and metanotal groove inconspicuous or absent. Metapleural bulla small, elliptical. Petiolar node as high as propodeum, upright, nearly trapezoidal; anterior margin and dorsum moderately convex, posterior margin nearly straight; subpetiolar process wedge. Prora absent. Gaster subconical, basal two intersegments contracted, apex with sting.

In dorsal view, pronotum widest in mesosoma, humeral corners bluntly rounded; lateral margins moderately convex. Mesonotum elliptical. Propodeum nearly rectangular, gradually narrowing from bottom to the top, forming a ridge. Petiolar node trapezoidal, front narrow and gradually widening backwards; anterior margin flat, posterior margin moderately convex.

Mandible with a row of hairy pits. Dorsal surface of body with densely hairy punctation. Mesopleuron and metapleural with longitudinally rugose. dorsal surface of body with sparsely erect or suberect hairs and densely sub-decumbent hairs. Body color brownish black, funiculus, mandible and legs yellowish brown.

Ecological notes. The new species was collected in the Huanglianshan National Nature Reserve, Yunnan. The holotype and one paratype were collected in the same soil nest in a *Eucalyptus* forest (plantation) at an altitude of 1500 m, and four paratypes were found in a monsoon broad-leaved evergreen forest at an altitude of 1500 m. In addition, 22 workers of this new species were found to be nesting in the soil and foraging on forest floor (Suppl. material 1: fig. S17).

Etymology. The specific name refers to the relatively minute size of the compound eye that characterizes workers of this species.

Brachyponera nigrita (Emery, 1895)

Fig. 26A–D

Ponera nigrita Emery, 1895 m: 459 (w.) Myanmar.

Type material. • Syntype workers, Myanmar ("Burma"), Carin Cheba, 500–1500 m., ii.-iii.1888 (L. Fea) (images of a syntype worker, CASENT0903936 available on AntWeb were examined).

Measurements and indices. Worker (Fig. 26A–D): HL 1.23, HLL 1.13, HLA 0.15, HW 1.17, ML 0.72, CML 0.19, CI 95, SL 1.24, SI 106, ED 0.24, PrL 0.83, PrH 0.71, PrW 0.83, WL 2.00, TL 6.0, PL 0.48, PH 0.88, DPW 0.63, LPI 182, PDPI 131.

Figure 26. *Brachyponera nigrita* worker (CASENT0903936, type) **A** head in full-face view **B** label **C** body in lateral view **D** body in dorsal view. Photographer Will Ericson.

Diagnosis. The species can be separated from other Chinese members of the genus based on the combination of the following characters: larger species, > 4.5 mm in total body length; head width > 0.9 mm; flagellar segments 1 and 2 longer than broad; posterior face of propodeum medially and petiole entirely smooth or very weakly punctate; gastral tergite 1 with fewer standing hairs, the number, excluding those on posterior margin of tergite, being usually < 10; body color usually dark brown.

Brief description. In full-face view, head longer than broad, roughly trapezoidal. Mandible triangular with nine teeth. Frontal carina short, frontal lobes well developed, covering antennal socket. Antennae 12-segmented, scape exceeds posterolateral corner, flagellar segments gradually increase in size toward the end. Eye medium in size and located in front of lateral margin of head. In lateral view, metanotal groove deeply impressed. Dorsal of propodeum nearly straight, longer than declivity; posterodorsal corner of propodeum broadly rounded.

Petiolar node as high as propodeum, upright, nearly trapezoidal; subpetiolar process forms a wedge. In dorsal view, pronotum anterior and lateral margins broad and round, posterior margin concave. Petiolar node crescent-shaped. Mandible densely punctate; head densely punctate; mesosoma smooth, pronotum finely punctate, and propodeum finely rugose; petiolar node and posteroventral area densely finely punctate. Body dorsally with abundant standing hairs and densely sub-decumbent hairs. Body black, appendages yellowish brown.

Brachyponera obscurans **(Walker, 1859)**

Fig. 27A–D

Formica obscurans Walker, 1859: 372 (q.) Sri Lanka.

Type material. type worker, Primary type locality: Sri Lanka (Ceylon). (images of a syntype worker, CASENT0902495 available on AntWeb were examined).

Measurements and indices. Worker (Fig. 26A–D): HL 0.86, HLL 0.79, HLA 0.10, HW 0.80, ML 0.50, CML 0.14, CI 93, SL 0.80, SI 99, ED 0.16, PrL 0.62, PrH 0.52, PrW 0.56, WL 1.37, TL 4.1, PL 0.30, PH 0.48, DPW 0.48, LPI 159, PDPI 158.

Diagnosis. The species can be separated from other Chinese members of the genus based on the combination of the following characters: smaller species, < 4.5 mm in total body length; head width < 0.9 mm; flagellar segments 1 and 2 each as long as broad, or broader than long; dorsum of propodeum nearly straight, longer than declivity, posterodorsal corner of propodeum broadly rounded; upper part of propodeum with densely sub-decumbent hairs; in dorsal view, petiolar node flat oval; body color usually yellowish brown to tan.

Brief description. In full-face view, head longer than broad, roughly trapezoidal, posterolateral corners of head narrowly rounded. Mandible triangular with nine teeth. Antennae 12-segmented, scape exceeds posterolateral corner, flagellar segments gradually increase in size toward the end. Eye medium in size and located in front of lateral margin of head. In lateral view, metanotal groove deeply impressed. Dorsum of propodeum nearly straight, longer than declivity; posterodorsal corner of propodeum broadly rounded. Petiolar node as high as propodeum, upright, nearly trapezoidal; subpetiolar process forms a wedge. In dorsal view, pronotum anterior and lateral margins broad and round, posterior margin concave. Petiolar node flat oval. Mandible densely punctate; head densely punctate; mesosoma, petiole and gaster finely punctate. Dorsum of body with abundant standing hairs and densely sub-decumbent hairs; upper part of propodeum with densely sub-decumbent hairs; body color dark brown, mandible, flagellar segments, and legs deep yellowish brown.

Brachyponera paraarcuata **Chen, Yu & Yi, sp. nov.**

https://zoobank.org/DD7E9165-CB0C-4770-A644-88586152784A

Fig. 28A–C

Type material. ***Holotype.*** worker, China: • Yunnan Province, Honghe Hani and Yi Autonomous Prefecture, Lvchun County, Banpo Township, Bayanhongdong, 24.63598'N, 102.34737'E, 1258 m above sea level, from soil in a monsoon

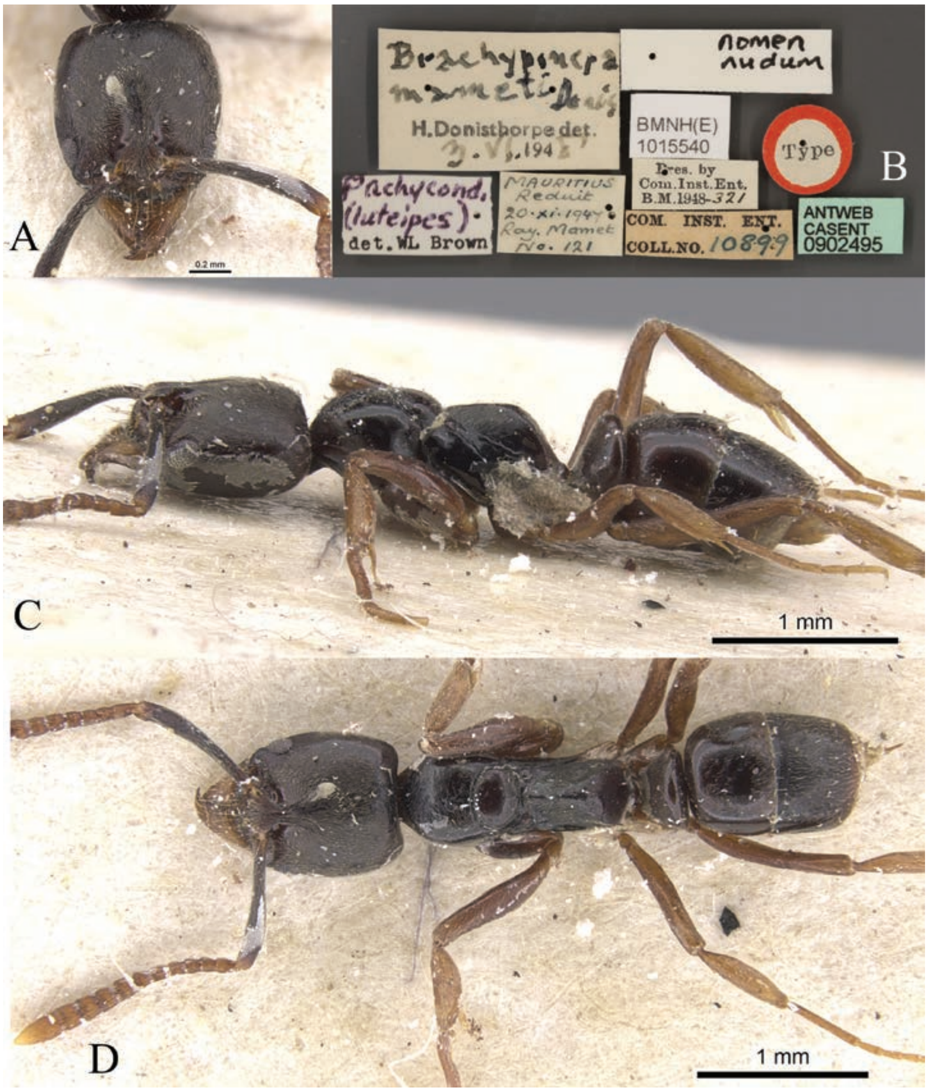

Figure 27. *Brachyponera obscurans* worker (CASENT0902495, type) **A** head in full-face view **B** label **C** body in lateral view **D** body in dorsal view. Photographer Will Ericson.

evergreen broadleaf forest, 10.X.2023, Bolun Li leg., No. KIZ20231657 (KIZ). ***Paratypes***: • 4 workers, same data as holotype (KIZ20231657A, KIZ20231657B deposited in SWFU, KIZ20231657C, KIZ20231657D deposited in GXNU).

Non-type material examined. 1 worker, China: Yunnan Province, Honghe Hani and Yi Autonomous Prefecture, Lvchun County, Banpo Township, mohelongtang, 22.61721'N, 102.33585'E, 1263 m above sea level, from mixed coniferous-broad forest, 13.iv.2023, Chao Chen leg., No. KIZ20230173 (KIZ); 2 workers, Honghe Hani and Yi Autonomous Prefecture, Lvchun County, Banpo Township, Bayanhongdong, 24.63598'N, 102.34737'E, 1258 m above sea level, monsoon evergreen broadleaf forest, 10.X.2023, Bolun Li leg., No. KIZ20230527.1-KIZ20230527.2 (KIZ); 2 workers, Honghe Hani and Yi Autonomous Prefecture, Lvchun County, Qimaba Township, dongma village, 22.68607'N, 102.30688'E, 1267 m monsoon evergreen broad-leaved forest, 18.iv.2023, Chao Chen leg., No. KIZ20230625.1- KIZ20230625.2 (KIZ).

Measurements and indices. *Holotype*: (Fig. 28A–C): HL 1.01, HLL 0.93, HLA 0.15, HW 0.91, ML 0.55, CML 0.13, CI 90, SL 0.98, SI 107, ED 0.13, PrL 0.65, PrH

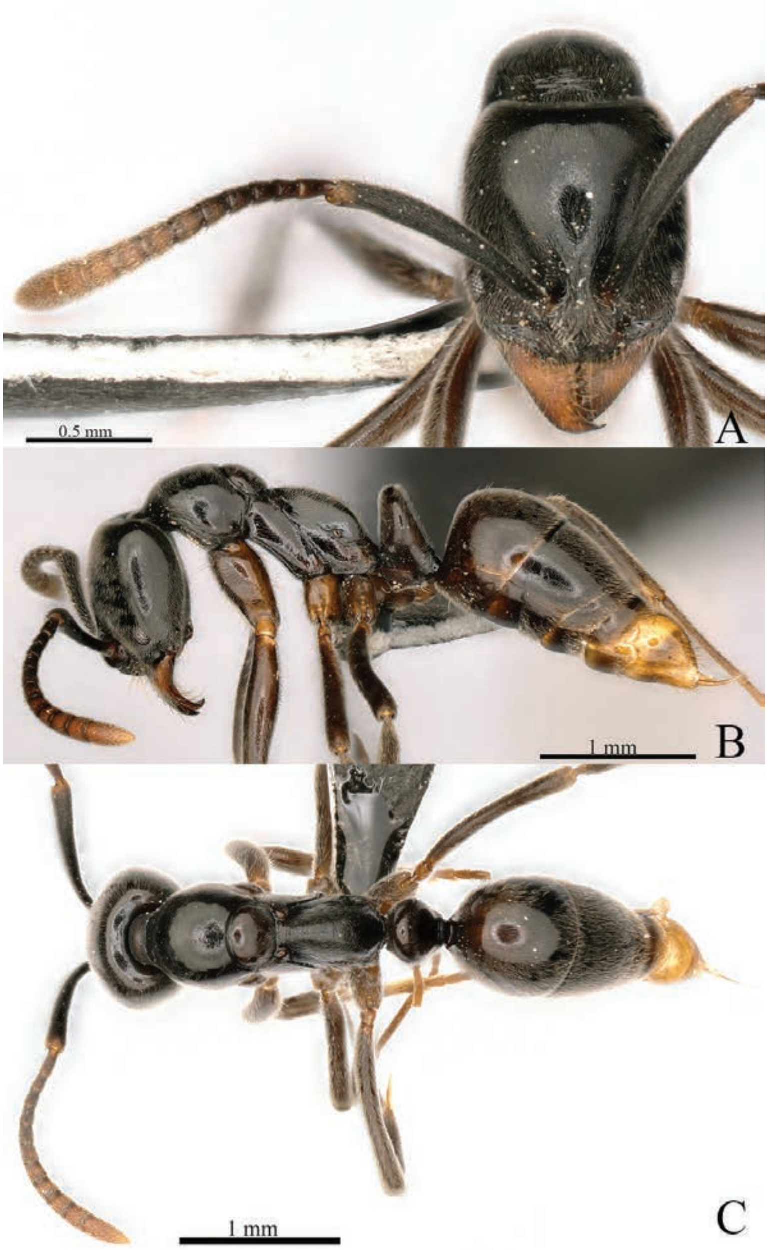

Figure 28. *Brachyponera paraarcuata* sp. nov. worker (holotype, No. KIZ20231657) **A** head in full-face view **B** body in lateral view **C** body in dorsal view. Photographer Chao Chen.

0.54, PrW 0.67, WL 1.51, TL 5.1, PL 0.36, PH 0.68, DPW 0.42, LPI 188, PDPI 117. ***Paratypes*** (n = 4): HL 0.98–1.09, HLL 0.92–0.97, HLA 0.14–0.15, HW 0.90–0.95, ML 0.55–0.57, CML 0.12–0.13, CI 87–92, SL 0.95–0.98, SI 103–105, ED 0.13, PrL 0.60–0.66, PrH 0.54–0.55, PrW 0.61–0.67, WL 1.46–1.51, TL 5.0–5.4, PL 0.34–0.37, PH 0.66–0.68, DPW 0.42–0.43, LPI 184–194, PDPI 116–124.

Diagnosis. The new species is similar to *Brachyponera arcuata* (Karavaiev, 1925), but it differs in lateral margins of head from mandible base to anterior edge of eye nearly straight (Fig. 12C), propodeal declivity smooth at the margin (Fig. 12D), body color black to brownish black. In *B. arcuata*, lateral margins of head between mandible base and anterior edge of eye are strongly convex (Fig. 12A), propodeal declivity is rugose at margin (Fig. 12B), and body color is brownish yellow.

Description. In full-face view, head longer than broad, roughly rectangular, posterior margin nearly straight, posterolateral corners narrowly rounded, lateral margins moderately convex. Mandible triangular with nine teeth, end tooth largest, and with a basal mandibular pit. Clypeus transverse, center of anterior margin weakly concave. Frontal carina short, frontal lobes well developed, covering antennal socket, frontal region with central longitudinal ridge. Antennae 12-segmented, scape exceeds posterolateral corner of head by 1/5 of its length, flagellar segments gradually increase in size toward the end. Eye medium to small and maximum diameter consists of eight ommatidia (ED 0.13 mm).

In lateral view, anterior margin of pronotum forms a cervical shield extending forward. Pronotum and mesonotum significantly higher than propodeum. Promesonotal suture seams evident, metanotal groove deeply impressed. Dorsal surface of propodeum continuously connected with declivity, forming a complete circular arc. Propodeal spiracle rounded, groove between spiracle and metanotal groove inconspicuous or absent. Metapleural bulla small, roughly elliptical. Petiolar node as high as propodeum, upright, nearly trapezoidal; anterior and posterior margin nearly straight, dorsum moderately convex; subpetiolar process triangular. Prora absent. Gaster subconical, basal two intersegments contracted, apex with sting.

In dorsal view, pronotum broadest, lateral margins moderately convex, humeral corners indistinct. Promesonotal suture and metanotal groove form an ellipse. propodeum rectangular, wide at the lower part and narrow at the upper part. Petiolar node broader than long, lateral and anterior margins convex, posterior margin flat.

Head, pronotum, mesonotum, and gaster with largely densely punctate. Mesopleuron, propodeum, petiolar node and legs with hairy punctations. Clypeus, mandible, coxa, propodeum, petiolar node and gaster with sparse erect or suberect hairs, dorsal surface of body with densely sub-decumbent hairs. Body color black to brownish black, funiculus, mandible, and legs yellowish brown.

Ecological notes. The new species was collected in the Huanglianshan National Nature Reserve in Yunnan. The type series was collected from the same soil nest in a monsoon evergreen broad-leaved forest at an altitude of 1250 m and 14 were collected foraging on the ground surface. One worker was collected in the soil of mixed coniferous and broadleaf forest at an altitude of 1000 m. Two workers were collected on the ground surface of the monsoon evergreen broadleaf forest at an altitude of 1250 m (Suppl. material 1: fig. S18).

Etymology. The specific epithet *paraarcuata* is a compound word meaning "similar to *arcuata*".

Brachyponera xui Chen, Yu & Yi, sp. nov.

https://zoobank.org/3AEDBAE9-C634-4790-AAF5-C9AC68B4C014

Fig. 29A–C

Type material. ***Holotype*** (worker) China: • Yunnan Province, Honghe Hani and Yi Autonomous Prefecture, Lvchun County, Sanmeng Township, laobianduan, 22.92752'N, 102.28553'E, 1749 m above sea level, from montane mossy evergreen broad-leaved forest, 24.iv.2023, Chao Chen leg., No. KIZ20231023 (KIZ). ***Paratypes***: • 1 worker, same data as holotype, No. KIZ20231004 (SWFU);

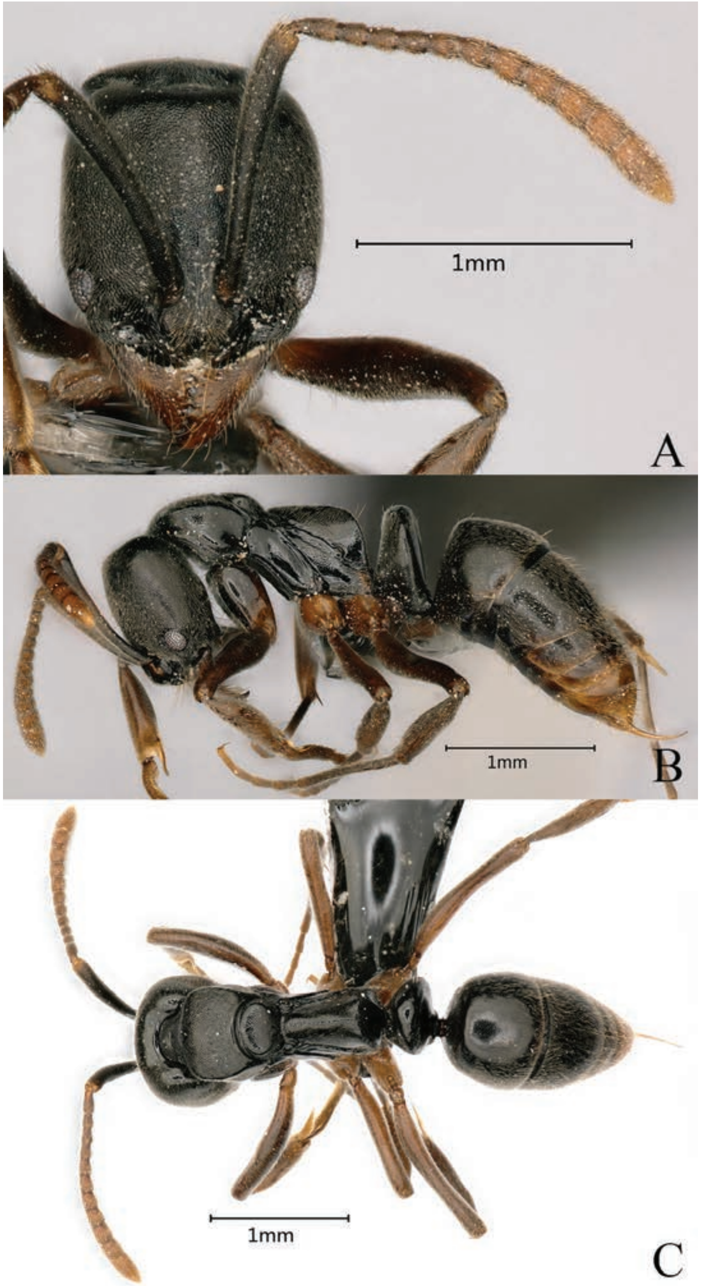

Figure 29. *Brachyponera xui* sp. nov. worker (holotype, No. KIZ20231023) **A** head in full-face view **B** body in lateral view **C** body in dorsal view. Photographer Chao Chen.

• 1 worker, Yunnan Province, Honghe Hani and Yi Autonomous Prefecture, Lvchun County, Qimaba Township, Dongma village, 22.69017'N, 102.33054'E, 744 m above sea level, from monsoon evergreen broad-leaved forest, 10.x.2023, Yu Yu leg., No. KIZ20231736 (GXNU).

Non-type material examined. • 2 workers, China: Yunnan Province, Honghe Hani and Yi Autonomous Prefecture, Lvchun County, Qimaba Township, lali village, 22.81959'N, 102.30435'E, 1263 m above sea level, montane mossy evergreen broad-leaf forest, 21.iv.2023, Chao Chen leg., No. KIZ20230837.1-KIZ20230837.2 (KIZ); • 1 worker,, Honghe Hani and Yi Autonomous Prefecture, Lvchun County, Qimaba Township, Xiaoheijiang, 22.69476'N, 102.33646'E, 510 m Tropical seasonal rainforest, 10.x.2023, Bolun Li leg., No. KIZ20231480 (KIZ);

Measurements and indices. ***Holotype*****:** (Fig. 29A–C): HL 0.97, HLL 0.92, HLA 0.13, HW 0.96, ML 0.54, CML 0.08, CI 99, SL 0.97, SI 101, ED 0.16, PrL 0.65, PrH 0.48, PrW 0.67, WL 1.56, TL 4.9, PL 0.38, PH 0.78, DPW 0.56, LPI 205, PDPI 147. ***Paratypes*** (*n* = 2): HL 0.96–1.05, HLL 0.91–0.94, HLA 0.12–0.15, HW 0.96–1.04, ML 0.53–0.55, CML 0.08, CI 99–100, SL 0.97–1.01, SI 97–101, ED 0.14–0.17, PrL 0.63–0.67, PrH 0.45–0.50, PrW 0.66–0.69, WL 1.54–1.58, TL 4.8–5.1, PL 0.38–0.39, PH 0.77–0.79, DPW 0.55–0.58, LPI203–205, PDPI 145–148.

Diagnosis. The new species is similar to *Brachyponera pilidorsalis* (Yamane), but it differs in head and pronotum with densely deeply punctate surface with small pits, eye relatively small, pronotum has edges (Fig. 9A), and dorsal surface of propodeum is longer. In *B. pilidorsalis*, head and pronotum are with sparsely lightly punctate sculpture with small pits, eye is relatively small, pronotum has weaker edges, and dorsal surface of propodeum is short.

Description. In full-face view, head nearly square, with length and width roughly equal, posterior margin nearly straight, lateral margins moderately convex, posterolateral corners narrowly rounded. Mandible triangular with nine teeth, end tooth largest, and with a basal mandibular pit. Clypeus transverse, center of anterior margin moderately concave. Frontal carina short, frontal lobes well developed, covering antennal socket, frontal region with central longitudinal ridge. Antennae 12-segmented, scape exceeds posterolateral corner of head by 1/5 of its length, flagellar segments gradually increase in size toward the end. Eye medium and maximum diameter consists of nine ommatidia (ED 0.16 mm).

In lateral view, lateral edge of pronotum has obvious edges. Pronotum and mesonotum significantly higher than propodeum. Promesonotal suture seams evident, metanotal groove deeply impressed. Mesonotum moderately convex. Dorsal surface of propodeum nearly straight, declivity steep slope, nearly straight, posterodorsal corner of propodeum broadly rounded. Propodeal spiracle rounded, there is a groove between spiracle and metanotal groove. Metapleural bulla small, roughly elliptical. Petiolar node as high as propodeum, upright, nearly trapezoidal; anterior margin nearly straight, posterior margin and dorsum moderately convex; subpetiolar process forms a wedge. Prora absent. Gaster subconical, basal two intersegments contracted, apex with sting.

In dorsal view, lateral edge of pronotum has obvious edges; equal width between upper and lower parts; pronotum broadest, lateral margins gradually narrower posteriorly. Mesonotum anterior margin convex, posterior margin slightly concave. propodeum nearly rectangular, gradually narrowing from the bottom to the top, forming a ridge. Petiolar node broader than long, anterior margin moderately convex, lateral margins strongly convex, posterior margin flat.

Mandible with sparsely punctate with small pits, head and pronotum with densely punctate with small pits. lateral face of pronotum, propodeum, petiolar node and gaster with hairy punctation. Mesopleuron, metapleural and lower part of lateral side of petiolar node smooth and shiny. dorsal surface of body with sparsely erect or suberect hairs and densely sub-decumbent hairs. Body color black, funiculus, mandible, and legs yellowish brown.

Ecological notes. The new species was collected in the Huanglianshan National Nature Reserve in Yunnan. The type series was collected while foraging on the ground surface of a montane mossy evergreen broadleaf forest at an altitude of 1750 m (Suppl. material 1: fig. S19), and one paratype was collected while foraging under a rock. One paratype was collected while foraging on the surface of a monsoon evergreen broad-leaved forest at an elevation of 750 m (Suppl. material 1: fig. S20). Another 107 workers of this new species were collected in seven sample plots in forest types including tropical seasonal rainforest, monsoon evergreen broadleaf forest, montane mossy evergreen broadleaf forest, mixed coniferous broadleaf forest, and deciduous broadleaf forest. Nesting sites included under rocks, in rotten wood, under rotten wood, and in soil. Foraging sites included surface and under stones. All sample plots were below 2000 m in elevation.

Etymology. The new species is named in honor of Professor Zhenghui Xu (Southwest Forestry University, China) for his outstanding contributions to the ant fauna of China.

Comments on the taxonomic position of *Euponera tianzun* (Terayama, 2009), comb. nov.

Euponera tianzun (Terayama, 2009), comb. nov.

Fig. 30A–D

Pachycondyla tianzun Terayama, 2009: 106, figs 31–35, 38 (w.). Type locality: Taiwan.
Brachyponera tianzun (Terayama, 2009): Schmidt and Shattuck 2014: 81.

Type material. Holotype worker of *E. tianzun* was examined in online database of the NIAES (http://www.niaes.affrc.go.jp/inventory/insect/inssys/hymlst.htm HYM-182, imaged by Hiraku Yoshitake & Takashi Kurihara). ***Holotype*** (worker). Type locality: China: Taiwan Province, Nantou Pref., Nanfeng-Cun, Nanshanxi, 12. viii. 1980 (M. Terayama). Type-depository: NIAES (National Institute for Agro- Environmental Sciences).

Diagnosis. This species is separated from *Euponera sharpi* Forel, 1901 by the angulate posterodorsal corner and much steeply sloped posterior margin of propodeum. Rather it resembles *E. sakishimensis* (Terayama, 1999) from the Ryukyus, Japan, and *E. pilosior* (Wheeler, 1928) from Japan and Korea. However, it is separated from the latter two by the narrow dorsal surface of propodeum and triangular subpetiolar process (Terayama 2009).

Measurements and indices. ***Holotype***: HL 1.18, HW 1.08, SL 0.80, WL 1.65, PL 0.40, PH 0.75, DPW 0.57, TL 4.7 CI 92, SI 74 (Terayama 2009).

Redescription of worker (Fig. 30A–D). In full-face view, head longer than broad, roughly rectangular, posterior margin weakly concave, posterolateral corners narrowly rounded, lateral margins moderately convex. Mandible triangular with ten teeth, and with a basal pit; masticatory margin meets with basal margin a right angle. Anterior margin of clypeus weakly convex, median clypeal ridge slightly raised. Frontal lobes well developed, covering antennal socket. Antennae 12-segmented; scape slightly exceeding posterior margin of head; flagellum obviously incrassate toward apex. Eye small, consisting of six or seven ommatidia, 0.04 mm in diameter.

In lateral view, dorsal and ventral margins of head slightly convex. Promesonotal suture and metanotal groove impressed. Mesonotum slightly convex. Dorsal surface of propodeum nearly straight, posterodorsal corner narrowly rounded, declivity steeply sloping (almost vertical), about equal to

Figure 30. *Euponera tianzun* worker (holotype) **A** head in full-face view **B** labels **C** body in lateral view **D** body in dorsal view. Photographers Hiraku Yoshitake, Takashi Kurihara.

length of dorsum. Spiracle circular and located at about midpoint of propodeal side. Metapleural bulla roughly elliptical. Petiolar node higher than long; in dorsal view anterior margin nearly straight and dorsal and posterior margins slightly convex; subpetiolar process triangular, with dully angulate ventral corner. Prora present on anterior margin of first gastral sternite. Gaster roughly elliptical, apex with sting.

With mesosoma in dorsal view, pronotum broadest, lateral margin moderately convex, humeral corner indistinct. Promesonotal suture and metanotal groove impressed. Mesonotum elliptical, its lateral margin moderately convex. Petiolar node broader than long, anterior and lateral margins slightly convex, posterior margin nearly straight.

Head and body surface weakly punctate. Clypeus, pronotum, petiolar node and gaster with sparse erect hairs, cranium, antennae, mesosoma and gaster with suberect hairs and pubescence. Body dark reddish brown to blackish brown; head darker than alitrunk; antenna, mandible, and legs reddish brown.

Comments. The species was transferred to *Euponera* because it bears morphological traits typical for this genus, among them: head rectangular, longer than wide (CI = 91), with concave posterior margin in full-face view; mandible with 10 teeth, and with a basal mandibular pit; anterior margin of clypeus weakly convex; antennal scape slightly exceeding the posterior margin of head; SI = 74; eye small, consisting of six or seven facets, 0.04 mm in diameter; alitrunk with straight dorsal margin in profile; propodeum with angulate posterodorsal corner and steeply sloped posterior margin in profile, in dorsal view dorsal surface relatively wide; petiole higher than long in profile, subpetiolar process triangular, with dully angulate ventral corner (Terayama 2009).

Discussion

In this study, we described four new species of *Brachyponera* distributed in China, and we hypothesize that the number is not definitive as there are most likely still undiscovered species of occurring in this country. The distribution range of this genus covers Oriental, Indo-Australian, and Palaearctic regions (Janicki et al. 2016), and further studies should provide more insights into the diversity of *Brachyponera* on a global scale. Also, studies on this genus are challenging due to the small morphological differences between species. However, the four new species described in this work are distinguished based on strong and well-defined characters.

The species group division proposed by Yamane (2007) was supplemented with additional sets of characters that should facilitate taxonomic studies on this genus. In summary, we distinguish 23 species of *Brachyponera* divided into eight species groups, i.e., *atrata* group, *lutea* group, *kumtongi* group, *chinensis* group, *xui* group, *arcuata* group, *nigrita* group, and *obscurans* group. The complexity of biomes can be simplified by grouping species with the same characteristics into one species group, making it easier to study and understand the structure and function of ecosystems.

By sequencing, we obtained the DNA sequences of mitochondrial COI of four new species and *B. brevidorsa*. In addition, sequences of nine species, including two outgroups, were downloaded from GenBank. The analysis showed that the smallest genetic distance between species was 7% (*B. croceicornis* and *B. obscurans*), and the largest genetic distance was 19.62% (*B. nakasujii* and *B. paraarcuata* sp. nov.). However, our results should be viewed cautiously, as trees based only on COI are considered unreliable, often disagreeing with those inferred from ultraconservative genes (Hebert et al. 2003; Pons et al. 2006). Collecting more specimens in subsequent surveys will allow for building a more complete phylogenetic tree and the future analyses should be based on UCEs. By this, it will be more likely to gain a better understanding of the phylogeny of *Brachyponera*.

During the field survey, we did not collect enough queens and males, which resulted in our inability to understand the complete life history of each species fully. We believe that further research on the *Brachyponera* will provide new insights into the morphological classification, genetic evolution, and biology of the genus.

Acknowledgments

We give special thanks to Prof. Zhenghui Xu (College of Forestry, Southwest Forestry University) for his great help in drafting the article and identifying the specimens. We would like to thank the staff of Huanglianshan Nature Reserve for their assistance in our field research (Mr Wenxiang Zhang, Mr Wen Wang). We Special thanks are also due to Prof. Seiki Yamane (Department of Earth and Environmental Sciences, Faculty of Science, Kagoshima University) for providing us with a large number of specimens that have helped us tremendously in writing this article. Furthermore, we extend our appreciation to the California Academy of Sciences (San Francisco) for granting us permission to utilize images from AntWeb. Special thanks to Dr Brian Lee Fisher (creator of AntWeb). We would like to thank the journal editor Dr Sebastian Salata for his valuable suggestions and careful revision and the valuable comments of the two reviewers Dr François Brassard and Dr Weeyawat Jaitrong.

Additional information

Conflict of interest

The authors have declared that no competing interests exist.

Ethical statement

No ethical statement was reported.

Funding

This study was supported by the Project of Huanglianshan National Nature Reserve Animal Diversity Expedition (No. E2023HLS001), Yunnan Agricultural Basic Research Joint Project (No. 202301BD070001-004) and the National Natural Science Foundation of China (No. 31660631).

Author contributions

Investigation: YY. Writing - review and editing: CY, CC.

Author ORCIDs

Chao Chen https://orcid.org/0009-0007-2983-9570
Yu Yu https://orcid.org/0009-0002-8775-1415
Chuanhui Yi https://orcid.org/0009-0008-9014-9947

Data availability

All of the data that support the findings of this study are available in the main text or Supplementary Information.

References

AntWeb (2024) AntWeb, California Academy of Sciences, San Francisco, California, USA. http://www.antweb.org/ [accessed 10 March 2024]

Antwiki (2024) AntWiki. https://www.antwiki.org/ [accessed on 10 March 2024]

Arimoto K (2017) Taxonomy of the *Leptogenys modiglianii* species group from southeast Asia (Hymenoptera, Formicidae, Ponerinae). ZooKeys 651: 79–106. https://doi.org/10.3897/zookeys.651.10336

Bingham CT (1903) The fauna of British India, including Ceylon and Burma. Hymenoptera. Vol. II. Ants and Cuckoowasps. Taylor and Francis, London, 506 pp.

Bolton B (1975) A revision of the ant genus *Leptogenys* Roger (Hymenoptera: Formicidae) in the Ethiopian region with a review of the Malagasy species. Bulletin of the British Museum (Natural History). Entomology 31: 235–305. https://doi.org/10.5962/bhl.part.29487

Bolton B (2003) Synopsis and classification of Formicidae. Memoirs of the American Entomological Institute 71: 1–370.

Bolton B (2024) An online catalog of the ants of the world. http://www.antcat.org/ [retrieved on 11 March 2024]

Dang AV, Yamane S, Nguyen DA, Eguchi K (2018) New combination and redescription of *Brachyponera mesoponeroides* Radchenko, 1993 (Hymenoptera: Formicidae: Ponerinae). Revue Suisse de Zoologie 125(2): 221–229. https://doi.org/10.5281/zenodo.1414203

Duanchay T, Buttachon S, Pinkaew N, Jaitrong W (2024) Two new cave dwelling species of the ant genus *Brachyponera* Emery, 1900 (Hymenoptera: Formicidae, Ponerinae) from Thailand. Far Eastern Entomologist 511: 1–12. https://doi.org/10.25221/fee.511.1

Emery C (1895) Viaggio di Leonardo Fea in Birmania e regioni vicine. LXIII. Formiche di Birmania del Tenasserim e dei Monti Carin raccolte da L. Fea. Parte II. Annali del Museo Civico di Storia Naturale 34[=(2)14]: 450–483. https://doi.org/10.5962/bhl.part.16764

Emery C (1900) Formicidarum species novae vel minus cognitae in collectione Musaei Nationalis Hungarici quas in Nova-Guinea, colonia germanica, collegit L. Biró. Publicatio secunda. Természetrajzi Fü zetek 23: 310–338.

Folmer O, Black M, Hoeh W, Lutz R, Vrijenhoek R (1994) DNA primers for amplification of mitochondrial cytochrome c oxidase subunit I from diverse metazoan invertebrates. Molecular Marine Biology and Biotechnology 3(5): 294–299.

Gotoh A, Ito F (2008) Seasonal cycle of colony structure in the ponerine ant *Pachycondyla chinensis* in western Japan (Hymenoptera, Formicidae). Insectes Sociaux 55: 98–104. https://doi.org/10.1007/s00040-007-0977-y

Guénard B, Weiser M, Gomez K, Narula N, Economo EP (2017) The Global Ant Biodiversity Informatics (GABI) database: a synthesis of ant species geographic distributions. Myrmecological News 24: 83–89.

Harris RA (1979) A glossary of surface sculpturing. California Department of Food and Agriculture, Bureau of Entomology. Occasional Papers in Entomology 28: 1–31.

Haskins CP, Haskins EF (1950) Note on the method of colony foundation of the ponerine ant *Brachyponera* (Euponera) lutea Mayr. Psyche (Camb.) 57(1): 1–9. https://doi.org/10.1155/1950/72123

Hebert PDN, Cywinska A, Ball SL, deWaard JR (2003) Biological identifications through DNA barcodes. Proceedings of the Royal Society of London: Series B, Biological Sciences 270(1512): 313–321. https://doi.org/10.1098/rspb.2002.2218

Ito F, Ohkawara K (1994) Spermatheca size differentiation between queens and workers in primitive ants. Naturwissenschaften 81: 138–140. https://doi.org/10.1007/BF01131772

Janicki J, Narula N, Ziegler M, Guénard B, Economo EP (2016) Visualizing and interacting with large-volume biodiversity data using client-server web-mapping applications: the design and implementation of antmaps.org. Ecological Informatics 32: 185–193. https://doi.org/10.1016/j.ecoinf.2016.02.006

Karavaiev V (1925) Ponerinen (Fam. Formicidae) aus dem Indo-Australischen Gebiet. (Fortsetzung). Konowia 4: 115–131.

Kikuchi T, Tsuji K, Ohnishi J, le Breton J (2007) Caste-biased acceptance of non-nestmates in a polygynous ponerine ant. Animal Behaviour 73: 559–565. https://doi.org/10.1016/j.anbehav.2006.04.015

Lattke JE (2011) Revision of the New World species of the genus *Leptogenys* Roger (Insecta: Hymenoptera: Formicidae: Ponerinae). Arthropod Systematics & Phylogeny 69(3): 127–264. https://doi.org/10.3897/asp.69.e31744

Letunic I, Bork P (2021) Interactive tree of life (iTOL) v5: an online tool for phylogenetic tree display and annotation. Nucleic Acids Res 49 (W1): W293-W296. DOI: https://doi.org/10.1093/nar/gkab301

Matsuura K (2002) Colony-level stabilization of soldier head width for head-plug defense in the termite Reticulitermes speratus (Isoptera: Rhinotermitidae). Behavioral Ecology and Sociobiology 51: 172–179. https://doi.org/10.1007/s00265-001-0426-2

Matsuura K, Kuno E, Nishida T (2002) Homosexual tandem running as selfish herd in *Reticulitermes speratus*: novel antipredatory behavior in termites. Journal of Theoretical Biology 214: 63–70. https://doi.org/10.1006/jtbi.2001.2447

Mayr G (1862) Myrmecologische Studien. Verhandlungen der Kaiserlich-Königlichen Zoologisch-Botanischen Gesellschaft in Wien 12: 649–776.

Menchetti M, Schifani E, Gentile V, Vila R (2022) The worrying arrival of the invasive Asian needle ant *Brachyponera chinensis* in Europe (Hymenoptera: Formicidae). Zootaxa 5115(1): 146–150. https://doi.org/10.11646/zootaxa.5115.1.10

Nei M, Kumar S (2000). Molecular Evolution and Phylogenetics. Oxford University Press, New York, 333 pp. https://doi.org/10.1093/oso/9780195135848.001.0001

Nelder MP, Paysen ES, Zungoli PA, Benson EP (2006) Emergence of the introduced ant *Pachycondyla chinensis* (Formicidae: Ponerinae) as a public health threat in the southeastern United States. Journal of Medical Entomology 43(5): 1094–1098. https://doi.org/10.1093/jmedent/43.5.1094

Ogata K (1987) A generic synopsis of the poneroid complex of the family Formicidae in Japan (Hymenoptera). Part 1. Subfamilies Ponerinae and Cerapachyinae. Esakia 25: 97–132. https://doi.org/10.5109/2494

Pons J, Barraclough TG, Gomez-Zurita J, Cardoso A, Duran DP, Hazell S, Kamoun S, Sumlin WD, Vogler AP (2006) Sequence-based species delimitation for the DNA taxonomy of undescribed insects. Systematic Biology 55: 595–609 https://doi.org/10.1080/10635150600852011

Ronquist F, Teslenko M, van der Mark P, Ayres DL, Darling A, Höhna S, Larget B, Liu L, Suchard MA, Huelsenbeck JP (2012) MrBayes 3.2: efficient Bayesian phylogenetic inference and model choice across a large model space. Systematic Biology 61(3): 539–542. https://doi.org/10.1093/sysbio/sys029

Schmidt C (2013) Phylogenetics of Ponerine ants (Hymenoptera: Formicidae: Ponerinae). Zootaxa 3647: 201–250. https://doi.org/10.11646/zootaxa.3647.2.1

Schmidt C, Shattuck SO (2014) The higher classification of the ant subfamily Ponerinae (Hymenoptera: Formicinae), with a review of ponerine ecology and behavior. Zootaxa 3817: 1–242. https://doi.org/10.11646/zootaxa.3817.1.1

Snelling RR (1981) Systematics of social Hymenoptera In: Hermann H.R. (ed.). Social Insects. Vol. 2. Academic Press, New York, 369–453. https://doi.org/10.1016/B978-0-12-342202-6.50012-5

Tamura K, Stecher G, Kumar S (2021) MEGA 11: Molecular Evolutionary Genetics Analysis Version 11. Molecular Biology and Evolution 38(7): 3022–3027. https://doi.org/10.1093/molbev/msab120

Terayama M (2009) A synopsis of the family Formicidae of Taiwan (Insecta: Hymenoptera). Research Bulletin of Kanto Gakuen University. Liberal Arts 17: 81–266.

Thompson JD, Gibson TJ, Higgins DG (2002) Multiple sequence alignment using ClustalW and ClustalX. Current Protocols in Bioinformatics 1: 2.3.1–2.3.22. https://doi.org/10.1002/0471250953.bi0203s00

Wheeler WM (1933) Colony-founding among ants, with an account of some primitive Australian species. Harvard University Press, Cambridge, 179 pp.

Wilson EO (1955) A monographic revision of the ant genus *Lasius*. Bulletin of the Museum of Comparative Zoology 113: 1–201.

Wilson EO (1958) Studies on the ant fauna of Melanesia III. Rhytidoponera in western Melanesia and the Moluccas. IV. The tribe Ponerini. Bulletin of the Museum of Comparative Zoology 119: 303–371.

Xu ZH (1994) A taxonomic study of the ant genus *Brachyponera* Emery in southwestern China (Hymenoptera Formicidae Ponerinae). [In Chinese.]. Journal of Southwest Forestry College 14: 181–185.

Xu ZH (2002) A Study on the Biodiversity of Formicidae Ants of Xishuangbanna Nature Reserve. Yunnan Science and Technology Press, Kunming, 181 pp.

Xu ZH, He QJ (2015) Taxonomic review of the ponerine ant genus *Leptogenys* Roger, 1861 (Hymenoptera: Formicidae) with a key to the Oriental species. Myrmecological News 21: 137–161.

Yamane S (2007) *Pachycondyla nigrita* and related species in Southeast Asia. In: Snelling RR, Fisher BL, Ward PS (Eds) Advances in ant systematics (Hymenoptera: Formicidae): homage to E. O. Wilson - 50 years of contributions. Memoirs of the American Entomological Institute, 650–663.

Yashiro T, Matsuura K, Guénard B, Terayama M, Dunn RR (2010) On the evolution of the species complex *Pachycondyla chinensis* (Hymenoptera: Formicidae: Ponerinae), including the origin of its invasive form and description of a new species. Zootaxa 2685: 39–50. https://doi.org/10.11646/zootaxa.2685.1.3

Supplementary material 1

Additional images

Authors: Chao Chen, Yu Yu, Chuanhui Yi

Data type: pdf

Link: https://doi.org/10.3897/zookeys.1230.140159.suppl1

ZooKeys 1230: 287–302 (2025)
DOI: 10.3897/zookeys.1230.142967

Research Article

A new species of the genus *Ovophis* Burger in Hoge & Romano-Hoge, 1981 (Serpentes, Viperidae) from southern Yunnan, China

Shuo Liu[1], Mian Hou[2], Mingzhong Mo[3], Mei Li[4], Biao Li[4], Xiong Luo[4], Dingqi Rao[5], Song Li[1,6]

1 *Kunming Natural History Museum of Zoology, Kunming Institute of Zoology, Chinese Academy of Sciences, Kunming, Yunnan 650223, China*
2 *College of Continuing (Online) Education, Sichuan Normal University, Chengdu, Sichuan 610066, China*
3 *Honghe Prefecture Forestry and Grassland Bureau of Yunnan Province, Mengzi, Yunnan 661199, China*
4 *Yuanyang Guanyinshan Provincial Nature Reserve Management and Protection Bureau, Yuanyang, Yunnan 662400, China*
5 *Kunming Institute of Zoology, Chinese Academy of Sciences, Kunming, Yunnan 650201, China*
6 *Yunnan Key Laboratory of Biodiversity Information, Kunming Institute of Zoology, Chinese Academy of Sciences, Kunming, Yunnan 650201, China*
Corresponding authors: Song Li (lis@mail.kiz.ac.cn); Dingqi Rao (raodq@mail.kiz.ac.cn)

Abstract

A new species of *Ovophis* is described from Yuanyang Guanyinshan Provincial Nature Reserve in southern Yunnan Province, China. The new species can be distinguished from congeneric species by the following combination of characters: ratio of tail length to total length 0.191–0.206, internasals separated by one or two scales, dorsal scales in 22-21-17 rows, ventrals 146–148, subcaudals 57–64, most subcaudals paired and a few unpaired, third supralabial larger than fourth, white spots on dorsal tail continuous. This study further reveals that the species diversity of *Ovophis* has been seriously underestimated, and there is still a lot of work to be done on the taxonomy of this genus.

Key words: cytochrome *b* gene, morphology, mountain pitvipers, systematics, taxonomy

Academic editor: Robert Jadin
Received: 28 November 2024
Accepted: 30 January 2025
Published: 6 March 2025

ZooBank: https://zoobank.org/AEDF6634-5A9E-422F-9727-1F99F871C886

Citation: Liu S, Hou M, Mo M, Li M, Li B, Luo X, Rao D, Li S (2025) A new species of the genus *Ovophis* Burger in Hoge & Romano-Hoge, 1981 (Serpentes, Viperidae) from southern Yunnan, China. ZooKeys 1230: 287–302. https://doi.org/10.3897/zookeys.1230.142967

Introduction

The genus *Ovophis* Burger in Hoge & Romano-Hoge, 1981 is a group of medium-sized venomous snakes that are widely distributed in mountainous areas of eastern Asia, southern Himalayas, and Indochina (Leviton et al. 2003; Neang et al. 2011; Che et al. 2020; Guo et al. 2022; Guo and Che 2024). Currently, this genus is recognized to contain seven species, namely *O. monticola* (Günther, 1864), *O. convictus* (Stoliczka, 1870), *O. makazayazaya* (Takahashi, 1922), *O. tonkinensis* (Bourret, 1934), *O. zayuensis* (Jiang, 1977), *O. anitae* David, Frétey & Vogel, 2024, and *O. jenkinsi* Qiu, Wang, Xia, Jiang, Zeng, Wang, Li & Shi, 2024 (Qiu et al. 2024). In addition, *Trimeresurus okinavensis* Boulenger, 1892 and *Trimeresurus gracilis* Oshima, 1920 may also belong to this genus since they share similar morphological characteristics with the above seven species (Uetz et al. 2025). However, these two species were not supported in *Ovophis* based on molecular data (Malhotra and Thorpe 2000, 2004; Li et al. 2020; Shi et al. 2021). Therefore, recent taxonomic studies did not include these two species in *Ovophis* (e.g., Zeng et al. 2023; Qiu et al. 2024).

Previously, *Ovophis monticola* was considered a widely distributed species, and the snakes of this genus occurring in Yunnan Province of China were all considered to be *O. monticola* (Zhao et al. 1998; Zhao 2006; Yang and Rao 2008). Afterwards, Malhotra et al. (2011) conducted a taxonomic revision of *Ovophis* and considered that more than one species of this genus is distributed in Yunnan, while the true *O. monticola* is not found in Yunnan. Subsequently, Zeng et al. (2023) conducted further evaluation of *Ovophis* and described a new species of this genus from Yunnan. However, David et al. (2024) considered that the nomen "*Ovophis malhotrae*" proposed by Zeng et al. (2023) is nomenclaturally unavailable and proposed for it a new nomen. Therefore, four species of *Ovophis* are distributed in Yunnan currently, namely *O. makazayazaya*, *O. zayuensis*, *O. anitae*, and *O. jenkinsi* (Zeng et al. 2023; David et al. 2024; Qiu et al. 2024).

During our recent fieldwork in southern Yunnan, China, some mountain pitviper specimens were collected from Yuanyang Guanyinshan Provincial Nature Reserve. Molecular and morphological comparison revealed that these specimens belong to a distinct taxon in the genus *Ovophis*. Herein, we describe this taxon as a new species.

Material and methods

Field surveys were conducted in Yuanyang Guanyinshan Provincial Nature Reserve, Yuanyang County, Honghe Hani and Yi Autonomous Prefecture, Yunnan Province, China, under the permit from Yuanyang Guanyinshan Provincial Nature Reserve Management and Protection Bureau. Specimens were preserved in approximately 75% ethanol and then deposited at Kunming Natural History Museum of Zoology, Kunming Institute of Zoology, Chinese Academy of Sciences (KIZ).

Total genomic DNA was extracted from liver tissues. Fragments of mitochondrial cytochrome *b* (*Cytb*) gene were amplified and sequenced using the primers L14910 and H16064 (Burbrink et al. 2000). Amplification and sequencing were completed by Sangon Biotech (Shanghai) Co., Ltd. Newly generated sequences have been deposited in GenBank and homologous sequences were obtained from GenBank (Table 1).

Sequences were aligned using MAFFT 7.471 (Katoh and Standley 2013). A Bayesian inference (BI) was performed in MrBayes 3.2.7 (Ronquist et al. 2012) using the GTR+F+I+G4 model and a maximum likelihood (ML) analysis was performed in IQ-TREE 1.6.12 (Nguyen et al. 2015) using the TN+F+I+G4 model, which was selected under the Akaike Information Criterion in ModelFinder (Kalyaanamoorthy et al. 2017). The technical computation methods for BI and ML phylogenetic analyses and genetic divergences calculation were the same as those in Liu et al. (2023).

Measurements were taken with a digital caliper to the nearest 0.1 mm. Measurement methodology followed David and Vogel (2012). Values for symmetric head characters are given in left/right order. The following morphological characteristics were noted:

Cep	cephalic scales, number on a line between the middle of supraoculars;
DSR	dorsal scale rows, at one head length behind the head, at midbody (namely at SVL/2), and at one head length before the vent, respectively;
HL	head length, from the tip of the snout to the angle of the jaw;

IL	infralabial scales;
SC	subcaudal plates;
SL	supralabial scales;
SVL	snout-vent length;
TaL	tail length;
TL	total length;
VEN	ventral plates.

Table 1. Samples used for the phylogenetic analyses in this study.

Species	Voucher	Locality	GenBank Accession
Ovophis zhaoermii sp. nov.	KIZ2023041	Yuanyang, Yunnan, China	PV035804
Ovophis zhaoermii sp. nov.	KIZ2024078	Yuanyang, Yunnan, China	PV035805
Ovophis zhaoermii sp. nov.	KIZ2024079	Yuanyang, Yunnan, China	PV035806
Ovophis zhaoermii sp. nov.	KIZ2024080	Yuanyang, Yunnan, China	PV035807
Ovophis anitae	GP 2041	Yunnan, China	OP441841
Ovophis anitae	GP 2053	Jinping, Yunnan, China	OP441842
Ovophis anitae	GP 2225	Jinping, Yunnan, China	OP441843
Ovophis anitae	ROM 39381	Lao Cai, Vietnam	HQ325160
Ovophis anitae	ROM 39382	Lao Cai, Vietnam	HQ325161
Ovophis anitae	ROM 39384	Lao Cai, Vietnam	HQ325162
Ovophis anitae	YBU 19103	Pingbian, Yunnan, China	OP441844
Ovophis convictus	AM B580	Cameron highlands, Pahang, Malaysia	HQ325129
Ovophis convictus	AM B628	Cameron highlands, Pahang, Malaysia	HQ325141
Ovophis convictus	AM B629	Pulau Langkawi, Malaysia	HQ325142
Ovophis jenkinsi	IOZ 002680	Yingjiang, Yunnan, China	PP171455
Ovophis jenkinsi	IOZ 002679	Yingjiang, Yunnan, China	PP171456
Ovophis jenkinsi	CAS 224424	Kachin, Myanmar	HQ325176
Ovophis jenkinsi	CAS 234763	Kachin, Myanmar	HQ325179
Ovophis jenkinsi	CAS 234866	Kachin, Myanmar	HQ325180
Ovophis jenkinsi	GP 1617	Myitkyina, Kachin, Myanmar	OP441885
Ovophis makazayazaya	AM A87	Taiwan, China	AF171907
Ovophis makazayazaya	AM B480	Yunnan, China	HQ325123
Ovophis makazayazaya	AM B482	China	AY352748
Ovophis makazayazaya	AM B578	China	HQ325128
Ovophis makazayazaya	AM B664	Sichuan, China	HQ325143
Ovophis makazayazaya	AM B665	Sichuan, China	HQ325144
Ovophis makazayazaya	AM B666	Sichuan, China	HQ325145
Ovophis makazayazaya	AM B669	Sichuan, China	HQ325146
Ovophis makazayazaya	AM B791	Yunnan, China	HQ325173
Ovophis makazayazaya	AM B793	Yunnan, China	HQ325174
Ovophis makazayazaya	AM B795	Yunnan, China	HQ325175
Ovophis makazayazaya	CAS 23440	Yunnan, China	HQ325178
Ovophis makazayazaya	GP 19	Hongya, Sichuan, China	OP441864
Ovophis makazayazaya	GP 20	Hongya, Sichuan, China	HQ325165
Ovophis makazayazaya	GP 21	Huili, Sichuan, China	OP441856
Ovophis makazayazaya	GP 23	Yunnan, China	AY763230
Ovophis makazayazaya	GP24/R01	Jingdong, Yunnan, China	HQ325166
Ovophis makazayazaya	GP 25	Hongya, Sichuan, China	HQ325167
Ovophis makazayazaya	GP 214	Anzhou, Sichuan, China	OP441863
Ovophis makazayazaya	GP 227	Hekou, Yunnan, China	HQ325170

Species	Voucher	Locality	GenBank Accession
Ovophis makazayazaya	GP 228	Hekou, Yunnan, China	HQ325171
Ovophis makazayazaya	GP 343	Shimen, Hunan, China	HQ325172
Ovophis makazayazaya	GP 1030	Yizhang, Hunan, China	OP441848
Ovophis makazayazaya	GP 2052	Jiangxi, China	OP441845
Ovophis makazayazaya	GP 2544	Hongkou, Sichuan, China	OP441866
Ovophis makazayazaya	GP 3831	Qianshan, Jiangxi, China	OP441846
Ovophis makazayazaya	GP 5058	Kaihua, Zhejiang, China	OP441847
Ovophis makazayazaya	GP 6748	Shangri-La, Yunnan, China	OP441857
Ovophis makazayazaya	GP 7749	Xuyong, Sichuan, China	OP441870
Ovophis makazayazaya	KIZ 02143	Luquan, Yunnan, China	OP441860
Ovophis makazayazaya	KIZ 03100	Youyang, Chongqing, China	OP441853
Ovophis makazayazaya	KIZ 037717	Fugong, Yunnan, China	OP441858
Ovophis makazayazaya	KIZ 037718	Fugong, Yunnan, China	OP441859
Ovophis makazayazaya	KIZ 09136	Pingbian, Yunnan, China	OP441852
Ovophis makazayazaya	NTNU B200800	Taiwan, China	DQ305463
Ovophis makazayazaya	SCUM035040	Huili, Sichuan, China	AY763229
Ovophis makazayazaya	YBU 061033	Anzhou, Sichuan, China	OP441867
Ovophis makazayazaya	YBU 091099	Changning, Sichuan, China	OP441871
Ovophis makazayazaya	YBU 09115	Changning, Sichuan, China	OP441865
Ovophis makazayazaya	YBU 11160	Leishan, Guizhou, China	OP441849
Ovophis makazayazaya	YBU 13314A	Shennongjia, Hubei, China	OP441869
Ovophis makazayazaya	YBU 13315A	Shennongjia, Hubei, China	OP441874
Ovophis makazayazaya	YBU 14212	Lincang, Yunnan, China	OP441854
Ovophis makazayazaya	YBU 14281	Mengzi, Yunnan, China	OP441850
Ovophis makazayazaya	YBU 15042	Wenshan, Yunnan, China	OP441855
Ovophis makazayazaya	YBU 15043	Wenshan, Yunnan, China	OP441851
Ovophis makazayazaya	YBU 15186	Muchuan, Sichuan, China	OP441873
Ovophis makazayazaya	YBU 15191	Muchuan, Sichuan, China	OP441872
Ovophis makazayazaya	YBU 18171	Hekou, Sichuan, China	OP441868
Ovophis makazayazaya	YPX 53011	Weixi, Yunnan, China	OP441861
Ovophis makazayazaya	YPX 53013	Weixi, Yunnan, China	OP441862
Ovophis makazayazaya	ZMB 70214	China	HQ325137
Ovophis makazayazaya	ZMB 70219	China	HQ325134
Ovophis makazayazaya	ZMB 70220	China	HQ325135
Ovophis makazayazaya	ZMB 70221	China	HQ325136
Ovophis monticola	ZMB 70216	Gandaki, Nepal	HQ325138
Ovophis monticola	ZMB 70218	Gandaki, Nepal	HQ325131
Ovophis monticola	GP 2028	Nyalam, Xizang, China	OP441883
Ovophis monticola	GP 2050	Nyalam, Xizang, China	OP441884
Ovophis tonkinensis	AM B581	China	HQ325130
Ovophis tonkinensis	AM B806	Hainan, China	HQ325181
Ovophis tonkinensis	GP 1632	Maoming, Guangdong, China	OP441875
Ovophis tonkinensis	GP 1665	Maoming, Guangdong, China	OP441876
Ovophis tonkinensis	GP 2140	Lingshui, Hainan, China	OP441877
Ovophis tonkinensis	GP 7703	Hainan, China	OP441878
Ovophis tonkinensis	KIZ 011602	Xuan Son, Phu Tho, Vietnam	OP441880
Ovophis tonkinensis	KIZ 022262	Xing ‘an, Guangxi, China	OP441881
Ovophis tonkinensis	MVZ 226627	Vinh Phuc, Vietnam	HQ325151
Ovophis tonkinensis	ROM 29763	Vinh Phuc, Vietnam	HQ325157
Ovophis tonkinensis	ROM 30776	Gia Lai, Vietnam	HQ325164
Ovophis tonkinensis	ROM 31082	Vinh Phuc, Vietnam	HQ325158
Ovophis tonkinensis	ROM 7798	Gia Lai, Vietnam	AY223572
Ovophis tonkinensis	YPX 28352	Lingshui, Hainan, China	OP441882

Species	Voucher	Locality	GenBank Accession
Ovophis tonkinensis	ZMB 70223	China	HQ325132
Ovophis tonkinensis	ZMB 70224	Lao Cai, Vietnam	HQ325133
Ovophis tonkinensis	ZMB 70225	China	HQ325139
Ovophis tonkinensis	ZMB 70226	China	HQ325140
Ovophis zayuensis	CAS 233203	Kachin, Myanmar	HQ325177
Ovophis zayuensis	GP 89	Mêdog, Xizang, China	OP441887
Ovophis zayuensis	GP 90	Zayü, Xizang, China	HQ325168
Ovophis zayuensis	GP 92	Gongshan, Yunnan, China	HQ325169
Ovophis zayuensis	GP 557	Bayi, Xizang, China	OP441889
Ovophis zayuensis	GP 594	Bayi, Xizang, China	OP441893
Ovophis zayuensis	GP 611	Bayi, Xizang, China	OP441891
Ovophis zayuensis	GP 713	Bomi, Xizang, China	OP441890
Ovophis zayuensis	GP 1388	Mêdog, Xizang, China	OP441886
Ovophis zayuensis	GP 1505	Zayü, Xizang, China	OP441892
Ovophis zayuensis	KIZ 010968	Mêdog, Xizang, China	MW111486
Ovophis zayuensis	KIZ 035124	Gongshan, Yunnan, China	OP441895
Ovophis zayuensis	KIZ 037721	Lushui, Yunnan, China	OP441894
Ovophis zayuensis	KIZYPX27835	Bomi, Xizang, China	MW133461
Ovophis zayuensis	KIZYPX27855	Zayü, Xizang, China	MW133460
Ovophis zayuensis	KIZYPX27857	Nyingchi, Xizang, China	MW133459
Ovophis zayuensis	YBU 071107	Bayi, Xizang, China	OP441888
Ovophis cf. *meridionalis*	ROM 39385	Lao Cai, Vietnam	HQ325163
Ovophis cf. *meridionalis*	ROM 39386	Lao Cai, Vietnam	HQ325154
Ovophis cf. *meridionalis*	ROM 39387	Lao Cai, Vietnam	HQ325155
Ovophis cf. *meridionalis*	ROM 39388	Lao Cai, Vietnam	HQ325156
Ovophis cf. *tonkinensis*	GP 2042	Guangxi, China	OP441879
Ovophis cf. *tonkinensis*	ROM 35310	Cao Bang, Vietnam	HQ325159
Ovophis sp.	FMNH 258632	Xe Kong, Laos	HQ325124
Ovophis sp.	FMNH 258633	Champassak, Laos	HQ325125
Ovophis sp.	FMNH 258634	Champassak, Laos	HQ325126
Ovophis sp.	FMNH 258635	Champassak, Laos	HQ325127
Ovophis sp.	ROM 37617	Kon Tum, Vietnam	HQ325152
Ovophis sp.	ROM 37618	Kon Tum, Vietnam	HQ325153
Protobothrops mucrosquamatus	GP 5683	Cuiping, Sichuan, China	OP441896

Results

The BI and ML analyses yielded a consistent topology, which was almost identical to that published in Zeng et al. (2023). The sequences of the specimens from Yuanyang Guanyinshan Provincial Nature Reserve formed a distinct clade sister to a clade consisting of sequences of specimens from Lao Cai, Vietnam with strong support by both BI and ML, and then they together formed a clade sister to *Ovophis zayuensis* with strong support by BI (Fig. 1). The uncorrected pairwise distance between the sequences of the specimens from Yuanyang Guanyinshan Provincial Nature Reserve and the clade consisting of sequences of specimens from Lao Cai, Vietnam was 4.0%, the uncorrected pairwise distance between the sequences of the specimens from Yuanyang Guanyinshan Provincial Nature Reserve and the sequences of *O. zayuensis* was 7.4%, and the uncorrected pairwise distances between the sequences of the specimens from Yuanyang Guanyinshan Provincial Nature Reserve and the sequences of other species of this genus ranged from 9.1% to 13.0% (Table 2).

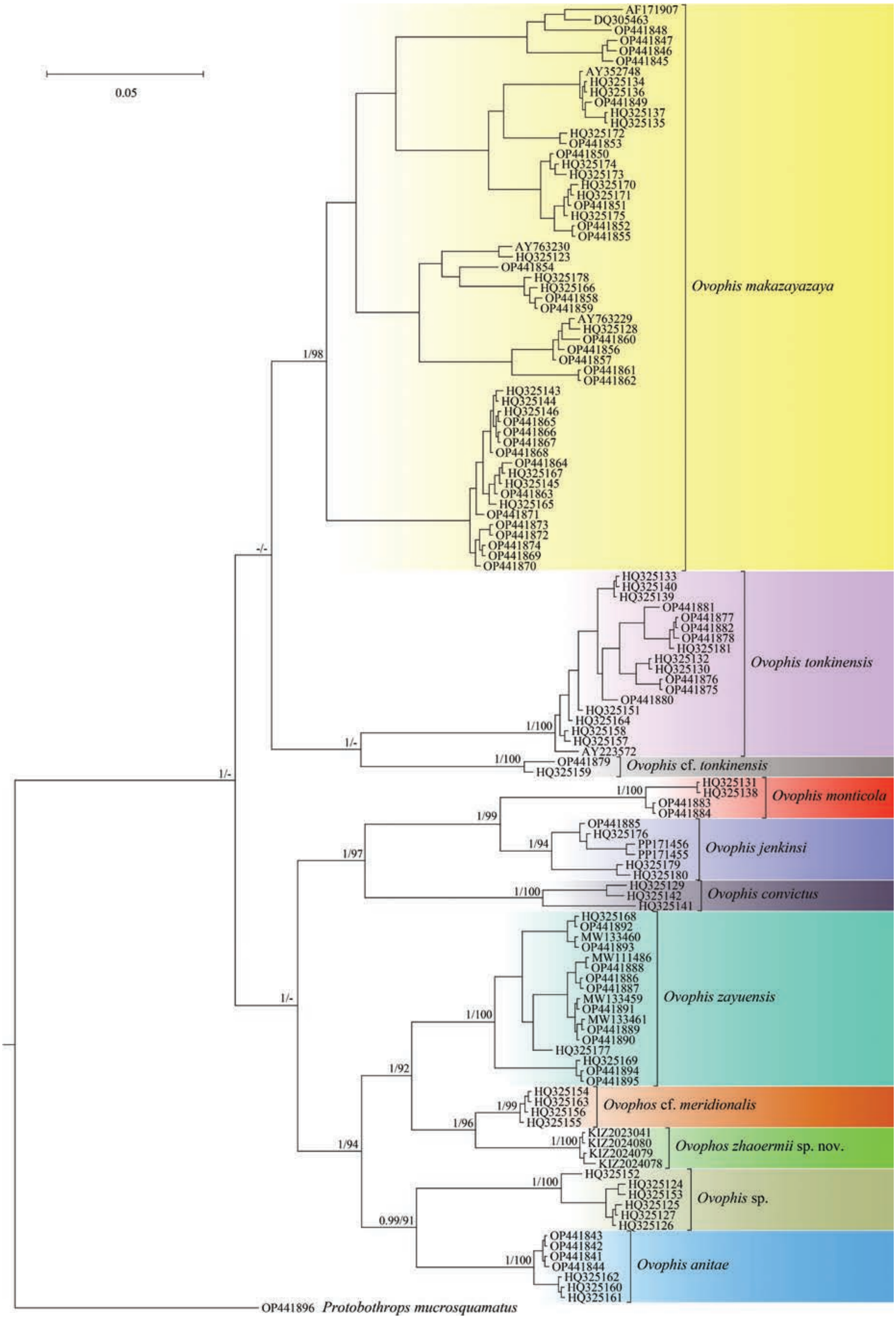

Figure 1. Bayesian phylogram of the genus *Ovophis* inferred from *Cytb* sequences. Numbers after and behind "/" are Bayesian posterior probabilities and ML ultrafast bootstrap values (only values above 0.90/90 are shown), respectively.

Table 2. Uncorrected pairwise genetic distances (%) estimated from *Cytb* sequences.

	1	**2**	**3**	**4**	**5**	**6**	**7**	**8**	**9**	**10**
1 *Ovophis zhaoermii* sp. nov.										
2 *Ovophis anitae*	9.1									
3 *Ovophis convictus*	11.6	10.9								
4 *Ovophis jenkinsi*	11.9	11.5	11.6							
5 *Ovophis makazayazaya*	11.6	10.8	12.7	11.9						
6 *Ovophis monticola*	13.0	12.4	12.2	7.2	13.3					
7 *Ovophis tonkinensis*	11.7	10.9	12.4	11.9	11.1	13.7				
8 *Ovophis zayuensis*	7.4	8.5	11.4	10.0	10.8	12.2	11.5			
9 *Ovophis* cf. *meridionalis*	4.0	7.5	9.8	10.6	10.3	13.1	10.5	6.2		
10 *Ovophis* cf. *tonkinensis*	12.4	10.6	12.9	12.0	10.2	13.8	9.2	11.1	11.0	
11 *Ovophis* sp.	9.6	8.1	12.6	11.4	12.1	12.6	11.8	9.1	8.9	11.3

Ovophis zhaoermii sp. nov.

https://zoobank.org/43381C87-E16A-455D-AB2A-DD7F15E88BA2
Figs 2–4

Material examined. ***Holotype*.** • KIZ2024078, adult male, collected on 23 July 2024 by Shuo Liu from Yuanyang Guanyinshan Provincial Nature Reserve, Yuanyang County, Honghe Hani and Yi Autonomous Prefecture, Yunnan Province, China (23°1'43"N, 102°56'11"E; 2400 m a.s.l.). ***Paratypes*.** • KIZ2023041, adult male, collected on 16 May 2023, and KIZ2024079–KIZ2024080, two adult males, collected on 16 July 2024, all by Shuo Liu from the same locality as the holotype.

Diagnosis. Ratio of tail length to total length 0.191–0.206, internasals separated by one or two scales, second supralabial bordering loreal pit, dorsal scales in 22-21-17 rows, ventrals 146–148, subcaudals 57–64, 3–11 subcaudals unpaired and other subcaudals paired, third supralabial larger than fourth, dorsal surface of head unpatterned, dorsal surface of body brownish-black or reddish-brown with rectangular black blotches, series of white spots on dorsal surface of tail continuous, iris off-white with a black mesh pattern.

Description of holotype. Adult male; body relatively slender, tail relatively short, SVL 541 mm, TaL 133 mm, TaL/TL 0.197; head approximately pear shaped, distinct from neck, HL/SVL 0.05; snout blunt and rounded, rostral trapezoidal, upper tip slightly visible from above; eye small, pupil vertically elliptic; supraocular 1/1, elongate, oval, largest scales on dorsal head, separated by six small scales; nostril close to snout tip; two internasals, approximately rectangular, separated by one small scale; two much smaller scales between rostral and internasals; loreal 1/1; preoculars 3/3; postoculars 2/3; suboculars 1/3, separated from supralabials by two rows of scales; supralabials 8/9, first and second in contact with nasal, second bordering loreal pit, third larger than fourth; infralabials 9/10, first pair contacting each other behind mental, first to third in contact with chin shields; mental triangular; one pair of chin shields, meeting in midline; dorsal scales in 22-21-17 rows, distinctly keeled except outer row; ventral scales 148, excluding four preventrals; subcaudal scales 61, first to eleventh unpaired, others paired; cloacal plate undivided.

***Color of holotype in life*.** Dorsal surface of head brownish-black; lateral surface of head dark reddish-brown, a wide brownish-black stripe behind eye on each side, a narrow discontinuous white stripe from mouth corner to lateral neck on each side;

Figure 2. Dorsal view (top) and ventral view (bottom) of the type series of *Ovophis zhaoermii* sp. nov. in preservative.

Figure 3. The holotype (KIZ2024078) of *Ovophis zhaoermii* sp. nov. in life **A** general view **B** dorsal view of the head **C** left view of the head **D** right view of the head **E** dorsal view of the tail.

lower lip reddish-brown with some irregular white blotches; dorsal surface of body brownish-black with many rectangular, large black blotches on dorsolateral surface, blotches of left and right sides arranged approximately in staggered pattern; two black spots below each black dorsolateral blotch; some irregular black blotches on ventrolateral part of body; anterior dorsal surface of tail dark brownish-black, posterior dorsal surface of tail white, composed of a continuous series of white spots on two medial rows of scales; ventral surface of head reddish-brown with some irregular white blotches; ventral surface of body and tail brownish-yellow with many irregular grayish-brown blotches; iris off-white with a black mesh pattern.

Variations. Morphometric and meristic data of the type series are provided in Table 3. The paratypes resemble the holotype in most aspects except for small differences in body size, relative tail length, and the number of unpaired subcaudals. In addition, the larger paratype (KIZ2024080) resembles the holotype in coloration, while the two smaller paratypes (KIZ2023041 and KIZ2024079) have lighter body coloration than the holotype.

Figure 4. The paratypes of *Ovophis zhaoermii* sp. nov. in life **A** KIZ2024079 **B** KIZ2024080 **C** KIZ2023041.

Table 3. Measurements (in mm) and scalation data of the type specimens of *Ovophis zhaoermii* sp. nov.

	KIZ2024078	KIZ2024079	KIZ2024080	KIZ2023041
	Holotype	Paratype	Paratype	Paratype
	Male	Male	Male	Male
SVL	541	396	543	461
HL	26.7	21.0	27.6	25.0
TaL	133	103	132	109
TL	674	499	675	570
TaL/TL	0.197	0.206	0.196	0.191
Cep	6	6	7	7
DSR	22-21-17	22-21-17	22-21-17	22-21-17
SL	8/9	9/9	8/8	8/8
IL	9/10	10/10	10/10	9/10
VEN	148	147	147	146
SC	61 (1st–11th unpaired)	64 (4th–11th unpaired)	61 (4th–6th unpaired)	57 (15th–23th unpaired)

Ecology notes. The specimens of the new species were found on the ground beside a stream at night. No other reptile species were found at the type locality of the new species, but many amphibian species were found in sympatry, including *Amolops minutus* Orlov & Ho, 2007, *A. viridimaculatus* (Jiang, 1983), *Atympanophrys gigantica* (Liu, Hu & Yang, 1960), *Feihyla fuhua* Fei, Ye & Jiang, 2010, *Hyla annectans* (Jerdon, 1870), *Leptobrachium ailaonicum* (Yang, Chen & Ma, 1983), *Nanorana aenea* (Smith, 1922), and *Zhangixalus duboisi* (Ohler, Marquis, Swan & Grosjean, 2000). Therefore, we presume the new species may prey on frogs in the wild.

Distribution. The new species is currently known only from Yuanyang Guanyinshan Provincial Nature Reserve in Yuanyang County, Honghe Hani and Yi Autonomous Prefecture, Yunnan Province, China (Fig. 5).

Etymology. Named after the renowned Chinese herpetologist, Prof. Ermi Zhao (1930–2016). The designation of this specific epithet honors his great contribution to herpetological research in China, especially in snake research. According to the type locality of this species, we suggest the English common name “Guanyinshan mountain pitviper” and the Chinese common name “观音山烙铁头蛇 (Pinyin: guān yīn shān lào tiě tóu shé)”.

Comparisons. *Ovophis zhaoermii* sp. nov. can be differentiated from *O. anitae* by having a relatively longer tail (TaL/TL 0.191–0.206 vs 0.133), having more subcaudal scales (57–64 vs 47), some of the subcaudal scales being unpaired (vs all of the subcaudal scales being paired), dorsal scales being in 22-21-17 rows (vs 27-23-19 rows), and the second supralabial bordering the loreal scale (vs the second supralabial being separated from the loreal scale).

Ovophis zhaoermii sp. nov. can be differentiated from *O. convictus* by having a relatively longer tail (TaL/TL 0.191–0.206 vs 0.064–0.128), having more subcaudal scales (57–64 vs 17–31), having more ventral scales (146–148 vs 120–140), some of the subcaudal scales being unpaired (vs all of the subcaudal scales being paired), and having continuous white spots on the dorsal surface of the tail (vs scattered white spots on the dorsal surface of the tail).

Ovophis zhaoermii sp. nov. can be differentiated from *O. makazayazaya* by having more subcaudal scales (57–64 vs 34–52), some of the subcaudal scales being unpaired (vs all of the subcaudal scales being paired), the third supralabial being larger than the fourth (vs the fourth supralabial being larger

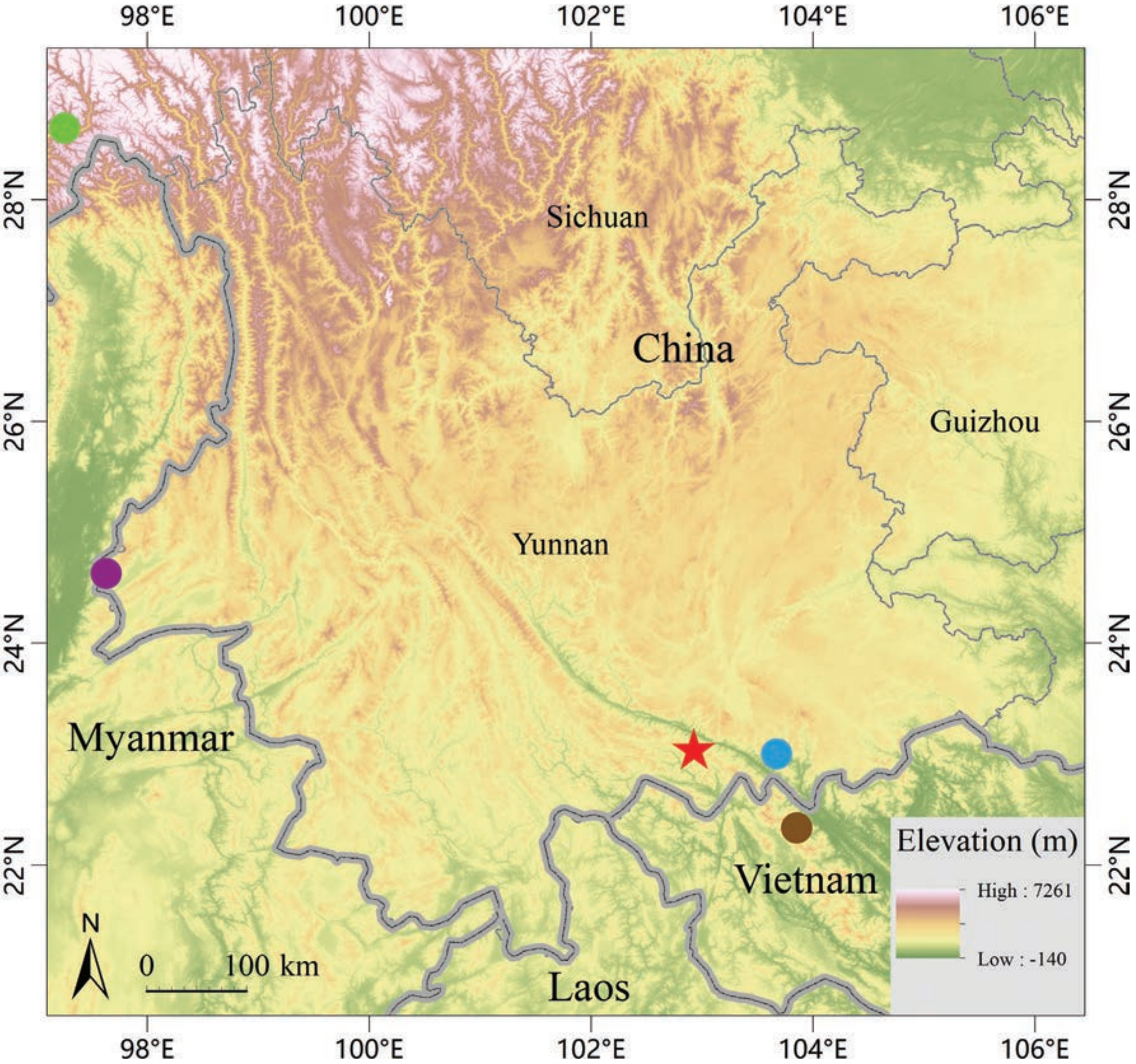

Figure 5. Map showing the type localities of *Ovophis zhaoermii* sp. nov. (red star), *O. anitae* (blue dot), *O. jenkinsi* (purple dot), *O. zayuensis* (green dot), and *Trimeresurus monticola meridionalis* (brown dot).

than the third), and having continuous white spots on the dorsal surface of the tail (vs scattered white spots on the dorsal surface of the tail).

Ovophis zhaoermii sp. nov. can be differentiated from *O. monticola* by having an unpatterned dorsal head surface (vs patterned dorsal head surface), having relatively more subcaudal scales (57–64 vs 37–58), some of the subcaudal scales being unpaired (vs all of the subcaudal scales being paired), the dorsal scales being in 22-21-17 rows (vs 23 or 21-23 or 21-19 rows), and having continuous white spots on the dorsal surface of the tail (vs scattered white spots on the dorsal surface of the tail).

Ovophis zhaoermii sp. nov. can be differentiated from *O. jenkinsi* by having a relatively longer tail (TaL/TL 0.191–0.206 vs 0.132–0.184), having more subcaudal scales (57–64 vs 40–52), having more ventral scales (146–148 vs 134–142), some of the subcaudal scales being unpaired (vs all of the subcaudal scales being paired), having an unpatterned dorsal head surface (vs patterned dorsal head surface), and having continuous white spots on the dorsal surface of the tail (vs scattered white spots on the dorsal surface of the tail).

Ovophis zhaoermii sp. nov. can be differentiated from *O. tonkinensis* by having more subcaudal scales (57–64 vs 39–49), having more ventral scales (146–148 vs 128–134), most of the subcaudal scales being paired (vs all or most of the subcaudal scales being unpaired), and the third supralabial being larger than the fourth (vs the fourth supralabial being larger than the third).

Ovophis zhaoermii sp. nov. can be differentiated from *O. zayuensis* by having fewer ventral scales (146–148 vs 160–177), most of the subcaudal scales being paired (vs all or most of the subcaudal scales being unpaired), the dorsal scales being in 22-21-17 rows (vs 25 or 27-23-19 or 17 rows), and having continuous white spots on the dorsal surface of the tail (vs no visible white spots on the dorsal surface of the tail).

Discussion

In the phylogenetic analysis, the sequences which were regarded as *Ovophis tonkinensis* by Zeng et al. (2023) formed two highly divergent clades, with a genetic distance of up to 9.2%. The first clade contained some sequences of specimens from southeastern China and northern and central Vietnam, which cover the type locality of *O. tonkinensis*, while the second clade contained two sequences of specimens from Guangxi of China and Cao Bang of Vietnam, respectively. Therefore, we consider that the first clade is *O. tonkinensis*, while the second clade may represent a cryptic species, and we temporarily refer to the second clade as *Ovophis* cf. *tonkinensis*.

Qiu et al. (2024) described *Ovophis jenkinsi* from Tongbiguan Township, Yingjiang County, Yunnan Province, China, which is closely related to *O. monticola*, based on morphological and molecular data. However, Qiu et al. (2024) did not include all available sequences of *O. monticola* in their phylogenetic analysis. In this study, we integrated all available sequences of *O. monticola* and the sequences of *O. jenkinsi*, and the analysis showed that among the sequences previously considered to belong to *O. monticola*, those corresponding to specimens from Gandaki of Nepal and Nyalam of China formed one clade, while those corresponding to specimens from Kachin of Myanmar formed another clade together with the sequences of *O. jenkinsi*; the genetic distance between these two clades was 7.2%. Therefore, according to the type locality of *O. monticola*, we consider the clade containing sequences of specimens from Nepal and Nyalam of China to be *O. monticola*, and the other clade to be *O. jenkinsi*. That is to say, *O. monticola* is restricted to Nepal and adjacent southern Xizang of China and northern India, while *O. jenkinsi* is also distributed in northern Myanmar in addition to western Yunnan.

David et al. (2024) considered that *Trimeresurus monticola meridionalis* Bourret, 1935 may be a distinct species, and it is likely that either *Ovophis anitae* or the *Ovophis* sp. 1 in Zeng et al. (2023) is a junior synonym of *T. m. meridionalis*. It can be confirmed that *Ovophis zhaoermii* sp. nov. is definitely not a junior synonym of *T. m. meridionalis*, although in both species the third supralabial is larger than the fourth one. *Ovophis zhaoermii* sp. nov. differs from *T. m. meridionalis* by having relatively more subcaudal scales (57–64 vs 47–54), having more ventral scales (146–148 vs 134–136), some of the subcaudal scales being unpaired (vs all of the subcaudal scales being paired), the dorsal scales being in 22-21-17 rows (vs 25-25-19 or 23-23-17 rows), and having continuous white spots on the dorsal surface of the tail (vs no visible white spots on the dorsal surface of the tail). However, it cannot be determined whether *O. anitae* or the *Ovophis* sp. 1 in Zeng et al. (2023) is conspecific with *T. m. meridionalis* currently. Until there is sufficient evidence, we retain the validity of *O. anitae* and refer to the *Ovophis* sp. 1 in Zeng et al. (2023) as *Ovophis* cf. *meridionalis* for the time being.

The area where *Ovophis zhaoermii* sp. nov. was discovered is located within Yuanyang Guanyinshan Provincial Nature Reserve, which is far away from human settlements. There are intact primary forests in the nature reserve, and they are legally protected. Therefore, we consider that this species is currently not threatened by humans.

Acknowledgments

We thank the forest rangers of Yuanyang Guanyinshan Provincial Nature Reserve for their assistance in the fieldwork and the editors and reviewers for their efforts on the manuscript. Thanks also to the curator and deputy curator of Kunming Natural History Museum of Zoology, Kunming Institute of Zoology, Chinese Academy of Sciences for their support of the field survey and taxonomic research.

Additional information

Conflict of interest

The authors have declared that no competing interests exist.

Ethical statement

No ethical statement was reported.

Funding

This work was supported by the project of Yuanyang Guanyin Mountains Provincial Nature Reserve Integrative Scientific Expedition (grant no. E2HX105B), Biological Resources Programme, Chinese Academy of Sciences, the Position of Bioclassonomist of Chinese Academy of Sciences (grant no. CAS-TAX-24), and the project of the Ministry of Ecology and Environment of China: Investigation and assessment of amphibians and reptiles in southern Yunnan.

Author contributions

Conceptualization: DR, HM, MM, ML, BL, XL. Formal analysis: SL (Shuo Liu), MH, SL (Song Li). Investigation: SL (Shuo Liu), SL (Song Li), MM, ML, BL, XL. Writing - original draft: SL (Shuo Liu). Writing - review and editing: SL (Shuo Liu), SL (Song Li), DR. Funding acquisition: SL (Song Li).

Author ORCIDs

Shuo Liu https://orcid.org/0000-0001-7825-3006
Mian Hou https://orcid.org/0000-0002-3322-6570
Dingqi Rao https://orcid.org/0000-0003-2680-1503
Song Li https://orcid.org/0000-0003-0834-5882

Data availability

All of the data that support the findings of this study are available in the main text.

References

Burbrink FT, Lawson R, Slowinski JB (2000) Mitochondrial DNA phylogeography of the polytypic North American rat snake (*Elaphe obsoleta*): A critique of the subspecies concept. Evolution; International Journal of Organic Evolution 54(6): 2107–2118. https://doi.org/10.1111/j.0014-3820.2000.tb01253.x

Che J, Jiang K, Yan F, Zhang YP (2020) Amphibians and Reptiles in Tibet—Diversity and Evolution. Science Press, Beijing, 603 pp.

David P, Vogel G (2012) On the status of *Trimeresurus monticola meridionalis* Bourret, 1935 (Squamata: Viperidae). Zootaxa 3304(1): 43–53. https://doi.org/10.11646/zootaxa.3304.1.3

David P, Frétey T, Vogel G (2024) The status of the nomen "*Ovophis malhotrae*" (Squamata, Serpentes, Viperidae, Crotalinae). Bionomina 38: 055–061. https://doi.org/10.11646/bionomina.38.1.5

Guo P, Che J (2024) Snakes in Qinghai-Xizang Plateau. Science Press, Beijing, 229 pp.

Guo P, Liu Q, Wu YY, Zhu F, Zhong GH (2022) Pitvipers of China. Science Press, Beijing, 249 pp.

Kalyaanamoorthy S, Minh BQ, Wong TKF, von Haeseler A, Jermiin LS (2017) ModelFinder: fast model selection for accurate phylogenetic estimates. Nature Methods 14: 587–589. https://doi.org/10.1038/nmeth.4285

Katoh K, Standley DM (2013) MAFFT multiple sequence alignment software version 7: improvements in performance and usability. Molecular Biology and Evolution 30: 772–780. https://doi.org/10.1093/molbev/mst010

Leviton AE, Wogan G, Koo M, Zug GR, Lucas R, Vindum J (2003) The dangerously venomous snakes of Myanmar. Illustrated key and checklist. Proceedings of the California Academy of Sciences 54(24): 407–462.

Li JN, Liang D, Wang YY, Guo P, Huang S, Zhang P (2020) A large-scale systematic framework of Chinese snakes based on a unified multilocus marker system. Molecular Phylogenetics and Evolution 148: 106807. https://doi.org/10.1016/j.ympev.2020.106807

Liu S, Yang MJ, Rao JQ, Guo YH, Rao DQ (2023) A new species of *Pareas* Wagler, 1830 (Squamata, Pareidae) from Northwestern Yunnan, China. Taxonomy 2023(3): 169–182. https://doi.org/10.3390/taxonomy3020013

Malhotra A, Thorpe RS (2000) A phylogeny of the *Trimeresurus* group of pit vipers: New evidence from a mitochondrial gene tree. Molecular Phylogenetics and Evolution 16(2): 199–211. https://doi.org/10.1006/mpev.2000.0779

Malhotra A, Thorpe RS (2004) A phylogeny of four mitochondrial gene regions suggests a revised taxonomy for Asian pitvipers (*Trimeresurus* and *Ovophis*). Molecular Phylogenetics and Evolution 32(1): 83–100. https://doi.org/10.1016/j.ympev.2004.02.008

Malhotra A, Dawson K, Guo P, Thorpe RS (2011) Phylogenetic structure and species boundaries in the mountain pitviper *Ovophis monticola* (Serpentes: Viperidae: Crotalinae) in Asia. Molecular Phylogenetics and Evolution 59(2): 444–457. https://doi.org/10.1016/j.ympev.2011.02.010

Neang T, Chhin S, Kris M, Hun S (2011) First records of two reptile species (Gekkonidae: *Hemidactylus garnotii* Dumeríl & Bibron, 1836; viperidae: *Ovophis convictus* stoliczka, 1870) from Cambodia. Cambodian Journal of Natural History 2: 86–92.

Nguyen L, Schmidt HA, von Haeseler A, Minh BQ (2015) IQ-TREE: A fast and effective stochastic algorithm for estimating maximum-likelihood phylogenies. Molecular Biology and Evolution 32(1): 268–274. https://doi.org/10.1093/molbev/msu300

Qiu XC, Wang JZ, Xia ZY, Jiang ZW, Zeng Y, Wang N, Li PP, Shi JS (2024) A new mountain pitviper of the genus *Ovophis* Burger in Hoge & Romano-Hoge, 1981 (Serpentes, Viperidae) from Yunnan, China. ZooKeys 1203: 173–187. https://doi.org/10.3897/zookeys.1203.119218

Ronquist F, Teslenko M, van der Mark P, Ayres DL, Darling A, Hçhna S, Larget B, Liu L, Suchard MA, Huelsenbeck JP (2012) MrBayes 3.2: Efficient Bayesian phylogenetic inference and model choice across a large model space. Systematic Biology 61(3): 539–542. https://doi.org/10.1093/sysbio/sys029

Shi JS, Liu JC, Giri R, Owens JB, Santra V, Kuttalam S, Selvan M, Guo KJ, Malhotra A (2021) Molecular phylogenetic analysis of the genus *Gloydius* (Squamata, Viperidae, Crotalinae), with descriptions of two new alpine species from Qinghai-Tibet Plateau, China. ZooKeys 1061: 87–108. https://doi.org/10.3897/zookeys.1061.70420

Uetz P, Freed P, Aguilar R, Reyes F, Kudera J, Hošek, J (2025) The Reptile Database. http://www.reptile-database.org [Accessed on: 2025-1-17]

Yang DT, Rao DQ (2008) Amphibia and Reptilia of Yunnan. Yunnan Publishing Group Corporation, Yunnan Science and Technology Press, Kunming, 411 pp.

Zeng YM, Li K, Liu Q, Wu YY, Hou SB, Zhao GG, Nguyen SN, Guo P, Shi L (2023) New insights into the phylogeny and evolution of Chinese *Ovophis* (Serpentes, Viperidae): Inferred from multilocus data. Zoologica Scripta 52(4): 358–369. https://doi.org/10.1111/zsc.12589

Zhao EM (2006) Snakes of China. Anhui Science Technology Publishing House, Hefei, 669 pp.

Zhao EM, Huang MH, Zong Y, Jiang YM, Huang QY, Zhao H, Ma JF, Zheng J, Huang ZJ, Wei G, Yang DQ, Li DJ (1998) Fauna Sinica Reptilia, Vol. 3: Squamata: Serpentes. Science Press, Beijing, 522 pp.

ZooKeys 1230: 303–333 (2025)
DOI: 10.3897/zookeys.1230.127858

Review Article

A taxonomic review of the genus *Rhinoceros* with emphasis on the distinction of *Eurhinoceros* (Perissodactyla, Rhinocerotidae)

Francesco Nardelli[1], Kurt Heißig[2]

1 *IUCN SSC Asian Rhino Specialist Group and Conservation Planning Specialist Group, Gland, Switzerland*
2 *Bayerische Staatssammlung für Paläontologie und Geologie, München, Germany*
Corresponding author: Francesco Nardelli (franardelli@gmail.com)

Academic editor: Alessio Iannucci
Received: 19 May 2024
Accepted: 15 January 2025
Published: 6 March 2025

ZooBank: https://zoobank.org/222AB4F0-334B-4B7D-A261-031B654B85BD

Citation: Nardelli F, Heißig K (2025) A taxonomic review of the genus *Rhinoceros* with emphasis on the distinction of *Eurhinoceros* (Perissodactyla, Rhinocerotidae). ZooKeys 1230: 303–333. https://doi.org/10.3897/zookeys.1230.127858

Abstract

This study examines the ecomorphological characteristics of two Asian rhinoceros species: the critically endangered Sundaic rhinoceros and the vulnerable Indian rhinoceros. Among the five living rhinoceros taxa, the three Asian species are notable for their tusked incisors. Fossil evidence highlights the divergence between *Rhinoceros* and *Eurhinoceros* in cheek tooth morphology, linked to different dietary specialisations. The Sundaic rhinoceros, a generalist browser restricted to the Ujung Kulon peninsula of Java, exhibits distinctive features such as a grey hide with polygonal patterns, a typical 'saddle' on the nape, a slender head shape and a protrusion instead of a horn in females. The latter is a unique trait among Rhinocerotini species. In contrast, the Indian rhinoceros, a variable grazer, inhabits riverine grasslands in northern India and southern Nepal, displaying deep skin folds and tubercles. Ecological behaviours differ significantly, with the Sundaic rhinoceros being solitary wanderers and Indian rhinoceros forming temporary crashes. Both species possess unique adaptations for survival, emphasising the importance of understanding their systematics for effective conservation. The study further examines the interrelationships among the one-horned Asian species of the Rhinocerotidae family, highlighting their distinct features. The revision delves into skull morphology, dentition, and ecological dynamics, revealing evolutionary patterns and ancestral traits. Both single horned rhinoceroses went a separate and diverging way of evolution that was not triggered by geographical separation but by niche partitioning. Comparative analyses shed light on the evolutionary trajectory and ecological adaptations of each species. The fossils, the ecological and morphological adaptations of both species, suggest designating '*Rhinoceros*' *sondaicus* as distinct from *Rhinoceros unicornis*, under the one-horned rhinoceros *Eurhinoceros*, as proposed by Gray (1868). *Eurhinoceros sondaicus* emerges as a persistently more primitive form.

Key words: Ecology, *Eurhinoceros sondaicus*, Indian rhinoceros, Javan, morphology, palaeontology, *Rhinoceros unicornis*, Sundaic rhinoceros, systematics

Introduction

"The forehead and the nose behind the base of the horn flat, both in the living animal and skull. *Eurhinoceros*." With these words, John Edward Gray (1868: 1009) described a new one-horned rhinoceros to classify the Sundaic rhinoceros. A century later Heißig (1972) considered valid the genus *Eurhinoceros* to significantly distinguish *E. sondaicus* (Desmarest, 1822), a separate one-horned rhinoceros from *Rhinoceros* to which belongs the Indian rhinoceros *Rhinoceros unicornis* Linnaeus, 1758. Nardelli (1988: 41) foresaw that '*Rhinoceros*' *sondaicus* could be classified in a separate genus from *Rhinoceros unicornis*, suggesting that differences in their morphology and behaviour – such as the distinct external features of '*R.*' *sondaicus*' head, especially its lips, and the fact that the former is a browser and the latter a grazer – support this distinction.

This work aims to examine the differing ecomorphological characters of *Rhinoceros* and *Eurhinoceros*. The results suggest that the single-horned rhinoceroses, *Rhinoceros unicornis* and *Eurhinoceros sondaicus*, followed separate evolutionary paths not due to geographical isolation but rather as a result of niche partitioning. This can be followed by a number of stepping stones from the Middle Miocene onwards.

Heißig (1972: 29) reported the parallel presence of *Gaindatherium* and *Eurhinoceros* aff. *sondaicus* in the Middle Miocene Nagri formation of the Siwalik region of Pakistan. Fossil records of ancient rhinoceros species provide insights into their evolutionary history and the environmental conditions they inhabited (MacFadden 1998). By examining the morphology and geographic distribution of fossils, researchers can uncover patterns of niche partitioning and evolutionary divergence. Extant examples include the browser *Diceros bicornis* Linnaeus, 1758 and the exclusive grazer *Ceratotherium simum* Burchell, 1817, which are sympatric today (MacFadden 1998: 282), as well as the variable grazer *Rhinoceros unicornis* and the generalist browser *Eurhinoceros sondaicus* (Pandolfi et al. 2021: 9 and references therein as *Rhinoceros*), which had some overlapping ranges.

Pandolfi and Maiorino (2016) provide data on the coexistence of *'Rhinoceros' sondaicus* and *Rhinoceros unicornis* in certain parts of their former ranges, with dietary specialisation playing a key role. The major distinctions between these two species are found in their dental morphology, indicating adaptation to different feeding strategies. *Eurhinoceros sondaicus* is more adapted to browsing on softer, leafy vegetation, while *R. unicornis* is more inclined towards grazing on tougher, more abrasive plants material. This divergence in feeding habits minimised direct competition for resources, thus facilitating their coexistence.

Despite some similarities in cranial features, their teeth reflect evolutionary adaptations to different ecological niches, with *R. unicornis* showing adaptations for grazing-related diets and *E. sondaicus* for browsing. This separation allowed these species to share habitats without exhausting common food sources (Pandolfi and Maiorino 2016).

Extant species of Rhinocerotini Gray, 1821 (sensu Pandolfi 2015) exhibit diverse feeding habits that include grazing, mixed feeding, and browsing. Likewise, the diets of Pleistocene species were varied. In their study, Hernesniemi et al. (2011) analysed mesowear patterns in both extant and Pleistocene species, comparing *Diceros bicornis*, *Ceratotherium simum*, *Dicerorhinus sumatrensis* (Fischer, 1814), *'Rhinoceros' sondaicus*, and *Rhinoceros unicornis* to fossil samples from Pleistocene Rhinocerotini, such as *Stephanorhinus kirchbergensis* (Jäger, 1839), *S. hemitoechus* (Falconer, 1859), *S. hundsheimensis* (Toula, 1902), and *Coelodonta antiquitatis* Blumenbach, 1799. When clustered by mesowear scores from the first and second molars, *Stephanorhinus kirchbergensis* grouped closely with *Dicerorhinus sumatrensis*, while *S. hundsheimensis* showed affinity with '*Rhinoceros*' *sondaicus*. These browsing species, together with the somewhat separate *Stephanorhinus hemitoechus*, were distinctly separated from *Rhinoceros unicornis*, a variable grazer, which clustered near the grazer *Coelodonta antiquitatis* and the exclusive grazer *Ceratotherium simum*.

In the case of *Rhinoceros unicornis* and *Eurhinoceros sondaicus*, the results of the present study imply that environmental pressures led to the development of differences in dental morphology, specialised feeding strategies, habitat adaptations and behavioural traits. Despite inhabited some overlapping areas, the two species evolved independently.

The Sundaic rhinoceros *Eurhinoceros sondaicus* (Desmarest, 1822)

Distribution and subspecies

The case of *E. sondaicus* distribution is a conundrum. If limited to the few human reports or artifacts, its range appears as fragmented patches throughout a vast area covering South and Southeast Asia. However, if inferred suitable habitats in the region of the documented locations are included, the range becomes much larger and contiguous (Fig. 1). The earliest known fossils of a *Rhinoceros* cf. '*R.*' *sondaicus* in Southeast Asia are from central Myanmar, dating back to 9–8 million years ago (Longuet et al. 2024). The taxon has been traced from the Miocene (Heißig 1972) as *Eurhinoceros* aff. *sondaicus* and to the Pleistocene in northern Pakistan (Khan 2009; Abdul et al. 2014; Siddiq et al. 2016), Myanmar (Zin-Maung-Maung-Thein et al. 2006, 2010), Cambodia (Beden and Guérin 1973), Thailand (Suraprasit et al. 2016), Vietnam (Bacon et al. 2004), and Indonesia (Koenigswald 1935; Hooijer 1964; Antoine 2012). During the Holocene epoch, the species was probably widespread across various regions.

The presence of '*Rhinoceros*' *sondaicus* has been confirmed in northeastern India and Bangladesh (Rookmaaker 1980, 1997, 2002), Myanmar (Loch 1937; Reynolds 1954), Thailand (McNeely and Cronin 1972), Cambodia (Poole and Duckworth 2005), Laos (Neese 1975), Vietnam (Loch 1937; Schaller et al. 1990), Malaysia (Sody 1959; Medway 1969), and Sumatra and Java (Sody 1959). Some reports on rhinoceroses from Bhutan exist, but actually pertain to *R. unicornis* (Rookmaaker 2016). The accounts originating from Hainan Island are unverified (Rookmaaker and Carpentier 2007). In Borneo, records of the species have been unclear (Rookmaaker 1977) or limited to a few fossils (Cranbrook 1986; Cranbrook and Piper 2007). The occurrence in southeastern China is uncertain (Rookmaaker 1980, 2006).

The Sundaic rhinoceros, also known as Javan or Lesser one-horned rhinoceros, is presently classified as 'Critically Endangered' by the International Union for Nature Conservation (IUCN). The species has been exterminated from most of its historical range, with only a small population of an unknown number, mostly males (Haryono et al. 2015; Nardelli 2016), confined within Ujung Kulon peninsula, the western tip of Java. In this location, it has become a 'refugee' species (Nardelli and Roboský 2023). Three subspecies have been recognised within the species *Eurhinoceros sondaicus*. The nominal *E. s. sondaicus* (Desmarest, 1822) inhabited Peninsular Malaysia, Sumatra, Java (Sody 1959); *E. s. annamiticus* (Heude, 1892) was detected in regions of Thailand, Cambodia, Laos, Vietnam (the Indochina Peninsula; Groves and Guérin 1980), and eventually southeastern China

Figure 1. *Eurhinoceros sondaicus*. Holocene (11500 BCE to present) distribution map based on reports and suitable habitats across space and time. Map based on Groves (1967: 224, fig. 1) and Rookmaaker (1980: 261, fig. 2); sea levels after Kim et al. (2023). Free vector and raster map data CC0 1.0.

(Rookmaaker 2006). *E. s. inermis* (Lesson, 1836) was identified in northeast India, Bangladesh (Rookmaaker 1997), and possibly Myanmar (Groves 1967). Some authors have suggested that these three taxa might be better treated as distinct phylogenetic species on biogeographical grounds (Gippoliti et al. 2013).

Morphology

Eurhinoceros sondaicus exhibits distinct characteristics that set it well apart from *Rhinoceros unicornis*. Only a few measurements of weight and size are available. Groves and Leslie (2011) indicate weight data with one female at 1500 kg, one male at 1200 kg and head-and-body lengths ranging from 305 to 344 cm, with shoulder heights between 120 and 170 cm. Today no statement can be made concerning any difference of body weight between the sexes. Their hide colour ranges from grey to dusky grey, making them easy to distinguish from *R. unicornis* that has brownish-grey coloration. Their body is covered by distinctive scale-like polygons that form a mosaic (Lydekker 1907; Peacock 1933; Harper 1945).

In contrast, the epidermal surface of *R. unicornis* exhibits limited patterns comprised of tubercles (Laurie et al. 1983) and its skin-folds differ from the arrangement typical of *E. sondaicus*: one behind the occiput close to the head, a transversal fold across the middle of the shoulders extending underneath the throat, another encompassing the entire body behind the shoulders and several folds that form distinctive patterns on the thighs and around the posterior. The posterior cervical fold extends over the nape of the neck, forming a distinctive, saddle-shaped shield, and serves as a diagnostic feature. Differently, the nape shield in *R. unicornis* is continuous. *Eurhinoceros sondaicus* has a rugose integument, covered with a cuticle consisting of small, angular plates. Its head is characterised by distinctive nasal, frontal, and occipital bones and is narrower and longer compared to that of *R. unicornis*. These taxa also differ in the upper lip shape and length, reflecting their adaptation to different feeding habits, given that *E. sondaicus* is a generalist browser (Nardelli 2013) and *R. unicornis* is a variable grazer (Hullot et al. 2019). The upper lip is long and flexible, almost prehensile (Sody 1959). Griffiths (1993) also noted that the presence of the distinguishing 'saddle' on the neck was a manifestation of sexual dimorphism, although the data needed to confirm this hypothesis is lacking.

Even though the species is generally described as hairless, a sparse hairy covering has been documented by some authors (Groves 1967; Cave 1969; Nardelli and Robovský 2023). According to these records, body hair is more prominent in juveniles and gradually disappears with age, whereby adults only retain ear fringes, eyelashes, and tail bristles. The tail is fully exposed in side view, clearly protruding from its hind quarters (Groves and Leslie 2011). In females, the horn is a mere protrusion, allowing easy differentiation from males (Hoogerwerf 1970; Groves 1971). This sexual dimorphism in horn development is a unique characteristic of the only species among the Rhinocerotini where only males have a horn, averaging 20 cm in length. Even if the horn is nearly absent, the skull construction is adapted to bear a substantial horn also in females.

Primary dental morphology

The strong lower incisors are directed almost straight forward (Fig. 4A). The cheek teeth are mesodont. The upper premolars are well molarised with a wide entrance in the central valley separating both lingual cusps (Fig. 6A [A]). On their labial side, there is no prominent metacone ridge, but the metacone is somewhat more lingually inclined like in molars (Fig. 6A [B]). The secondary folds are confined to the crochet, a crista is lacking (Fig. 6A [C]). On the lingual side, more or less complete cingula prevent lesions of the gingiva (Fig. 6A [D]). These observations were made on specimens of the Bavarian Zoological State Collection.

Ecology

The behaviour of *Eurhinoceros sondaicus* suggests a strong reliance on lowland forests (Nardelli and Robovský 2023) while mountainous excursions were likely situational or historically influenced by advancing anthropisation and competition with conspecifics at the time (Sody 1959 and references therein as *Rhinoceros sondaicus*). *Rhinoceros unicornis* is documented to establish dominance hierarchies (Dinerstein 2003, 2011). In contrast, the study by Wilson (2021) indicates that both male and female '*R.*' *sondaicus* primarily lead non-social lives. This solitary and retiring species, constrained to lowland areas, can still cover 15–20 km in a day. Nonetheless, most individuals occupy smaller patches for extended periods under favourable feeding conditions. Individual home ranges are not fixed for a lifetime and may shift based on the circumstances. A typical male's territory can range from 12.5 to 21 square kilometres, whereas a female's territory is smaller, spanning only 2.6–13.4 square kilometres (Amman 1986). Overall, female home ranges during seasonal periods are, on average, half the size of those of males (Setiawan et al. 2017). Female territories also overlap, allowing males to breed with multiple females. In contrast, male territories overlap only at the periphery (Hariyadi et al. 2016), resembling the behaviour of *D. sumatrensis*, also a browser and a rainforest dweller (van Strien 1985). Males are usually intolerant of each other, although sightings of two bulls wallowing together have been reported (Hoogerwerf 1970). They navigate a network of trails, not always continuous, linking wallows, pools, or river courses in which they swim (Sody 1959). Showing preference for easier routes, as a clear indication of adaptation to lowlands, they establish well-trodden tracks through thick scrub, while making detours around dense vegetation or steep slopes. In some cases, these tracks may turn into low tunnels shared with other animals.

Males as well as females often frequent wallows, approximately every two days, formed in depressions filled with rainwater that are concealed by vegetation, which can sometimes be quite deep and measure 20–35 m^2. Although they show preference for fresh water, they are also attracted by muddy river banks and tidal forest margins. They often urinate while wallowing and this behaviour is assumed to be triggered by contact with water. This species is most highly active during night time and in the early morning, while resting during the day, especially around noon. As it needs to remain vigilant, it often rests in standing position, dozing with its head lowered and its ears constantly flicking (Nardelli 1988).

Aside from a few bamboo shoots, there is no evidence indicating feeding on grass. Its diet includes leaves from more than 200 plant species (Hariyadi et al. 2016). Occasionally, this foraging can be supplemented by browsing on rattan (*Calamus* spp.), palms (*Pandanus* spp.), young bamboos, mango, and fig fruit (Amman 1986).

Individuals mostly communicate through olfactory means, due to which they leave urine traces across their territory by squirting on vegetation. While males typically urinate in short, upward squirts—sometimes reaching up to 2 m, likely for dominance assertion and territory marking—females urinate in a continuous stream between their hind legs, scenting the ground. While moving along their trails, both males and females leave urine-scented mud from their wallows on the surrounding vegetation.

Rhinoceros unicornis and *Eurhinoceros sondaicus* exhibit distinct behaviours for marking trails with secretions from their foot glands. The first scatters dung by kicking it around from their dung piles, whereas the latter, without forming piles, drags one hind foot through its faeces. Despite these differences, both species share the habit of scattering or dragging their hind feet through their dungs, leaving trails marked with glandular secretions that can extend for several meters (Hoogerwerf 1970; Amman 1986; Bhattacharya 2020b). The elusive nature of the species, combined with its remote and often inaccessible habitat, makes it challenging for researchers to observe and document the behaviours comprehensively. This indicates that a perception of *E. sondaicus* having a minimal range of vocalisations (Sody 1959 as *Rhinoceros sondaicus*) could be attributed to their geographical isolation, small population size and the scarcity of research on the species (Wilson 2021 as *Rhinoceros sondaicus*). Nevertheless, the analysis of video recordings from camera traps yielded insights into the vocalisations, identifying eight distinct call types. These recordings, comprising 196 individual calls, allowed the creation of detailed sonograms, a first for this species (Wilson 2021).

Although information on the breeding behaviour is scarce, based on the photographic and video evidence, it is identified that the females precede their calves akin to black rhinoceros *Diceros bicornis*. Conversely, *R. unicornis* females follow theirs (Nardelli and Robovský 2023), sharing the behaviour of white rhinoceros *Ceratotherium simum* in Africa. Owing to this distinction, black rhinoceros calves are vulnerable to predation, particularly by spotted hyena *Crocuta crocuta* (Erxleben, 1777), whereas there are no recorded instances of white rhinoceros calves succumbing to the same predator (Hitchins 1986). Consequently, it is likely that in the past calves faced significant predation from tigers *Panthera tigris* (Linnaeus, 1758), which would have played a significant role in the species demise.

The Indian rhinoceros *Rhinoceros unicornis* Linnaeus, 1758

Distribution

The presence of *R. unicornis* in China and Southeast Asia during the Neogene and Quaternary epochs cannot be substantiated without more detailed fossil evidence. Reports from existing sources indicate that most of these fossils would be more accurately attributed to *Rhinoceros sinensis* Owen, 1870 (Laurie et al. 1983; Yan et al. 2023) or ‘*Rhinoceros*’ *sondaicus* (Rookmaaker 1980, 2006).

The *Rhinoceros unicornis* range covered the entire Indo-Gangetic plain: India, northern Bangladesh, Assam, Nepal, southern Bhutan, and north and eastern Pakistan with a few records from the south and one from Afghanistan (Choudhury 1985; Rookmaaker 2000). Today it is restricted to eleven main protected areas (Fig. 2) and listed 'Vulnerable' by the International Union for Nature Conservation with an in-situ population of ~ 4000 individuals. While Zschokke et al. (2011), Zschokke (2016), and Ghosh et al. (2022) highlighted genetic variability within the remaining populations of *R. unicornis*, there seems to be no recognised subspecies in the extant species.

Morphology

Rhinoceros unicornis is considerably larger than *Eurhinoceros sondaicus*, superseded in size only by the elephant and the white rhinoceros, with males weighing more than 2,000 kg and females reaching 1,600 kg. As one of the world’s largest land mammals, its shoulder height ranges from 160 to 190 cm and its length reaches nearly 400 cm (Laurie et al 1983). Adult males and females differ in only a few characteristics. Both sexes have a grey-brown hide and their skin folds have a pinkish hue. In contrast to *E. sondaicus* with five

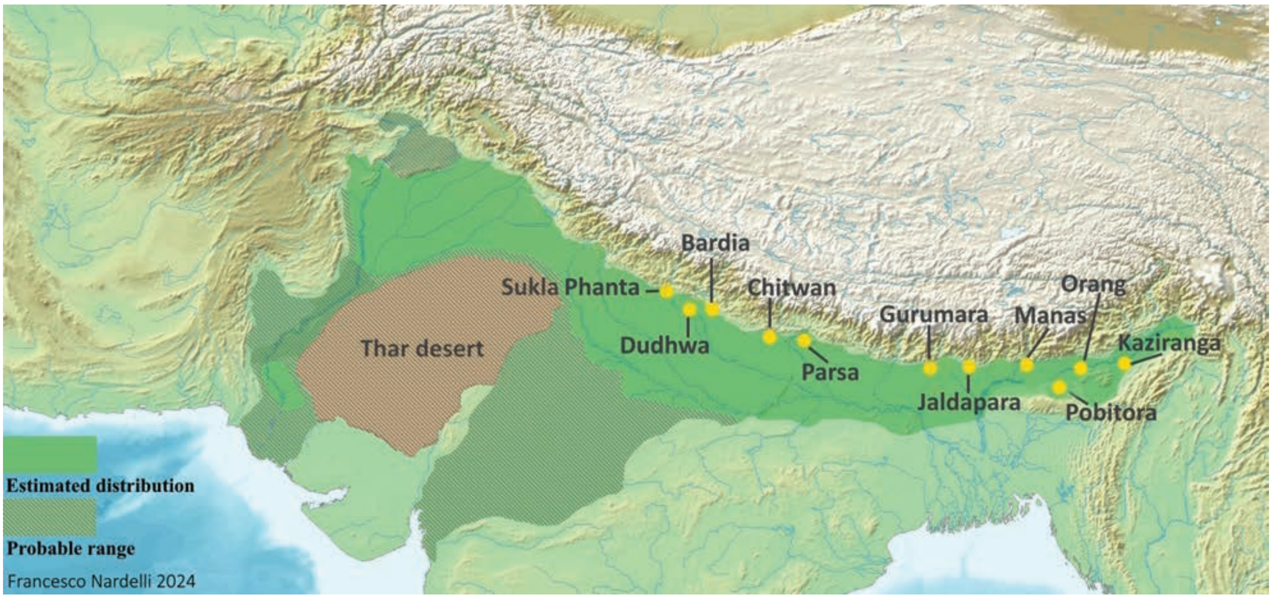

Figure 2. *Rhinoceros unicornis*. Holocene (11500 BCE to present) distribution map based on reports and suitable habitats across space and time. Yellow dots represent the current locations of *R. unicornis*. Map based on Rookmaaker (2000: 71, fig. 5). Free vector and raster map data CC0 1.0.

main skin folds, *R. unicornis* has four, which are more pronounced in males than in females. However, each individual has distinct skin fold patterns and raised tubercles on the hide; in fact these individual characteristics allowed Laurie (1978) to distinguish each of the animals in Royal Chitwan National Park in southern Nepal he studied between 1972 and 1976.

Males have significantly larger neck musculature and can also be distinguished from females by the distinctive deep folds behind and across the shoulders, on the neck, and before and across the thighs, while featuring a thick patch of skin on the upper part of the chest. Both males and females have a single horn ranging 20–40 cm in length, which is wider at the base in males.

Primary dental morphology

The lower incisors are turned sideways (Fig. 4B). Their length is greater in adult males compared to females. The cheek teeth are subhypsodont, and block-like. The parastyle fold is reduced (Fig. 6B [A]), whereas a blunt, narrow metacone ridge is present on the labial side of the not-inclined metacone of the upper premolars (Fig. 6B [B]). In these teeth, the molarisation is not perfect, because the lingual cusps are still fused from the base to a varying height, leaving only a narrow slit between them in fresh premolars (Fig. 6B [C]). Crista and crochets are present and may unite to isolate a small medifossette from the central valley (Fig. 6B [D]). Lingual cingula are lacking or confined to small ridges (Fig. 6B [E]). These observations were made on specimens of the Bavarian Zoological State Collection.

Ecology

The social structure differs in several aspects from that of *E. sondaicus*, including its semi-territorial behaviour, as individual superiority is asserted primarily through dominance (Laurie 1978, 1982; Dinerstein 2003), exhibiting complex intraspecific activities. These interactions can include dominance hierarchies, territorial disputes, mating behaviours, and social bonding. Factors such as age, sex, and individual temperament influence these interactions, leading to a diverse range of patterns within their populations (Bhattacharya 2020a). While usually solitary, individuals can occasionally form temporary groups at wallows or within seasonal feeding grounds. Some authors have observed crashes of up to a dozen rhinoceroses, predominantly sub-adults, wallowing simultaneously (Laurie 1978, 1982; Dinerstein 2003; Bhattacharya and Chakraborty 2016) and noted that they can sustain a higher population density in smaller areas than other Asian rhinoceroses (Hazarika and Saikia 2010). Research suggests that the species may possess some of the smallest annual and seasonal home ranges observed among mega-herbivores (Dinerstein 2011). Laurie (1978, 1982) also documented cases of young males being in close proximity to or lying near their elders while wallowing, but would be inevitably chased away after a while. Immature males tend to exhibit more gregarious behaviour than adults or immature females and young females might occasionally accompany an older cow and her calf. However, male calves spend a long time with their mothers or other sub-adult males due to their heightened vulnerability to attacks from adult males (Laurie 1982).

Rhinoceros unicornis has historically occupied various habitats, including marshes, alluvial plains, grasslands, and arid forests on the flood plains of major rivers such as the Indus, the Ganges, and the Brahmaputra, which they still share with elephants *Elephas maximus* Linnaeus, 1758, and water buffaloes *Bubalus bubalis* (Linnaeus, 1758); (Laurie 1978, 1982; Laurie et al. 1983; Dinerstein 2003). They spend part of the day in water, especially during the hot and rainy monsoon season from June to September. Bathing not only helps them lower their body temperature and ward off biting insects, but also provides opportunities for socialising with other rhinoceroses. After exiting the water, they often rub their heads, necks, flanks, or horns against nearby trees, leaving mud deposits on the surrounding vegetation. The species exhibits a noteworthy behaviour by utilising communal defecation sites as they traverse their familiar habitats (Bhattacharya 2020b). Individuals of all age and sex groups in Chitwan National Park, Nepal, were observed using dung piles, as documented by Laurie (1978).

Laurie (1978, 1982) and Laurie et al. (1983) highlighted that rhinoceroses and hippopotamuses of the genus *Hexaprotodon* Falconer & Cautley, 1836, previously occupied similar ecological niches in India and although the latter have disappeared from India, the presence of *Hippopotamus amphibius* Linnaeus, 1758 in Africa, where they have asserted their dominance over water bodies, might explain why African rhinoceroses avoid swimming. They are most active during the night and tend to follow established trails linking salt licks, water sources and favoured foraging grounds. Individual ranges are not exclusive and are smaller than those of *E. sondaicus* and include areas covered by mixed pasture. Laurie (1978, 1982) documented ranges spanning from less than 0.5 km^2 to nearly 9 km^2. An adult would typically have a home range of ~ 3 km^2, while sub-adults would have slightly larger ranges. Mature males in breeding condition show preference for establishing exclusive territories in the most fertile habitats, although no correlation between successful mating and territorial exclusivity has been established. In search of females, males may roam in several overlapping territories, each of approximately 6 km^2, where the female population is the greatest. On the other hand, sub-adult males would seek areas less likely to be defended by dominant males. In contrast to mature *E. sondaicus* females, *R. unicornis* females cover more extensive ground and may contend for the most appealing settings.

Rhinoceros unicornis occupies a diverse habitat comprising grasslands, swamps, and riverine forests, where they graze on grasses and herbaceous plants from various families. They are highly flexible and adjust their diet not only to their habitat, but also to the grass season, especially during the monsoon rains, which increases their feeding resources.

The taxon is identified as a variable grazer, consuming 60–90% grasses with seasonal dietary shifts. Microwear patterns on its teeth show that, while primarily grass-eating indicated by the low complexity and high anisotropy on the grinding surfaces, it also processes a variety of plants material using its shearing surfaces (Hullot et al. 2019). Its lips are also well adapted to curl around short grasses, as well as allowing the stems of taller varieties to be pushed down, revealing the leaf blades. Laurie (1978, 1982) documented 183 plant species from 57 families in the dietary intake, 70–90% of which, depending on the season, is derived from 50 species of herbaceous plants. In addition to harvesting aquatic plants, a valuable source of sodium, by submerging their heads up to one meter underwater for 45 seconds at a time, they have been documented leaving hillside sal (*Shorea robusta*) forests to graze on grass shoots in newly burned areas. Tall grasses, those reaching up to 4–7 m in height, particularly *Pennisetum purpureum*, as well as *Saccharum* species and grass of the genus *Narenga* are favoured sources of nutrition. They are abundant in the spring, but during the monsoon, shorter grasses are also consumed. The remaining portion of dietary intake comprises leaves or branches from shrubs, sedges, ferns, and aquatic plants.

Laurie (1982), and Dinerstein (2003, 2011) identified ten distinct vocalisations, each associated with specific behavioural contexts. Bhattacharya (2020b) further researched in depth vocal signals; though no sonograms analysis was performed.

Genetic insights

This study briefly reports on the results of DNA analyses conducted separately on *E. sondaicus* and *R. unicornis* so far. While these studies provide valuable insights into the genetic makeup of each species individually, no direct comparative analysis has been performed between the two. As a result, specific genetic variations that could support the classification of these species into separate genera remain unconfirmed. The potential chromosomal differences between these taxa are reported here based on what is known from separate studies. While these discussions are informed by existing data, they are inherently speculative due to the lack of a direct comparative genetic analysis. Future research that includes direct molecular comparisons using consistent methodologies will be essential to define their evolutionary relationship more accurately.

Despite low genetic diversity being a long-term feature of rhinoceroses (Willerslev et al. 2009; Liu et al. 2021), the modern species exhibit the lowest levels of diversity, likely exacerbated by recent anthropogenic-driven population declines (Liu et al. 2021). The study by Margaryan et al. (2020) on '*Rhinoceros*' *sondaicus* identifies genetic diversity within the species, represented by historical sequences and extinct subspecies, emphasising the importance of preserving genetic diversity to maintain evolutionary potential. This study reveals fluctuations in genetic diversity over time, influenced by factors such as population size changes and environmental pressures. Examination of mitochondrial DNA (mtDNA) sequences from ancient specimens highlights evidence of recent lineage extinction events within populations (Margaryan et al. 2020). This suggests that certain genetic lineages or haplotypes present in ancestral communities are no longer found in recent ones, indicating a decline or loss in genetic diversity.

Due to the poor DNA quality of ancient specimens, e.g., *'Rhinoceros' sondaicus*, Liu et al. (2021) could not assemble their genomes directly. Instead, they mapped them against other species genomes which, according to the authors, may introduce 'biases'. They further acknowledge the need for caution in interpreting results. Since only part of the Rhinocerotidae was studied, a considerable gap remains in understanding their evolutionary history until more comprehensive genome sequencing is conducted.

Genetic analysis of *Rhinoceros unicornis* reveals strong genetic structuring across different Indian states, with distinct genetic clades corresponding to specific geographical regions, suggesting limited gene flow and possible isolation mechanisms (Ghosh et al. 2022). Microsatellite analysis conducted by Ghosh et al. (2022) provides insights into genetic variation within populations. By analysing all frequencies and microsatellite loci, they identified specific genetic markers that exhibit variation across populations, indicating differences in genetic structure and connectivity. mtDNA analysis was also used by Ghosh et al. (2022) to infer the maternal evolutionary history and phylogeographic structure of extant populations.

Fossil evidence (Heißig 1972) suggests that the divergence of the *Rhinoceros* clade possibly took place during the Middle Miocene epoch 16–11.6 Mya. Some molecular studies estimate the divergence at 11.7–1.9 Mya (Tougard et al. 2001) and 13.4–13.2 Mya (Willerslev et al. 2009). Other studies, such as those by Margaryan et al. (2020) and Liu et al. (2021), calculate the divergence during the Pliocene 5.3–2.6 Mya (Fig. 3). During these periods, various factors such as changes in climate, habitat, and resource availability would have influenced the evolutionary trajectory of these taxa (Cerling et al. 1997; Longuet et al. 2023, 2024).

Findings and implications

"The key differences between *R. unicornis* and *R. sondaicus* are most apparent in their teeth, whereas the morphology of the skull is rather similar" (Pandolfi and Maiorino 2016: 10). Among the five extant species, the Asian ones stand out for possessing tusk-like incisors, a feature absent in African species. The synapomorphy of a sloped orbital floor connects these species without incisors. The three Asian forms can be categorised on a scale of increasing specialisation, ranging from *Dicerorhinus sumatrensis* with two horns to *Eurhinoceros sondaicus* and *Rhinoceros unicornis* with a single horn. The shape and posture of the skull align with this scale, but the same cannot be said for the morphology of the molars. While the molar and premolar type of *R. unicornis* can be understood as a high-crowned specialisation form of the primitive *D. sumatrensis*, the type of *E. sondaicus* diverges, showing similarities to African forms in the weakening of the metaconus rib, molarisation of the premolars, and strengthening of the inner cingulum (Heißig 1981).

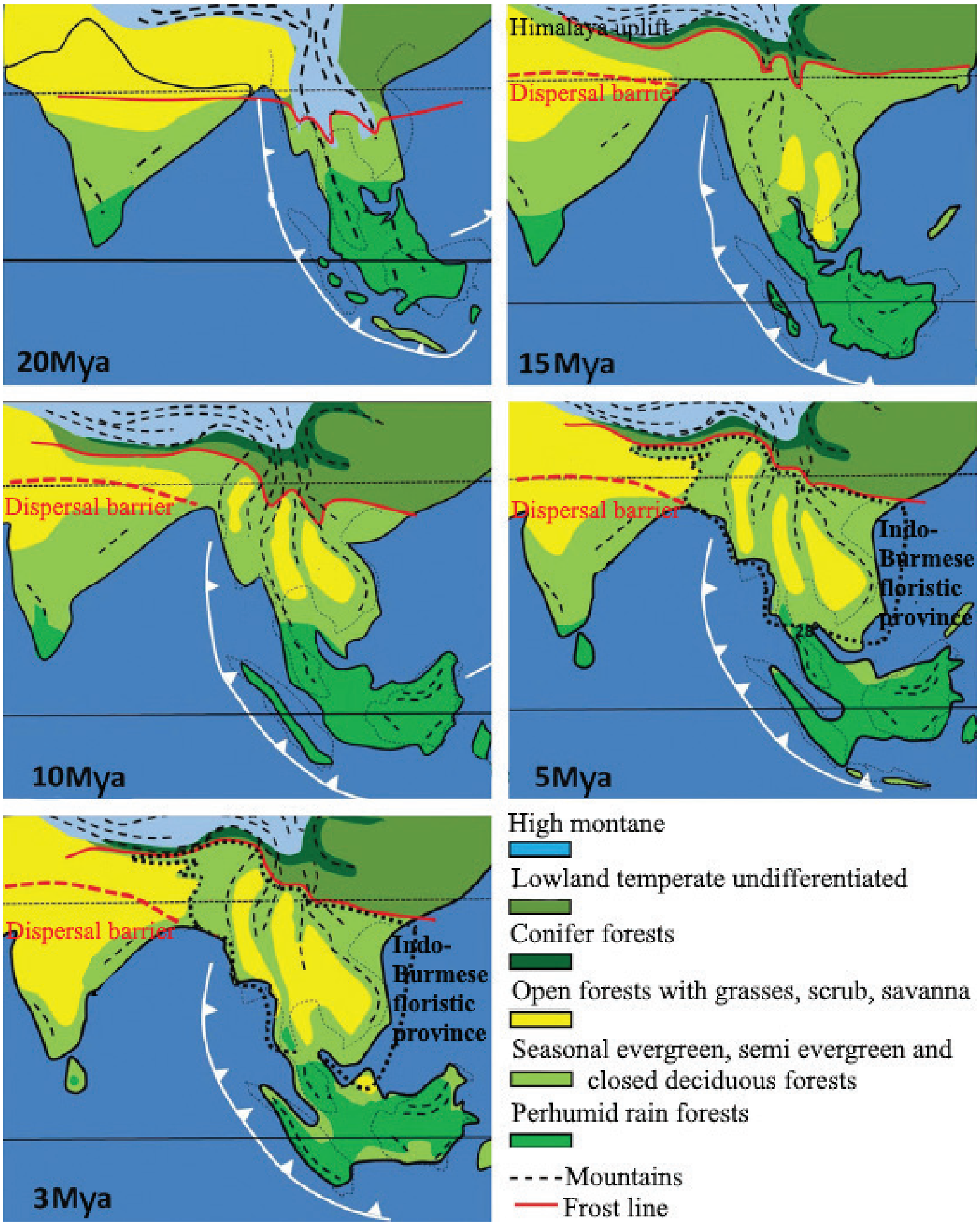

Figure 3. Palaeogeography, climate, and dispersals from the Early Miocene to the Late Pliocene. Adapted with permission from Morley (2018: 218).

The significance of the distinctions in cheek tooth morphology (Table 1) can be estimated only with a look at the paleontological evidence. Nearly all paleontological knowledge depends on the tooth morphology because skulls are rarely preserved. Cheek teeth with similarities to *Rhinoceros* and *Eurhinoceros* are known from Lower Miocene deposits in the Himalayan foreland basin (Forster-Cooper 1934). Other less complete specimens from the Lower Miocene Bugti beds, stored in the Natural History Museum, London show the fusion of lingual cusps more or less high above the enamel basis, the presence of a narrow metacone ridge in the upper premolars, and of both crista and crochet as in *Rhinoceros* (Forster-Cooper 1934: fig. 36). The first skulls with single horns and comparable tooth morphology are known from the Middle Miocene of Europe

Table 1. Dental differences of upper cheek teeth in extant one-horned rhinoceroses (credit KH).

Character	*Rhinoceros unicornis*	*Eurhinoceros sondaicus*
1. Crown height	subhypsodont	mesodont
2. Ectoloph of molars	flat	sinuous
3. Parastyle	short to reduced	long, prominent
4. Crista in molars	present	lacking
5. Crista in premolars	present	lacking
6. Lingual cusps of premolars	partly fused	widely separated
7. Metacone ridge of premolars	narrow, prominent, blunt	flattened and depressed
8. Lingual cingulum of premolars	vestigial or lacking	strong, sometimes continuous

with *Lartetotherium* Ginsburg, 1974 and South Asia with *Gaindatherium browni* Colbert, 1934, the latter with somewhat higher tooth crowns.

The series with increasing tooth height continues to *Rhinoceros sivalensis* Falconer & Cautley, 1847, which already has the typical skull profile of *Rhinoceros*. Differences in the combination of crown height, secondary folds, and cingulum formation show that this phylogenetic lineage was more complexly branched so that it is not easy to find the direct line to the living *Rhinoceros*. It makes no sense to distinguish primitive and progressive morphologies, as these are due to diverging dietary specialisations. Whereas *Eurhinoceros* was constantly a non-selective browser, the early relatives of *Rhinoceros* managed the transition from selective browsing to grazing, following the increasing dominance of grasses in the vegetation (Barry et al. 2002). As proposed by Singh et al. (2012), several sub-basins located south of the Himalayas experienced a gradual increase in aridity from approximately 12 million years ago to the present. This environmental shift likely has influenced the dietary habits of the rhinoceroses.

Owing to its confined habitat and the openness of its environment, as well as ex situ breeding programs, the ecological dynamics of *R. unicornis* are closely monitored and well documented. Extensive studies have been conducted on this species, yielding substantial data and allowing Laurie (1978, 1982), Laurie et al. (1983), Dinerstein (2003), and Bhattacharya (2020a) to provide comprehensive insights into the physical characteristics, socialisation, mating, feeding habits, and other patterns. Despite a fairly extensive body of literature on *E. sondaicus*, this species has not been given sufficient attention in investigations on the phylogenetic development of the Rhinocerotidae family. As a result, there is presently no consensus on their phylogenetic attributes. Several comparisons bring forth specific facts that would emerge from these studies. As shown in Tables 1, 2, *E. sondaicus* can be differentiated from *R. unicornis* based on several key characteristics of the teeth and the skulls as these features are more primitive in *E. sondaicus*, suggesting a harmonic developmental growth that uniformly impacts nearly all aspects of cranial and dental anatomy. According to Colbert (1942), this clear progression in the skull and tooth characters from *E. sondaicus* to *R. unicornis* is unique, allowing certain Pleistocene species of the one-horned rhinoceroses to assume intermediary positions between these two extant forms.

Based on skeletal morphology highlighted by current evidence in this study, *E. sondaicus* is considered the most primitive member of the one-horned rhinoceroses, exhibiting structural features that, through subsequent develop-

Table 2. Divergences in skulls between *R. unicornis* and *E. sondaicus* (after Colbert 1942: 2).

Rhinoceros unicornis	***Eurhinoceros sondaicus***
1. Large and robust	1. Slenderer and lighter than *R. unicornis*
2. Nasals expanded into large, rounded horn boss	2. Less expansion in the nasals; horn boss pointed rather than rounded, very small in females
3. Occipital surface high and narrow. Skull deep	3. Occipital surface comparatively low and broad. Skull comparatively shallow
4. Deep 'saddle' in profile of skull between nasal and occipital vertex	4. Rather shallow 'saddle' in cranial profile
5. Zygomatic arch rounded at posterior termination	5. Zygomatic arch angular at posterior termination
6. Posterior margin of palate concave or with small median projection	6. Posterior margin of palate with median projection
7. Mesopterygoid fossa, basisphenoid and basi-occipital bones narrow	7. Mesopterygoid fossa, basisphenoid and basi-occipital bones comparatively broad
8. Pterygoids compressed and grooved	8. Pterygoids flattened and laterally expanded
9. Vomer thick and united to sides of pterygoid	9. Vomer thin, lamelliform, pointed and free
10. Premaxillaries broad	10. Premaxillaries relatively narrow

ments and adaptations became distinctive for Pleistocene species such as *Rhinoceros sinensis*, *Rhinoceros sivalensis*, and the contemporaneous *Rhinoceros unicornis* (Colbert 1942; Hooijer 1946: 675). *Eurhinoceros sondaicus* is the sole Asian rhinoceros species well represented by a substantial number of specimens from Pakistan, Myanmar, Thailand, Cambodia, and Vietnam fossil deposits, allowing us to trace its evolutionary history from the Miocene (Heißig 1972) through the early Late Miocene (Longuet et al. 2024) to Plio-Pleistocene (Beden and Guérin 1973; Bacon et al. 2004; Zin-Maung-Maung-Thein et al. 2006, 2010; Khan 2009; Abdul et al. 2014; Suraprasit et al. 2016; Siddiq et al. 2016). In its dentition and skeletal characteristics, the representatives of Pleistocene *E. sondaicus* mirror the extant Sundaic rhinoceros.

Heißig's (1981) cladistic analysis suggests that *R. unicornis* and *E. sondaicus* share a common ancestral lineage. However, the considerable diversity of fossil Rhinocerotini in South Asia, particularly in the Siwalik beds, presents challenges in attributing isolated remains to specific taxa, obscuring evolutionary inferences. Therefore, the relationship of fossil Rhinocerotini to extant species must be based primarily on dental characters. In most systematics studies, diet and cheek tooth morphology are often thought to be of less importance than other characters, even though dental microwear texture analysis can be employed to deduce ancient diets (Hullot et al. 2019: 398).

Following Heißig's initial discovery (1972), more findings emerged to confirm the ancient presence of *Eurhinoceros* in the Siwalik beds of Pakistan. Khan (2009) examined several fossil rhinoceros species from the Pleistocene Siwalik beds, identifying the dental characteristics of some specimens as belonging to *Eurhinoceros sondaicus* (as *R. sondaicus* and *R.* aff. *sondaicus*). Abdul et al. (2014) recorded the finding of Pleistocene rhinocerotid fossils from localities of Siwalik beds in the Gujrat district at Sar Dhok in Pabbi hills, where specimens belonging to *Rhinoceros sivalensis*, *'Rhinoceros' sondaicus*, and *Rhinoceros unicornis* were recovered as well as finds from Jari Kas in Mirpur district which belong to *Eurhinoceros sondaicus* and *Rhinoceros platyrhinus* Falconer & Cautley, 1847. These fossils, dating from the Tatrot and Pinjor stages of the Soan Formation ~ 3.5–0.9

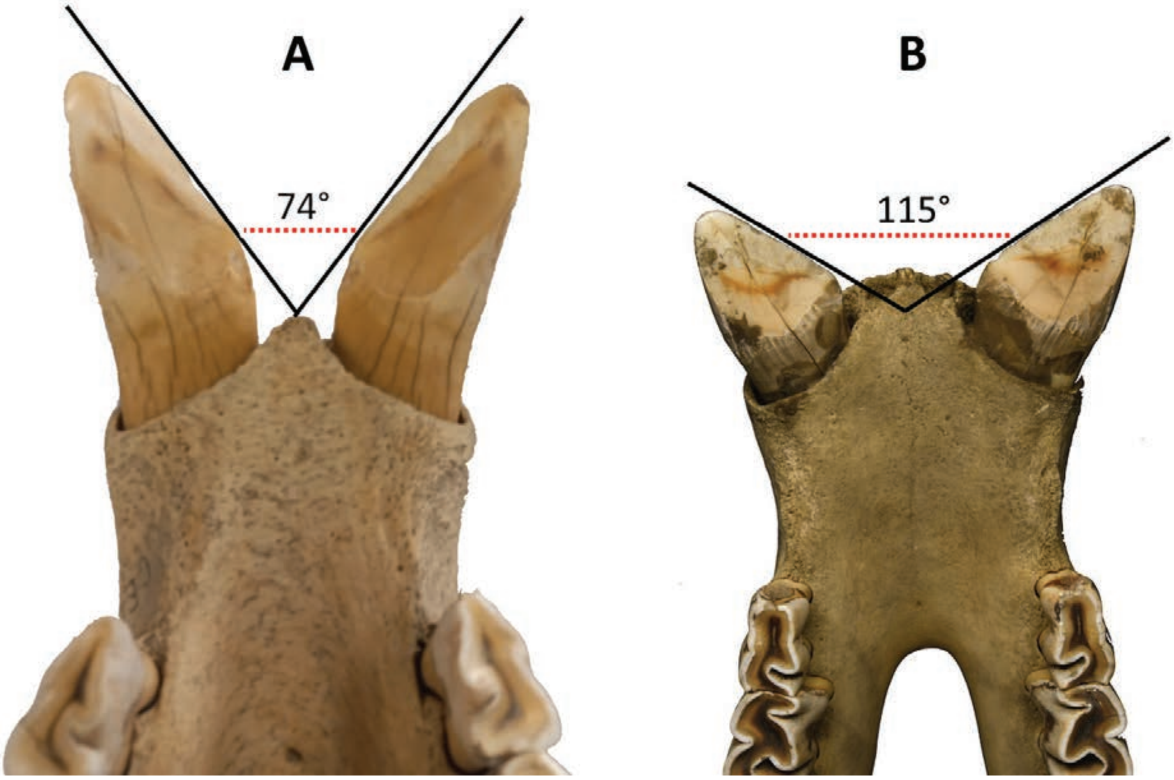

Figure 4. Lower incisors of **A** *Eurhinoceros sondaicus* and **B** *Rhinoceros unicornis*. The images highlight a distinct difference in the angles and orientation of the incisors as they emerge from the mandible, reflecting specific characteristics. **A** Specimen no. 294 from the Museum of Natural History 'Giacomo Doria' of Genoa. Collected by G. B. Ferrari in 1873. Origin: Banten Province, Java. Photograph by Giuliano Doria **B** female specimen NHMUK ZD 1883•10•23•3 from the collections of the British Museum of Natural History, London. Collected by H.R.H. The Prince of Wales in 1883. Origin: Terai of Nepal. Photograph by Phaedra Kokkini.

million years ago include well-preserved maxillary and mandibular fragments, in addition to isolated teeth (Abdul et al. 2014). Siddiq et al. (2016) described fossil *Rhinoceros* aff. '*R*'. *sondaicus* collected from various Siwalik bed localities, including the areas of Sar Dhok in Gujrat district, Tatrot in Jhelum district, Jari Kas in Mirpur district of Azad Jammu and Kashmir regions. These samples include maxillary and mandibular fragments, as well as isolated teeth.

Fossils of *Eurhinoceros* have been also found in Myanmar, Thailand, Cambodia, and Vietnam. Zin-Maung-Maung-Thein et al. (2006) identified right and left maxillae of *'Rhinoceros' sondaicus* from the upper part of the Irrawaddy (Ayeyarwady) Formation. Additional cranial remains, including upper teeth, were recovered along the Irrawaddy sediments in central Myanmar (Zin-Maung-Maung-Thein et al. 2010). Fossil specimens of *Rhinoceros* cf. '*R.*' *sondaicus* consisting of post-cranial remains were collected from the Tebingan area in the Magway Region of Myanmar (Longuet et al. 2024). The mammalian fauna from the Irrawaddy Formation is estimated based on the presence of several genera with well-established chronological distributions in the Siwalik deposits (Longuet et al. 2023, 2024). Deposits at Khok Sung in the Nakhon Ratchasima province of Thailand have preserved *'Rhinoceros' sondaicus* cranial, mandibular, and dental fossils (Suraprasit et al. 2016). At the Phnom Loang, Middle Pleistocene to the Holocene site in Cambodia, Guérin (1973) identified *'Rhinoceros' sondaicus guthi*

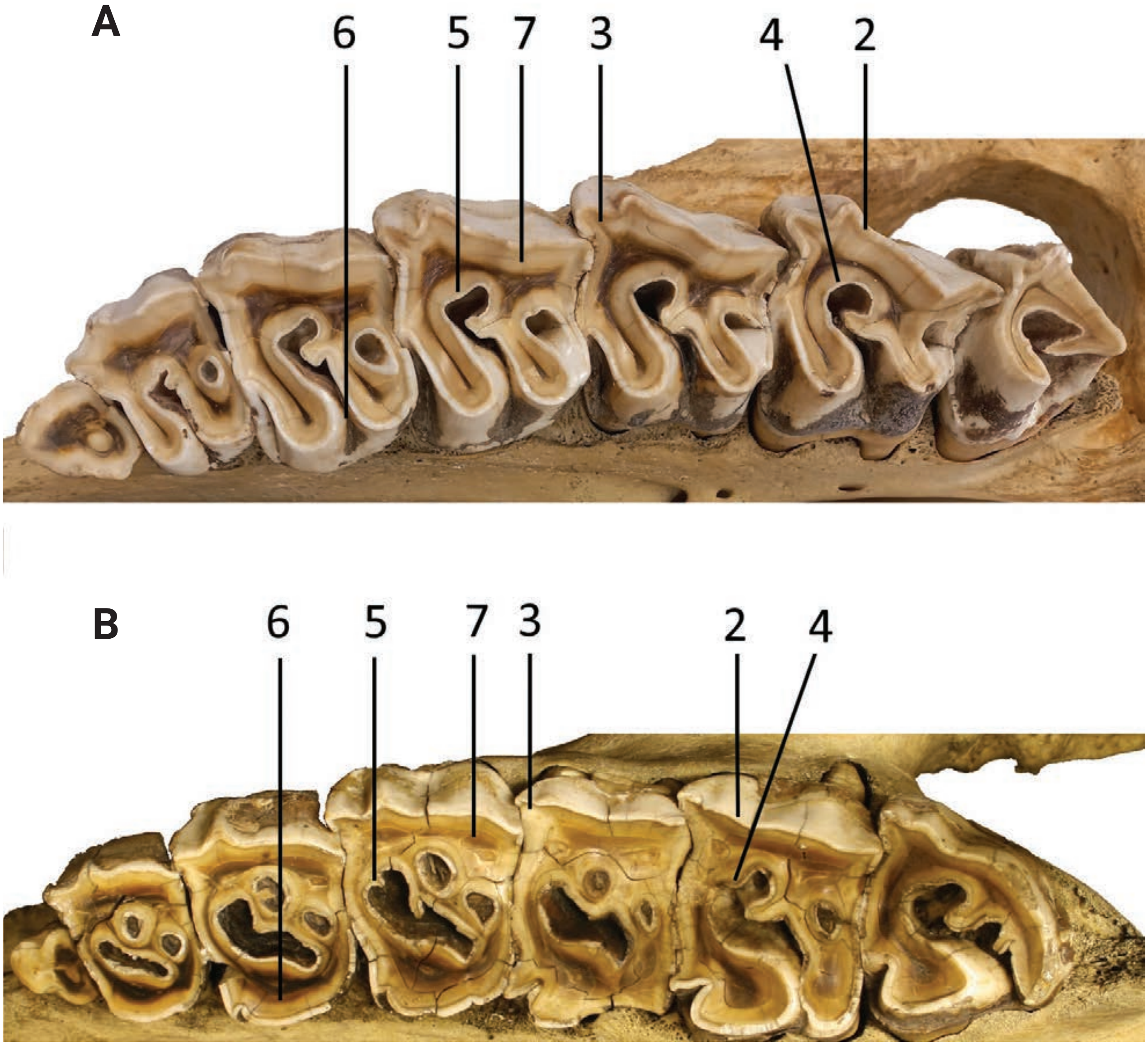

Figure 5. **A** Upper teeth of the left maxilla in occlusal view of *Eurhinoceros sondaicus*, specimen no. 294, from the Museum of Natural History 'Giacomo Doria' of Genoa. Collected by G. B. Ferrari in 1873. Origin: Banten Province, Java. Photograph by Giuliano Doria **B** upper teeth of the left maxilla in occlusal view of *Rhinoceros unicornis*, specimen NHMUK ZD 1951•11•30•2, from the British Museum of Natural History, London. Collected by H. R. H. The Prince of Wales in 1883. Origin: Terai of Nepal. Photograph by Luca Pandolfi. Refer to Table 1 for numbered annotations.

Guérin, 1973 fossil specimens. Molar fossils provisionally referred to *'Rhinoceros'* cf. *sondaicus*, were identified at the Pleistocene Ma U'Oi cave, northern Vietnam (Bacon et al. 2004). In the above-mentioned studies four taxa were identified based on dental morphology and dimensions. Fossils of Rhinocerotini occur as early as in the Lower Miocene of the Bugti beds. Some of these single finds, stored in the Museum of Natural History, London are still undescribed.

The differences, especially in the premolars, can be associated with the dissimilar diets of *R. unicornis* and *E. sondaicus* (Hullot et al. 2019). *Rhinoceros unicornis* is a variable grass eater and has high-crowned, block-like upper cheek

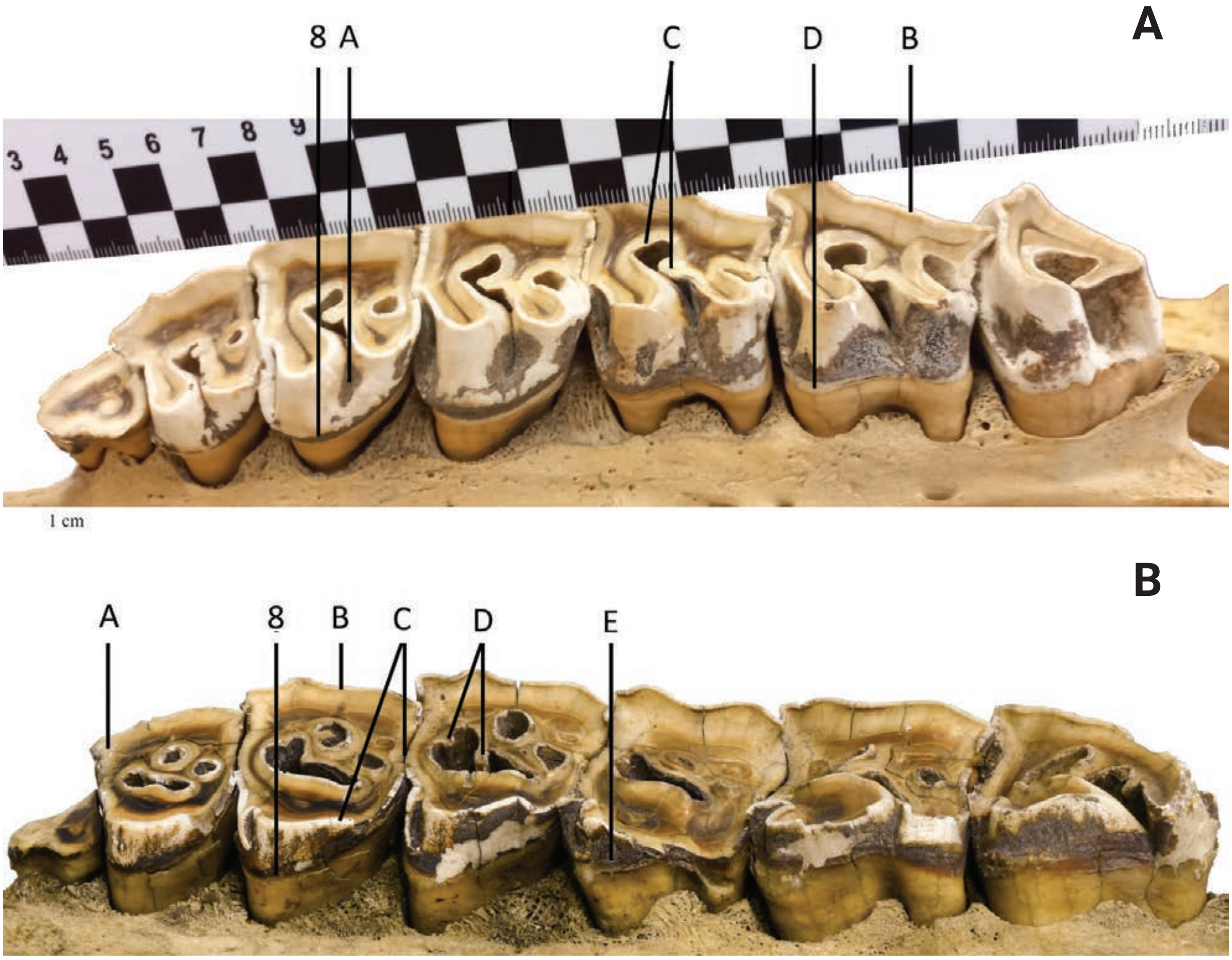

Figure 6. A Upper teeth of the left maxilla in lingual view of *Eurhinoceros sondaicus*, specimen no. 294, from the Museum of Natural History 'Giacomo Doria' of Genoa. Collected by G. B. Ferrari in 1873. Origin: Banten Province, Java. Photograph by Giuliano Doria **B** upper teeth of the left maxilla in lingual view of *Rhinoceros unicornis*, specimen NHMUK ZD 1951•11•30•2, from the British Museum of Natural History Collections, London. Collected by H. R. H. The Prince of Wales in 1883. Origin: Terai of Nepal. Photograph by Phaedra Kokkini. Refer to Table 1 for numbered annotations.

teeth that can withstand, for a lifetime, the abrasion caused by fibres and silicic acid. On the other hand, *E. sondaicus* is a generalist browser, exposing its premolars to twig fragments, requiring cingula to prevent lesions of the gums. Without the stress of strong abrasion, the teeth could stay mesodont. The premolars possess a narrow metacone rib and a high lingual wall, even if the lingual cusps are separated by lingual and labial furrows. A lingual cingulum may be present or absent, and this stage of molarisation was defined as 'paramolariform' by Heißig (1969: 16). It is rather widespread in the tribe Rhinocerotini and still present in the living *R. unicornis*.

Members of the *Rhinoceros* clade are well represented in the Siwalik beds, starting with the genus *Gaindatherium* which is characterised by the absence of a lingual cingulum and a distinct metacone rib. This lineage appears to transition into the higher-crowned *Rhinoceros sivalensis* and eventually leads to the even more high-crowned extant species, although earlier and contemporaneous specimens of *R. sivalensis* appear to be too high-crowned to be considered direct ancestors of *Eurhinoceros*. *Eurhinoceros* seems to have arrived relatively early in

Java during the Pleistocene, potentially with an ancestor referred to as *'Rhinoceros' sivasondaicus* Dubois, 1908. Evidence of this evolutionary pathway can be traced through fossil specimens found at Ngandong, Sangiran, Djetis, and Trinil Pleistocene localities in Java (Koenigswald 1935; Hooijer 1964; Antoine 2012).

Looking for earlier members of the *Eurhinoceros* lineage in the Siwalik collections, Heißig (1972: 29) described two premolars from Sethi Nagri and an upper molar and some lowers from two localities of the Chinji Formation in Pakistan. The specimens come from Dehm's expeditions to the Siwalik Hills in Pakistan (winter 1955/1956), housed in the Bavarian State Collection of Paleontology and Geology, Munich and the University of Utrecht Collection, Netherlands. They all differ from *Gaindatherium* by the formation of cingula. The complete set of characters foreshadowing the morphology of the recent *Eurhinoceros* shows the upper premolar described by Heißig (1972: 18) from the Dhok Pathan Formation of Parlewali. It differs from the premolar figured by Matthew (1929: figs 33–34) with the probable provenance Dhok Pathan by the loss of the metacone rib, the deeper separation of the lingual hills and the formation of a lingual cingulum around the protocone base.

The two premolars were identified as *Eurhinoceros* aff. *sondaicus* due to their resemblance to the extant species. Heißig (1972: 30) detailed a M2 and two m3, one of them on a mandible fragment from the Middle Miocene of the Chinji Formation as a probable *Eurhinoceros* sp. as illustrated by Heißig (1972: pl. 5, figs 8, 9; pl. 7, figs 1, 2). The upper molar, albeit somewhat fragmentary, aligns with the features of the extant species in the faint antecrochet and the subtle protocone constriction, typical traits of most Rhinocerotini. Additionally, it shares the development of a lingual cingulum and the absence of a metacone rib. The absence of the cingulum in the external groove of the lower molars is also not observed in all living Rhinocerotini e.g., *Diceros* and *Dicerorhinus* (Heißig 1972: 30). If this determination is correct, these specimens would prove a separation of the one-horned rhinoceroses from the main stock of Rhinocerotini around the Middle Miocene.

At first sight, *R. unicornis* and *E. sondaicus* display similarity in traits such as the head position and the partly or nearly complete armour of the skin, although both are distinctly different when analysed in depth. The relatively high position of the head in the variable grazer *R. unicornis*, compared to the exclusive grazer *C. simum*, as shown by the forward inclination of the occipital plane, corresponds to its feeding habits, which include consuming very tall elephant grass (*Pennisetum purpureum*) and reaching for high-hanging twigs in dense forest vegetation (Bales 1996: 274). The armour, however, is not easily understood as convergence and may have been a characteristic of shared ancestral lineage. According to Endo et al. (2009), the development of skin folds in *R. unicornis* is considered a thermoregulatory adaptation, serving to protect the rhinoceroses from heat.

The morphology of the skull shows a strong correlation with the hypsodont index (Piras et al. 2010). This indicates that adaptations to different feeding habits occur deeper within the rhinoceros evolutionary tree, rather than limited to the species level. These adaptations include distinct modifications to the posterior part of the skull, which is known to vary with feeding behaviour: while the mandible and skull are more constrained by phylogeny and their developmental integration, the upper tooth row is less influenced by this relationship and teeth are the most adaptable cranial structure in evolutionary terms (Piras et al. 2010).

The skull dimensions in adults of the two living species are as follows: the occipito-nasal distance range is 613–694 mm in *unicornis* and 567–669 mm in *sondaicus*; the maximum width at the zygomatic arches is 355–435 mm in *unicornis* and 324–365 mm in *sondaicus*; *unicornis* has a mandibular length of 526–600 mm and a condylar height of 277–309 mm, while *sondaicus* has a mandibular length of 467–518 mm and a condylar height of 208–247 mm (Guérin 1980). At this point, it is practical to delineate the disparities in the skull between the two extant species (Table 2). These distinctions carry significant importance for prospective discussions regarding the phylogenetic position of each taxon in relation to the other (Colbert 1942).

The skull morphology of the two genera differs, with *R. unicornis* having, in proportion, a larger and heavier skull compared to *E. sondaicus*. Additionally, the occiput of *R. unicornis* is higher and narrower, making the dorsal outline of the skull very concave. Overall, while both genera share certain anatomical features, they also exhibit distinct differences in skull morphology (Fig. 7). The analysis of one *'Rhinoceros' sondaicus* specimen from the Manchester Museum, UK by Cave (1985) reveals several key features that are characteristic of *E. sondaicus* cranial morphology. The occipital plane is inclined forward. The orbital-aural length is longer than the orbito-nasal dimension. This ratio of orbital-aural length to orbito-nasal dimension is characteristic of *E. sondaicus* and contributes to its unique cranial proportions. The infra-orbital foramen is positioned above the second premolar tooth, which is a characteristic feature of its cranial anatomy. The mode of anterior attachment of the petro-sphenoidal ligament serves as a distinguishing feature between *E. sondaicus* and *R. unicornis*. In *E. sondaicus*, the anterior attachment of the petro-sphenoidal ligament is characterised by a small tubercle located at the termination of the Eustachian crest. This tubercle serves as the point of connection for the petro-sphenoidal ligament. On the other hand, in *R. unicornis*, there is no corresponding tubercle at the termination of the Eustachian crest. Instead, the petro-sphenoidal ligament attaches subtly to the posterior free margin of the alisphenoid bone. This difference in the anterior attachment of the petro-sphenoidal ligament between the two taxa is a significant anatomical distinction that aids in the identification and classification of their respective crania (Cave 1985). By examining these features, it is possible to differentiate between their specimens and gain insights into the unique cranial morphology of each species.

"The (skulls) shape in the lateral view reflects ecological niche, in particular feeding type from browsing to grazing, and it also represent taxonomic discrimination" (Pandolfi et al. 2021: 1). The lateral shape of rhinoceros skulls plays a crucial role in reflecting their ecological niches, particularly distinguishing feeding habits ranging from browsing to grazing. Browsing species, typically exhibit different skull structures compared to grazing species. In the lateral view, the shape helps identify these feeding behaviours by highlighting morphological traits adapted to their diets, such as the orientation of the occipital area and the development of other cranial features. This differentiation in skull forms also serves as an important indicator of taxonomic distinctions among rhinoceros species, aiding in the classification and understanding of their evolutionary adaptations. These anatomical differences are consistent with the feeding habits, as grazing rhinoceroses like the white and Indian rhinoceroses feed closer to the ground, while browsing species such as the Sundaic and the Asiatic two-

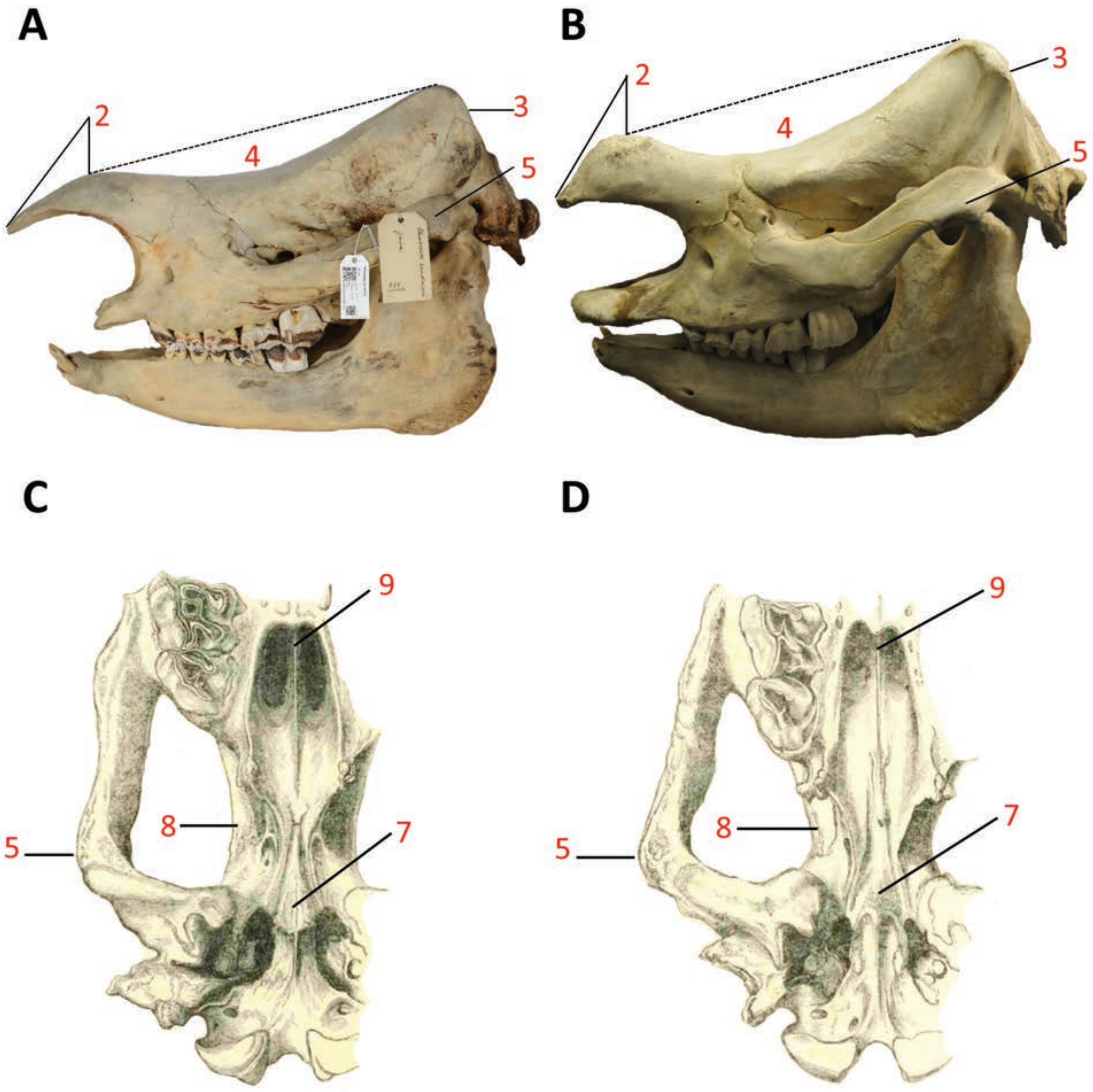

Figure 7. A Left side view of the skull of *Eurhinoceros sondaicus* (juv.), specimen NHM-DMA-26801/1, collected in Java, 1838. Credit: Natural History Museum, Oslo. Adapted from Matschiner (2021: 4842), with permission from Elsevier Eds. Photograph by Lars Erik Johannessen **B** left side view of the skull of *Rhinoceros unicornis* (juv.), Smithsonian NMAH. Licensed under CC BY-SA 4.0. The image has been modified by isolating the skull and inverting its position horizontally. Photograph by David J. Stang **C** partial ventral view of the cranium of *Eurhinoceros sondaicus* **D** partial ventral view of the cranium of *Rhinoceros unicornis*. Adapted from Flower (1876: 446, 447). Main cranial differences outlined following Colbert (1942). Refer to Table 2 for numbered annotations.

horned rhinoceroses feed on leaves and saplings. This connection between skull morphology and dietary preferences can also be traced through fossil records, demonstrating how rhinoceroses adapted to varying environments and food sources over time (Pandolfi et al. 2021). As shown in Fig. 8, a smaller angle **o** suggests a posteriorly extended occipital crest, which corresponds to a downward-oriented skull posture. When the lateral semicircular canals (LSC) are aligned horizontally, the palatal plane in *E. sondaicus* is nearly horizontal (Fig. 8A), whereas in *R. unicornis*, the rostrum and palatal plane tilt slightly downward

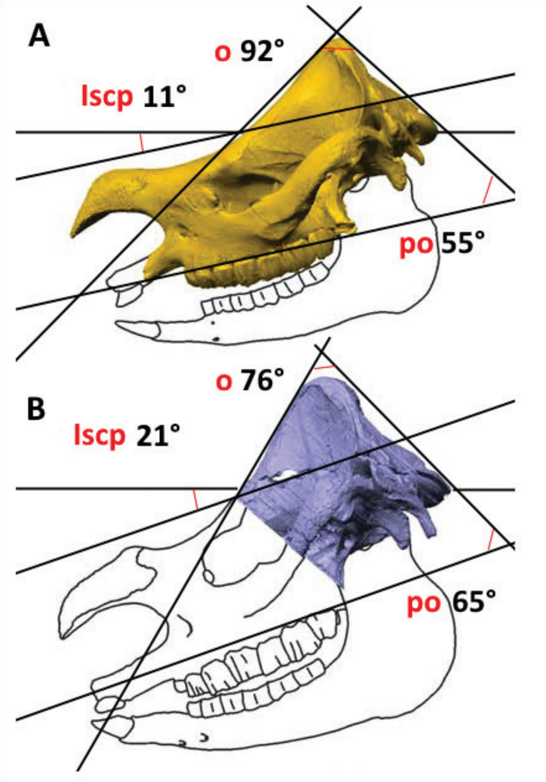

Figure 8. Polygonal surface model of **A** *Eurhinoceros sondaicus* skull (in yellow) and **B** *Rhinoceros unicornis* skull (in blue) with measured angles. Abbreviations: **lscp**–angle between plane spanned between the lateral semicircular canals (LSC) of both inner ears and the palatal plane; **o**–angle of the occipital crest between the occipital plane and the parietal plane; **po**–angle between occipital plane and palatal plane. Skull drawings and colours have been maintained from the original. Adapted with permission from Schellhorn (2018: 53).

towards the ground (Fig. 8B). The angle between the plane defined by the LSC of both inner ears and the palatal plane is also smaller in *E. sondaicus*.

Schellhorn (2018) highlights that the connection between the shape of the occiput and head posture has been recognised for a long time (Zeuner 1934; Bales 1996). Zeuner (1934) was the first to quantitatively analyse the shape of the occiput, specifically the angles **o** and **po**, and found that the angle **o** that is formed between the parietal and occipital planes is smaller in grazing rhinoceroses compared to browsing species. Schellhorn (2018: 58) also affirms: “These results also support the hypothesis that rhinoceroses with large lower second incisors but one small nasal horn, like *R. sondaicus*, have a horizontal head posture”.

Heißig (1972, 1989) suggested that fossil rhinoceroses with strong lower tusks likely used them as defensive weapons against predators, similar to the behaviour of extant Asian rhinoceroses. This inference is based on the well-documented behaviour of the living species, which use their tusks in combat (Sody 1959; Owen-Smith 1988). In contrast, the African species, which have completely reduced incisors, rely on their large horns for fighting (Dinerstein 2011). Dinerstein (2011) further proposed a potential link between these behaviours and typical head posture, noting that rhinoceroses with strong lower tusks might favour a horizontal head posture, which would facilitate the use of their tusks as weapons.

This idea is reinforced by the observation that a downward head posture is predominantly seen in both living and fossil rhinoceroses with large horns and without lower second incisors (Heißig 1973). Schellhorn (2018) and Benoit et al. (2020) emphasise the intricate relationship between anatomical features, such as the LSC orientation and occipital shape, and behavioural aspects like feeding preferences and head posture. While Benoit et al. (2020) underline the complexity and potential limitations in reconstructing these features accurately in extinct species, Schellhorn (2018) demonstrates a practical application in extant rhinoceroses, providing new insights that could potentially be adapted to fossil records. A pivotal insight from the work of Benoit et al. (2020) is the pronounced influence of phylogenetics on all examined variables in ungulates. Their findings propose that, in ungulates, LSC orientation predominantly corresponds to evolutionary relationships. For a more precise understanding, upcoming research endeavours should scrutinise each subclade independently, demanding a broader sample size for each (Pandolfi et al. 2021).

Conclusions

The one-horned Asiatic rhinoceroses are examples of evolutionary histories driven by ecological pressures. Adaptations of large terrestrial mammals to various environments are linked to the diversity of food items they can consume, which is reflected in the variation of their dental and cranial morphologies. In rhinoceroses, these adaptations are identified in their teeth structure and head posture. Evidence on feeding habits aligns with the positioning of skulls within the morphospace, allowing us to infer the existence of distinct feeding types or ecomorphotypes.

Ecological niche modelling studies have demonstrated differences in habitat preferences and ecological requirements, suggesting niche partitioning as a mechanism for coexistence and evolutionary divergence. These models predict distinct distributions and habitat suitability for each taxon also within overlapping geographical ranges.

Behavioural observations of *R. unicornis* and *E. sondaicus* in their natural habitats have provided insights into their substantial dissimilar dietary intake, marked activity patterns and distinct habitat utilisation. These observations indicate specific behaviours supporting the notion of niche partitioning to reduce competition. This separation of ecological niches not only prevented direct competition but also contributed to their distinct evolutionary trajectories. The fossils support this divergence, with evidence indicating that *E. sondaicus* evolved to exploit a browsing niche, while *R. unicornis* became increasingly specialised as a grazer. The significant distinctions in tooth morphology, including the variation in wear patterns, reflect their adaptation to different diets and ecological settings over extended geological timescales.

Genetic assessments were not feasible in this study due to the lack of comparative genetic research. Studies on population dynamics and demographic history reveal patterns of genetic diversity, gene flow, and population structure within *R. unicornis* and *E. sondaicus* populations.

The morphological and ecological differences between the two taxa are not merely superficial adaptations to different dietary intakes, but significant structural changes that have evolved over paleontological epochs. The distinctions reflect deep evolutionary adaptations, not short-term ecological plasticity. The study identifies key divergences, not minor traits but fundamental anatomical features tied to their evolutionary adaptations. These diversities are expected to be satisfactory in taxonomy to justify genus-level distinctions, as seen in other genera like *Ceratotherium* and *Diceros*. Since the extant African rhinoceroses are classified into different genera, it is reasonable to separate *Rhinoceros* and *Eurhinoceros* due to their similar dietary adaptations, among a number of other characteristics. By integrating evidence from paleontological records, ecological niche modelling, morphology, behavioural observations and population dynamics, this assessment substantially supports the idea of distinct evolutionary trajectories for *Rhinoceros unicornis* and *Eurhinoceros sondaicus*.

Available data do not provide justification for classifying *Eurhinoceros sondaicus* as a congeneric species with *Rhinoceros unicornis* or as a subgenus within *Rhinoceros*. In our view, the phenotypic and adaptive differences observed between the two lineages warrant a reassessment of its taxonomic status at the genus level. This approach not only reflects their evolutionary separation but also provides a clearer framework for better understanding of their distinct characteristics within a phylogenetic context.

Acknowledgements

We extend our sincere gratitude to the editors and anonymous peer reviewers for their significant and constructive feedback, which greatly improved the manuscript, in particular Nathalie Yonow for skillfully polishing the final text. We are grateful to Robert and Harsanti Morley and Rico Schellhorn for their generous authorisation to use Figs 3 and 8, respectively. We especially thank Luca Pandolfi (University of Basilicata) and Giuliano Doria (Museum of Natural History 'Giacomo Doria' of Genoa) for providing original photographs of specimens featured in Figs 4(A), 5(A, B), and 6(A), and for kindly granting permission for their inclusion in this work. We received extraordinary support from Phaedra Kokkini (British Museum of Natural History) for taking photographs in lingual view of the Indian rhinoceros maxilla, possibly the first ever published for this species, in Fig. 6(B), as well as the image in Fig. 4(B). Spartaco Gippoliti and Tommaso De Francesco are sincerely acknowledged for their insightful suggestions. The Rhino Resource Centre (RRC) website is recognized as the most valuable repository, providing access to the majority of the papers cited below: http://www.rhinoresourcecenter.com/.

Additional information

Conflict of interest

The authors have declared that no competing interests exist.

Ethical statement

No ethical statement was reported.

Funding

No funding was reported.

Author contributions

Both authors have contributed equally.

Author ORCIDs

Francesco Nardelli https://orcid.org/0000-0001-9317-5376

Data availability

All of the data that support the findings of this study are available in the main text.

References

Abdul AM, Cerdeño E, Akhtar M, Khan MA, Siddiq Kh (2014) An account of the Upper Siwalik rhinocerotids of Pakistan. Abstract volume of the 4th International Palaeontological Congress, Mendoza, Argentina, 549 pp.

Amman H (1986) Contributions to the ecology and sociology of the Javan rhinoceros (*Rhinoceros sondaicus*, Desmarest). Basel University, Inaugural Dissertation.

Antoine P-O (2012) Pleistocene and Holocene rhinocerotids (Mammalia, Perissodactyla) from the Indochinese Peninsula. Comptes Rendus Palevol, Elsevier 11: 159–168. https://doi.org/10.1016/j.crpv.2011.03.002

Bacon AM, Demeter F, Schuster M, Vu TL, Nguyen KR, Antoine P-O, Sevket S, Ha HN, Nguyen MH (2004) The Pleistocene Ma U'Oi cave, northern Vietnam: palaeontology, sedimentology and palaeoenvironments. Geobios 37: 305–314. https://doi.org/10.1016/j.geobios.2003.03.010

Bales GS (1996) Skull evolution in the Rhinocerotidae (Mammalia, Perissodactyla): Cartesian transformations and functional interpretations. Journal of Mammalian Evolution 3 (3): 261–279. https://doi.org/10.1007/BF01458183

Barry JC, Morgan ME, Flynn LJ, Pilbeam D, Behrensmeyer AK, Raza SM, Khan AI, Badgley C, Hicks J, Kelley J. (2002) Faunal and environmental change in the late Miocene Siwaliks of northern Pakistan. Paleobiology 28 (S2): 1–71. https://doi.org/10.1666/0094-8373(2002)28[1:FAECIT]2.0.CO;2

Beden M, Guerin C (1973) Le gisement des vertébrés du Phnom Loang (Province de Kampot, Cambodge). Travaux et Documents de l'ORSTOM 27: 3–97.

Benoit J, Legendre LJ, Farke AA, Neenan JM, Mennecart B, Costeur L, Merigraud S, Manger PR (2020) A test of the lateral semicircular canal correlation to head posture, diet and other biological traits in "ungulate" mammals. Scientific Reports 10: 1–21. https://doi.org/10.1038/s41598-020-76757-0

Bhattacharya A (2020a) Ecology, behaviour and management practices of Great Indian one Horned Rhinoceros at Gorumara, Jaldapara and Kaziranga national parks, India. Thesis presented to Raiganj University.

Bhattacharya A (2020b) Communication types in Indian Rhinoceros (*R. unicornis*, Linnaeus). International Journal of Trend in Research and Development 7(4): 188–194.

Bhattacharya A and Chakraborty K (2016) Defecation behaviour of great Indian one horned rhinoceros (*R. unicornis*, Linnaeus). International Journal of Science and Research 5 (7): 923–978.

Blumenbach JF (1799) Handbuch der Naturgeschichte. Sechste Ausgabe (6th ed). Johann Christian Dieterich, Goettingen, 703 pp.

Burchell WJ (1817) Ueber eine neue Gattung Nashorn. Isis (Oken) 1: 1318–1319. [figs 1, 2]

Cave AJE (1969) Hairs and vibrissae in the Rhinocerotidae. Journal of Zoology, London 157(2): 247–257. https://doi.org/10.1111/j.1469-7998.1969.tb01700.x

Cave AJE (1985) An unrecorded specimen of the Javan rhinoceros (*Rhinoceros sondaicus*). Journal of Zoology, London 207: 527–535. https://doi.org/10.1111/j.1469-7998.1985.tb04949.x

Cerling T, Harris J, MacFadden B, Leakey MG, Quade J, Eisenmann V, Ehleringer J.R (1977) Global vegetation change through the Miocene/Pliocene boundary. Nature 389: 153–158. https://doi.org/10.1038/38229

Choudhury A (1985) Distribution of Indian one-horned rhinoceros (*Rhinoceros unicornis*). Tiger Paper 12(2): 25–30.

Colbert EH (1934) A new rhinoceros from the Siwalik beds of India. American Museum Novitates 749: 1–13. https://doi.org/10.70249/9798893981964-002

Colbert EH (1942) Notes on the Lesser one-horned rhinoceros, *Rhinoceros sondaicus*, 2. The position of *Rhinoceros sondaicus* in the phylogeny of the genus *Rhinoceros*. American Museum Novitates 1207: 1–5.

Cranbrook Earl of (1986) A review of fossil and prehistoric remains of rhinoceroses of Borneo. Sabah Museum and Archives Journal 1(1): 50–110.

Cranbrook Earl, Piper PJ (2007) The Javan rhinoceros *Rhinoceros sondaicus* in Borneo. Raffles Bulletin of Zoology 55 (1): 217–220.

Desmarest AG (1822) Mammalogie, ou description des espèces des Mammifères. Veuve Agasse, Paris, 277–555.

Dinerstein E (2003) The return of the unicorns: natural history and conservation of the Greater one-horned rhinoceros. Columbia University Press, New York, 316 pp. https://doi.org/10.7312/dine08450

Dinerstein E (2011) Family Rhinocerotidae (Rhinoceroses). In: Handbook of the mammals of the world, vol. 2: Hoofed mammals. Lynx, New York, 144–181.

Dubois E (1908) Das geologische Alter der Kendeng-oder Trinilfauna. Tijdschrift van het Koninklijk Nederlandsch Aardrijkskundig Genootschap (2)25: 1235–1270.

Endo H, Kobayashi H, Koyabu D, Hayashida A, Jogahara T, Taru H, Oishi M, Itou T, Koie H, Sakai T (2009) The morphological basis of the armor-like folded skin of the Greater Indian Rhinoceros as a thermoregulator. Mammal Study 34(4): 195–200. https://doi.org/10.3106/041.034.0403

Erxleben JCP (1777) Systema regni animalis per classes, ordines, genera, species, varietates, cum synonymia et historia animalium. Weygandianis, 636 pp. https://doi.org/10.5962/bhl.title.15933

Falconer H, Cautley PT (1847) Fauna antiqua sivalensis, being the fossil zoology of the Sewalik Hills, in the North of India Illustrations, part VIII: Suidae and Rhinocerotidae. Smith, Elder and Company, London, pls 69–80. https://doi.org/10.5962/bhl.title.61447

Falconer H (1859) [In Gaudin CT (Ed.)] Modifications apportés par Mr. Falconer a la faune du Val d'Arno. Bulletin de la Société Vaudoise des Sciences Naturelles 6(44): 130–131.

Falconer H, Cautley PT (1836) Note on the fossil hippopotamus of the Siwalik Hills. Asiatic Researches 19(3): 39–53.

Flower WH (1876) On some cranial and dental characters of the existing species of rhinoceroses. Proceedings of the Zoological Society of London 1876 May 16: 443–457. https://doi.org/10.1111/j.1096-3642.1876.tb02583.x

Forster-Cooper C (1934) The extinct Rhinoceroses of Baluchistan. Philosophical Transactions of the Royal Society of London (B) 223: 569–616. https://doi.org/10.1098/rstb.1934.0013

Ghosh T, Kumar S, Sharma K, Kakati P, Sharma A, Mondol S (2022) Consideration of genetic variation and evolutionary history in future conservation of Indian one-horned rhinoceros (*Rhinoceros unicornis*). BMC Ecology and Evolution 22(92): 1–13. https://doi.org/10.1186/s12862-022-02045-2

Ginsburg L (1974) Les Rhinocérotidés du Miocène de Sansan (Gers). Compte Rendu des Séances de l'Académie des Sciences, Paris 278 (5) D: 597–600.

Gippoliti S, Cotterill FPD, Groves CP (2013) Mammal taxonomy without taxonomists: a reply to Zachos and Lovari. Hystrix Italian Journal Mammalogy 24: 145–147.

Gray JE (1868) Observations on the preserved specimens and skeletons of the Rhinocerotidae in the collection of the British Museum and Royal College of Surgeons, including the description of three new species. Proceedings of the Zoological Society of London: 1003–1032.

Griffiths M (1993) The Javan rhino of Ujung Kulon: an investigation of its population and ecology through camera trapping. Directorate General of Forest Protection and Nature Conservation and the World Wide Fund for Nature Indonesia Program, Jakarta, 1–92.

Groves CP (1967) On the rhinoceroses of South-East Asia. Säugetierkundliche Mitteilungen 15(3): 221–237.

Groves CP (1971) Species characters in rhinoceros horns. Zeitschrift fur Saugetierkunde 36 (4): 238–252. [figs 1–22]

Groves CP, Guérin C (1980) Le *Rhinoceros sondaicus annamiticus* d'Indochine: distinction taxinomique et anatomique; relations phylogénétiques. Geobios 13(2): 199–208. https://doi.org/10.1016/S0016-6995(80)80028-3

Groves CP, Leslie Jr DM (2011) *Rhinoceros sondaicus* (Perissodactyla: Rhinocerotidae). Mammalian Species 43(887): 190–208. https://doi.org/10.1644/887.1

Guérin C (1973) Rhinocerotidae: 19–50, pls. 1–4. In Beden M and Guérin C (1973) Le gisement des vertébrés du Phnom Loang (Province de Kampot, Cambodge). Travaux et Documents de l'ORSTOM 27: 3–97.

Guérin C (1980) Les rhinocéros (Mammalia, Perissodactyla) du Miocène terminal au Pléistocène supérieur en Europe occidentale; comparaison avec les espèces actuelles. Documents du Laboratoire de Géologie de la Faculté des Sciences de Lyon 79: 3–1183.

Hariyadi ARS, Sajuthi D, Astuti DA, Alikodra HS, Maheshwari H (2016) Analysis of nutrition quality and food digestibility in male Javan rhinoceros (*Rhinoceros sondaicus*) in Ujung Kulon National Park. Pachyderm 57: 86–96. https://doi.org/10.69649/pachyderm.v57i.408

Harper F (1945) Extinct and vanishing mammals of the old world. New York, American Committee for International Wild Life protection, Special Publication no. 12: 1–850. https://doi.org/10.5962/bhl.title.19520

Haryono M, Rahmat UM, Daryan M, Raharja AS, Muhtarom A, Firdaus AY, Rohaeti A, Subchiyatin I, Nugraheni A, Khairani KO, Kartina (2015) Monitoring of Javan Rhino population in Ujung Kulon National Park. Pachyderm 56: 82–86. https://doi.org/10.69649/pachyderm.v56i.374

Hazarika BC, Saikia PK (2010) A study on the behaviour of great Indian one-horned rhinoceros (*Rhinoceros unicornis*) in the Rajiv Gandhi National Park, Assam, India. NeBio 1(2): 62–74. https://doi.org/10.5402/2012/259695

Heißig K (1969) Die Rhinocerotidae (Mammalia) aus der oberoligozänen Spaltenfüllung von Gaimersheim bei Ingolstadt in Bayern und ihre phylogenetische Stellung. Verlag der Bayerischen Akademie der Wissenschaften; in Kommission bei der Beck'schen CH Verlagsbuchhandlung, München: 1–133.

Heißig K (1972) Paläontologische und geologische Untersuchungen im Tertiär von Pakistan, 5. Rhinocerotidae (Mammalia.) aus den unteren und mittleren Siwalik-Schichten. Bayerische Akademie der Wissenschaften Mathematisch–Naturwissenschaftliche Klasse, Abhandlungen, München. Neue Folge 152: 1–112.

Heißig K (1973) Die Unterfamilien und Tribus der rezenten und fossilen Rhinocerotidae (Mammalia). Säugetierkundliche Mitteilungen 21: 25–30.

Heißig K (1981) Probleme bei der cladistischen Analyse einer Gruppe mit wenigen eindeutigen Apomorphien: Rhinocerotidae. Palaeontologisches Zeitschrift 55(1): 117–123. https://doi.org/10.1007/BF02986041

Heißig K (1989) 21 The Rhinocerotidae. In: Prothero DR and Schoch RM (Eds) The Evolution of Perissodactyls. Oxford University Press, New York, 399–417.

Hernesniemi E, Blomstedt K, Fortelius M (2011) Multi-view stereo three-dimensional reconstruction of lower molars of Recent and Pleistocene rhinoceroses for mesowear analysis. Palaeontologia Electronica: 1–15.

Heude PM (1892) Études odontologiques. 1. Herbivores trizygodontes et dizygodontes. Mémoires concernant l'histoire naturelle de l'Empire Chinois 2: 65–84.

Hitchins PM (1986) Earlessness in the black rhinoceros–a warning. Pachyderm 7: 8–10. https://doi.org/10.69649/pachyderm.v7i1.634

Hoogerwerf A (1970) Udjung Kulon, the land of the last Javan rhinoceros. With local and general data on the most important faunal species and their preservation in Indonesia. Brill RJ, Leiden, 512 pp. https://doi.org/10.1163/9789004646698

Hooijer DA (1946) The evolution of the skeleton of *Rhinoceros sondaicus* Desmarest. Proceedings of the Koninklijke Nederlandse Akademie van Wetenschappen, Amsterdam 49 (6): 671–676.

Hooijer DA (1964) New records of mammals from the middle pleistocene of Sangiran, central Java. Zoologische Mededelingen 40 (10): 73–88.

Hullot M, Antoine P-O, Ballatore M, Merceron G (2019) Dental microwear textures and dietary preferences of extant rhinoceroses (Perissodactyla, Mammalia). Mammal Research 64: 397–409. https://doi.org/10.1007/s13364-019-00427-4

Jäger GF (1839) Über die fossilen Säugethiere welche in Württemberg in verschiedenen Formationen aufgefunden worden sind, nebst geognostischen Bemerkungen über diese Formationen. Verlag Carl Erhard, Stuttgart. Abtheilung 2: 1–214.

Khan AM (2009) Taxonomy and distribution of rhinoceroses from the Siwalik Hills of Pakistan. PhD Thesis, University of the Punjab, Lahore.

Kim HL, Li T, Kalsi N, Nguyen HTT, Shaw TA, Ang KC, Cheng KC, Ratan A, Peltier WR, Samanta D, Pratapneni M, Schuster SC, Horton BP (2023) Prehistoric human migration between Sundaland and South Asia was driven by sea-level rise. Commununications Biology 6: 1–10. https://doi.org/10.1038/s42003-023-04510-0

Koenigswald GHR van (1935) Die fossilen Säugetierfaunen Javas. Proceedings van de Koninklijke Nederlandse Akademie van Wetenschappen 38: 88–98.

Laurie WA (1978) The ecology and behaviour of the greater one-horned rhinoceros. Ph.D. dissertation. University of Cambridge, Cambridge.

Laurie WA (1982) Behavioural ecology of the Greater one-horned rhinoceros (*Rhinoceros unicornis*). Journal of Zoology, London 196(3): 307–341. https://doi.org/10.1111/j.1469-7998.1982.tb03506.x

Laurie WA, Lang RM, Groves CP (1983) *Rhinoceros unicornis*. Mammalian Species 211, The American Society of Mammalogists: 1–6. https://doi.org/10.2307/3504002

Lesson RP (1836) Complement des œuvres de Buffon ou histoire naturelle des animaux rares découverts par les naturalistes et les voyageurs depuis la mort de Buffon, vol. 10: Oiseaux et Mammifères. Histoire naturelle générale et particulière des mammifères et oiseaux découverts depuis la mort de Buffon: Oiseaux et mammifères. Pourrat Frères et Roret, Paris, 414 pp.

Linnaeus C (1758) Systema naturae per regna tria naturae, secundum classes, ordines, genera, species, cum characteribus, differentiis, synonymis, locis Editio decima, reformata [edn 10]. Holmiae, Laurentii Salvii: i–iv, 1–824. https://doi.org/10.5962/bhl.title.542

Liu S, Dalen L, Gilbert T, Rookmaaker LC and 35 others (2021) Ancient and modern genomes unravel the evolutionary history of the rhinoceros family. Cell 184: 4874–4885. https://doi.org/10.1016/j.cell.2021.07.032

Loch CW (1937) *Rhinoceros sondaicus*: the Javan or Lesser one-horned rhinoceros and its geographical distribution. Journal of the Malayan Branch of the Royal Asiatic Society 15(2): 130–149.

Longuet M, Zin-Maung-Maung-Thein, Thaung-Htike, Man-Thit-Nyein and Masanaru TM (2023) New fossil remains of Rhinocerotidae (Perissodactyla) from the early Late Miocene Tebingan area, central Myanmar, Historical Biology: 1–14. https://doi.org/10.1080/08912963.2024.2408617

Longuet M, Handa N, Maung-Thein ZM, Htike T, Nyein MT, Takai M (2024) Post-cranial remains of Rhinocerotidae from the Neogene of central Myanmar: morphological descriptions and comparisons with ratios. Historical Biology: 1–15. https://doi.org/10.1080/08912963.2024.2408617

Lydekker R (1907) The game animals of India, Burma and Tibet. Being a new and revised edition of "The great and small game of India, Burma and Tibet". Rowland Ward, London: 1–409. https://doi.org/10.5962/bhl.title.16137

MacFadden BJ (1998) Tale of two rhinos: isotopic ecology, paleodiet, and niche differentiation of *Aphelops* and *Teleoceras* from the Florida Neogene. Paleobiology 24(2): 274–286. https://doi.org/10.1666/0094-8373(1998)024[0274:TOTRIE]2.3.CO;2

Margaryan A, Sinding MS, Liu S, Vieira FG, Chan YL, Nathan S, Moodley Y, Bruford MW, Gilbert MTP (2020) Recent mitochondrial lineage extinction in the critically endangered Javan rhinoceros. Zoological Journal of the Linnean Society 190(1): 372–383. https://doi.org/10.1093/zoolinnean/zlaa004

Matschiner M (2021) Museum specimens tell the history of rhinoceroses. Cell 184(19): 4841–4842. https://doi.org/10.1016/j.cell.2021.08.026

Matthew WD (1929) Critical observations upon Siwalik Mammals. Bulletin of the American Museum of Natural History, New York 56(7): 437–560.

Matthew WD (1931) Critical observations on the phylogeny of the rhinoceroses. University of California Publications, in Geological Science 20: 1–8.

McNeely JA, Cronin EW (1972) Rhinos in Thailand. Oryx 11(6): 457–460. https://doi.org/10.1017/S0030605300010735

Medway L (1969) The wild mammals of Malaya and offshore islands, including Singapore. Kuala Lumpur, Oxford University Press: 1–127.

Morley RJ (2018) Assembly and division of the South and South-East Asian flora in relation to tectonics and climate change. Journal of Tropical Ecology 34(4): 209–234. https://doi.org/10.1017/S0266467418000202

Nardelli F (1988) The Rhinoceros: a Monograph. Basilisk Press, London, 133 pp.

Nardelli F (2013) The mega-folivorous mammals of the rainforest: feeding ecology in nature and in controlled environment: A contribution to their conservation. International Zoo News 60(5): 323–339.

Nardelli F (2016) Current status and conservation prospects for the Javan rhinoceros *Rhinoceros sondaicus* Desmarest 1822. International Zoo News 63(3): 180–202.

Nardelli F, Robovský J (2023) New data on the ecology and conservation of the Javan rhinoceros *Rhinoceros sondaicus* Desmarest, 1822 (Perissodactyla, Rhinocerotidae). Gazella (Praha) 49(2022): 183–205.

Neese HC (1975) Survival of the Javan rhinoceros in Laos. Report: 1–27.

Owen R (1870) On fossil remains of mammals found in China. Quarterly Journal of the Geological Society London 26: 417–434. https://doi.org/10.1144/GSL.JGS.1870.026.01-02.40

Owen-Smith RN (1988) Megaherbivores: The influence of very large body size on ecology. Cambridge University Press, Cambridge, 369 pp. https://doi.org/10.1017/CBO9780511565441

Pandolfi L (2015) Sistematica e filogenesi dei Rhinocerotini (Mammalia, Rhinocerotidae). Dissertation presented to the University of Rome, Italy.

Pandolfi L, Maiorino L (2016) Reassessment of the largest Pleistocene rhinocerotine *Rhinoceros platyrhinus* (Mammalia, Rhinocerotidae) from the Upper Siwaliks (Siwalik Hills, India). Journal of Vertebrate Paleontology 36(2): 1–12. https://doi.org/10.1080/02724634.2015.1071266

Pandolfi L, Bartolini-Lucenti S, Cirilli O, Bukhsianidze M, Lordkipanidze D, Rook L (2021) Paleoecology, biochronology, and paleobiogeography of Eurasian Rhinocerotidae during the Early Pleistocene: The contribution of the fossil material from Dmanisi (Georgia, Southern Caucasus). Journal of Human Evolution 156: 1–13. https://doi.org/10.1016/j.jhevol.2021.103013

Peacock EH (1933) A game book for Burma and adjoining territories. H&F, Witherby G, London, 292 pp.

Piras P, Maiorino L, Raia P, Marcolini F, Salvi D, Vignoli L, Kotsakis T (2010) Functional and phylogenetic constraints in Rhinocerotinae craniodental morphology. Evolutionary Ecology Research 12: 897–928.

Poole CM and Duckworth JW (2005) A documented 20th century record of Javan Rhinoceros *Rhinoceros sondaicus* from Cambodia. Mammalia 69(3–4): 443–444. https://doi.org/10.1515/mamm.2005.039

Reynolds EAP (1954) Burma rhino. Burmese Forester 4(2): 104–108.

Rookmaaker LC (1977) The rhinoceros of Borneo: a 19th century puzzle. Journal of the Malayan Branch of the Royal Asiatic Society 50(1): 52–62.

Rookmaaker LC (1980) The distribution of the rhinoceros in Eastern India, Bangladesh, China and the Indo-Chinese region. Zoologische Anzeiger 205(3/4): 253–268.

Rookmaaker LC (1997) Records of the Sundarbans rhinoceros (*Rhinoceros sondaicus inermis*) in India and Bangladesh. Pachyderm 24: 37–45. https://doi.org/10.69649/pachyderm.v24i1.903

Rookmaaker LC (2000) Records of the rhinoceros in Pakistan and Afghanistan. Pakistan Journal of Zoology 32(1): 65–74.

Rookmaaker LC (2002) Historical records of the Javan rhinoceros in North-East India. Newsletter of the Rhino Foundation of Nature in North-East India 4: 11–12.

Rookmaaker LC (2006) Distribution and extinction of the rhinoceros in China: review of recent Chinese publications. Pachyderm 102: 102–106. https://doi.org/10.69649/pachyderm.v40i1.1267

Rookmaaker LC (2016) On the alleged presence of the two-horned Sumatran rhinoceros and one-horned Javan rhinoceros in the Himalayan Kingdom of Bhutan. Pachyderm 57: 116–117. https://doi.org/10.69649/pachyderm.v57i.399

Rookmaaker LC and Carpentier H (2007) Early references to the rhinoceros on the Chinese island of Hainan. Journal of the Royal Asiatic Society Hong Kong Branch 45(2005): 235–236.

Schaller GB, Dang NX, Thuy LD, Son VT (1990) Javan rhinoceros in Vietnam. Oryx 24(2): 77–80. https://doi.org/10.1017/S0030605300034712

Schellhorn R (2018) A potential link between lateral semicircular canal orientation, head posture, and dietary habits in extant rhinos (Perissodactyla, Rhinocerotidae). Journal of Morphology 279: 50–61. https://doi.org/10.1002/jmor.20753

Setiawan R, Gerber B, Ujang MR, Daryang D, Firdaus AY, Haryono M, Khairani KO, Kurniawan Y, Long B, Lyet A, Muhiban M, Mahmud R, Muhtarom A, Purastuti E, Ramono W, Subrata D, Sunarto S (2017) Preventing global extinction of the Javan Rhino: Tsunami risk and future conservation direction. Conservation Letters 11(1): 1–9. https://doi.org/10.1111/conl.12366

Siddiq MKh, Akhtar M, Khan MA, Ghaffar A, Sarwar Kh, Khan AM (2016) New fossils of rhinoceros (Rhinocerotidae) from the Soan Formation (Plio-Pleistocene) of Northern Pakistan. Pakistan Journal of Zoology 48(3): 657–664.

Singh S, Parkash B, Awasthi AK, Singh T (2012) Palaeoprecipitation record using O-isotope studies of the Himalayan Foreland Basin sediments, NW India. Palaeogeography, Palaeoclimatology, Palaeoecology 331–332: 39–49. https://doi.org/10.1016/j.palaeo.2012.02.031

Sody HJV (1959) Das Javanische Nashorn, *Rhinoceros sondaicus*, historisch und biologisch. Zeitschrift fur Saugetierkunde 24(3/4): 109–240.

Strien NJ van (1985) The Sumatran rhinoceros in the Gunung Leuser National Park, its distribution, ecology and conservation. Doorn, Van Strien: 1–207.

Suraprasit K, Jaeger JJ, Chaimanee Y, Chavasseau O, Yamee C, Tian P, Panha S (2016) The Middle Pleistocene vertebrate fauna from Khok Sung (Nakhon Ratchasima, Thailand): biochronological and paleobiogeographical implications. ZooKeys 613: 1–157. https://doi.org/10.3897/zookeys.613.8309

Tougard C, Delefosse T, Hoenni C, Montgelard C (2001) Phylogenetic relationships of the five extant rhinoceros species (Rhinocerotidae, Perissodactyla) based on mitochondrial cyctochrome b and 12s rRNA genes. Molecular Phylogenetics and Evolution 19(1): 34–44. https://doi.org/10.1006/mpev.2000.0903

Toula F (1902) Das Nashorn von Hundsheim *Rhinoceros* (*Ceratorhinu*s Osborn) *hundsheimensis* nov. form. mit Ausführungen über die Verhältnisse von elf Schädeln von *Rhinoceros* (*Ceratorhinus*) *sumatrensis*. Abhandlungen der Kaiserlich-Königlichen Geologischen Reichsanstalt 19: 1–92.

Willerslev E, Gilbert M, Binladen J, Ho S, Campos P, Ratan A, Tomsho L, Fonseca R da, Sher A, Kuznetsova T, Nowak-Kemp M, Roth T, Miller W, Schuster S (2009) Analysis of complete mitochondrial genomes from extinct and extant rhinoceroses reveals lack of phylogenetic resolution. BMC Evolutionary Biology 9: 1–30. https://doi.org/10.1186/1471-2148-9-95

Wilson SG (2021) Factors shaping the conservation of the critically endangered Javan Rhinoceros–*Rhinoceros sondaicus*. Ph.D. thesis, School of Biological Sciences, University of Queensland, Brisbane.

Yan Y, Wang Y, Zhu M, Zhang Y, Qin D, Jin C (2023) New rhino remains from Middle to Late Pleistocene of Chongzuo, Guangxi with discussion on Quaternary Rhinoceros evolution in Southern China. Quaternary Sciences 43(3): 777–792.

Zeuner FE (1934) Die Beziehungen zwischen Schädelform und Lebensweise bei den rezenten und fossilen Nashornern. Berichte der Naturforschenden Gesellschaft zu Freiburg im Breisgau 34: 21–80.

Zin-Maung-Maung-Thein, Thaung-Htike, Tsubamoto T, Takai M, Egi N, Maung-Maung (2006) Early Pleistocene Javan rhinoceros from the Irawaddy Formation, Myanmar. Asian Paleoprimatology, Primate Research Institute, Kioto University 4: 197–204.

Zin-Maung-Maung-Thein, Takai M, Tsubamoto T, Egi N, Thaung-Htike, Nishimura T, Maung-Maung, Zaw-Win (2010) A review of fossil rhinoceroses from the Neogene of Myanmar with description of new specimens from the Irrawaddy Sediments. Journal of Asian Earth Sciences 37(2): 154–165. https://doi.org/10.1016/j.jseaes.2009.08.009

Zschokke S (2016) Genetic structure of the wild populations of the Indian rhinoceros (*Rhinoceros unicornis*). Indian Journal of History of Science 51(2.2): 380–389. https://doi.org/10.16943/ijhs/2016/v51i2.2/48451

Zschokke S, Armbruster GFJ, Ursenbacher S, Baur B (2011) Genetic differences between the two remaining wild populations of the endangered Indian rhinoceros (*Rhinoceros unicornis*). Biological Conservation 144: 2702–2709. https://doi.org/10.1016/j.biocon.2011.07.031

ZooKeys 1230: 335–346 (2025)
DOI: 10.3897/zookeys.1230.144099

Research Article

First record of the genus *Cochleopsaltria* Pham & Constant (Hemiptera, Cicadidae, Cicadinae) from China, with a description of the second species

Cheng-Bin Wang[1], Zhi-Jian Liu[2]

1 *Engineering Research Center for Forest and Grassland Disaster Prevention and Reduction, Mianyang Normal University, 166 Mianxing West Road, Mianyang 621000, Sichuan Province, China*
2 *School of Marxism, Fuzhou University, 2 Xueyuan Road, Fuzhou 350108, Fujian Province, China*
Corresponding author: Cheng-Bin Wang (entomologist@qq.com)

Abstract

Cochleopsaltria Pham & Constant, 2017 (Hemiptera, Cicadidae, Cicadinae) is no longer monospecific: *C. huboliao* **sp. nov.** from Fujian Province of China is described and illustrated. A key to the two species of *Cochleopsaltria* is presented.

Key words: Cicada, Dundubiini, key, morphology, new genus record, new species, Oriental region, taxonomy

Introduction

The monotypic genus *Cochleopsaltria* (Hemiptera, Cicadidae, Cicadinae, Dundubiini, Dundubiina) was erected by Pham and Constant in 2017 for *C. duffelsi* Pham & Constant, 2017, based on a single male from northern Vietnam (Pham and Constant 2017). Since then, there has been no report on the discovery of this species or the genus.

In the present study, a new species of *Cochleopsaltria* is described from Huboliao National Nature Reserve, Fujian, China, representing a new national record for genus. Therefore, the number of the genera in the subtribe Dundubiina from China amounts to four: *Cochleopsaltria* Pham & Constant, 2017, *Dundubia* Amyot & Audinet-Serville, 1843, *Macrosemia* Kato, 1925 and *Platylomia* Stål, 1870 (Metcalf 1963; Chou et al. 1997; Sanborn 2013; Wang 2014). Illustrations of the diagnostic characters of the new species, a distribution map of the genus, and a key to the two species are provided.

Material and methods

Four males and three females of the new species were collected from Huboliao National Nature Reserve of Fujian Province (China) on 25 October 2023. After fieldwork, the specimens were kept in a freezer (-20 °C). About half a year later, the specimens were relaxed and softened in water

OPEN ACCESS

Academic editor: Allen Sanborn
Received: 10 December 2024
Accepted: 12 February 2025
Published: 6 March 2025

ZooBank: https://zoobank.org/7BA1DB65-E0AC-48C9-A94B-B7C9BAA9CF63

Citation: Wang C-B, Liu Z-J (2025) First record of the genus *Cochleopsaltria* Pham & Constant (Hemiptera, Cicadidae, Cicadinae) from China, with a description of the second species. ZooKeys 1230: 335–346. https://doi.org/10.3897/zookeys.1230.144099

at room temperature for 12 h and then placed in distilled water for cleaning and dissection. To examine the male genitalia, the pygofer (containing the aedeagus), together with sternite VIII, were detached by fine-point tweezers and cleared with a trypsin solution at room temperature for 12 h. Then, they were placed in a 70% ethanol solution to remove the remaining trypsin. After examination, the body parts were mounted on a slide using Euparal mounting medium for future studies. Images were taken with a Canon MP-E 65 mm 1–5× macro lens on a Canon EOS 5DsR. Images of the same object at different focal planes were combined using Zerene Stacker 1.04 stacking software. Adobe Photoshop CS6 was used for post-processing. The description was carried out on dry specimens. Morphological terminology follows Moulds (2005, 2012) and higher taxonomy follows Marshall et al. (2018) and Simon et al. (2019). Measurement criteria in millimetres (mm) follow Wang and Liu (2022).

The type material of the new species is deposited in the following collections: **CLYQ**—Chonglinyequ Cultural Creativity Co., Ltd., Fuzhou, China; **MYNU**—Invertebrate Collection of Mianyang Normal University, Mianyang, China.

Taxonomy

Family Cicadidae Batsch, 1789
Subfamily Cicadinae Batsch, 1789
Tribe Dundubiini Atkinson, 1886
Subtribe Dundubiina Atkinson, 1886

Genus *Cochleopsaltria* Pham & Constant, 2017
Chinese common name: 勺蝉属

Cochleopsaltria Pham & Constant, 2017: 227 (description; 1 sp.); Marshall et al. 2018: 27, 39 (higher taxonomy; list).

Type species. *Cochleopsaltria duffelsi* Pham & Constant, 2017, by original designation and monotypy.

Note. 2 species; Oriental region.

Diagnosis. The genus *Cochleopsaltria* Pham & Constant, 2017 can be separated from all other genera in the subtribe Dundubiina by the combination of the following characters: **Male.** Head not wider than pronotum while wider than mesonotum; rostrum at least reaching posterior coxae; pronotum shorter than mesonotum; pronotal collar with median length long, about 0.4 times as long as pronotal disc; forewings with infuscations; opercula spoon-shaped, broad and strongly convex in about apical 2/3, with apices broadly rounded, at least reaching posterior margin of sternite VI; abdomen almost as long as distance from head to cruciform elevation; pygofer upper lobes absent; uncus bifurcate with lobes stout, fused at base. **Female.** Abdominal tergite 9 with dorsal beak elongate, longer than anal styles; ovipositor sheath extremely elongate.

Cochleopsaltria duffelsi **Pham & Constant, 2017**

Chinese common name: 笛氏勺蝉

Cochleopsaltria duffelsi Pham & Constant, 2017: 227, figs 1–4 (description; illustrations).

Type locality. "Hoa Binh 2, Quan Chu, Dai Tu, Thai Nguyen Province, 200–300 m".

Distribution. Vietnam.

Cochleopsaltria huboliao **sp. nov.**

https://zoobank.org/1AEF95BD-8D9B-41D4-B03F-FC0931EE64EA

Figs 1A–C, 2A–C, 3A–E, 4A–E, 5A–C, 6A, B

Chinese common name: 虎伯寮勺蝉

Type locality. China, Fujian: Zhangzhou City, Huboliao National Nature Reserve [虎伯寮国家级自然保护区], Letu District [乐土片].

Type material. 4 ♂♂ 3 ♀♀. ***Holotype*****:** • ♂ (MYNU), **China, Fujian:** Zhangzhou City, Huboliao National Nature Reserve [虎伯寮国家级自然保护区], Letu District [乐土片], 25.X.2023, Liang Guo, Qun-Zhen Wu & Zu-Bin Chen leg. (MYNU). ***Paratypes*****:** • 3 ♂♂ 3 ♀♀ (1 ♀ in MYNU and 3 ♂♂ 2 ♀♀ in CLYQ), same data as holotype.

Etymology. The specific epithet is from the Chinese name (in Pinyin) of the type locality "Huboliao". The name is a noun in apposition.

Description. Male (Figs 1A, B, 6A, B). ***Measurements*** (mm, *N* = 2, including smaller holotype). Body 37.3–39.2 long. Lengths of different body parts: head (2.6–2.9), pronotum (5.8–6.3), mesonotum (10.1–10.5), forewing (49.4–50.5), abdomen (18.8–19.5); width: head (13.0–13.2), pronotum (13.4–13.7), mesonotum (8.3–8.7), forewing (13.9–14.4), tergite 3 (12.0–12.3). Ratios of different body parts: (body length)/(head width) = 2.9; (pronotal length)/(head length) = 2.2; (mesonotal length excluding cruciform elevation)/(pronotal length) = 1.5; (abdominal length)/(head + pronotal + mesonotal length) = 1.0; (head width)/(pronotal width) = 1.0; (head width)/(mesonotal width) = 1.6; (tergite 3 width)/(mesonotal width) = 1.4; (forewing length)/(forewing width) = 3.6.

Head**.** Ground colour ochraceous, with following black markings: longitudinal median fascia broad, bifurcate in posterior part, enclosing three ocelli, reaching frontoclypeal suture and posterior margin of head, without extended lateral parts; lateral fasciae broad except distinctly narrowed posterior part, reaching anterolateral and posterior margins of head; transverse fascia narrowly along posterior margin of head; paired small spots against posterior margin of head. Compound eyes ochraceous. Ocelli orangish. Distance between lateral ocellus and corresponding eye about 2.8 times as wide as distance between lateral ocelli. Antennae brown to fuscous. Postclypeus moderately swollen, mostly ochraceous, with paired brown oblique fasciae just anterior to frontoclypeal suture and a long "Y"-like brown median fascia ventrally, with 10–11 wide transverse grooves on each side. Anteclypeus ochraceous along median carina and brown laterally. Gena ochraceous, with oblique black fascia in anterior part. Lorum black in about posterior half and ochraceous in about anterior half. Rostrum ochraceous with blackish apical part, reaching middle of sternite **II**.

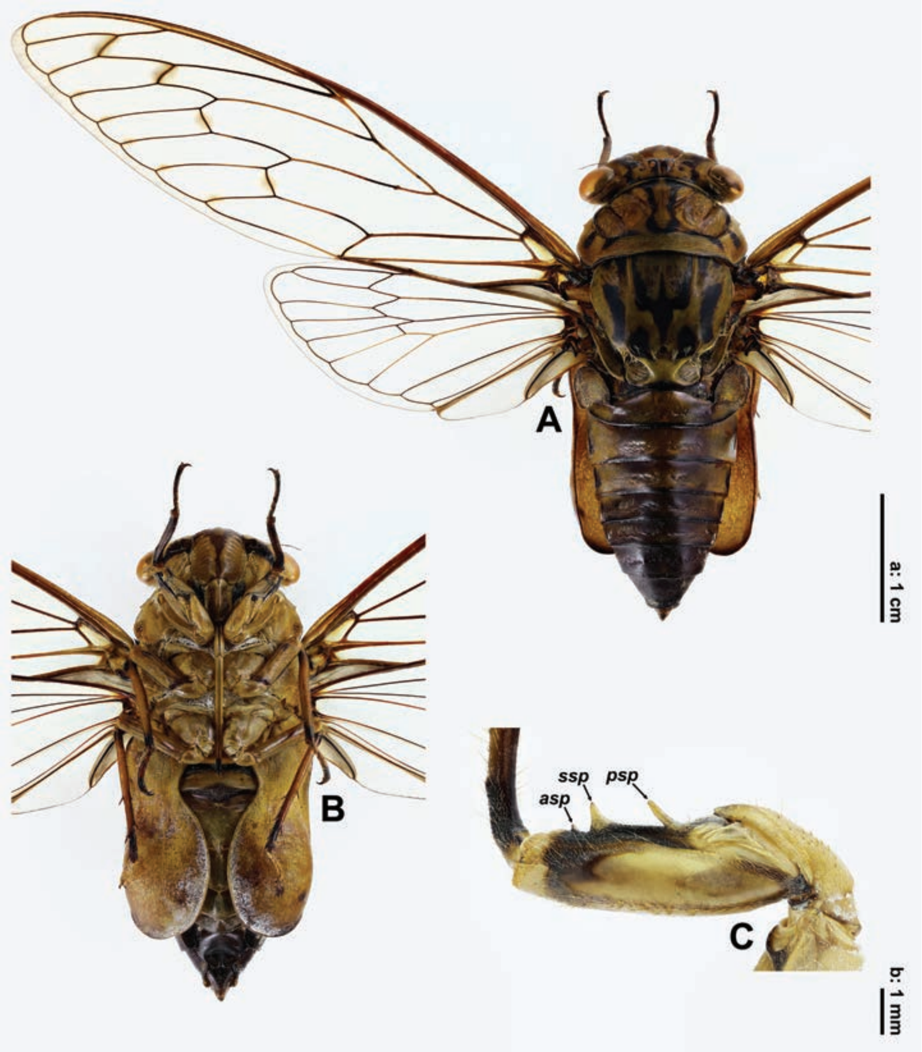

Figure 1. *Cochleopsaltria huboliao* sp. nov., ♂, holotype **A** habitus, dorsal view **B** ditto, ventral view **C** right fore femur, lateral view. Abbreviations ***asp*:** apical spine ***psp*:** primary spine ***ssp*:** secondary spine. Scale bar **a** for A, B and **b** for C.

***Thorax*.** Pronotum ochraceous, slightly tinged with greenish on pronotal collar, with following black markings: submedian fasciae long, extending from anterior margin of pronotum to ambient fissure, broadened at both anterior and posterior ends; fascia along ambient fissure, broadening anterolaterally; two paired large elongate spots on pronotal collar, joining ambient fissure; no fasciae along paramedian and lateral fissures. Pronotal collar with median length long, about 0.4 times as long as pronotal disc, moderately ampliate posterolaterally; lateral margins with acute lateral teeth at about anterior 1/3, orientating laterally; posterolateral angles widely rounded; surface transversely grooved. Mesonotum greenish ochraceous, with following black markings: median fascia fusiform, broadened in middle part, strongly tapering anteriorly and reaching anterior 1/6 of mesonotum excluding cruciform elevation, moderately tapering posteriorly and not reaching anterior margin of cruciform elevation; submedian fasciae slender, along parapsidal sutures, moderately tapering anteriorly and broadening posteriorly, joining median fascia; accessory fasciae short, between submedian fasciae and accessory spots, not joining lateral fasciae posteriorly; lateral fasciae wide, gently

Figure 2. *Cochleopsaltria huboliao* sp. nov., ♀, paratype **A** habitus, dorsal view **B** ditto, ventral view **C** right fore femur, lateral view. Abbreviations ***asp*:** apical spine ***psp*:** primary spine ***ssp*:** secondary spine. Scale bar **a** for A, B and **b** for C.

curved, starting from anterior 2/7 of mesonotum excluding cruciform elevation, extending posteriorly just near anterior arms of cruciform elevation; accessory spots small, lateral to accessory fasciae; posterior spots large, occupying scutal depressions. Cruciform elevation bright ochraceous, with paired black markings on anterior arms. Wing groove ochraceous. Ventral side ochraceous, basisternum 2 with paired oblique black rhombic markings, basisternum 3 with paired small black spots, surface densely with short setae.

***Legs*.** Bicoloured, ochraceous to brown with blackish markings. Profemur (Fig. 1C) with three spines: primary spine slender, digitiform, obliquely inserted, with apex rounded; secondary spine subtrianglular, with apex rounded; apical spine rather small, subtrianglular, with apex rounded. Meracanthi ochraceous, slender and slightly curving medially.

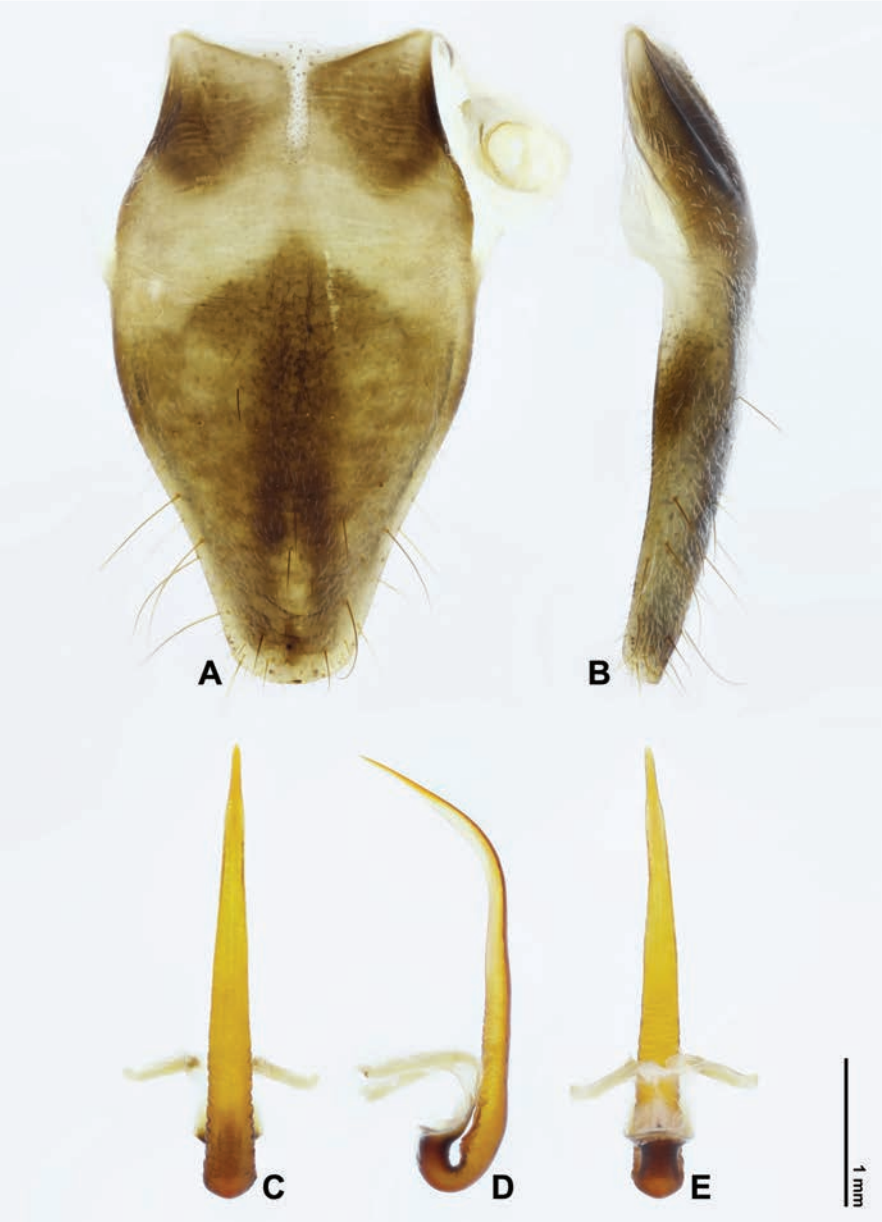

Figure 3. *Cochleopsaltria huboliao* sp. nov., ♂, holotype **A** sternite VIII, ventral view **B** ditto, lateral view **C** aedeagus, dorsal view **D** ditto, lateral view **E** ditto, ventral view.

Wings. Hyaline. Forewing with eight apical cells; ulnar cell 3 about twice as long as apical cell 5; RA_2 vein with distal portion about 1.9 times as long as proximal portion; venation color mixed with ochraceous, brown and fuscous; infuscations present on r, r-m, m and m-cu crossveins, and paler on apices of longitudinal veins of apical cells; nodal line absent; basal cell greyish ochraceous; basal membrane greyish ochraceous. Hindwing with six apical cells; venation color mixed with ochraceous, brown and fuscous, 3A blackish; jugum and longitudinal margins of vannus greyish ochraceous.

Operculum. Mostly ochraceous, with basal part of lateral margin blackish; spoon-shaped, constricted around basal 2/7, broad and strongly convex in about apical 2/3; apex broadly rounded, extending beyond posterior margin of sternite VI; separated from each other about 1/5 width of one of them; lateral margin slightly bisinuate while medial margin strongly so.

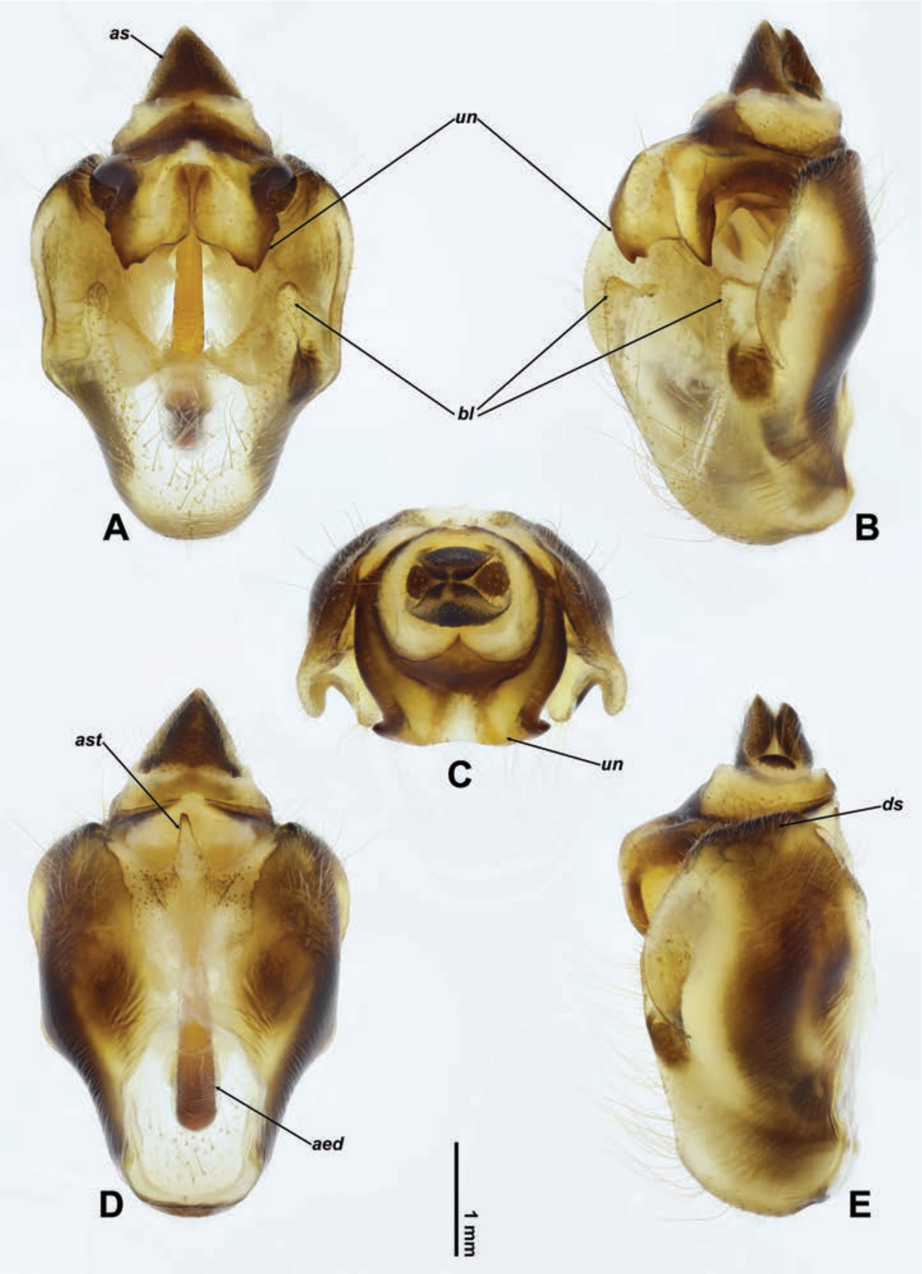

Figure 4. Pygofer of *Cochleopsaltria huboliao* sp. nov., ♂ **A** ventral view **B** ventrolateral view **C** apical view **D** dorsal view **E** lateral view. Abbreviations ***aed*:** aedeagus ***as*:** anal styles ***ast*:** apical stylus ***bl*:** basal lobe ***ds*:** distal shoulder ***un*:** uncus.

***Abdomen*.** Obconical, in dorsal view generally brownish in basal part and fuscous apically. Tergite 1 fuscous to blackish; tergites 2–8 with posterior margins narrowly blackish; tergites 3–6, each with one fuscous spot at lateral side. Timbal cover oval, ochraceous with narrow brown margin, covered with greyish hairs, especially in lateral part, completely concealing timbal in dorsal view. Sternites III–VI mostly ochraceous to brown; sternite VII fuscous except ochraceous in posterior part, subhexagonal, inconspicuously emarginate at posterior margin, with longitudinal median groove in posterior part; sternite VIII (Fig. 3A) ochraceous with brown median fascia and paired anterior markings, drop-like, rounded at posterior margin, anterolateral apodemes subtriangularly developed.

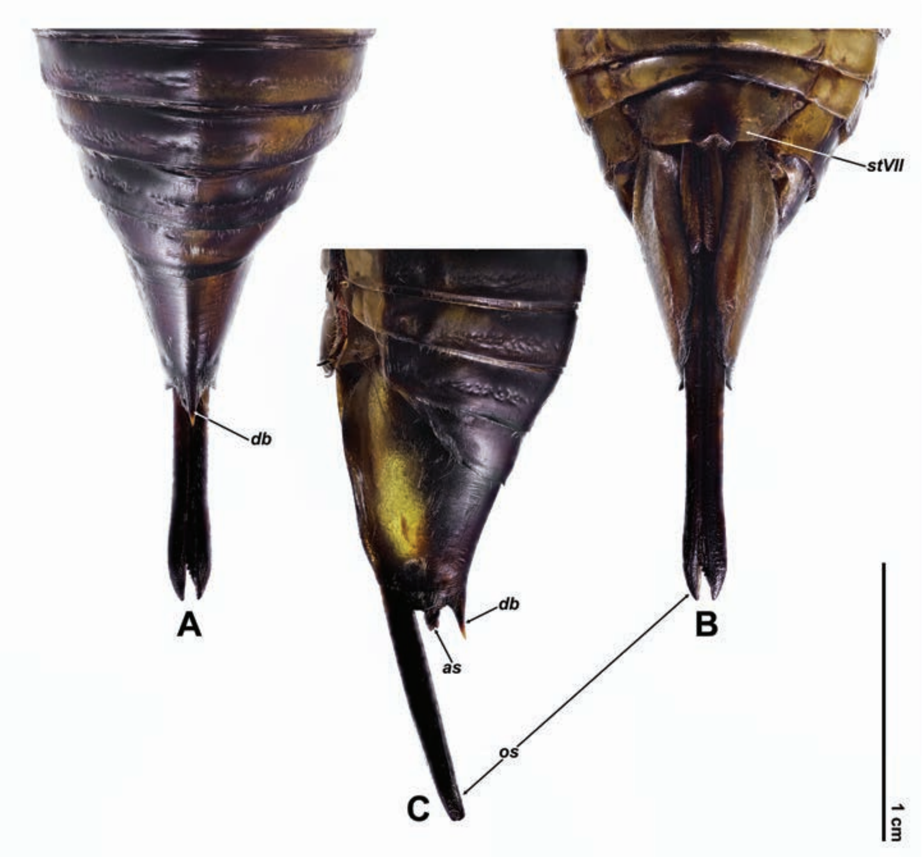

Figure 5. Female terminalia of *Cochleopsaltria huboliao* sp. nov., paratype **A** dorsal view **B** ventral view **C** lateral view. Abbreviations ***as*:** anal styles ***db*:** dorsal beak ***stVII*:** sternite VII ***os*** ovipositor sheath.

***Genitalia*.** Pygofer suboval, more or less narrowing anteriorly in ventral and dorsal views (Fig. 4A, D); anal styles relatively large, moderately sclerotised, densely covered with short setae (Fig. 4A–E); apical stylus relatively large, slender, lightly sclerotised, digitiform (Fig. 4D); basal lobes in ventral view elongate (Fig. 4A), in ventrolateral view subtriangular in apical parts (Fig. 4B); upper lobes absent; distal shoulders obliquely truncated at apices in lateral view (Fig. 4E). Uncus bifurcate; lobes stout, fused at base, rather narrowly separated from each other medially, in ventral view angulate at apices, crenulate at lateral margin and bisinuate at medial margin (Fig. 4A), in ventrolateral view further one bidentate at apices (Fig. 4B). Aedeagus thin and slender, gradually narrowing towards apex, without processes (Fig. 3C, E); in lateral view, strongly turning ventrally in apical 1/3 and almost straight in basal 2/3 (Fig. 3D).

Female (Fig. 2A, B). *Measurements* (mm, N = 2). Body 42.1–45.8 long. Length of different body parts: head (1.9–2.7), pronotum (4.9–5.9), mesonotum (9.1–10.0), forewing (50.8–52.6), abdomen (26.2–27.2); width: head (12.6–13.1), pronotum (13.5–13.9), mesonotum (9.5–10.1), forewing (14.2–14.7), tergite 3 (13.1–13.5). Ratios of different body parts: (body length)/(head width) = 3.5; (pronotal length)/(head length) = 2.1; (mesonotal length excluding cruciform elevation)/(pronotal length) = 1.4; (abdominal length)/(head + pronotal + mesonotal length) = 1.5; (head width)/(pronotal width) = 1.0; (head width)/(mesonotal width) = 1.3; (tergite 3 width)/(mesonotal width) = 1.3; (forewing length)/(forewing width) = 3.6.

Figure 6. Field observations of *Cochleopsaltria huboliao* sp. nov. at Huboliao National Nature Reserve (© Qun-Zhen Wu) **A** a living male perching on a branch, posterodorsal view **B** ditto, lateral view **C, D** habitat and host plant.

Rostrum extending beyond posterior margin of abdominal sternite II; profemur (Fig. 2C) similar to that of male; abdomen subconical, gradually converging apically; operculum short, rounded at posterior margin, extending slightly beyond posterior margin of abdominal sternite II and separated from each other by about 1.7 times width of one of them; abdominal sternite VII (Fig. 5B) subroundly incised at middle of posterior margin, with paired protuberances flanked incision; abdominal tergite 9 with dorsal beak (Fig. 5A, C) elongate, roundly sharp, longer than anal styles; ovipositor sheath (Fig. 5A–C) blackish, extremely elongate.

Variation. All male or female types without evident variation.

Field observations. A living male of the new species is shown in Fig. 6A, B and its habitat in Huboliao National Nature Reserve is shown in Fig. 6C, D. According to the collectors' recollection, during the collecting trip in late October, this cicada was abundant in the reserve, but the individuals were difficult to capture. They were in the canopy and not attracted to light traps at night, so the collectors had to climb up the trees to capture them.

Distribution. China (Fujian) (Fig. 7).

Differential diagnosis. The new species well resembles its only congener *C. duffelsi* from Vietnam in general appearance, but it is not difficult to distinguish them using the following key.

Additionally, although many species in Cicadinae exhibit morphological variations in markings and operculum length, they still have certain reference characteristics:

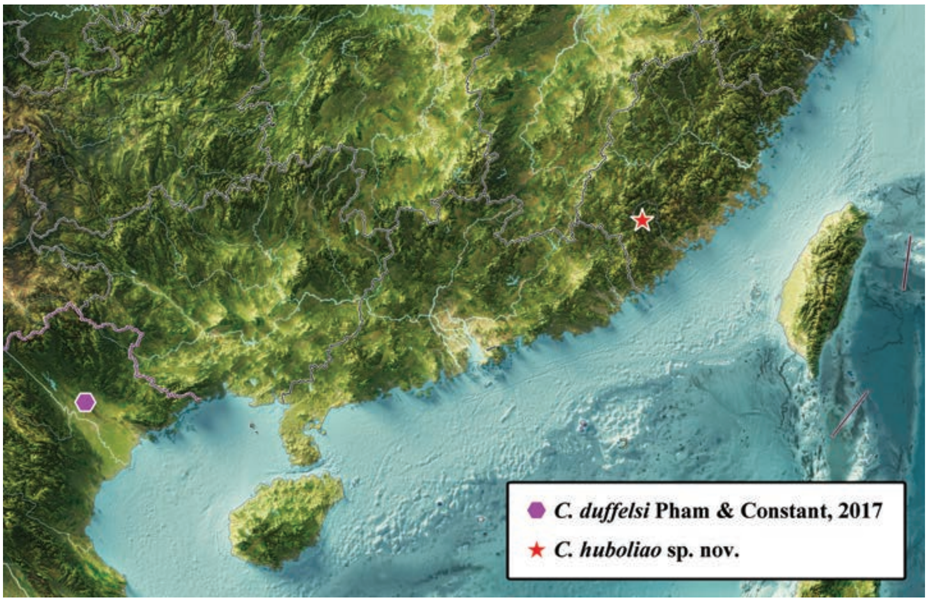

Figure 7. Distribution map of *Cochleopsaltria* species.

In *C. duffelsi*, pronotal collar with three paired large spots (Pham and Constant 2017: figs 2A; 3A); mesonotum with median fascia moderately tapering anteriorly and weakly so posteriorly, lateral fasciae relatively slender, accessory spots absent (Pham and Constant 2017: figs 2A; 3A); opercula reaching posterior margin of sternite VI (Pham and Constant 2017: figs 2B; 3B). In *C. huboliao* sp. nov., pronotal collar with two paired large spots (Fig. 1A); mesonotum with median fascia strongly tapering anteriorly and moderately so posteriorly, lateral fasciae relatively wide, small accessory spots lateral to accessory fasciae (Fig. 1A); opercula extending beyond posterior margin of sternite VI (Fig. 1B).

Key to males of *Cochleopsaltria* Pham & Constant, 2017

1 Pygofer basal lobes in ventrolateral view rounded in apical parts (Pham and Constant 2017: fig. 4B); uncal lobes in ventral view rounded at apices, simply arcuate at both lateral and medial margins (Pham and Constant 2017: fig. 4C), in ventrolateral view further one rounded at apices (Pham and Constant 2017: fig. 4B) .... ***C. duffelsi* Pham & Constant, 2017**

– Pygofer basal lobes in ventrolateral view subtriangular in apical parts (Fig. 4B); uncal lobes in ventral view angulate at apices, crenulate at lateral margin and bisinuate at medial margin (Fig. 4A), in ventrolateral view further one bidentate at apices (Fig. 4B) .... ***C. huboliao* sp. nov.**

Acknowledgements

We are indebted to Zu-Bin Chen, Liang Guo, Peng-Yu Liu and Qun-Zhen Wu (all CLYQ) for providing the specimens of the new species. We would like to express our sincere gratitude to Michel Boulard (Villeneuve-la-Comtesse, France), Chang-Chin Chen (Tianjin, China), Lei Feng (Weifang, China), Jin-Yuan Jiang (Wuxi, China), Xiao-Feng Li (Ehime university, Matsuyama, Japan), Yu-Tang Wang and Hao Xu (both MYNU), and Jin Zhang (Zhangjiakou, China) for their considerable help in this study. We thank Yu-jian Li (Qufu Normal University, China), Jeng-Tze Yang (National Chung Hsing University, Taichung, China), and an anonymous reviewer for their constructive comments on earlier versions of the manuscript.

Additional information

Conflict of interest

The authors have declared that no competing interests exist.

Ethical statement

No ethical statement was reported.

Funding

This study was financially supported by the Natural Science Foundation of Huaguoshan (花果山自然科学基金NSFH-2025).

Author contributions

Conceptualization: C-B Wang & Z-J Liu. Project administration: C-B Wang. Resources: Z-J Liu. Supervision: C-B Wang. Visualization: C-B Wang. Writing–original draft: C-B Wang. Writing–review and editing: C-B Wang & Z-J Liu.

Author ORCIDs

Cheng-Bin Wang https://orcid.org/0000-0002-7913-8779
Zhi-Jian Liu https://orcid.org/0009-0000-2129-1861

Data availability

All of the data that support the findings of this study are available in the main text.

References

Chou I, Lei Z-R, Li L, Lu X-L, Yao W (1997) The Cicadidae of China (Homoptera: Cicadoidea). Tianze Eldoneio, Hong Kong, 380 pp.

Marshall DC, Moulds MS, Hill KBR, Price BW, Wade EJ, Owen CL, Goemans G, Marathe K, Sarkar V, Cooley JR, Sanborn AF, Kunte K, Villet MH, Simon C (2018) A molecular phylogeny of the cicadas (Hemiptera: Cicadidae) with a review of tribe and subfamily classification. Zootaxa 4424(1): 1–64. https://doi.org/10.11646/zootaxa.4424.1.1

Metcalf ZP (1963) General Catalogue of the Homoptera. Fascicle VIII. Cicadoidea. Part 1. Cicadidae. North Carolina State College, Raleigh, No. 1502, 919 pp.

Moulds MS (2005) An appraisal of the higher classification of cicadas (Hemiptera: Cicadoidea) with special reference to the Australian fauna. Records of the Australian Museum 57(3): 375–446. https://doi.org/10.3853/j.0067-1975.57.2005.1447

Moulds MS (2012) A review of the genera of Australian cicadas (Hemiptera: Cicadoidea). Zootaxa 3287: 1–262. https://doi.org/10.11646/zootaxa.3287.1.1

Pham H-T, Constant J (2017) A new genus and species of cicada from Vietnam: *Cochleopsaltria duffelsi* gen. et sp. nov. (Hemiptera: Cicadomorpha: Cicadidae). Bulletin de la Société Royale Belge d'Entomologie 153: 226–230.

Sanborn AF (2013) Catalogue of the Cicadoidea (Hemiptera: Auchenorrhyncha). With Contributions to the Bibliography by Martin H. Villet. Elsevier/Academic Press, London, 1001 pp. https://doi.org/10.1016/B978-0-12-416647-9.00001-2

Simon C, Gordon ER, Moulds MS, Cole JA, Haji D, Lemmon AR, Lemmon EM, Kortyna M, Nazario K, Wade EJ, Meister RC, Goemans G, Chiswell SM, Pessacq P, Veloso C, McCutchen JP, Łukasik P (2019) Off-target capture data, endosymbiont genes and morphology reveal a relict lineage that is sister to all other singing cicadas. Biological Journal of the Linnean Society 128(4): 865–886. https://doi.org/10.1093/biolinnean/blz120

Wang X (2014) Taxonomic study of Cicadini from China (Hemiptera: Cicadidae). Master's Thesis, Northwest Agriculture & Forestry University, Yangling, 267 pp.

Wang C-B, Liu P-Y (2022) A new species of *Polyneura* Westwood, 1842 from Yunnan, China (Hemiptera, Cicadidae, Cicadinae). Biodiversity Data Journal 10: e84554. https://doi.org/10.3897/BDJ.10.e84554